



The
University
Of
Sheffield.

Heart failure syndrome and predicting response to cardiac resynchronisation therapy

Patient specific models, biomarkers and biophysical properties.

David Roy Warriner

Submitted for the degree of Doctor of Philosophy

Medical Physics Group

Department of Infection, Immunity and Cardiovascular Science

Faculty of Medicine, Dentistry and Health

July 2016

Abstract

Heart failure results from the heart pumping insufficient quantities of blood to meet the body's metabolic requirements. This condition affects around 600,000 people in the United Kingdom and carries with it a significant morbidity and mortality. Patients typically complain of reduced exercise capacity and a poor quality of life. Whilst there are various pharmaceutical options available to clinicians, none directly augment cardiac function. Cardiac resynchronisation therapy (CRT) is proven to reverse the progression of left ventricular systolic dysfunction, the most common cause of heart failure. The device resynchronises inefficient cardiac function, reducing symptoms and improving stroke volume and life expectancy. However, only two thirds of patients typically derive benefit from this pacemaker, it being unclear why. Finding a sensitive and specific predictor of response would be invaluable, preventing potential harm to patients, reducing waste and targeting the patient groups who will derive benefit.

In this body of work, the heart failure syndrome is delineated; the evidence underpinning CRT discussed and the difficulties in defining response outlined. There are 2 main research themes in this body of work, measuring and predicting response to CRT. In the former, the role of patient specific three-dimensional computational models and biophysical properties are investigated, and, in the latter, the influence of CRT on the heart failure syndrome using biomarkers.

It is concluded that CRT response can be predicted using patient specific computational models of the left ventricle, but they are too complex for routine clinical use. Biophysical markers have more merit in the immediate future, being simpler and quicker, with measures of endothelial and skeletal muscle function, demonstrating promise in a small cohort of patients. Finally, there exists a significant level of undiagnosed pathology in this patient group, such as hyperuricaemia and hyperparathyroidism, but it remains unclear what impact CRT has on this comorbidity.

Acknowledgments

Firstly, a big thanks to my brilliant supervisors, Professor Pat Lawford and Dr Paul Sheridan, I couldn't want for two more approachable, brilliant and friendly individuals to support me along my PhD journey.

I want to thank my parents and brother for their unwavering support and encouragement over the last 6 years. My fellow medical physics PhD candidates, in particular Angela, Dani, Paul, Iwona, Alastair, Richard, Claudia and Jeroen. Also to the rest of the friendliest department I've ever worked in, including Steve, Andy, John, Susheel, Martin and Yubing. The fabulous staff in the cardiology, echocardiography and pulmonary function departments in Sheffield, in particular Pauline, Debbie, Jane, Justin, Debbie and Tracey, for their hardwork, flexibility and professionalism.

I want to thank all 21 of the patients who took part in the Sheffield arm of the Grand Challenge project and gave up 5 precious days of their lives to make this happen.

Also a huge thank you to Beth for giving me the time and space to finish the 'albatross' around my neck for the past 6 years and proof reading the final copy numerous times.

Finally, this thesis is dedicated to the memory of Robert "Bob" Glew (1917-2015) a huge influence on my life and without whose encouragement; none of this would have been possible.

Publications

Papers

Gonzalez G, **Warriner DR**, Jackson T, Zacur E, Hose DR, Razavi R, Smith NP & Lamata, P (2016). Adverse Left Ventricular Remodelling Patterns Predict Response to Cardiac Resynchronization Therapy. In progress.

Warriner DR, Sheridan PJ and PV Lawford (2016).

Cardiac resynchronisation therapy improves handgrip strength.

Cardiol Research, 7(3):95-103 doi.org/10.14740/cr475w

Forms the basis for section 7.1.4.

Warriner DR, Lawford PV and Sheridan PJ (2016).

Measures of endothelial dysfunction predict response to cardiac resynchronisation therapy. OpenHeart, 3(1). doi:10.1136/openhrt-2015-000391

Forms the basis for section 7.1.2.

Warriner DR, Brown AG, Varma S, Sheridan PJ, Lawford P, et al. (2014).

Closing the Loop: Modelling of Heart Failure Progression from Health to End-Stage Using a Meta-Analysis of Left Ventricular Pressure-Volume Loops. PLoS ONE, 9(12): e114153. doi: 10.1371/journal.pone.0114153 **Forms the basis for section 6.4.**

Reviews

Warriner DR, Sheridan PJ & Lawford PV (2015).

Heart failure: not a single organ disease but a multisystem syndrome.

Br J Hosp Med;76(6):330-6. doi: 10.12968/hmed.2015.76.6.330.

Warriner DR & Sheridan PJ (2014).

End-stage heart failure non-pharmacological therapy: recent advances in pacemakers, pressure monitors, pumps and other devices

Postgrad Med J;90:1061. doi:10.1136/postgradmedj-2012-131288

Poster Presentations

Warriner DR, Sheridan PJ & Lawford PV (2016).

Cardiac resynchronisation therapy leads to improvements in handgrip strength.

BCS Annual Conference, Manchester, UK.

http://heart.bmj.com/content/102/Suppl_6/A2.1.abstract?sid=aafb9eef-f067-4777-acaf-6b60778807d8

Warriner DR, Lawford PV & Sheridan PJ (2016).

Measures of endothelial dysfunction predict response to cardiac resynchronisation therapy.

BCS Annual Conference, Manchester, UK.

http://heart.bmj.com/content/102/Suppl_6/A39.1.abstract?sid=ac665136-73a4-4a90-9cf8-76b2f15d20e1&trendmd-shared=0

Gonzalez G, **Warriner DR**, Jackson T, Sammut E, Zacur E, Hose DR, Razavi R, Smith NP & Lamata, P (2015).

Adverse Left Ventricular Remodelling Patterns Predict Response to Cardiac Resynchronization Therapy.

AHA Scientific Sessions, Orlando, USA.

http://circ.ahajournals.org/content/132/Suppl_3/A16108.abstract

Warriner DR (2013).

Modelling the progression of heart failure, from health to end stage.

Insigneo (Institute for *in silico* medicine) Showcase, Sheffield, UK.

Abbreviations

Technical terms:

2D – 2 Dimensional

3D – 3 Dimensional

6MWD – 6 Minute walk distance

6MWT – 6 Minute walk test

ACC – American College of Cardiology

ACE-I – Angiotensin converting enzyme inhibitor

Ach – Acetylcholine

ACR – Albumin creatinine ratio

ADH – Anti-diuretic hormone

ADL – Activities of daily living

ADP – Adenosine diphosphate

AF – Atrial fibrillation

AHA – American Heart Association

ALP - Alkaline phosphatase

ALS – Advanced life support

A_m – Late diastolic myocardial atrial velocity

AMI – Acute myocardial infarction

ANP – Atrial natriuretic peptide

ARB – Angiotensin receptor blocker

AS – Aortic stenosis

ASHT – American Society of Hand Therapists

AT – Anaerobic threshold

ATS – American Thoracic Society

AV – Atrioventricular

AVNA – Atrio-ventricular nodal ablation

B-FFE - Balanced fast field echo

BBB – Bundle branch block

BCG - Ballistocardiography

BCS – British Cardiac Society

BiV - Biventricular
BMJ – British Medical Journal
BNP –Brain natriuretic peptide
BP – Blood pressure
BSE – British Society of Echocardiography
CCS – Clinical composite score
CFD – Computational fluid dynamics
CFM – Colour flow mapping
CHQ - Chronic heart failure questionnaire
CKD – Chronic kidney injury
cMR – Cardiac magnetic resonance
CNP – C natriuretic peptide
COPD – Chronic obstructive pulmonary disease
CPET – Cardiopulmonary exercise testing
CRF – Clinical research facility
CRP – C reactive protein
CRS – Cardio renal syndrome
CRT – Cardiac resynchronisation therapy
CRT-D - Cardiac resynchronisation therapy defibrillator
CRT-P – Cardiac resynchronisation therapy pacemaker
CS – Coronary sinus
CT – Computed tomography
CVBRU – Cardiovascular Biomedical Research Unit
CVS – Cardiovascular system
CW – Continuous wave
CXR – Chest x-ray
DCM – Dilated cardiomyopathy
dFT – Diastolic filling time
DICOM – Digital imaging and communication in medicine
DM – Diabetes mellitus
DNA – Deoxyribonucleic acid
dP/dt – Rate of pressure rise
DS - Dyssynchrony

ECG – Electrocardiogram

EDPVR - End diastolic pressure volume relation

EDRF - Endothelium derived relaxation factor

EDTA - Ethylenediaminetetraacetic acid

EF – Ejection fraction

eGFR – Estimated glomerular filtration rate

E_m – Early diastolic myocardial velocity

E_{max} – Maximal elastance

E_{min} – Minimal elastance

eNOS – Endothelial nitric oxide synthase

EPSRC – Engineering and Physical Sciences Research Council

ESC – European Society of Cardiology

ESPVR – End systolic pressure volume relation

ESR – Erythrocyte sedimentation rate

EuroQoL EQ-5D - European quality of life 5 dimensions

FEA – Finite element analysis

FIESTA - Fast imaging employing steady-state acquisition

FMD – Flow mediated dilation

FSM – Frank-Starling mechanism

GC – Grand challenge

GCP – Good clinical practice

GE - Gradient echo

GIMIAS - Graphical interface for medical image analysis and simulation

GP – General practitioner

GST – Guys and St Thomas’

GTN – Glycerine trinitrate

HCM – Hypertrophic cardiomyopathy

HGS – Grip strength

HF – Heart failure

HF-LVSD – Heart failure left ventricular systolic dysfunction

HFPEF – Heart failure with a preserved ejection fraction

HFREF – Heart failure with a reduced ejection fraction

HR – Heart Rate

HRUK – Heart Rhythm United Kingdom
hs-CRP – High sensitivity c reactive peptide
hs-TNT - High sensitivity troponin t
HTN - Hypertension
IA – Invasive angiography
IABP – Intra aortic balloon pump
ICD – Implantable cardioverter defibrillator
ICER - Incremental cost effectiveness ratio
ICL – Imperial College London
IHD – Ischaemic heart disease
IL – Interleukin
IPR - Intellectual Property Rights
IVCD – Interventricular conduction delay
IVMD – Interventricular mechanical delay
JVP – Jugular venous pulse
KCCQ - Kansas city cardiomyopathy questionnaire
KCL – Kings College London
LAP – Left atrial pressure
LBBB – Left bundle branch block
LPM – Lumped-parameter model
LTR – Length tension relationship
LV-PEP – Left ventricular pre ejection period
LVAD – Left ventricular assist device
LVD-36 - Left ventricular dysfunction questionnaire
LVDD – Left ventricular diastolic dysfunction
LVEDD – Left ventricular end-diastolic dimension
LVEDP – Left ventricular end diastolic pressure
LVEDV – Left ventricular end diastolic volume
LVESV – Left ventricular end systolic volume
LVH – Left ventricular hypertrophy
LVOT – Left ventricular outflow tract
LVSD – Left ventricular systolic dysfunction
MET – Metabolic equivalents

MI – Myocardial infarction
MLWHFQ – Minnesota living with heart failure questionnaire
MRA – Mineralocorticoid antagonist
MRI – Magnetic resonance imaging
MS – Medical School
MSU – Mid stream urine
MV – Mitral valve
NGAL - Neutrophil gelatinase associated lipocalin
NGH – Northern General Hospital
NIHR - National Institute for Health Research
NIV – Non-invasive ventilation
NMD – Nitrogen mediated dilation
NO – Nitric oxide
NP – Natriuretic peptide
NRES – National Research Ethics Service
NT-proBNP – N terminal pro brain natriuretic peptide
NYHA – New York Heart Association
OA - Osteoarthritis
ODE – Ordinary differential equations
OMT – Optimal medical therapy
PAH – Pulmonary arterial hypertension
PCWP – Pulmonary capillary wedge pressure
PDE – Partial differential equations
PFU – Pulmonary function unit
PIS – Patient information sheet
PMH – Past medical history
PNS – Phrenic nerve stimulation
PRF – Pulse repetition frequency
PTH – Parathyroid hormone
PV – Plasma volume
PVD – Peripheral vascular disease
PVR – Peripheral vascular resistance
PW – Pulsed wave

QALY – Quality of life years
QLQ-SHF - Quality of life in severe heart failure questionnaire
QOL – Quality of life
QRSd – QRS duration
R&D – Research and development
RAAS – Renin angiotensin aldosterone system
RCR – Resistor capacitor resistor
RCT – Randomised controlled trial
RER - Respiratory exchange ratio
RF – Radio frequency
RPE – Rating of perceived exertion
RV – Right ventricle
RV-PEP – Right ventricular pre ejection period
RVF – Right ventricular failure
RVOT - Right ventricular outflow tract
SA – Sinoatrial
SAB - Scientific advisory board
SABCG – Signal average ballistocardiography
SAECG – Signal averaged electrocardiogram
SCD – Sudden cardiac death
SD – Standard deviation
SE – Spin echo
 S_m – Systolic myocardial velocity
SNR – Signal to noise ratio
SNS – Sympathetic nervous system
SOD - Superoxide dismutase
SPWMD – Septal to posterior wall mechanical delay
SSFP – Steady state free precession
STDEV – Standard deviation
STHT – Sheffield Teaching Hospitals Foundation Trust
SVI – Stroke volume index
TAH – Total artificial heart
TDI – Tissue Doppler imaging

Tn - Troponin
TnC – Troponin C
TNF – Tumour necrosis factor
TnI – Troponin I
TnT – Troponin T
TOE – Transoesophageal echocardiogram
TrueFISP - Fast imaging with steady state precession
TSI – Tissue synchronisation imaging
TTE - Transthoracic echocardiography
TTP – Time to peak
TV – Tricuspid valve
TVI – Tissue velocity imaging
UA – Uric acid
UACR – Urinary albumin creatinine ratio
UCL – University College London
ULF – Ultra low frequency
UMA – Urinary microalbuminuria
UPF - Universitat Pompeu Fabra
USFD – University of Sheffield
USS - Ultrasound
VCO₂ – Carbon dioxide production
V_E – Ventilatory rate
VitD – Vitamin D
VO₂ – Oxygen consumption
VR – Venous return
VT - Ventricular tachycardia

Collaborator abbreviations:

BB – Bojan Blazevic, PhD Student, Kings College London

DW - David Warriner, the author

DDS – Dani Da Silva Soto, computer scientist, Royal Hallamshire Hospital, Sheffield

DWL - Debbie Wilkinson-Lil, Cardiac Physiologist, Northern General Hospital, Sheffield

TG – Tim Gillot, Head of Clinical Chemistry, Northern General Hospital, Sheffield

TS - Tobias Shaeffter, Professor of Biomedical Engineering, Kings College London

TH - Tracey Hughes, Pulmonary Physiologist, Northern General Hospital, Sheffield

JA - Justin Adams, Cardiac Physiologist, Northern General Hospital, Sheffield

JM – Jean Maloney, Cardiac Nurse Specialist, Northern General Hospital, Sheffield

NS – Neil Simms, Professor of Mechanical Engineering, University of Sheffield

MB - Mark Black, Research Associate, Liverpool John Moores University

PL – Pablo Lamata, Henry Dale Fellow, Kings College, London

PS - Paul Sheridan, Consultant Cardiologist, Northern General Hospital, Sheffield

PVL – Patricia Lawford, Professor of Physiological Modelling, University of Sheffield.

PW – Phil Whitfield, Head of immunochemistry, Northern General Hospital, Sheffield

RR – Reza Razavi, Professor of Paediatric Cardiovascular Science, King's College London

DRH – Rod Hose, Professor of Computational Biomechanics, University of Sheffield

Warriner DR, Sheridan PJ and PV Lawford (2016). Cardiac resynchronisation therapy improves handgrip strength. *Cardiol Research*. **Forms the basis for section 7.1.4.**

Warriner DR, Lawford PV and Sheridan PJ (2016). Measures of endothelial dysfunction predict response to cardiac resynchronisation therapy. *OpenHeart*, 3(1). **Forms the basis for section 7.1.2.**

Warriner DR, Brown AG, Varma S, Sheridan PJ, Lawford P, et al. (2014).

Closing the Loop: Modelling of Heart Failure Progression from Health to End-Stage Using a Meta-Analysis of Left Ventricular Pressure-Volume Loops. *PLoS ONE*, 9(12). **Forms the basis for section 6.4.**

Contents

ABSTRACT	2
ACKNOWLEDGMENTS.....	3
PUBLICATIONS	4
ABBREVIATIONS	6
CONTENTS	14
TABLE OF FIGURES.....	20
TABLE OF TABLES	23
CHAPTER 1 INTRODUCTION.....	27
1.1 The challenge	27
1.2 Aims and Objectives.....	28
1.3 Chapter content	29
CHAPTER 2 HEART FAILURE	31
2.1 Introduction	31
2.2 Epidemiology.....	31
2.2.1 Frequency.....	31
2.2.2 Mortality	32
2.2.3 Morbidity	32
2.2.4 Ethnicity	33
2.2.5 Gender	33
2.3 Aetiology	34
2.4 Pathophysiology.....	35
2.4.1 Systolic Dysfunction	36
2.4.2 Frank-Starling Mechanism	36
2.4.3 Hormonal regulation.....	38
2.4.4 Sympathetic nervous system	40
2.4.5 Vascular Changes	40
2.4.6 Cardiac remodelling	41
2.4.7 Other changes	41
2.4.8 Diastolic Dysfunction.....	42
2.5 Dyssynchrony	42
2.5.1 Introduction	43

2.5.2	Myocardial electrical activation sequence.....	43
2.5.3	Heart Failure	45
2.5.4	Aetiology	47
2.5.5	Epidemiology.....	47
2.5.6	Assessment	48
2.6	Diagnosis	61
2.6.1	Symptoms and Signs	61
2.6.2	Investigations	62
2.7	Classification	65
2.7.1	Symptoms	65
2.7.2	LV function	66
2.8	Treatment	67
2.9	Conclusions	68
CHAPTER 3 CARDIAC RESYNCHRONISATION THERAPY		69
3.1	Introduction	69
3.2	Brief history.....	69
3.3	Indications.....	70
3.4	Device.....	72
3.5	Procedure.....	72
3.6	Cost	73
3.7	Challenges	74
3.8	Complications.....	75
3.9	Follow-up	75
3.10	Benefits	77
3.10.1	Observational Trials	77
3.10.2	Randomised controlled trials	78
3.11	Response.....	88
3.11.1	Introduction	88
3.11.2	Subjective.....	88
3.11.3	Objective	90
3.11.4	Other markers.....	94
3.12	Failure of Response	94
3.13	Conclusions	96

CHAPTER 4 MATERIALS AND METHODS	97
4.1 Background	97
4.2 Ethics	97
4.2.1 Details	97
4.2.2 Patient Selection	99
4.2.3 Recruitment of Sheffield Patients	100
4.2.4 Patients at baseline	101
4.2.5 Statistics	103
4.3 Conclusions	104
CHAPTER 5 ASSESSMENT OF RESPONSE	105
5.1 Introduction	105
5.1.1 Six Minute Walk Test	106
5.2 Cardiopulmonary Exercise Test.....	113
5.2.2 Minnesota Living with Heart Failure Questionnaire	122
5.2.3 Left Ventricular Volumes.....	128
5.2.4 Surrogate markers.....	138
5.3 Discussion.....	141
5.4 Conclusions	143
CHAPTER 6 MODELLING.....	144
6.1 Introduction	144
6.1.1 Computational Cardiovascular models	145
6.1.2 Cardiovascular models in Clinical Use	146
6.1.3 Model dimensionality	146
6.1.4 Boundary conditions	148
6.2 Pressure-Volume loops	148
6.3 Zero-Dimensional Models	151
6.3.1 Introduction	151
6.3.2 Cardiac models.....	154
6.3.3 Gap in the evidence	155
6.3.4 Problems with lumped parameter cardiovascular models	155
6.3.5 Models of the progression heart failure	156
6.4 Lumped parameter modelling of HF progression	157
6.4.1 Introduction	157

6.4.2	Methods.....	159
6.4.3	Results.....	164
6.4.4	Discussion.....	170
6.4.5	Conclusions	174
6.5	Lumped parameter modelling of response to CRT	174
6.5.1	Introduction	174
6.5.2	Methods.....	177
6.5.3	Hypotheses.....	177
6.5.4	Results.....	178
6.5.5	Discussion.....	182
6.5.6	Conclusions	186
6.6	3D Models.....	187
6.6.1	Introduction	187
6.6.2	Segmentation.....	192
6.6.3	Method	196
6.6.4	Results.....	200
6.6.5	Discussion.....	203
6.7	Geometrical model	205
6.7.1	Introduction	205
6.7.2	Method	206
6.7.3	Statistics	207
6.7.4	Results.....	207
6.7.5	Discussion.....	215
6.7.6	Conclusions	216
6.8	Electrophysiological model	217
6.8.1	Introduction	217
6.8.2	Methods.....	218
6.8.3	Results.....	221
6.8.4	Discussion.....	223
6.8.5	Conclusions	226
6.9	Discussion.....	226
6.10	Conclusions	228
CHAPTER 7	BIO AND BIOPHYSICAL MARKERS.....	230

7.1	Biophysical Markers	230
7.1.1	Introduction	230
7.1.2	Flow Mediated Dilatation (FMD).....	230
7.1.3	Ballistocardiography.....	249
7.1.4	Hand Grip Strength	278
7.2	Biomarkers	289
7.2.1	Introduction	289
7.2.2	Uric acid	289
7.2.3	Troponin T.....	297
7.2.4	Brain Natriuretic Peptide	303
7.2.5	Parathyroid Hormone/Vitamin D.....	310
7.2.6	High sensitivity C-Reactive Peptide.....	319
7.2.7	Proteinuria	326
7.3	Conclusions	333
CHAPTER 8 EVALUATION OF CLINICAL RELEVANCE		334
8.1	Models	334
8.2	Biophysical	337
8.3	Biomarkers	339
8.4	Conclusions	340
CHAPTER 9 DISCUSSION, CONCLUSIONS AND FUTURE WORK.....		341
9.1	Discussion.....	341
9.2	Conclusions	347
9.3	Future Work.....	347
9.3.1	General.....	347
9.3.2	Modelling	348
9.3.3	Biophysical	348
9.3.4	Biomarkers	349
PERMISSIONS		350
APPENDIX.....		351
Minnesota Living with Heart Failure Questionnaire		351
Borg Breathlessness scale		352
Borg Rating of Perceived Exertion (RPE) scale		353
Patient Information Sheet		354

Protocol.....	362
Consent form	373
Letter of invitation	374
GP letter.....	375
REFERENCES.....	376

Table of Figures

Figure 1: Frank-Starling mechanism and effect on contractility and afterload	37
Figure 2: Effect of increasing EDV on SV in various physiological states	37
Figure 3: The complexities of the Renin-Angiotensin-Aldosterone System.....	39
Figure 4: The conduction pathways of the heart.....	44
Figure 5: 12 lead ECG demonstrating LBBB	48
Figure 6: ECG leads V1 and V6 demonstrating LBBB	48
Figure 7: An apical 4 chamber trans-thoracic echocardiogram	49
Figure 8: M mode echocardiogram the LV in parasternal short-axis view	50
Figure 9: Echocardiographic measurement of atrioventricular dyssynchrony	53
Figure 10: Echocardiographic measurement of interventricular dyssynchrony	54
Figure 11: TSI displays colour-coded time-to-peak tissue Doppler velocities.....	56
Figure 12: Speckle-tracking time–strain curves in a HF patient with LBBB.....	58
Figure 13: Acquisition of 3D LV image (left) and analysis of the 16 segments (right)....	59
Figure 14 : cMR with LV in diastole (left) and systole (right) in the coronal plane	61
Figure 15: CXR demonstrating acute pulmonary oedema	63
Figure 16: CXR with CRT-D in situ	72
Figure 17: Grand Challenge Modelling project workflow and division of labour	98
Figure 18: 6MWD in responders (white) and non-responders black.....	108
Figure 19: Patient-undergoing 6MWT with purpose built walkway	109
Figure 20: Peak VO ₂ in responders (white) and non-responders (black)	117
Figure 21: Patient undergoing CPEX testing on bicycle ergometer	118
Figure 22: MLWHFQ score in responders (white) and nonresponders (black)	124
Figure 23: Simpson's method using apical 4 (left) and 2 chamber (right) views	129
Figure 24: LVEDV in responders (white) and nonresponders (black)	131
Figure 25: LVESV in responders (white) and nonresponders (black)	131
Figure 26: LVEF in responders (white) and nonresponders (black)	132
Figure 27: Diagram showing increasing complexity of models from 0-3D	147
Figure 28: Cardiac cycle and PV loop	149
Figure 29: Measurement and formation of a LV PV loop	150
Figure 30: A 2-component Windkessel model.....	153

Figure 31: A lumped parameter model with 2-element afterload	159
Figure 32: PV conductance catheter in the LV.....	159
Figure 33: Screenshot using Sourceforge software to digitize a PV loop.....	162
Figure 34: Screenshot using OpenCell to model cardiovascular haemodynamics.....	163
Figure 35: Mean (triangles) and individual LV PV loops (lines) from Stage D	167
Figure 36: Mean (thick) and individual PV loops (thin) from all HF Stages	168
Figure 37: Modelled (lines) and mean (shapes) loops according to HF stage.....	169
Figure 38: Calculation of error in modelling the mean Stage A LV PV loop	170
Figure 39: PWTDI measurement (right to left) of E, E' septal and E' lateral	176
Figure 40: LV PV loop at baseline in responders (dashed) and nonresponders (solid)	180
Figure 41: Non-invasive LV PV loops in responders.....	180
Figure 42: Non-invasive LV PV loops in nonresponders.....	181
Figure 43: Correlation between measured and modelled LV PV data.....	182
Figure 44: 3D model workflow.....	191
Figure 45: Mock-up 3D LV models demonstrating various biophysical properties	192
Figure 46: Automated cMR segmentation (shaded red) axial and sagittal.....	195
Figure 47: Automated segmentation mesh (left) with actual cMR image (right)	196
Figure 48: 3D SSFP cMR in 3 orthogonal planes, sagittal, axial and coronal.....	197
Figure 49: Process of hand segmentation of the LV endocardial surface.....	197
Figure 50: Hand-segmented LV surface epicardial (left) and endocardial (right)	198
Figure 51: 3D whole heart segmentation using the UCL tool	199
Figure 52: Outer (left) and inner (right) LV surface from using the UCL tool.....	199
Figure 53: Hand (green) and semi-automated (red) LV surfaces overlaid	201
Figure 54: LV surfaces of hand (white) and semi-automated (colour) segmentation .	202
Figure 55: Comparing the distance between corresponding voxels in each surface...	202
Figure 56: The 3 stages of the mesh personalisation process	208
Figure 57: Variances of the modes of shape variation from PCA	209
Figure 58: Differences between responders and nonresponders by variation modes	210
Figure 59: Mean LV shape (left) and overlay of responder and nonresponder (right)	210
Figure 60: Distribution of shape coefficients in PCA coordinates 4 and 5	211
Figure 61: Comparison of differences between statistical averages of LV shapes	212
Figure 62: Illustration of the anatomical changes encoded by Mode 4 and Mode 5 ..	213
Figure 63: Comparison of AUC based on combinations of PCA modes of variation....	214

Figure 64: Type I (right) and Type II (left) activation patterns of the LV	217
Figure 65: Mesh construction process	220
Figure 66: Model pacing locations versus ex-vivo electrical mapping in human heart	221
Figure 67: Correlation between measured and modelled QRSD	222
Figure 68: Activation time (ms) visualised on the epicardium. Not to scale.....	223
Figure 69: FMD acquisition; patient, brachial USS, sphygmomanometer and arm jig	233
Figure 70: MIA-IIc brachial analyser software with B-mode USS of brachial artery	233
Figure 71: FMD response following cuff deflation at frame 1800	234
Figure 72: NMD response following administration of GTN at frame 600	234
Figure 73: FMD (mean and SD) in responders (white) and nonresponders (black).....	242
Figure 74: NMD (mean and SD) in responders (white) and nonresponders (black)	242
Figure 75: Logistic regression of probability of CRT response and baseline FMD	243
Figure 76: FMD and NMD box plots at baseline in responders and nonresponders ...	243
Figure 77: BCG and ECG data, from a healthy adult over 10 minutes	250
Figure 78: Number of publications in BCG and SHM over 60 years.....	253
Figure 79: BCG and ECG data, from various HF failure patients	255
Figure 80: Use of BCG to optimise interventricular delay in CRT.....	256
Figure 81: Kistler signal amplifier, force plate and metal platform	257
Figure 82: Configuration screens for g.Recorder software	259
Figure 83: Configuration screens for Kistler charge amplifier.	259
Figure 84: Connection guide for BCG and ECG leads into g.USBamp	260
Figure 85: Example figure of SABCG and ECG results	263
Figure 86: SABCG from responders at all time points.....	266
Figure 87: SABCG from responders at all timepoints (II)	266
Figure 88: SABCG from responders pre and post optimisation of CRT device.....	267
Figure 89: BCG signal averaged data from the nonresponder at all time points.....	268
Figure 90: SABCG at baseline in responders and nonresponder	269
Figure 91: SABCG at baseline in responders, demonstrating SD	269
Figure 92: Correlation between M wave and LVEDV, at 6 months, in responders.....	271
Figure 93: Correlation between N wave and peak VO ₂ , at 6 months, in responders ..	271
Figure 94: Correlation between K wave and QRSD, at 12 months, in responders	271
Figure 95: Correlation between I wave and PP, at baseline, in responders	272
Figure 96: The muscle hypothesis of HF symptoms.....	279

Figure 97: Picture of the Jamar hand dynamometer	281
Figure 98: Left and right HGS in responders (grey) and non-responders (black).....	285
Figure 99: Screen shot of the Seattle Heart Failure Model.....	291
Figure 100: UA in responders (white) and nonresponders (black)	294
Figure 101: hsTnT in responders (white) and nonresponders (black)	300
Figure 102: NT-proBNP levels in responders (white) and nonresponders (black)	307
Figure 103: Serum PTH in responders (white) and nonresponders (black)	316
Figure 104: Serum Vitamin D in responders (white) and nonresponders (black).....	316
Figure 105: Serum hsCRP in responders (white) and nonresponders (black).....	323
Figure 106: UACR in responders (white) and nonresponders (black).....	330
Figure 107: Correlation between 6MWD and GS in the left (A) and right (B) hands ...	345
Figure 108: Correlation coefficient between UA and peak VO ₂ and UA and LVEDV....	345

Table of Tables

Table 1: Major causes of HF	34
Table 2: A summary of HF aetiology in 8 studies published between 1996 to 2010	35
Table 3: Specificity and sensitivity of signs and symptoms of HF	62
Table 4: Blood tests used in the investigation of HF	62
Table 5: Levels of natriuretic peptides required for the diagnosis of HF	63
Table 6: NYHA functional classification of symptom severity in heart failure	65
Table 7: AHA/ACC classification of HF.....	66
Table 8: CRT clinical trial names and their acronyms.	70
Table 9: A summary of the important CRT clinical trials.....	70
Table 10: NICE 2014 guidelines for implantation of CRT	71
Table 11: International guidelines for the selection of patients for CRT	71
Table 12: Summarising the 21 patients recruited to the study at baseline Error! Bookmark not def	
Table 13: Summarising scar position, device, manufacturer and lead position.	103
Table 14: 6MWD comparing responders and nonresponders at baseline	107
Table 15: 6MWD in responders comparing baseline results with follow-up.....	107
Table 16: 6MWD for nonresponders at baseline and follow-up.....	107
Table 17: Mean 6MWD at baseline and at 6 months in the CRT trials	113

Table 18: Baseline CPET metrics in responders and nonresponders.	116
Table 19: CPET metrics in responders at baseline and during follow-up.....	116
Table 20: CPET metrics in nonresponders at baseline and during follow-up.	116
Table 21: Baseline and 6 months values of peak VO ₂ in the CRT trials.....	119
Table 22: MLWHQ at baseline in responders and nonresponders	124
Table 23: MLWHQ in responders at baseline and follow-up	124
Table 24: MLWHFQ in nonresponders at baseline and follow-up	124
Table 25: Mean MLWHFQ score and improvement from the CRT trials	127
Table 26: LVEF and LV volumes in responders and nonresponders	130
Table 27: LVEF and LV volumes in responders.....	130
Table 28: LVEF and LV volumes in nonresponders	130
Table 29: BSE reference range for LV volumes in men and women	136
Table 30: LVEDV at baseline and follow-up in the CRT trials	137
Table 31: LVESV at baseline and follow-up in the CRT trials.....	137
Table 32: EF at baseline and follow-up in the CRT trials.....	137
Table 33: Surrogate markers at baseline in responders and nonresponders	140
Table 34: Surrogate markers in responders at baseline and follow-up	140
Table 35: Surrogate markers in nonresponders at baseline and follow-up.....	141
Table 36: Pearson’s correlation coefficient between markers of response	143
Table 37: Components of LPM models, their meaning and units of measurement	151
Table 38: AHA/ACC stages of HF	157
Table 39: HF studies used in LV PV loop modelling	161
Table 40: Demographics and aetiology of HF	164
Table 41: Comparison of data for each HF stage, using 2-tailed Student’s T-test	165
Table 42: LPM variables for each model, compared using 2-tailed Student’s T-test...	166
Table 43: LV parameters according to each ACC/AHA HF stage, mean and (SD)	168
Table 44: LPM input variables and AHA/ACC stage of HF.....	170
Table 45: Model input parameters at baseline and follow-up in responders.....	178
Table 46: Model input parameters at baseline and follow-up in nonresponders	178
Table 47: The 6 model outputs in responders at baseline and follow-up.	179
Table 48: The 6 model outputs in nonresponders at baseline and follow-up.	179
Table 49: All model outputs versus measured parameters at baseline and follow-up.	179
Table 50: Mean, SD, maximum distance and number of individual voxels.	201

Table 51: Characterization of cohorts based on left ventricular volumes	208
Table 52: Results of sweeps alongside clinical QRSd for 10 of the Sheffield cases.....	222
Table 53: Biodomain parameters converted into monodomain	224
Table 54: Typical FMD values in HF studies	236
Table 55: Baseline brachial artery parameters in responders and nonresponders	241
Table 56: Brachial artery parameters in responders	241
Table 57: Brachial artery parameters in nonresponders	241
Table 58: Markers of response in responders during follow-up	264
Table 59: Parameters at which may influence SABCG	264
Table 60: SABCG force and time at baseline and follow-up	265
Table 61: Comparing the force and timing of each SABCG wave in responders	265
Table 62: HGS values from studies conducted on HF patients	281
Table 63: Patient demographics at baseline	283
Table 64: Baseline HGS of responders and nonresponders	284
Table 65: HGS of responders at baseline and during follow-up	Error! Bookmark not defined.
Table 66: HGS of nonresponders at baseline and during follow-up	284
Table 67: UA levels in heart failure and their significance	290
Table 68: Baseline characteristics of responders and nonresponders	293
Table 69: UA and renal function in responders at baseline and follow-up.....	293
Table 70: UA and renal function in nonresponders at baseline and follow-up	294
Table 71: Universal classification of myocardial infarction.....	298
Table 72: Tn levels in heart failure and their significance.....	298
Table 73: Baseline hsTnT in responders and nonresponders	300
Table 74: hsTnT in responders	300
Table 75: hsTnT in nonresponders.....	300
Table 76: NP's in HF and CRT and their significance	304
Table 77: NT-proBNP level in responders and nonresponders.....	306
Table 78: NT-proBNP levels in responders.....	306
Table 79: NT-proBNP levels in nonresponders	306
Table 80: PTH levels found in HF.....	313
Table 81: Calcium metabolism of responders and nonresponders at baseline	314
Table 82: Calcium metabolism of responders at baseline and follow-up.....	315
Table 83: Calcium metabolism of nonresponders at baseline and follow-up.....	315

Table 84: Typical values of CRP in HF	320
Table 85: hsCRP in responders and nonresponders at baseline	322
Table 86: hsCRP in responders at baseline and follow-up	322
Table 87: hsCRP in nonresponders at baseline and follow-up	322
Table 88: Levels of UMA in HF	327
Table 89: Baseline UACR in responders and nonresponders	329
Table 90: UACR in responders at baseline and during follow-up	330
Table 91: UACR in nonresponders at baseline and during follow-up	330

Chapter 1 Introduction

1.1 The challenge

Heart failure (HF) is a result of the heart's reduced ability to pump blood due to a number of aetiologies, such as loss of effective contractile tissue due to myocardial infarction or a fall in cellular contractility, such as cardiomyopathy. Subsequent changes, referred to as adverse modelling of the diseased left ventricle, such as dilatation and loss of synchronous contraction further reduce effective contractility and lead to a worsening cycle of deteriorating cardiac function. However, HF is not simply a single organ disease but is, rather, a complex syndrome, resulting in impairment of many other organs and tissues due to reduced tissue perfusion. HF is a common condition with a UK prevalence of over 900,000 ¹. Optimal pharmacological therapy such as beta-blockers, angiotensin-converting enzyme inhibitors and mineralocorticoid receptor antagonists for HF confer clinical benefit, but there is still considerable morbidity, accounting for approximately 120,000 admissions per year in the UK ¹. The annual mortality attributable to heart failure is around 60% ² and costs to the health care system are among the highest of a single disease ³ and increasing as a result of the ageing population. Cardiac resynchronisation therapy (CRT) is a relatively new treatment for HF, improving the mechanical efficiency of the heart by artificially pacing both the left and right ventricles to re-coordinate the timing of electrical stimulation and thus synchronous mechanical contraction. This correction of dyssynchrony is associated with improvements in left ventricular (LV) systolic function ⁴, myocardial oxygen consumption ⁵, morbidity and mortality ⁶.

Recent advances in cardiac imaging allow accurate measurement of cardiac geometry, wall motion and chamber flow patterns and combining these with electro-anatomical mapping systems and high-fidelity invasive pressure measurement provide high resolution data sets for characterising individual HF patients. In addition, the clinic record, integrated with epidemiological data provides an additional resource with which to personalise care. In order to best use these advances, there is increasing momentum behind a paradigm shift away from predefined clinical indices determining

treatment options and a towards true personalisation of care based on imaging and modelling an individual's specific physiology.

An exciting and highly promising strategy underpinning this shift is the assimilation of multiple image sets into personalised state of the art biophysical models. The development of such models provides the ability to capture the multi-factorial cause and effect relationships, which link the underlying pathological mechanisms. Furthermore, using a biophysical basis presents unique opportunities to assist with treatment decisions through the derivation of quantities that cannot be imaged but are likely to play a key mechanistic role in HF e.g. tissue stress and pump efficiency.

A number of key developments are beginning to allow clinical translation, including 3D image acquisition, image processing advances, improved numerical methods and increased performance per unit cost of computing, which allow the use of complex computational models in a clinical setting. Such finite element based models accurately represent both anatomy and detailed microstructure. The mathematical descriptions serve as spatial frameworks for embedding cellular models of electrical activation and tension generation, producing cardiac contraction. Through the activation of multi-scale approaches these cell and organ models can be coupled together to produce increasing sophisticated simulations of cardiac physiology, in health and disease. The proposition of using personalised multi-scale models of patients to map disease and model therapies and remains a tantalising possibility.

1.2 Aims and Objectives

The aims of the project were threefold;

- to assist in the design of patient-specific biophysical models of left ventricle based on data acquired from cardiac imaging that are able to predict the response of the LV to CRT,
- to investigate how the patient's routine clinical record might be used to inform a patient-specific models and finally,
- to investigate novel methods of characterising the HF failure syndrome which may have additional value in assisting the prediction and measurement of response to this therapy.

The work was founded on the success of an earlier pilot study from the same partners. For the pilot, image acquisition was carried out in a state of the art research-intensive clinical imaging centre at Kings College, London (KCL). The objectives of this study were to improve both patient selection for, and maximise response to, CRT by:

- Identification of predictors and markers of response to CRT – using novel biomarkers and biophysical markers.
- Using a robust approach to the assessment of clinical response to CRT – including LV function, patient symptoms and cardiorespiratory performance.
- Creating patient-specific models, which could be used to predict response to CRT using, personalised anatomical, electrophysiological and mechanical data.
- Device personalisation through optimisation of atrioventricular and interventricular delays at 6 weeks post CRT implantation, thus ensuring that the device best compliments the patient’s native electrophysiology.
- Determine the feasibility of translating the workflow from a specialist high-volume academic cMR unit to a routine hospital setting (STHT) with a different cMR scanner, sequences and staff, laying the groundwork for a large multicentre randomised control trial.

1.3 Chapter content

The next two chapters continue to provide the background to the project. Chapter 2 presents our current clinical understanding of heart failure including the concepts of left ventricular systolic dysfunction, cardiac dyssynchrony, heart failure and the heart failure syndrome and the associated epidemiology, aetiology, pathophysiology and pharmacology of treatment. Chapter 3 focuses on the introduction of cardiac resynchronisation therapy (CRT) as a recent treatment for left ventricular systolic dysfunction-heart failure and the history of its development and proposed mechanism of action. It also provides information on the implantation procedure and highlights the complexities and resulting challenges in trying to measure a response to CRT including the potential ways in which a positive response might be defined. Finally, the current clinical evidence base for the use of CRT is presented.

The cohort of 21 patients recruited in Sheffield are presented in Chapter 4. This chapter gives a comprehensive account of how the patient cohort was selected, details of the ethical approval, the characteristics of the cohort at baseline before cardiac

resynchronisation therapy implantation and the materials and methods used to study the patients. Chapter 5 defines the way in which a response to cardiac resynchronisation therapy has been defined for the purposes of this PhD, and describes more traditional, albeit very comprehensive, assessment of the patients at baseline and then at 6 and 12 months following implantation to assess their response in 4 separate domains, including symptoms and quality of life, left ventricular size and function, 6 minute walk duration and cardiopulmonary exercise testing.

Chapters 6, 7 and 8 describe new approaches to assessment and novel tools including the development of patient-specific computational models of the heart created using data from their routine clinical record (Chapter 6). Pre-existing data from the literature was also used to map function of the failing left ventricle in an attempt to measure response to cardiac resynchronisation therapy, using lumped parameter models and subsequently 3D models of the left ventricle from cardiac magnetic resonance imaging in an attempt to predict response. Chapter 7 considers the use of biomarkers such as parathyroid hormone and biophysical markers such as hand grip strength in an attempt to both predict and measure response to cardiac resynchronisation therapy and what insights such markers offer into the heart failure syndrome. The clinical utility of the models, biomarkers and biophysical markers in terms what they add to existing measures and predictors of response and how they could be used in a routine clinical setting are brought together and discussed in Chapter 8.

The final chapter brings together all aspects of the work in the form of a general discussion and final conclusions and highlights areas which might benefit from further investigation based on the findings of the PhD.

Heart Failure

In this chapter the epidemiology, aetiology and pathophysiology of heart failure will be discussed, along with how it is diagnosed, the role of dyssynchrony and it's treatment.

1.4 Introduction

According to Dickstein et al (2008) heart failure (HF) is defined as "a complex clinical syndrome that can result from any structural or functional cardiac disorder that impairs the ability of the ventricle to fill with or eject blood"⁸.

A diagnosis of HF depends on evidence of impairment of cardiac function in the context of symptoms, and signs, of salt and water retention. As described by Dickstein et al (2008), HF can be classified by time (acute vs. chronic), anatomy (right vs. left), physiology (systolic vs. diastolic), aetiology (ischaemic vs. non-ischaemic), genetics (inherited vs. acquired) and sequelae (low vs. high-output)⁸.

It is important to recognise that HF is not simply an insult affecting a single organ but is, rather, a multifaceted syndrome which can result in impairment of psychological, musculoskeletal, haematological, pulmonary, endocrine, endothelial, renal and hepatic systems. Whilst the presence of these broader effects is not prerequisite for the diagnosis of HF, related non-cardiac tissue, or indeed whole organ dysfunction may influence both the perception and severity of symptoms in HF patients. Many of these potentially important aspects have yet to be investigated in relation to HF therapies, for example, the influence of resynchronisation of a failing heart on other organ dysfunction is not known nor, more importantly, is whether baseline markers of such dysfunction pre-implantation can predict the response to CRT.

1.5 Epidemiology

1.5.1 Frequency

In the 21st century, the prevalence of HF in the UK is estimated to be 7.1-13.5/1000 persons with an incidence 1.3-2/1000 person years⁹⁻¹¹. Whilst estimates regarding the frequency of HF in the UK vary, there is general agreement within the literature that

the problem is increasing and that, increasing age is accompanied by increasing risk of developing HF ¹²⁻¹⁴. As discussed by Najafi et al (2009), the increasing caseload observed may simply be a function of an expanding population, even if the incidence of heart failure *per se* is static ¹⁵. However, there are concerns that the problem is under-estimated. This may be due to erroneous hospital discharge summaries ¹⁶, incorrect documentation of diagnoses ¹⁷ or cases that remain undetected clinically ¹⁸.

1.5.2 Mortality

In the mid-21st century, the 5-year survival for patients with HF was estimated to be between 25% and 53%, with a mean value worse than that for bladder, bowel, prostate and breast cancer ^{13 14 19}. Such data are based upon observational work, retrospective studies or randomised controlled trials (RCTs) for highly selected populations, making comparisons between, and generalisations to, other populations difficult ^{20 21}.

Despite the increase in prevalence, the mortality of HF appears to be falling, mirroring that of ischaemic heart disease (IHD), the main cause of HF ^{22 23}. It follows that the increasing number of patients with IHD, who survive their index event e.g. myocardial infarction (MI), go on to develop HF, because more patients receive preventative, more effective and timely reperfusion therapy following their MI, and so more lives and myocardium is saved ^{24 25}. Thus, rather than dying from a single MI, patients are living long enough to suffer recurrent MIs and/or develop subsequent LV impairment and the resulting clinical signs and symptoms of HF.

1.5.3 Morbidity

In the last few years HF has become established as the most common cause of hospitalisation in the over 65s with the average length of inpatient stay approaching 1 week ²⁶, and the readmission rate in the 6 months following discharge almost 50% ²⁷. HF accounts for over 2% of the annual NHS budget (£2 billion), with the vast majority of this sum spent on costly admissions to hospital and subsequent inpatient episodes ¹. HF is associated with a marked reduction in quality of life, determined not just by impairment of physical health (many patients having greater physical impairment than those with arthritis or chronic lung disease) but also by deterioration of mental health.

Clinically significant depression is present in over a fifth of HF patients, the degree and prevalence increasing with the severity of HF²⁸. This is important, as the perception of symptoms of chronic medical conditions, such as HF, is closely intertwined with the mood of the patient.

1.5.4 Ethnicity

There is currently a paucity of evidence relating to ethnic differences in HF and low recruitment of ethnic minorities to RCTs continues to present a challenge. Possible reasons for low recruitment include; distrust of the medical community, failure to actively recruit such minorities and lack of knowledge within ethnic communities about research and therefore clinical trials²⁹. Some researchers have argued that ethnicity should be the basis for the design of RCTs as this would ensure active recruitment of such minorities whilst others counter argue that trials should concentrate on diversity and inclusivity. In consequence, a strategy of recruitment based on positive discrimination has been trialled but is yet to be adopted globally³⁰. This is particularly important as there is evidence to suggest that the relative risk of HF and subsequent morbidity is greatest in South Asians³¹. This may reflect differences in the aetiology of HF³², the prevalence of risk factors, difficulties in managing patients in whom English may not be their first language³³ or other factors such as response to treatment³⁴.

1.5.5 Gender

Prevalence of HF varies between genders, with prevalence in females estimated at 7.8-11.5/1000 persons compared to 6.4-28.5/1000 for males and the incidence is estimated at 3.9-5.6/1000 person years for females compared to 4.1-4.4/1000 for males^{10 11 15}. Women typically have a better prognosis, following a diagnosis of HF, but there is debate as to whether this is independent of the ejection fraction (EF) or aetiology³⁵⁻³⁷. At diagnosis, women are typically older, with greater frequency of hypertension (HTN), diabetes mellitus (DM) and symptoms but are less likely to smoke or have known IHD³⁸. Women are significantly under-represented in clinical HF trials and reasons for this include specific exclusion criteria limiting female participation in order to avoid pregnant women, and also age; with women with HF tending to be older^{39 40}. Women are also less likely to receive treatment due to concerns over lack of prospective data, and possible gender-specific effects of treatment⁴¹⁻⁴³.

Specifically, with reference to the key CRT trials, well over 70% of patients recruited are male ^{6 44-49}.

1.6 Aetiology

HF can be classified by time, anatomy, physiology, genetics and sequelae, all of which will have varying aetiology. As mentioned above, the most common cause of HF in the UK is IHD, accounting for over two thirds of cases, usually as a result of coronary atherosclerosis leading to myocardial infarction, death of myocardium and subsequent development of myocardial scar, LVSD and HF-LVSD ⁵⁰. Whilst there are many other possible causes of HF, the relative frequency and distribution of these will of course depend on the population studied. The next section briefly outlines the causes of HF and discusses the causes of HF-LVSD in more detail. The causes of HF *per se* are summarised in table 1.

Table 1: Major causes of HF

Cause	Example	Ventricle	Incidence
Vascular dysfunction	Ischaemic heart disease	Left	Common
Rhythm disturbance	Atrial fibrillation	Both	Common
Valvular dysfunction	Mitral regurgitation	Left	Common
Lifestyle	Obesity	Left	Common
Pulmonary disease	Pulmonary embolus	Right	Intermediate
Idiopathic	Dilated cardiomyopathy	Both	Intermediate
Infective	Viral myocarditis	Both	Rare
Infiltrative diseases	Amyloidosis	Both	Rare
Autoimmune disease	Hyperthyroidism	Both	Rare
Inherited	Atrial-septal defect	Right	Rare
Drug side-effect	Bleomycin chemotherapy	Both	Rare
Physiological state	Post-partum cardiomyopathy	Both	Rare

As suggested by a review of studies published ^{11 50-56} between 1991 and 2010 (table 2), the ratio of the aetiology of HF between ischaemic and non-ischaemic disease has remained constant at 50:50. As these studies are drawn from different populations, with varying cohort sizes, follow-up, and methodologies it is difficult to draw firm conclusions. However, it appears that there has been a steady increase in HF attributed to valvular heart disease (VHD) and a rise, followed by a fall, in HTN.

Influences of other factors, e.g. alcohol consumption, remain unchanged. This seems to make sense; the incidence of degenerative valve disease is increasing as the population ages and expands, leading to consequences such as HF. HTN on the other hand, is being diagnosed and managed more aggressively and so one would naturally expect cases of HF due to HTN, typically that due to chronic and poorly controlled HTN, to fall. Finally, risk factors for, and prevalence of, alcohol excess during this period have remained relatively constant. As McMurray and Stewart (2000)⁵⁷ have commented, for patients with multiple risk factors it is very difficult to attribute HF to a single cause; patients may have undiagnosed or subclinical risk factors, treated differently, and with variable effect, all of which could have contributed to HF.

Table 2: A summary of HF aetiology in 8 studies published between 1996 to 2010

Author		Maggioni	Fonarow	Mozaffarian	Baldasserroni	Fox	Cowie	Packer	Mair	
Reference		51	52	53	54	50	11	55	56	
Year of publication		2010	2008	2007	2002	2001	1999	1999	1999	
Duration of follow-up (years)		1	0.25	1.6	1	1.5	1.5	5	1	
No of participants		5118	20,118	10,538	5517	332	220	3192	266	
Demographics	Age (years)	Mean	67	61	65	63	76	76	64	69
		SD (+/-) or Range	13	14.5	18-96	N/A	37-95	25-85	10	35-75
	Male participants (%)		67	61	76	76	54	N/A	79	41
Aetiology	Ischaemic		44	54	62	46	52	36	64	45
	Non-ischaemic	Dilated Cardiomyopathy	56	46	38	36	48	76	35	55
		Hypertension				13	4	14	20	2
		Valvular Heart Disease				N/A	10	7	6	18
		Atrial Fibrillation				N/A	3	5	N/A	N/A
		Other e.g. alcohol				6	8	5	N/A	9
		Unknown (idiopathic)				N/A	13	35	N/A	N/A

1.7 Pathophysiology

This is a complex area, depending on aetiology and also rate of development. The section, which follows, discusses HF-LVSD in depth and briefly describes LV diastolic dysfunction. These may coexist. In addition, systolic function of the right ventricle (RV) can become impaired resulting in right ventricular failure (RVF) in isolation, or both ventricles may develop simultaneous systolic dysfunction, leading to biventricular or congestive cardiac failure (CCF). As these are not the primary focus of this thesis,

for the sake of brevity, they are not considered here. Why, and at what point, patients with LVSD without symptoms develop symptomatic HF-LVSD, remains unclear.

1.7.1 Systolic Dysfunction

The primary pathophysiological mechanism in LVSD is a reduction in stroke volume and a subsequent fall in cardiac output, despite a compensatory rise in heart rate. This results in a reduction in the supply of blood to the tissues from the left ventricle (LV). LVSD may arise from a reduction in functioning myocardium following an MI, LV outflow obstruction e.g. as in aortic stenosis, an increase in the systemic after-load increasing cardiac work, e.g. as in HTN or an increase in the systemic pre-load e.g. iatrogenic fluid overload. This fall in CO leads to changes in the Frank-Starling mechanism (FSM), hormonal regulation, autonomic nervous system and the vascular system, leading to adverse cardiac remodelling and impairment in other tissues downstream. These pathophysiological changes determine the presence of symptoms and signs in HF⁵⁸ and have been addressed by effective treatment modalities (via the renin-angiotensin-aldosterone system [RAAS] using angiotensin converting enzyme inhibitors [ACE-I], for example) as well as being used as biomarkers in HF diagnosis and prognosis⁵⁹ e.g. brain natriuretic peptide (BNP).

1.7.2 Frank-Starling Mechanism

In health, the FSM⁶⁰ links increasing venous return with increased SV and therefore CO (see figure 1). This is due to the unique length-tension relationship (LTR) of cardiac muscle whereby increasing the length of the sarcomere increases the number of possible actin-myosin interactions. Unlike skeletal muscle, cardiac muscle cells are not at their optimum length at rest, and thus increasing venous return (VR) pre-stretches the myocardium, increasing the length of the muscle fibres, which increases the left ventricular end-diastolic volume (LVEDV) number of potential actin-myosin interactions and so produces a more forceful contraction, increasing the stroke volume (SV). However, the FSM is also central to the pathophysiology of LVSD. Sustained increases in VR combined with myocardial necrosis and scarring cause pathological over-stretching of the myocardium, disrupting the LTR, reducing the number of potential actin-myosin interactions, and thus the force of contraction (see figure 2)⁶¹.

Figure 1: Frank-Starling mechanism and effect on contractility and afterload

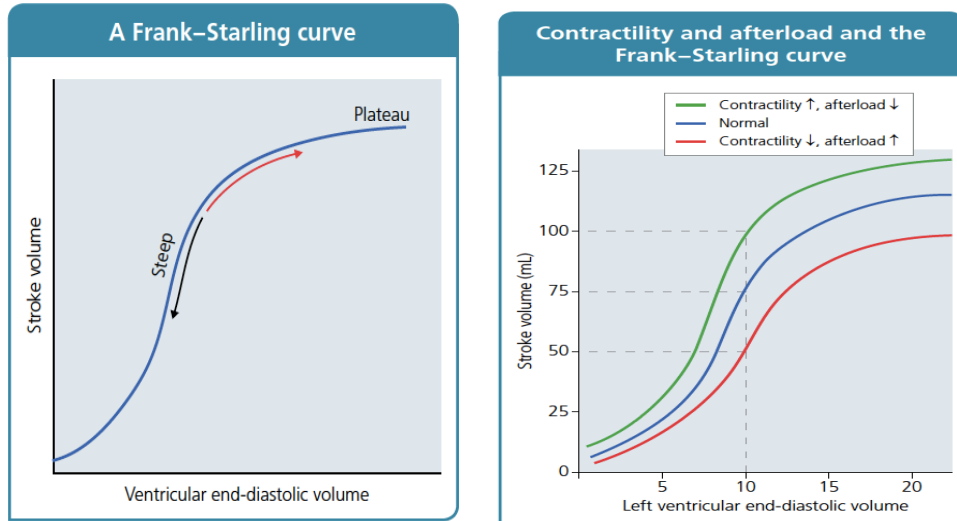


Figure on the left demonstrating the S shaped relationship between stroke volume (SV) and left ventricular end diastolic volume (EDV), with stroke volume increasing with increasing end-diastolic volume, to a point. Figure on the right, again demonstrating the S shaped relationship between SV and LVEDV with the influence of contractility (positive) and afterload (negative) on both.

Figure 2: Effect of increasing EDV on SV in various physiological states

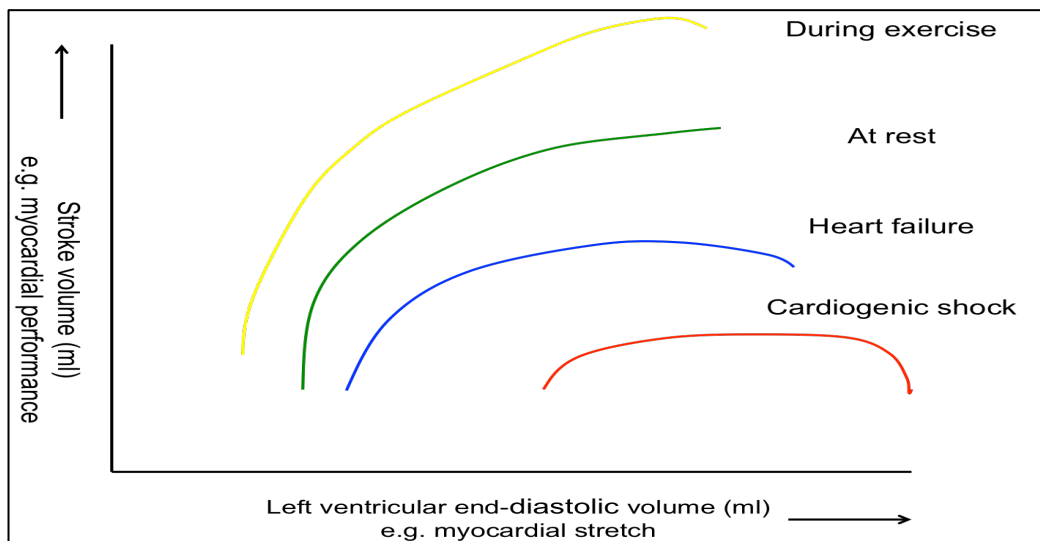


Figure 2 demonstrating the relationship between SV and LVEDV in the presence of a range of conditions, from exercise, at rest, with heart failure and in cardiogenic shock, the SV increasing as the EDV increases until a point when the heart begins to fail.

1.7.3 Hormonal regulation

LVSD leads to the upregulation of the several neuro-hormones, specifically; the RAAS, natriuretic peptides and anti-diuretic hormone (ADH). Initially these act to compensate for failing ventricular function, maintaining tissue perfusion but as the disease progresses they eventually catalyse both the development and the progression of HF.

1.7.3.1 Renin-Aldosterone-Angiotensin System

Upregulation of the RAAS leads to increasing blood concentrations of renin, angiotensin II and aldosterone. A reduction in CO results in a fall in renal perfusion, which is detected by the juxtaglomerular apparatus of the afferent arteriole in the kidney as a decrease in the afferent pressure. This stimulates the release of renin, which catalyses the production of angiotensin I from angiotensinogen and then ACE catalyses the conversion to angiotensin I to II (figure 3).

Angiotensin II mediates its effects in 5 ways by; increasing sympathetic nervous system (SNS) activity, increasing Na^+ and Cl^- absorption from the ascending loop of Henle, stimulating the release of aldosterone from the adrenal cortex, stimulating arteriolar vasoconstriction (systemic and renal) and stimulating the secretion of anti-diuretic hormone from the posterior lobe of the pituitary gland.

The net effect is retention of salt and water. This increases plasma volume (PV) and hence blood pressure, which, for the short term, improves tissue perfusion. However, this short-term gain comes at a long-term cost of an increasing workload on an already failing myocardium, thus exacerbating LV dysfunction. Aldosterone release is stimulated not only by angiotensin II but also by atrial stretch and mediates its effect by stimulating the receptors in the distal tubule and collecting ducts of the kidney, augmenting the return of Na^+ to the plasma and the retention of K^+ in the filtrate, ultimately increasing PV, VR and therefore CO.

Figure 3: The complexities of the Renin-Angiotensin-Aldosterone System

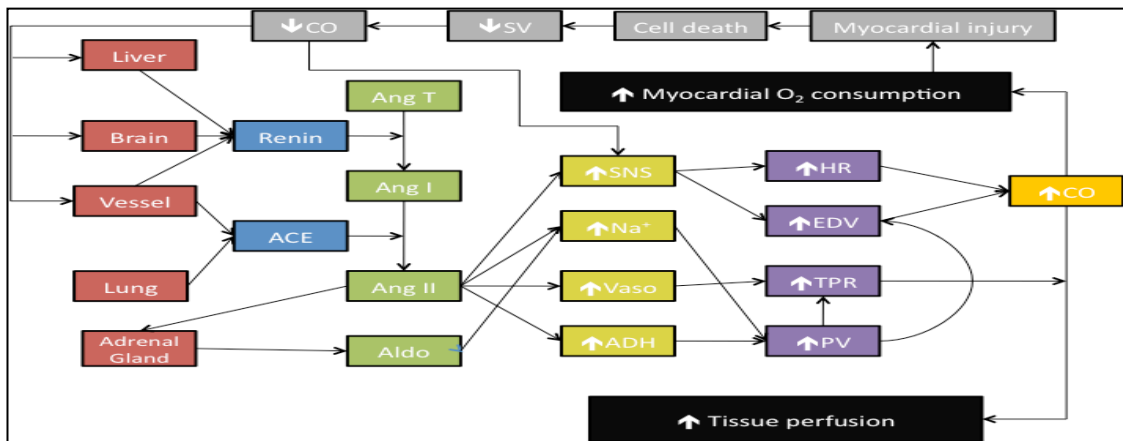


Figure 3 demonstrates the complexities of the RAAS, with its effects downstream on the sympathetic nervous system, vasculature, salt and water retention.

ACE = angiotensin converting enzyme, ADH = anti-diuretic hormone, Aldo = aldosterone, Ang = angiotensin, Ang II = angiotensin II, Ang T = angiotensinogen, CO = cardiac output, EDV = end-diastolic volume, HR = heart rate, PV = plasma volume, TPR = total peripheral resistance, SV = stroke volume, Vaso = vasoconstriction

1.7.3.2 Natriuretic Peptides

Natriuretic peptides (NPs) comprise atrial (ANP), brain (BNP) and C-type (CNP) peptides, produced by the atria, ventricles and vascular endothelium, respectively. Each is released in response to several stimuli but the unifying stimulus is stretch, due to increased plasma volume. All are significantly elevated in HF-LVSD. BNP is synthesised and stored as pre-pro-BNP (inactive), cleaved to proBNP (inactive) and then to BNP, which is released from the cardiac myocyte along with its N terminal component (NT-proBNP), a 76 amino acid biologically inactive fragment. Both ANP and BNP augment natriuresis, reduce plasma volume and reduce BP by relaxing arterioles, hence protecting the failing heart. In contrast, the actions of CNP remain to be fully elucidated. Although it may have a protective function, its role remains controversial^{62 63}. The use of BNP as a clinical marker has increased in the past decade, particularly in primary care, and it is included in the European Society of Cardiology (ESC) guidelines for the clinical diagnosis of HF⁸, it is also used for research purposes, and in secondary care, when assessing response to HF-LVSD treatments, such as CRT

44 .

1.7.3.3 Anti-diuretic hormone

ADH is synthesised in the hypothalamus and is released from storage in the posterior lobe of the pituitary gland. It acts on the aquaporin channels of the distal tubule and collecting duct in the kidney, increasing the volume of water reabsorbed, thus producing more dilute plasma and more concentrated urine. The resulting increase in plasma volume increases cardiac preload and it also acts to increase systemic vascular resistance. This process has been the focus of, as yet unsuccessful, therapies (such as Tolvaptan), which block ADH and act to treat fluid overload in HF-LVSD⁶⁴.

1.7.4 Sympathetic nervous system

Reduction in CO is detected as a drop in pressure by baroreceptors in the aortic arch and carotid bodies, stimulating a release of noradrenaline from the SNS, increasing peripheral resistance (and therefore BP) via α_1 receptors and increasing cardiac contractility (inotropy) and heart rate (chronotropy) via β_1 receptors. However, as before, this short-term measure to increase CO and maintain tissue perfusion results in an increase in workload for the heart and thus exacerbates HF in the longer term.

1.7.5 Vascular Changes

As mentioned previously, in HF there is a progressive increase in peripheral vascular resistance (PVR), stimulated by upregulation of SNS and angiotensin II amongst other factors. The blood vessels themselves are not merely passive conduits, but they (or rather their endothelium) produce paracrine mediators that influence their tone.

Endothelin is an example of one such mediator. Endothelin is a potent vasoconstrictor, which increases PVR and Na^+ uptake by vasoconstriction of the afferent arteriole thus increasing BP. Its release is stimulated by angiotensin II and ADH and inhibited by nitric oxide (NO). Endothelin levels correlate with the severity of HF-LVSD and can be used to stratify patients in terms of prognosis. Unfortunately, despite the development of endothelin antagonists, targeting endothelin has yet to yield a successful treatment modality for HF-LVSD⁶⁵. This is presumably because endothelin is an epiphenomenon of the HF-LVSD syndrome rather than a causal agent.

Conversely, the release of NO, a potent vasodilator, is reduced in HF-LVSD. The balance of vascular mediators acting upon the vascular endothelium, causing

vasodilation and vasoconstriction is referred to as *endothelial function*. This is a measure of the severity of HF⁶⁶ and is improved by medication⁶⁷ and aerobic exercise⁶⁸. Endothelial function can be assessed in several ways, one of which is through use of a technique known as flow-mediated dilatation (FMD), measuring the percentage increase in the diameter of the brachial artery immediately following a set period of occlusion.

1.7.6 *Cardiac remodelling*

Myocardial ischaemia, valvular disease and increased LV afterload (due to hypertension or diabetes) leads to upregulation of neuro-hormones and decreased myocyte contractility hypertrophy, and ultimately, cell death. LV hypertrophy (LVH) is typically eccentric and follows a period of focal cardiac ischaemia, resulting in death of the infarcted tissue and compensatory regeneration of the surrounding tissue. The hypertrophic response is a homeostatic attempt to overcome the increase in LV wall shear stress according to Laplace's law. LVH initially serves to augment the pump function of the failing heart by increasing contractility, but this also results in increased myocardial stiffness and reduced ventricular relaxation. Eventually, however this compensatory mechanism is overcome, leading to LV dilation and changing shape of the LV, from a hemi-ellipse to a near spherical shape.

1.7.7 *Other changes*

As mentioned previously, HF-LVSD is not a disease specific to the heart but rather it is a syndrome affecting many systems, including kidney, thyroid⁶⁹, parathyroid⁷⁰, bone⁷¹, lungs⁷² and skeletal muscle⁷³. With reference to skeletal muscle, HF leads not only to a loss of muscle mass, but alterations in muscle power⁷⁴, fibre distribution⁷⁵, metabolism⁷⁶, mitochondrial structure⁷⁷ and function⁷⁸, nutritive flow⁷⁹ and respiration⁸⁰. This sarcopenia explains many of the symptoms of HF such as fatigue and breathlessness and indicates why aerobic exercise, employed in cardiac rehabilitation centres, may be beneficial by halting or partially reversing some of these changes. It also suggests that evaluation of skeletal muscle strength in patients with HF-LVSD may prove fruitful to assess or predict response to therapies. For example, it may be shown that it is skeletal, not cardiac muscle, driving symptoms; hence they

experience no symptomatic improvement in their HF despite optimal medical therapy, and so cardiac rehabilitation with a graded exercise prescription might be beneficial.

Moreover, it has been discovered that biomarkers, such as urinary micro-albumin ⁸¹ (UMA) and parathyroid hormone ⁷⁰ (PTH), elevated in a response to the systemic effects of HF-LVSD, can help in the estimation of the morbidity and mortality of such disease. Uric acid ⁸² and C-reactive protein ⁸³ (CRP), markers of inflammation, are implicated in the pathogenesis of IHD and HF-LVSD and have been found to correlate with overall prognosis in both conditions.

1.7.8 Diastolic Dysfunction

In contrast to LVSD, the pathophysiology of diastolic dysfunction is poorly understood. Diastolic dysfunction refers to the failure of the myocardium to relax during diastole, due to increased stiffness and reduced compliance. In the presence of symptomatic HF, with near/normal systolic function isolated diastolic dysfunction is referred to as heart failure with a preserved ejection fraction (HFPEF); this often coexists with LVSD. In HFPEF, LV diastolic dysfunction typically arises from sustained and elevated afterload due to, for example, poorly controlled HTN. The increase in afterload results in marked compensatory LVH, the net effect of which is a thick ventricular wall and small ventricular cavity. This causes raised left ventricular end-diastolic pressure (LVEDP), inadequate filling of the ventricle, a reduction in SV and, as in LVSD, a reduction in CO. This is clinically significant as approximately 70% of ventricular filling is passive and occurs during ventricular diastole. The remaining 30% of ventricular filling is active due to atrial systole, the so-called 'atrial kick'. There is some evidence to suggest that there is an active fibrotic process involved and that such stiffness in the ventricular wall limits coronary perfusion and may cause microvascular ischaemia ^{84 85}. Debate continues as to whether HFPEF is truly a discrete entity or marks a transitional phase between the normal heart and HF-LVSD, and furthermore whether HFPEF is truly the same condition as diastolic heart failure, another term frequently used. The rest of the thesis focuses on HF-LVSD exclusively.

1.8 Dyssynchrony

Dyssynchrony (DS) is an absence of synchrony between or within cardiac chambers.

1.8.1 Introduction

In patients with HF-LVSD, the contractile function of the LV is impaired and heavily dependent on preload and afterload. In this situation, any conduction delay will lead to a further reduction in contractile performance, impairment of mechanical efficiency and unfavourable energy consumption. The electrical delay can occur anywhere in the conduction system, from the sinoatrial (SA) node to the Purkinje fibres and ventricular myocardium, and can manifest as a mechanical delay between the synchronised contractions of the cardiac chambers, this is termed dyssynchrony (DS). DS or electro-mechanical delay between the atria and ventricles is termed atrioventricular DS (AV DS), between the left and right ventricles, interventricular DS (InterV DS) and finally, within the left ventricle itself, intraventricular dyssynchrony (IntraV DS).

1.8.2 Myocardial electrical activation sequence

In brief, the SA node spontaneously fires, activating the atria, which then contract, filling the ventricles actively after passive filling. This same signal, after a delay, passes through the AV node, to the ventricles, via the bundle of His and Purkinje fibres, resulting in ventricular contraction and expulsion of blood to the pulmonary from the right ventricle and the systemic circulation from the left. So in healthy individuals, the atria contract then the ventricles and the ventricles then contract at the same time.

1.8.2.1 Atrial and Atrioventricular conduction

All cardiac tissue is electrically active, and so, many areas of the heart can act as potential pacemakers (see figure 4). However if all such regions competed against each other, the cardiac cycle would become disorganised and so there is a hierarchy, with the fastest pacemaker always assuming control over slower ones. For example, the SA node has an intrinsic rate of 100, the AV node 70, the Bundle of His 30-40 and ventricles < 30 depolarisations/min, respectively. Thus, in health, the normal electrical activation sequence originates from the sinoatrial (SA) node, located between the superior vena cava and the right atrium.

Figure 4: The conduction pathways of the heart

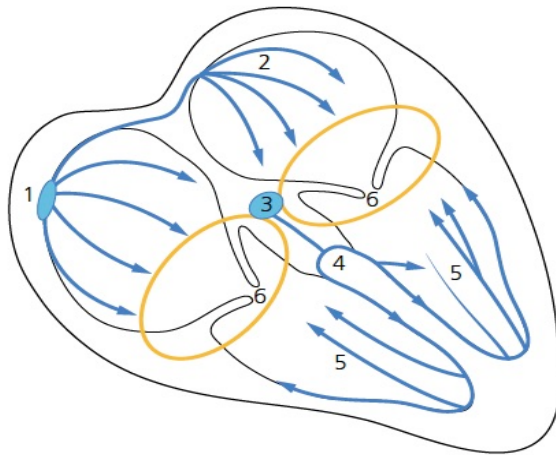


Figure 4 demonstrates the conduction pathways of the heart, within and between the atria, atria and ventricles and the ventricles themselves.

1: SA node, 2: Bachmann's bundle, 3: AV node, 4: Bundle of His, 5: Purkinje fibres and 6: Fibrous trigone.

The SA node contains electrically active P cells, which automatically and spontaneously depolarise at a regular interval. Depolarisation can be influenced by the sympathetic and parasympathetic nervous systems, increasing or decreasing the rate respectively. The resulting atrial depolarisation is seen as the P wave on the ECG. The wave of cardiac depolarisation is conducted from the atria, by specialised conducting pathways, which run anteriorly, centrally, and posteriorly to the AV node and takes around 100ms.

The heart is a functional syncytium, and because the annulus fibrosus, between the atria and ventricles, electrically isolates the upper chambers from the lower chambers, the AV node is the only intrinsic pathway connecting the two. The AV node slows the transmission of the depolarisation wave and depolarisation takes approximately 80ms to travel from the atrial to the ventricular side of the node⁸⁶. This ensures that atrial systole is completed after passive ventricular filling but prior to ventricular systole, optimising ventricular preload. This delay, together with the P wave duration, represents the PR interval on the ECG, which is typically around 40-200ms duration.

From the AV node, the signal is transmitted along the septum via the bundle of His, itself travelling along the interventricular septum. Due to a higher concentration of gap junctions, transmission along this pathway is conducted at 3-4m/s; significantly faster than transmission through the ventricular myocardium which is 0.3-1m/s⁸⁷.

1.8.2.2 Ventricular conduction

The bundle of His splits into 2 branches, right and left bundle branches; as the latter is comprised of anterior and posterior fascicles, the whole structure is termed trifascicular. The bundles are electrically isolated, electrically coupling to the myocardium via the Purkinje-myocardial junctions located sub-endocardially in the ventricles only. These bundles then divide to give a large reticular structure, known as the Purkinje fibres. In health, the rapid conduction and broad reach of the fibres ensures a high degree of electrical and therefore mechanical synchronicity (both inter- and intraventricular) during ventricular depolarisation/systole. It takes around 20ms for the signal to travel from the bundle to initiate ventricular depolarisation⁸⁷. This can be seen as the QRS complex on the ECG.

In health, the first site of ventricular electrical activation is the LV at the interventricular septum. This is followed shortly afterwards (10ms) by activation of the RV⁸⁸. Following this activation, the wave-fronts then proceed simultaneously in both ventricles from apex to base and from septum to lateral wall. In health, there is near simultaneous ventricular contraction, the interventricular mechanical delay (IVMD) is close to 0ms and total ventricular activation time normally takes 50-80ms corresponding to a QRS duration of a similar duration⁸⁸. The last regions of right and left ventricles to be depolarised are the basal areas of the pulmonary conus and the posterolateral region respectively.

1.8.3 Heart Failure

In HF-LVSD the presence of both structural and functional changes in both ventricles leads to abnormal electrical activation and propagation. As a result, sinus node incompetence, atrial arrhythmias and bundle branch blocks (BBB) are common. The loss of normal synchronous sequence of electrical activation means that the signal is unable to pass rapidly from the atria to the ventricles via the specialised conduction system. Instead, depolarisation passes between the myocytes via gap junctions. This transmission path is up to 4 times slower, resulting in asynchronous and pathological activation and atrioventricular uncoupling and leading to electromechanical DS as mentioned above.

1.8.3.1 Atrial conduction

There is frequently bi-atrial dilatation in HF-LVSD with diffuse fibrosis and focal scarring due to a combination of ischaemia, inflammation and increased mechanical stress⁸⁹. This can lead to alteration in gene expression, dysfunction of Ca²⁺ ion channels and resulting slow and abnormal conduction. Commonly, there is also sinus node dysfunction, leading to both chronotropic and inotropic incompetence. As a result, there is significantly reduced atrial systolic function in HF-LVSD.

1.8.3.2 Ventricular conduction

A left bundle branch block (LBBB) refers to a conduction block in any part of the left intraventricular conduction pathway, from the main bundle to the fascicles. As a consequence there is rapid activation of the RV via the RBB but slow activation of the left ventricle via the working myocardium. This results in early activation and contraction of the interventricular septum and late activation of the posterior and lateral walls. This leads to posterolateral stretching as the septum contracts followed by late posterolateral contraction as one wall exerts forces on its corresponding contralateral partner. The consequence is a heterogeneous distribution of LV stress (the amount of tension developed in the LV wall during systole) and strain (the percentage change describing the degree of deformation of the LV during systole). Conventional catheter-mapping techniques and 3D non-contact mapping show that, in patients without disease of the conduction system, there is a homogenous and continuous activation sequence in the LV, which takes 50-80ms. However, in LBBB a functional conduction block leads to discrete, U-shaped LV activation. In patients with QRSd < 150ms the block is usually positioned laterally but for those where the QRSd > 150ms the block is located anteriorly LV activation takes 80-150ms⁸⁶.

Right bundle branch block (RBBB) describes a conduction block in any part of the right interventricular conduction pathway, specifically anywhere from the distal His bundle to the main right bundle. As a result there is rapid activation of the LV via the LBB but slow activation of the right ventricle via the working myocardium. In the presence of RBBB, the earliest activation site is the LV septum followed by the RV septum from where, after a considerable delay, the wavefront spreads from cell to cell, to the anterior and lateral RV walls and finally the right ventricular outflow tract. Similar to LBBB, it is the anterolateral regions that have delayed activation as takes 80-120ms.

1.8.4 Aetiology

DS may arise as consequence of IHD, which damages not only the myocardium (leaving scar tissue following myocardial infarction, for example) but also the conducting system e.g. sinoatrial node, atrioventricular node, bundle of His or Purkinje fibres. This damage results in a delay in electrical activation of the myocardium and dyssynchronous contraction of the heart. DS is common in populations with HF-LVSD, carries a poorer prognosis than HF-LVSD without DS and results in impairment of ventricular filling, systolic function and worsening of functional mitral regurgitation.

1.8.5 Epidemiology

Estimates of the prevalence of DS depend on the type, definition and instrument used, all of which vary between studies.

Atrioventricular DS, as determined by a prolonged PR interval, has a prevalence of 1-2% in a healthy cohort⁹⁰ but is more common in populations with HF-LVSD, in isolation (10%) and in association with interV DS (4%)⁹¹. It is important to note that, none of the major CRT trials comment on the prevalence of AV DS in their study populations.

InterV DS, as determined by a prolonged QRSd, has a prevalence of 1% in healthy adults at 50 years of age, increasing to 17% at 80 years of age^{92 93}. However, in a general population without underlying symptomatic structural heart disease, RBBB is not typically considered to be a sign of underlying disease. In contrast, LBBB is often pathological; prevalence increasing with diseases such as diabetes and IHD. Specifically, in a HF-LVSD population, prevalence is 30% irrespective of age⁹⁴.

If echocardiography, rather than surface ECG, is used to assess the interV DS, by measuring the IVMD as performed in the CARE-HF trial for example, then the prevalence increases to over 60%⁴⁴. Prevalence of interV DS also increases as the QRSd increases, for example with QRSd of < 120ms, 120-150ms and > 150ms the prevalence of interV DS, as defined by the presence of an IVMD greater than 40ms, is reported to be 12.5%, 52.4% and 72% respectively⁹⁵.

There are no reported studies of intraV DS in healthy adult populations, presumably because in the absence of disease this is both uncommon and implausible. The prevalence of intraV DS in a HF-LVSD population increases with increasing QRSD. For example for durations of < 120ms, 120-150ms and > 150ms the prevalence was reported to be 29.5%, 57.1% and 71% respectively as determined by a > 50ms difference among regional pre-ejection periods ⁹⁵. Similarly, Emkanjoo et al (2007)⁹⁶ reported the prevalence of intraV DS to be 45.1% and 23% in patients with a prolonged versus normal QRSD respectively when measured using echocardiographic tissue Doppler imaging (TDI). This suggests that mechanical DS may be present, and demonstrable, by echocardiography even when electrical DS cannot be detected by surface ECG and that the broader the QRSD the greater the likelihood of both mechanical intra- and inter DS.

1.8.6 Assessment

Assessment of DS can be performed using a variety of different modalities.

1.8.6.1 Electrocardiography

Figure 5: 12 lead ECG demonstrating LBBB

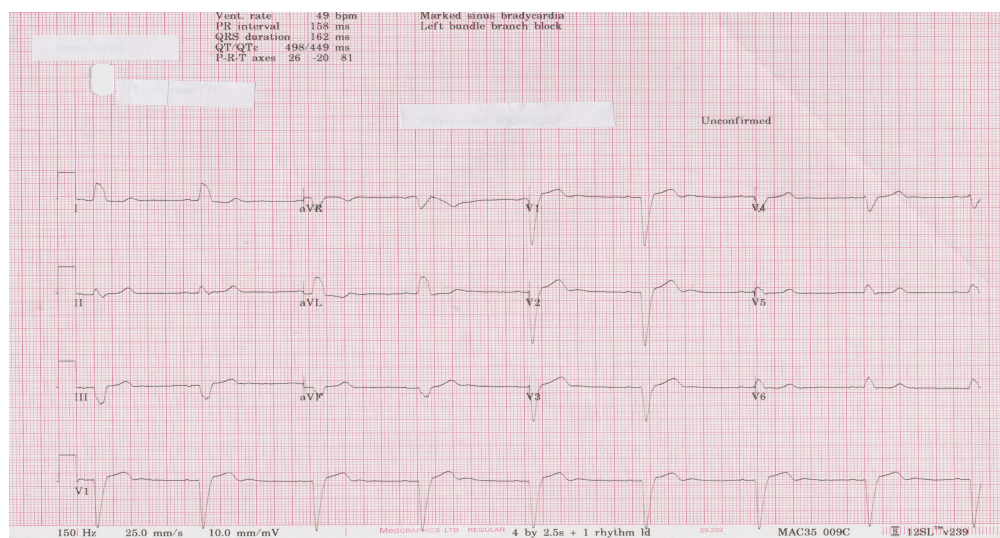


Figure 5 demonstrates a 12 lead ECG of a patient with left bundle branch block, demonstrating classical rS pattern in leads V1-3.

Figure 6: ECG leads V1 and V6 demonstrating LBBB

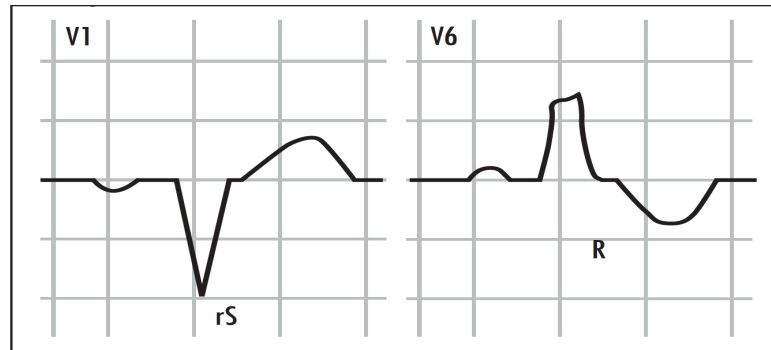


Figure 6 demonstrates a close up of LBBB as seen in leads V1 with classic rS pattern and V6 with classic R pattern.

The electrical changes occurring in the heart can be recorded by electrodes placed on the surface of the chest. The resulting ECG (figure 5) may give the first indication of DS if there is PR prolongation ($> 0.2\text{ms}$) denoting AV delay or a prolonged QRSd ($> 0.12\text{ms}$) with an atypical morphology, e.g. LBBB or RBBB.

1.8.6.2 Echocardiography

Figure 7: An apical 4 chamber trans-thoracic echocardiogram

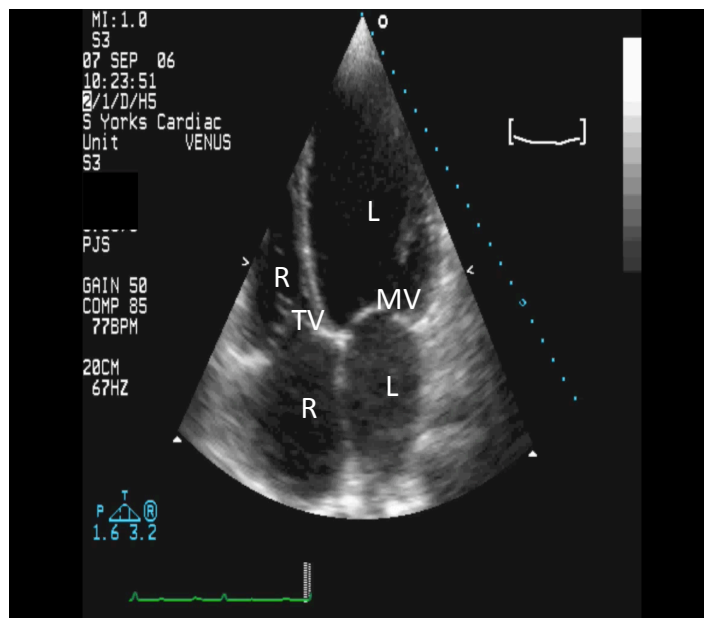


Figure 7 demonstrates a B-mode 2 dimensional image of heart as seen from the cardiac apex, with both ventricles and both atria, hence 4 chambers.

LA = left atrium, LV = left ventricle, MV = mitral valve, RA = right atrium, RV = right ventricle, TV = tricuspid valve.

Echocardiography is a non-invasive specialised imaging technique, which uses a probe containing piezo-electric crystals producing high frequency ultra-sound (USS) waves. The emitted waves are reflected by the intra-thoracic structures to differing degrees. These reflected waves are then detected by the probe and transduced into an

electrical signal, which builds an image of the heart (figure 7). Whilst the ECG provides a screening tool for gross electrical DS, AV and interV, the echocardiogram can provide more detailed information about mechanical DS, in particular IntraV DS. Echocardiography has the advantages of speed, portability and ease of use but it can have limitations in terms of field of view and also suffers from poor penetration (e.g. for bone) and an inability to discriminate and differentiate between types of soft tissue.

As highlighted below, a variety of specific echocardiographic modalities have been developed, enabling both the structure and function of the heart to be interrogated.

M-mode (figure 8 bottom) produces a single discrete beam of USS in a series of juxtaposed parallel lines creating a continuous strip, or 1D image, which allows a specific myocardial region of interest to be sampled. This modality enables the distance of structures from the transducer to be recorded and can be used to measure LV diameter, for example.

B mode (figure 8 top) produces real-time dynamic images of the heart in cross section. An array of crystals, are activated and inactivated in phase, producing an arc of USS lines, numbering around 100 per sector. These are then compiled into a 2D image. Repetition of this process at 100 times per second enables visualisation of cardiac motion. This is used for gross assessment of cardiac function - for discrimination between mild – moderate – or severe LV systolic dysfunction, for example. This can be utilised by transthoracic (TTE) or trans-oesophageal (TOE) echocardiographic probes.

Figure 8: M mode echocardiogram the LV in parasternal short-axis view

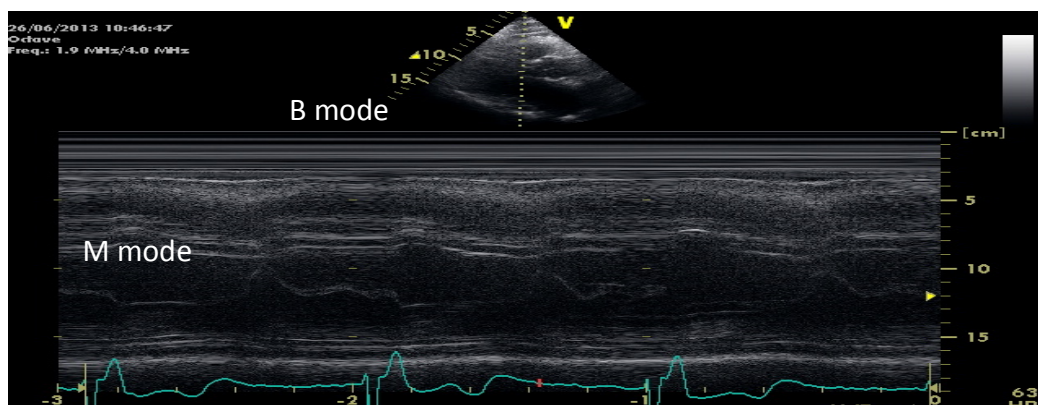


Figure 8 demonstrates an black and white M mode echocardiogram (bottom) taken the in long axis parasternal view, with B mode (top) and cursor seen through the mitral valve and finally ECG recording in blue.

Doppler ultrasound is used to assess the speed and direction of blood flow through the heart and is particularly useful for detecting and assessing valve dysfunction. As blood is continuously moving, the frequency of the reflected USS beam alters, this change in frequency is known as the Doppler shift. An increase in frequency denotes movement towards the transducer and a decrease in frequency, movement away, providing that the vector of flow is in line with the USS beam. Doppler USS has 3 different modes, pulse wave (PW), continuous wave (CW) or colour flow mapping (CFM). PW uses discrete pulses of USS and has a high spatial resolution but low velocity resolution. Velocities exceeding the detectable range result in aliasing, leading to 'wrapping' of the image and subsequent under sampling which leads to inaccuracies in the measured velocity. CW uses continuous emission of USS waves. This avoids the velocity issues affecting PW but limits spatial resolution. CFM gives a pictorial representation of the flow field with colours indicating the speed and direction of blood flow.

More recently, pulse wave tissue Doppler imaging (PW TDI) has been developed. This is able to measure the direction and speed of the contracting or relaxing myocardium using a specific filter threshold to detect the low frequency, high amplitude signals produced by the heart as it moves.

Several small single centre trials indicate that echocardiographic parameters such as septal-posterior wall motion delay (SPWMD) and interventricular mechanical delay (IVMD) are predictive of response to CRT^{97 98}. However, the PROSPECT trial⁹⁹, a large multicentre trial with central analysis and standardised training assessing 12 separate parameters, was unable to demonstrate any single echocardiographic measure of DS which predicted response to CRT, either through LVESV or a clinical composite score. However, this outcome may be related more to "technical and interpretative factors" according to Chung et al (2008)⁹⁹ rather than the measurements themselves. Other potential echocardiographic metrics to quantify DS and predict response, such as

strain, strain rate and speckle tracking, have been investigated¹⁰⁰⁻¹⁰². Whilst current evidence looks promising, these techniques remain confined to use as research tools and so the QRS duration on the surface ECG currently remains one of the few, if not the only, robust predictors of response to CRT¹⁰³. However, in the absence of a prolonged QRSD, it has become apparent following the EchoCRT trial¹⁰⁴, that searching for and treating intraV DS can actually lead to harm.

3D echocardiography

Three dimensional echocardiography, available in transthoracic or trans-oesophageal probes, consists of a matrix array of 2400 elements which can be focused and steered, sampling the heart in a multitude of directions, which with combined a proprietary processing system, reconstructs a pyramidal volume dataset, such as a 3D still or 4D movie. The image seen is either comprised of a series of 2D images, taken over consecutive heart beats and “stitched” together, or more recently a complete dataset can be acquired in a single heartbeat, termed real-time 3D.

1.8.6.2.1 Atrioventricular Dyssynchrony

The presence of mechanical AV DS delays the onset of ventricular systole in relation to atrial filling, shortening the passive ventricular filling period and leading to suboptimal ventricular filling due to superimposition of active atrial contraction with early passive filling. This leads to suboptimal preload, causing a reduction in SV and late diastolic (presystolic) functional mitral regurgitation. AV DS is typically measured using echocardiography (figure 9), from the apical 4-chamber view, using trans-mitral PW Doppler with the imaging plane between the tips of the fully open mitral valve, to study ventricular inflow. The total diastolic filling interval (dFT), also known as mitral valve ejection time (MVET), comprises the E wave (ventricular relaxation) and the A wave (atrial systole) indicating early passive and late active ventricular filling, respectively. In the presence of AV DS, there is a reduction in the E wave duration and the dFT is reduced to less than 40% of the corresponding cycle length, measured on the ECG below, and so the E and A waves begin to fuse.

Figure 9: Echocardiographic measurement of atrioventricular dyssynchrony

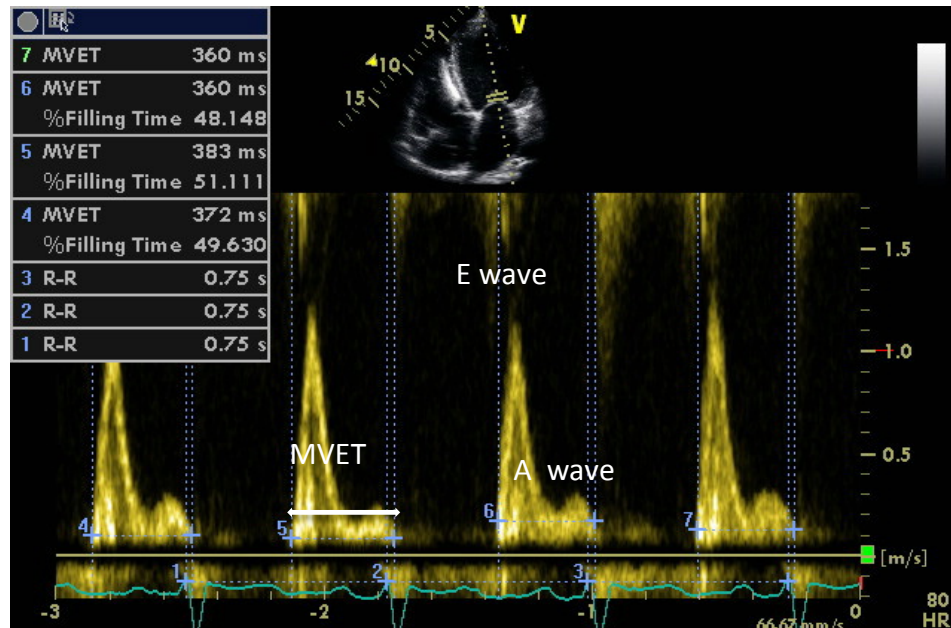


Figure 9 demonstrates a B mode 4 chamber echocardiogram (top) with continuous wave Doppler (bottom) used to measure the passive (E wave) and active (A wave) contributions to LV filling.

1.8.6.2.2 Interventricular Dyssynchrony

IVMD or InterV DS is measured by echocardiography using pulse wave Doppler flow. In health, the total ventricular activation time is 60-80ms corresponding to a QRS width of 70-80ms and, as mentioned previously, there is almost simultaneous biventricular contraction and a IVMD of close to zero. However, in BBB, the IVMD is typically increased to 40ms in the presence of a QRSd of > 150ms indicating significant interV DS. IVMD is derived from a series of measurements of both ventricles, primarily the time from the onset of the Q wave of the QRS complex on the ECG, denoting ventricular depolarisation, to the onset of flow through the ventricular outflow tract e.g. the delay between electrical activation to mechanical contraction. Flow is measured using CW Doppler and represents the onset of mechanical contraction of the ventricle (figure 10). The time from the Q wave to the onset of flow is known as the pre-ejection period (PEP) or ejection time (ET). The procedure is carried out similarly for the LV and RV, giving the LV-PEP or AVET and RV-PEP or PVET. The time difference between the onset of LV contraction to the onset of RV contraction should be < 40ms; a time greater than this is pathological and represents significant IVMD.

Figure 10: Echocardiographic measurement of interventricular dyssynchrony

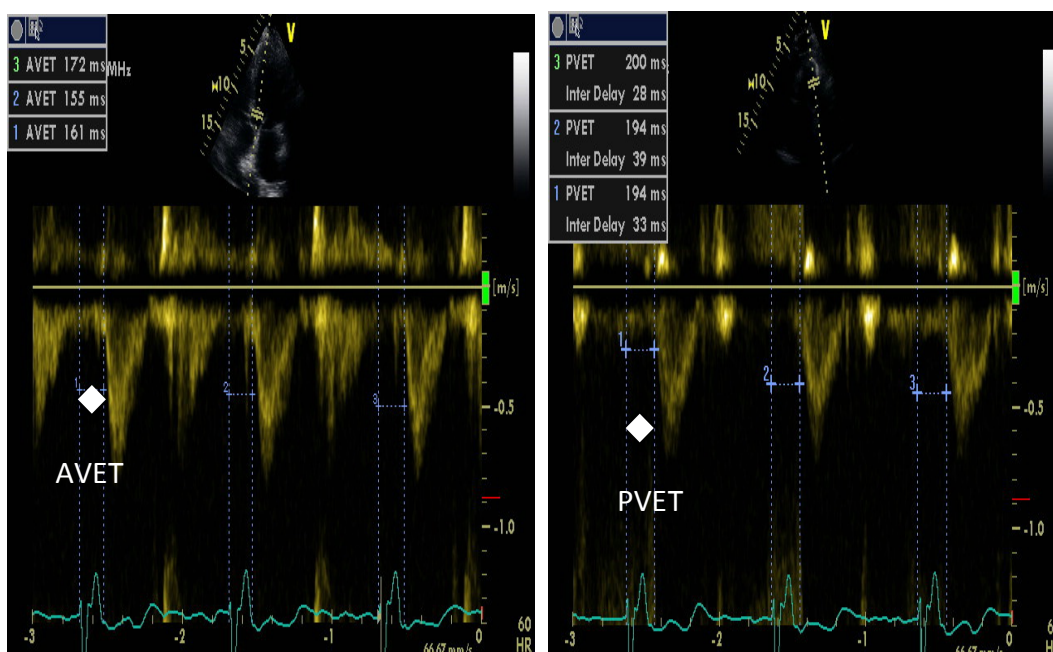


Figure 10 demonstrates measurement of the aortic valve ejection time (left) and the pulmonary valve ejection time (right), using continuous wave Doppler through the respective valves to measure the duration from the Q or S wave to the onset of flow.

1.8.6.2.3 Intraventricular dyssynchrony

IntraV DS refers to the early or late contraction of ventricular wall segments due to electrical conduction delays within the LV resulting in electromechanical uncoupling. Measurement of IntraV DS is more challenging to determine than its interventricular counterpart; being open to interpretation and influenced by method of assessment. It also lacks a standardised approach or agreed defined cut-off. It can be measured by several modalities including M-mode, 2D and 3D echocardiography and cardiac magnetic resonance imaging.

M-mode ultrasound imaging

The septal to posterior wall motion delay (SPWMD) is the time delay between septal and posterior wall systolic contraction (normal < 130ms). In a parasternal short axis view, the M mode cursor is positioned perpendicular to the septum and posterior wall and, with reference to a single cardiac cycle, the time difference between the onset of the Q wave component of the QRS complex on the ECG and the peak inward septal

and posterior wall motion is measured. M-mode is a simple, quick and readily-available tool but is dependent upon good echocardiographic windows. Disadvantages include the inability to measure DS in other LV regional walls. Septal or posterior wall akinesis due to previous MI or abnormal RV pressure/volume load will also influence septal motion leading to erroneous measurement. In advanced HF-LVSD, all inward wall motion is severely reduced, therefore determining a true peak can be challenging.

Pulse-wave tissue Doppler imaging

Pulse-wave TDI (PW TDI) can be used to measure intraventricular dyssynchrony since its temporal resolution enables the clinician to determine systolic myocardial velocities (S_m). Most commonly, the time from the onset of the QRS complex and the S_m peak (time to S_m peak) and the time from the onset of the QRS complex and the onset of S_m (time to S_m onset), are recorded. A period of > 65ms recorded for the time to S_m peak between LV segments is considered a significant delay. Using apical 2-, 4- and 5-chamber views, the cursor is placed in the wall of the ventricle at both mid and basal regions, creating a 12-segment model. The apical segment is not used as the resulting data is considered to be unreliable. The Doppler trace creates a signal comprising three waves: the systolic myocardial velocity (S_m) moving towards the transducer and the early diastolic myocardial velocity (E_m) and the late diastolic myocardial atrial (A_m) velocity both moving away from the transducer. PW TDI is considered a useful method for assessing intraventricular dyssynchrony, which has been used successfully to predict CRT response in small trials¹⁰⁵.

However, since it is impossible to view all the segments in a single image, multiple cardiac cycles are required to measure all the velocities. This may introduce inaccuracies due to inherent variability between cycles, especially in patients with AF or ectopy. Furthermore, the technique is time-consuming, operator dependant and presents a steep learning curve for echocardiographers.

Colour TDI

There are a variety of techniques based on colour TDI, including Tissue Synchronisation Imaging (TSI) and Tissue Velocity Imaging (TVI)

TSI and TVI are post-processing techniques, which are carried out offline, using previously acquired colour images, from apical views. The main advantages over PW Doppler as alluded to by Galderisi et al (2007)¹⁰⁶, is that these techniques allow measurement of the dyssynchrony of both opposing walls and different regions within the same wall, from a single view and a single cardiac cycle.

In TSI the velocity of the myocardial tissue is analysed to determine a peak velocity within a selected portion of the cardiac cycle and, since the peaks occur in the context of global motion, a delay in peak wall motion will produce a delayed peak velocity (figure 11). As for PW tissue Doppler, apical views are used to build a 12-segment model including apical and basal regions. The delay (in ms) within the myocardium being viewed is automatically assigned a colour from green indicating synchrony (regions reaching peak velocity at the same time), to red indicating dyssynchrony (regions reaching peak velocity at different times). Colour relates to the amount of delay rather than tissue velocity and so, when applied across the 2D LV image, produces a colour-coded map of wall motion delay allowing a quick 'eyeball' assessment of DS. Individual segments can also be interrogated with an inter-segmental difference of > 40ms indicating DS.

Figure 11: TSI displays colour-coded time-to-peak tissue Doppler velocities

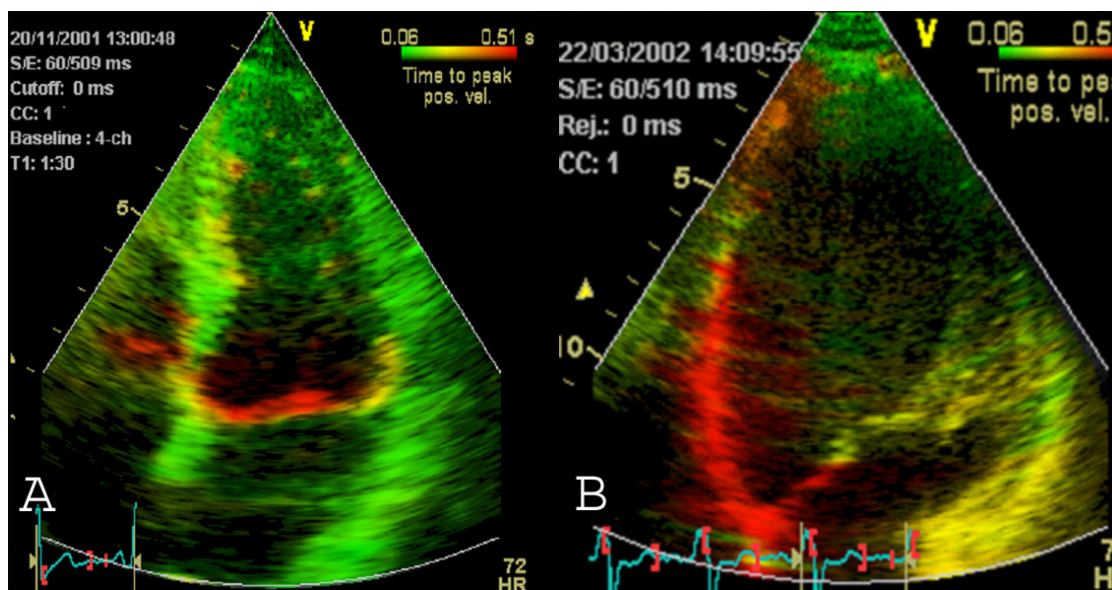


Figure 11 demonstrates tissue synchronisation imaging view of the left ventricle in 4 (left) and 2 chamber views (right). On the left, all the walls are green demonstrating no intra-ventricular dyssynchrony as the walls contract at the same time, on the right, the postero-lateral wall is red and the antero-septum is amber, demonstrating intra-ventricular dyssynchrony.

Similarly TVI reports longitudinal myocardial velocities (cm/sec) and can be displayed using pulsed, colour or M-mode Doppler.

PW TDI is a technically demanding technique with a steep learning curve. During TDI acquisitions, the frame-rate must be high, the sector width narrow, gains adjusted in order to view TDI clearly and, prior to measurement, aortic valve opening and closing must be marked in order to differentiate normal from post-systolic contraction.

Other techniques include the measurement of strain (amount of myocardial deformation). Strain is calculated throughout the cardiac cycle by means of a post-processing technique enabling the time to minimal or maximal strain to be assessed in different regions of the LV. Strain rate (e.g. the rate of change of strain) imaging can also be used. In theory, both of types of strain measure are superior to TDI as they facilitate differentiation of active and passive myocardial motion.

Finally, speckle tracking is a modality, which detects and traces the movement of pixels in the moving myocardium and can be used to calculate strain. Longitudinal and transverse in can be recorded from apical views and radial and circumferential strain from short-axis views (see figure 12). The STAR trial demonstrated that radial and transverse strain measured by speckle tracking was predictive of response to CRT ¹⁰².

Figure 12: Speckle-tracking time-strain curves in a HF patient with LBBB

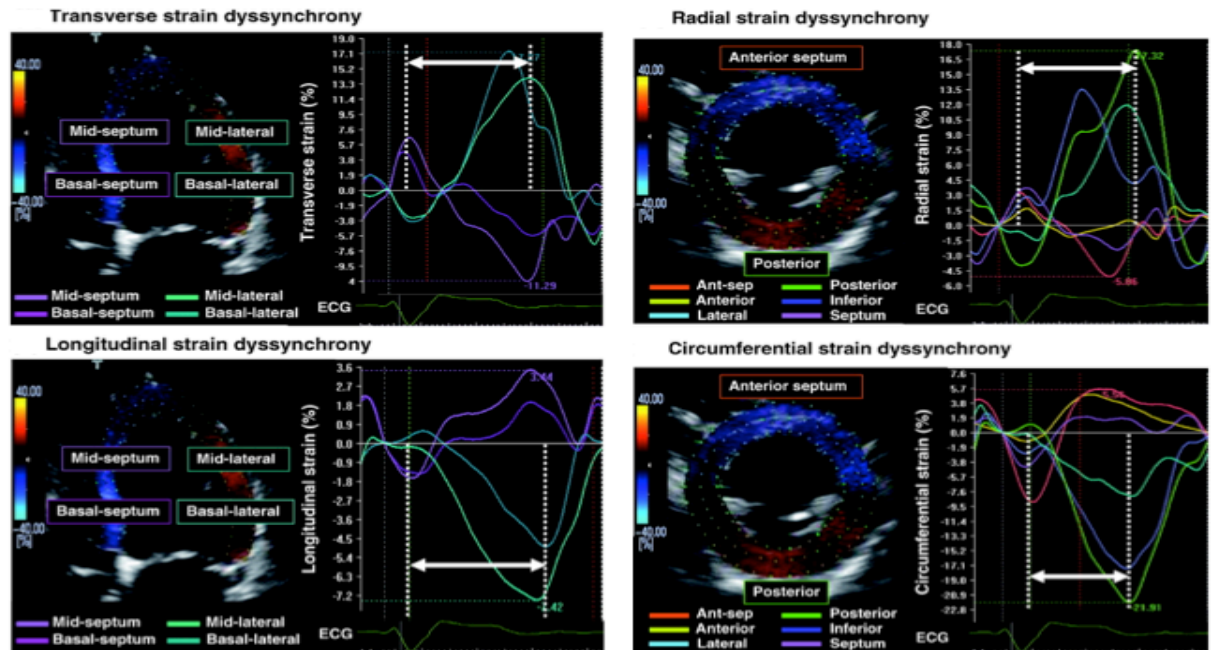


Figure 12 demonstrates the four measurements of strain from the left ventricle, transverse and longitudinal from the apical four chamber and radial and circumferential from the parasternal short axis. Each demonstrating dyssynchrony, between the septal and lateral or anterior and posterior walls respectively.

3D echocardiography

According to Galderisi et al (2007)¹⁰⁶, the advent of 3D transthoracic echocardiography (3DTTE) enabled “intraventricular dyssynchrony to be evaluated by analysing LV wall motion in multiple apical planes during the same cardiac cycle” and it also “offers better spatial resolution than a single plane”. This representation of the 3D LV volume (figure 13), was used by Kapetanakis et al (2005) to quantify global LV mechanical dyssynchrony derived from the standard deviation of the time taken for each of the 16 LV segments to reach minimum end systolic volume¹⁰⁷. The main advantage of using 3DTTE is that all 16 segments can be assessed simultaneously for intraventricular dyssynchrony and all aspects of LV systolic function including radial, longitudinal and circumferential contraction can also be evaluated. 3DTTE allows for more accurate volume assessment than 2DTTE. This is important for assessing markers of response such as LVEDV.

3DTTE has several shortcomings, these include less than optimal feasibility; images must be of high quality to calculate volumes, which can prove to be more time-consuming than conventional 2DTTE. Temporal resolution is currently lower than for 2DTTE, there is a narrower angle of image acquisition thus large LV volumes may be curtailed, and finally image analysis must be performed off-line using proprietary software, such as TomTec (Tomtec Imaging Systems GmbH, Fulda, Germany). Unlike strain, or strain-rate, imaging, active and passive motion cannot be differentiated. Akinetic segments may move due to being pushed or pulled by adjacent segments, leading to incorrect assumptions and inaccurate calculations of wall motion or volume. Acquisition is not possible for most patients with AF or ectopy with current echocardiography machines; as multiple cardiac cycles are needed to construct a moving image in 3D, and so arrhythmias create artefacts. 3DTTE is also very technically demanding and operator dependent.

Figure 13: Acquisition of 3D LV image (left) and analysis of the 16 segments (right)

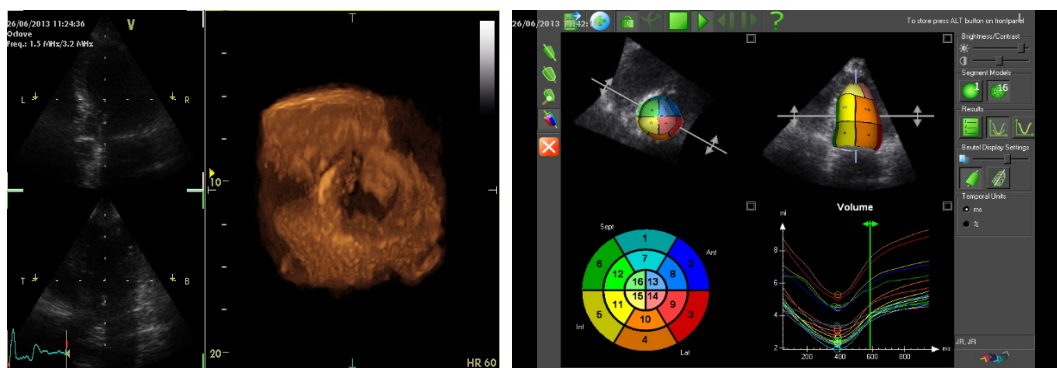


Figure 13 demonstrates the real time acquisition of the 3D whole heart image on the with two and three dimensional images of the left ventricle in the four chamber view (left) with off line analysis of the relative synchrony the 16 colour coded left ventricular segments (right).

1.8.6.3 Cardiac Magnetic Resonance

Cardiac magnetic resonance (cMR) imaging is a non-invasive imaging technique, which creates 2D and 3D, static and dynamic (albeit not real-time) images of the heart (see figure 14). This modality can be used to delineate the geometry, tissue architecture and function of the heart. Unlike USS, it is costly, time- and staff-intensive and not portable but it has the advantage of high spatial resolution.

cMR, uses the principle of nuclear magnetic resonance, the phenomenon atomic nuclei resonating in response to radiofrequency waves (RF) and can discriminate between different tissue types by virtue of their different concentrations of H atoms. A cMR sequence refers to a particular combination of radiofrequency pulses and gradients that produce images with a specific appearance. There are 2 fundamental types of cMR sequence, namely gradient (GE) and spin (SE) echo sequences. With GE sequences blood and adipose tissue appear white, resulting in what is known colloquially as 'white-blood' imaging. With SE, blood appears black whilst adipose tissue is white. This is referred to as 'black-blood' imaging. Fast imaging with steady state free precession (SSFP) is a variant of GE, and is commonly used to determine areas of focal myocardial dysfunction. SSFP is referred to as TrueFISP (fast imaging with steady state precession), FIESTA (fast imaging employing steady-state acquisition) and b-FFE (balanced fast field echo), by vendors Siemens, GE and Philips, respectively.

Due to the disparity between the cardiac cycle and the time taken to acquire cMR images, ECG gating and breath-hold is used to minimise respiratory and cardiac motion artefacts. It can take many cardiac cycles to acquire a single cMR image of the whole heart; images are usually acquired during diastole, triggered by the QRS complex on the ECG.

Factors such as arrhythmias, dysfunctional breathing and adiposity can lead to image degradation. Methods employed to increase the signal to noise ratio (SNR) and improve contrast between tissues include premedication with agents to slow the heart rate (prolonging diastole) and the use of intravenous gadolinium contrast agents. The latter is also used for assessment of ischaemia and fibrosis. More recent scanners use a more powerful 3 Tesla (3T) magnetic coil (rather than 1.5T) and so benefit from increased SNR and spatial and temporal resolution but, as consequence, specific absorption rate and acoustic noise are increased, degrading the quality of the image and leading to potential errors in volume assessment or tissue delineation. Cardiac structure and function can be assessed using cMR based on comparison of absolute volumes to the normal population or calculation of changes in volume with the cardiac cycle e.g. EF%. Intraventricular dyssynchrony can be assessed using techniques such as

myocardial tagging, allowing the quantification of regional wall motion, by strain and strain rate.

Figure 14 : cMR with LV in diastole (left) and systole (right) in the coronal plane

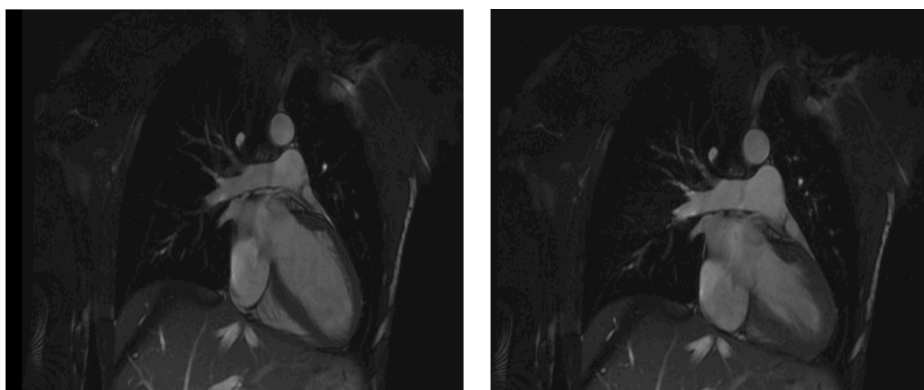


Figure 14 demonstrates 2 still images taken from the cine of a healthy patient during cMR with ventricular diastole on the left and ventricular systole on the right.

1.9 Diagnosis

The working diagnosis of heart failure is generated from a combination of the patient's history, symptoms and signs and is confirmed or refuted by investigations performed.

1.9.1 Symptoms and Signs

The presence of incidental LVSD is not sufficient to make a diagnosis of HF-LVSD since, as mentioned earlier; HF-LVSD is defined as LVSD in the presence of the symptoms/signs of HF e.g. salt and water retention. This is related to the fact that, as McDonagh et al (1997) ¹² showed, nearly 50% of patients with LVSD are asymptomatic and, even when severe, LVSD may cause no functional limitations ¹⁰⁸. However, these groups of patients remain at high risk of subsequently developing symptomatic HF-LVSD.

A patient, typically with a past medical history (PMH) including HF-LVSD risk factors, will present *de novo* with symptoms of ankle swelling, cough, dyspnoea and fatigue. Of these, orthopnoea, dyspnoea and paroxysmal nocturnal dyspnoea (PND) are moderately sensitive and specific symptoms of HF-LVSD ¹⁰⁹. On examination, a patient may have signs of pulmonary congestion, fluid overload or reduced organ perfusion. A raised jugular venous pulse (JVP), the presence of a third heart sound (S3) and tachycardia are specific to HF-LVSD but lack sensitivity (table 3).

Table 3: Specificity and sensitivity of signs and symptoms of HF

	Clinical Feature	Sensitivity (%)	Specificity (%)
Sign	Tachycardia	7	99
	Raised JVP	10	97
	Third heart sound	31	95
	Peripheral oedema	10	93
	Pulmonary crepitations	13	91
Symptom	Orthopnoea	21	81
	Pedal oedema	23	80
	Paroxysmal nocturnal dyspnoea	33	76
	Dyspnoea	66	52

The American Heart Association/American College of Cardiology (AHA/ACC) guidelines¹¹⁰ state that there is a poor relationship between cardiac performance and symptoms and discuss other cardiac factors influencing symptomatology, including “ventricular distensibility, valvular regurgitation, pericardial restraint, conduction disturbance, cardiac rhythm and right ventricular function.” together with non-cardiac factors such as abnormal “peripheral vascular function, skeletal muscle physiology, pulmonary dynamics, neurohormonal and reflex autonomic activity, and renal sodium handling.

1.9.2 Investigations

According to the National Institute for Health and Care excellence (NICE) guidelines, when diagnosing HF-LVSD, one should assess “severity, aetiology, precipitating factors, type of cardiac dysfunction and correctable causes” which will guide management¹¹¹. Blood tests are necessary (table 4), as abnormalities in these can lead to symptoms suggestive of HF-LVSD (as anaemia causing breathlessness for example) or exacerbate pre-existing HF-LVSD (as in cardio-renal anaemia, for example).

Table 4: Blood tests used in the investigation of HF

Blood test	Reason
Full Blood Count	Anaemia or Infection
Renal Function	Renal failure
Liver Function	Liver failure
Thyroid Function	Thyroid disease
Lipids	Hypercholesterolaemia
Glucose	Diabetes mellitus

The accuracy of diagnosis of HF-LVSD is often poor, due to a combination of misdiagnosis ¹¹² and a lack of confidence amongst clinicians ¹¹³. As a result, in areas such as primary care, which lack easy and rapid access to investigations such as radiography and echocardiography, many patients routinely have blood samples taken and NPs measured as part of their diagnostic work up (table 5) to support the working diagnosis of HF-LVSD. Indeed, a health technology appraisal concluded that BNP was a more sensitive and specific diagnostic test for HF-LVSD than any other currently available but this assumes that no other cause of raised BNP is found ¹¹⁴.

Table 5: Levels of natriuretic peptides required for the diagnosis of HF

Natriuretic Peptide		
BNP	NT-proBNP	Diagnosis
Level (pg/ml)	Level (pg/ml)	
< 100 pg/ml	< 400 pg/ml	Unlikely
100-400 pg/ml	400-2000 pg/ml	Uncertain
> 400 pg/ml	> 2000 pg/ml	Likely

Figure 15: CXR demonstrating acute pulmonary oedema

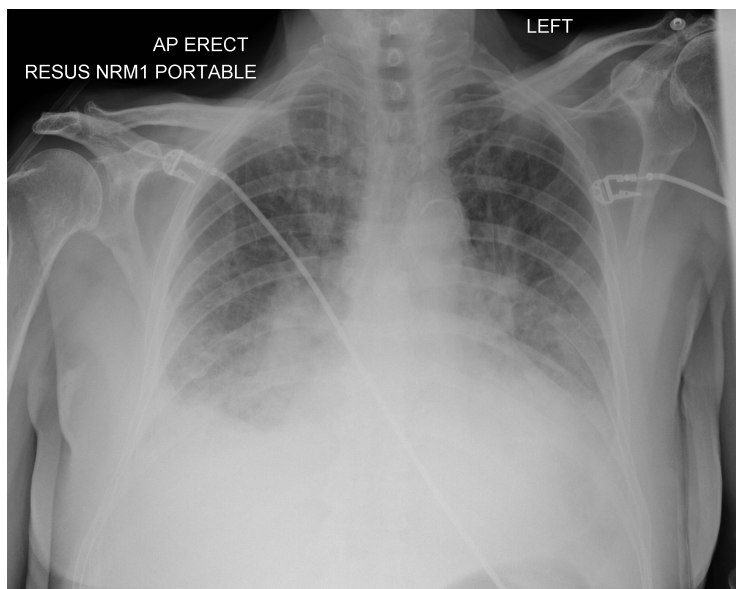


Figure 15 is a plain film anterior-posterior chest x-ray of a patient with acute left ventricular failure demonstrating bilateral frank alveolar oedema.

A chest x-ray (CXR) may indicate signs of HF-LVSD (see figure 15) such as alveolar oedema, pulmonary venous hypertension, cardiomegaly or an alternative diagnosis, such as pulmonary fibrosis, for example. ECG findings in HF-LVSD are typically non-specific but include LVH, BBB, pathological Q waves, AF and ST or T wave changes. Whilst this only demonstrates an abnormality of cardiac electrophysiology,

and not the degree of any abnormality nor any impact on myocardial mechanics, a normal ECG makes the diagnosis of LVSD unlikely (< 10%)⁸.

All patients with suspected HF-LVSD should have an early TTE to interrogate the structure and function of the heart. This allows the clinician to assess the volume of the heart chambers and identify any underlying pathology such as valvular defects or abnormalities of contractility of the myocardium. LV systolic function can be assessed either by subjective gross visual appearance e.g. for mild, moderate or severe LVSD or by objective volume assessment to calculate the stroke volume (SV) or ejection fraction (EF).

Equation (1) stroke volume:

SV = LV end diastolic volume (LVEDV) - LV end systolic volume (LVESV)

Equation (2) ejection fraction:

EF = SV/LVEDV

This relationship is widely used to describe the systolic function of the LV as it defines the fraction of blood pumped out of the LV with each cardiac contraction. If a patient has symptoms and signs of HF but the EF is normal (> 55%) then they are said to suffer from HFPEF. In contrast, if the EF is low (< 55%) then this is referred to as HF-LVSD or HF with a reduced EF (HFREF). To stratify LVSD further, mild LVSD corresponds to an EF of 45-55%, moderate 35-45% and severe < 35%. There are other measurements, which may be abnormal in heart failure, including left atrial size, aortic outflow velocity time integral and inferior vena cava flow. Diastolic dysfunction can be diagnosed by analysis of diastolic filling patterns at the mitral valve, according to the E/A ratio, which is a Doppler measure of passive (E) and active (A) LV filling through the mitral valve. Other imaging modalities maybe indicated depending on the exact clinical scenario; including trans-oesophageal echo (TOE) for valvular disease, cardiac magnetic resonance (cMR) imaging for myocarditis and cardiac computed tomography (CT) or invasive angiography (IA) for co-existing IHD.

1.10 Classification

1.10.1 Symptoms

As mentioned above, HF is defined as abnormal ventricular systolic or diastolic function, in the presence of symptoms and signs due to salt and water retention. Symptoms are classified clinically using the subjective, symptom-based New York Heart Association (NYHA) functional classification (table 6) as opposed to the objective, qualitatively-based and distinct, American Heart Association/American College of Cardiology (AHA/ACC) stages of HF (table 7) categorises HF in terms of development and progression.

Table 6: NYHA functional classification of symptom severity in heart failure

Class	Symptoms	Limitation	Example
I	None	None	Normal activity
II	Mild	Slight	Breathless on incline
III	Moderate	Moderate	Comfortable only at rest
IV	Severe	Severe	Breathless even at rest

The AHA stages are not intended to replace the NYHA classification but, rather, emphasise risk prevention and highlight progression and treatment of HF from ‘at risk’ to end-stage, particularly as the NYHA classification only refers to patients with overt and symptomatic HF. The newer staging system is not widely understood and furthermore lacks simple quantitative measures, such as EF or BNP for example, which help to categorise and compare patients¹¹⁵. The NYHA functional classification, whilst poorly reproducible and open to misinterpretation¹¹⁶, is an otherwise useful stratifying tool and correlates well with mortality¹¹⁷. Finally, there are also more specific classification systems, including the Killip⁵⁸ and Forrester¹¹⁸ classification for assessing HF severity post-myocardial infarction.

Table 7: AHA/ACC classification of HF

HF Stage	Description	Example	NYHA class
A	High risk without SHD or signs/symptoms of HF	HTN, DM	I
B	SHD without signs/symptoms of HF	LVH, LVSD	II/III
C	SHD with current/previous signs/symptoms of HF	Clinical HF	
D	SHD and refractory signs/symptoms of HF	Heart transplant	IV

AHA = American heart association, ACC = American college of cardiology, DM = diabetes mellitus, HTN = hypertension, HF = heart failure, LVH = left ventricular hypertrophy, LVSD = left ventricular systolic dysfunction, SHD = structural heart disease.

1.10.2 LV function

In nephrology, the equivalent of HF is chronic renal failure (CRF) with the staging used is both quantitative; from stage 1 (normal kidney function) to stage 5 (end stage renal failure), and quantitative, by means of the estimated glomerular filtration rate (eGFR). The availability of a similar tool for HF would benefit clinicians and patients alike. Unfortunately, the situation is more complex for HF since, unlike the estimate glomerular filtration rate for the kidney, there are many markers of cardiac (dys-) function. One of the most commonly-used markers of LVSD employed in diagnosis of HF-LVSD is LVEF but this has several specific shortcomings, including;

- It takes no account of LV twist, longitudinal shortening and diastolic function ¹¹⁹.
- LVEF may be preserved in HF or reduced due to other diseases ¹²⁰.
- It can be measured by several methodologies, which are not interchangeable ¹²¹.
- The relationship between symptoms and LVEF is poor ¹²².
- In the measurement of LVEF, inter-observer reliability is poor ⁸.

Thus, whilst a reduction of LVEF is associated with a poorer prognosis, LVEF has significant limitations in the context of the search for a universal diagnostic tool ¹²³.

The value of biochemical markers has yet to be determined fully but recent studies have shown that it is possible to differentiate AHA HF stages using clinical and neuro-hormonal profiling and these stages correlate with prognosis so perhaps it is neuro-hormonal profiling rather than 2DTTE that should be used to diagnose and stratify patients with HF ¹²⁴. It has also been suggested that the concentration of serum natriuretic peptide correlates with the degree of LVSD and so the severity of HF-LVSD.

1.11 Treatment

Suitable strategies for the treatment of HF-LVSD can be deduced from an understanding of the pathophysiology. Including;

- Removal of excess fluid; salt and water retention, which manifests as pulmonary and peripheral oedema, can be treated with diuretics.
- Augmentation of the pump function; β -blockers slow the heart rate, lengthening the duration of diastole, improving myocardial filling and reducing myocardial oxygen demand.
- Reducing afterload; ACE inhibitors reduce the afterload on the heart by reducing total peripheral resistance and so reduce myocardial work.
- Treating any underlying causes; it is important to ascertain the cause of the LVSD, as many are treatable and some are potentially reversible.

A common treatment strategy therefore includes the use of loop diuretics, β -blockers and ACE inhibitors; to reduce fluid overload, improve heart contractility and to reduce adverse remodelling and afterload respectively ^{2 125 126}. Diuretics aside, all these treatments have been proven to reduce mortality and morbidity in HF-LVSD populations. Other treatments employed in refractory cases include; aldosterone antagonists, hydralazine, nitrates, thiazide diuretics and digoxin. Patients may have frequent exacerbations requiring up-titration of therapy. Despite monitoring and adjustment of drug therapy, some patients require admission into hospital, for specialist assessment and further investigations and in extreme cases intravenous

therapy; including diuretics and inotropes, intra-aortic balloon pumps (IABP) and non-invasive ventilation (NIV).

Advanced therapies for patients whose symptoms remain refractory to oral medications (NYHA III-IV) include intravenous therapy, devices, surgery or transplant. Surgical therapies can include removal of infarcted, and thus dead, myocardium (left ventricular restoration), mitral valve repair for mitral regurgitation, using left ventricular assist devices (LVADs) as a bridge to transplant or as a destination therapy and, most radically and rarely, the use of a total artificial heart (TAH). The ultimate, curative, therapy for HF-LVSD is a heart transplant but demand for donor hearts greatly outweighs the supply and, in cases where a donor heart is available, there remains significant morbidity and mortality following such a procedure.

The focus of this thesis is examining the use of CRT to treat patients with moderate to severe HF-LVSD. CRT, also known as biventricular pacing or multi-site left ventricular pacing is a relatively new therapy for the treatment of HF-LVSD. Whilst both the acute and chronic effects of CRT on the cardiovascular system are well documented, its effects on other organ systems in the body in HF-LVSD are less well known and it remains unclear why a third of patients don't respond to CRT despite meeting evidence based pre-implant criteria. This body of work will seek to address these points using novel biomarkers and patient specific models, and, in doing so, attempt to further refine the definition of response.

1.12 Conclusions

This chapter has discussed how HF is common, costly and deadly and the many effects it can have on other organs. In the next chapter we shall discuss, how cardiac resynchronisation, a therapy specifically developed for LVSD can improve morbidity and mortality in HF.

Chapter 2 Cardiac Resynchronisation Therapy

This chapter discusses how cardiac resynchronisation therapy (CRT) was developed, how it is implanted, which patients benefit, the evidence and the difficulty in measuring and defining response.

2.1 Introduction

Dyssynchrony has been identified as a therapeutic target for patients with HF-LVSD. CRT can be used to electrically resynchronise the cardiac chambers, with the aim of restoring mechanical synchrony. In essence, CRT rewires the right atrium (RA), RV and LV and restores electrical synchronicity, and thus mechanical synchronicity, of atrial and ventricular contractions.

The goals of CRT are to improve patient's symptoms, to reduce hospitalisation, reduce death and finally reduce the economic burden of HF-LVSD on local healthcare systems.

2.2 Brief history

In the late 1990s researchers began to investigate ways in which cardiac dyssynchrony, could be corrected using pacemakers to pace both ventricles, i.e. through biventricular (BiV) pacing. It was becoming apparent that LV function deteriorated in patients undergoing long-term RV apical pacing, despite normal function prior to implantation¹²⁷. Early trials concluded that "biventricular pre-excitation could restore mechanical synchrony and improve acute left ventricular mechanics, energetic efficiency and regional metabolism"¹²⁸.

Subsequent clinical trials such as VIGOR¹²⁹ and PATH-HF¹³⁰ demonstrated that BiV pacing led to reverse remodelling. Trials such as IN-SYNC¹³¹, MUSTIC¹³², CONTAK CD¹³³ and MIRACLE ICD⁴⁹ developed this concept further, establishing the safety of such devices in large populations and the pivotal work of the CARE-HF⁴⁴ and COMPANION¹³⁴ trials established that such treatments led to reductions in morbidity and mortality. Most recently, the large RAFT¹³⁵ trial, found significant benefit, in terms of both morbidity and mortality, in mild-moderate symptomatic HF-LVSD. For a summary of the names, acronyms and data from the important CRT trials, see tables 8 and 9.

Table 8: CRT clinical trial names and their acronyms.

CRT Clinical Trials	
Acronym	Full Title of Study
CARE HF	Effect of Cardiac Resynchronization on Morbidity and Mortality in Heart Failure Trial
COMPANION	Cardiac-Resynchronization Therapy with or without an Implantable Defibrillator in Advanced Chronic Heart Failure Trial
CONTAK CD	CONTAK (name of the device) Cardioverter Defibrillator trial
IN SYNC	INSYNC (name of the device)
MADIT	Multicentre Automatic Defibrillator Implantation Trial with Cardiac Resynchronization Therapy
MIRACLE	Multicentre InSync Randomized Clinical Evaluation
MIRACLE ICD	Multicentre InSync Randomized Clinical Evaluation Implantable Cardioverter Defibrillator Trial
MUSTIC	Multisite Biventricular Pacing in Patients with Heart Failure and Intraventricular Conduction Delay Trial
PATH-CHF	Pacing Therapies in Congestive Heart Failure Trial
RAFT	Resynchronization–Defibrillation for Ambulatory Heart Failure Trial
RETHINQ	Cardiac-Resynchronization Therapy in Heart Failure with Narrow QRS Complexes Trial
VIGOR	Effects of long-term biventricular stimulation for resynchronization on echocardiographic measures of remodelling.

Table 9: A summary of the important CRT clinical trials

Trial	Patients (No)	Age (mean)	Male (%)	NYHA				Year of publication	Device		Characteristics		Endpoint					Follow-Up months		
				1	2	3	4		P	D	EF%	QRSd	SR	Death	Hospitalisation	Safety	Re-Modelling		Symptoms	
RAFT	1798	66	82					2010			< 30	>120								40
MADIT CRT	1820	65	75					2009			< 30	> 130								54
RETHINQ	172	59	65					2007			< 35	< 130								6
CARE HF	813	66	73					2005			< 35	> 120								29
COMPANION	1520	68	69					2004			< 35	> 120								16
CONTAK CD	490	66	84					2003			< 35	> 120								6
MIRACLE ICD	369	67	77					2003			< 35	> 130								6
IN SYNC	84	64	91					2002			< 35	> 130								3
MIRACLE	453	65	68					2002			< 35	> 130								6
VIGOR	53	58	57					2002			< 35	> 120								4
PATH-CHF	25	60	49					2001			< 35	> 120								6
MUSTIC	67	63	75					2001			< 35	> 150								3

2.3 Indications

The recent NICE guidance (2014)¹³⁶ provides an essential update to the 2007 technology appraisal ¹³⁷. Previous practice in the UK was to recommend patients for CRT if they had symptomatic HF-LVSD with an ejection fraction < 35% and were on optimal medical therapy (OMT). OMT means patients are taking both ACE-I and a β -blocker, at doses as high as can be tolerated, unless the drugs are specifically contraindicated. Symptoms should have been severe (NYHA III-IV) with patients

having a QRSd > 150ms or a QRSd of 120-150ms together with a positive dyssynchrony study. An exact definition of a 'positive dyssynchrony' study was not given.

In line with recent guidance from other regions of the world^{122 138}, current UK technology appraisal is explicit depending on the NYHA class and QRS duration (table 10 and 11). The level of severity of HF-LVSD (EF < 35%) and OMT remain key requirements but now CRT is suggested in patients with less severe heart failure (NYHA class II). Patients with NYHA IV should only be considered if they are ambulatory e.g. not bed-bound and the threshold for consideration based on QRSd is now > 120ms rather than > 150ms, reflecting recent evidence. A further distinction is the absence of a requirement for a positive echocardiography dyssynchrony study in patients with a QRSd < 150ms, due to the lack of evidence of such studies to predict response.

Table 10: NICE 2014 guidelines for implantation of CRT

QRSd (ms)	NYHA class			
	I	II	III	IV
< 120	ICD if there is a high risk of sudden cardiac death			ICD and CRT not clinically indicated
120 – 149 without LBBB	ICD	ICD	ICD	CRT-P
120 – 149 with LBBB	ICD	CRT-D	CRT-P or CRT-D	CRT-P
≥ 150	CRT-D	CRT-D	CRT-P or CRT-D	CRT-P

Table 11: International guidelines for the selection of patients for CRT

Region		UK	USA	Europe	
Clinical criteria	QRSd	ms	> 120 *	> 120	> 120
	NYHA	/IV	II-IV~	II-IV~	II-IV~
	OMT	Y/N	Y	Y	Y
	LVEF	%	< 35	< 35	< 35
Evidence	Class	I - III	I	I	I
	Level	A - C	A	A	A
Obtained	Body		NICE	AHA	ESC
	Date		2014	2012	2012

LVEF = left ventricular ejection fraction, OMT = optimal medical therapy,

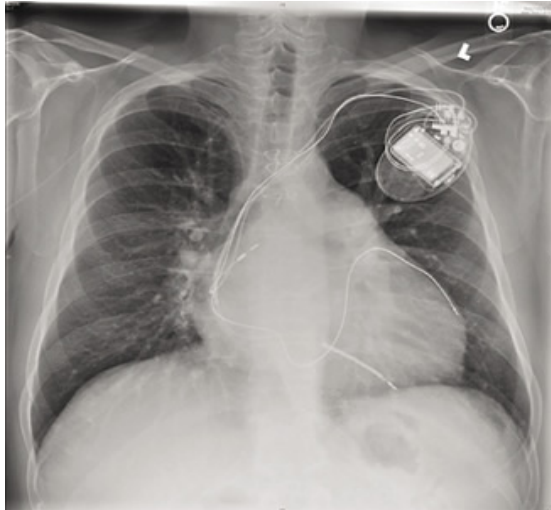
NYHA = New York Heart Association, QRSd = QRS duration.

* With LBBB.

~ Class IV patients must be ambulatory.

2.4 Device

Figure 16: CXR with CRT-D in situ



A plain film antero-posterior chest x-ray demonstrating the presence of the CRT-D box under the left clavicle, the atrial lead in the right atrial appendage, the right ventricular lead (with shocking coil) in the right ventricular apex and the left ventricular lead in the postero-lateral branch vein of the coronary sinus.

A CRT device (see figure 16) is essentially a pacemaker, which consists of a metal box and leads. The box, houses a computer, circuitry and a battery sealed within titanium metal case. The box is approximately the size of a pocket watch and weighs about 75g. There are between 2 to 3 leads, which are screwed into the box and then into specific chambers in the heart, in order to pace them appropriately. The device may also have an implantable cardioverter defibrillator (ICD) function, termed CRT-D, which can either provide anti-tachycardia pacing or defibrillation function, if a malignant ventricular rhythm, such as ventricular tachycardia or fibrillation develops. If the device does not have a defibrillator function, it is termed CRT-P (pacing).

2.5 Procedure

The procedure takes between 1.5-3 hours and is carried out in an electrophysiology laboratory. The patient is sedated and local anaesthetic is administered. Typically, an incision is made in the left pectoral region and a subcutaneous pocket made which will serve to retain the pacemaker generator, including the battery and circuitry. Venous

access is gained to the subclavian, cephalic or axillary veins, using radiographic and/or venographic guidance (with radio-opaque contrast). The vessels and heart are imaged using fluoroscopy as the leads (right atrial and right ventricular) are placed endovascularly to the endocardium of the RA (usually within the appendage), and to the endocardium of the RV, typically at the apex or septum. The leads used are typically active fixation leads, which have a small retractable screw at the tip, which is deployed when the lead is in position ensuring a secure placement. The left ventricular lead, also inserted via the endovascular route, is introduced via the coronary sinus ostium and advanced retrogradely to one of the tributary coronary veins on the epicardial surface of the LV it is held in place passively and as a result is the lead most at risk of displacement. Following implantation of the CRT device, the patient is usually kept in hospital for monitoring overnight, with a CXR performed to ensure that the 3 leads are positioned correctly and that there is no pneumothorax. Finally, a 12 lead ECG is performed before discharge to ensure appropriate biventricular capture e.g. QRSd and morphology, as baseline for future comparison e.g. to detect loss of capture or lead displacement and especially if there are changes made to the programmed AV or VV delays.

2.6 Cost

The 2014 NICE Health Technology Appraisal¹³⁶ updated the systematic review of the cost effectiveness of CRT therapy based on data from the CARE-HF, COMPANION, CONTAK, MIRACLE and MUSTIC trials. According to data obtained in 2011 from across the NHS, the average cost of a CRT-P device is £3411 and a CRT-D device costs around £12293. With implantation costs this rises to £8281 and £17,849 respectively. Median time to device failure was established as 10.4 years for CRT-P and 5.8 years for CRT-D.

The systematic review looked at the incremental cost effectiveness ratio or ICER (defined as $\text{Cost CRT} - \text{Cost OMT} / \text{No of QALYs CRT} - \text{No of QALYs OMT}$) in conjunction with the quality-adjusted life years. Quality adjusted life years (QALYs) are calculated as the product of both remaining expected life quantity and quality and so a year of perfect life is 1, less than perfect < 1 and death 0. In the UK, NICE approves technologies, provided they do not exceed an ICER per QALY of > £30,000 e.g. compared to the current best treatments, an additional year of perfect life will cost

£30,000 using this therapy. The review judged that CRT-P was associated with an ICER per QALY of £10,494 and a QALY gain of 0.70 (equivalent to 256 days of full health) when compared with OMT. CRT-D on the other hand was associated with an incremental cost of £25,200 and a QALY gain of 0.99 (equivalent to 361 days of full health) compared with OMT.

It is worth revisiting the technology appraisal from 2007¹³⁷, as this concluded that “implanting a CRT device in 13 people would result in the saving of one additional life over a 3-year period, compared with optimal medical therapy” and that CRT-P becomes cost effective after 3.5 years of therapy and CRT-D after 7.5 years of therapy. Interestingly, it also concluded that CRT would be rendered cost-ineffective if the risk of death from worsening HF-LVSD fell below 15% per annum or if the CRT-D battery failed in less than 3.5 years. Thus cost-effectiveness is influenced not only by the suitability of the patient but also by the longevity of the device.

2.7 Challenges

According to the most recent European CRT survey in 2009¹³⁹, the UK is the 10th highest user of CRT devices, with just over 60 implanted per million head of population, however, this falls short of the Heart Rhythm UK (HRUK) target of 140 implanted per million population¹⁴⁰, achieved in countries such as Denmark, Germany and Italy. This suggests that, in the UK and in other countries, there might be patients who are suitable for a device such as CRT, but are not receiving them. This could be due to many reasons e.g. poor awareness of guidelines, loss to follow-up, patient wishes, contraindications, failed implantation, unfavourable anatomy but overcoming the barriers preventing suitable patients from receiving a device is clearly the first challenge to ensuring such a laudable target is met e.g. is this a conscious decision.

Difficulties in device implantation are reported for around 5-10% of cases, thus even eligible patients who are referred for a CRT device may, in the end, not have one implanted. In such cases the patient may be offered a second attempt at implantation with a more experienced clinician, at a higher volume centre or with a surgically placed epicardial LV lead.

There are a number of different factors, which may lead to failure of implantation;

- Difficulty visualising and cannulating the coronary sinus
- Highly variable anatomy and is often tortuous coronary sinus
- Difficulty accessing the area with the greatest electrical or mechanical delay
- Scar tissue may prevent stimulation or capture of that area of myocardium
- Unstable LV lead position
- Phrenic nerve stimulation causing patient discomfort

Of course, there are also the problems associated with any implantable permanent pacemaker, such as difficulties in venous access for example.

2.8 Complications

Peri-procedural complications include; pocket haematoma, coronary vein dissection/perforation, pneumothorax or death.

Phrenic nerve stimulation (PNS) may become apparent during the procedure, or more frequently, following discharge. Developments such as a quadripolar LV lead, comprising 4, rather than the typical 2, independent electrodes, is designed to stimulate the LV in 4 separate locations, increasing the number of potential pacing vectors from 3 to 10, allowing the pacing vector which causes PNS to be avoided, without the need to reposition the LV lead.

2.9 Follow-up

Post procedure all patients should be seen, approximately once every three months, by a technician in the ECG clinic, to ensure that their device (pacemaker +/- defibrillator) is working correctly. Any problems are relayed to the implanting clinician and the patient is brought back to see the clinician three months post-implantation to check the degree of improvement, if there are any problems with the device but also to see that the wound has healed well. In the interim the patient has access by telephone to a nurse specialist and are given advice on what to do in certain circumstances e.g. if they should receive a shock. At 3-month follow-up, if the patient is deemed to have responded i.e. they feel better, they are discharged from the tertiary devices clinic, back to either the referrer such as their tertiary heart failure specialist, secondary care cardiologist or even general practitioner. There are guidelines set by the HRUK on this device aftercare¹⁴¹.

Some manufacturers offer remote follow-up on certain devices, providing weighing scales and automated sphygmomanometers for the patient to use in their own home. There is daily collection of device data via Wi-Fi. The physician has access to such data but this is primarily controlled and monitored by the manufacturer. This provides an early warning system to pre-empt clinical deterioration and is part of the ongoing development of telemedicine in this area.

Longer-term complications, occurring within 4 years of implantation are common with 50% of devices needing revision due to battery depletion and 14% due to unanticipated events such as lead displacement or infection ¹⁴².

Implantation onto the epicardial surface of the LV offers an option for patients, who cannot have the LV lead implanted trans-venously via the CS. This procedure can be carried out thorascopically by a cardiothoracic surgeon. Finally, through its increasing role and availability, cMR imaging delineation of the coronary sinus to aid the implantation of the technically difficult LV lead and the mapping of scarring to guide lead placement, may also lead to improved identification of suitable patients.

Some patients may be termed 'nonresponders' to CRT despite successful implantation of the and even objective improvement of cardiac function post-implant. This affects up to a third of patients receiving CRT and whilst it remains unclear why such patients don't derive benefit, it may be longer because it is no longer the heart that is driving their symptoms ¹⁴³. Indeed, the only 2 cardiac measurements, which are required to satisfy implantation criteria, are QRSd and LVEF. In the original CRT trials, most patients had isolated HF-LVSD in the apparent absence of explicit comorbidities such as peripheral vascular disease, depression, malignancy or other chronic organ failure, all of which are common in HF-LVSD populations, but are not be addressed directly by CRT. The complications listed above are not insignificant, particularly so if the patient does not go on to gain any benefit from their device. Clearly, a robust means of identifying all patients who would benefit from a CRT device, prior to implantation, would prove valuable to physicians, researchers, patients and device manufacturers.

2.10 Benefits

2.10.1 *Observational Trials*

During the mid to late-1990s, many observational trials were conducted. These paved the way for the development of clinical guidelines and for further research into CRT, assessing both acute haemodynamic and chronic functional improvements in patients with HF-LVSD.

Cazeau et al (1994)¹⁴⁴ performed the first-in-man observational trial of a biventricular pacemaker demonstrating that 4-chamber pacing was feasible in a single patient with refractory end-stage HF-LVSD, LBBB and interatrial conduction delay. By 6 weeks post-implantation, there was improvement in clinical status, from NYHA IV to II and a 17kg weight loss due to the resolution of peripheral oedema.

Foster et al (1995)¹⁴⁵ demonstrated acute haemodynamic improvement, in terms of increased cardiac index and decreased systemic vascular resistance, for 18 patients between 12 and 36 hours after coronary artery bypass surgery using biventricular pacing, as opposed to RV pacing alone. However, it is important to note that these patients did not have HF-LVSD.

Cazeau et al (1996)¹⁴⁶ compared the virtue of different pacing configurations such as RV apex, RVOT, RA apex-LV pacing and RVOT-LV pacing in a group of 8 end-stage HF-LVSD patients with broad QRSd and NYHA class III-IV, who were ineligible, for heart transplantation. The authors were able to demonstrate a significant increase in cardiac index and decrease in pulmonary capillary wedge pressure immediately following implantation with LV and biventricular pacing configurations only. During the follow-up period of 3 months, 4 patients died, but the survivors showed an improvement in functional class from NYHA IV to II, demonstrating both the acute haemodynamic and chronic functional benefits of the biventricular pacemaker.

In the following year, Blanc et al (1997)¹⁴⁷ published a study supporting the findings of Cazeau's earlier work, demonstrating acute haemodynamic benefit (in terms of systolic blood pressure or pulmonary capillary wedge pressure) for 27 patients with end stage

HF-LVSD and AV or interV DS. Again, this benefit was only associated with LV or BiV pacing configurations and not RV apex or RVOT.

Similarly, both Kass et al (1999)¹⁴⁸ and Leclercq et al (1998)¹⁴⁹ demonstrated acute haemodynamic benefits (measured by improvements in dP/dt and cardiac index respectively) in a total of 36 end-stage HF-LVSD (NYHA III-IV) patients with significant interventricular dyssynchrony, when using LV or biventricular but not RV apex or RV septal pacing configurations.

Saxon et al (1998)¹⁵⁰ demonstrated an improvement in LV fractional area as measured using intraoperative transoesophageal echocardiography in patients with depressed LV function post cardiac surgery. Gras et al (1998)¹⁵¹ showed that such a pacing modality led to gains in QoL, NYHA class and 6 minute walk distance at 3 month follow-up in the preliminary results of the first multicentre observational study of biventricular pacing in patients with end-stage HF-LVSD (NYHA III/IV) and significant interventricular dyssynchrony. In a final analysis of this study, Gras et al (2002)¹³¹ were able to demonstrate the benefit of biventricular pacing in the same patient group at 12 months.

2.10.2 Randomised controlled trials

To date, more than 12,000 HF-LVSD patients have been recruited to randomised clinical trials of CRT, showing that CRT in combination with OMT has significant benefits in terms of morbidity and mortality compared to OMT alone, or to OMT with ICD. The majority of these trials had restrictive inclusion criteria, based on the observational trials described above or on the established contemporary guidelines at the time of recruitment. Thus patients were required to have symptomatic HF-LVSD (NYHA class II-IV), with interventricular conduction delay (QRSd > 120ms), with normal sinus rhythm and with/or without an indication for an ICD. More recent trials have investigated patients with less symptomatic HF-LVSD, and those with AF and/or a shorter QRSd.

Most trials relied upon primary endpoints, such as the 6-minute walk distance (6MWD), NYHA functional class and quality of life (QoL) assessment. Others used a combination of metrics, such as the clinical composite score (CCS)¹⁵², based on a

combination of NYHA class, symptom severity and outcomes including heart failure, hospitalisation and death. The most recent large trials use clinical composite primary endpoints, including cardiac mortality, all-cause mortality and HF hospitalisation. Secondary endpoints included levels of neuro-hormonal biomarkers such as BNP, a reduction in LV volume as measured by 2DTTE and peak VO₂ measured during graded exercise on a treadmill or bicycle ergometer.

The RCTs have been broadly consistent in terms of improvements in the primary endpoints detailed above, with the 6MWD, NYHA functional class and QoL all improving, with some exceptions, as will be discussed below. Similarly, there has been consistency in improvements of secondary endpoints. In the case of peak VO₂, there have been consistent reports of improvements in this endpoint, apart from in the recent RETHINQ trial. All trials have shown reductions in both the degree of MR and LV volume but, to date, only CONTAK-CD has failed to show a reduction in HF hospitalisation.

In addition to observational trials, there have been 14 major randomised controlled trials investigating the role of CRT. Each is considered in turn, in the sections below.

2.10.2.1 MUSTIC SR/MUSTIC AF

Cazeau et al (2001)⁴⁸ conducted a single-blind randomised, controlled crossover study (the pacemaker was either switched off initially and then on or vice versa) of 67 patients in sinus rhythm but with severe HF-LVSD (NYHA class III), receiving OMT, LVEF < 35%, 6MWD < 450m, and with a QRS duration of > 150ms. This was called the MUSTIC-SR study. Only 47 patients completed the study, with 9 withdrawn before randomisation and 10 failing to complete both phases. It was shown that for the remaining patients 6MWD (primary endpoint), MLWHFQ score (assessing QoL), peak VO₂ and HF hospitalisations (secondary endpoints) were significantly improved at 24 weeks of follow-up. The patients expressed preference for the 12-week period when the CRT device was switched on, compared to when it was switched off.

In 2002, the AF extension of the MUSTIC trial, called MUSTIC-AF¹⁵³, used similar inclusion criteria but recruited 33 patients in persistent or permanent AF, with a QRSD > 200ms on RV pacing, demonstrating significant improvements in the primary and

secondary endpoints, excluding QoL. However this was a small study, with < 25% female participants, with significant drop out at 50% (including death and failure to pace the LV) and again single-blinded, which somewhat weakens the results.

These were the first randomised trials assessing biventricular pacing in man.

2.10.2.2 PATH-CHF/PATH-CHF II

In the PATH-CHF study, Auricchio et al (2002)¹³⁰ conducted a single blind, randomised, controlled crossover study on 41 patients followed up over 12 months. Once again dropout rates were high with only 29 patients completing the study. The aim was to investigate both the acute haemodynamic and long-term clinical benefit of different pacing modalities such as RV, LV or BiV in severe HF-LVSD patients. Inclusion criteria included severe HF-LVSD (NYHA III-IV), OMT, QRSd > 120ms and PRd > 150ms. Significant improvements were seen in both the primary (peak VO₂ and 6MWD) and the secondary endpoints (QoL assessed by MLWHFQ and NYHA functional class). Furthermore, greater haemodynamic improvement was observed in terms of dP/dt and pulse pressure with LV rather than RV pacing. Unusually for a HF clinical trial, there was an even gender split (50:50) thus applicability of the results to the female population is credible. However, as for the MUSTIC trials, numbers were small, with a significant dropout rate and the trial was only single-blinded. In addition contrary to what might be expected, the functional improvements failed to return to baseline when the pacing was either switched off or during the wash out period suggesting that there might be a placebo effect e.g. the mere implantation of the device led to patients feeling better, even when it was turned off.

The PATH-CHF II trial¹⁵⁴, was a similar trial (single-blinded, randomized, controlled, crossover), which recruited 86 HF-LVSD patients, in sinus rhythm, NYHA functional class > II and a QRSd > 120ms. The aim was to assess the effect of both uni- and bi-ventricular pacing modalities on acute haemodynamic and chronic symptomatic outcomes. Patients were stratified 1:1 according to QRSd, with both long (> 150ms) and short (120-149ms) groups and followed up over 6 months, with 3 months of inactive and 3 months of active pacing. The primary endpoint was peak VO₂ and secondary endpoints were 6WMD and QoL assessed by MLWHFQ. A significant number of patients could not be randomised (12) or did not complete the study (17).

The prolonged QRSd group improved in terms of all primary and secondary endpoints, the short QRSd group none. This trial was pivotal in influencing the CRT eligibility criteria, determining that QRSd of > 150ms was needed and demonstrating that patients with NYHA class of II may benefit from CRT; not included in earlier trials.

2.10.2.3 MIRACLE/MIRACLE ICD/MIRACLE ICDII

The MIRACLE trial by Abraham et al (2002)¹⁵⁵ was the first CRT trial conducted in a multi-centre, double-blinded, parallel controlled manner with a large cohort of patients (453). It was also the first trial to assess CRT, against OMT without crossover, in patients with severe HF-LVSD (NYHA III-IV, QRSd > 130ms, LVEF < 35%) and sinus rhythm but with no prior pacing indications. The primary endpoint was the 6MWD and secondary endpoints included NYHA functional class, QoL assessed by MLWHFQ, peak VO₂, hospital admissions, patient preference and mortality. Significant improvements were seen in all primary and secondary endpoints with pacing compared to the control group. However it should be noted that whilst > 90% patients were receiving diuretics or ACE-I, less than two thirds were receiving β -blockers. In addition, the majority of patients were white males and follow up was limited to 6 months. Ideally, all patients with HF-LVSD should take β -blockers (unless not tolerated or contra-indicated) and thus one would expect that OMT would include a much higher proportion e.g. > 90% of patients on β -blockers. Furthermore, since the cohort was mainly comprised of white males, applicability of the results to minority and female populations is problematic.

The MIRACLE ICD trial by Young et al (2003)⁴⁹ was designed in a similar way to the MIRACLE trial but, rather than studying CRT alone, the combinations of ICD with OMT versus CRT-D with OMT were investigated. Inclusion criteria and endpoints were the same, apart from an indication for ICD for all 369 patients. With the CRT switched on, the patients showed significant gains in terms of QoL, functional class and exercise capacity (assessed by peak VO₂ rather than 6MWD). This outcome was similar to that reported for the CRT-alone group in the MIRACLE trial. However, it is important to note that the duration of follow-up was short (6 months) and the study was not powered to detect either morbidity or mortality benefits between the groups.

In contrast to the more symptomatic HF-LVSD patients who benefited in earlier trials, the MIRACLE ICD II trial¹⁵⁶ set out to investigate the use of CRT in a less symptomatic

patient group (specifically those in NYHA class II). A total of 186 patients were recruited, with inclusion criteria based on NYHA class II alone, QRS > 130ms, LVEF < 35%, OMT and an ICD indication. As before, patients were randomised to either CRT-D with OMT or ICD with OMT. The primary endpoint was peak VO₂ and the secondary endpoints were QoL, NYHA functional class, 6MWD, LV volumes and LVEF. There was no significant difference between the control and the intervention groups in terms of peak VO₂, 6MWD and NYHA functional class. However at 6 months patients within the intervention groups showed significant reductions in LV volumes and significant increases in LVEF when compared with controls. As the authors note, follow-up was relatively short and patients with milder heart failure have better preserved exercise tolerance than those with severe HF-LVSD so the lack of improvement in cardiorespiratory fitness was perhaps not unexpected. The authors concluded that CRT offered important benefits to patients with mildly symptomatic HF-LVSD, but in the absence of any functional improvement, and in the light of the not insignificant risk of complications, further research would be required before routine use of CRT in NYHA II could be recommended.

2.10.2.4 VENTAK/CONTAK-CD

Reported by Higgins et al (2003), this was a randomised, controlled, double blinded study comparing CRT-D patients with pacing turned on or off. This was a parallel crossover design and included patients with HF-LVSD, NYHA class II-IV, EF < 35%, QRSd > 120ms in normal sinus rhythm¹³³. The study's initial intention was to follow up patients for 3 months, but this was extended to 6 months and the primary endpoint was changed from peak VO₂ to a composite endpoint of a reduction in heart failure events. This was presumably because the primary endpoint was not reached at 3 months. Despite the large number of patients recruited (581) no significant improvement in the primary endpoint was observed. However in the NYHA III-IV subgroup, peak VO₂, 6MWD, QoL, NYHA class and LV volumes were significantly improved in the active pacing group but only LV volumes were improved in the NYHA class II subgroup. This adds further weight to the absence of clinical, if not LV remodelling, benefit in these patients. Furthermore, over 80% of the patients were male yet only 50% were taking β-blockers, despite the patients being reported as receiving OMT. This made translation of the results to a female population and the

influence of β -blockers in determining response unclear, as the majority of other CRT trials report that over 90% of patients received β -blockers.

2.10.2.5 COMPANION

The COMPANION trial, as reported by Bristow et al (2004)⁶ was the largest trial of CRT and compared OMT versus OMT+CRT versus OMT+CRT-D undertaken at the time with more than 1500 patients recruited. Inclusion criteria included HF-LVSD, NYHA class III-IV, QRSd > 120ms, PRd > 150ms, sinus rhythm and no pre-existing clinical indication for a pacemaker or defibrillator. The trial was randomised, but not blinded, and the primary composite endpoint was a combination of all-cause mortality and hospitalisation. The duration of follow up was 12 months for the OMT group and 18 months for the CRT group. The trials primary endpoint was all-cause mortality and hospitalisation and in this regard it achieved a 20% reduction with device therapy compared to medication alone. CRT reduced the relative risk of death due to any cause by 24% and CRT-D reduced this by 36%. As the authors highlighted, the devices implanted became commercially available during the trial; this led to a high number of withdrawals from the OMT-only group to allow the clinicians to implant a CRT device. Such patients were excluded from the primary endpoint but were re-consented so that they could be included in the intention to treat analysis.

2.10.2.6 CARE-HF

This trial reported by Cleland et al (2005)⁴⁴ examined the influence of CRT on long-term mortality and morbidity in patients with severe HF-LVSD. Over 800 patients were recruited and followed up for 2.5 years. The inclusion criteria were; NYHA III-IV, EF < 35%, OMT and QRSd of either > 150ms or 120-149ms but with 2/3 echocardiographic criteria of dyssynchrony (IVMD > 40ms, delayed activation of the posterolateral left ventricular wall or aortic pre-ejection delay of > 140ms). The trial was international, multicentre and randomised to either CRT or OMT (stratified according to NYHA class) but not blinded. The majority of the patients were men in NYHA III class, with over 90% using an ACE-I and 70% a β -blocker. The primary outcomes were time to death from any cause or an unplanned hospitalisation for a cardiovascular event. Secondary outcomes included death from any cause or unplanned hospitalisation with worsening heart failure. Continuous outcomes included NYHA class, QoL measured by both the MLWFHQ and the European Quality of Life–5 Dimensions (EuroQoL EQ-5D) instrument.

The trial reached its primary endpoint, with the CRT group achieving a significant ($p < 0.001$) 16% absolute risk reduction. Fifty-five percent of the group receiving OMT alone died or had an unplanned hospitalisation for a cardiac event, compared with 39% of the CRT group. The trial also achieved significance in all of the secondary outcomes ($p < 0.001$), with 30% of the OMT alone group suffering death from any cause compared with 20% in the CRT group. The CRT group also had significant improvements ($p < 0.001$) in IVMD, mitral regurgitation, LV volumes, LVEF, QOL (as measured by MLWHFQ and EuroQoL EQ-5D), systolic BP and NT-proBNP. This study proved to be pivotal in terms of standard of care the UK and in Europe, significantly influencing the criteria for patient selection for CRT in clinical guidelines.

2.10.2.7 RD-CHF

This trial by Leclercq et al (2007)¹⁵⁷ was unique in that it recruited patients in HF-LVSD who already had a pacemaker *in situ*, upgrading them from a single chamber RV pacemaker to CRT. Patients with AF, previously excluded from such trials, were also included. Inclusion criteria included HF-LVSD, NYHA III-IV, LVEF $< 35\%$, interventricular dyssynchrony defined as IVMD > 40 ms and intraventricular delay defined as an aortic pre-ejection time of > 180 ms, both measured by 2DTTE. The trial was a randomised crossover design, comparing RV vs. BiV pacing, in 2 separate 3-month blocks. Despite being a multicentre study, only 56 patients were enrolled, with 12 patients dropping out before randomisation when BiV pacing was found not to be feasible and a further 12 not followed up after randomisation due to death, infection or other reasons. This was the first paper to base inclusion on echocardiographic rather than ECG parameters e.g. QRSd. More than 90% of the patients were male and not all patients were in NYHA III-IV despite this being one of the stated inclusion criteria.

The primary or secondary endpoints are not explicitly stated in the paper. However, there were significant improvements in NYHA class, 6MWD and QOL in the BiV group, compared to the RV-only group and no increase in ventricular arrhythmias in the BiV group. The authors concluded that such an upgrade was safe and feasible, but with such a high dropout rate, their findings will need to be repeated on a much larger patient group before firm conclusions can be made.

2.10.2.8 MADIT CRT

This trial by Moss et al (2009)¹⁵⁸ was designed to investigate whether CRT would reduce the risk of death or HF events in those with mild or asymptomatic HF-LVSD (NYHA class I-II). Over 1800 patients were recruited, with inclusion criteria of LVEF < 30% and QRSd > 130ms and followed up for over 2.5 years. Patients were randomly assigned to either ICD alone or CRT-D in a 3:2 ratio. The vast majority of patients were white (> 90%) males (> 75%) with NYHA II symptoms. Over 97% of patients were receiving ACE-I or ARB therapy and over 93% of patients were receiving a β -blocker. Whilst no mention is made of whether OMT was an essential inclusion criteria this is one of the few trials where nearly all patients were taking some form of OMT. The primary endpoint was death from any cause or a non-fatal HF event. The primary endpoint was achieved, with a significantly lowered risk of death in the CRT-D group, but this was primarily restricted to a sub-group with a QRSd > 150ms. The CRT-D group also had significantly lower LV volumes and improved LVEF at follow-up. No measure of functional improvement e.g. NYHA class, QOL, 6MWD or peak VO₂ was reported and, whilst it could be argued that NYHA Class I is asymptomatic making it difficult to demonstrate improvement, this could have been measured using a QOL questionnaire. It would also have been interesting to compare functional reserve between Classes (I and II) to see what differences, if any, were present at baseline or follow up in terms of peak VO₂ for example.

Significantly, the outcome of this trial led to an extension of USA guidelines to include patients with NYHA functional class II HF-LVSD.

2.10.2.9 RETHINQ

This trial by Beshai et al (2007)¹⁵⁹ was a double-blinded, randomised, controlled, multicentre clinical trial aiming to answer the question of benefit of CRT in patients with a narrow QRS but with an ICD indication. Inclusion criteria included QRSd < 130ms, HF-LVSD, LVEF < 35%, NYHA class III and mechanical dyssynchrony demonstrated on 2DTTE. The primary endpoint was an increase in peak VO₂ > 1ml/kg/min at 6 months post implantation.

Over 170 patients were recruited and underwent subsequent randomisation, all had a CRT-D implanted and were either actively paced (CRT group) or not (control group). Although no p-values are given, there appears to be a greater number of men in the

active pacing group. Over > 90% of patients in both groups were taking an ACE-I or β -blockers. At 6 months there was no significant difference between the groups in peak VO_2 , or indeed 6MWD, QOL (measured by MLHFQ) or LV volumes but the CRT group did have a significantly improved NYHA Functional Class a subjective and secondary endpoint. There was a high complication rate, of around 20%, in both groups.

Similar to other studies using 2DTTE to measure dyssynchrony (and hence eligibility for CRT) it is possible that the choice this specific criterion rather than QRSd could account for the lack of benefit since the authors state that 96% of patients in their study qualified for inclusion based on tissue Doppler measurement of an opposing wall delay of > 65ms, rather than the SPWMD of > 130ms measured using M-mode which would have included only 4% of their patient population. Clearly, as this was a multi-centre trial, it was important to choose a measure of dyssynchrony that was both feasible and reproducible, but as found in the PROSPECT trial, even extensive training of echocardiographers cannot guarantee that the same metric is being measured consistently. This is further evidenced by the fact that a subgroup of patients with QRSd 120-130ms did derive benefit, reinforcing the difficulty of using 2DTTE to measure DS, the notion that the QRSd is the best predictor of CRT response and that a prolonged QRSd is necessary to derive benefit.

2.10.2.10 RAFT

This trial by Tang et al (2010)¹³⁵ aimed to discover if the addition of a defibrillator to CRT + OMT would reduce mortality and morbidity, in patients with moderate-severe HF-LVSD with indications for an ICD. This was a randomised controlled multicentre trial, but not blinded, 1798 patients were randomly assigned to CRT-D or ICD with inclusion criteria of LVEF < 30% and QRSd 120ms. Initially, the trial recruited NYHA II-III patients but later, in February 2006, this was revised to recruit only NYHA II patients, reflecting emerging clinical trial data and guideline changes. Patients were followed up for over 3 years. The primary endpoint was death from any cause or HF leading to hospitalisation. The majority (> 80%) of patients were male and in NYHA class II. Twelve percent had permanent AF or atrial flutter and more than 90% were using a β -blocker and 96% an ACE-I. There was a significant reduction in the primary endpoint in the CRT-D group compared to the ICD alone group, with a 7% absolute risk reduction. Once again, subgroup analysis demonstrated that a QRSd > 150ms was associated with

increased benefit from CRT. This trial was unable to show that mildly symptomatic patients derived functional benefit from CRT but, as VENTAK/CONTAK CD had failed to show, and MADIT-CRT had failed to investigate, it did show that there was a significant reduction in death and hospitalisation for this patient group. However, worryingly, more than 15% of patients in the CRT-D group developed complications such as haematoma, infection and pneumothorax before 30 days. So whilst the lives of patients in NYHA class II may be saved, they may not necessarily feel any better and may have a significant risk of complications.

2.10.2.11 BLOCK-HF

The most recent CRT large trial to be reported is that by Curtis et al (2013)¹⁶⁰. This was designed to answer a clinical question that has troubled clinicians for several years. In patients with chronotropic incompetence and a corresponding indication for a pacemaker due to AV block, there is good evidence that, whilst an adequate heart rate may be restored, long-term RV apical pacing can lead to impairment of LV systolic function. This begs the question would using a BiV pacing strategy from the outset be less harmful to LV function?

In this prospective, multicentre, randomised, double blind trial 691 patients were implanted with a CRT-P or CRT-D (if they also had an indication for a defibrillator) and then randomly assigned to RV or BiV pacing. Inclusion criteria included a pacemaker indication due to AV block, NYHA class I-III and a LVEF < 50%. Exclusion criteria are not stated. The primary outcome recorded was the “time to death from any cause, an urgent care visit for heart failure that required intravenous therapy, or a 15% or more increase in the left ventricular end-systolic volume index”. Patients were followed up for over 3 years and the primary outcome occurred in 55.6% of patients assigned to the RV compared to 45.8% of the BiV pacing group leading the investigators to conclude that a BiV pacing strategy should be carried out from the outset. There are, however, several problems with this study; 23% of the patients died (this is high compared to other CRT studies, especially given the mild severity of HF-LVSD), the population was heterogeneous (LVEF was between 40 +/- 8.3% and thus accounts for a whole spectrum of LV dysfunction from normal/preserved/reduced) and the sample size was small. Over 73% of the patients recruited were male with an average participant age of participant in the mid-70s making translation to other groups e.g. young females, difficult. On the whole, the 2 groups were similar but there is no

statistical comparison of medical therapies included in the study e.g. percentage of patients on OMT, which could both skew and confound the results. Finally, 23% of patients crossed over from the RV to the BiV pacing group. Although there is no accepted best practice for dual chamber devices, other available RV target pacing options (His bundle, for example) were not investigated in this study. It is possible that these alternatives could lead to less deleterious effects on LV function and thus the requirement for BiV pacing. In summary, this initial study suggests that BiV pacing for patients with an indication for a pacemaker with mild-moderate HF-LVSD leads to improved outcomes when compared to RV pacing alone.

2.11 Response

2.11.1 Introduction

Response to CRT can be defined according to 2 domains:

- Subjective (in terms of symptoms); NYHA functional class and QOL assessment.
- Objective (in terms of heart function); imaging, biomarker and cardiovascular performance assessment.

It has become apparent that only 70% of patients implanted with CRT are thought to derive benefit from the procedure and are deemed responders. A smaller percentage deriving maximal benefit are termed 'super' responders and the remaining patients may either not respond at all or respond negatively becoming worse, reflecting perhaps the inexorable progression of the disease, rather than as a direct result of the CRT device or procedure.

2.11.2 Subjective

2.11.2.1 NYHA class

As discussed previously, most CRT clinical trials use NYHA functional class to assess patients and to define response but as also mentioned, NYHA classification is not without problems. Nevertheless CRT has been shown to reduce NYHA functional class by an average of 0.5-0.8^{46-48 133}. For example in the MIRACLE, MIRACLE ICD and CONTAK CD trials, 68%, 72% and 63% of patients improved by one or more class, compared with 38%, 54% and 48% of controls. According to Yu et al (2008) in some randomised control trials (RCTs) following CRT, 30-50% of patients improved

symptomatically, despite the fact that their pacemaker was not turned on⁸⁶. The reported improvement in symptoms in the control, and perhaps also the intervention, group, maybe a result of natural variation in end-stage organ failure and/or a placebo effect associated with having the CRT device implanted in the first place.

2.11.2.2 Quality of life questionnaire

The MLWHFQ is a disease-specific questionnaire designed to measure quality of life (QOL) in patients with HF (see appendix). Similar tools include Quality of Life in Severe Heart Failure Questionnaire (QLQ-SHF)¹⁶¹, the Chronic Heart Failure Questionnaire (CHQ)¹⁶², the Kansas City Cardiomyopathy Questionnaire (KCCQ)¹⁶³ and the Left Ventricular Dysfunction Questionnaire (LVD-36)¹⁶⁴. First developed in 1984 at the University of Minnesota, the MLWHFQ, has been validated and is widely used¹⁶⁵. It is designed to measure exactly how a patient's HF is impacting on their day-to-day life. There are 21 questions, all of which start with the same common stem "Did your heart failure prevent you from living as you wanted during the past month (4 weeks) by..." for example question 1 "...causing swelling in your ankles or legs?". Each question is given a rating on a 6-point Likert scale from 0 (no) to 5 (very much), giving an overall score out of 105 (see appendix).

The questionnaire covers a wide range of issues such as; the side effects of treatments, hospital admissions, symptoms, mood, sex life and appetite. As it is American in origin, some questions, such as the cost of healthcare, are less relevant in the UK. Furthermore as HF patients often have a large burden of comorbidity, they may feel unwell for a variety of reasons, wrongly attribute this to HF, and hence score highly on the questionnaire. Many would argue such a QOL assessment, asking the question "Does the patient feel better?" is the most important measure of response as after all that is why we develop treatments, to reduce morbidity and also mortality. Measurement may be also influenced by a placebo effect, as simply by having the device fitted the patient may feel better as evidence by NYHA class improving with the pacemaker switched off. Investigator bias can be an issue, particularly if the trial is not blinded, because they want to make the patient feel better or to influence their results. Also, the presence of a spouse may have an influence, as if the patient has suggested to their spouse that they feel better (even if they do not), they may not want to suggest otherwise on the questionnaire.

Whilst a patient may feel better and have a lower score following a procedure, this does not necessarily mean that they will have physiologically benefited from the procedure, as evidenced by a worsening LVEDV, pVO₂ or 6MWD, for example. Also, as discussed previously, QoL may not be able to discriminate between severities of heart failure it is simply the LVEF that determines this. There is regression to the mean with patients scoring high initially but lower later and vice versa and the presence of comorbidity, such as IHD or COPD, makes correct discrimination of symptoms caused by one pathology from another difficult¹⁶⁶⁻¹⁶⁸.

The questionnaire is quick to complete, easy to administer, simple to understand and there is the capacity to obtain scores pertaining both to the physical and psychological fields. The advantage over simply asking a patient if they feel better or using their answer to stratify their NYHA group, is that it is the patient who rates their own health, not an interpretation by a clinician. It is a detailed, yet qualitative, assessment of the impact of HF on a patient's day-to-day life and can be repeated at time intervals and the scores compared. CRT leads to an improvement in MLWHFQ by 10-30 points on average and so reduction in MLWHFQ score by 10 points (out of 105) or more is considered a significant improvement and thus a positive response in the QoL domain^{46-48 133 169}.

2.11.3 Objective

2.11.3.1 LV reverse remodelling

Change in LV volumes and EF% are both used to assess patients' response in CRT trials, as these are believed to reflect the reverse remodelling of the LV following device therapy. On average, CRT increases EF by 4-6% and reduces LV volumes by 8-15%^{6 44 46 47 48 133 170}. These are surrogate markers at best, as arguably the main purpose of CRT is to improve the patient's symptoms. Several trials have defined a reduction in LV volume by more than 10% as a positive response to CRT and consensus opinion considers a reduction of this magnitude to be a significant improvement and thus a positive response in the LV reverse remodelling domain⁸⁶. However, the correlation between a significant reduction in LV volume and symptomatic improvement as assessed by NYHA class is not strong. For example Bleeker et al (2006)¹⁰⁵ found that

whilst 70% of CRT responders improved by at least one NYHA functional class, only 56% of patients had > 15% reduction in LVEDV, with just 51% meeting both criteria. This highlights both inter- and intra-reliability problems of serial LV volume assessment using 2DTTE. The use of echocardiography machines and probes from different manufacturers, combined with different operators and techniques in different settings can lead to the measurement of apparent volumetric differences which may not be real. What is required is homogeneity of all of these factors. This is often not feasible in large trials, which take place across multiple centres, languages and time domains. Ideally, volume assessment should be carried out using cMR; this is the gold standard for volume measurement of the cardiac chambers, particularly in the presence of structural heart disease. However, safety concerns prohibit the use of cMR in the presence of existing pacemakers, due to the risk of lead migration or local heating effects, although cMR compatible devices are now available, they were not at the time of this work.

2.11.3.2 Cardiorespiratory Fitness

2.11.3.2.1 Cardiopulmonary Exercise Testing (CPET)

Cardiopulmonary exercise testing (CPET) is the gold standard for the assessment of functional capacity and fitness. This is a non-invasive and objective maximal exercise test which is continued to exhaustion. The individual runs or cycles against a progressively increasing resistance, with heart rate, ECG, O₂ uptake (VO₂), CO₂ production (VCO₂), ventilation (V_E) blood pressure and work (watts) recorded simultaneously. This allows for the analysis of gas exchange at rest, exercise and recovery. VO₂ is the volume of oxygen taken up, transported and used by an individual during exercise and is measured in units of ml (of O₂) per kg (of body mass) per min (of exercise). VO₂ Max is the highest attainable value of VO₂, seen as a plateau of the VO₂ trace or defined by Lupton and Hill (1923) as “the oxygen intake during an exercise intensity at which actual oxygen intake reaches a maximum beyond which no increase in effort can raise it”¹⁷¹. Sedentary individuals will have a score of 30-40 ml/kg/min, elite athletes around 70-90 ml/kg/min and patients with end stage HF-LVSD around 10-20 ml/kg/min.

When seeking to assess patients with organ failure, a more pragmatic alternative to VO_2 Max is peak VO_2 , the highest value of VO_2 attained, but not necessarily attainable. This is a useful approach because conducting maximal exercise test on patients with end-stage organ failure, such as HF-LVSD, is dependent on both the good will of the patients and their willingness to attend for repeated testing. To insist on measuring VO_2 Max would be unethical, poorly tolerated, potentially unsafe with a high dropout rate. Peak VO_2 is largely governed by the patient's symptoms, with encouragement to continue performance until exhaustion. A score $< 15\text{ml/kg/min}$ or less than 50% of their age predicted value, is of prognostic significance in HF-LVSD as it denotes increased risk of mortality. Expert opinion suggests "it is challenging to obtain complete datasets in patients with repeat cardiopulmonary exercise tests because of the acceptance of the study by the patients or their condition at the time of follow-up study"⁸⁶. Patients with HF-LVSD will have reduced peak VO_2 , due to a reduction in cardiac output, impaired muscle metabolism and reduction in O_2 uptake, but with a positive response to CRT, cardiac output is found to improve, allowing the patients to exercise more, improving muscle metabolism and so increasing peak VO_2 .

Other data obtained from CPET includes, peak wattage, anaerobic (or lactate) threshold, respiratory exchange ratio (RER), rest and maximal heart rate and rest and maximal blood pressure. As wattage is determined by workload, the patient is typically limited by their HF-LVSD symptoms. With a positive response to CRT one would expect this to increase in as overall cardiorespiratory fitness improves. The anaerobic or lactate threshold is the point at which CO_2 production exceeds O_2 uptake and so as the body is in oxygen debt, there is switch to anaerobic metabolism with the production of lactic acid. This level can be improved with exercise and so, like peak wattage, one would expect LT to mirror any VO_2 peak improvement. The RER is the ratio between CO_2 exhaled and O_2 inhaled in one breath. At rest this is around 0.8 but during intense exercise the value approaches a value approaching or above 1, suggesting that more oxygen is being used by muscles leading to greater carbon dioxide production. Indeed an $\text{RER} > 1$ is used as a surrogate endpoint for VO_2 peak. The VE/VCO_2 slope representing the ratio of ventilation against VCO_2 exhalation is typically 25 ml/kg/min in healthy adults but $> 34\text{ ml/kg/min}$ in HF-LVSD and is inversely related to cardiac output at peak exercise.

Subjective measures of exertion are recorded immediately after the test is finished, including the rating of perceived exertion (RPE) scale and the Borg scale of breathlessness (BSB). The RPE (see appendix) is a 15-point Likert scale ranging from 6 (no exertion at all) to 20 (maximal exertion), which correlates highly with heart rate (RPE x 10 = HR e.g. 6 – 60bpm and 20 – 200bpm). Similarly, the BSB (see appendix) is a 10-point Likert scale, from 0 (not breathless at all) to 10 (maximal severity of breathlessness). These allow the exercise physiologist and clinician to ensure that the patient has performed a maximal test, as there may be disparities between how hard the patient claims to have exercised and their physiological results. Furthermore, one can see whether the patient might be able try harder, as a result of improved cardiac function, following response to CRT.

In the CRT trials^{48 49 133 155}, peak VO₂ in responders has been shown to increase by 0.8-1.2 ml/kg/min, from a baseline of 10-15ml/kg/min, representing a 6-10% improvement at 6 months. Only four trials have specifically included peak VO₂ assessment in responders with a maximum follow up period of 12 months. Currently, an improvement greater than 1ml/kg/min in peak VO₂ is considered a significant improvement in the CPET¹⁷² and thus a positive response in terms of cardiovascular fitness.

2.11.3.2.2 Six Minute Walk Test (6MWT)

First used in the mid-1980s, the 6MWT provides a simple, objective and reproducible assessment of functional capacity¹⁷³. Initially, a 12-minute walk test was proposed, but it was subsequently found that shortening its duration did not reduce its utility. Rather than asking the patient how far they can walk, which is inherently problematic due to over/underestimation or recall bias, it measures the 6-minute walk distance (6MWD). The 6MWD is the distance walked in 6 minutes at a normal pace on a flat, hard, even surface. Patients can use their normal walking aids and are allowed to rest, but are encouraged to continue on afterwards. It is used as a measure of functional capacity in HF, to monitor response to treatment and also as a predictor of morbidity and mortality. In a meta-analysis Olsson et al (2005) found the average increase in 6MWD following interventions such as ACE-inhibitors, β-blockers and exercise training was

32m¹⁷⁴. This clearly demonstrates that it is not just CRT that can lead to such improvements.

In a similar way to CPET, the 6MWT evaluates the integration and performance of the various systems required for exercise, including cardiac, pulmonary, musculoskeletal, haematological, vascular and neurological systems. However whilst there is good correlation between CPET and 6MWT, the 6MWT is not a measure of peak VO₂ nor does it determine the cause of exercise limitation¹⁷⁵. The reference range for healthy individuals (571 ± 90m) depends largely on both age and gender of the individual but will also be determined by weight and height¹⁷⁶. On average an increase in 6MWD by 10-20% is observed following 6 months of CRT and thus a more than 10% improvement in the 6MWD is considered a significant improvement in this metric and a positive response in terms of cardiovascular fitness¹⁷².

2.11.4 Other markers

Since improvements in LV synchrony lead to augmented systolic performance, measures of dyssynchrony such as MV filling % or IVMD might be used to try to categorise responders. However, improvement of myocardial mechanics is far removed from improving patient symptoms and there is often discordance between symptoms and haemodynamic improvements e.g. dP/dt or SV. Similarly, it would be expected that patients with IVMD who improve, would also have a reduction in the QRSd, denoting reduced inter-ventricular dyssynchrony. Other subjective measures of response might be the absence of clinical events, such as admission with acute HF exacerbation or a reduction in pharmacological requirement of diuretics for example, as cardiac function improves. However, if the patient has an absence of clinical events or a reduced requirement for diuretics, but feels no better, is it still fair to categorise them as a responder? For this reason, neither of these has been included in many clinical trials nor are they used in this thesis.

2.12 Failure of Response

Failure to respond to CRT may either reflect poor patient selection (inclusion of those without significant dyssynchrony, for example) or the limitations of how 'response' is defined (in terms of improvements in morbidity, mortality, exercise capacity, EF or NYHA class, for example). As response to other therapies, such as oral medication, is

not uniform; being influenced by many factors such as aetiology, “genetics, gender, age, disease state, environment and race”, perhaps the degree of heterogeneity of response to CRT is not surprising^{177 178}. Furthermore, since HF-LVSD is not a single organ insult but a multi-organ syndrome, improving the pump function of the heart will not necessarily improve symptoms, morbidity or mortality, as it is not the heart alone that determines these.

When a patient fails to respond the clinician first assesses for deterioration in terms of other diseases such as renal failure or COPD, which could influence CRT response. For example for many CRT trials, patients with such comorbidities were excluded or at least their presence was not documented, but unfortunately this does not reflect the HF-LVSD patient population as a whole as many of these diseases coexist.

Next, the clinician determines whether optimal CRT is being delivered. Optimal CRT delivery requires the patient to receive biventricular pacing (BiVP%) more than 95% of the time, any less than this and it is likely the patient will not respond. Possible reasons for a drop in BiVP% include the development of atrial tachyarrhythmia or significant ventricular ectopy leading to a drop in the proportion of paced ventricular beats. If atrial tachyarrhythmia accounts for the drop in BiVP%, β -blocker therapy can be up-titrated or the patient can undergo AV node ablation (AVNA). This has been shown to lead to significant reduction in mortality and morbidity in patients with AF and CRT compared to CRT and OMT alone in observational trials¹⁷⁹, but is yet to be demonstrated in RCTs.

If, despite optimal BiVP%, the patient is found to be a nonresponder and if other comorbidities remain stable they are referred for echocardiographic-based CRT device optimisation. There are two components to optimisation, AV and interV optimisation, depending on whether the patient has atrial fibrillation and an atrial lead (and hence AV cannot be optimised), or not. Several methods can be used for CRT optimisation, including echocardiography (eg Ritter), aortic VTI or iterative, using non-invasive cardiac output monitoring such as finger plethysmography, ECG and finally invasive haemodynamic assessment eg dP/dt.

The optimisation process used in Sheffield is outlined below:

AV optimisation –

The iterative method involves increasing the timing delay between the RA and LV in a stepwise fashion (by approximately 20ms), during which echocardiography is used to image the mitral inflow Doppler, measuring the inflow into the LV from the LA, both passive e.g. ventricular diastole (E wave) and active e.g. atrial systole (A wave). The shortest AV delay that does not truncate the A wave is chosen, allowing for maximal LV filling duration.

InterV optimisation –

The aortic VTI method involves increasing the timing delay, between the LV and RV in a stepwise fashion (by approximately 20ms), during which echocardiography is used to image the LV outflow tract to measure the aortic VTI, approximating to the LV stroke volume. The timing corresponding to the largest aortic VTI (averaged over 3 cycles) is chosen. Recently work has concentrated on specific subgroups that have previously been excluded from clinical trials or failed to respond such as patients with AF¹⁸⁰ or milder HF-LVSD¹³⁵. It is apparent, that patients with RBBB perform less well in CRT trials than their LBBB counterparts. The reason for this is as yet unknown, but such patients may require multi-site RV pacing for the RBBB, like the LBBB patients receive for their LV.

2.13 Conclusions

In this chapter the rationale for using CRT in a pre-specified patient cohort has been outlined and the evidence base for doing so. The challenges in predicting response to CRT was also discussed and the utility of optimising the device to individuals. Building on Chapters 2 and 3, Chapter 4 will then cover the background to this work on patients with HF and predicting their response to CRT.

Chapter 3 Materials and methods

In this chapter the patient cohort studied in this project is delineated, including what tests and treatments they underwent, at what time point and why.

3.1 Background

This work was part of a larger multicentre study entitled “Translating biomedical modelling into the heart of the clinic” between the University of Sheffield (USFD)/STHT, University College London (UCL), King’s College London (KCL) and Imperial College London (ICL) and was funded by an Engineering and Physical Sciences Research Council (EPSRC) grant (R/125661-11-1) as part of the “Grand Challenges” call; “Significant problems that need a long-term, coordinated approach from researchers to overcome” (see appendix). The overarching aim was to construct a robust, intuitive workflow, which would enable the creation of 3D predictive cardiac model, based on patient-specific anatomy and cardiac function. The four participating Universities each provided specific, complimentary, expertise (see figure 17), encompassing image acquisition, processing, modelling, data collection and clinical application.

3.2 Ethics

The project was conducted in compliance with the principles of the Declaration of Helsinki October 2008 and the principles of Good Clinical Practice (GCP). The project was approved by the National Research Ethics Service (NRES) number 10/H0802/71. The study was undertaken under the auspices of the former National Institute for Health Research, Cardiovascular Biomedical Research Unit (CVBRU) in Sheffield using the clinical research facility at the Northern General Hospital (NGH) part of STHT and it was also required to meet local requirements under the auspices of STHT local governance, the CVBRU patient panel and the Sheffield Scientific and Advisory Board (SAB).

3.2.1 Details

3.2.1.1 Patients

A total of fifty patients selected for CRT were recruited to the study. Twenty patients were recruited under PS at STHT and thirty were recruited at Guys and St Thomas’s

NHS Trust (GST) under RR. The total cohort size was determined by a power calculation, assuming a two-thirds responder rate to CRT with 95% confidence interval ($\pm 17\%$ for sensitivity and $\pm 23\%$ for specificity) predicting response. This also allowed for a worst-case scenario where the computer models perform no better than chance (i.e. sensitivity and specificity = 50%) at predicting response. All patients were assessed at baseline, 6 and 12 months post implantation (+/- 2 weeks) in terms of; cardiac structure and function, objective and subjective measures of exercise capacity and levels of neurohormonal biomarkers.

Figure 17: Grand Challenge Modelling project workflow and division of labour

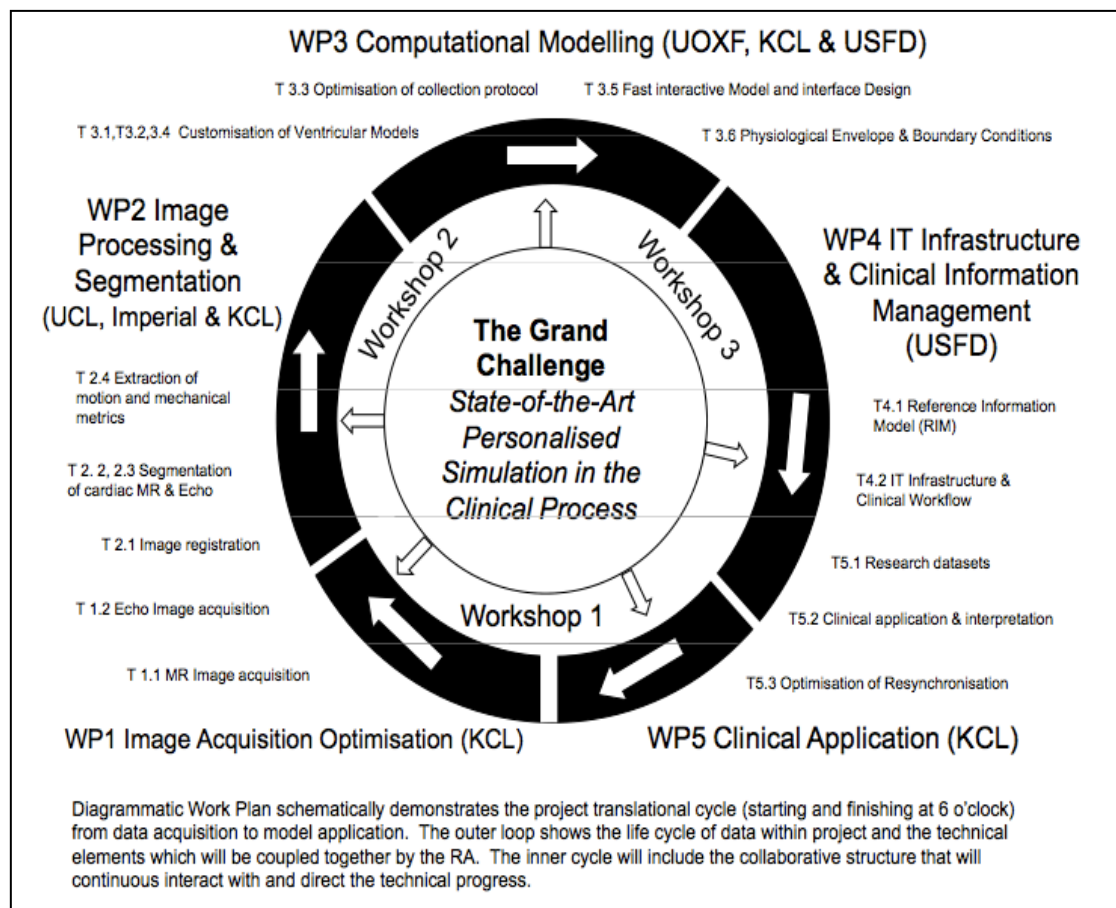


Figure 17 demonstrates the division of labour, data flow, various workpackages (WP) and partners involved in the Grand Challenge modelling project.

3.2.1.2 Sheffield sub-set of 20 patients

A number of different tests were selected for evaluation as potential novel predictors or novel markers of response. A *predictor* would be able to demonstrate a significant difference at baseline between responders and nonresponders whereas a *marker*

would demonstrate a significant difference during follow-up when compared to baseline.

Tests were chosen based on a gap in the evidence from the existing literature on predicting and measuring response to CRT:

- Blood Biochemistry
 - Uric acid (UA)
 - High sensitivity c-reactive peptide (hsCRP)
 - High sensitivity Troponin T (hsTnT)
 - Parathyroid hormone (PTH)
 - Vitamin D (VitD)
- Urinary Biochemistry
 - Microalbuminuria (UMA)
- Endothelial function
 - Flow mediated dilation (FMD)
- Skeletal muscle function
 - Handgrip strength (HGS)
- Non-invasive cardiac haemodynamics
 - Ballistocardiography (BCG)

3.2.2 Patient Selection

The inclusion criteria for both GSTT and STHT, in terms of patients deemed suitable for CRT reflected the NICE (2007) health technology appraisal¹³⁴ which, in turn, was based heavily on evidence from the CARE-HF study^{44 137}. Patients were eligible, if they suffered from HF-LVSD, experienced, or had recently experienced, symptom severity of NYHA class III-IV, were currently on optimal medical therapy (OMT) e.g. maximal tolerated doses (if not contra-indicated) of β -blockers and ACE-I/ARB and had a QRSd greater than 150 ms or 120-149 ms with a positive dyssynchrony echo study (demonstrating significant atrio-, inter- or intraventricular delay). Exclusion criteria related mainly to contraindications to cMR as patients were required to have a scan at baseline in order to create the personalised 3D model. For this reason, patients with a pre-existing pacemaker (some patients are upgraded to CRT from a conventional dual-chamber device already *in situ*), claustrophobia (due to the narrow confines of the cMR scanner), pregnancy (due to concerns about the interaction between magnetic

resonance and pregnancy) and an estimated glomerular filtration rate (eGFR) < 25ml/min/1.73 m² to avoid the risk of nephrogenic systemic fibrosis (NSF) in patients with severely impaired renal function following accumulation of the Gadolinium contrast agent used in cMR.

3.2.3 Recruitment of Sheffield Patients

Recruitment commenced in June 2012 and twenty-one patients were recruited over a 12-month period. Approval was given to recruit an additional patient following early withdrawal of one patient due to failed LV lead implantation.

The aim was to follow up twenty patients for 12 months, with assessment at baseline (within 2 weeks pre-CRT implantation), echocardiography guided optimisation of the device at 6 weeks post-CRT implantation and assessments at 6 months and 12 months (\pm 2 weeks) post implantation to assess clinical response and to investigate novel predictors/markers of response.

The patients were mainly lower/middle class, white, British men. As discussed in the introduction, recruiting ethnic minorities and women to clinical HF trials is difficult. Unfortunately a single Afro-Caribbean patient that was approached declined to join the study and no other suitable patients from ethnic minorities were identified during the 12-month recruitment window. Similarly, only 2 females were recruited to the study and whilst a third female was approached unfortunately she died before she could take part in the study. The patient cohort was homogenous; being comprised of predominantly white males in their late 60s and thus similar to other CRT studies, but perhaps does not reflect the demographic make-up of South Yorkshire as a whole.

The patients came from a variety of locations around South Yorkshire, including Sheffield, Barnsley, Rotherham and Chesterfield and areas further afield such as Nottinghamshire and Derbyshire. They also came from a variety of employment backgrounds including mining, accountancy, pharmacy, nursing, engineering, farming and heavy goods driving. In terms of marital status, 18 of the patients were married, one was single, one divorced and one a widower. Potential patients for recruitment to the project were identified in one of several ways:

- By direct referral to PS either within STHT or externally from another hospital.

- From a biweekly review of the joint CRT/ICD waiting list by DW and PS.
- From a list of dyssynchrony studies from the STHT echocardiography department.
- From a specialist nurse (JM) who pre-assessed all patients referred for CRT in STHT.
- All consultants and trainees in STHT were asked and reminded for suitable patients.

Once the patients had been identified, but before they were formally approached, their hospital notes were reviewed to ensure they met all of the inclusion criteria and none of the exclusion criteria. In the first instance, DW contacted the patients via telephone. The project was discussed briefly and then a patient information sheet (PIS) was sent (see appendix). The patient was contacted again two weeks later by phone, this ensured that they had adequate time to read the material, discuss it with their partner or next of kin and establish if they had any questions.

If the patient did not wish to take part, no further questions were asked. If they did, then a date was agreed with the patient for their first appointment. In some cases this was the cMR scan and in others a baseline assessment including echocardiography, exercise and blood tests was carried out. On arrival the patients all gave their written consent to take part in the project (see appendix) and any questions they had were addressed. A letter (See appendix) was also sent to their general practitioner (GP) informing them that they would be taking part.

Delays in obtaining ethical and R&D approval these centered around discussions over the research protocol and the appropriate costing of tests locally and presented a challenge to starting recruitment. Recruitment finally commenced some 10 months after the project had officially started and was finished in 12 months. In total, 60 patients were considered for recruitment, 20 were not approached as they failed to meet the inclusion criteria, despite initial promise, and 19 were approached but declined for various reasons, including frailty and lack of time.

3.2.4 Patients at baseline

Tables 12 and 13 summarises all the patients at baseline. All the patients were in NYHA class III, the majority of the patients had HF-LVSD of ischaemic aetiology and twenty

patients had a LBBB morphology. Nearly all the patients were overweight or obese according to their BMI, reflecting the high prevalence of obesity in the UK, despite the ‘cardiac cachexia’ commonly found in patients with end-stage HF-LVSD. If the QRSd was 120-149 ms, then the criteria for a positive dyssynchrony echo included; mean AV delay calculated by mitral valve filling was < 40%, interV delay (IVMD) calculated by the delay between the aortic and pulmonary pre-ejection periods > 40ms and intraV delay, using PW TDI to calculate the difference in peak septal-lateral wall motion > 40ms. The majority of the patients were taking β -blockers and an ACE-I or ARB at the maximally tolerated dose, similarly nearly all the patients were taking a loop diuretic and over a half a mineralocorticoid receptor antagonist (MRA). For the patients who were not taking either a β -blocker or an ACE-I/ARB, it was clarified with the treating physician (PS) before recruitment that this was because of intolerance or another contraindication. At the time of recruitment, a variety of comorbidities were recorded, with a most patients suffering from several conditions other than their HF-LVSD. This table demonstrates that the inclusion criteria were met.

Table 12: Summarising the 21 patients recruited to the study at baseline

Patient No		1	2	3	4	5	6	7	8	9	10	11	12	13	14	15	16	17	18	19	20	21	Mean	SD
Demographics	Age (years)	75	66	64	75	58	74	67	67	80	80	49	67	73	77	70	57	71	76	74	72	69	69.6	7.8
	Gender	M	M	M	M	M	M	M	F	F	M	M	M	M	M	M	M	M	M	M	M	M	19/21	
	BMI (kg/m ²)	32.7	22.4	24.5	26.1	31.3	22.8	33.0	26.0	28.6	31.6	29.1	38.3	25.0	27.9	36.0	22.5	29.4	28.6	30.7	35.0	28.7	29.0	4.5
Past medical history	Cholesterol	Y	Y	Y	Y	Y	Y	Y	N	Y	Y	Y	N	Y	Y	Y	N	N	N	Y	Y	N	15/21	
	IHD	Y	Y	Y	Y	Y	Y	N	N	N	Y	N	N	Y	N	N	Y	N	N	N	N	Y	10/21	
	HTN	N	Y	N	Y	Y	Y	Y	N	N	Y	Y	Y	N	N	N	N	Y	N	N	N	Y	10/21	
	AF	N	Y	Y	N	Y	N	N	N	Y	Y	Y	N	N	Y	N	N	N	Y	N	N	N	10/21	
	MI	Y	Y	Y	Y	Y	Y	N	N	N	N	N	N	Y	N	N	Y	N	N	N	N	N	8/21	
	CKD	N	Y	Y	Y	Y	Y	Y	N	N	N	N	N	N	Y	N	N	N	N	N	N	Y	7/21	
	Depression	N	Y	N	Y	N	Y	Y	Y	N	N	N	N	Y	N	N	N	N	N	N	N	N	6/21	
	Diabetes	N	N	N	N	Y	N	Y	N	Y	N	N	N	N	N	N	Y	N	N	N	N	Y	5/21	
	COPD	N	Y	N	Y	N	Y	N	Y	N	Y	N	N	N	N	N	N	N	N	N	N	N	5/21	
	CABG	N	N	N	Y	N	N	N	N	N	Y	N	N	N	N	Y	N	N	N	N	N	Y	4/21	
	Stroke	N	N	N	N	Y	Y	N	N	N	N	N	N	Y	N	N	N	N	N	N	N	N	3/21	
Functional assessment	QRSd (ms)	168	129	156	138	196	188	163	177	138	164	167	200	152	192	138	128	167	163	162	151	163	161.9	20.9
	EF (%)	24	34	20	33	24	22	23	27	32	32	28	8	23	17	30	16	35	32	33	20	12	25.0	7.6
	NYHA Class	III	III	III	III	III	III	III	III	III	III	III	III	III	III	III	III	III	III	III	III	III	21/21	
Medications	ACEI/ARB	Y	Y	Y	Y	N	Y	Y	Y	Y	Y	Y	Y	Y	Y	Y	N	Y	Y	N	Y	Y	18/21	
	B-blocker	Y	Y	Y	Y	N	Y	Y	Y	Y	Y	Y	Y	N	Y	Y	N	Y	Y	Y	Y	Y	18/21	
	Loop diuretic	Y	Y	Y	Y	Y	Y	Y	Y	Y	Y	Y	Y	N	Y	Y	Y	Y	Y	Y	Y	Y	20/21	
	MRA	Y	N	Y	Y	Y	Y	N	N	N	N	Y	Y	Y	N	Y	Y	Y	Y	Y	N	N	13/21	

6MWD = 6 minute walk distance, ACEI = angiotensin converting enzyme inhibitor, AF = atrial fibrillation, ARB = angiotensin receptor blocker, BMI = body mass index, CABG = coronary artery bypass grafts, CKD = chronic kidney disease, COPD = chronic obstructive pulmonary disease, EF = ejection fraction, HTN = hypertension, M = male, MRA = mineralocorticoid receptor antagonist, MLWHFQ = Minnesota living with heart failure questionnaire, NYHA = new york heart association, QRSd = QRS duration.

Table 13: Summarising scar position, device, manufacturer and lead position.

Patient no	Scar position	CRT	Manufacturer	Lead position		
				RA	RV	LV
1	N/A	P	Boston	RAA	Apex	Posterior vein
2	N/A	D	Boston	Mid RA	Apex	Lateral vein
3	N/A	D	St Jude	RAA	Apex	Lateral vein
4	Anteroseptal	D	Medtronic	RAA	Apex	Posterior vein
5	Anteroseptal	P	Guidant	RAA	Apex	Middle vein
6	N/A	P	Boston	RAA	Apex	Lateral vein
7	Anteroapical	P	Guidant	RAA	Apex	Lateral vein
8	Septal	P	Guidant	RAA	Apex	Epicardial
9	N/A	P	St Jude	RAA	Apex	Lateral vein
10	N/A	P	St Jude	N/A	Apex	Lateral vein
11	Anterior	D	St Jude	N/A	Apex	Lateral vein
12	N/A	D	Boston	RAA	Apex	Lateral vein
13	N/A	D	St Jude	Low RA	Apex	Lateral vein
14	Anterior	D	Boston	N/A	Apex	Lateral vein
15	N/A	P	Boston	RAA	Apex	Lateral vein
16	Anteroseptal	D	Boston	RAA	Apex	Lateral vein
17	Anteroseptal	D	Boston	RAA	Apex	Lateral vein
18	N/A	P	Guidant	N/A	Apex	Lateral vein
19	N/A	D	Boston	N/A	Apex	Lateral vein
20	N/A	D	Boston	N/A	Apex	Epicardial
21	Apex	D	St Jude	RAA	Apex	Posterior vein

3.2.5 Statistics

Statistical analyses were performed using SPSS version 18.0 (SPSS, Inc). Variables were tested for normality using the Shapiro-Wilk test, with $p < 0.05$ considered to be significant and indicate non-parametric distribution. Values are expressed as either mean \pm standard deviation for parametric data, percentages for nominal data or median and interquartile range for non-parametric data, as appropriate. Differences between groups were compared using independent T-tests or Mann Whitney U (unpaired data) and Wilcoxon Sign Rank tests (paired data) for normally and non-normally distributed variables respectively. For all parametric data, a 2-tailed Student's T-test was used to examine statistical significance; unpaired for comparing between

groups at baseline. Comparison of data within groups during follow up was performed using one-way ANOVA with repeated measures. Categorical data was analysed using a two-tailed Fisher's exact. Pearson's correlation coefficient was used to examine the strength of correlations in parametric data and Spearman Rank, for non-parametric data. A p value of < 0.05 was considered significant.

3.3 Conclusions

In this chapter the patient cohort who will undergo CRT and then be investigated as part of the Grand Challenge project have been identified at baseline. In the following chapter, their assessment of response will be assessed following CRT implantation, which will be used to inform Chapters 6 and 7 when their response is attempted to be predicted using computer models and measured using novel biophysical and biomarker surrogates.

Chapter 4 Assessment of Response

In this chapter the definition of a CRT responder is defined and the Sheffield cohort of patients undergo multi-modal measures of response, at baseline and at 6 and 12 months following CRT implantation. This definition and these measures are then used to inform the modelling, biomarker and biophysical marker work.

4.1 Introduction

Patients were assessed for response using a 3 pronged approach, namely; improvements in symptoms, cardiovascular fitness and LV function measured using the Minnesota Living with Heart Failure Questionnaire (MLWHFQ), cardiopulmonary exercise testing (CPET)/ six minute walk distance (6MWD) and left ventricular end-diastolic volume (LVEDV) respectively. This evidence-based approach was defined by:

- Cardiovascular fitness
 - An increase of 1ml/kg/min or more in peak VO_2 ¹⁷².
 - An increase by 10% or more in 6MWD⁸⁶.
- LV reverse remodelling
 - A decrease in LVEDV by 10% or more¹⁵⁸.
- Symptoms
 - A decrease in the MLWHFQ score by 10 points or more¹⁶⁹.

Patients were classified as true responders only if they met all four of the criteria and therefore nonresponders if they met three or less, or scored worse in any way, when compared to their baseline results, at the 6 and 12 month follow-up assessments. The groups were mutually exclusive and therefore one patient could not belong to both groups.

In subsequent chapters of this thesis the terms 'responder' and 'nonresponder' will be based on these criteria. These are based on widely used definitions for assessing response for CRT. However, whilst they are used collectively and robustly when assessing clinical response, when predicting response they are often used selectively and individually.

This approach was selected as an objective, multimodal and robust assessment of the patient and their response to CRT, rather than relying on one modality alone. Furthermore whilst a patient may feel pressured to say they feel better (due to the presence of a medical professional or relative), improvement on all 4 fronts, would be less likely to be due to chance or bias. This was the first time that such a robust approach to the prediction of response has been chosen, as clearly the definition of response must be agreed *a priori*.

Other possible surrogate markers of response, such as QRSd, weight and BP will also be considered, to rule out possible confounding factors.

4.1.1 Six Minute Walk Test

4.1.1.1 Introduction

The 6MWT is an objective, well-used and validated test of cardiorespiratory performance. It measures the 6MWD, which is the distance walked (in metres) in 6 minutes at a patients normal pace on a flat, hard, even surface.

4.1.1.2 Methods

The test was administered according to the 2002 American Thoracic Society (ATS) guidelines¹⁸¹. A corridor, meeting the 30m required length, within the Pulmonary Function Unit (PFU) of the NGH in Sheffield was used. The test was supervised and recorded by the investigator (DW) and TH, a senior respiratory physiologist. Patients were asked to wear comfortable clothes and footwear, were given a light breakfast several hours before and the test was conducted at the same time of day (11:30-12:30) to minimise potential confounding factors. All patients were rested for 10 minutes prior to beginning the 6MWT and a baseline assessment of breathlessness, was taken using the Borg scale (see appendix).

Once rested, patients were directed to the start of the walkway and asked to walk in a straight line to the end of the corridor (and back), at their normal walking pace, and to repeat this as often as they could in 6 minutes. The 6 minutes was timed and the number of laps recorded. They were allowed to use their normal walking aid (where appropriate) and were told they could stop if needed to rest, for whatever reason, no

encouragement was given other than to continue on following a rest or to check that they were not in distress. There were chairs along the corridor the patients could use if needed. Members of staff conducting the 6MWT were trained in Advanced Life Support (ALS) and a crash-trolley with oxygen, defibrillator and medicines was kept to hand should an urgent need arise.

The presence of a relative had to be controlled for, as the patient's spouse often accompanied them to the assessment and their presence may have influenced the patients to walk further than they would have otherwise. This influence was minimised where possible, by keeping the spouse away from the 6MWT area. There was a change in the walk area 18 months into the project, which was unavoidable due to a relocation of the PFU within STHT. This meant there was now a purpose built 6MWT area within the department. Following the procedure, the patients were offered a glass of water; a further assessment of breathlessness was made using the Borg scale and then the patients rested for 10 minutes before leaving the department.

4.1.1.3 Results

Table 14: 6MWD comparing responders and nonresponders at baseline

6MWD (m)		Responders		Nonresponders		Student's T-test
		Mean	SD	Mean	SD	P value
Time (months)	Baseline	374.3	112.8	337.4	144.7	0.23

Table 15: 6MWD in responders comparing baseline results with follow-up.

6MWD (m)		Responders		One way ANOVA with repeated measures	
		Mean	SD	P value	
Time (months)	Baseline	374.3	112.8	Baseline vs.	
	6	391.0	108.1	6 months	< 0.05
	12	418.5	105.3	12 months	< 0.05

Table 16: 6MWD for nonresponders at baseline and follow-up

6MWD (m)		Nonresponders		One way ANOVA with repeated measures	
		Mean	SD	P value	
Time (months)	Baseline	337.4	144.7	Baseline vs.	
	6	279.2	155.5	6 months	0.34
	12	279.6	113.8	12 months	

Figure 18: 6MWD in responders (white) and non-responders black

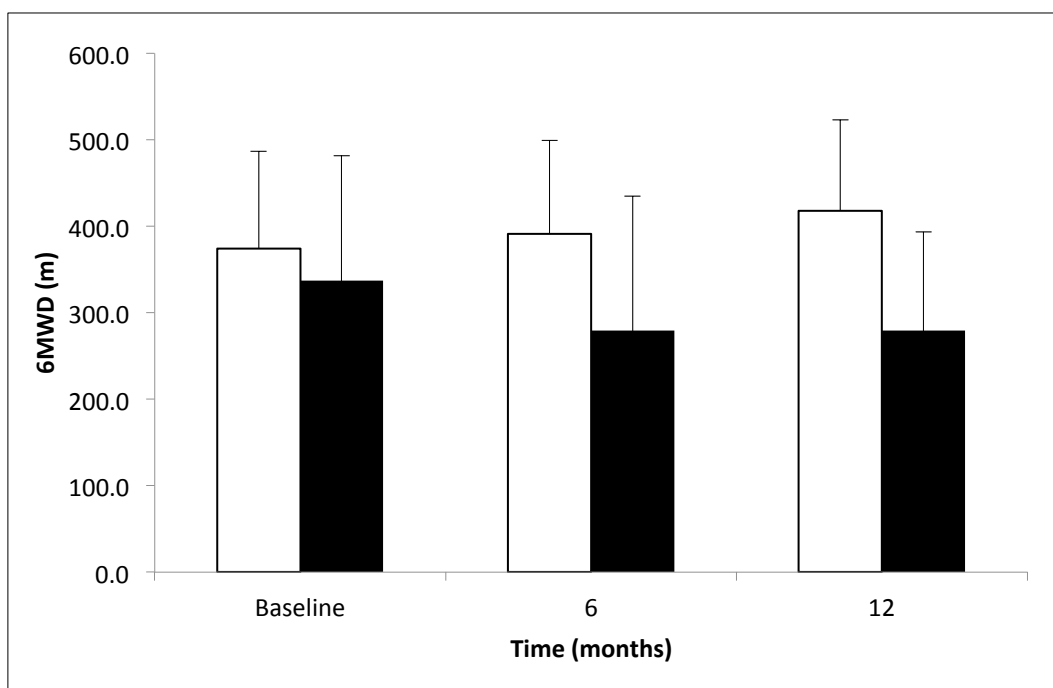


Figure 18 demonstrates the differences in the 6 minute walk duration in responders and non-responders at baseline and at 6 and 12 months following CRT implantation.

Using a two-tailed Student's T-test at baseline, there was no statistically significant difference in 6MWD between responders and nonresponders (see table 14). Responders showed an improvement at both 6 and 12-month follow-up (see table 15 and figure 18). According to one way ANOVA with repeated measures and Greenhouse-Geisser correction determined this difference over 12 months was significant ($F(1.93, 21.03) = 22.67, p < 0.01$). Post-hoc analysis using the Bonferroni correction demonstrated responders had statistically significant differences between baseline and six months and baseline and twelve months. There was a decrease in the 6MWD in nonresponders at 6 and 12 months, but this trend was not statistically significant (see table 16 and figure 18).

4.1.1.4 Discussion

Figure 19: Patient-undergoing 6MWT with purpose built walkway



Figure 19 demonstrates one of the grand challenge patients undertaking the 6 minute walk test in the purpose built walk way in the lung function unit at the Northern General Hospital, with pulse oximeter on their right hand.

Of the cohort of 19 patients followed up for 12 months, 15 demonstrated a significant increase (10%) in the 6MWD. Accordingly, fourteen of these were categorised as a responders and one was categorised as a nonresponder using the criteria mentioned previously. Although a difference was recorded between the groups at baseline, this was not statistically significant, suggesting that the groups had a similar level of capability in terms of this particular metric before CRT implantation. In terms of responders, 6 demonstrated > 10% increase at 6 months with a further 8 at 12 months. The non-responder demonstrated a > 10% increase at 6 months, sustained at 12 months and a further non-responder demonstrated a < 10% increase at 12 months.

Every effort was taken to ensure that the test was performed in a standardised and controlled fashion but there were some limitations, which should be noted (see figure

19). During the initial 18 months of the project, the 6MWT was carried out along a specific corridor in the PFU at the NGH, where similar clinical tests were carried out for HF-LVSD and COPD. This location was not ideal as it was often busy with clerical and medical staff and other patients attending the PFU and it had many doors opening on to it. Patients were told that people would get out of their way and members of staff were also told be aware of patients using the corridor for this purpose and so disruption was kept to a minimum. However, being a clinical environment it was impossible to predict, measure, or avoid other people using the corridor and at the time there was no alternative site at the NGH, which was suitable for undertaking the test. As the PFU was some 10 minutes' walk away from the ECG department where the other tests were carried out, whenever possible the patients were taken by wheelchair. This ensured they were as rested as possible before the test. To ensure patients did not feel patronised, their decision to walk had to be respected and for those who walked every effort was made, once they arrived, to ensure that they were not out of breath and adequately rested before undertaking the test.

The learning effect in 6MWT performance is well known; healthy individuals have been shown to improve when assessed on consecutive days, an improvement which is stable at 2 months ¹⁸². However, it is unclear whether this translates to a HF-LVSD population and furthermore, whether this is relevant as patients were assessed three times over a 12 month period, with gaps of six months ¹⁸³. Indeed, other studies on repeated 6MWT on HF-LVSD patients found performance was not always improved and questioned the feasibility of repeat performance of 6MWT in a clinical setting ¹⁸⁴.

In December 2012, the PFU moved to a new building with a purpose built 6MWT corridor. This was a wide corridor, with no doors, windows or other impedances or distractions. It is difficult to say what influence this may or may not have had on performance of the patients on the 6MWT. At this point 10 patients had completed the study, 7 patients were awaiting 12-month follow-up and 2 patients had yet to reach 6-month follow-up, so over two-thirds of the assessments had already taken place. There was certainly no statistically significance difference in the 6MWD recorded for patients following the move in this study or during subsequent routine clinical assessments out width this study ¹⁸⁵. However, the change in venue this may

limit the reproducibility of results and perhaps should be considered an extraneous variable.

Due to time, financial and logistical constraints, the 6MWT was performed on the same day as the peak VO₂ test. Furthermore, whilst the investigator (DW) was always present e.g. a constant influence, different members of staff from the PFU (depending on availability) would help perform the assessment. However, all staff, investigator included, were unaware of the patient's previous 6MWT performance.

Given that a 10% improvement in the 6MWD is considered significant, absolute improvement depends upon the distance measured at baseline; for example, an increase of 40m will not be significant if the baseline is 450m but will if the baseline was 200m. In a meta-analysis of HF-LVSD RCTs by Olsson et al (2005) 32m was the average increase in 6MWD recorded following interventions such as ACE-inhibitors, β -blockers and exercise training, with a significant improvement following intervention noted in only 9 of 47 trials. For this reason it was concluded that it was an insufficiently robust test for pharmacological intervention, although it was greater value in patients with more advanced heart failure e.g. CRT trials, where it may function as a maximal exercise test, hence being used in this study and others¹⁷⁴.

Several of the patients had knee or hip osteoarthritis (OA) and found the walk challenging due to pain from their degenerative joints. At the time of the test, all of the patients had taken their daily medications including analgesia, but clearly OA was a limiting factor in their performance. Beyond the end of the trial, one responder had a replacement operation. With reduced pain one might expect them to be able to walk further but as this was outside the timeframe of the study this was not tested.

It is important to highlight that the patients in this study were not simply HF-LVSD patients, many of them had other chronic organ diseases, such as renal failure and COPD, all of which may have had an impact on their 6MWD; thus underperformance might not simply be due to non-response to CRT. As mentioned previously, none of the previous CRT trials comment on other major comorbidities and, in this regard, it is difficult to compare and contrast these results with those. Most patients will have HF-

LVSD due to IHD, following cigarette smoking, HTN and/or DM, which will also increase the likelihood of other functionally limiting diseases such as CKD, COPD and PVD. Equally, mood and motivation vary on daily basis even in healthy individuals, and this type of measure of function, ignores such variables. Due to the time constraints of the project, the patients could not be tested repeatedly or brought back at other times. With patients in the project having a mean comorbidity of 5 diseases it is perhaps not surprising that they may have been functionally limited due to other reasons.

Patients, who responded to CRT, often performed worse on repeated testing of the 6MWD, despite recording a higher peak VO_2 subsequently on CPET, which seems illogical. Clearly peak VO_2 and 6MWD relate to different aspects of the cardiorespiratory fitness, thus one might not expect necessarily any improvement in peak VO_2 to be mirrored in 6MWD and 6MWD is more subjective than peak VO_2 . Yet 6MWD is more 'real world' and subsequently of greater importance to the patients e.g. "I can I now walk to the shops and back".

In the context of data from other trials (see table 17), the 6MWD at baseline in the CRT trials listed ranges between 244m to 363m. The lowest distance is from the COMPANION trial and the highest from the RAFT trial, reflecting their inclusion criteria of NYHA functional class III-IV and II-III respectively. Our responder group at baseline (average 394m) appear somewhat fitter than baseline groups from other studies. However, taken together as a whole, the groups are similar. A 394m walk in 6 minutes along busy corridor, means the patients may already at their physiological limit, with a walking speed of 1m/s or 2.5mph, not dissimilar to that expected from healthy individuals. The 12% increase in 6MWD 12 months is in keeping with the studies below, albeit at 6 months but at the time of writing there are no published studies, which report 6WMD in CRT patients at 12 months.

Table 17: Mean 6MWD at baseline and at 6 months in the CRT trials

Trial	Mean 6MWD (m) in CRT responder group		
	Baseline	6 months	Increase (%)
COMPANION	244	284	16.3
CONTAK	316	351	11.0
MADIT	363	N/A	N/A
MIRACLE	305	344	12.7
MUSTIC	320	350	9.3
PATH	342	386	12.8
RAFT	355	N/A	N/A

4.1.1.5 Conclusion

The 6MWT was carried out to the best of our ability, with regards to standardisation, local protocols and national guidelines. There was no statistically significant difference between the groups at baseline and but there was a significant improvement in responders, 6 at 12 months and 14 at 12 months. There is anecdotal evidence that the PFU has found the 6MWT to be unreliable in clinical use, when compared to CPET and derived measures such as peak VO_2 ¹⁸⁵.

4.2 Cardiopulmonary Exercise Test

4.2.1.1 Introduction

The cardiopulmonary exercise test (CPET) is an objective and scientific measure of cardio-respiratory fitness. As mentioned in Chapter 3, the CPET is used to record the patient's peak VO_2 , this is the maximal value attained, but not necessarily attainable, during exercise testing to exhaustion. The individual is asked to cycle (or run) against an increasing load during which gas exchange, electrocardiograph, blood pressure and work are monitored and recorded. Considered by some to be the 'gold standard' for HF-LVSD functional assessment, others regard it as more expensive and time-consuming version of the 6MWT.

4.2.1.2 Method

The patients had a light breakfast several hours before testing and were rested for 10 minutes immediately before the test. The tests were all conducted around the same time of day, between 12:30-13:30, to minimise the risk of any confounding factors. The tests were conducted by a senior physiologist (TH). Both the physiologist and the

investigator were trained in advanced life support and a crash trolley containing oxygen, defibrillator and emergency medications was kept in the room during the test, in case of urgent clinical need.

The patient's name, date of birth and hospital number, height and weight were entered into the CPET workstation station (Masterscreen, Carefusion, UK).

The patient was asked to sit in a chair and ECG electrodes were attached, for the 4 limb leads: right arm (RA), left arm (LA), right leg (N) and left leg (F). The patient was shaved if there was poor contact between the electrode and skin. In order to prevent entanglement during cycling, the 2 limb electrodes were located in the right and left inguinal fossae and the arm electrodes in the subclavicular areas. The 6 chest leads, from V1 – V6 were then placed in the usual manner, from 4th intercostal space (right parasternal) to 5th intercostal space (left mid-axillary).

The patient was then taken to the bicycle ergometer (ViaSprint 150, Carefusion, UK), the saddle height adjusted to ensure optimum comfort and pedalling ergonomics, with around 5 degrees of knee flexion at the bottom end of the pedal stroke. The handlebar height was adjusted for comfort; neither the saddle nor handlebars were adjustable fore or aft. The patient's feet were then secured onto the pedals using toe-straps.

The patient was connected to the 10 ECG leads, a blood pressure sphygmomanometer and a transcutaneous oxygen saturation monitor. The correct size of breathing mask was established and placed over the patient's mouth, ensuring a tight seal. The patient was asked not to talk for the duration of the test, but to gesture by tapping the handlebar if they felt unwell and to shake or nod their head in response to yes/no questions.

Baseline data (blood pressure, ECG, heart rate, oxygen saturations, ventilation rate (V_E), VO_2 and VCO_2) were collected over several minutes, with the patient at rest and breathing freely.

The patient cycled for 5 minutes against no resistance, to warm up and to ensure that resting VO_2 had plateaued. Any necessary adjustments to the recording apparatus were made before a load was added incrementally (20 watts per minute), by increasing the pedalling resistance. The ECG was monitored continuously for signs of cardiac ischaemia or arrhythmia, along with BP and O_2 saturation recordings. The patient was asked intermittently if they were experiencing chest pain or dizziness and they answered by nodding or shaking their head. The test was continued until the patient could cycle no more, either because they were too breathless or their legs were too painful, whilst ensuring that the respiratory exchange ratio (RER) was > 1 . This RER level indicated that the patient was nearing the limit of their cardiorespiratory capacity. The load was then removed and the patient was encouraged to pedal gently to allow them to recover and to cool down.

During the cool down, monitoring was continued and the data recorded until baseline levels were re-established. Finally the patient was assessed using the Borg and RPE scales (see appendix) to record how hard they had worked and how breathless they were at the peak of the test.

Specific criteria needed to be met if the patient was to be stopped from finishing the test, such as significant ST depression or fall in oxygen saturations, but this was not encountered during any of the 57 assessments. The patient then sat in a chair for a further 10 minutes, until they had fully recovered, before they were allowed to leave the department with DW.

4.2.1.3 Results

Table 18: Baseline CPET metrics in responders and nonresponders.

Baseline		Responders		Nonresponders		Student's T-test
		Mean	SD	Mean	SD	P value
Load	W	82.3	16.9	81.1	24.3	= 0.29
AT	ml/kg/min	9.2	1.2	9.2	1.8	= 0.16
Peak VO ₂	ml/kg/min	12.5	1.4	13.9	2.7	= 0.12
Borg	1 - 10	4.4	2.2	4.5	1.0	= 0.76
RPE	6 - 20	15.6	2.4	15.9	2.7	= 0.46

Table 19: CPET metrics in responders at baseline and during follow-up.

Responders		Time (months)						One way ANOVA with repeated measures	
		Baseline		6		12		Baseline vs	
		Mean	SD	Mean	SD	Mean	SD	6 months	12 months
Load	W	82.3	16.9	104.0	23.4	101.0	32.5	= 0.06	
AT	ml/kg/min	9.2	1.2	9.3	1.3	8.6	1.9	= 0.74	
Peak VO ₂	ml/kg/min	12.5	1.4	14.1	1.6	14.7	1.5	< 0.05	< 0.05
Borg	1 - 10	4.4	2.2	3.9	0.8	4.0	0.9	= 0.97	
RPE	6 - 20	15.6	2.4	14.3	2.2	14.8	2.0	= 0.26	

Table 20: CPET metrics in nonresponders at baseline and during follow-up.

Nonresponders		Time (months)						One way ANOVA with repeated measures	
		Baseline		6		12		Baseline vs	
		Mean	SD	Mean	SD	Mean	SD	6 months	12 months
Load	W	79.6	24.5	78.5	26.8	68.4	27.8	= 0.45	
AT	ml/kg/min	9.7	1.5	8.1	1.8	8.2	2.2	= 0.42	
Peak VO ₂	ml/kg/min	13.9	2.7	11.5	4.4	12.8	3.8	= 0.21	
Borg	1 - 10	5.3	1.7	4.3	1.3	4.8	1.3	= 0.65	
RPE	6 - 20	16.6	2.9	16.0	2.3	15.6	0.9	= 0.22	

Figure 20: Peak VO₂ in responders (white) and non-responders (black)

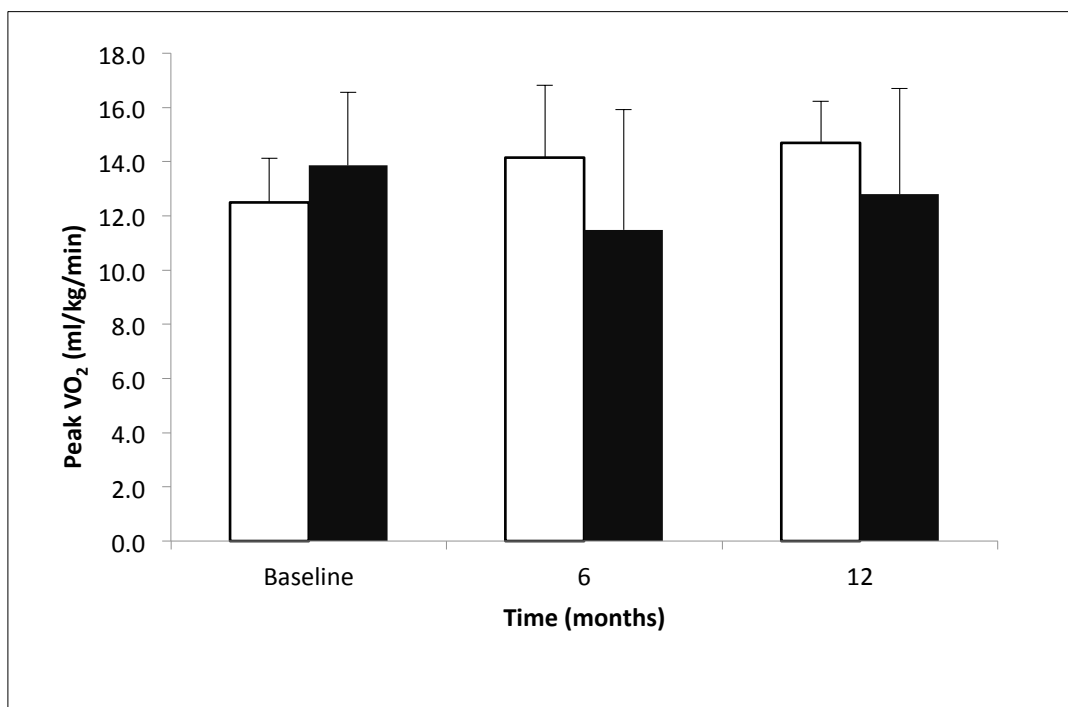


Figure 20 demonstrates the differences in the peak VO₂ in responders and non-responders at baseline and at 6 and 12 months following CRT implantation.

Using a 2-tailed Student's T-test, there were no statistically significant differences between responders and non-responders at baseline (see table 18).

A one-way ANOVA with repeated measures and Greenhouse-Geisser correction used to assess any difference in responders (see table 19) over 12 months found that RPE ($F(1.10, 8.83) = 1.41, p = 0.26$), Borg score ($F(1.37, 13.70) = 0.15, p = 0.97$ or AT ($F(1.65, 13.21) = 0.26, p = 0.74$) were not significantly different, so post hoc analysis with pairwise comparison was not undertaken (see table 19). A one-way ANOVA with repeated measures that did not violate Mauchly's test of sphericity determined that workload in responders approached statistical significance ($F(2, 22) = 4.45, p = 0.06$). Finally, a one-way ANOVA with repeated measures and Greenhouse-Geisser correction determined that peak VO_2 ($F(1.27, 13.9) = 9.26, p < 0.01$) was significantly different over the 12 months (see figure 20) and post-hoc analysis using the Bonferroni correction demonstrated responders had statistically significant differences between baseline and six months ($p < 0.05$) and baseline and twelve months ($p < 0.05$).

A one-way ANOVA with repeated measures and Greenhouse-Geisser correction assessed any difference in non-responders over the 12 months found that Load ($F(1.2, 0.37) = 0.91, p = 0.45$), AT ($F(1.26, 3.78) = 0.91, p = 0.42$), peak VO_2 ($F(1.26, 5.03) = 1.89, p = 0.21$), Borg score ($F(1.56, 4.7) = 0.45, p = 0.65$) or RPE ($F(1.39, 2.78) = 2.25, p = 0.22$) were not significantly different, so post hoc analysis with pairwise comparison was not undertaken (see table 20).

4.2.1.4 Discussion

Figure 21: Patient undergoing CPEX testing on bicycle ergometer



Figure 21 demonstrates a patient undergoing CPEX testing on a static ergometer bicycle in the pulmonary function unit, connected to pulse oximetry, 12 lead ECG, and breathing apparatus to measure gas exchange.

The lack of statistically significant differences at baseline in CPET (see figure 21) between the responder and nonresponder groups is important. This suggests that the groups were similar (at least in terms of cardiorespiratory function) before the CRT device was implanted and thus any subsequent differences in CPET metrics can be attributed to the intervention alone.

As detailed previously, patients were classed as responders if they achieved an increase in peak VO₂ of more than 1ml/kg/min during follow-up in conjunction with significant improvements in 2 other areas. As can be seen, 14 patients were categorised as responders using these criteria and the group achieved not just an arbitrary but, rather, a statistically significant increase in peak VO₂ at 6 months ($p < 0.05$), which was sustained at 12 months ($p < 0.05$). In contrast, nonresponders showed deterioration with respect to peak VO₂ during follow-up but this change was not significant. This demonstrates that CRT leads to significant gains in cardiorespiratory fitness; this most likely due to improved cardio-metabolic function.

Table 21: Baseline and 6 months values of peak VO₂ in the CRT trials

Trial	Mean Peak VO ₂ (ml/kg/min) in CRT group		
	Baseline	6 months	Increase (%)
RETHINQ	12.4	12.8	3.2
MUSTIC	13.7	16.2	18.2
MIRACLE ICD	13.3	14.4	8.2
MIRACLE	14.0	15.1	7.8
CONTAK	12.0	12.8	6.6

In terms of other CPET metrics, there was a measurable increase in the maximum load responders were able to tolerate during follow-up testing. A fall was recorded for nonresponders, although this was not statistically significant. This means that, for the same degree of breathlessness and fatigue as measured by the Borg and RPE scale respectively, responders performed a greater level of work. In terms of anaerobic threshold, there was deterioration in the nonresponders whilst responders seemed to be stable during follow-up, this makes sense as this is the component of cardiorespiratory fitness that is trainable, in contrast to VO₂ Max which is believed to be largely genetically predetermined and can be influenced only slightly by training or by reducing body mass.

The baseline mean of 13.0ml/kg/min for peak VO₂ in this patient cohort (from both groups) is in agreement with the data from other trials (table 21) which range between

12-14ml/kg/min. However, the trials do not comment upon other metrics such as AT, Borg or RPE score. A low peak VO_2 score ($< 15\text{kg}/\text{min}/\text{ml}$) is not only considered (amongst other criteria) to be an indication for heart transplant but is also associated with increased mortality, demonstrating that this is a very unwell patient group. Currently there is no 12 month CPET data in the published literature; earlier trials that used CPET as a criterion appear to have stopped follow-up at 6 months whilst subsequent larger trials which continued follow-up for over 2 years did not use CPET. Some cite the patients' lack of acceptance or their condition at follow-up as deterring researchers from such long term CPET follow-up; it is also possible that such data may exist but remains unpublished.

Average Borg and RPE scores of 4-6 and 15-16 in all patients across all time points, equates to "somewhat severe-severe breathlessness" and "hard-very hard" effort respectively. This is equivalent to exertion at around the anaerobic threshold and means that the patients, symptomatically at least, considered this a near-maximal test. This is important; if the patients scored poorly on one of these then it would suggest the test was submaximal. Furthermore, values for peak VO_2 , AT and work would have questionable interpretations as it could be argued that the patient had not tried as hard as they could and the limitation might be psychological, not physiological. The degree of functional impairment in this patient group is such that, even at 80 watts the mean workload achieved for the cohort as a whole, patients again considered this to be near maximal test. Cycling with a load less than 100 watts or 16km/h is considered to be light effort equivalent to 5-6 metabolic equivalents of task (METs) or metabolic equivalents. A MET is a measure of the metabolic cost of exercise during a particular physical activity compared to a reference activity, with 1 MET (1 kcal/ kg x hr) equivalent to an effort of 3.5ml/kg/min. This is a further demonstration of the functional limitations of this group.

The improvement of 1.6ml/kg/min, recorded for the responders at 6 months, is higher than that reported in other trials, which averaged 1ml/kg/min in similar patient groups. The reason for this degree of benefit is unclear since, at baseline, these patients appear to be similar to cohorts from other CRT trials. The improvement may be due to CRT alone by improving stroke volume, cardiac output and cardiorespiratory

fitness or it is possible CRT allows patients to exercise more, further improving their skeletal, respiratory and cardiac physiology and adding to the gains from the CRT device. The 12-month data is of particular interest, as at the time of writing, there is no published follow-up data at 12 months for peak VO_2 . The improvements seen at 6 months were maintained, and in 3 cases, improved upon, at 12 months. Peak VO_2 proved to be the most powerful of all the measure of response; if a patient improved significantly in terms of this domain then they improved in terms of all the other markers of response, except the 6MWD.

There was only one large change in the other CPET metrics at follow-up, bordering on significance, namely an increase in work in responders. This makes sense as, with improvements in cardiac function, the patients might be expected to achieve a higher workload than at baseline. Whilst the anaerobic threshold is known to improve with training, it is unlikely that any of the patients will have been exercising to such an extent in their day-to-day life to improve this threshold and hence large improvements would not be expected. The lack of significant difference in the Borg or RPE scores, suggests that the patients did not feel they were trying any harder following CRT, but their workload and peak VO_2 were actually higher. This is important as significant differences in Borg or RPE scores following CRT implantation might suggest that it was because they were 'trying' more e.g. the difference was psychological rather than physiological. For nonresponders, there were no statistically significant differences in any of the metrics, suggesting that whilst they had not deteriorated significantly during the follow-up period, neither had they significantly improved. This defines a nonresponder.

The intrinsic difficulty in using a symptom limited (VO_2 peak) rather than the maximal test (VO_2 Max), is that although patients are encouraged to continue once they feel that they have reached their limits they will stop, regardless of whether or not they could in reality continue. Furthermore an inherent issue in serial testing is ensuring that patients comply, and continue, with the research project. If they feel that their health is being negatively impacted or their autonomy overridden, then they may withdraw jeopardising the project. The investigator chose not to encourage patients during testing in case this was deemed to be coercion, but the clinical staff encouraged

patients as per their usual practice. Neither the investigator, clinical staff nor the patient was allowed to know previous performance on this, nor any other marker of response, until the assessment was completed, so as not to influence outcomes.

The patients were all very willing to perform the CPET test and voiced no concerns or complaints. Occasional difficulties included; erratic breathing which settled upon adding resistance, patients complaining of claustrophobia when the mask was placed and non-compliance with instructions not to talk during the test all of which are common in CPET testing of HF-LVSD patients. Anecdotally, it was the first time many of the patients had been on a bike for years.

Peak VO₂ is an objective and rigorous assessment of a patient's physical fitness in a more controlled and controllable environment than 6MWT. However, due to issues such as illness, staffing, and clinical case-load, there were often different numbers and members of staff helping with the CPET assessment. The senior physiologist was usually TH, but on occasion it was CR and although there is a specific protocol to follow, such differences may lead to alterations in the patients performance.

4.2.1.5 Conclusion

Responders to CRT demonstrated a significant improvement in peak VO₂ and work measured during CPET at 6 months. This is first study to measure peak VO₂ in patients at 12 months post-CRT and this improvement was sustained, and further improved upon, at 12 months. There were no such improvements in nonresponders at 6 or 12 months. In the present study, peak VO₂ was a powerful marker of response. Patients who improved in terms of this metric improved on all the others. In comparison to the 6MWT, CPET may be considered to lack ecological validity but, within the current study, it proved to be a more robust, objective and reproducible measure of cardiorespiratory fitness and response to CRT.

4.2.2 Minnesota Living with Heart Failure Questionnaire

4.2.2.1 Introduction

The Minnesota Living with Heart Failure questionnaire (MLWHFQ) is a validated, widely used quality of life (QoL) questionnaire, developed specifically for HF. As

discussed in chapter 3, there are 21 questions covering topics such as side effects of treatments, recent hospital admissions, symptoms, mood, sex life and appetite. Each question starts with the same common stem “Did your heart failure prevent you from living as you wanted to during the past month (4 weeks) by...” for example “...causing swelling in your ankles and legs” the answer to which is then rated on a 6 point Likert scale, from 0 (no) to 5 (very much).

4.2.2.2 Method

The authors of the questionnaire provide no specific instructions on its administration so a local protocol was devised. The MLWHFQ (see appendix) was administered with the patient sitting in a quiet room, with the investigator spending several minutes with them, explaining its purpose, how the questions are structured and the rating scale used. This process was repeated at each time point. The patients were then left to fill out the 21 questions in their own time with the investigator present throughout to answer any questions that they might have.

The patients received a blank questionnaire on each occasion. They were not reminded how they had scored last time, nor were their previous scores checked prior to reassessment. The questionnaire was administered at 08:30, the same time during each point of assessment in case exertion experienced, or medications administered during testing might influence their scores. If a relative accompanied the patient, their involvement was kept to a minimum. As was the case for the other markers of response, the patients were informed of their performance only at the end of the assessment session.

4.2.2.3 Results

Table 22: MLWHQ at baseline in responders and nonresponders

MLWHFQ		Responders		Nonresponders		Student's T-test
		Mean	SD	Mean	SD	P value
Time (months)	Baseline	44.4	21.9	52.8	22.7	0.33

Table 23: MLWHQ in responders at baseline and follow-up

MLWHFQ		Responders		One way ANOVA with repeated measures	
		Mean	SD		
Time (months)	Baseline	44.4	21.9	Baseline vs.	
	6	24.4	19.1	6 months	< 0.05
	12	24.3	22.3	12 months	< 0.05

Table 24: MLWHFQ in nonresponders at baseline and follow-up

MLWHFQ		Nonresponders		One way ANOVA with repeated measures	
		Mean	SD		
Time (months)	Baseline	52.8	22.7	Baseline vs.	
	6	37.0	20.6	6 months	= 0.31
	12	36.4	26.7	12 months	

Figure 22: MLWHFQ score in responders (white) and nonresponders (black)

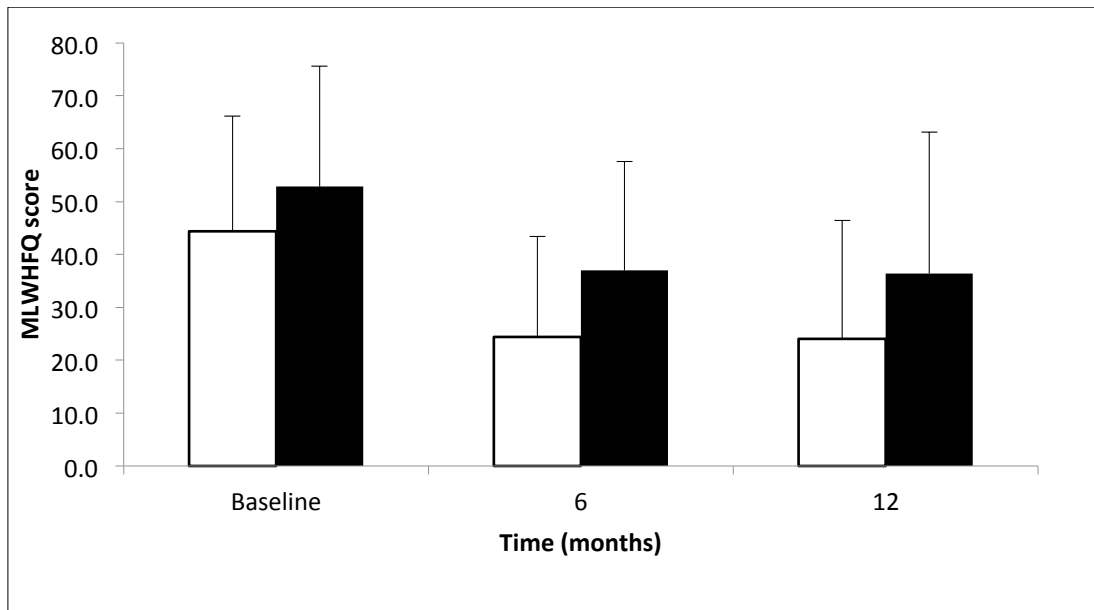


Figure 22 demonstrates the differences in the MLWHFQ in responders and non-responders at baseline and at 6 and 12 months following CRT implantation.

Using a 2-tailed Student's T-test, there were no statistically significant differences between responders and non-responders at baseline (see table 22).

A one-way ANOVA with repeated measures and Greenhouse-Geisser correction determined that MLWHFQ in responders ($F(1.97, 21.76) = 7.40, p < 0.01$) but not nonresponders ($F(1.8, 7.45) = 5.82, p = 0.31$) was statistically different (see table 24) between time points during follow-up. Post-hoc analysis using the Bonferroni correction demonstrated responders (see figure 22 and table 23) had statistically significant differences between baseline and six months ($p < 0.05$) and baseline and twelve months in responders ($p < 0.05$).

4.2.2.4 Discussion

Responders had significantly lower MLWHFQ scores during follow-up than at baseline. However, almost all patients reported that they felt better symptomatically, whether they had improved significantly in terms of other markers of response or not. This suggests there may be a significant placebo effect when measuring response to CRT therapy by the MLWHFQ. Responders appeared to be less symptomatic at baseline, which was also reflected in other markers of response such as 6MWT for example, but these differences were not statistically significant.

There is a notable similarity between the cohort of 19 patients (see table 25) at baseline and those from the large clinical trials, although it would appear that in the current project, responders are less symptomatic at baseline and show greater improvement at 6 months when compared to the trial data. This is despite there being no statistically significant difference at baseline in this or any other of the metrics of response. Unfortunately, as mentioned previously, similar comparisons at 12 months cannot be made due to a lack of published data. Interestingly, in CRT crossover trials such as CONTAK and MUSTIC, there was a 10-20% reduction in symptoms following 3 months of inactive 'pacing', again demonstrating a possible placebo effect. This could also perhaps explain the symptomatic improvement in the nonresponders in this study.

Responders maintained their improvement in terms of symptoms at 12 months, with some deteriorating or improving slightly. This was not reflected in any other marker of response and the slight deterioration could reflect the inherent variability of symptoms in chronic disease. Patients were not given access to their previous scores nor the completed questionnaire itself, so as not to unduly influence the results. This being said, it might have been interesting to allow this, in order for them to see how they fared at the previous assessment and so perhaps enable them to gauge more precisely how they were feeling in light of their previous results.

Table 25: Mean MLWHFQ score and improvement from the CRT trials

Trial	Mean MLWHFQ score in CRT group		
	Baseline	6 months	Decrease (%)
COMPANION	N/A	N/A	25
CONTAK	56	49	31
MIRACLE	59	41	18
MUSTIC	51	30	41
PATH	49	24	51

Three of the questions are problematic when it is used in the UK; first question 15, refers to paying for treatments, which is not relevant. Second, question 8, refers to earning a living, which is not relevant as, given the average age of a HF patient at diagnosis, most have retired. Finally, question 2 refers to working around the yard and is worded oddly. The above did lead to some confusion and/or a default answer of 0 and so perhaps the score should not be considered out of 105 but rather 99 or 93, for example.

It is interesting that by 12 months follow-up both groups were stable in reference to their 6-month score, despite improvements or deterioration in other markers of response such as 6MWD or VO₂ peak. This suggests that perhaps the placebo effect was not short-lived and highlights the logic behind following up patients for more than 6 months. However, as both groups had improvements in symptoms, albeit only significantly in the responders, it is important to not categorise response on patient's symptoms alone, otherwise all 19 patients would have been classed as responders.

4.2.2.5 Conclusions

For responders, as recorded by the MLWHFQ, symptoms improved significantly by over 45% at 6 months, this was maintained at 12 months and, for nonresponders, symptoms improved by 29%, increasing to 31% by 12 months. For nonresponders this was not a statistically significant difference and this group did not improve significantly in any other regard. The responders had less marked symptoms at baseline but this was not significant, suggesting, that at least according this metric, the two groups were very similar. Finally, the improvement in the MLWHFQ score in nonresponders highlights the importance of using a multi-model approach to assess response rather than relying on symptoms alone.

4.2.3 *Left Ventricular Volumes*

4.2.3.1 **Introduction**

Assessment of left ventricular (LV) size is commonly performed to assess LV dilation secondary to LVSD (as discussed in chapter 2). A reduction in LV size is an accepted surrogate marker of improvement, providing evidence of reverse LV remodelling, as a result of improved LV systolic function. Accepted metrics include LV end diastolic dimension (LVEDD), LV end diastolic volume (LVEDV) and LV end systolic volume (LVESV). The latter, as used in this study, is measured with 2D transthoracic echocardiography (2DTTE), and calculated using modified Simpson's biplane method of discs.

4.2.3.2 **Method**

Data was obtained during the routine echocardiographic follow-up assessment. Images were acquired and measured by either DWL or JA who were both senior echocardiographers in the echocardiography department in NGH.

Images of the LV were acquired in the conventional manner from two orthogonal planes in the apical view (4 and 2 chamber) over several cardiac cycles. The volume of the LV was measured at end-diastole (immediately after mitral valve closure, when the LV chamber is at its largest). The edges of the endocardium were traced free-hand along the endocardial border, from one hinge point of the mitral valve to the other, encapsulating the black LV blood pool, using the General Electric (GE Healthcare, Princeton, US) Vivid 7 ultrasound machine during acquisition of a full study.

The modified Simpson's rule for calculation of LV volume is based on a stack of elliptical disks, the cross sectional area of each disc is calculated from the diameter obtained in both the 2 and 4 chamber views and the thickness of each disc represents a fraction (1/20 approximately) of the LV long axis. The accepted convention is to exclude trabeculations and papillary muscles when tracing the endocardium, and this methodology was followed throughout (see figure 23).

Equation (3) volume of each disc:

$$\pi (D_{4c} \times D_{2c}) L / 4n$$

D_{4c} = internal diameter of left ventricle in 4 chamber view.

D_{2c} = internal diameter of left ventricle 2 chamber view.

L = length of each disc.

Equation (4) total ventricular volume:

$$\frac{\pi}{4} \sum_{1}^{20} D_{4c} \times D_{2c} \times L / 20$$

D_{4c} = internal diameter of left ventricle in 4 chamber view.

D_{2c} = internal diameter of left ventricle 2 chamber view.

20 = total number of discs.

L = length of each disc.

Figure 23: Simpson's method using apical 4 (left) and 2 chamber (right) views

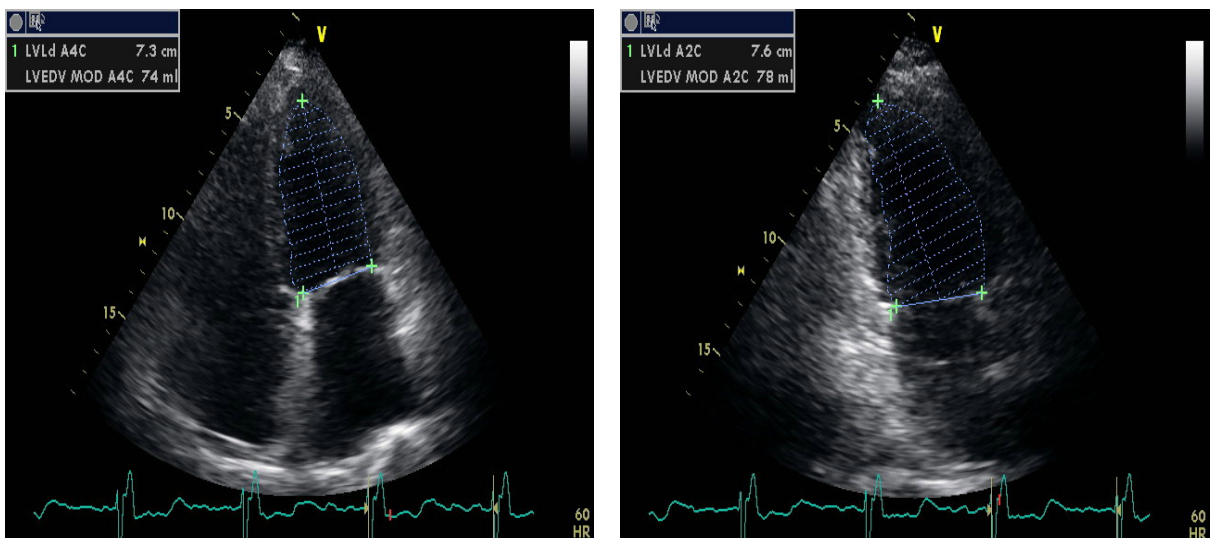


Figure 23 demonstrates the measurement of the left ventricular volume using Simpson's modified rule, with an apical 4 chamber and apical 2 chamber view of the left ventricle on the left and right respectively. The 3 green crosses indicate either side of the mitral valve annulus and the apex of the left ventricle and the hashed blue line is drawn around the internal surface of the left ventricle, which following calculation, results in the LV volume as seen in the top left hand corner.

4.2.3.3 Results

Table 26: LVEF and LV volumes in responders and nonresponders

LV volume		Responders		Nonresponders		Student's T-test
		Mean	SD	Mean	SD	P value
Baseline	LVEDV (ml)	201.0	128.4	153.2	87.8	= 0.58
	LVESV (ml)	156.7	114.1	122.5	59.9	= 0.25
	EF (%)	25.6	8.1	25.8	8.0	= 0.96

Table 27: LVEF and LV volumes in responders

LV volume	Time point	Responders		One way ANOVA with repeated measures	
		Mean	SD	P value	
LVEDV (ml)	Baseline	201.0	128.4	Baseline vs.	
	6 months	181.5	125.6	6 months	< 0.05
	12 months	173.6	132.2	12 months	< 0.05
LVESV (ml)	Baseline	156.7	114.1	Baseline vs.	
	6 months	134.1	108.9	6 months	< 0.05
	12 months	127.2	111.1	12 months	< 0.01
EF (%)	Baseline	25.6	8.1	Baseline vs.	
	6 months	33.6	10.0	6 months	= 0.07
	12 months	33.0	8.3	12 months	

Table 28: LVEF and LV volumes in nonresponders

LV volume	Time point	Nonresponders		One way ANOVA with repeated measures	
		Mean	SD	P value	
LVEDV (ml)	Baseline	153.2	87.8	Baseline vs.	
	6 months	172.4	126.2	6 months	= 0.63
	12 months	145.2	88.8	12 months	
LVESV (ml)	Baseline	122.5	59.9	Baseline vs.	
	6 months	144.4	117.6	6 months	= 0.54
	12 months	118.8	72.2	12 months	
EF (%)	Baseline	25.8	8.8	Baseline vs.	
	6 months	34.8	5.0	6 months	= 0.29
	12 months	34.9	6.7	12 months	

Figure 24: LVEDV in responders (white) and nonresponders (black)

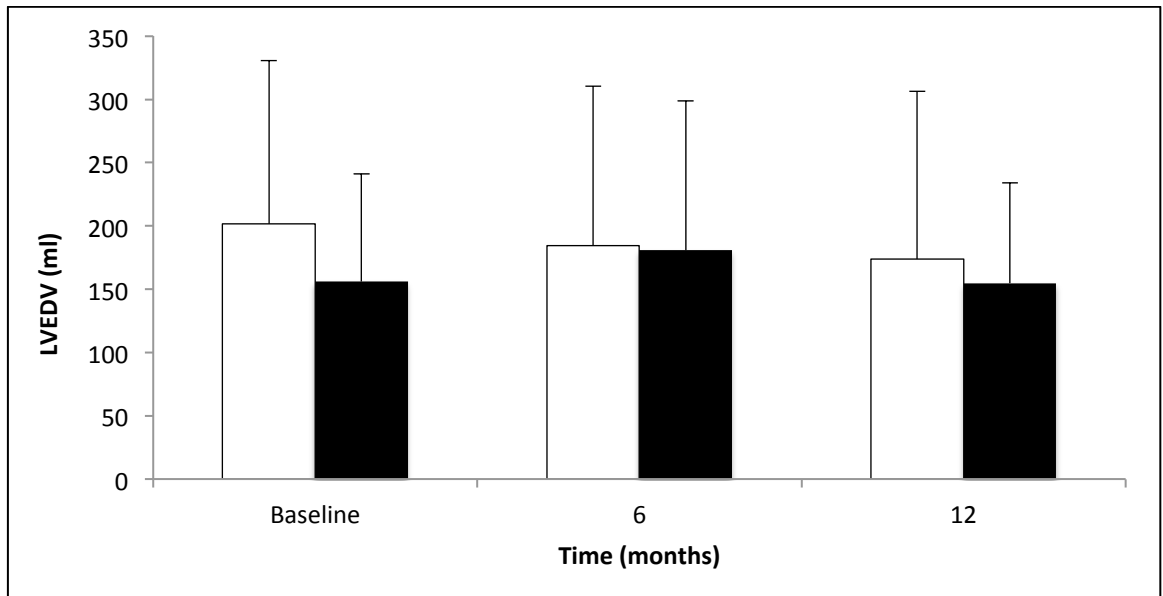


Figure 24 demonstrates the differences in the MLWHFQ in responders and nonresponders at baseline and at 6 and 12 months following CRT implantation.

Figure 25: LVESV in responders (white) and nonresponders (black)

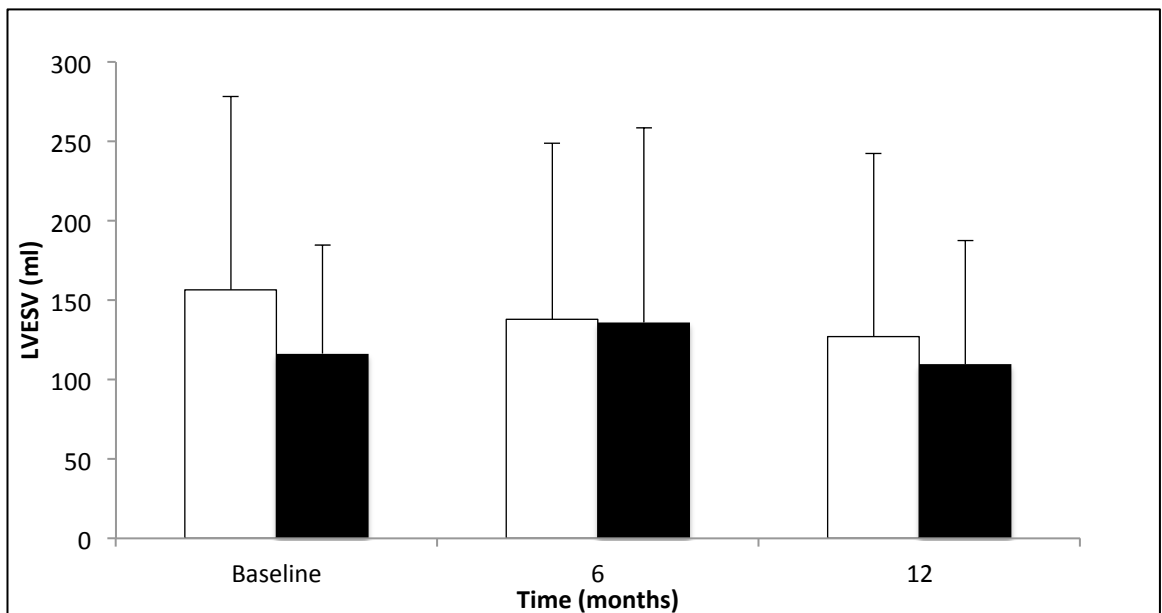


Figure 25 demonstrates the differences in the MLWHFQ in responders and nonresponders at baseline and at 6 and 12 months following CRT implantation.

Figure 26: LVEF in responders (white) and nonresponders (black)

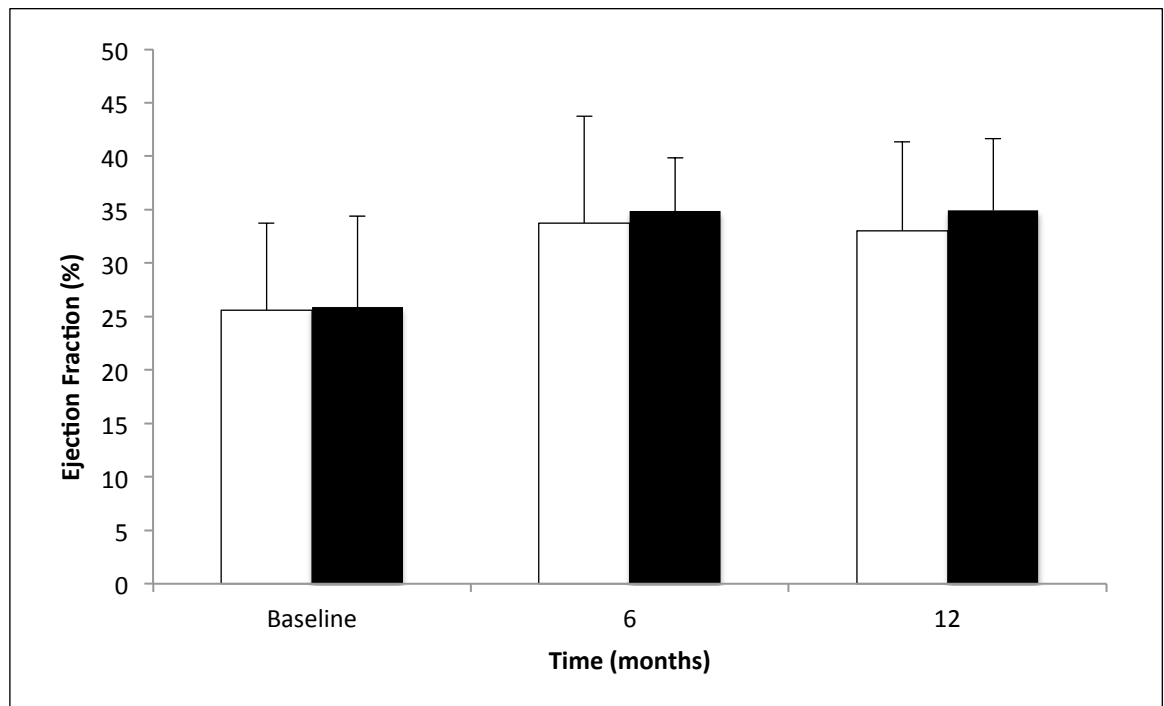


Figure 22 demonstrates the differences in the MLWHFQ in responders and non-responders at baseline and at 6 and 12 months following CRT implantation.

Using a 2-tailed Student's T-test, there were no statistically significant differences between responders and non-responders at baseline (see table 26 and figures 24-26).

A one-way ANOVA with repeated measures and Greenhouse-Geisser correction determined that LVEDV ($F(1.73, 17.43) = 6.37, p < 0.01$), LVESV ($F(1.59, 17.52) = 11.92, p < 0.01$) but not EF ($F(1.50, 16.52) = 3.38, p = 0.07$) in responders was statistically different between time points during follow-up (see table 27). Post-hoc analysis using the Bonferroni correction demonstrated responders had statistically significant differences between baseline and six months for LVEDV ($p < 0.05$) and LVESV ($p < 0.05$) and baseline and twelve months for LVEDV ($p < 0.05$) and LVESV ($p < 0.01$).

4.2.3.4 Discussion

In terms of responders, 14 patients demonstrated a significant reduction in LVEDV observed at 6 months showing further improvement at 12 months.

At the time of defining the criteria determining a 'responder' in the context of this study (prior to recruitment) LVESV was not considered to be significant marker *a priori* but, for the sake completion it is included in the results. Of the 14 responders, all demonstrated reductions in LVESV at 6 and 12 months with the majority showing a decrease of LVESV of > 10%. The sustained reduction in LV volumes at 12 months, in conjunction with improvements in the 2 other markers, suggests that these 14 patients were true CRT responders and the results are not a result of chance. The lack of significant correlation with the LV volumes or EF and other markers of response is as expected, as whilst a reduction in LV size is related to clinical outcomes, e.g. to morbidity and mortality, it is not related to symptomatic response.

Two of the nonresponder group had > 10% reductions in LVEDV at 12 months, others had small, non-significant increases or reductions in LV volumes (LVEDV or LVESV), and showed no significant improvement in any other marker of response. LV volumes in the nonresponder group appear to show a simple random variation with regression to the mean at 12 months. The observed improvement in EF% in nonresponders is more difficult to explain but may be related to both inter- and intra-operator variability in measurement of the relatively small LV volumes; the smaller the volume the greater the impact of measurement error.

Unfortunately, for logistical reasons, it was not possible to have the same patient assessed by the same echocardiographer at every time point. This introduced potential variability to the assessment. Ideally, each patient would be assessed by a single echocardiographer or, perhaps preferably, by both sonographers at each time point and each then measuring the LVEDV on all the acquired images. This would produce 4 measurements of volume enabling a mean and SD to be obtained. Unfortunately, due to clinical commitments, and in the absence of a dedicated research sonographer, this did not prove to be feasible. In addition, in order to

minimise inconvenience to the patient, all the required tests were scheduled for a single day; the necessary synchronisation across departments further constrained the possible assessment time points. In the event, the operator depended on which echocardiographer was free on the day.

The Vivid 7 echocardiography machine and 3D probe (Siemens GmbH, Erlangen, Germany) used in Sheffield, required multiple cardiac cycles to build a single 3D image, making it impractical for patients with significant ectopy or atrial fibrillation, hence it was not considered practical after consultation with the investigators and sonographers to perform 3DTTE scans on every patient at every time point. As a result, 2DTTE was used for all patients at all time points, despite potential limitations and only these volumes recorded at baseline and follow-up were used in the assessment of response. Newer scanners since can acquire a 3D image from a single cardiac cycle. This is ideal for patients with arrhythmias as in this study but, at the time, this was not available in SHTT. Indeed, many of the patients did not have echo windows that were considered excellent and most were overweight-obese, leading to poor endocardial definition and inadequate studies; hence the LV volumes and any variation must be considered in this light.

To avoid introducing any possible extraneous variables, the investigators played no part in the acquisition of images or the measurement of volumes. In addition, to avoid influencing the echocardiographers, they were blinded to the results of other tests or markers of response.

According to Lang et al (2006)¹⁸⁶ the advantages of using modified Simpson's rule include the fact that it allows for an irregularly shaped LV and it also minimises mathematical assumptions. However, when imaging the LV, it is important to avoid foreshortening of the LV apex. This can give an erroneous reduction in the measured long axis and underestimation of the LV volume and poor images with signal drop out in the endocardium can result in inaccuracies in tracing the endocardial border. For these reasons it is important to acquire good images on axis. Despite these considerations this technique remains the most commonly used method for assessing

LV volume in clinical practice; it is the recommended technique by the European Society for Cardiology (ESC) and the value/technique quoted typically in the literature. Whilst improvements in EF% are common, these are rarely quoted and indeed no threshold for improvement has been set in previous trials. The responders in this study had a statistically significant increase in EF of 8%; a much larger increase than that reported in most clinical trials albeit with only 6 months follow-up, unlike 12 months here. One possible explanation for this is that some of these individuals are super responders, the CARE-HF trial found improvements in EF% at 18 months of 6.9%, similar to this patient cohort, with 3.7% at 3 months only, demonstrating further improvement the longer the device was *in situ*. Clearly, this cohort of patients is small and the possibility of differences due to chance and/or error cannot be excluded.

There is a fundamental difficulty of defining CRT response, which must be binary for clinical trials regardless of the metric(s) used, even though in reality it is never as clear cut as noted previously by Bleeker et (2006)¹⁰⁵. Furthermore, the inherent variability of serial LV volume measurements due to the influence of external factors such as equipment and the patient's acoustic window and internal factors such as inherent inter-operator variability and variability due to experience, technique and time pressure is widely recognised. The variation in LV volume measurements at multiple time points is in the region of 10%. This is why a sustained reduction in LV volumes is important, suggesting that the reduction is real, not erroneous¹⁸⁷. In this study, limited to a single centre, using one echocardiography machine and 2 experienced echocardiographers, less inherent variability might be expected than in multicentre trials, involving using different machines, conventions, and echocardiographers of varying experience. It is worth noting that LVEF is not measured routinely at this centre, instead visual assessment of LVSD severity is categorised as mild/moderate/severe, highlighting a lack of experience with this measure and explaining possible variation in LVEF in this cohort.

As discussed in Chapter 3, in most CRT trials, a reduction of 10-15% in LVEDV or LVESV during serial assessment is typically considered to be significant. However, the lower the threshold is used, the more patients would appear to be responders and equally, the higher the threshold used, the fewer patients will be deemed as responders, at

least in terms of this metric. Yu et al (2008) noted that in routine clinical practice, measurement of LV volume is not performed with the same rigor as in clinical trials and so the change in LV volume will only be useful as an indicator if it is large ⁸⁶. It is likely most patients will have LV volumes unchanged or changed slightly following CRT and so such differences must be viewed with respect to the rigor and variability of how such a method is performed. This is just one method of assessing a single element of response to CRT; the patient may have responded in other ways hence the importance of the multi-modal approach adopted in this work.

Table 29: BSE reference range for LV volumes in men and women

LV size		Normal	Mild	Moderate	Severe
Men	ml	67 - 155	156 - 178	179 - 201	> 202
	ml/m ²	35 - 75	76 - 86	87- 96	> 97
Women	ml	56 - 104	105 -117	118 - 130	> 131
	ml/m ²	35 - 75	76 - 86	87- 96	> 97

Using the approach of normalisation to body surface area, patients in this cohort had a mean LVEDV of 107ml/m² at baseline. This is similar to value of 117ml/m², reported at baseline in CARE-HF for a predominantly European cohort ⁴⁴. Indeed, comparing our cohort, in terms of LVEDV measured in both ml and ml/m² to the reference range (see table 29) provided by the British Echocardiography Society (BSE) we find that all the patients in our study had grossly abnormal LV volumes ¹⁸⁸.

Whilst other studies (MUSTIC¹⁵²,MIRACLE¹⁵⁵, COMPANION⁶, RD-CHF¹⁵⁴ and PATH-CHF¹²⁷) have used the baseline LV end-diastolic dimension (in mm), rather than the LVEDV, as a measure of LV size, most did not record the difference at follow-up. The CARE-HF trial used a LVEDV volume index normalised to body surface area at baseline but again failed to report any changes during follow-up. As can be seen from tables 30, 31 and 32, CARE-HF⁴⁴, MIRACLE⁶, MADIT¹⁵⁸ and RETHINQ¹⁵⁹ trials all demonstrated a relative reduction in LV volumes of between 6 and 30% and an absolute increase in LVEF% of between 1 and 3.7%.

The patients in our study appear to have volumes smaller than those recorded in the aforementioned clinical trials. The reason for this is unclear, but it could be related to patient size, which might become apparent if the data was normalised for body surface

area. Over 70% of our patients were below average height for the UK (< 161cm females and < 175cm males) and, as a consequence, would be expected to have reduced LV size and mass.

Table 30: LVEDV at baseline and follow-up in the CRT trials

Trial	Mean LVEDV (ml) in CRT group		
	Baseline	6 months	Decrease (%)
MIRACLE ICD II	337	296	12.1
MADIT-CRT	251	194	22.7
MIRACLE ICD	322	302	6.2
RETHINQ	210	194	7.6

Table 31: LVESV at baseline and follow-up in the CRT trials

Trial	Mean LVESV (ml) in CRT group		
	Baseline	6 months	Decrease (%)
MIRACLE ICD II	275	225	18.1
MADIT-CRT	175	123	29.7
MIRACLE ICD	N/A	N/A	N/A
RETHINQ	163	95	41.7

Table 32: EF at baseline and follow-up in the CRT trials

Trial	EF% in CRT group		
	Baseline	6 months	Increase
CARE-HF	25	28.7	3.7
MADIT-CRT	N/A	N/A	1.0
MIRACLE ICD	24	26.1	2.1
RETHINQ	25	26.2	1.2

4.2.3.5 Conclusions

Our patient cohort had similar LV volumes at baseline to patients from the CARE-HF and when compared to normalised values from the BSE, LV size was found to be severely abnormal. At 6-month follow-up, responders demonstrated a statistically significant reduction of 9% and 14% in LVEDV and LVESV respectively. This improvement continued to be seen at 12 months with reductions of 14% and 18%. Non-responders, demonstrated no such significant changes. This reduction in LV volumes in responders was similar to that reported by the large CRT trials.

4.2.4 *Surrogate markers*

When comparing outcomes in two groups, it is important to ensure they are as similar as possible before the intervention, to avoid confounding variables influencing the results. Whilst the other markers of response have already been considered, it is important to consider the physiological make-up of the cohort at baseline and during follow-up. To this end, surrogate markers of response were compared between the groups at baseline and within each group during follow-up. Using a Student's 2 tailed T-test demonstrates that there was no significant difference between the groups at baseline (see table 33).

In responders, a one-way ANOVA with repeated measures and Greenhouse-Geisser correction (see table 34) was used to analyse the difference over the 12 months. There was no significant difference in systolic ($F(1.40, 15.4) = 0.47, p = 0.56$), diastolic ($F(1.64, 18.08) = 0.85, p = 0.42$), pulse ($F(1.09, 11.9) = 1.00, p = 0.35$) or mean arterial ($F(1.92, 21.17) = 0.84, p = 0.44$) blood pressure. Similarly, there was no significant difference in weight ($F(1.92, 21.2) = 0.03, p = 0.97$), QRS duration ($F(1.66, 16.59) = 0.07, p = 0.88$), body mass index ($F(1.82, 20.06) = 0.12, p = 0.98$) or percentage of biventricular pacing ($F(1.33, 13.37) = 2.72, p = 0.11$).

The same test was used to analyse the difference in surrogate markers over the 12 months in non-responders (see table 35). In terms of non-responders there was no significant difference in systolic ($F(1.07, 4.27) = 0.82, p = 0.47$), diastolic ($F(1.93, 7.73) = 0.35, p = 0.70$), pulse ($F(1.19, 4.79) = 0.82, p = 0.43$) or mean arterial ($F(1.32, 5.29) = 0.32, p = 0.65$) pressure. Similarly, there was no significant difference in weight ($F(1.42, 5.70) = 0.96, p = 0.40$), QRS duration ($F(1.80, 7.21) = 0.85, p = 0.45$), body mass index ($F(1.47, 5.91) = 1.71, p = 0.25$) or percentage of biventricular pacing ($F(1.07, 4.27) = 0.82, p = 0.45$).

The two groups were largely similar before CRT implantation and the only difference of note was the larger weight and subsequent higher BMI of the responder group. Rather than presenting with the anticipated cardiac cachexia, both groups were overweight-obese, with the responders more so. This may suggest that the group were "healthier" at baseline, were better conditioned and had a milder form of HF-LVSD syndrome.

However, without an assessment of lean- versus fat- mass, it could be these patients were too breathless to exercise and so tended towards weight gain. Furthermore, any increase in weight during follow-up, could be due to increase in lean mass, fat mass or fluctuations in fluid-balance. Investigation using bio-impedance methods could delineate this further.

It was predicted that CRT would lead to a reduction in QRSd due to more physiological e.g. quicker interventricular conduction and subsequent restoration of synchrony, which in turn would lead to an increase in SV and therefore BP. However, there were no significant changes in the groups during follow-up nor any trending towards significance. CRT trials, to date, have used various surrogate markers such as a reduction in QRS duration and increase in systolic BP to assess CRT response. Indeed in all patients implanted with CRT versus OMT the CARE-HF⁴⁴ and COMPANION¹³⁴ studies reported significant and sustained increases in systolic BP at 3 months and 18 months of 2-6mmHg respectively and the MIRACLE¹⁵⁵ study reported a significant decrease in QRSd of 20ms. Despite similarities between such patient cohorts and these, this finding was not repeated in this work. However, this sample size was orders of magnitude smaller and the study was not powered to detect such small differences. Finally, it is well known those patients who receive less than 95% biventricular pacing, are less likely to derive clinical benefit from their CRT device¹⁸⁹. Reductions in pacing may be due to tachyarrhythmia, lead dislodgement and loss of LV capture¹⁹⁰. In our study, whilst responders appear to have received a lower % than the nonresponders initially, both groups were receiving over 95% biventricular pacing by 12 months. Whilst the differences are not statistically significant, this does demonstrate that the lack of response was not due to inadequate biventricular pacing.

In summary, there was no significant difference at baseline between the groups or during follow-up within the groups in terms of surrogate markers of response or possible confounding factors. Finally, during the 12 months follow-up, there were no hospital admissions or deaths in either group so these events cannot be used as a marker of response either. These results will be used in the following chapters, when investigating novel predictors and markers of CRT response, in this patient cohort.

Table 33: Surrogate markers at baseline in responders and nonresponders

Baseline*		Units	Responders		Nonresponders		Student's T-test
			Mean	SD	Mean	SD	P value
Blood Pressure	Systolic	mmHg	126.8	12	126.2	21.4	= 0.94
	Diastolic	mmHg	73.3	10.4	74.6	6.5	= 0.89
	PP	mmHg	53.5	14.2	52.2	19.4	= 0.87
	MAP	mmHg	91.1	11.9	91.3	9.9	= 0.97
Physical	Weight	Kg	92.8	17.8	80.6	20.8	= 0.20
	Height	m	1.74	0.1	1.72	0.1	= 0.68
	BMI	Kg/m ²	30.4	4.2	27.7	4.5	= 0.11
CRT	BiVP	%	91.1	13.8	98.3	8.8	= 0.63
ECG	QRSd	ms	162.3	23.4	163	23.1	= 0.50

BMI = body mass index, BiVP = biventricular pacing, BP = blood pressure, CRT = cardiac resynchronisation therapy, ECG = electrocardiography. PP = pulse pressure, MAP = mean arterial pressure, QRSd = QRS duration. Baseline refers to pre-CRT implantation other than for BiVP where it refers to approximately 6 weeks post CRT implantation.

Table 34: Surrogate markers in responders at baseline and follow-up

Responders		Units	Baseline*		6 months		12 months		One way ANOVA with repeated measures	
			Mean	SD	Mean	SD	Mean	SD	Baseline vs. 6	6 vs. 12
Blood Pressure	Systolic	mmHg	126.8	12.0	129.9	18.7	132.1	19.8	= 0.56	
	Diastolic	mmHg	73.3	10.4	76.4	11.1	75.5	13.7	= 0.42	
	PP	mmHg	53.5	14.2	53.5	10.7	58.3	16.7	= 0.34	
	MAP	mmHg	91.1	11.9	94.2	13.3	94.9	14.5	= 0.44	
Physical	Weight	Kg	92.8	17.8	92.8	16.9	89.7	17.5	= 0.97	
	Height	m	1.7	0.1	1.7	0.1	1.7	0.1	N/A	
	BMI	Kg/m ²	30.4	4.2	32.4	4.0	29.4	4.0	= 0.98	
CRT	BiVP	%	91.1	13.8	94.2	9.4	96.2	6.7	= 0.11	
ECG	QRSd	ms	162.3	23.4	159.8	27.5	165.7	28.8	= 0.88	

BMI = body mass index, BiVP = biventricular pacing, BP = blood pressure, CRT = cardiac resynchronisation therapy, ECG = electrocardiography. PP = pulse pressure, MAP =

mean arterial pressure, QRSd = QRS duration. *Baseline refers to pre-CRT implantation other than for BiVP where it refers to approximately 6 weeks post CRT implantation.

Table 35: Surrogate markers in nonresponders at baseline and follow-up

Nonresponders		Units	Baseline*		6 months		12 months		One way ANOVA with repeated measures	
			Mean	SD	Mean	SD	Mean	SD	Baseline vs 6	6 vs 12
Blood Pressure	Systolic	mmHg	126.2	21.4	119.8	9.9	119.4	9.1	= 0.74	
	Diastolic	mmHg	74.6	6.5	73.6	8.0	76.0	8.0	= 0.70	
	PP	mmHg	52.2	19.4	46.2	3.9	43.4	5.4	= 0.43	
	MAP	mmHg	91.3	9.9	89.0	8.5	90.5	8.0	= 0.65	
Physical	Weight	Kg	80.6	20.8	83.2	19.6	81.5	16.0	= 0.40	
	Height	m	1.7	0.1	1.7	0.1	1.7	0.1	N/A	
	BMI	Kg/m ²	27.7	4.5	27.8	4.1	27.3	3.2	= 0.25	
CRT	BiVP	%	98.3	8.8	95.0	5.7	96.4	5.3	= 0.45	
ECG	QRSd	ms	163.0	23.1	161.0	22.9	166.8	19.4	= 0.50	

BMI = body mass index, BiVP = biventricular pacing, BP = blood pressure, CRT = cardiac resynchronisation therapy, ECG = electrocardiography. PP = pulse pressure, MAP = mean arterial pressure, QRSd = QRS duration. *Baseline refers to pre-CRT implantation other than for BiVP where it refers to approximately 6 weeks post CRT implantation.

4.3 Discussion

At 12 months, out of the 21 patients, two of whom were unable to be implanted conventionally and within time frame of this study and therefore were excluded, 14 were classified as responders and 5 as nonresponders according to the criteria set *a priori*. However, as discussed, the response to CRT is not binary. This is best evidenced by the fact that nearly all patients reported that they had improved symptomatically in terms of their responses to the MLWHFQ, but only 16 of these did so in conjunction to any degree with any other parameter, albeit inconsistently and not meeting the pre-specified thresholds. In particular there was no significant improvement in terms of any objective measure such as LVEDV or peak VO₂. This is consistent with the power of the placebo-effect of having a CRT implanted, as found in the earlier CRT crossover trials, when CRT was implanted but left switched off and it could be argued that, once this became apparent, the MLWHFQ should have been removed as marker of response, as when a metric improves in all patients MLWHFQ then its discriminatory power is somewhat limited. This being said the difference in MLWHFQ was significant in responders but not so in nonresponders.

Response *a priori* was defined as an increase of 1ml/kg/min or more in peak VO₂, an increase by 10% or more in 6MWD, a decrease in LVEDV by 10% or more, and a decrease in the MLWHFQ score by 10 points. Responders were those patients that met all four of the criteria and nonresponders those that met less than three, or scored worse in any way, when compared to their baseline results, at the 6 and 12 month follow-up assessments. This nomenclature is used throughout the rest of this body of work. The responder-rate in this study was 14/19 or 74%. This in agreement with figures reported in the large randomised controlled trials irrespective of the multi-modal and more robust approach that was adopted to defining response, the high proportion (50%) of patients with AF who are typically excluded from CRT trials, or the level of comorbidity.

It is clear that different criteria could have been selected at the outset to increase the yield of 'responders' but then question as to whether the level of response was clinically meaningful would need to be addressed. It would also have been possible to optimise the choice of criteria based on emerging trends as the project progressed; by limiting the judgement to single criterion, a reduction in LVEDV, for example but this ignores the inherent variability of such a measure.

The strongest and only significant correlation between markers of response occurred between 6MWD and MLWHFQ, perhaps as these are both real world tests of how HF influences an individual on a day-to-day basis and so it makes sense that those with the most severe symptoms can walk the least. The correlation direction was negative, demonstrating that the further an individual could walk, the less severe their symptoms, which is logical. The lack of significant correlation with other markers of response (see table 36), may be due to small cohort size, the role of chance and variation in serial assessment of markers such as LVEDV or difficulties in 6MWD testing as reported. As already discussed, there is no absolute categorisation of positive or negative response and it does not necessarily follow that response in one criterion will lead to response in another. These are all specific and unique tests of an individual's HF condition and not interchangeable.

Table 36: Pearson’s correlation coefficient between markers of response

Correlation	PVO ₂		LVEDV		MLWHFQ	
	r	p	r	p	r	p
PVO ₂						
LVEDV	-0.24	0.93				
MLWHFQ	-0.24	0.79	0.22	0.71		
6MWD	0.34	0.11	0.11	0.37	-0.42	< 0.01

It is difficult to say how this correlation fits with the data from other trials as no correlations were drawn between different markers of response in CRT studies by other authors. However, this correlation is well known and has been demonstrated in other HF-LVSD trials¹⁹¹. Any other correlations that did exist, albeit non-significantly, were in the direction expected, for example a positive correlation between peak VO₂ with 6MWD and a negative correlation between MLWHQ score and LVEDV e.g. as the patient’s cardiorespiratory function improves as measured by increased peak VO₂ or reduced LVEDV, the patient can walk further and has fewer symptoms.

This is the first CRT study which reports follow-up data over 12 months, with measures of the cardiorespiratory performance such as peak VO₂. Importantly, it demonstrates that gains made in responders at 6 months are maintained at 12 months. Responders had significantly improved LV function, symptoms and cardiorespiratory fitness and thus are defined as deriving maximal benefit from their CRT device. Furthermore, the study demonstrates that peak VO₂, in addition to being arguably the ‘gold standard’ for cardiorespiratory function in HF-LVSD assessment, potentially has a role as the ‘gold standard’ for assessing response since only those patients who showed significant improvements in VO₂ demonstrated significant improvements in the remaining criteria. Finally, the study indicates that the potential placebo effect of CRT is not short-lived, with most nonresponders maintaining symptomatic improvements at 12 months based on the MLWHFQ, despite no significant improvement in other markers of response.

4.4 Conclusions

Fourteen of the nineteen patients have been classified as responders, the following chapters will investigate where this response could have been identified a priori but also whether there are other ways in which CRT improves the heart failure syndrome.

Chapter 5 Modelling

In this chapter, what a computational model is and isn't will be discussed, a number of models will be used in an attempt to model the heart as it fails but also to predict whether the response of the 14 patients to CRT could have been identified at baseline. The work in the following chapter was conducted in collaboration with others. Specifically in the lumped parameter work DW ran, analysed and interpreted the results of a pre-existing model created by Dr Yubing Shi and, similarly, in the 3D modelling work, DW created the meshes and analysed and interpreted the results but did not run or create the models used. These latter aspects were carried out by members of the group at KCL led by Professor Nic Smith.

5.1 Introduction

There are various types of models used in cardiovascular research from *in vitro* models of the myocyte, to *in vivo* animal models such as murine or porcine, to *in silico* computational models which employ mathematical equations to represent the cardiovascular system and complex computational software to solve them, both of which can be used to model the human heart and vasculature in health or in diseased states.

The purpose of a mathematical model is to investigate and predict results of scientific theories. Statistical analysis may reveal correlation between variables, but modelling can provide insight into the underlying mechanisms. The individual contribution of each component can be manipulated and assessed and there are fewer problems with ethics, scale or validity. The process is less resource intensive and is not reliant upon the presence of the actual item being modelled e.g. the failing heart. A model has been defined as a "a simplified or idealised description or conception of a particular system, situation, or process, often in mathematical terms, that is put forward as a basis for theoretical or empirical understanding, or for calculations, predictions, etc.; a conceptual or mental representation of something"¹⁹². Therefore it is a simplification, rather than an exact copy of reality, and as such it should contain only the essential elements and not be so complex that it becomes a 'replica'.

5.1.1 Computational Cardiovascular models

Whilst a cardiovascular model should capture the 'essence' of a specific problem and attempt to simplify the heart and/or vasculature in a way that is easy to manipulate, understand and quantify, for many years bioengineers have striven to compete with more and more complex models but it has become increasingly clear that, if such models are going to be used in clinical practice, they need to be as simple as possible. When considering using a computational model of physical process, the problem must first be precisely defined, secondly a mathematical model created and finally the model used to simulate the process.

When specifying a model, challenges include choosing what specific features to incorporate (or to exclude). Simple models provide elegant solutions, relying on parsimony and adopting the simplest assumptions when formulating a theory. They can aid understanding by allowing specific input parameters to be manipulated in real-time (which might be impossible in a living system), for example *if total peripheral resistance is increased by 50% what effect does this have on the cardiac output?* This can then lead to the generation of new hypotheses and further experiments, to confirm the findings. However, complex modelling techniques (which have been, more often than not, originally developed to address complex engineering problems) are increasingly being applied to clinical problems and, whilst it is perhaps understandable that high levels of complexity are often justified in the context of providing a better representation of reality, the so called "personalised model", more complex is not always the most useful. The ultimate goal is to develop a model which is tractable; input data required to run the model (which might include; images, physiological measurements, demographic data and so on) must be available and of adequate quality and models with high levels of complexity are often not easy or impossible to validate. They may also require significant time and computational resource to run.

There are various issues with the clinical deployment of such models in clinical medicine and to a large degree, they are treated with a degree of scepticism by clinicians, due to lack of understanding, concerns regarding legal implications e.g. what if it is wrong, time constraints and applicability to the individual patient. Critically, it is imperative that the model is validated, to ensure that it fits the data well and therefore provides robust answers to the questions posed.

5.1.2 Cardiovascular models in Clinical Use

Examples of models currently in use include the Seattle Heart Failure Model (SHFM); a well-validated model, which can be used to predict prognosis of HF-LVSD. It is Open Source (www.depts.washington.edu/shfm/) and accessible online. The required input parameters include patient- specific information such as current clinical status, therapy and laboratory results⁵³. There also exists a validated prediction model to aid clinicians in the diagnosis of HF-LVSD in the acute setting, with age, pre-test probability and NT-proBNP as input parameters

¹⁹³. This latter model has been further developed by using a statistical technique known as a support vector machine, utilising Bayesian theory to fill in missing data and analysing parameters such as Na⁺, BNP and EF. The use of the model is reported to improve diagnostic accuracy from 25-50% to 75%¹⁹⁴. These examples give insight into benefits that can be gained from simplifying the critical elements of a complex process (in this case prognosis and diagnosis) and representing them in terms of a model.

5.1.3 Model dimensionality

Computational models have varying degrees of complexity, from simple zero-dimensional or 'lumped-parameter' (LPM) models to sophisticated 3 dimensional models (see figure 27). According to Shi (2011) LPMs "assume a uniform distribution of the fundamental variables (pressure, flow and volume) within any particular compartment (organ, vessel or part of vessel) of the model at any instant in time" and are based upon ordinary differential equations (ODEs)¹⁹⁵. Other, more complex, distributed parameter models in 1-, 2- or 3-D recognise the variation of these parameters in space and use partial differential equations (PDE) to describe arterial pressure and flow¹⁹⁶. Thus the different dimensional levels can be considered in the following way; a LPM can be thought of as representing a time-dependent function as a single point in space, a 1-D model as a line modelling various points along the length (x axis) with time, a 2-D model as a plane modelling various points along length (x axis) and width (y axis) with time and the 3-D model extends across all three planes modelling various points along length (x), width (y) and depth (z axis). There is also the concept of a 4-D model, this is a unable to be implanted 3-D model with a time dimension, as seen for example during the contraction of the LV. However, due to demands in terms of computer processing, such models are very slow to run and can

take hours-weeks to create and run. In addition whilst technically and scientifically interesting, in general, they are of limited clinical use, certainly in the acute clinical setting when decisions need to be made in seconds or minutes.

There are two different types of multi-scale model, referring to either multiple spatial and temporal scales or multi-dimensions (i.e. zero-, 1-, 2-, or 3-D). In the former, the behaviour of a system is predicted using information from different spatial or temporal levels, for example knowledge of the cell, tissue, organ and then the system. In the latter, the term 'multi-scale' refers to coupling of a lower order model to a higher order, coupling a 3D model to a LPM model, for example. These can be used to answer complex questions without the need to model the whole domain of interest in 3-D. The EU FP7 project, euHeart (www.euheart.eu) is one example of a project which employed this approach.

Figure 27: Diagram showing increasing complexity of models from 0-3D

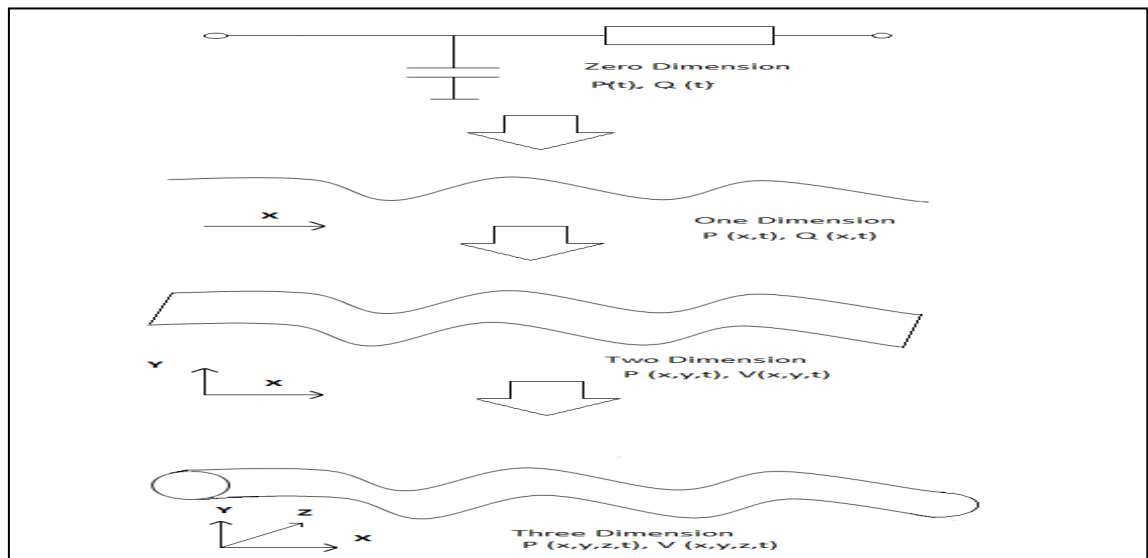


Figure 27 demonstrates the varying complexity of computational models from zero dimensions e.g. lumped parameter model where a time-dependent function is a single point in space, to three dimensions,

$P = \text{pressure}$, $Q = \text{flow}$, $V = \text{volume}$, $t = \text{time}$, $x = \text{length}$, $y = \text{width}$ and $z = \text{depth}$.

Here, simple LPM models were used to represent the afterload whilst complex 3-D models can then be used to predict the detailed fluid dynamics within the ventricle,

the myocardial wall mechanics or the dynamic electrophysiological excitation map. This combination of modelling techniques allows an area of interest to be modelled in detail, perhaps based on information from clinical images, leading to the development of patient-specific models, whilst keeping computing resources to a minimum.

5.1.4 Boundary conditions

When modelling complex physiological systems, the equations used rarely yield analytical solutions and so the systems are discretised by sampling at points within the domain to make them tractable for computational solution. Computer models required mathematical assumptions to reduce the complexity, time and cost of the simulation. Thus boundary conditions can be considered pre-specified, time varying values of displacement, velocity, pressure or derived properties. In computational biomedicine, the combination of material properties of the system and boundary conditions can be used to describe the unique physiological conditions to make the model patient specific. An example of a boundary condition in CFD would be the vessel wall, for example. The argument for using approximated values e.g. population averages for material properties and boundary conditions lies on the ability to collect more precise readings and the level of confidence in the measurements. However, the simulation must be specific enough to truly represent the system of interest, thus there is inherent conflict between the desire to make the model as patient-specific as possible and the resulting requirement to make an ever increasing number of measurements to achieve this end.

5.2 Pressure-Volume loops

There are several ways of quantifying the performance of the LV, ranging from non-invasive measurements such as EF (%) and cardiac index ($l/min/m^2$) to invasive measurements such as dP/dt and elastance (E_{max}). Whilst there are advantages and disadvantages to each method, when constructing a cardiovascular model, elastance acquired using a pressure-volume (PV) loop is preferred as it is load-independent measure of LV performance where as EF% and dP/dt are dependent on several extra-cardiac e.g. preload, afterload and intra-cardiac factors e.g. synchronicity of contraction and heart rate. Whilst performing invasive measures such as E_{max} carry clinical risk, because they are load and heart rate dependent it is felt they are more

robust, reproducible, specific and accurate measure of the intrinsic work of the system of interest.

To create a PV loop of the LV, a cardiac catheter tipped with a micro-manometer is passed trans-femorally to the LV apex, where it records real-time pressures. The volume of the LV can be calculated with left ventriculography using the conductance method (via the same catheter) or by using simultaneous real-time echocardiography. Pressures and volumes can be sampled repeatedly during a single cardiac cycle, and pressures plotted against volumes to create a loop (figures 28 and 29). LV filling conditions can be manipulated (using caval occlusion to reduce the pre-load or adrenaline to increase the afterload, for example) and the resulting changes in the PV loop mapped, with HR kept constant by the use of a temporary pacing wire. If the data points acquired at maximal pressure and minimal volume, are connected from the range of loops described, they will describe the end-systolic pressure-volume relation (ESPVR), the slope of which is the end-systolic elastance which represents systolic contractility. Similarly if the data points acquired at minimal pressure and maximal volume are connected, the end diastolic pressure volume relation (EDPVR) is described. The slope of this is the E_{min} , representing diastolic stiffness. The shape and size of the loops are characteristic of different disease states, such as HF, LVH and LVSD, which affect systolic and diastolic function to differing degrees.

Figure 28: Cardiac cycle and PV loop

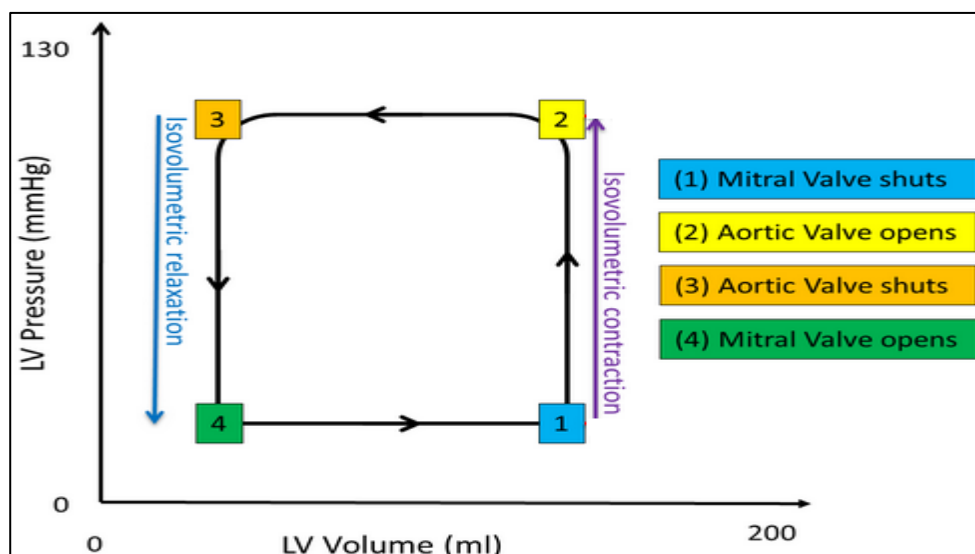


Figure 28 demonstrates a schematic of a pressure-volume loop of the left ventricle, demonstrating the changes in pressure and volume according to the phase of the cardiac cycle.

Figure 29: Measurement and formation of a LV PV loop

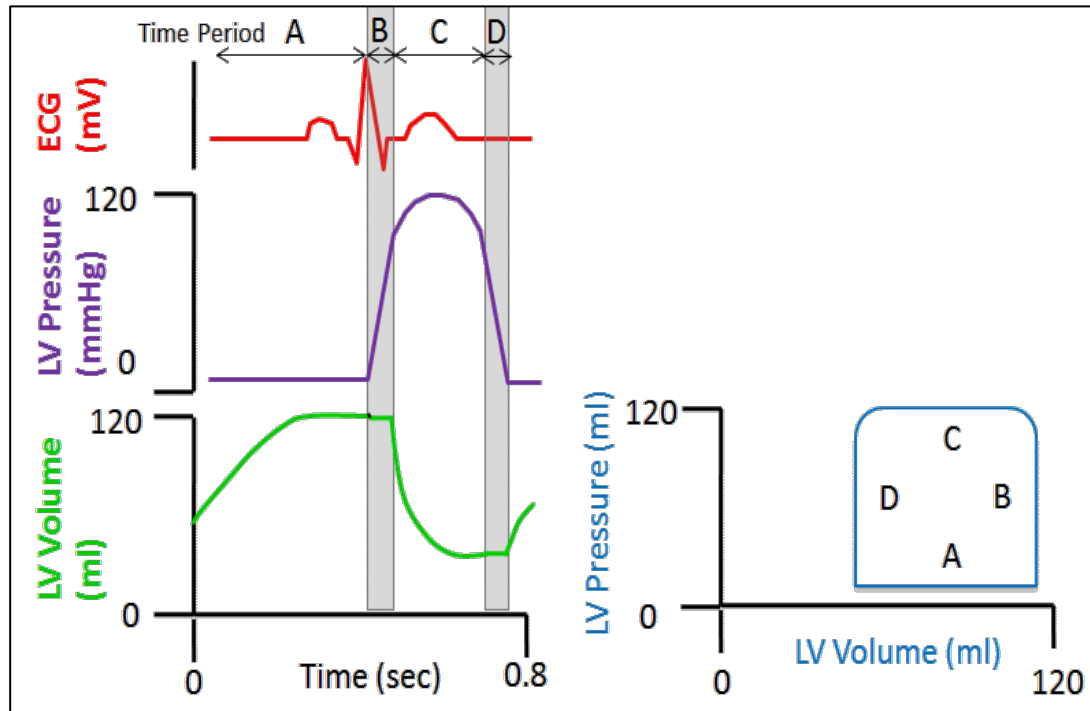


Figure 29 demonstrates how the PV loop is derived, on the left, from the ECG at the top denoting the phase of the cardiac cycle, the LV pressure and LV volume below, with time along the x axis, which is converted into a loop seen on the right.

PV loops are often used in animal models and in clinical heart failure experiments but are not performed routinely in clinical practice. This is primarily due to the preference for EF%, which like Emax is a late-systolic index of LV performance but is conceptually simple, non-invasive and easy to determine and reproduce. Furthermore it has extensively documented clinical utility, using a variety of imaging modalities. In contrast, the PV loop is dependent on LV volume and mass and its use is limited by age- and gender-dependent variability. Also, changes in RV filling pressure can affect the position of the interventricular septum, altering LV diastolic pressure and thus the resulting PV-relationship. Despite these reservations the PV loop can provide valuable insight. In engineering terms it describes the work carried out by a system; the case of

the heart the LV-PV loop describes the work expended by the LV during contraction. For this reason, the PV loop offers valuable insight into the behaviour of the LV during HF-LVSD and response to treatment such as CRT.

5.3 Zero-Dimensional Models

5.3.1 Introduction

Blood flow in the circulation obeys the laws of physics, which govern energy, mass and momentum conservation. LPM models are best thought of in terms of hydraulic-electrical analogues; just as in an electrical circuit the voltage gradient determines the flow of current, the flow of blood in the cardiovascular system is determined by the pressure gradient and so such LPM can be used to simulate physiology and pathophysiology of the cardiovascular system, furthering understanding.

Table 37: Components of LPM models, their meaning and units of measurement

Symbol	Meaning		Units
	Electrical	Physiological	
<i>C</i>	Capacitance	Vessel compliance	mmHg/ml
<i>R</i>	Resistance	Frictional losses	mmHg*sec/ml
<i>L</i>	Inertance	Blood rheology	mmHg*sec/ml

Factors influencing flow in an electrical circuit are the capacitance (*C*), resistance (*R*) and inertance (*L*); and the corollaries of these in the human circulation are the elasticity of the blood vessel wall, the frictional losses encountered and the rheology of the blood respectively (table 37). Parameters of the electrical model can be adjusted to simulate various pathological conditions and the consequences of such adjustments can be explored, for example increasing resistance and reducing capacitance can simulate systemic hypertension. As in an electrical circuit, components can be organised in series or in parallel, which will influence the current and the voltage measured.

In an electrical circuit, a capacitor typically comprises 2 electrical conductors, separated by an insulator; it functions to store electrical energy. The capacitance is the ratio of the charge on each conductor (*Q*) to the voltage (*V*) between them

(Capacitance = Q/V). In a vascular circuit, its corollary is compliance, which can be defined as the change in volume with change in pressure (Compliance = V/P). Compliance represents the elasticity of the large central arteries. For example, the aorta buffers the pulsatile nature of the flow ejected the left ventricle at systole and then, during diastole, elastic recoil of the aorta returns energy to the blood to help to maintain forward flow. Compliance is the reciprocal of stiffness. Thus the greater the change in volume mediated by a change in pressure, the greater the compliance and vice versa. Elastance is represented in LPM by a variable capacitor, whose capacity can be changed intentionally and repeatedly, representing the volume of blood in a cardiac chamber, such as the atria or ventricles.

In the electrical analogue, resistance can be described by Ohm's law ($I = V/R$), where resistance (R) is the ratio of the voltage (V) across the resistor's terminals to the magnitude of the current (I) in an electrical circuit. In a vascular circuit, the equivalent to electrical resistance is peripheral resistance (PR) which is governed, primarily, by the small distal arteries and arterioles. Together these provide a variable resistance, via vessel calibre change, to ensure the blood supply to the periphery remains constant. PR can be defined as the change in pressure gradient across the vascular tree with change in flow ($R = \Delta P/Q$), therefore the greater the change in pressure mediated by a change in flow, the greater the resistance and vice versa.

Inertance can be defined as the pressure gradient in the fluid that is needed to change the flow rate with time ($L = P \times l/A$), determined by the density of the fluid (P), the length of the tube (l) and the cross sectional area of the tube (A). In the human, this accounts for the inertia of the entire vascular tree. Therefore, the greater the density (of blood) and longer the length of the tube (vascular tree) the greater the inertia, and the greater the cross sectional area of the tube (vessel) the smaller the inertia.

Figure 30: A 2-component Windkessel model

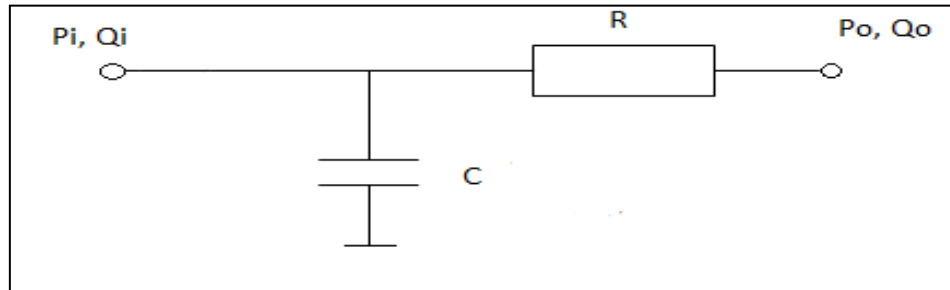


Figure 30 demonstrates a simple 2 component “Windkessel” lumped parameter model with a capacitor and a resistor, representing total arterial compliance and systemic vascular resistance respectively.

Diodes are used as electrical analogues of valves. A diode contains two leads, like a resistor but Ohm’s law does not apply; the resistance is low in one direction and high in the other. Similarly, valves in heart, when competent, have a very high resistance to backward flow and very low resistance to forward flow.

Together all of these components can be used to create models, which are electrical analogues of varying levels of complexity representing the cardiovascular system; the arterial system is thus comprised of capacitors and resistors and the heart chambers represented by capacitors and diodes.

The earliest form this type of model originates from 1899 and is called the ‘Windkessel’ model, a term meaning ‘air chamber’ in German. In this model, Otto Frank described the arterial system as a single elastic chamber (Figure 30), comprising two elements; a capacitor representing the large arteries, which determine total arterial compliance (C) and a resistor representing the smaller vessels, which determine the peripheral vascular resistance (R). These factors affect the ingoing (i) pressure and flow thus giving the outgoing (o) pressure and flow.

This simple model is still used today with many currently-used models still based on expansion of the simple RC unit with the addition of further R, C or, indeed, L components. Whilst being able to model the basic behaviour of the arterial tree, the 2-element model lacks accuracy in terms of the high frequency behaviour of the

system. Accuracy can be improved by adding an extra element - the characteristic impedance of the system -representing the proximal aorta in terms of local blood inertia and vessel compliance. Since the resulting 3-element model still tends to overestimate C and R, inclusion of a 4th element, the inertance, was proposed by Segers et al (2008) ¹⁹⁷.

A large number of LPM models varying levels of complexity can be found in the literature. These range from the simple single-compartment RLC models such as the Windkessel model where the whole of the systemic or pulmonary vasculature is treated as a single entity, to multi-compartment models where the vascular system is discretised into units, with the aorta, arteries, arterioles, capillaries and veins each having their own unique properties. In this way, the entire cardiovascular system can be modelled using a series of resistances, inductances and compliances without following anatomical convention.

Some researchers have adopted an alternative approach attempting to map out the entire human anatomical vascular tree by creating a multi-branched multi-compartmental model. The obvious caveat here is that increasing complexity parameters may be accompanied by increasing potential for error ¹⁹⁸. Models can also be divided into those which are open loop, in that a specified pressure or flow is applied to a given afterload and the results recorded, or closed loop where there is conservation of blood volume throughout the circulation and the output is affected by preload and afterload.

5.3.2 Cardiac models

LPMs can be further sub-divided into non-pulsatile¹⁹⁹ or pulsatile²⁰⁰ models. In the former, Starling's Laws are used to describe heart function but for pulsatile models the heart chambers are based on a time-varying elastance function and, as mentioned above, the heart valves are represented by diodes. The time-varying elastance model is simple to comprehend and use and as a consequence, has been widely adopted by the modelling community.

5.3.3 *Gap in the evidence*

Whilst LPM models have been used to attempt to understand the behaviour of the failing and the response to therapy (with support from an LVAD, for example) there has been no attempt to triage the importance of the various components and therefore understand precisely what impact the parameters have on the output of the model. Is the LV more important than the R and C in determining LV output or the patient's symptoms, for example? Furthermore, none have been employed to model response to therapy, such as CRT.

Yuexian et al (2009), used a complex model, based on a Windkessel circulation with embedded autonomic nervous system and renal blood volume adjustment, reduced the contractility of the LV, modelled with a variable capacitor, by 50% to simulate HF-LVSD²⁰¹. The rationale for this approach is not clear; it is unlikely that a 50% reduction of LV contractility will be relevant to all cases of HF-LVSD and the authors fail to give a reason, reference or justification for such a value. Other researchers²⁰² have tried to model biventricular failure in a pig with a VAD device *in situ*, by reducing LV and RV contractility, rather than that of the LV alone. This is a step forward but ignores the potential role of other components such as the LA. Similarly, Hsu et al (2008)²⁰³ looked at end-stage HF-LVSD by halving the LV contractility whilst increasing the LV volumes, systemic and total arterial resistances but this again ignores the potential role of many other components which are known to change in end-stage HF-LVSD such as the RV. A more realistic model of HF would encompass changes in all these components and more. For example, Di Molfetta et al (2010)²⁰⁴ used a variable elastance model of the ventricles including the septum, which enabled intra- and inter-ventricular delay and the result of biventricular stimulation to be modelled, coupled with a LPM of the downstream systemic vasculature. The researchers used the model in an attempt to improve biventricular synchronisation in CRT and "reproduce clinical data and also estimate the trend of parameters which are difficult to measure".

5.3.4 *Problems with lumped parameter cardiovascular models*

According to Shi et al (2011), once a reference range has been found for the parameters, the majority of input variables must be derived by a process of trial and error to see if these match the measured output data¹⁹⁵. There is an immediate problem here, for whilst these may be valid mathematically, this does not necessarily

mean that they will have a clinical correlate. In addition, this process is long and slow and there is a lack of consistency amongst researchers when choosing parameters such as LV elastance, for example²⁰⁵⁻²⁰⁸. This is a result of difficulties in parameter setting. First, because of the invasive nature of measuring such values *in vivo* many of these are unknown. Second, individual models may have more than one combination of input variables, which give the same desired output. And third, different models may use different components and thus entirely different parameters. It is clear that within the clinical community, such studies will not be considered valid and robust the absence of real (e.g. *in vivo* measured) variables using data associated with the specific human heart being modelled rather than arbitrary numbers. Whilst there is a general paucity of data available for healthy control subjects, some studies have attempted to address this by using parameters taken from by comparing simulated model performance with *in vivo* measurements, such as aortic pressure recordings using catheters in both healthy normal¹⁹⁷ and patients with HTN²⁰⁹ or HF^{206 210}. Other aspects of the cardiovascular circulation which have not been interrogated include the influence of AV or interventricular dyssynchrony. From a clinical perspective, LPMs are, at best, rudimentary but they have the advantages of being simple, easy to manipulate, quick to run, and place low demands on computing resources. It is important to reiterate that whilst more complex models may give a richer set of results, they do not necessarily give more accurate results, but rather, the model must be fit for the purpose for which it is employed.

5.3.5 Models of the progression heart failure

To date no model has systemically attempted to show the progression of heart failure from normality, through onset to end stage. However researchers have been able to show differences in vascular compliance, resistance and also left ventricular elastance. A single paper by Tsuruta et al (1994)²¹¹ demonstrated that it is possible to simulate the various stages of the Forrester classification of HF-LVSD, using hypothetical patient parameters, but as previously mentioned, this represents acute decompensated HF-LVSD after MI and does not describe other aetiologies, such as non-ischaemic disease. Arnold et al (1991)²¹² used pulsed wave velocity (PWV) to demonstrate that brachial artery diameter and compliance decreased as HF-LVSD symptom severity increased, using a propagative model derived from the Moens-Korteweg formula, used to model

the relationship between PVW and the compliance of the arterial wall. Furthermore, Duprez et al (1998) ²¹³, in one of the first high profile uses of lumped parameter models in a clinical paper, showed that there was an inverse relationship between large artery compliance and aldosterone, despite treatment with full dose ACE-inhibitors and diuretics. Unfortunately patients were not stratified according to HF severity, but this was proven to be the case in a similar study, albeit on patients with HFPEF ²¹⁴.

5.4 Lumped parameter modelling of HF progression

5.4.1 Introduction

In 2001, the joint AHA/ACC taskforce guidelines²¹⁵ attempted, for the first time, to categorise HF and its progression in terms of pathophysiology (see table 38). This initiative was intended to “complement” the pre-existing New York Heart Association (NYHA) functional classification and describe the development of LV dysfunction from patients with a high risk of HF e.g. hypertension (Stage A) to those with severe and symptomatic HF e.g. requiring transplant (Stage D). However, this classification is qualitative; focusing on describing each stage and open to misinterpretation ¹¹⁵.

It is clear that definition of quantitative measures for each stage could be of significant benefit since they could be used to chart the pathophysiology, improve risk-stratification and the prediction of response to clinical interventions. To date, attempts to categorise patients into individual stages have concentrated on indirect measures, such as biomarkers e.g. BNP, which nonetheless improve prognostication ¹²⁴.

Table 38: AHA/ACC stages of HF

Stage	Description	Examples
O*	No risk, heart disease or symptoms	Healthy adults
A	Risk of HF but without structural heart disease	Hypertension
B	Structural heart disease without signs or symptoms of HF	Previous myocardial infarction
C	Structural heart disease with prior or current symptoms of HF	Requiring routine HF drugs
D	Refractory HF requiring specialist intervention	Heart transplant

*O – this stage is not included in the AHA/ACC classification but has been added for completeness.

The focus of the current study is the population of patients with HF-LVSD. This decision was based on both pragmatic and therapeutic considerations since only patients with HF-LVSD have therapeutic interventions that are associated with significant impact on morbidity and mortality. There have been many studies looking at LV PV loops in patients with heart disease, but this is the first attempt to collate and compare these.

When seeking to model LV performance, quantitative data is vital to ensure that what is being modelled is an accurate representation of reality. Previous attempts to model the heart as it fails, and the effect of potential therapies, pre-date the AHA/ACC classification and apply hypothetical haemodynamic states according to Forrester class¹¹⁸ rather than actual patient data^{211 216}. Current computational models of HF-LVSD, whether zero-dimensional or multi-scale, choose arbitrary parameters for the LV such as reducing elastance by 50% or use boundary conditions such as resistance and compliance, which are not directly based on data from HF-LVSD patients. The aim of this work was been to provide specific LV performance and systemic vascular data on a population basis, from a healthy to a failing heart.

Figure 31: A lumped parameter model with 2-element afterload

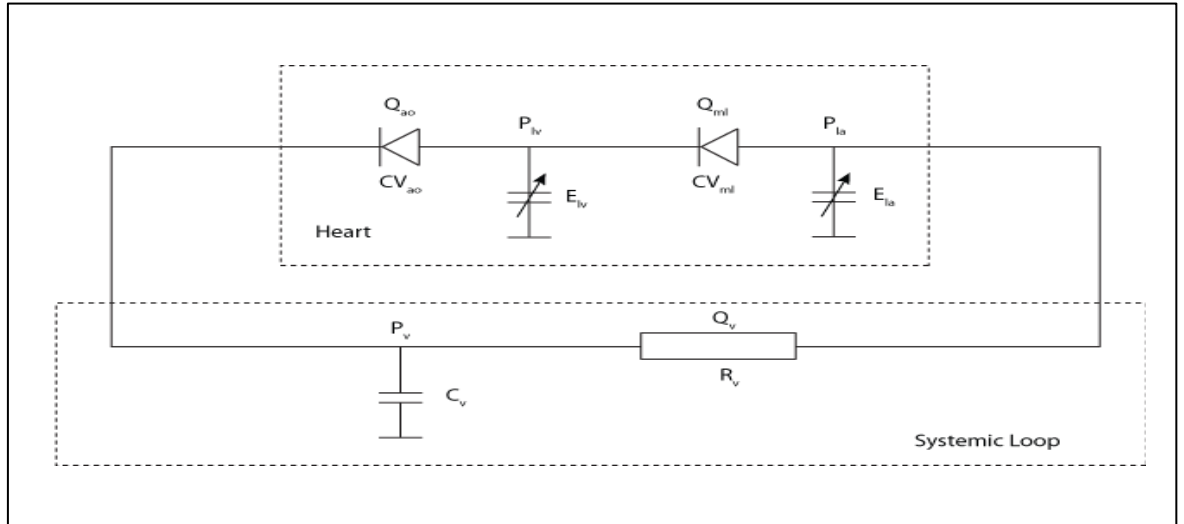


Figure 31 demonstrates a closed loop lumped parameter model with diodes for aortic (CV_{ao}) and mitral valves (CV_{mi}), variable capacitors for left ventricle (E_{lv}) and left atrium (E_{la}) and a capacitor and resistor representing the systemic circulation, used in this chapter to model the left ventricle as it fails.

This would provide a quantitative assessment of each AHA/ACC stage of HF and, for the first time, define risk and onset and progression of HF-LVSD according to changes in the physical properties of the left ventricle as represented by left ventricular pressure-volume loops. The choice of the pressure-volume (PV) loop in this context is based on its direct description of the performance of the LV in real time making it superior to the blunt instrument of measuring systolic function through fractional shortening or ejection fraction (LVEF). The PV loop allows appropriate classification and understanding of the process by which heart failure develops, irrespective of whether it is related to systolic or diastolic dysfunction.

5.4.2 Methods

5.4.2.1 Pressure Volume loops

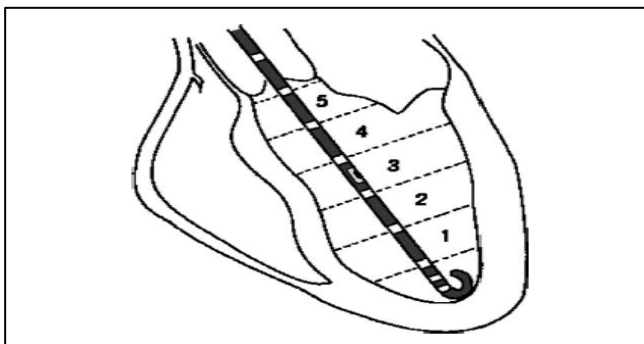


Figure 32: PV conductance catheter in the LV

Figure 32 demonstrates the PV ‘pig-tail’ shaped catheter in the left ventricle, with manometer at level 3 and multiple electrodes along the

catheter used to divide the LV into segments and using conductance measure the change in volume of each segment.

The methodology for PV loop acquisition has been described in detail previously ²¹⁷. Briefly, a catheter is inserted via the femoral artery to the apex of the LV cavity under fluoroscopy. Real-time measurement of pressure is performed using a micro-manometer on the catheter. Ventricular volume is recorded using the conductance method, in which multiple electrodes situated along the catheter measure the electrical conductance of arbitrary segments within the LV blood pool; the summation of these represents the total volume of the LV cavity (see figure 32).

To collect data for a meta-analysis of PV loops from the published literature an online search of Pubmed, Web of Knowledge, Medline and Google images was conducted, using the search term “pressure-volume loop”. In order to be included in the final analysis the resulting references were studied to check that they met specific criteria (see table 39).

5.4.2.2 Inclusion criteria:

- Studies with complete LV PV loops in adult humans.
- (and) Studies representing any AHA/ACC stage including healthy normal subjects.
- (and) HF, if present, due to LV systolic dysfunction only.

5.4.2.3 Exclusion criteria:

- Diastolic heart failure or HFPEF.
- HF secondary to an uncertain or uncommon cause such as Chagas’ disease.
- An unclear past medical, symptom or drug history.
- Absence of pictorial representations of entire loop e.g. diastolic limb only.
- Acquisition during experimental treatment without baseline measure.

Table 39: HF studies used in LV PV loop modelling

Class		Author	Year	
NYHA	ACC/AHA			
N/A	O and A	Kelly	1992	
		Redington	1988	
I	B	Magorien	1983	
		Thormann	1990/91/92	
		Thormann	1990	
		Schreuder	1991	
		Kelly	1992	
		Hayward	2001	
		Urheim	2002	
		ten Brinke	2010	
II	C	Smith	1974	
		Sonntag	2004	
		Thormann	2008	
		Remmelink	2009/10	
III		Feldman	1996	
		Macgowan	1998	
		Kim	1999	
		Dekker	2004	
		Steendijk	2006	
		Kashimura	2007	
IV		D	Herrmann	1987
			Aroney	1989
	Schreuder		1995	
	Kass		1995	
	Lorusso		1997	
	Hayward		1999	
	Kawaguchi		2001	
	Schreuder		2005	
	Ferrari		2005	
	Tulner		2006	
	ten Brinke		2010	

Of the 351 papers identified only 31²¹⁷⁻²⁴⁷ satisfied all of the inclusion, and none of the exclusion, criteria and were subsequently included in the final analysis. These included data from 203 patients.

The graphical images of PV loops captured from the papers online using a screenshot, were uploaded into an open access analysis software package (Engauge digitizing software <http://digitizer.sourceforge.net/>) and converted into numbers (see figure 33)

Figure 33: Screenshot using Engauge software to digitize a PV loop

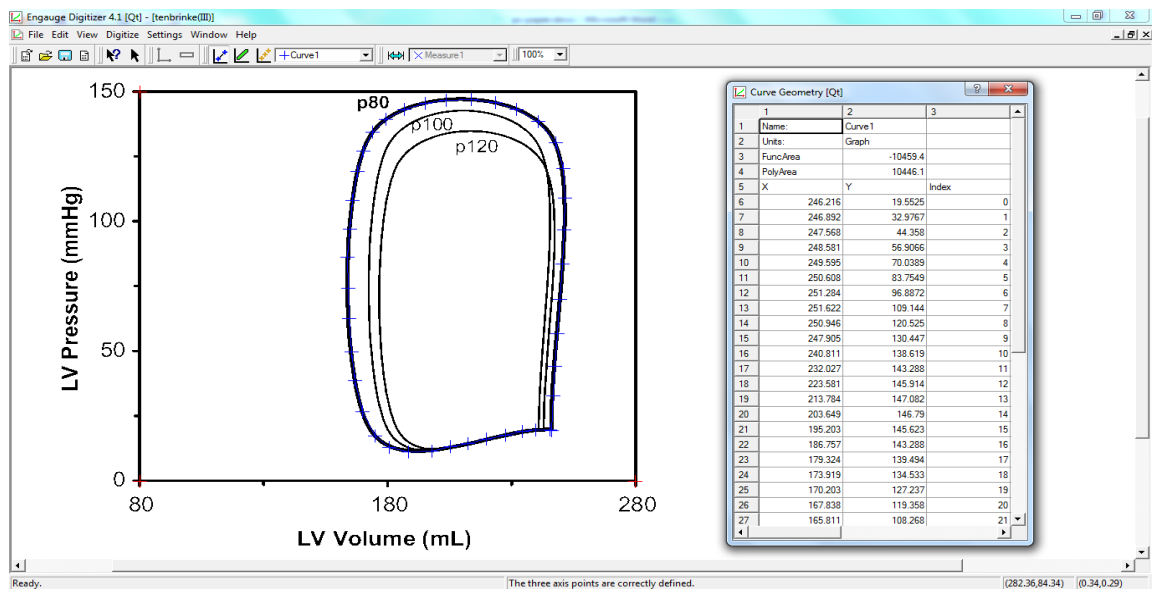


Figure 33 demonstrates the use of Engauge software to digitise an existing PV loop from a published study, on the left is a PV loop, the red crosses are used to set the axes, the blue crosses auto-populate the loop and this results in the database on the right.

5.4.2.4 Modelling the PV loops

As discussed numerous computational models of the cardiovascular system, of different levels of complexity, ranging from simple lumped parameter models, to more complex 3 dimensional models can be found in the literature. Lumped parameter models can describe the changes in pressure, volume and flow that occur over the cardiac cycle as a function of cardiac performance and systemic afterload. This model presents the numerical values of the four parameters in the simplest possible representation of the heart and systemic circulation, the components of which are

described below. The progression of heart failure is thus expressed in terms of the evolution of these four parameters. Furthermore it is suggested that the values of the components that represent the systemic afterload might be used to determine appropriate boundary conditions for the modeller who is interested in using such representations to provide boundary conditions for complex, anatomically-accurate 3D models of the left ventricle.

For this study, a LPM (see figure 31) with a variable elastance LV and 2 element (R and C) Windkessel afterload was chosen to model the LV in HF²⁴⁹. This was downloaded from the CellML (<http://www.cellml.org/>) model repository, (a free-to-access store of computer- based mathematical models) and run using OpenCell, an open source platform for working with CellML models²⁵⁰.

To model the mean AHA/ACC PV loops, the Matlab (The Mathworks Inc, Cambridge, UK) optimisation toolbox was used to find the combination of parameters that best fitted the data of both the mean and the individual loops. The resulting model PV loop data was exported to an excel spread sheet (Microsoft Inc, Redmond, US) and compared against the mean PV loop.

Figure 34: Screenshot using OpenCell to model cardiovascular haemodynamics

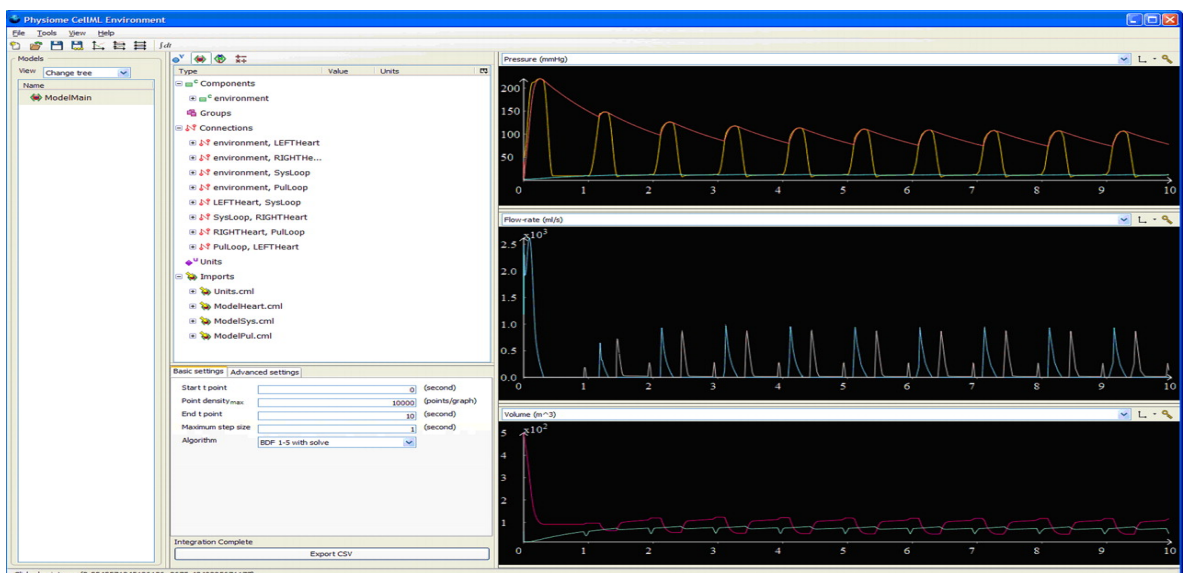


Figure 34 demonstrates a screenshot of Opencell, with different components of the model listed on the left and on the right, the aortic and left ventricular pressure in the

top frame, pulmonary and aortic flow in the middle frame and left atrial and left ventricular volume in the bottom frame.

5.4.3 Results

5.4.3.1 Mean Pressure Volume loops

The majority of the patients within each AHA/ACC category are males in their late fifties (table 40) and some AHA/ACC HF-LVSD stage groups have more patients than others. Group A is dominated by patients with ischaemic heart disease (IHD), rather than other risk factors such as obesity or diabetes. However there is a balanced distribution of HF aetiologies in groups C and D, with both ischaemic and idiopathic dilated cardiomyopathy (DCM) accounting for approximately 50% of cases in each.

Table 40: Demographics and aetiology of HF

HF Stage			O	A	B	C	D			
Demographics	Patients	N =	2	65	6	42	88			
	Gender	% male	100	65	83	88	81			
	Age	mean	29	56	59	60	58			
Aetiology	HTN	%		7						
	IHD	%		93						
	MI	%						100		
	Ischaemic	%							50	54
	Non-ischaemic	%								50

For brevity, raw and mean loops are just shown for a single stage, AHA/ACC D (figure 35) but from these, it is evident that even within end-stage HF, there is significant individual variation, both in terms of LV pressure and volume.

Table 41: Comparison of data for each HF stage, using 2-tailed Student's T-test

AHA/ACC HF Stage	Parameter	Unit	O	A	B	C	D
O	LVEDV	(ml)		$p = 0.31$	$p = 0.27$	$p < 0.05$	$p < 0.05$
	LVESV	(ml)		$p = 0.22$	$p = 0.13$	$p < 0.01$	$p < 0.05$
	SV	(ml)		$p = 0.49$	$p = 0.13$	$p = 0.11$	$p < 0.001$
	EF	(%)		$p = 0.19$	$p < 0.05$	$p < 0.001$	$p < 0.001$
A	LVEDV	(ml)			$p = 0.37$	$p < 0.001$	$p < 0.001$
	LVESV	(ml)			$p = 0.05$	$p < 0.001$	$p < 0.001$
	SV	(ml)			$p < 0.05$	$p < 0.01$	$p < 0.001$
	EF	(%)			$p < 0.01$	$p < 0.001$	$p < 0.001$
B	LVEDV	(ml)				$p < 0.01$	$p < 0.01$
	LVESV	(ml)				$p < 0.01$	$p < 0.001$
	SV	(ml)				$p = 0.39$	$p < 0.001$
	EF	(%)				$p < 0.01$	$p < 0.001$
C	LVEDV	(ml)					$p = 0.09$
	LVESV	(ml)					$p = 0.08$
	SV	(ml)					$p = 0.40$
	EF	(%)					$p < 0.05$

Table 42: LPM variables for each model, compared using 2-tailed Student's T-test

AHA/ACC HF Stage	Parameter	Unit	O	A	B	C	D
O	E _{max}	(mmhg/ml)		$p = 0.76$	$p = 0.81$	$p < 0.001$	$p < 0.001$
	E _{min}	(mmhg/ml)		$p = 0.71$	$p = 0.65$	$p = 0.98$	$p = 0.77$
	LV Volume	(ml)		$p = 0.76$	$p = 0.81$	$p = 0.17$	$p < 0.001$
	Resistance	(mmhg•s/ml)		$p = 0.06$	$p = 0.25$	$p = 0.48$	$p = 0.37$
	Capacitance	(ml/mmhg)		$p = 0.67$	$p = 0.93$	$p = 0.71$	$p = 0.80$
A	E _{max}	(mmhg/ml)			$p = 0.63$	$p < 0.001$	$p < 0.001$
	E _{min}	(mmhg/ml)			$p = 0.06$	$p < 0.05$	$p < 0.001$
	LV Volume	(ml)			$p = 0.27$	$p < 0.05$	$p = 0.53$
	Resistance	(mmhg•s/ml)			$p = 0.36$	$p = 0.21$	$p = 0.08$
	Capacitance	(ml/mmhg)			$p = 0.41$	$p = 0.06$	$p = 0.07$
B	E _{max}	(mmhg/ml)				$p < 0.01$	$p < 0.001$
	E _{min}	(mmhg/ml)				$p = 0.16$	$p < 0.001$
	LV Volume	(ml)				$p = 0.88$	$p = 0.35$
	Resistance	(mmhg•s/ml)				$p = 0.88$	$p = 0.35$
	Capacitance	(ml/mmhg)				$p = 0.63$	$p = 0.35$
C	E _{max}	(mmhg/ml)					$p = 0.43$
	E _{min}	(mmhg/ml)					$p = 0.25$
	LV Volume	(ml)					$p = 0.25$
	Resistance	(mmhg•s/ml)					$p < 0.05$
	Capacitance	(ml/mmhg)					$p = 0.9$

Table 41 demonstrates, that there is no statistically significance differences between stages O and A or B, but together they are significantly different from stages C and D in all variables. There are no significant differences between stages C and D. Table 42 demonstrates, that whilst there is no statistically significance difference between model parameters between stages O and A or B, they are significantly different from stages C and D in Emax only. There were no significant differences between stages C and D.

Figure 35: Mean (triangles) and individual LV PV loops (lines) from Stage D

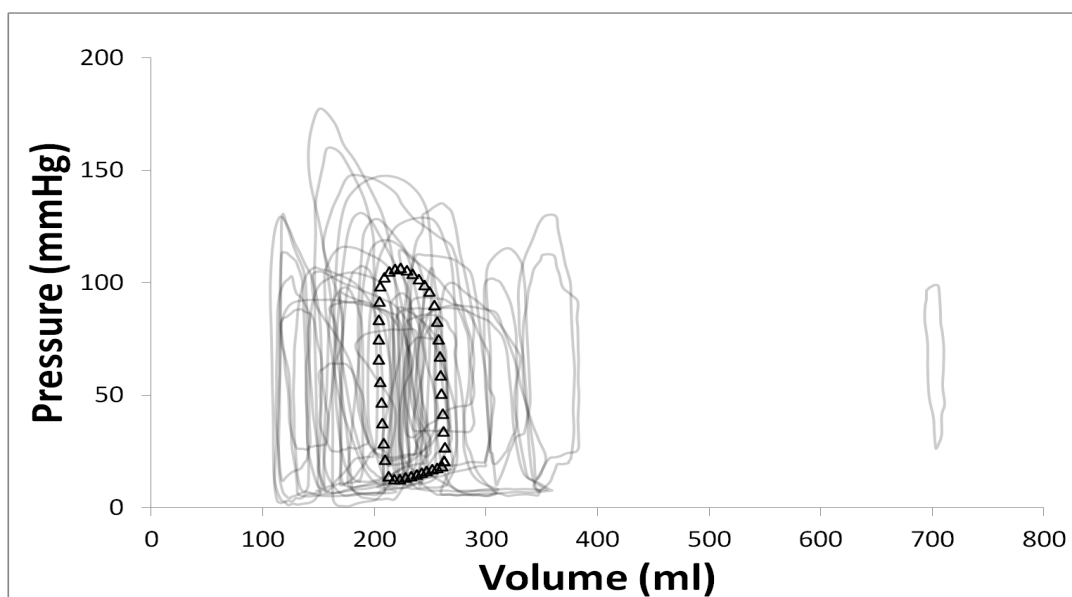


Figure 37 demonstrates the pressure volume loops of all the patients who comprise stage D in solid grey, with the mean pressure volume loop in black triangles.

As can be seen from figure 37, there is a conformational difference not only between all HF-LVSD groups (O, A, B, C, D) but also between asymptomatic and at risk groups O, A, B and those in symptomatic HF groups C, D. Table 41 shows that as a patient progresses from normal LV function to symptomatic LVSD-HF, LV volumes and diastolic pressures rise, and stroke volume (SV), ejection fraction (EF%) and systolic pressure fall. Furthermore, elastance and contractility of the LV fall as HF-LVSD progresses.

Figure 36: Mean (thick) and individual PV loops (thin) from all HF Stages

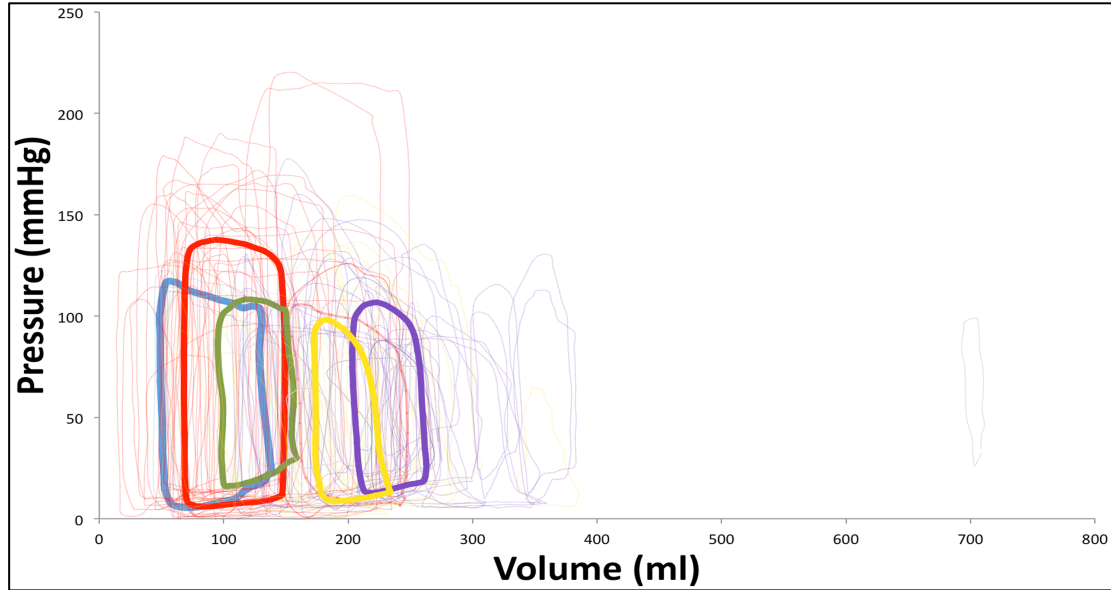


Figure 36 demonstrates the individual patients which make up each stage and are colour coded accordingly (thin faint lines) with the mean loops of each stage (solid thick line). Blue = Stage O (healthy individuals), Red = Stage A (risk of LVSD), Green = Stage B (asymptomatic LVSD), Yellow = Stage C (symptomatic HF-LVSD) and Purple = Stage D (end stage HF-LVSD)

Table 43: LV parameters according to each ACC/AHA HF stage, mean and (SD)

Stage		O	A	B	C	D
LV parameters	LVESV (ml)	48.2 (6.4)	65.9 (50.3)	93.5 (48.1)	165.6 (61.4)	210.3 (96.1)
	LVEDV (ml)	138.2 (21.8)	154.1 (30.1)	161.7 (49.1)	236.6 (62.2)	271.8 (98.4)
	SV (ml)	89.9 (143.3)	88.4 (29.1)	68.1 (23.3)	70.9 (21.4)	68.4 (30.6)
	EF (%)	0.65 (0.01)	0.57 (0.10)	0.45 (0.16)	0.32 (0.10)	0.25 (0.10)
	E _{max} (mmHg/ml)	2.23 (0.26)	2.27 (0.29)	1.32 (0.73)	0.63 (0.36)	0.55 (0.23)
	E _{min} (mmHg/ml)	0.17 (0.01)	0.09 (0.06)	0.10 (0.03)	0.06 (0.04)	0.08 (0.04)

5.4.3.2 Modelled Pressure Volume loops

For the modelled PV loops (see figure 37) on gross appearance it appears there is a more accurate fit, in terms of shape and size, for the loops representing the earlier

AHA/ACC HF stages, which reduces as LV contraction deteriorates and the HF-LVSD stage progresses. Table 43 shows how the modelled LV elastance falls from a normal LV to end-stage HF- LVSD; the volume of the LV increases whilst the resistance and compliance of the systemic vasculature remain unchanged.

Figure 37: Modelled (lines) and mean (shapes) loops according to HF stage

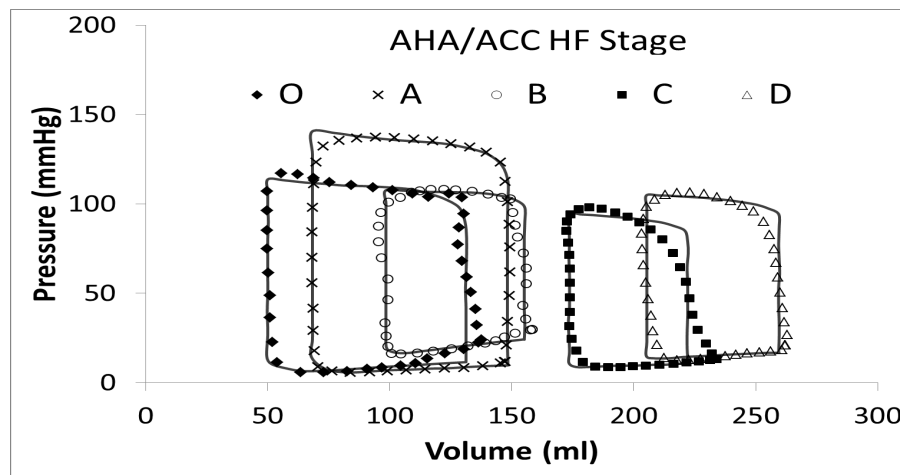


Figure 37 demonstrates the mean pressure volume loop from each stage in different shapes with the modelled loop in solid black line.

Finally, a comparison was made between the area error for the modelled loops and the mean, to give a measurement of accuracy (figure 38). Since the modelled loops are based on mean data, modelling the area as well as the shape of the PV loops is important. Thus a comparison was made between the overlapping area of the mean and modelled loops as a measure of closeness-of-fit against that area which did not overlap. Using Matlab, the area error for each mean PV loop versus its modelled counterpart PV loop was calculated (see also table 44), this gave an overall mean error for all stages of less than 10%. In order to gain insight into how well the model coped with modelling the individual PV loops from each patient, the individual loops comprising each stage were also modelled, using the same process but without any averaging.

Table 44: LPM input variables and AHA/ACC stage of HF

Windkessel input	units	Stage of HF				
		O	A	B	C	D
LV Elastance	mmhg/ml	2.50	2.20	1.14	0.55	0.52
LV Stiffness	mmhg/ml	0.08	0.06	0.15	0.04	0.06
Systemic Resistance	mmhg•s/ml	1.15	1.51	1.50	1.65	1.58
Systemic Compliance	ml/mmhg	3.19	2.90	5.34	3.87	4.33
Percentage error	%	7.5	3.0	7.5	15.0	10.6

Figure 38: Calculation of error in modelling the mean Stage A LV PV loop

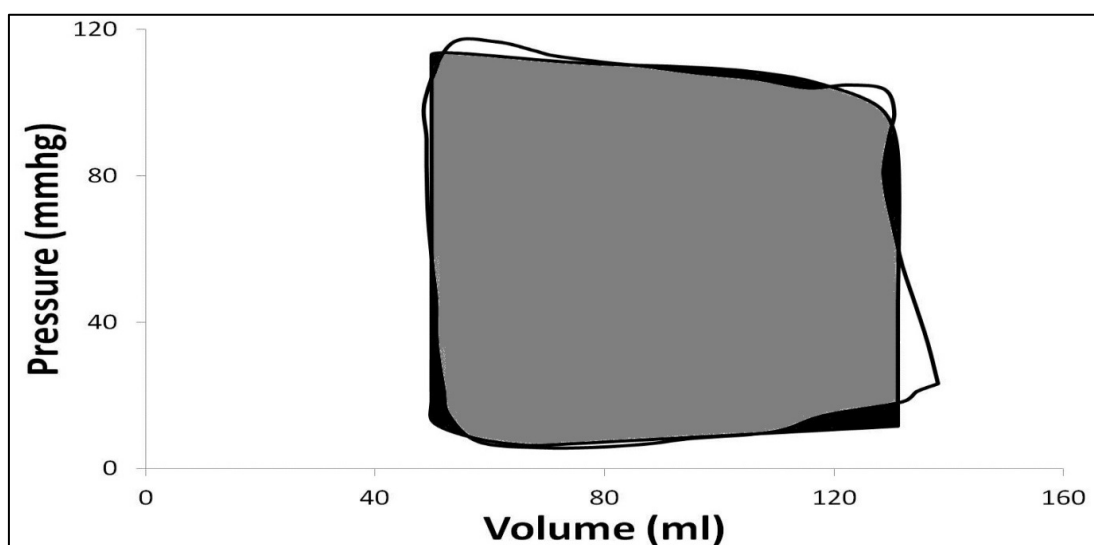


Figure 38 demonstrates the overlap between the mean and the modelled pressure volume loop from stage A, with the overlapping area in grey e.g. modelled correct and the erroneous area in black or white.

5.4.4 Discussion

5.4.4.1 Pressure Volume loops from the Literature

This study shows that pressure-volume data reported in the literature supports the physiological paradigm for heart failure due to left ventricular systolic dysfunction; as the left ventricle fails, it dilates. Thus, the force of contraction is impaired and the volume ejected with each beat (stroke volume) is reduced. The study also highlighted the quantitative changes occurring between each AHA/ACC stage. As AHA/ACC HF stages (particularly stages C and D) are descriptive and qualitative, it is remarkable how the AHA/ACC qualitative stages could be delineated quantitatively in this study.

5.4.4.2 Pressure Volume loops modelled the LPM

The LPM models true in physiological sense; predictably the pump function of the left ventricle deteriorates as the HF-LVSD progresses; the left ventricular chamber dilates and the afterload and plasma volume increase affecting both the resistance (R) and the compliance (C). The pressure-volume loops output from the model capture each stage as expected. Thus: Stage O is indeed healthy, with normal left ventricular parameters as would be expected from a disease-free population. For patients in Stage A, the vast majority of whom have IHD, the systolic pressure rises, reflecting increased afterload, and the EF% and SV fall. All these parameters are still within normal limits. Following a (likely) ischaemic insult to the myocardium in Stage B, there is a rise in LVEDP reflecting increased stiffness due to scar, a fall in systolic pressure due to impaired contractile force and corresponding reduction in both the ejection fraction and the stroke volume. What is somewhat surprising is that, whilst there is an increase in volume from stage C to D, both the systolic and diastolic pressures rise. However here it is important to remember that the process of HF is not a simple mechanical process but it reflects the contribution of the compensatory mechanisms driven by the sympathetic drive and by the endocrine responses driven by the RAAS as well as the sympathetic nervous system.

The patients in stages A-B are asymptomatic from the heart failure viewpoint despite the fact that relative to Stage O, the systemic resistance and compliance increase by over 60%, and LV Emax falls by up to 60%. The remaining contractile force is sufficient to meet the demands of the body. The difference between the asymptomatic patients with structural heart disease (Stage B) and those with symptoms of HF-LVSD (Stage C) is the reduction in LV Emax by a further 50%. The difference between symptomatic HF-LVSD and refractory HF-LVSD is a further modest (13%) reduction in Emax (which translates into an absolute fall of 75% compared to Stage O). This is an important observation that illustrates the delicate tipping point between physiological compensation and decompensation.

There is wide distribution of PV loops within each stage, as demonstrated in figure 34 (other stages are similar but for brevity are not shown). This highlights the challenge

of stratifying the disease condition based on current measures of LV function. The mean loops from stages B, C also fit within the range of data for patients in stage D and the AHA/ACC classification, due to the subjective nature of classification, rather than being based on objective data of physiological variables. But also because these are different patients at different time points on their HF-LVSD trajectory, not the same patients followed up over time. The potential overlap amongst the disease stages highlights further the importance of a physiologically-based criterion for the objective differentiation of HF-LVSD stages, rather than reliance on subjective assessment (although the latter is clinically important) and objective echocardiographic measurements as in current clinical practice. Reproducible, objective and independent parameters, such as elastance, could be used to improve patient-stratification but would require validation in clinical longitudinal studies. In the interim, this work has benchmarked reference ranges for each AHA/ACC HF stage (see table 43 and 44), for use by clinicians and modellers.

It might be argued that the distribution of PV loops within each AHA/ACC HF stage is an indication of a lack of strong correlation between AHA stage and LV performance. However, there are many other factors which might lead to the level of variability observed, including; the degree of natural variation within groups, involvement of factors beyond the simple mechanical process of impaired LV pump function such as compensatory neuroendocrine factors, other types of heart failure such as HFPEF or HF due valve disease or arrhythmia. Moreover, in this study, we were unable to control for medication or patient size, both of which may influence volume and pressure. To model HF accurately, other variables such as right ventricular function and renal function would need to be considered; the current work was confined to the consideration of the elastance and volume of the LV and the compliance and resistance of the systemic vasculature.

In terms of individual PV loops, the calculated error was much higher due to the difficulty of the model in simulating the more unusual shaped PV loops. This may have been due to errors in PV loop sampling, dyssynchrony or another variable. As a consequence some of the resulting individual patient loops had 'non-physiological'

shapes with marked pressure fluctuations during diastole and non-linear decreasing volumes during systole, for example. This was most notable in Stages C and D. Perhaps not surprisingly, the model is unable to take account of such aberrations. It is possible that such variations might be better fitted and errors reduced by adding more elements to the model, for example by using a 3-element afterload with inertance, or by including the right heart and pulmonary circulation, but what this would actually mean is unclear as such variables were not measured in these studies.

5.4.4.3 Future work

It would also be useful to compare PV loops from patients with HF of different aetiologies, such as those with ischaemic versus non-ischaemic DCM, and to model the effects of various therapies on the different parameters. Furthermore, comparing PV loops of patients with different isolated risk factors for HF (obesity or essential hypertension) or with different structural heart diseases (such as asymptomatic aortic stenosis or left ventricular hypertrophy, for example) to see how they progress from symptomless risk to symptomatic HF would also be of interest. Unfortunately, such data is not currently available. More PV loops are needed to inform stages O and B, where the mean loops, and therefore the models, are based on a small number of cases. However, it is unlikely that ethical approval for invasive PV loop analysis would now be granted for healthy subjects.

5.4.4.4 Drawbacks

For the majority data used in this meta-analysis the information provided on patients could not be linked to a specific PV loop given and so it proved to be impossible to control for age, body mass, sex, medications and other relevant comorbidities (both cardiac such as mitral regurgitation and non-cardiac such as renal failure) which might have an impact on loop shape, size and position with respect to the axes²⁴⁰. Some curves had already been averaged already from the patient population (hence the number of patients represented is greater than the number of loops) and what may have been classified as AHA Group D in previous decades, may be considered to be Group C today due to advances in treatments.

It was also impossible to control for any differences in methodology across the papers and most of the data is from middle-aged, male patients, reflecting the fact the women are under-represented in HF clinical trials; it cannot be assumed that groups who are not represented, or who are poorly represented, will have the same characteristics. As can be seen from figures 35 and 36, the averaging process leads to smoothing and loss of detail present in the raw data; this an individual patient in stage D will not necessarily fit the mean, but may fall within the range of values given.

Due to the duration of time (mean of 18 years) that has passed since the original publication of many of the papers, only a small number of authors were contactable and only 2 replied to a request for access to the raw data. Subsequently, a digitisation process was employed to allow access to the data underlying each PV loop, but clearly is not as accurate as modelling original data itself and adds an additional layer of error.

5.4.5 Conclusions

For the first time, a visual and quantitative representation of the AHA/ACC stages of HF-LVSD (from normal to end-stage) has been created. This could be used by clinicians, when making decisions about prognosis and treatment of patients, and those at risk of developing, HF-LVSD. Furthermore, the modelled PV loops establish previously unknown physiological parameters for each AHA/ACC stage of HF-LVSD and set the precedent for using LV elastance as a robust, reproducible and load-independent measure of LV performance and its deterioration at a population level. Such information will enable cardiovascular modellers with an interest in HF to create more personalised models of the LV for each patient in the context of considering essential boundary conditions such as systemic arterial compliance and total peripheral resistance. Finally, since there was no consistent pattern, for any of the parameters modelled, other than for elastance, this means the best afterload for more complex LV models in HF remains unclear or perhaps is unimportant, as it is clearly elastance that drives HF-LVSD rather than the characteristics of the peripheral circulation.

5.5 Lumped parameter modelling of response to CRT

5.5.1 Introduction

A key objective of the Grand Challenge modelling project was to determine how data from the patient's existing clinical record might be used to inform a personalised 3D cardiac model, when choosing appropriate boundary conditions, for example. Invasive data, such as the pressure-volume relationship, is not recorded routinely in HF patients, pre-CRT or otherwise. However, one of the requirements of the project was to attempt to use data that was collected in the course of routine clinical practice to inform personalised models that could be used to predict clinical response to CRT. How could non-invasive patient data from those recruited to the Grand Challenge project be used to create patient specific simulations? In this regard, the patient's clinical record was reviewed to assess potential input variables e.g. systemic blood pressure for the LPM as used earlier, which demonstrated utility in mapping the progression of HF-LVSD and were simple, elegant and quick to run. The potential of using the LPM to model these changes in LV physiology following CRT implantation, might offer insight into the boundary conditions of systemic vascular resistance and total arterial compliance governing the cardiovascular system of each patient and therefore also influence their response to CRT. Furthermore, these could variables could then be used to inform personalised models, for example creating patient specific simulations using a 3D segmentation of their LV from cMR coupled to a LPM afterload modelled from derived from the clinical record, rather than simply the same arbitrary afterload for all patients.

Whilst invasive PV loops are already used to demonstrate acute and chronic improvements in LV volume, LV pressure and elastance, non-invasive PV loops have not, as yet, been used to map the response to CRT, to attempt to predict response nor to investigate changes in systemic afterload vs. elastance in chronic CRT remodelling²²⁴. The output from a lumped parameter model can be converted into a PV loop, by extracting the P and V data from a single cardiac cycle. Chen et al (2001)²⁵¹ devised the 'non-invasive' PV loop, using 5 parameters; the brachial artery pressure measured using a sphygmomanometer, LV volumes measured using echocardiography and a constant (the estimated normalised ventricular elastance at arterial end-diastole). Together these were used to create the 4 points of a non-invasive PV loop and calculate elastance (E). It should be noted that, in this case, LVESP was estimated using systemic blood pressure measured with a standard automated sphygmomanometer

and a formula (brachial systolic pressure x 0.9), taken from earlier work by Kelly et al (1992)²⁴⁷. In the aforementioned work LVEDP, was assumed to be zero and so was not calculated nor estimated. However, LVEDP may well be elevated in HF-LVSD regardless of the aetiology and a value for LVEDP is required to complete a non-invasive LV PV loop, particularly if this is then to be modelled using a LPM. A method of estimating LVEDP from non-invasive 2D echocardiography measurements has previously been developed. This robust, validated, widely-cited and widely-used method by Nagueh et al (1997)²⁵² uses the mitral Doppler E/e' ratio (ratio of mitral inflow velocity/mitral annular velocity). The assumption is made that PCWP \approx mLAP \approx LVEDP and that E/e' can be used to estimate the LVEDP according to the equation: E' (average) = (E' lateral + E' septal) / 2 and PCWP = 1.24 (mean E/E') + 1.9.

Using 2DTTE to measure LVEDV and LVESV, sphygmomanometry to measure systolic BP (thus giving the LVESP) and the E/E' ratio the LVEDP from mitral Doppler (see figure 39), all could be taken from the patient's clinical record. By knowing such outputs for each patient, at baseline and follow-up, the LPM could be used to model PV data. Thus each patient could be represented at each time-point (baseline, 6 and 12 months post-CRT) to quantify any changes. Left ventricular volumes might be expected to fall and pressures and elastance to increase over time in responders to CRT.

Figure 39: PWTDI measurement (right to left) of E, E' septal and E' lateral

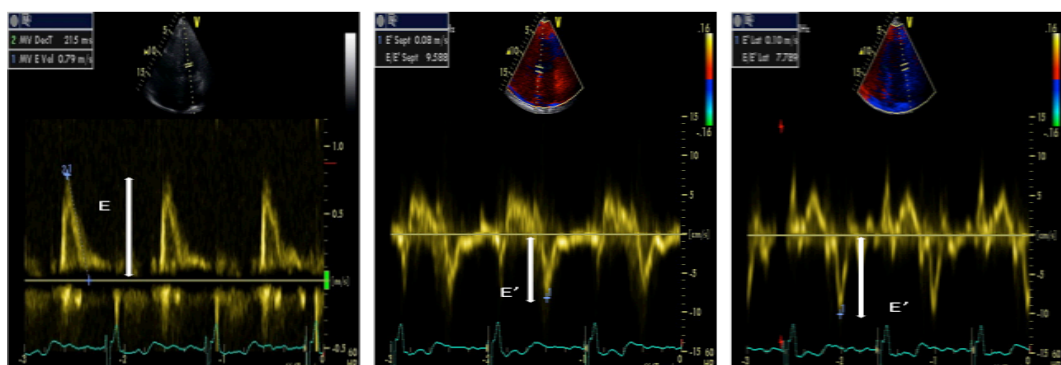


Figure 39 demonstrates pulsed wave Doppler either through the mitral valve (left) or pulsed wave tissue Doppler of the septum or lateral wall being used to calculate E and E' respectively.

5.5.2 Methods

The following measurements were made for each time point (at baseline (< 2 weeks pre-CRT implantation) and at 6 and 12 months post-CRT implantation) in 9 patients. Ten patients with AF were excluded as E/E' is not validated for such patients.

- BP data (recorded using a clinical automated sphygmomanometer BP machine) to give the brachial systolic pressure, which was then multiplied by 0.9 to give the LVESP.
- 2D echocardiographic volumes (LVEDV and LVESV) measured using the Simpson's method of discs from apical 4 and 2 chamber views (see Chapter 5).
- E/E' ratio measured using LV inflow and mitral annular tissue Doppler from the apical 4 chamber view, averaged over 5 cycles.

A non-invasive PV loop, was created for each patient using the above parameters. Data were recorded in an Excel spread sheet (Microsoft Inc, Redmond, USA) and the changes plotted from baseline to 12-month follow-up. Then, using the LPM model, the non-invasive PV loop was modelled using an optimisation function in Matlab (Mathworks Inc, Cambridge, UK). This ran the model repeatedly until the input parameters e.g. elastance, R & C created a PV loop which best fitted the output parameters of LV pressure and volume.

5.5.3 Hypotheses

Working hypotheses –

1) LV PV loop parameters alter significantly in patients classed as responders to CRT as determined from a combination of symptoms, echocardiography and CPET testing.

2) The clinical response to CRT can be predicted from baseline non-invasive LV PV loop parameters.

Null hypotheses –

1) LV PV loop parameters do not alter significantly in patients who are classed as responders to CRT as determined from a combination of symptoms, echocardiography and CPET testing.

2) The clinical response to CRT cannot be predicted by baseline non-invasive LV PV loop parameters.

5.5.4 Results

It took between 5-40 iterations of each model to create a patient specific LV loop at each stage. The mean number of iterations was 20. Whilst the process of optimisation was automated using a function in Matlab, baseline parameters had to be chosen. This choice was of baseline parameters were informed from modelling the AHA/ACC HF stages.

Table 45: Model input parameters at baseline and follow-up in responders

Responders			Baseline		6 months		12 months		One way ANOVA with repeated measures P value	
			Mean	SD	Mean	SD	Mean	SD	Baseline vs 6	Baseline vs 12
Inputs	LV Emax	mmHg/ml	1.40	1.15	2.02	1.55	2.28	1.70	= 0.05	
	LV Emin	mmHg/ml	0.17	0.10	0.17	0.11	0.16	0.09	= 0.88	
	R	mmHg•s/ml	2.03	0.78	2.20	0.88	2.29	0.78	= 0.49	
	C	ml/mmHg	3.61	0.29	3.56	0.32	3.58	0.30	= 0.37	

Table 46: Model input parameters at baseline and follow-up in nonresponders

Nonresponders			Baseline		6 months		12 months		One way ANOVA with repeated measures P value	
			Mean	SD	Mean	SD	Mean	SD	Baseline vs 6	Baseline vs 12
Inputs	LV Emax	mmHg/ml	1.18	0.63	1.05	0.86	0.98	0.86	= 0.26	
	LV Emin	mmHg/ml	0.13	0.07	0.13	0.09	0.12	0.06	= 0.84	
	R	mmHg•s/ml	2.20	0.91	1.43	0.41	1.63	0.16	= 0.24	
	C	ml/mmHg	3.76	0.32	3.81	0.34	3.81	0.34	= 0.39	

Table 47: The 6 model outputs in responders at baseline and follow-up.

Responders			Baseline		6 months		12 months	
			Mean	SD	Mean	SD	Mean	SD
Outputs	LVEDP	mmHg	23.5	6.3	19.2	2.9	16.5	5.9
	LVESP	mmHg	114.8	21.8	115.0	20.1	109.3	7.1
	LVEDV	ml	178.6	106.8	160.6	120.2	134.0	89.5
	LVESV	ml	132.2	85.2	110.4	96.0	90.6	78.6
	SV	ml	46.4	23.4	50.2	27.1	43.4	14.1
	EF	%	0.28	0.07	0.37	0.13	0.39	0.13

Table 48: The 6 model outputs in nonresponders at baseline and follow-up.

Nonresponders			Baseline		6 months		12 months	
			Mean	SD	Mean	SD	Mean	SD
Outputs	LVEDP	mmHg	19.8	9.3	20.0	6.2	21.8	5.0
	LVESP	mmHg	106.7	7.9	93.5	8.9	95.6	11.1
	LVEDV	ml	166.5	90.4	186.5	71.3	213.8	114.5
	LVESV	ml	123.3	76.0	135.5	72.2	170.8	117.6
	SV	ml	43.3	15.6	51.0	14.6	43.0	5.0
	EF	%	0.28	0.07	0.31	0.14	0.26	0.16

Table 49: All model outputs versus measured parameters at baseline and follow-up.

All			Pre CRT		6 months		12 months	
			Patient	Model	Patient	Model	Patient	Model
Outputs	LVEDP	mmHg	21.86	21.17	20.39	20.39	18.06	17.98
	LVESP	mmHg	111.20	111.16	106.40	105.99	102.26	102.04
	LVEDV	ml	173.22	173.11	184.22	184.33	157.33	157.33
	LVESV	ml	128.22	128.11	137.22	136.78	110.56	110.22

Tables 45 and 46 demonstrate the model outputs at baseline and during subsequent follow-up. In responders, LVEDP, LVESV and LVEDV decreased consistently during follow-up at 6 and 12 months. In non-responders LVEDP, LVESV and LVEDV increased consistently during follow-up. Table 47 compares the mean modelled versus measured data during follow-up in all patients. The mean differences between the data were 0.26 mmHg and 0.20 ml with standard deviations of 0.23 mmHg and 0.14 ml respectively (see table 49).

Figure 40: LV PV loop at baseline in responders (dashed) and nonresponders (solid)

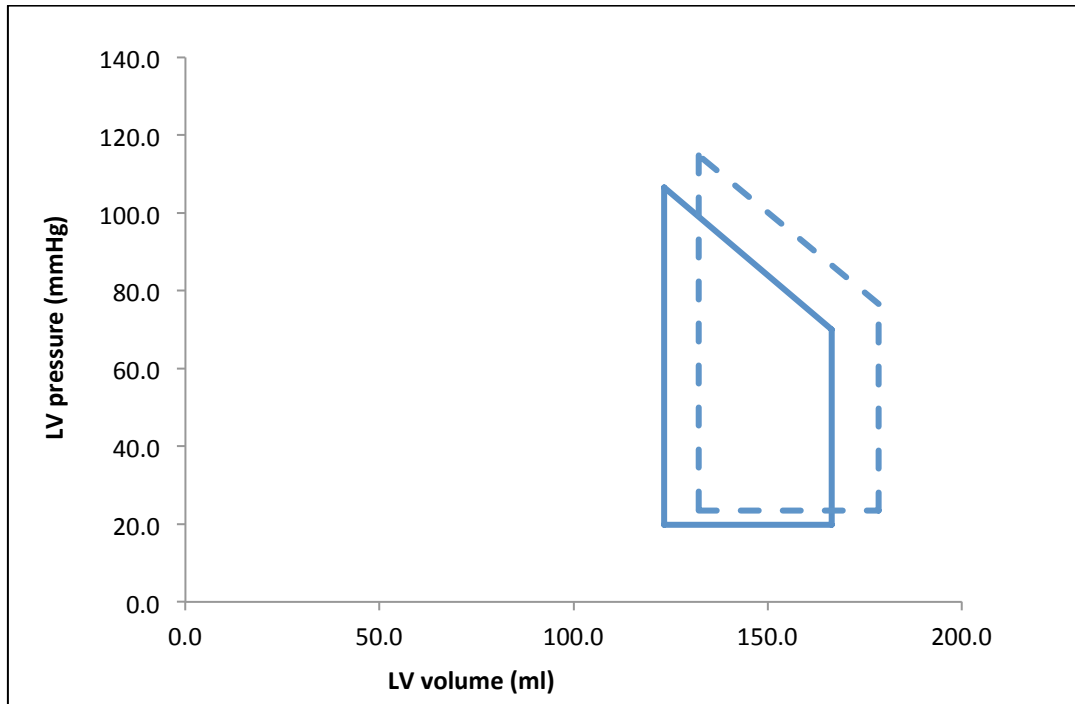


Figure 40 demonstrates the difference between the mean pressure volume loop of responders (dashed) and non-responders at baseline e.g. prior to CRT implantation.

Figure 41: Non-invasive LV PV loops in responders

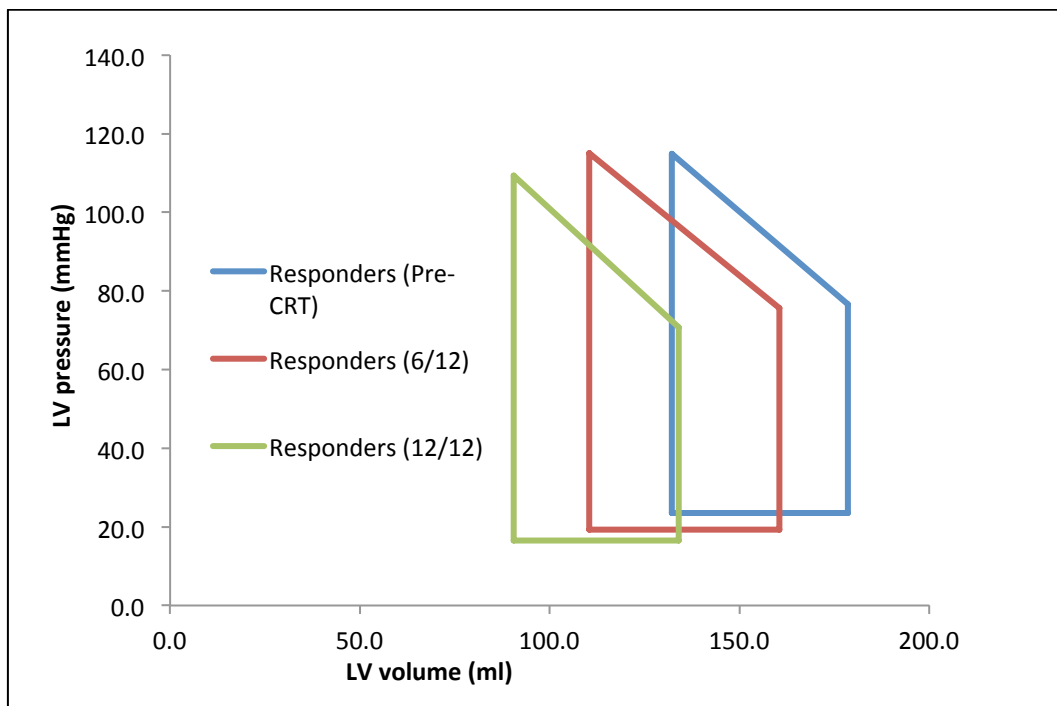


Figure 41 demonstrates the difference between the mean pressure volume loop of responders at baseline and following CRT implantation.

Figure 42: Non-invasive LV PV loops in nonresponders

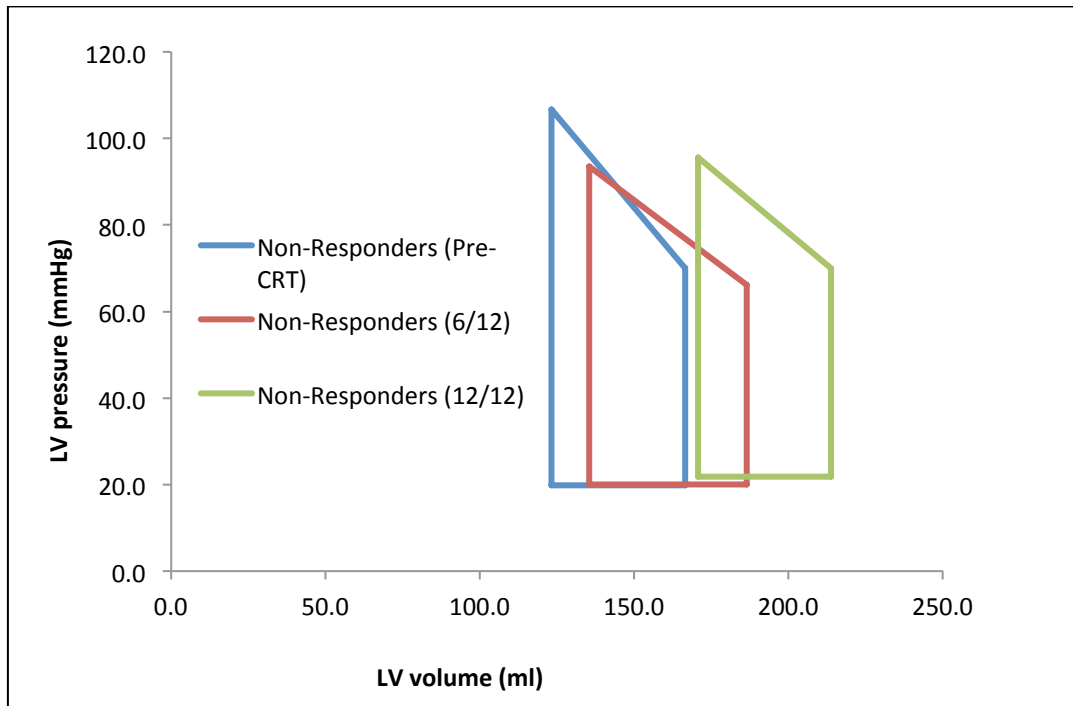


Figure 42 demonstrates the difference between the mean pressure volume loop of non-responders at baseline and following CRT implantation.

Using a two-tailed Student's T-test, model output parameters at baseline were not found to be significantly different between responders and nonresponders, with respect to pressure ($p = 0.80$) or volume ($p = 0.80$). Changes and statistical differences in LV volumes and BP during follow-up as a marker of CRT response have been dealt with in chapter 5 already and thus will not be considered further here. Using a 2-tailed Student's T-test, there was no significant difference between responders and nonresponders in terms of model input parameters at baseline. A one-way ANOVA with repeated measures was used to compare the difference between the model input parameters at baseline and follow-up. As can be seen in table 43, only E_{max} trended towards significance during follow-up in responders, with no significance changes in non-responders. There was no significant correlation between any of the input parameters, such as E_{max} , E_{min} , R or C and markers of response, such as peak VO_2 , MLWHFQ or 6MWD. Figure 43 using demonstrates the close fit between the modelled and measured parameters, statistically significant using Pearson's correlation coefficient.

Figure 43: Correlation between measured and modelled LV PV data

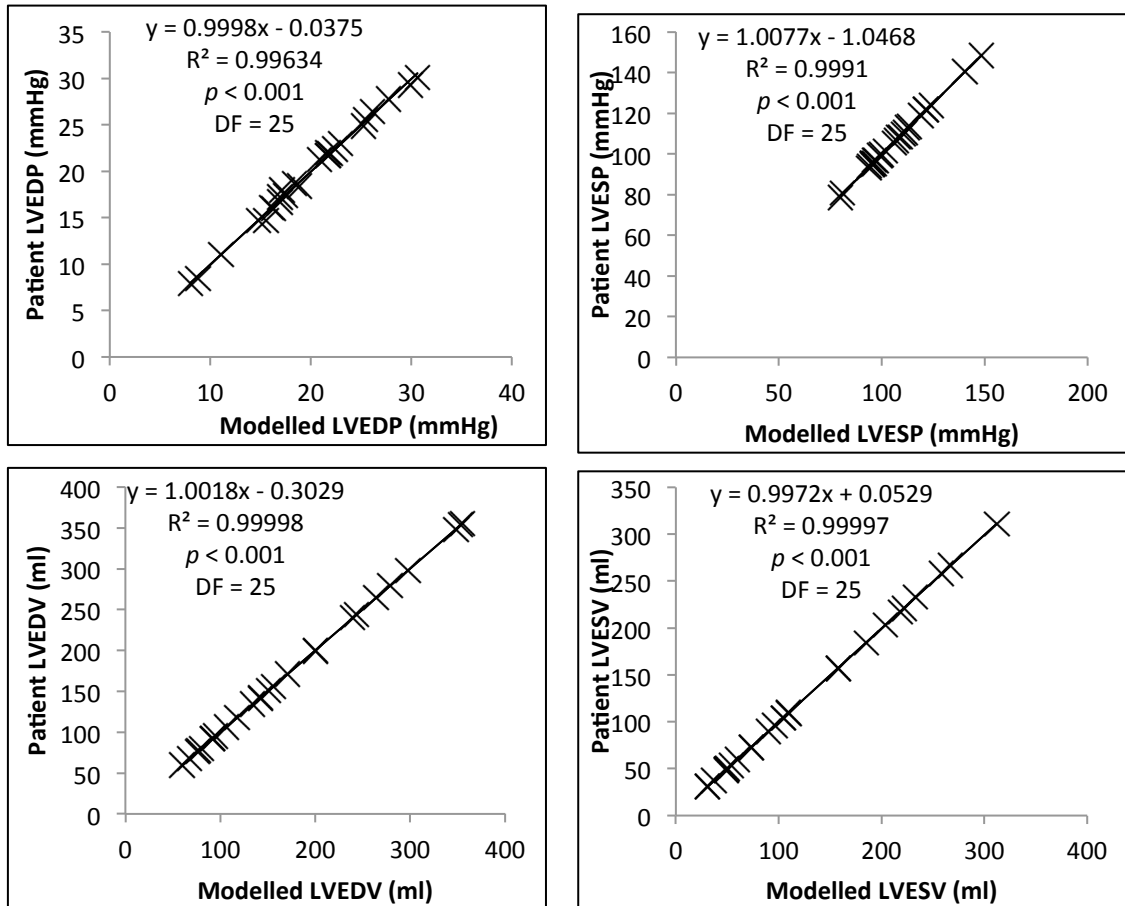


Figure 43 demonstrates the correlation between the measured and modelled left ventricular pressure volume parameters, all demonstrating statistical significance.

LVEDP = left ventricular end-diastolic pressure, LVEDV = left ventricular end-diastolic volume, LVESP = left ventricular end-systolic pressure, LVESV = left ventricular end systolic volume.

Thus, the first working hypothesis - that '*LV PV loop parameters alter significantly in patients who are classed as responders to CRT*' can be rejected and the null hypothesis is therefore accepted and the second working hypothesis is rejected and hence the null hypothesis, *that clinical response to CRT is not predicted by non-invasive LV PV loop parameters at baseline* can be accepted

5.5.5 Discussion

For the first time, non-invasive pressure volume loops have been created from patient data at baseline and during follow-up following CRT implantation. These loops were subsequently modelled using a LPM using a WKM, allowing insight into the behaviour

of both the patients' cardiovascular system following CRT implant but also the use of personalised LPM to model such changes.

This study demonstrates that mean LV Emax in responders, which was found to be 1.4mmHg/ml at baseline, increases by 43% to 2.02 at 6 months and then by 62% to 2.28 at 12 months, relative to baseline and trends towards significance. Other studies, using specific LV PV catheters, with P measured using a micro-manometer and V measured using a conductance or an angiographic method not 2DTTE, report baseline values of 0.7-0.8mmHg/ml for LV Emax increasing to 1.0 mmHg/ml immediately following implantation, sustained at 6 months^{224 225 253}. There was no such increase in Emax in nonresponders, indeed the Emax appeared to fall, but this change was not significant. The increase in Emax makes physiological sense, as CRT improves atrioventricular, inter and intraventricular synchronicity, leading to improved diastolic filling, reduced functional mitral regurgitation and increased stroke volume. The lack of change in Emin is unsurprising, as ventricular stiffness and reduced relaxation e.g. diastolic dysfunction is a different pathological process to HF-LVSD and other similar studies have failed to show an impact of CRT on such properties. Furthermore, whilst both systolic and diastolic dysfunction can co-exist in a patient with HF, CRT is not licenced for the treatment of HF-PEF in isolation.

The lack of significant difference in R and C during follow-up, suggests that CRT has no significant impact on ventricular-arterial coupling, systemic vascular resistance and total arterial compliance even at 12 months following implantation. Whilst R did fall in nonresponders (by 43%), this difference was not significant nor was it seen in responders. The only published study that could be found that looked at this property followed up 25 patients at 1 month post-CRT implantation and demonstrated a significant decrease in R but did not comment on C. The methodology used pulse wave velocity waveforms measured at the ascending aorta with a transfer function to derive arterial elastance changes and so cannot be readily applied to the 19 patients studied here²⁵⁴. Improvements in vascular biomechanics would be anticipated with CRT due to increased vessel wall shear stress, following increases in SV. This in turn would lead to; improved endothelial function, inhibition of the RAAS and up-regulation of vagal tone, resulting in relaxation of vascular smooth muscle. So simply, a fall in R

and a rise in C would be expected in patients following CRT implantation, particularly in responders. It is possible that the population in this study is simply too small to be able to detect such changes or that the LPM used was too simple to demonstrate such nuances.

In the modelling work on the AHA/ACC stages of HF-LVSD, it was demonstrated that a value of LV Emax 2.5mmHg/ml was normal in healthy individuals but patients in NYHA class III HF-LVSD would be expected to have a much lower LV Emax (0.63mmHg/ml). In this work the mean LV Emax at baseline for the HF-LVSD patients, all of whom were NYHA class III, was 1.2 mmHg/ml; somewhat higher than expected. It is possible that both systolic BP and LVESV were over- and under- estimated respectively, resulting in a falsely elevated LV Emax and this appears to have been consistent throughout this work as all the LV Emax values are higher than might be expected. Furthermore, it is well known that the correlation between LV volumes measured non-invasively by echocardiography and invasively by LV angiography or conductance is fair and that such measures are not interchangeable, which may also account for such differences in Emax between the 19 patients studied here and the work in on the ACC/AHA stages of HF. Also, whilst it has been demonstrated that 0.9 x systemic systolic blood pressure measured using automated sphygmomanometry is significantly correlated with invasively measured end-systolic LV pressure ($r^2 = 0.98$, $p < 0.001$, offset 0.17) using a conductance catheter, these should be considered different measures of the same system and so may not perhaps behave in the same way²⁴⁷.

The close fit of patient measured (or derived) data and model output parameters such as LVEDV, LVEDP, LVESP and LVEDP demonstrates the performance with which the LPM was able to model the patients. What cannot be modelled, unless an invasive LV PV study is conducted, is the shape of the loop. However, it is the 4 points that comprise the loop which are of significance and not the intermediate points in between.

It is disappointing that there was no correlation between measures of CRT response and the model parameters, particularly Emax and other measures of LV function such as NT-proBNP, peak VO₂. Clearly, like the non-invasive LV PV loops, these are all

indirect measures of LV function, which are influenced by many other factors, not simply the heart alone. Many of these are too complex to be modelled accurately or make mathematical assumptions for such as motivation, musculoskeletal function and comorbidities such as respiratory and renal disease.

The fall in LV Emax in nonresponders despite CRT implantation gives insight as to why such patients feel worse during follow-up, in that they experience a 0.2 mmHg/ml (17%) fall in LV contractility over the 12-month period of follow-up. Recalling the AHA/ACC stages HF-LVSD work, the difference between symptomatic HF (NYHA III) and end-stage HF (NYHA IV) was a modest 0.08 mmHg/ml (13%) reduction in Emax. Whilst this difference was not statistically significant, it remains unclear why despite all patients meeting current guidelines for, undergoing successful implantation of, CRT, that this group of patients should experience a deleterious effect on their LV function.

There are other possible measures of diastolic function such as pulmonary venous flow and velocity of flow progression, but neither of these have the strong evidence base associated with E/E' . Furthermore, there can be technical issues obtaining a reliable pulmonary venous flow signal (even with TOE) and neither can be used reliably to calculate LVEDP.

Problems with the use of 2DTTE and Simpson's method of discs to calculate LV volumes were considered in Chapter 5. Ideally, cMR would be employed to measure LV volumes but there were no cMR-compatible CRT devices on the market at the time of this study; it would not be valid to measure cMR at baseline and then use 2DTTE to follow-up, as LV volumes measured using these methodologies are non-interchangeable. Time limitations at follow-up resulted in patients having a single BP measurement using an automated sphygmomanometer, but this was following 10 min period lying quietly in a dark room. In hindsight, measuring the BP several times and using the mean value could give a more representative value or perhaps considering the use of a 24-hour BP monitor.

There are many ways to model a single PV loop depending on the parameters chosen and a more accurate fit might be achieved using a more sophisticated LPM model,

including the right heart and pulmonary vasculature, but many of the necessary input variables would be impossible to be measure, and therefore accurately model. In addition for some, inertance for example, do not have precise equivalents in terms of physiological measurement.

The cohort size for this particular sub-study was small due to prevalence of AF (> 50%) rendering measures of diastolic function such as E/E' inaccurate and reducing the number of patients from 19 to 9. E/E' is an instantaneous measure of LV filling, influenced by preload and afterload, and may change over time thus, as with other clinical and haemodynamic indices, multiple measures and calculation of the mean may have been preferable. All patients were fasted prior to their 2DTTE so this may mitigate some variation. The average E' velocity obtained from both the septal and lateral sides of the mitral annulus was used in this study to calculate LVEDP as is usual practice and used in the Nagueh formula. Septal E' is usually lower than lateral E' and so E/E' derived from a septal value, is higher than E/E' lateral and so an average value is preferential to mitigate for this variation. Mitral disease is known to affect mitral annular velocity and resulting E' values, no patients included in this study had mitral stenosis and only a minority had trivial-mild mitral regurgitation, common in such a population. According to Nagueh (1997)²⁵² “annular velocities vary with the site of sampling, and thus, the utility of this method is dependent on the location of the sample volume”. This raises the possibility of intra- and inter-operator variability, since 2 echocardiographers scanned the patients in this study. It would have been preferable for both to scan all patients, but funding, time and logistics would not allow this.

5.5.6 Conclusions

This is the first study to create non-invasive LV PV loops, model them in patients with HF-LVSD and following CRT implantation. As there were no significant differences in the non-invasive PV loop or derived LPM model data at baseline between responders and nonresponders, on the basis of this study, such parameters cannot be used as a predictor of CRT response. In terms of the derived input LPM parameters, such as E , R and C , the only difference that trended towards significance during follow-up, in either group, was an increase in E_{max} in responders. The lack of change in R and C suggests

that, not only are these unaffected by CRT (either acutely or chronically) but, more importantly, for modellers using more complex multi-level or 3D LV models with a LPM afterload, the exact choice of R and C is not as critical as previously assumed. This reflects the work on the AHA/ACC stages of HF showing that there is no statistically significant difference between R and C in individuals with risk of developing HF-LVSD (AHA/ACC stage A or NYHA I) and those with end-stage HF-LVSD (AHA/ACC Stage A or NYHA IV), at least in terms of modelled parameters. Further work on a larger cohort will be required in order to investigate whether response can be predicted as baseline and whether the results of this study, namely; a significant increase in LV Emax in responders but no significant difference in any other variable in either group, are maintained.

5.6 3D Models

5.6.1 Introduction

The first 3D computational cardiac models, developed in the 1960's, simply described the heart as a geometrical shape e.g. an ellipsoid. In the 1970's more detailed anatomical models emerged. These were based, typically, on explanted hearts or pathological specimens with information from pro-sections enabling the incorporation of cardiac fibre orientation. The development of computer aided design (CAD) in the 1990's and the exponential rise in medical imaging application such as MRI and CT in the early 2000's, has augmented the proliferation of 3D patient-specific cardiac models. The basis for such a model starts with extracting specific geometrical data for the heart of interest. Data may include the geometrical descriptions for all, or some, of the LV, RV, LA, RA and great vessels.

In order to build a 3-D electromechanical model of the heart, relevant, individual components parts must be described. For example, in addition to the anatomy of the chambers and great vessels, information on the structure and properties of the myocardium, the sequence of electrical activation and the resulting flow of blood through the heart are required in order to conceptualise cardiac function and construct a robust model. This approach employs anatomy, physics and biochemistry to describe the working action of the heart.

3-D models may start from a single myocyte, detailing the action of ion channels, calcium handling or myofilament interactions, building up to the orthotropic behaviour of the cardiac tissue and, then ultimately, creating a full heart model. But, as Hunter (2003)²⁵⁵ highlighted, our understanding of processes such as metabolic pathways, e.g. ATP production, and signalling, e.g. G-protein coupled receptors, are still in their infancy and so detailed multi-scale and multi-modal models remain some time away. The ultimate aim is to create patient-specific heart model that can be 'exercised' to investigate the interaction between patient variables, their disease profile and potential therapies. Patients with HF-LVSD and dyssynchrony, who are being considered for CRT where, for two similar patients one responds and one does not would be an example of this type of modelling application. However, it is important to note that no "global biophysical model of cardiac electrophysiology is suitable for all the clinical applications" and so specific models must be developed for a specific purpose²⁵⁶.

As Hunter (2003)²⁵⁵ stated, "models are all derived from the systems of physical equations underlying the heartbeat: (a) the electrical activation process, described by reaction-diffusion equations with current sources associated with membrane ion channels; (b) the soft tissue mechanics described by large deformation elasticity theory with orthotropic passive tissue properties and actively generated myofilament forces; and (c) ventricular and coronary fluid mechanics, based on Navier-Stokes equations and coupled to the soft tissue mechanics of myocardium".

As discussed previously, modelling is necessarily mathematically based, typically using both ordinary (ODEs) and partial differential equations (PDEs), whereby the dependent variable (or unknown function) is expressed as a function of a single independent variable or multiple independent variables and their derivatives. PDEs are used to describe complex concepts such as fluid flow whereas ODEs are used to describe rates of chemical reactions, where quantities are described by the rate of change of other quantities. The equations are linear if the unknown function and its derivatives appear to the power one e.g. the input is directly proportional to the output, but are otherwise non-linear. As the number of differential equations that can be solved by explicit analytic formulae is small, numerical approximations are used to solve such

DEs, extracting meaningful answers and so gaining an understanding as to the behaviour of the solutions. There are broadly three numerical approaches, namely; finite element, finite difference and finite volume methods.

In brief: finite element methods are numerical techniques which can be used to find approximate mathematical solutions to boundary conditions for PDEs. The complex mathematical problem is subdivided into smaller tractable problems, termed *finite elements*, which are then solved in relation to each other. The implementation of this method is known as *finite element analysis* (FEA) and is used for structural, thermal and electrical analysis. Finite difference methods typically employ the Laplace or Poisson equations. Finite volume is used to calculate variables averaged across a volume, but differs from finite difference in that a structured mesh is not strictly required. This method is typically used when modelling fluid flow. Use of the Navier-Stokes equations enables finite element techniques to be applied to study fluid mechanics; this technique is known as computational fluid dynamics or more frequently, CFD.

3-D models of the heart are conceptually interesting but mathematically challenging and computationally very demanding, requiring accurate modelling of the anatomy, the electrophysiology, fluid dynamics and myocardial mechanics. The 3D architecture of the heart is complex, not only in terms of geometry, but also in the context of muscle fibre orientation, connective tissue organisation, the anatomy conducting system and the coronary circulation and so on. Such models may describe not only the origin of myocardial activation from the sinoatrial node, but its propagation across the myocardium and the roles of the annulus fibrosus, the AV node and the His-Purkinje system. The mechanical properties of the myocardium govern motion, deformation and strain during the resulting cardiac cycle and modelling fluid dynamics may incorporate flow both within the heart chambers and within the coronary tree. In reality of course, these aspects are interrelated and even the most complex 3-D models will attempt to encompass some, but not all, of these components.

In the context of this thesis a 3D model is defined as a mathematical representation of a three dimensional anatomical structure and the related physiology. In this chapter

the method of constructing a 3D model of the human heart, its relevance to predicting response to CRT and its role in the Grand Challenge (GC) project are discussed.

The first step in developing a personalised 3D model of the heart is the acquisition of suitable image data from the individual patient (see figure 44). The advent of cMR, coupled with ECG gating, respiratory navigation and intravenous gadolinium- based contrast agents, allows the acquisition of a single high-resolution whole heart image during free breathing within 10 minutes or so. Whilst this can produce a clear depiction of the left ventricle, similar delineation of the atrial and right ventricular myocardium is relatively sub-optimal due to the limits of voxel reconstruction, which is limited to 1 mm. CT and 3DTTE can also be used. CT is the most accurate and robust method due to high temporal and spatial resolution but is limited due to the use of ionising radiation. 3DTTE is the quickest and simplest method has the limitations of poor signal to noise ratio and variable field of view.

Following acquisition of the appropriate 3D whole heart cMR image sequence, the cardiac geometry must be segmented (i.e. extracted from the image) to give the personalised anatomy required as the foundation for the patient-specific model. This can either be done by hand (slice by slice), using semi-automated methods such as snakes or level- sets (often with manual correction after the process) or fully automated by combining morphological operators and snakes (which are active computer generated curves which seek out object boundaries in an image).

Within this project, a technique was used for rapid construction of a patient-specific model; the patient data is fitted (morphed) to a pre-existing template (in this body of work, the ventricles only) creating a computational mesh. The mesh is a representation of an idealised geometry (in this case the LV. This then provides the domain for solving the mathematical derivation of physiological processes (see figure 45)²⁵⁷.

Good correspondence between the segmentation and the template is key to the success of this method. In addition whilst the segmentation may not be smooth, the mesh is required to be smooth with good quality elements or the resulting simulation

may be unstable. Ultimately, a trade-off between mesh quality, surface smoothing and geometrical precision is often sought.

Furthermore, if the patient geometry is extremely abnormal there may be significant discrepancies between the patient geometry and idealised anatomy. If this cannot be accounted for within the confines of the template, the morphing process may fail or the resulting model may not be representative of the patient. Alternatively, statistical atlases which represent the average anatomy of group of patients can be used but, of course, these are not specific for the individual patient. Another alternative is construction of a model from scratch but this is extremely time-consuming making it unsuitable for routine clinical use.

Typically, the template is described a linearly interpolated tetrahedral mesh, which defines the LV, which is curved, using linear polynomials and creating new data points in between known point. These types of mesh are simple, readily available and well characterised²⁵⁸. An alternative is to use a cubite Hermite mesh, which encodes “not only with the 3D Cartesian coordinates of nodes, but also with the derivatives of shape versus local finite element coordinates.”²⁵⁷.

The overarching aim of the GC project was to create a workflow that could be used by all partners in the project to produce a standardised and seamless process from collection of the cMR data, segmentation, meshing, solving, running and then validation of the model. The original plan was to investigate an initial cohort 50 patients, long with the collection of physiological information on response, such as NPs, VO_2 peak, 6MWD and MLWHFQ, before applying the workflow to a much large randomised population.

Figure 44: 3D model workflow

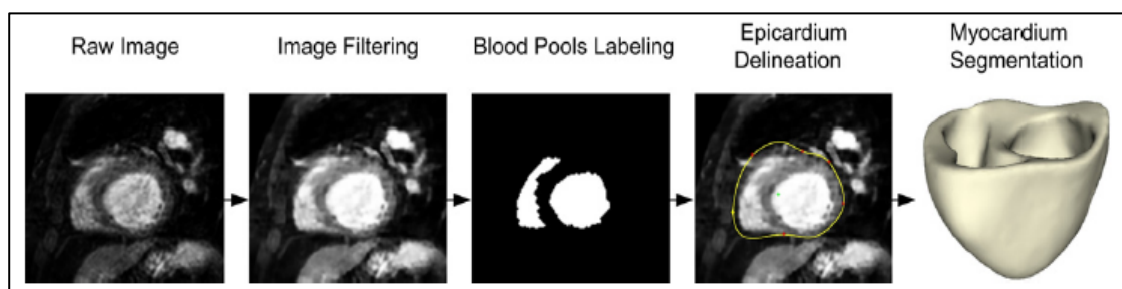


Figure 44 demonstrates the workflow used in the project, the raw image, filters used to improve subsequent endo and epicardium delineation and create the segmented myocardium.

Figure 45: Mock-up 3D LV models demonstrating various biophysical properties

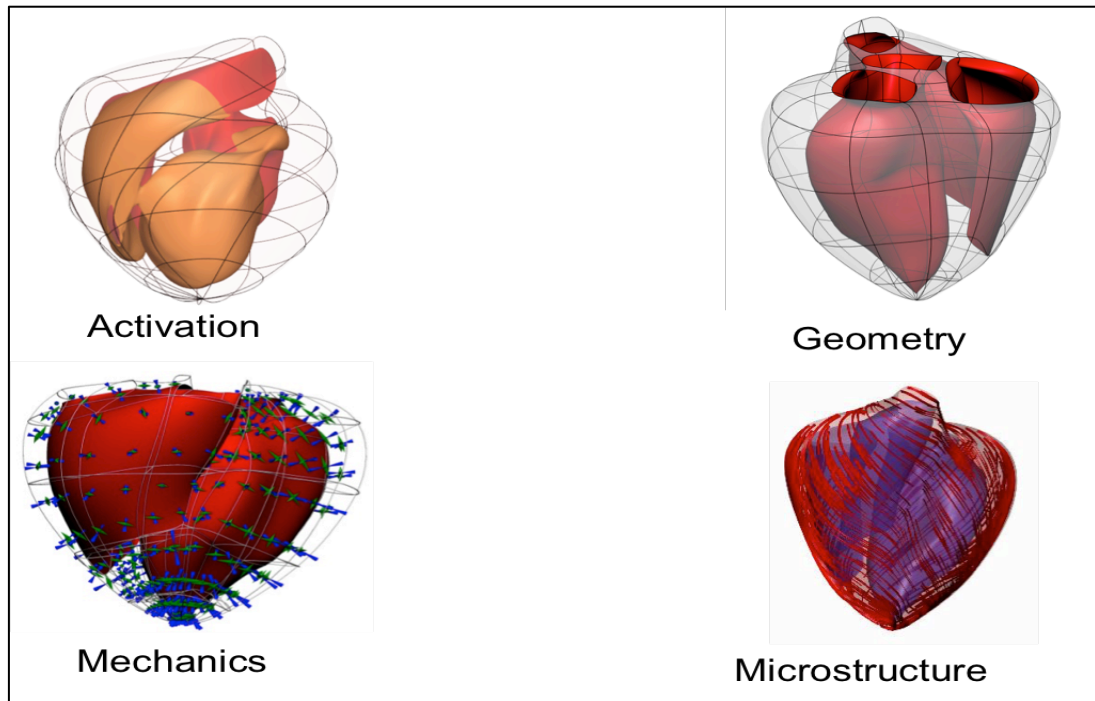


Figure 45 represents a mock-up of various 3D LV models, including ‘*Activation*’ depicts the propagation of the depolarising wavefront through the heart; ‘*Geometry*’ demonstrates the anatomical composition of the various chambers, ‘*Mechanics*’ the deformation of the myocardium during the cardiac cycle and ‘*Microstructure*’ the arrangement of the muscular fascicles composing the cardiac walls.

5.6.2 Segmentation

This work was completed with DDS.

As discussed in Chapter 2, cardiac MR (cMR) is considered to be the gold standard for LV and RV volume assessment and assessing the anatomy of the heart as a whole based on its superior spatial resolution, accuracy, reliability and lack of issues such as optimal ‘windowing’.

At USFD/STHT, a standard Siemens 1.5 Tesla Cardiac MR scanner was used to acquire 3D whole heart steady-state free precession (SSFP) images. This used true fast imaging with steady state precession (TrueFISP) which, as mentioned previously, is a technique that is optimised for speed and contrast between the blood pool and myocardium. This creates a series of data files in digital imaging and communications in medicine

(DICOM) format; the standard file format for medical images. This series of files can then be imported into a segmentation software package (e.g. GIMAS (graphical interface for medical image analysis and simulation, University of Pompeu Fabra, Barcelona, Spain). The term 'segmentation' refers to the process of determining which pixels in an image belong to which structure. This process can be carried out either by hand where the user identifies the 2 LV boundaries, both endocardial (between the blood pool and myocardium) and epicardial (between the myocardium and surrounding extra-cardiac tissue), or by an automated process. This is repeated for each slice of the heart, in all 3 axes (axial, sagittal and anteroposterior) the sum of which creates a 3D segmentation. Hand segmentation is time consuming, more than 100 slices may be included in each axis and each will need to be assessed multiple times. However it is considered the gold standard, as the expert operator can choose the correct surface where the automated tool might struggle to discriminate correctly, or fail to discriminate between tissues.

Automated tools are usually intensity-based and can often have difficulty in discriminating between tissues of similar intensity, for example between the myocardium and adjacent extra-cardiac tissues. One example of a situation where intensity-based methods do work well would be at the border between the blood pool and endocardium which, even without contrast is typically well defined. Consequently, whilst segmenting by hand is the most accurate method it is also the most labour-intensive, whereas the automated method is very quick (few minutes) but potentially fraught with errors, which, unless checked by hand, could lead to problems, such as errors in LV volumes. This is particularly important when measuring response to CRT (e.g. LVEDV/LVESV) or indeed assessing patient suitability (e.g. EF%) when accurate volume assessment is key.

The 3D whole heart sequence cannot give a true instantaneous representation of the heart, in the sense that the image is built up over many heart beats, with images acquired at end-systole. Artefacts due to breathing, movement or arrhythmias can degrade images; the region of interest may have moved or acquired at the wrong time in the cardiac cycle. This is particularly a problem in HF-LVSD, as up to 1/3 of patients will have coexisting atrial and ventricular arrhythmias. Furthermore, 20% of may

coexist in HF-LVSD patients and this, coupled with the fact that the patients are being asked to lay flat and in a confined space, means that the images produced are often poor, increasing demands on the automated segmentation software.

The automated segmentation software is optimised on healthy normal volunteers who can hold their breath for long periods and who have “typical” cardiac anatomy, in contrast to patients who may have dilated, scarred and morphologically-abnormal cardiac chambers. As a result, despite myocardial nulling, rather than clear delineation between the blood pool and myocardium or myocardium and mediastinal tissue 3D whole heart SSFP images can appear as heterogeneous shades of grey. Whilst 21 patients were recruited, only 20 had 3D SSFP images as one patient became unwell during scanning. The 3D SSFP images used a slice thickness was 8mm, taking around 15-20 min to capture a 3D image with 60-100 slices in each of the axial, sagittal and anteroposterior planes, depending on patient anatomy and cardiac size and shape.

A key aim of the project and one role for USFD/STHT was to evaluate the automated software used by partners in the GC and compare it to the gold standard of hand segmentation. If a model is to be used successfully to predict response to CRT *a priori*, the workflow must be accurate, robust and require minimal user input; it is not feasible to expect the clinician to spend significant time learning how to use the software and then several hours segmenting heart for each patient.

A challenge of the project was using the segmentation tool developed by UCL and Phillips, originally CT based and then refined on optimal images acquired from healthy subjects at KCL using a Phillips MRI scanner. Significant effort had to be made to carry out similar optimisation on the Siemens MRI scanner in Sheffield. The first images acquired in Sheffield were not optimal and whilst they all could be segmented by hand, there were issues when using the automated segmentation tool. The STHT cMR department received a great deal of input from KCL before images of acceptable quality could be acquired.

For the semi-automated segmentation, the shape of the LV was often found to be quite accurate and the endocardial border clearly defined due to the bright blood pool

and nulled myocardium, but the epicardial border was often poorly defined and generally overestimated. The surrounding non-cardiac tissue was of similar intensity and so the software had difficulty differentiating one from another. If the epicardial border is over-estimated and the endocardial border is accurate, the LV volume, i.e. the volume of blood, will be correct but LV mass and total LV volume will not. Furthermore, the underlying model guarantees that the resulting mesh will resemble the expected shape of the four chambers regardless of the accuracy of the fit.

Preliminary work used a fully automated tool, developed in GIMIAS was to compare fully automated, semi-automated and manual segmentation techniques. This tool required the user to load the cMR 3D SSFP files into the interface and select the LV apex, MV and AV annulus. Then using an intensity-based segmentation process, the tool differentiated cardiac tissue and great vessels from the extra-cardiac structures. However, this work and the use of this tool were abandoned since, as can be seen in figures 46 and 47, the accuracy was questionable on even on gross, qualitative analysis. As can be seen in the figure, different shades should correspond to different anatomical structures. However, the tool appears to have mistaken the position of the LA for the descending thoracic aorta. This is likely to be a consequence of sub-optimal cMR 3D SSFP images, with poor delineation between thoracic structures, atypical cardiac anatomy that the pre-existing GIMIAS heart template was unable to reconcile and the inability to make manual adjustments to the process of segmentation using the GIMIAS interface, despite it clearly segmenting the wrong structures.

Figure 46: Automated cMR segmentation (shaded red) axial and sagittal

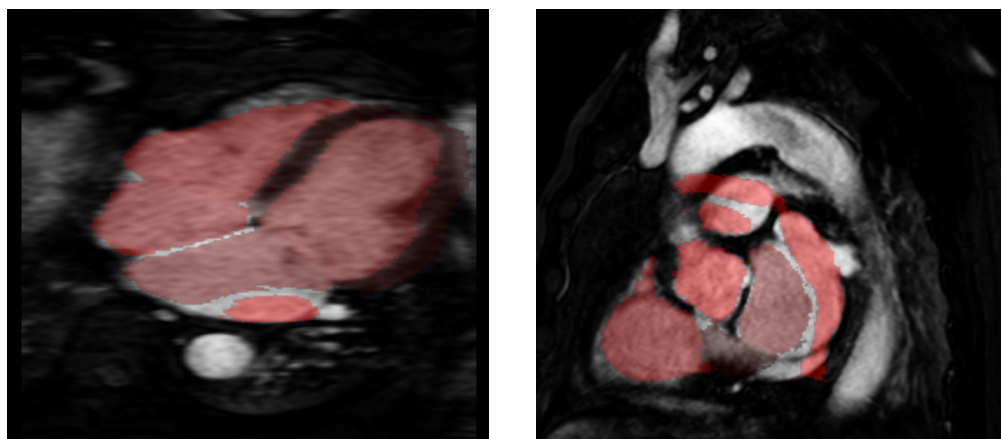


Figure 46 demonstrates the poor automated segmentation with the bright blood pool and grey myocardium from the cMR and various shades of red overlaid from the segmentation, which are not delineating the cardiac borders but overlapping with various extra-cardiac structures.

Figure 47: Automated segmentation mesh (left) with actual cMR image (right)

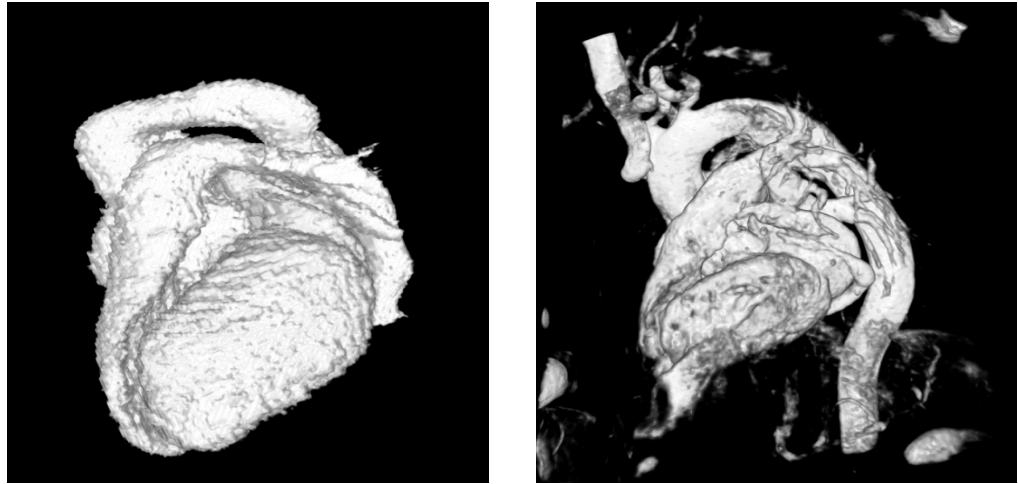


Figure 47 demonstrates on the left, the resulting 3D whole heart segmentation from created using the automated segmentation tool, versus what it should look like on the right, note the severely truncated aortic arch and lack of distinction between left atrium and ventricle

5.6.3 Method

5.6.3.1 Manual Segmentation

The images were segmented by first loading the 3D SSFP DICOM files into ITKSnap, Open Source 3D segmenting software (<http://www.itksnap.org/pmwiki/pmwiki.php>). The endocardial surface was segmented initially in the sagittal plane by tracing the outline of the LV between the blood pool and endocardium. Once all the segments in the sagittal plane were outlined, the images and segmentations were reviewed in the axial plane and then the anteroposterior plane, adjusting as necessary to ensure the best fit possible. This cycle was then repeated, until there was a smooth rendering of the LV endocardial surface, which was then used to create a 3D marching cubes mesh. A marching cubes mesh is polygonal mesh of an iso-surface from a three-dimensional field, comprised of voxels. Voxels consist of volume and pixel, and a pixel comprises a picture and an element. A marching cubes mesh is typically used for visualising medical data from MRI or CT. Since what might appear correct in one plane was often

incorrect in another, the 3D mesh could be updated and reviewed contemporaneously after every adjustment, the, to ensure that best fit and anatomical correctness was retained. Following the current convention, papillary muscles, trabeculations and valvular apparatus were excluded from the segmentation. This method took about 2 hours to complete per LV surface; a total of 4 hours per patient. Figure 48 demonstrates the 3D whole heart cMR DICOM images and figure 49 shows the same images loaded into segmentation software, in this case ITKsnap, with images being segmented, in particular the endocardial surface seen as the red shaded area. In figure 50, the end result can be seen after the 3D endocardial surface has been segmented by hand.

Figure 48: 3D SSFP cMR in 3 orthogonal planes, sagittal, axial and coronal

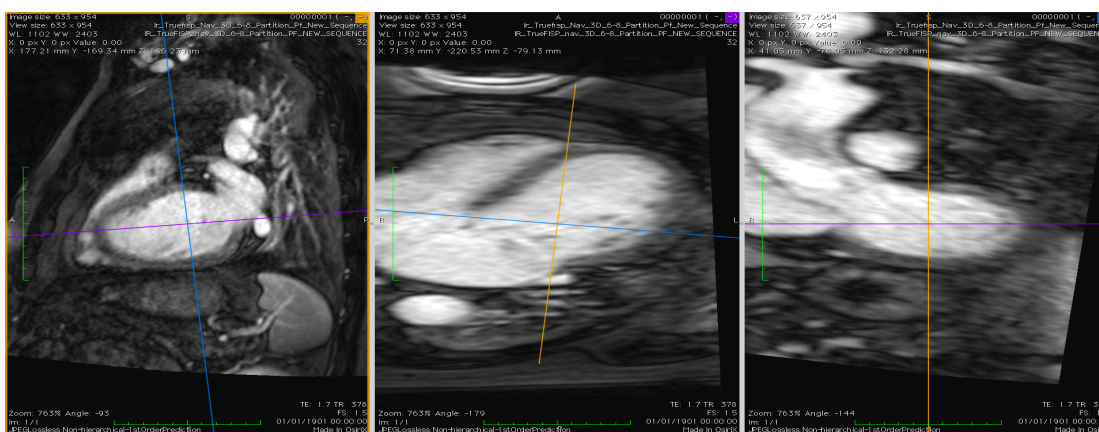


Figure 48 demonstrates the 3 orthogonal views possible following a 3D whole heart acquisition, which can then be used to create a 3D segmentation of the left ventricle.

Figure 49: Process of hand segmentation of the LV endocardial surface

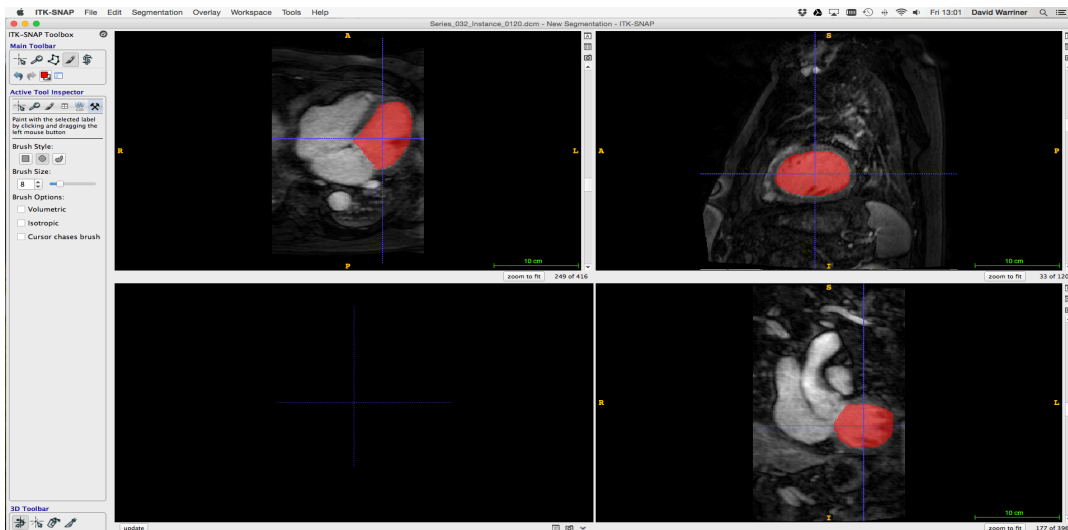


Figure 49 demonstrates the 3 orthogonal views seen during the process of hand segmentation of the left ventricle, with the areas shaded in red denoting the endocardial surface and volume, using ITKsnap.

Figure 50: Hand-segmented LV surface epicardial (left) and endocardial (right)

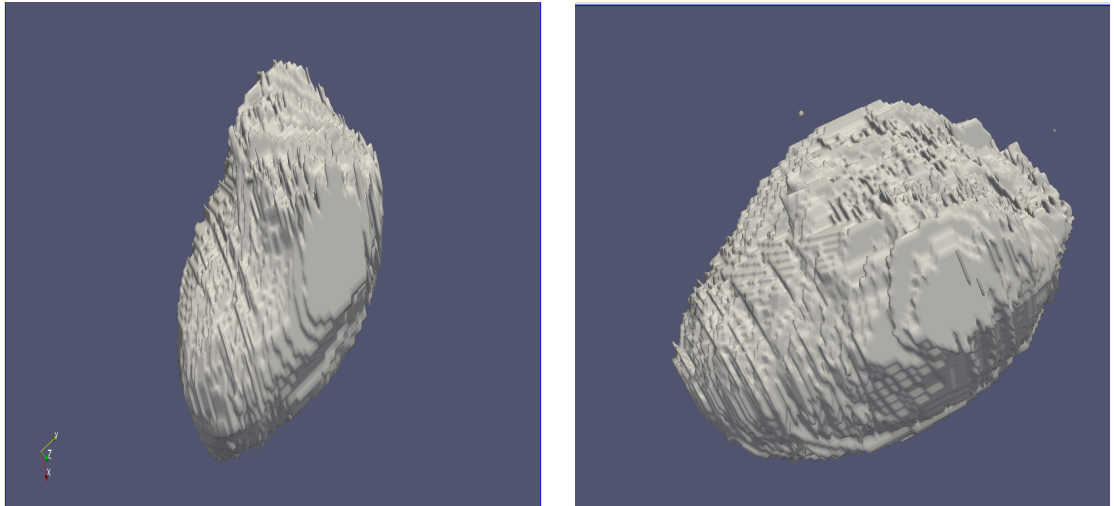


Figure 50 demonstrates the 2 3D surfaces created by hand segmenting the left ventricle, the epicardial surface on the left and the endocardial on the right. Note the large number of ridges present when segmenting by hand, each representing an individually delineated (shaded) section, not seen when using other techniques.

5.6.3.2 Semi-Automated segmentation

The semi-automated segmentations were created using a tool developed by UCL and Philips²⁵⁹ (see figure 51 and 52). It was proposed that this would be used for the GC workflow to ensure standardisation across both KCL and USFD. The 3D SSFP files were loaded into the tool and the 3 points (LV apex, MV and AV annulus) selected. Using intensity-based segmentation process, the tool differentiates cardiac from non-cardiac tissue, the 4 cardiac chambers and great vessels and most importantly (for this work) the bright and white blood pool from the nulled and dark myocardium. Importantly, the segmentation fit to the 3D whole heart cMR could be adjusted and re-run to create a best fit, hence the description 'semi-automated'. The pre-existing template is "fitted" to the cMR image.

Figure 51: 3D whole heart segmentation using the UCL tool

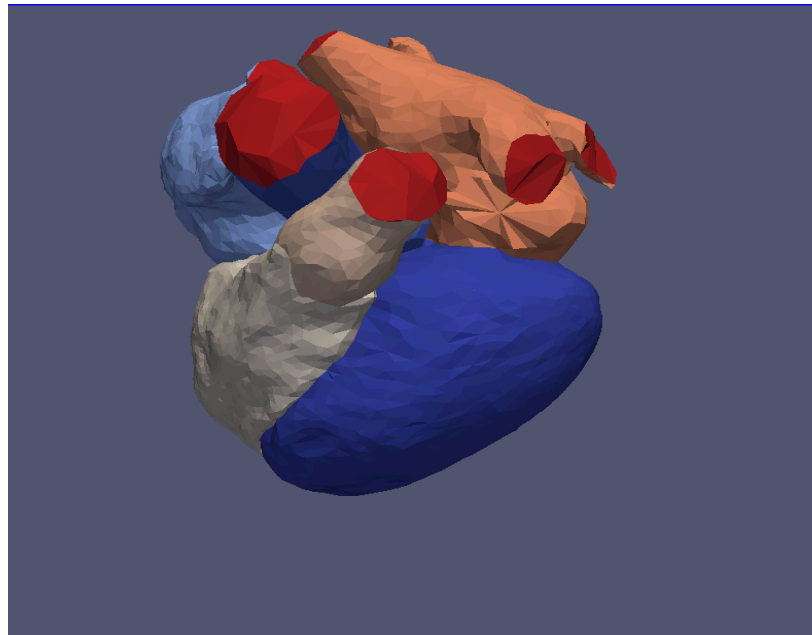


Figure 51 demonstrates a 3D whole heart segmentation using the UCL semi-automated tool, with left ventricle in dark blue, right ventricle in white, pulmonary artery in brown, right atrium in light blue and left atrium in orange. Note how much smoother the surface is.

Figure 52: Outer (left) and inner (right) LV surface from using the UCL tool

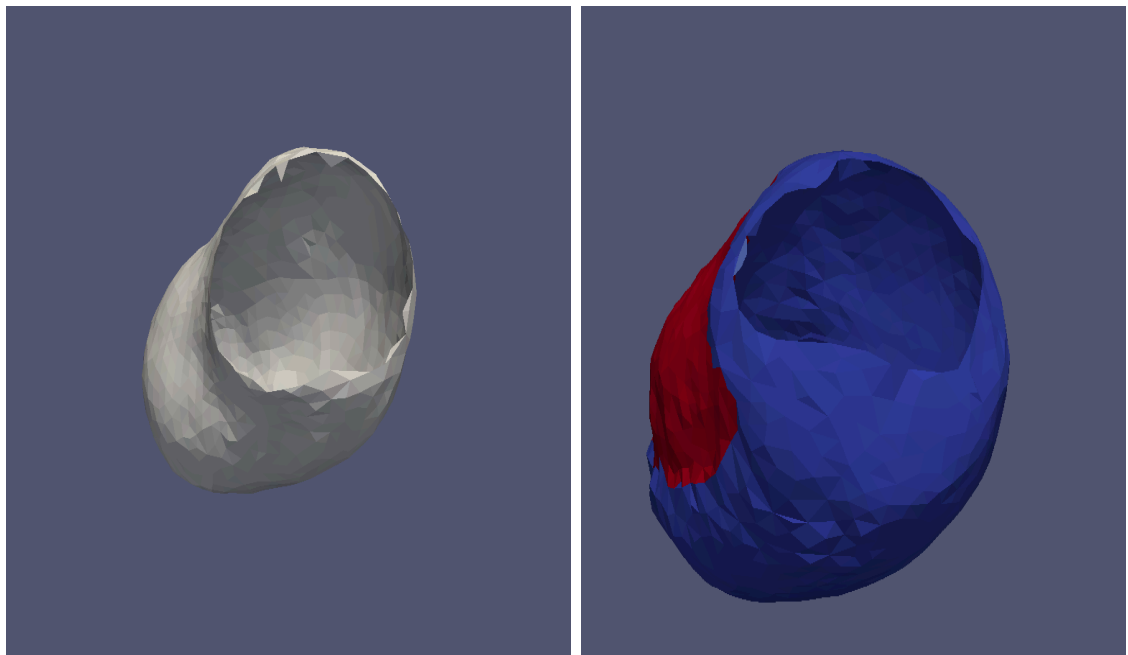


Figure 52 demonstrates the left ventricular surfaces segmented using the UCL semi-automated tool, with left ventricle epicardium in dark blue, and endocardium in white.

5.6.3.3 Comparison between Hand and Semi-Automated Segmentation

To ensure like was compared with like, for both the semi-automated and hand-segmented images, the LV segmentations were divided into 2 surfaces (epi- and endocardial) rather than a single LV volume. Code was developed in Matlab (The Mathworks Inc, Cambridge, UK) from at USFD for comparing surfaces. For each of the surfaces 4 points were selected manually, 1 at the LV apex and 3 on the LV base, in order to align the 3D images in space, using a coordinate system, X, Y and Z. The images had to be rotated and then translated, as the coordination systems for both the UCL and ITKsnap tools were slightly different, which meant they did not completely overlay in 3D space. The code compared the position in 3D space of each voxel, comprising the same point of each surface. This calculated the number of voxels compared between each surface and gave the mean, SD and maximum distance of the voxels from each other. The closer the voxels, the smaller the mean, SD and maximum distance and thus the more accurate the 3D segmentation compared to the gold standard of hand segmentation.

5.6.4 Results

The 3 figures demonstrate first an example of the overlay for corresponding hand and automated segmentations (figure 53), second a heat map demonstrating the distance of each voxel in the automated segmentation from its equivalent in the hand segmentation (figure 54) and finally a histogram with the number of points along the y axis and distance along the x axis, along with the mean and median distance of each voxel (figure 55). Table 50 gives a summary of all 20 patients, with the mean, SD and maximum distance between the two surfaces compared, demonstrating that the endocardial surfaces were more closely matched than the endocardial surfaces. The SD is greater than the mean in some circumstances, as the distance between the voxels could be positive or negative e.g. more endocardial or epicardial. Between 40,000-70,000 voxels were compared for each surface. The segmentations produced using Philips's UCL tool have a voxel size of 2.0 by 2.0 by 2.0 mm and the segmentations produced by hand have a voxel size of 1.5 by 0.77 by 0.77 mm. Unlike the semi-automated segmentation, the hand segmented surfaces did not consistently define where the ventricular surface ended and in others it ended prematurely. For this

200 | Page

reason, both surfaces were trimmed arbitrarily 5 mm from a manually defined basal plane, to ensure like was compared with like. This is also important as the template mesh of the ventricle did not include features such as the aortic or mitral valve, apparatus or valvular LV inflow/outflow continuity.

Table 50: Mean, SD, maximum distance and number of individual voxels.

Segmentation	Mean (mm)	SD (mm)	Max (mm)	Number
Inner	2.82	3.51	14.67	43141.80
Outer	4.79	3.85	18.20	76086.33
All	3.80	3.68	16.43	59614.07

Figure 53: Hand (green) and semi-automated (red) LV surfaces overlaid

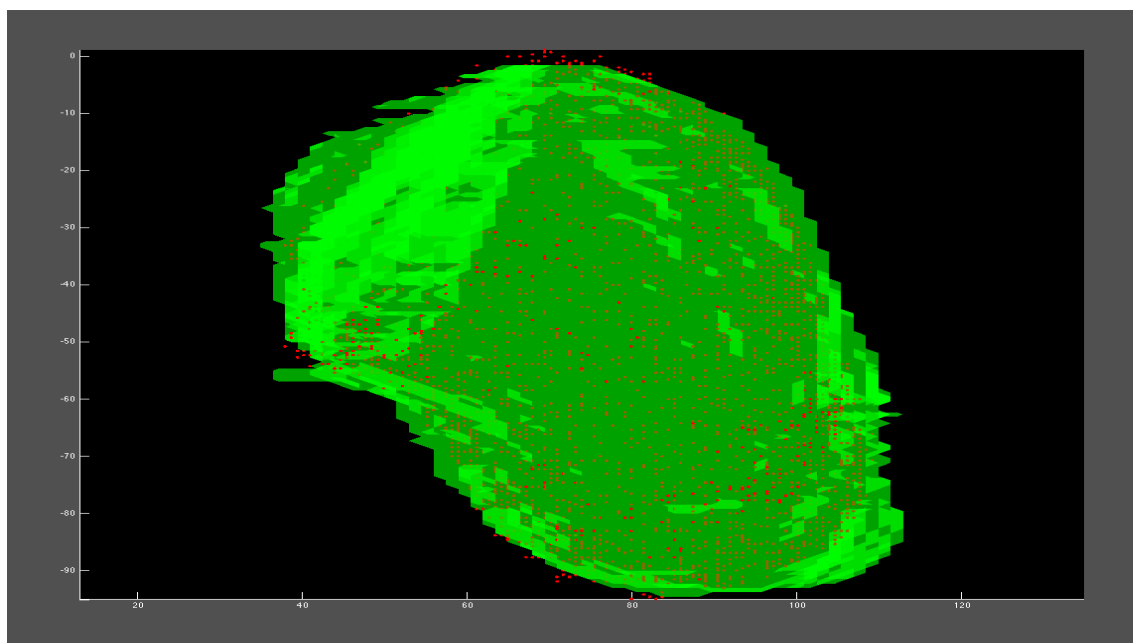


Figure 53 demonstrates the segmented endocardial left ventricular surfaces overlaid in MatLab, with the hand segmented surface in solid green and the semi-automated surface in red dots.

Figure 54: LV surfaces of hand (white) and semi-automated (colour) segmentation

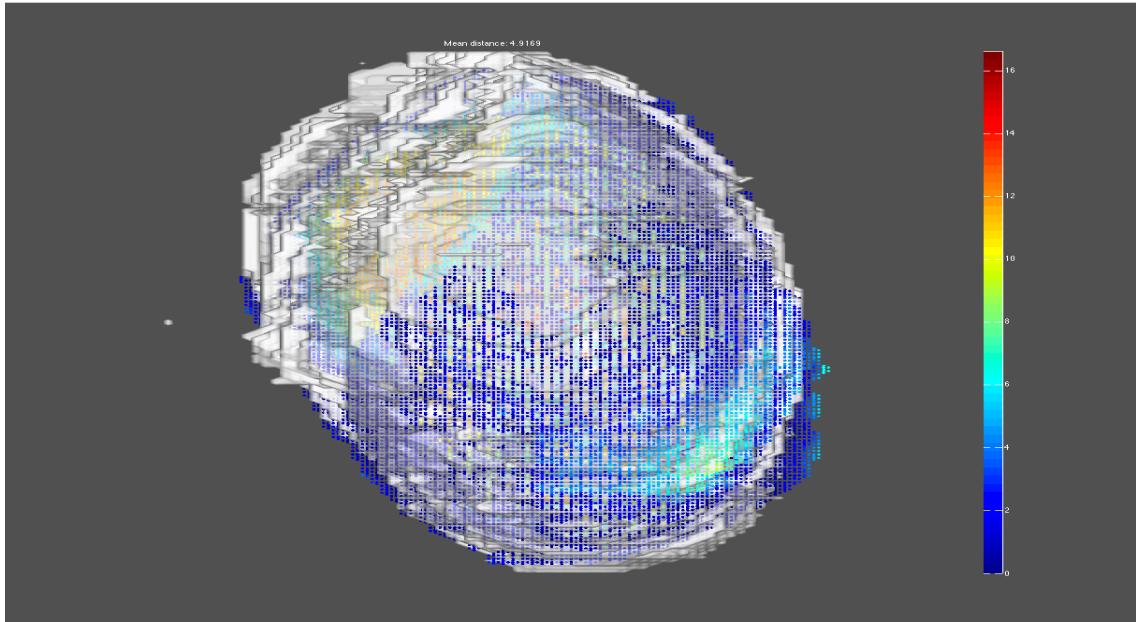


Figure 54 demonstrates the segmented epicardial left ventricular surfaces overlaid in MatLab and shown as a heat map, with the hand segmented surface in white and the semi-automated surface shown in rainbow colouration, from blue to red, depending on the proximity of the two voxels compared from each surface.

Figure 55: Comparing the distance between corresponding voxels in each surface

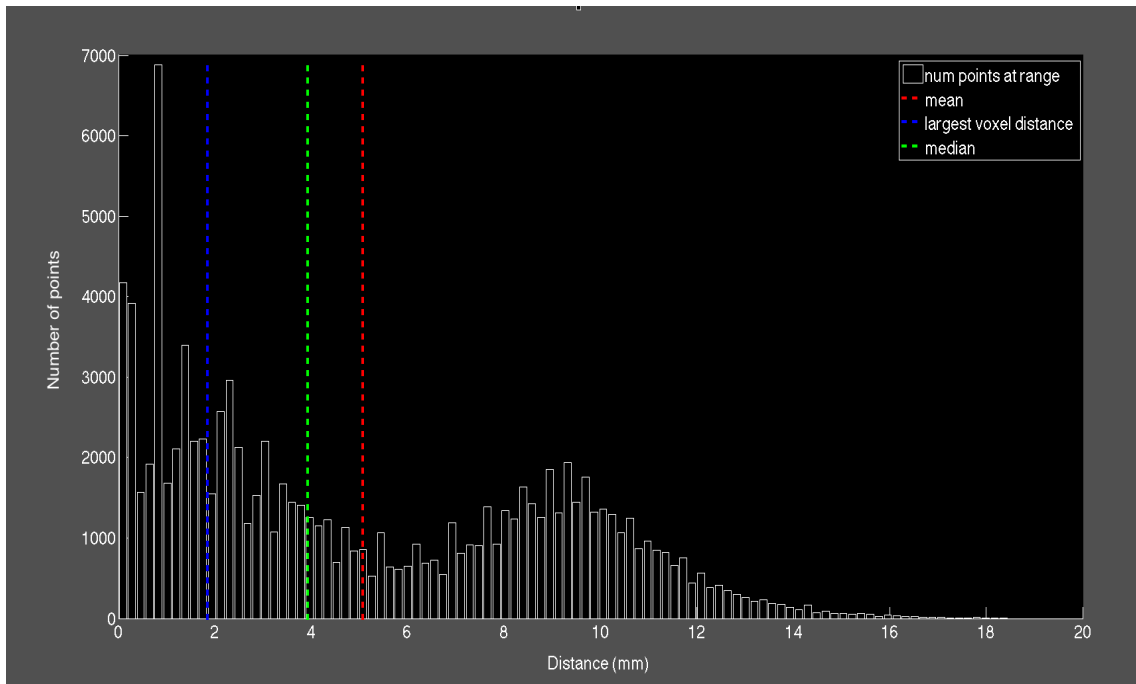


Figure 55 demonstrates the distance between the voxels in the left ventricular segmented surfaces, created by hand or by semi-automated tool.

5.6.5 Discussion

The aim of this aspect of the project was to compare the gold standard of hand segmentation with the semi-automated tool from developed and used by UCL and Phillips to assess its accuracy. If the GC was successful in predicting response to CRT with the available cohort of 50 patients, then the next stage would be an RCT using the segmentation tools and 3D models for multiple sites with potentially hundreds of patients. For the workflow to run smoothly and be automated, the same robust, standardised and consistent segmentation process would need to be used across all sites. Whilst giving good results, the process of hand segmentation took over a week to complete 20 cases. This was crucial for the development of the tool but clearly is not a sustainable use of a clinician's time. Both tools were easy to use but the automated tool saved many hours of work. What was clear was that the semi-automated tool was developed on healthy patients with high quality cMR images and normal LV geometry. The automated tool struggled to cope with dilated ventricles and where the geometry changed from half an ellipse to a windsock, with the accuracy falling subjectively to the naked eye and objectively when using the comparison tool. Furthermore it is clear that the mean, SD and maximum distances for comparing the endocardial surface were more accurate than when comparing the epicardial surface. This is a result of the gadolinium-based contrast, which clearly delineates the blood pool from the myocardium and thus demarcates the inner surface. For the outer surface the myocardium had to be distinguished from other extra-cardiac structures, without the strong difference in signal intensity this was difficult with the naked eye even when using 3 orthogonal plains, and proved to be extremely challenging for the automated tool. The accuracy of automatic segmentation is largely dependent on the quality of the 3D images, which, in turn, is determined by the scanner set-up, the radiographer, and the characteristics of the patient. This being said, clearly the hand-segmentations have a very irregular shape, being create in a slice wise fashion, other errors included incomplete regions and unintended artefacts. Similarly, the semi-automated tool arbitrarily divided the inter-ventricular septum into two surfaces, the right and left ventricle, creating an anatomically incorrect surface appearance.

At first glance, the mean difference in distance between the voxels (2.8-4.79mm) seems acceptable, although the sample is small making statistically comparisons

unreliable. However the maximum distance of up to 18.2mm between corresponding voxels, is less impressive suggesting that the automated tool is far from accurate for this purpose. From gross observation, it was the shape of LV that the automated software had greatest difficulty interpreting, rather than its size. This, in part is because the software tries to fit a pre-existing cardiac template to the images it analyses and thus the boundary conditions are predetermined. Significant deviations from this cannot be accommodated and subsequently important shape characteristics will be lost e.g. the windsock is forced into hemi-ellipse. Indeed, normal LV thickness is < 12mm and in most cases, patients with HF-LVSD have dilated and thinned hearts; a mean difference of even 2.8 – 4.79mm could give a 23 - 39% error in terms of over- or under- estimating LV volume and mass.

Both hand- and semi-automated- segmentation were carried out by a single operator (DRW), and whilst hand segmentation is felt to be the gold standard, this too will depend largely on the operator-experience in reviewing cardiac images (not just those in cMR) and is subject to both intra- and inter- observer variability. In this regard, DRW was the most experienced member of the project and thus it was felt having a non-clinician attempt to segment the LV, especially by hand and with poor images, would not be beneficial. DW had also viewed the 2D and 3D TTE images of the patients. In the future, it could be useful to explore this by exposing the automated tool to several untrained operators for segmenting the same LVs and comparing these to the gold standard. Furthermore, at the time of writing, the automated segmentations have not been used to create any meaningful models, which, whilst not a criticism of this work, means that the significance of such findings are somewhat limited.

Most automated LV segmentation algorithms use thresholding, region growing, edge detection, and clustering, based on short-, long- or multi-axis images. Also, the majority of previous work has been carried on dogs and pigs *in vivo* and *ex vivo* with CT rather than cMR. As two different applications used in this study, ITKsnap (creating LV 2 surfaces, not a single LV volume) and UCL (creating a 3D volume) direct comparisons of ventricular volume or mass cannot be made. Similar studies, albeit using different methods, have found automated tools to produce LV segmentations with 60-93% accuracy compared to the gold standard^{260 261}. Studies comparing hand versus

semi/fully automated segmentation of the LV are on-going but, as yet, hand-segmentation retains its position as the gold standard with few studies looking at patient data, but rather, data from healthy volunteers with “normal” hearts. The ideal approach would be semi-automated, whereby the operator chooses the initial areas of interest, which are then populated by the tool and then errors can be corrected manually afterwards. This would combine the speed advantage of the automated process with the accuracy of the manual one.

At the time of writing no cMR compatible CRT devices exist and a follow-up cMR was therefore not included in the GC ethics but such information with accompanying 3D segmentation would be fascinating to track exactly how the LV changes in size, shape and function. This could also be used for further validation of the automated segmentation process. The findings of this work were fed back to partners in the GC project in order to improve the automated segmentation process for future patients.

5.7 Geometrical model

This work was completed with PL.

5.7.1 Introduction

Cardiac anatomical remodeling is one of the main clinical features of HF-LVSD. As heart disease progresses into HF-LVSD, the ventricles become larger and more spherical with deteriorating cardiac function and symptoms becoming evident. Slowing, or reversing, remodelling is a therapeutic target in HF of all aetiologies and is thus regarded as an important sign by which HF-LVSD can be stratified and monitored. Currently, reverse-remodelling is mainly characterised through changes in EF or in myocardial mass.

In the past, technical factors and differences of interpretation have led to inconsistencies of results when assessing ventricular size and shape remodelling²⁶². Recent advances in imaging and computational techniques now allow 3D reconstruction and detailed comparison of the anatomy through the construction of statistical atlases. More specifically, cMR imaging is a non-invasive modality

considered the gold standard to assess left ventricular morphology²⁶³. Statistical atlases of cardiac anatomy built from CMR studies have been used to analyse shape differences within populations or to assess inherent bias between acquisition protocols^{264 265}. In such atlas studies, a 3D mesh represents the shape of each individual's anatomy, and it becomes an accurate virtual reconstruction able to capture subtle changes in the subject's anatomy.

The aim of this work was to conduct a comprehensive shape analysis of LV anatomy in a cohort of subjects that were selected for CRT and to test the existence of differences in between responders and nonresponders on the cohort of 50 patients (including the 20 patients from Sheffield). Shape analysis is a potential selection criterion that has not yet been studied, this perhaps surprising since left ventricular reverse remodeling is a widely-used and cited for assessing CRT response as it has been shown to accurately predict long-term survival^{266 267}.

5.7.2 Method

A statistical anatomical atlas gives a representation of an average shape and its variation within a given population. A robust and reproducible methodology is used to extract the shape of the LV from clinical images, and then encode and describe that shape with a consistent mathematical framework. In this study, the LV from each clinical case was represented in two ways; by a virtual 3D reconstruction of the anatomy and by a dual set of shape coefficients.

Segmentation of the LV anatomy was performed manually as described previously. Subsequently, 3D geometrical meshes were automatically fitted to the resulting segmented masks using methodology described in Lamata et al (2011)²⁵⁷. Each reconstructed mesh consists of a set of control points that describe the vertices of the shape and the curvature between vertices, totaling to 3504 degrees of freedom. The control points that describe the ventricular shapes of the population were then collectively analysed using Matlab 2013b (The MathWorks, Natick, MA) to create a computational atlas. In order to identify the main modes of variation in the left ventricular shapes, a complex statistical process, called principal component analysis

(PCA) was undertaken. PCA is a statistical technique used to emphasise variations and highlighting any patterns in a dataset. PCA uses orthogonal transformation to convert a range of possibly correlated variables, called principle components into a set of values of linearly uncorrelated variable. The goal of PCA is to describe the maximum amount of variance with the lowest number of principal components. Directions of anatomical change that explain the largest variance within the population under study were extracted. Each geometrical mesh is then projected into these axes of anatomical change to find the shape coefficients that describe the anatomy of each subject.

5.7.3 *Statistics*

Identification of CRT-response, based on either EDV or ESV rate changes, was used as the basis for patient stratification. Fisher's linear discriminant was used to identify the modes of variation that provide the best separability between the shape coefficients corresponding to the cohorts of responders and nonresponders. The area under of the receiver operating characteristic curve (AUC) was used to analyse the performance of the categorisation together with sensitivity and specificity. Values of $p < 0.05$ were considered to be statistically significant.

5.7.4 *Results*

5.7.4.1 *Characteristics of the participants under study*

Of the 50 subjects in the combined cohort, 76% were male. The mean age was 69 years (± 11), 50% had HF-LVSD of ischaemic aetiology, the mean QRSd was 153 ms (± 21), the average NYHA class was III and 88% had LBBB. 28 patients (56%) were identified as responders and 22 (44%) as nonresponders corresponding to a minimum 10% decrease cut-off in the LVESV, as described by Yu et al (2005)²⁶⁸. As seen in table 51, Using LVEDV as definition of response for the same volume change rate of 10% there were 25 responders (50%) and 25 nonresponders (50%). The mean reduction of left ventricle LVEDV for responders was $46.92 \pm 12.0\text{mL}$ ($p < 0.01$) and their LVESV decreased to $45.17 \pm 13.64\text{ mL}$ ($p < 0.05$). There was no significant difference between nonresponders at baseline and follow-up when the comparison was based on LVEDV. However, there was a significant increase of LVESV before and after 6 months of CRT implantation in the nonresponder group.

Table 51: Characterization of cohorts based on left ventricular volumes

	LVEDV			LVESV		
	Baseline	6 months	<i>p</i> value	Baseline	6 months	<i>p</i> value
Responders	183.8 ± 61.2	139.9 ± 49.2	< 0.01	144.5 ± 90.3	99.3 ± 76.7	< 0.05
Nonresponders	186.6 ± 92.8	214.9 ± 91.4	0.30	130.8 ± 43.6	164.1 ± 55.0	< 0.05

5.7.4.2 Construction of the statistical atlas of left ventricular anatomy

The creation of the cardiac statistical atlas involved fitting a 3D mesh to each of the segmented myocardial anatomy cases (figure 56).

Figure 56: The 3 stages of the mesh personalisation process

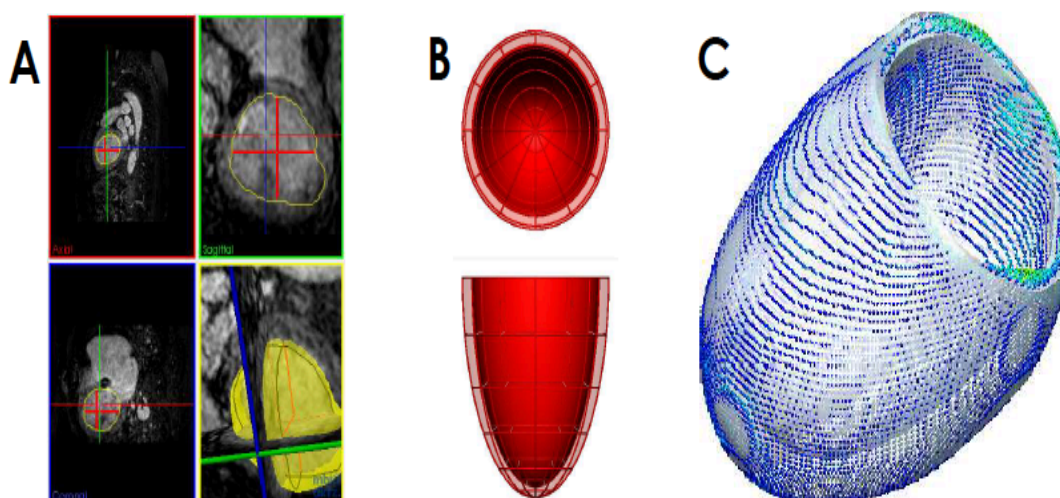


Figure 56 demonstrates the stages of the mesh personalization process, A displays the manual segmentation, where 3D interpolation is performed from a discrete set of 3D contours, B mesh template with 72 elements and C result of the mesh personalization (white mesh) overlaid to segmentation (colour-coded by fitting error).

The resulting mean fitting error for the 50 cases was 0.45mm. Subsequently, the first five modes of shape variation of the left ventricle were identified by means of PCA

these were mode 1 and 2 for 3D orientation, mode 3 for size, mode 4 for spherical remodeling and mode 5 for length. In overall, these five modes accounted for 72.5% of the variance of left ventricular anatomy in the population (see figure 56).

Figure 57: Variances of the modes of shape variation from PCA

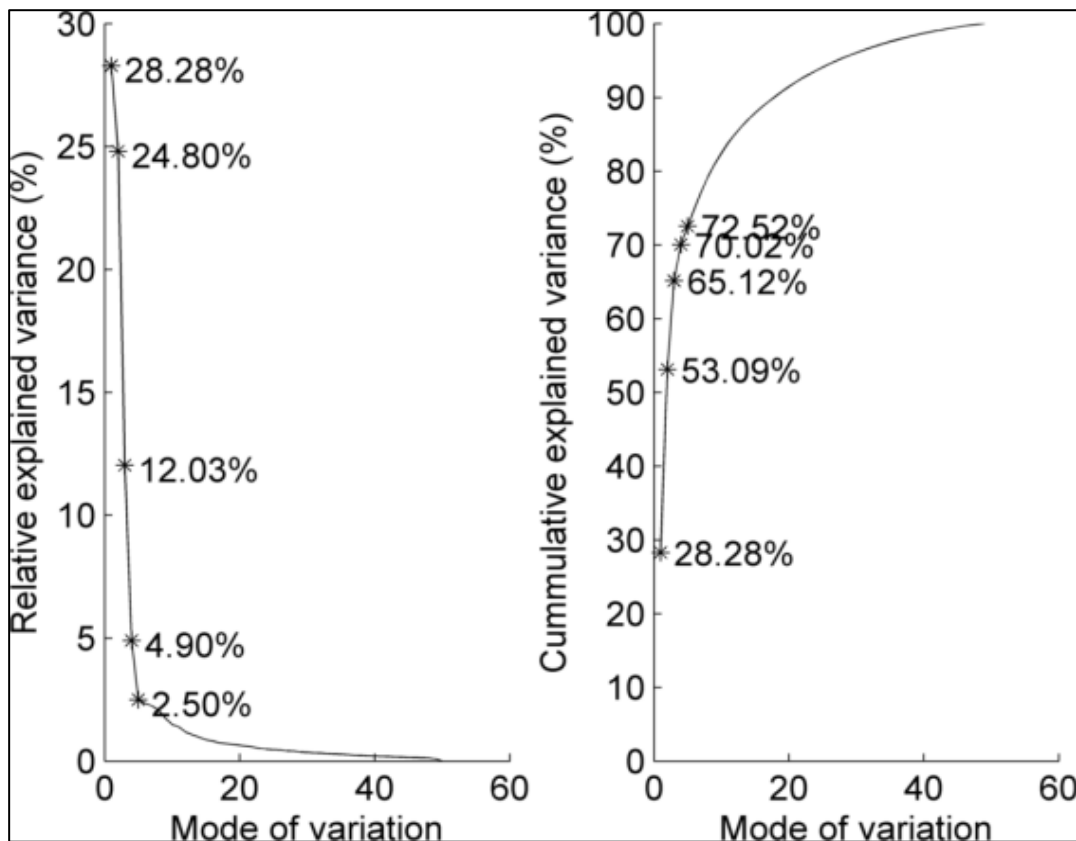


Figure 57 demonstrates the relative (left) and cumulative (left) explained variance against the mode of variation, demonstrating how the 5 modes could explain 72.5% of the variance in left ventricular shape between the responders and non-responders.

5.7.4.3 Changes of left ventricular geometry between cohorts

The groups of responders and nonresponders, as determined by a change in LVEDV and LVESV, were different in shape by the fifth and the fourth mode of anatomical variation, respectively (figure 57). Other modes of anatomical variation showed lower statistically significant differences between groups, accounting for very small changes and thus were discarded.

Figure 58: Differences between responders and nonresponders by variation modes

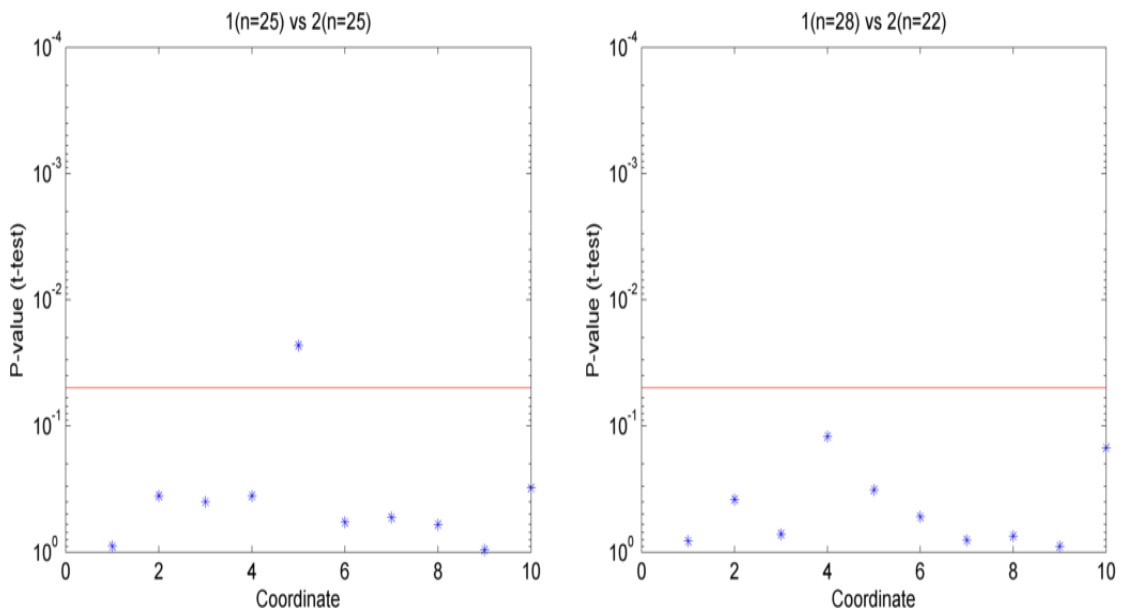


Figure 58 demonstrates the differences in left ventricular shape variation between responders and non-responders. The red line indicates a significance of $p = 0.05$. Left, comparison between cohorts using end-diastolic volume rate change of 10% as definition of response, demonstrating that mode of variation 5 was significantly different. Right, comparison based on end-systolic volume rate change of 10% as definition of response where mode of variation 4 was the closest mode to show statistically significant differences between cohorts.

Figure 59: Mean LV shape (left) and overlay of responder and nonresponder (right)

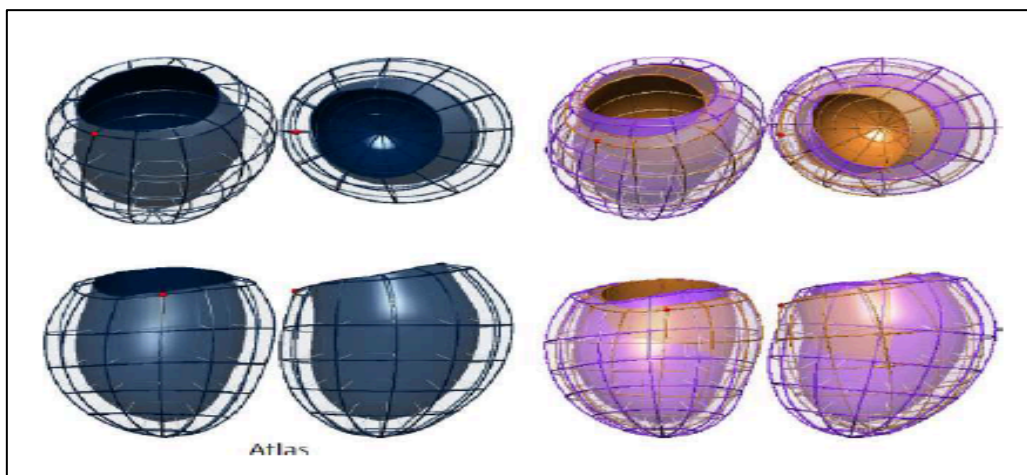


Figure 59 demonstrates the average LV anatomy of the statistical atlas on the left (dark blue) compared to the extreme geometry of the responder (purple) and

nonresponders (gold) groups, computed by the linear discriminant analysis combining modes 2 and 5. The small red sphere is located at the septal wall. The adverse remodeling shows a shorter septal wall and angle basal plane

The geometrical changes of the left ventricle meshes that correspond to the fourth and fifth modes of variation described earlier. This was visually assessed by overlaying 3D models that represent ± 2 standard deviations of the mean shape and colour-coding the differences among their corresponding node coordinates (see figure 61), illustrating the subjects that were identified as responders and nonresponders based on LVEDV and end-systolic volume (LVESV). The fourth mode of variation, predictor of response in ESV, was related to changes in the sphericity (height to width ratio of the left ventricle²⁶⁵). This spherical shape variation can be noticed as both concentric remodeling (changes in endocardium) and eccentric remodeling (differences in epicardium nodes) have a more regular pattern around the mid-ventricular section as compared to mode 5.

Accordingly, the average shapes presented remarkable similarities; responders generally presented thinner walls compared to nonresponders, and this reduction was more accentuated when ESV was used as definition of response.

Figure 60: Distribution of shape coefficients in PCA coordinates 4 and 5

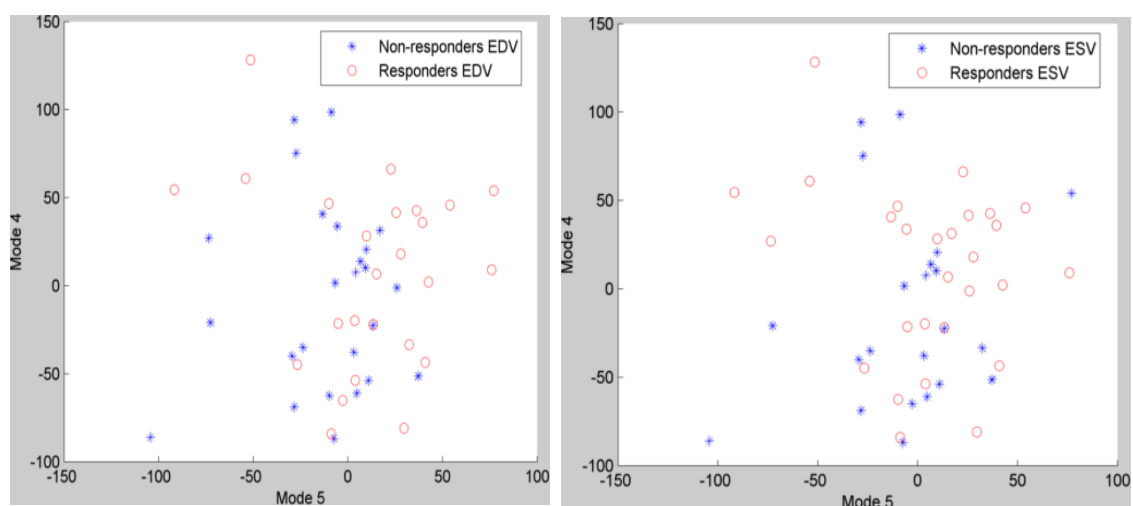


Figure 60 demonstrates the large overlap of cases corresponding to responders and nonresponders depending on the EDV and ESV criteria, as illustrated in PCA coordinates 4 and 5.

Figure 61: Comparison of differences between statistical averages of LV shapes

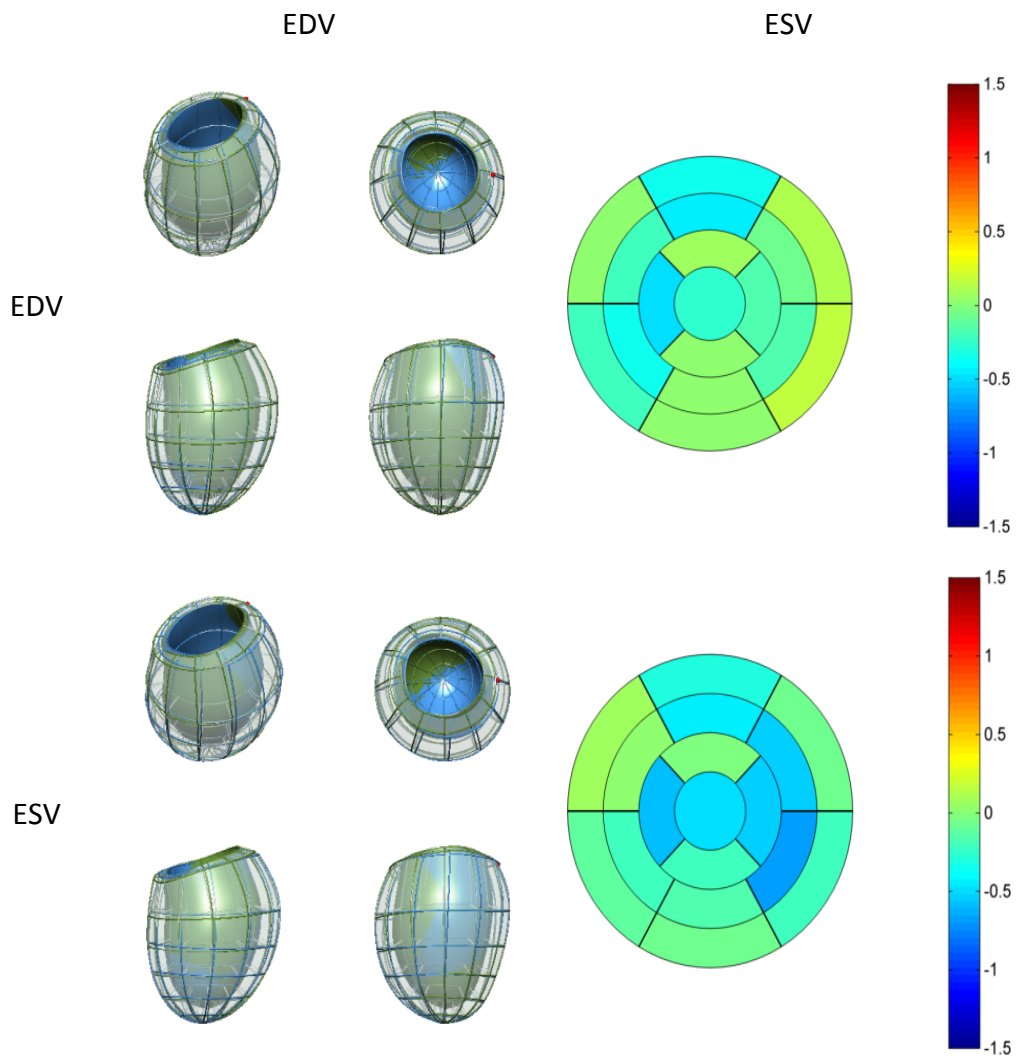


Figure 61 demonstrates, left, the overlay of average shapes corresponding to responders (blue) and nonresponders (green) and right, bull's eye plots illustrating the differences in wall thickness between nonresponders and responder average shapes (responders present thinner walls).

Figure 62: Illustration of the anatomical changes encoded by Mode 4 and Mode 5

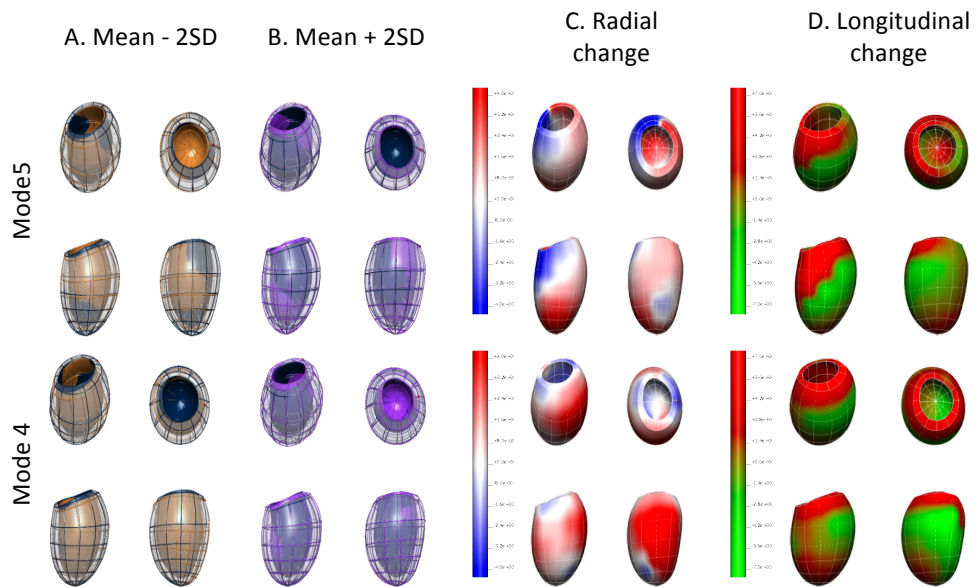


Figure 62 illustrates the different anatomical changes encoded by PCA modes 4 and 5. Specifically, panels A and B show the average left ventricular mesh in dark blue with superimposed orange and purple meshes representing - 2 and + 2 standard deviations respectively, with an opaque endocardial surface and semitransparent epicardial surface, panel C illustrates the + 2 standard deviation mesh colored accordingly to concentric (red) and eccentric (blue) remodeling (- 2 standard deviation shape and colors are symmetric and not shown) and finally panel D represents elongation (red) and shortening (green) changes.

5.7.4.4 Classification performance by using the power of modes of variation

The classification performance was analysed by the discriminant power of the modes of variation using Fisher's linear discriminant as the basis for separability between responders and nonresponders. All possible combinations of the first four and five modes of anatomical variation, corresponding to LVESV and LVEDV respectively, taking 1 to $k-1$ number of modes at a time (where $k = 4$ for ESV and $k = 5$ for EDV) for each combination. As seen in figure 63 the best performance, as measured by the AUC, is obtained when a combination of different modes of variation is used in Fisher's linear discrimination rather than a single mode. Using ESV as the definition of response, the best combination is found when modes 1, 3 and 4 are used together (AUC = 0.66, sensitivity = 0.71 and specificity = 0.63), whereas the best combination for EDV comprises modes 2, 3, 4 and 5 (AUC = 0.73, sensitivity = 0.72 and specificity 0.76). Interestingly, the AUC values obtained using a single mode of variation approximate the mean of all the possible combinations using that mode ($AUC_{ESV} = 0.64$ and $AUC_{EDV} = 0.71$).

Figure 63: Comparison of AUC based on combinations of PCA modes of variation

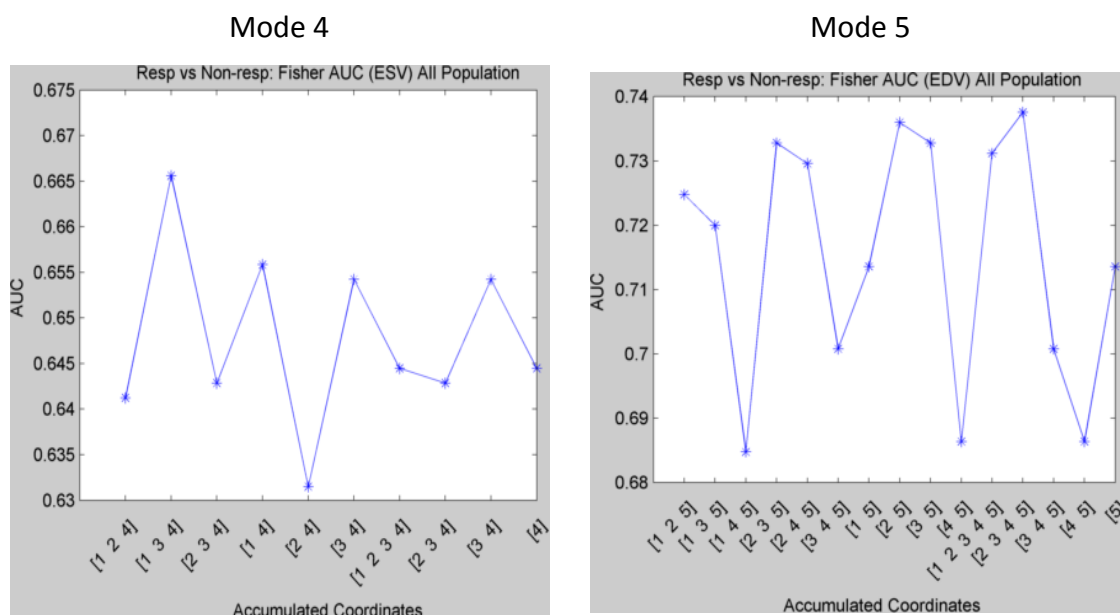


Figure 63 demonstrates principle component analysis mode 4 and end-systolic volume (left) and mode 5 and end-diastolic volume (right), in terms of the accumulated coordinates along the x axis and then the area under the curve along the y axis.

5.7.5 Discussion

Ventricular remodeling describes the changes occurring in the abnormal ventricular anatomy, including the morphological configuration of chambers and their increased volume over time ²⁶³. Remodeling due to HF-LVSD is the result of a combination of several factors that involve restructuring of myocytes, intercellular matrix components, and vessels in response to physiological or pathological stimuli ²⁶⁹. Depending on the etiology of HF, left ventricular remodeling could be categorised based on the extent of the modified shape. For example, the effects of remodeling due to hypertension and its prognosis can be classified in 3 geometric patterns based on measurements of mass index and relative wall thickness: concentric remodeling, eccentric hypertrophy and concentric hypertrophy ^{270 271}. The use of a computational atlas enables an extremely detailed description of these anatomical changes, based on a solid mathematical foundation, and this work is the first step towards the identification of heart failure remodeling patterns.

The reduction in LVESV and LVEDV after CRT implantation was better identified by a combination of different anatomical modes rather than a single mode of shape variation. This may be due to dependence on the selection of the response criteria, in which each of the two cardiac phases encodes different pathophysiological changes. It would be expected that this large overlap in the classification will decrease as further cases are studied. Indeed, in a larger cohort, the presence of ischemia could be used to further sub-divide the group of subjects. In addition, this whilst this work focused on a follow-up period of six months a longer follow-up also demonstrated many of the benefits of CRT ²⁷².

The choice of the criterion to define response is a critical aspect of any study of CRT. In this study, the reduction of ESV and EDV were chosen as the defining criteria, analysed independently at two institutions. Through experimental results identified that a reduction in LVESV of 10% represents a clinically relevant reverse remodeling factor and in this work significant reductions in both LVEDV and LVESV were found in responders; however, changes in LV shape coefficients were significantly different in LVEDV ²⁶⁸. This indicates that the selection of a definition of response could be

considered as a relative parameter and other parameters can be used as surrogates. In this study a similar percentage between responders and nonresponders to CRT using either LVEDV and LVESV as definitions of response was identified, whereas it has been documented that only about 70% of the patients which have undergone CRT show signs of a significant positive response to the procedure^{172 273 274}. With respect to the selection of criteria in predicting response, ejection fraction has proven to be a good predictor for cases related to super-responders^{275-278 279}. Nevertheless, left ventricular volumes and mass are more related to prognosis and the overall impact of therapy compared to ejection fraction²⁶³. Similarly, there is no universal agreement in the best single criterion or combination of clinical and echocardiographic criteria to use for long-term prediction²⁸⁰. In this work, the two factors that provide a more meaningful understanding of the morphological changes in vascular remodeling were chosen. It was observed that the fifth mode of variation in LVEDV – the mode with significant differences between responders and nonresponders – is a mode capable of detecting subtle anatomical shape variation in a cohort of individuals following CRT therapy.

5.7.6 Conclusions

This work presents the use of computational cardiac atlases for the extraction of potential shape markers of response to CRT. Recent advances in this field have demonstrated the ability of this technology to characterise cardiac disease and compare populations of patients^{264 265 281 282}. Assessment of LV shape prior to CRT implantation as observed in this study provided insight about the remodeling process in distinct stages and etiologies of heart failure. The findings indicate that the shape of the left ventricle is a potential biomarker to characterise response to CRT.

5.8 Electrophysiological model

This work was completed with BB.

5.8.1 Introduction

Figure 64: Type I (right) and Type II (left) activation patterns of the LV

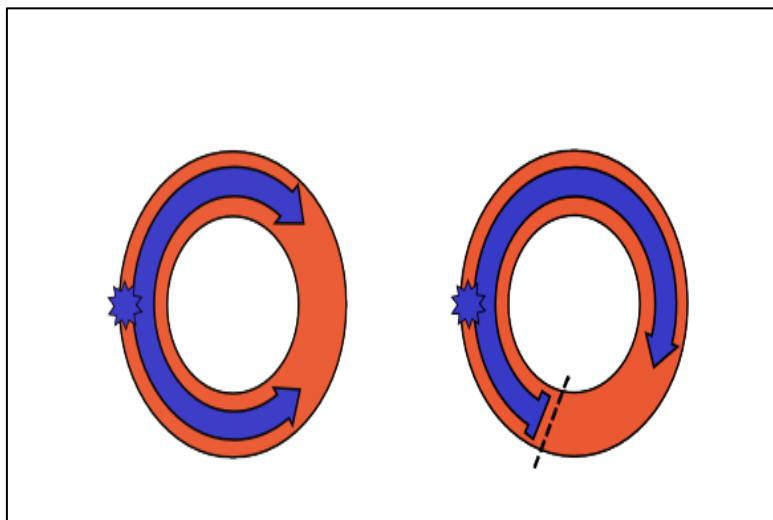


Figure 64 demonstrates the different activation patterns of the left ventricle. The star represents the septum, the arrow the direction of depolarisation and the hashed line, area of block.

It is believed that the underlying electrical activation pattern in the LV is a determining factor in the patient's response to CRT ²⁸³. Specifically, patients with a Type II or U-shaped activation pattern, characterised by a line of conduction block show a better response to CRT, than those with a Type I pattern, where activation begins at the septum and spreads in both directions to the lateral wall. Patients with Type II activation patterns are more likely to respond to CRT & are more common amongst patients with HF-LVSD of a non-ischaemic aetiology. This distinction is schematically seen in figure 64. Despite the relevance of this classification extracting activation patterns by a non-invasive means that is compatible with clinical practice remains challenging. There has been some success using mechanical activation sequences from tagged cMR as a surrogate, but as yet, these remain to be validated within a prospective clinical trial ^{284 285 286}. Furthermore, the use of mechanical activation sequences remains controversial given the negative conclusions of the PROSPECT and echoCRT trials.

Modelling offers a novel and alternative avenue to demarcate the different activation patterns, taking into account the patient's LV geometry and being driven by non-invasive clinical data, from ECG and cMR. The aim was to constrain the conductivity

parameter of a patient specific electrophysiology (EP) model, using the QRSd from a standard 12 lead ECG. The hypotheses are that the conductivity derived in this manner is consistent with the activation pattern using the methods described by Manav et al (2013)²⁸⁵ and that this will demonstrate predictive value for CRT. The model generation process is described; how the personalised geometry was created, the details of the model necessary to replicate physiological behaviour and how to determine the best estimate conductivity from the ECG.

Only Sheffield cases were used for this simulation, and of the Sheffield cases, only 10 simulations were found to be stable.

5.8.2 Methods

5.8.2.1 Mesh Construction

For EP simulation, high spatial resolution tetrahedral finite element meshes were required. These were generated in 3 steps, as illustrated in figure 65:

Figure 65: Mesh construction process

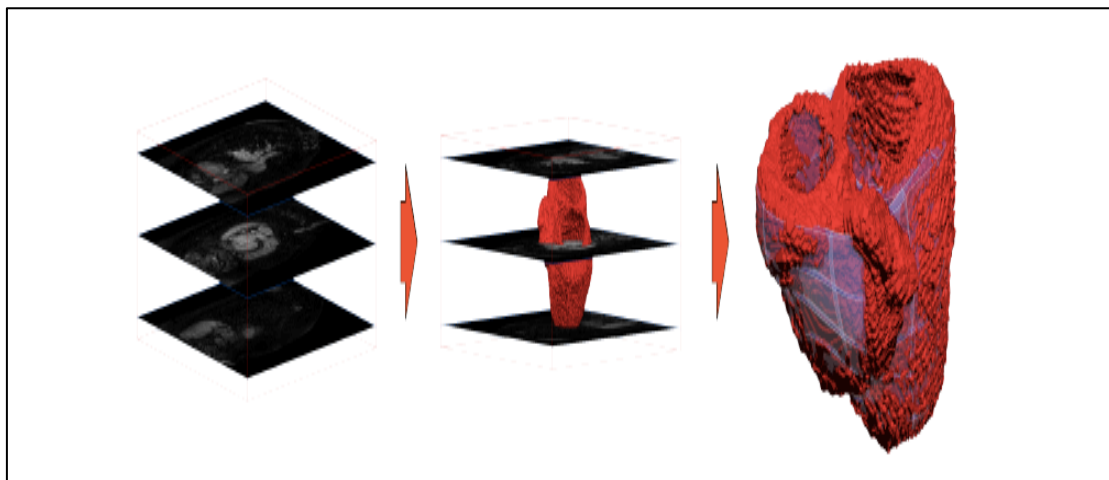


Figure 65 demonstrates the construction of the mesh, on the right first the myocardium was segmented from the cMR, in the middle, next a smooth low resolution mesh was fitted to the segmentation and finally on the right, a high resolution mesh was created from the smooth mesh.

A semi-automated segmentation of the myocardium was carried on the anatomical MRI volumes using a research tool created by collaborators at UCL²⁵⁹. This segmentation was compatible with simulation software, created a segmentation of

both ventricles (key for EP simulation) and also created a volume not a series of surfaces. The region of interest included both the left and right ventricles, from the valve plane to the apex. A smooth hexahedral cubic-Hermite mesh was created to define an internal coordinate system for the myocardium. A variational least squares minimisation approach was used to morph a template mesh to the segmented volumes from each patient ²⁸⁷. The least squares is an approach used in regression analysis, to identify an approximate solution to problem, in which there are more knowns than unknowns, the least squares referring to the minimisation of the sum of the squares of the errors made in each equation. Subsequently, commercial meshing software was used to generate a high-resolution tetrahedral mesh spatially embedded within the smooth mesh. Individual patient tetrahedral meshes consisted of between 98-280 million volume elements.

A generic fibre orientation based on data from human and canine histological studies was defined with respect to the cubic Hermite elements and mapped onto the tetrahedral mesh. Late gadolinium MR images were manually segmented to identify areas of scar in the myocardium. These domains were mapped onto the tetrahedral mesh by transforming both, into the canonical cMR coordinate system.

5.8.2.2 Biophysical model

The well-accepted biophysically-based pair of equations representing the spread of an action potential in tissues are the bi-domain equations; these represent the conservation of current within 2 spatially overlapping electrical potential domains separated by a permeable membrane ²⁸⁸. These domains represent the intra- and extra- cellular spaces. Under an assumption that the conductivity tensor (an object that describes linear relations between geometric vectors, scalars and other tensors) is not uniformly scaled and not rotated between domains, this pair of equations reduces to the mono domain equation:

Equation (5):

$$\nabla \cdot (\sigma \nabla V_m) = A_m (C_m \frac{\partial V_m}{\partial t} + I_{ion} + I_{applied})$$

Symbol	Description	Units	Rank
V_m	Membrane voltage	V	0 (scalar)
σ	Conductivity	S/m	2 (tensor)
A_m	Surface to Volume ratio	1/m	0 (scalar)
C_m	Membrane Capacitance	F/m ²	0 (scalar)
$I_{applied}$	Transmembrane Current	A/m ²	0 (scalar)
I_{ion}	External Current	A/m ²	0 (scalar)

The term I_{ion} is determined by the ten Tusscher human myocardial cell model²⁸⁹. This is mathematical model of the action potential of human ventricular cells that has considerable EP detail, but remains competitive in terms of computational cost, to be used in large-scale spatial simulations for the study of arrhythmias. According to ten Tusscher (2004)²⁸⁹ the model uses experimental data on the major ionic currents: “the fast sodium, L-type calcium, transient outward, rapid and slow delayed rectifier, and inward rectifier currents” and “basic calcium dynamics, allowing for the realistic modeling of calcium transients, calcium current inactivation, and the contraction staircase”. Finally, the model reproduces human epicardial, endocardial, and M cell action potentials and demonstrates that differences can be explained by differences in the transient outward and slow delayed rectifier currents.

The conductivity tensor σ is defined with respect to the fibre direction and a fix ratio of 0.35 between the primary fibre direction and the orthogonal plane (transversely isotropic e.g. the same properties in all directions), resulting in one free parameter that becomes the target of personalisation²⁹⁰. The system was solved using Cardiac Arrhythmia Research Package (CARP) (<https://carp.meduni-graz.at>) with a time-step of 10ms and mesh resolution of 250 μm necessary to achieve acceptable accuracy with biophysically detailed EP simulations.

5.8.2.3 Boundary Conditions

Figure 66: Model pacing locations versus ex-vivo electrical mapping in human heart

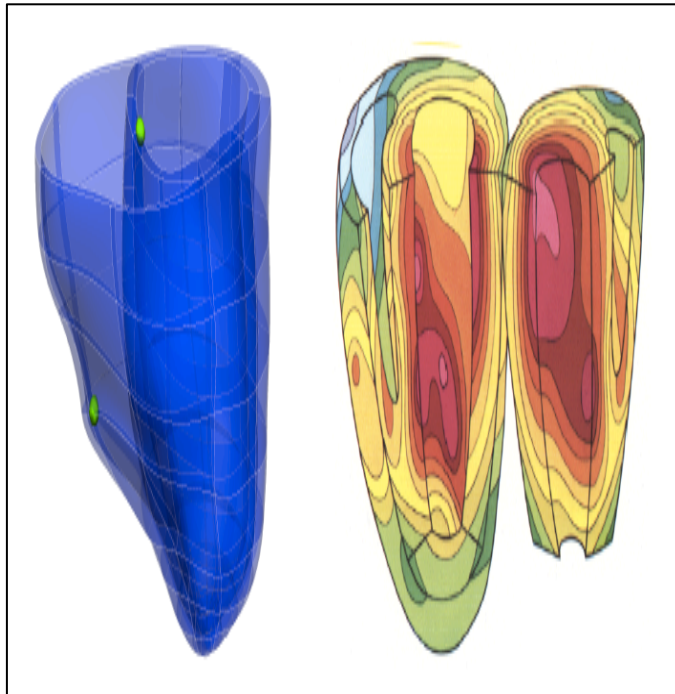


Figure 66 shows the pacing sites used to model intrinsic activation in this study. On the left, the blue biventricular mesh with the green balls demonstrating the pacing points chosen in the model and on the right, a biventricular mesh with heatmap demonstrating actual conduction in a human heart via electrical mapping.

Right ventricular Purkinje activation is replaced by point activation in the RV lateral wall. Pacing locations on the computational model were chosen to replicate the underlying pathophysiological state. This is a good approximation due to the limited extent of the Purkinje endpoints in this region, as shown in Figure 66⁸⁸. The left ventricular Purkinje network has an influence on a large part of the endocardium, but due to the presence of LBBB in these patients we stimulate at the AV node, near the probable site of Purkinje network failure. The pacing locations were consistent between cases as they were defined with respect to the smooth cubic-Hermite mesh. The septal activation occurred 10ms after the RV lateral wall site.

5.8.3 Results

A grid search was performed to estimate conductivity: simulations were carried out for conductivity values of $\sigma \in \{0.2, 0.3, 0.4, 0.5, 0.6, 0.7\}$ and the total activation time of the simulation was calculated as the time between the first point of activation (at the RV pacing site) and the last point of activation (see figure 64). This value was taken to

be representative of the QRS duration and the corresponding conductivity that best fit (seen in bold) the clinically measure pre-implant QRSD was calculated (see table 52). Patient 2 required a wider sweep to constrain the activation time.

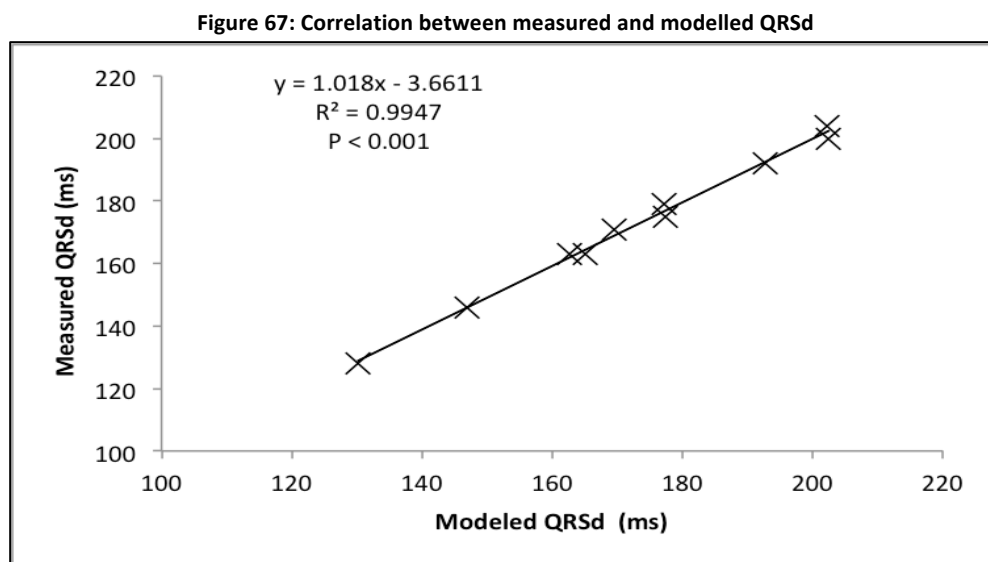


Figure 67 demonstrates the correlation between the modelled QRS duration in the electrophysiological models of the 10 Sheffield cases with the measured QRSD from the same patients using a 12 lead ECG.

Table 52: Results of sweeps alongside clinical QRSD for 10 of the Sheffield cases.

Case	Scar	0.2	0.3	0.4	0.5	0.6	0.7	0.8	QRS	σ
SHF001	N	286.7	230.4	198.5	177.3	162.1	150.5		179	0.49
SHF002	N	276.3	222.2	191.8	171.7	157.2	146.1	130.2	128	0.94
SHF003	N	310.1	262.2	225.5	200.9	183.1	169.5		171	0.69
SHF004	Y	262.3	210.1	180.6	161.1	147.1	136.3		146	0.61
SHF005	Y	310.1	264.3	226.9	202.2	184.4	170.8		204	0.49
SHF006	N	310.1	275.9	237.1	211.3	192.7	178.6		192	0.61
SHF007	Y	293.5	235.4	202.4	180.7	165.1	153.2		163	0.62
SHF008	Y	257.1	206.1	177.4	158.4	144.6	134.2		175	0.41
SHF012	N	310.1	289.7	248.9	221.9	202.5	187.6		200	0.62
SHF018	N	310.1	251.3	215.7	192.2	175.3	162.6		163	0.71

Figure 68: Activation time (ms) visualised on the epicardium. Not to scale

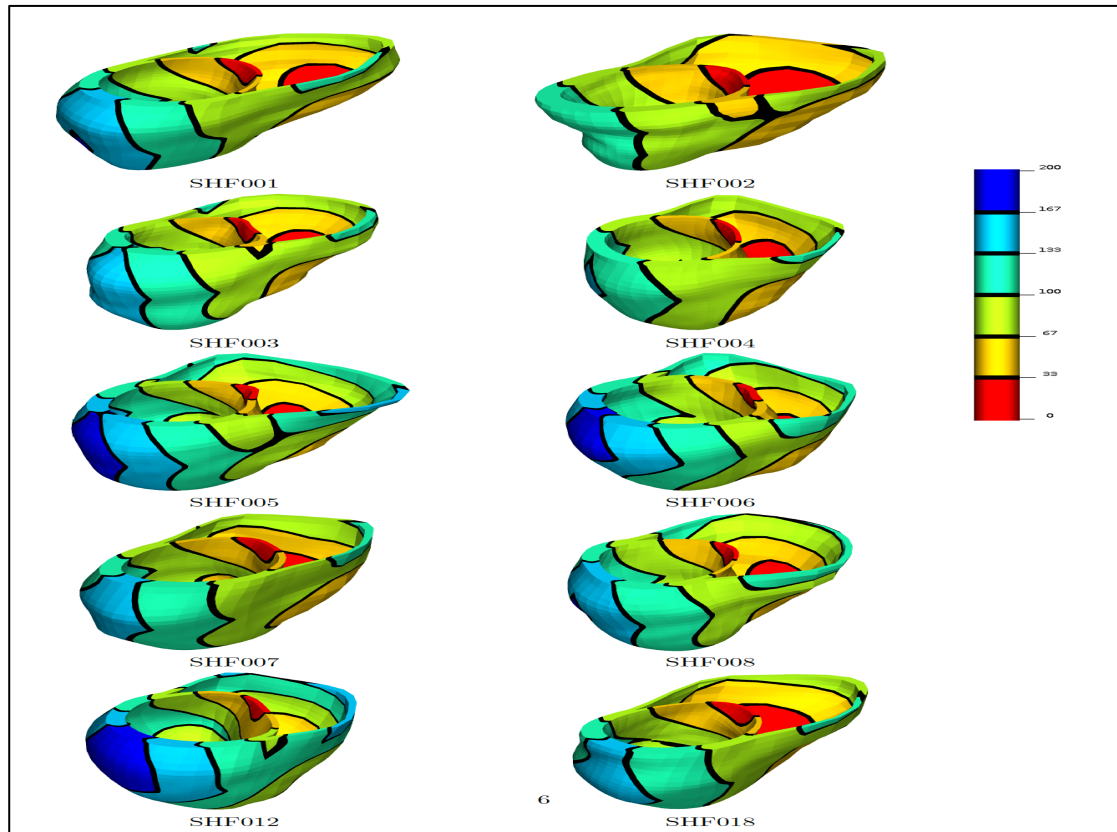


Figure 68 demonstrates the activation time across both ventricles for each of the 10 modelled Sheffield cases, from red (0 milliseconds) to dark blue (200 milliseconds) and note the non-physiological shape of the right ventricle in many of the cases.

5.8.4 Discussion

The conductivity measurements derived in the present study, are the first conductivity values reported for a cohort of human cases. The range of value is 0.41-0.94 S/m (mean 0.62 S/m, SD 0.15 S/m). The simulations represent a Type I activation pattern; activation without the presence of a functional block. Conduction values from this simulation indicate a longer observed QRS than would be expected with this activation pattern given the size of the patients' hearts. Hence, it would be expected cases with low conductivity to show conductivity closer to the population after the inclusion of functional block. In particular SHF001, 005 and 008 have conductivity below 0.5 S/m and as such are potential candidates for the Type II activation pattern. Sohal et al (2013), observed a rate of Type II activation of 48%, which is consistent with at least the aforementioned 3/10 cases being likely to have Type II activation ²⁸⁵.

SHF001 and SHF005 and were indeed responders to CRT, but unfortunately case 8 was withdrawn from the study due to unsuccessful LV lead implantation. The aetiology of cases 1 and 5 was ischaemic and case 8 non-ischaemic and cases 5 and 8 had septal and anteroseptal scar respectively. There appears to be no other similarities between these cases. The study was not powered to predict response to CRT in only 10 patients and thus statistical analysis of these results was not performed, however there was a close fit between the modelled and measured QRSd (see figure 67). Figure 68 demonstrates the activation time for each case, visualised on the epicardium.

Limited direct measurements of the conductivity exist for human ventricular tissue for the purposes of comparison. However, direct conductivity measurements have been carried out in mammalian cardiac tissue ²⁹¹⁻²⁹³. Biodomain parameters for these studies are seen in table 53 following Roth (1997) ²⁹⁴. A conversion to a monodomain equivalent conductivity, assuming that both intra and extracellular domains have equal ratios of anisotropy, was carried out using the relation $\sigma = \sigma_i \sigma_e / (\sigma_i + \sigma_e)$ to enable comparison to the values in the present study:

Table 53: Biodomain parameters converted into monodomain

	Clerc (1976)	Roberts (1979)	Roberts (1982)
	Reported Biodomain Parameters (S/m)		
σ_{il}	0.17	0.28	0.4
σ_{it}	0.019	0.026	0.06
σ_{el}	0.62	0.22	0.12
σ_{et}	0.24	0.13	0.08
	Calculated Monodomain Parameters (S/m)		
σ_l	0.13	0.12	0.092
σ_t	0.018	0.022	0.34

Subscripts 'e', 'i' correspond to the extracellular, intracellular domains; 'l', 't' to the longitudinal and transverse fibre directions. Mono-domain parameters were converted using the formula $\sigma = \sigma_i \sigma_e / (\sigma_i + \sigma_e)$ applied to each direction

independently. Clerc (1976)²⁹³ used excised calf trabeculae while Roberts (1979, 1982)^{291 292} carried out experiments on *in situ* canine ventricles.

The conductivity parameters derived in this study fall outside of the mono-domain-conductivity measurements summarised in table 51. The lowest longitudinal conductivity in this study (0.41) is greater than the largest corresponding value (0.13). This discrepancy has a large number of possible causes, including; differences in species human vs. bovine/canine; differences in physiological conditions, *in vivo* vs. *ex vivo/in situ*; differences in experimental measures, QRS duration vs local electrical potential and conduction velocity and simulation errors e.g. error in the total activation time due to mesh size. Since conduction velocity grows as the square of conductivity ($C_v^2 \propto \sigma$), any errors in the data propagate a squared error onto conductivity estimates²⁹⁵.

This work was based around an inverse model or “electrocardiographic” imaging, in that the QRSd was taken as an input into the model and this was used in an attempt to reconstruct the events that led up to it. However, this is one signal from the surface ECG that is used in an attempt to model the behaviour of the 2,000,000,000 myocytes underlying it and with such a huge number of cells, there is an almost infinite number of possible configurations and therefore sources of error. Since the 1990’s with the advent of the mono- or bi-domain models, it became possible to make calculations on the whole heart, by coupling many membrane models together, but even today, dealing individually with each of these myocytes is impossible. Of course, this is where mathematical assumptions are relied upon, for example that the myocardium (out with the regions of scar) has isotropic conductivity and can be considered homogenous tissue, but is unable to account for areas of functional block for example.

Further simulations, with models that include functional block and a paced protocol will allow corroboration of the high conductivity values obtained thus far. This will also allow insight into the optimum AV and VV delays for each patient’s anatomy. A literature comparison using conduction velocity instead of conductivity may also yield more insight as conduction velocity is reported more readily. On-going simulations will also allow us to test our hypothesis that underlying activation patterns can be

predicted from the QRS duration and ventricular geometry using biophysical modelling. It will be interesting to investigate whether retrograde activation of the Purkinje system contributes CRT response, by simulating LBBB with and without retrograde activation in patient specific models. In the future, with the use of diffusion tensor cMR, electromechanical models will be able to account for more detailed structural anisotropy between patients and what influence the presence of scar and then CRT may have the behaviour of local myocytes, their laminar arrays and the heart as a whole e.g. a true electromechanical model. This point is particularly important given the current disconnect between electrical and mechanical dyssynchrony. Finally, a comparison of these non-invasive methods *in silico* with invasive mapping of myocardial conductivity *in vivo* along with assessment of the type of activation pattern would give added credibility.

5.8.5 Conclusions

This work highlights the challenges and opportunities of using predictive 3D LV models. Due to issues associated with cMR segmentation, only 10 cases (all from the Sheffield cohort) provided data of the quality required to inform personalised conduction models. Nonetheless, from amongst these, the simulations were able to identify 3 cases with a type II conduction pattern, 2 of which were subsequently identified as responders. However, the simulations were time-consuming to perform and would need streamlining and automating before introduction into the clinical arena. Furthermore, the models were non-invasively assessing the conduction pattern, and whilst pre CRT implant factors e.g. QRSd and scar were considered post implant factors e.g. LV lead location and how these patients might therefore respond to CRT was not.

5.9 Discussion

The segmentation work demonstrates the potential problems with using fully-automated segmentation software, particularly the absence of quality control and especially as part of the planning or decision-making process for device therapy. Whilst the fully-automated tool was rapid, once run there was no option for manual adjustments, even if aberrations were seen. At the other extreme, the manual segmentation, takes considerable time to perform, but in the hands of an “expert” e.g. cardiologist, equates to the gold standard for cardiac segmentation, which can then be

used to create LV model that is true both in size and shape. In the middle, is the semi-automated approach; in theory this may represent the best of both worlds combining accuracy, speed and ability to correct errors. Indeed, the proprietary semi-automated segmentation tool developed by UCL and used by all of the other partners in this project was easy to use and consistent but had difficulty in segmenting the epicardial surface. At KCL it was found that any geometrical differences observed between responders and nonresponders at baseline from manual segmentation were lost when the compared to using the semi-automated tool, thus for the atlas work, only manual segmentations were used. Clearly more work would be needed before such an automated tool could be used as part of a randomised control clinical trial, but also factors such as patient selection, choice of cMR, experience of cMR doctor and radiographer, sequence and contrast agent would need to be addressed, along with and a more robust segmentation tool for hearts of neither a standard shape or size. The quality of segmentation is also dependant on the quality of the images available so clearly, the tool cannot be singled out at being the single weak link in the workflow process. In this regard, the tool performed better on the Sheffield 3D SSFP images following the involvement of TS, because the images and therefore tissue differentiation upon which the intensity based automated tool was dependent, had improved. The semi-automated tool was certainly easy to use, and in contrast to the manual process, was able to segment all 4 cardiac chambers and great vessels in a matter of minutes. This would have taken many hours, if not days to achieve by hand. Whilst the segmentations produced looked convincing to the human eye, mathematical comparison between semi-automated and hand segmentations revealed significant errors. Nevertheless, as seen above, the semi-automated segmentation appeared grossly more realistic than that achieved by hand due to a smoother cardiac contour, and so in this regard could be useful in discussing patient's and planning treatments such as CRT, for example coronary sinus and cardiac veins for the LV lead.

The atlas work demonstrates that the 3D model has merit in its own right even without running a simulation. By accurately reproducing the shape of the LV a statistical atlas is able to give insight into reverse remodelling enabling this to be correlated with predictors of response. It makes sense that of all the markers of response, it is LV reverse remodelling, which is predicted by such a geometrical study of these HF-LVSD

patients. However, as discussed previously, LVEDV/LVESV is not the only marker of response and using a single metric brings into question how response is defined. This work also sheds further light on the issues of using segmentation tools with a degree of automation and issues over quality control of the accuracy of epicardial delineation.

The EP modelling work demonstrates the potential for personalised models, combining both personalised LV anatomy and QRSd. However, the simulations took several days to run and many were inherently unstable. Ultimately only 10/21 Sheffield cases could be used and since these did not include assessment of the biomechanics, myocardial structure or fluid dynamics these models were comparatively simple. However, through the types of activation patterns generated by the models it was possible to correctly identify the response to CRT in 2 patients who received a device. Models were personalised to the patient at baseline with no attempt made to suggest a location for the LV lead (the positioning of which is quite variable) or to include a LV reverse remodelling response to CRT, both of which will have an impact on the resulting activation pattern, QRSd and LV volume. As a consequence of this work and the difficulties faced, the group have returned to simpler models, moving away (at least at present) from the concept of multi-modal models and perhaps re-emphasising that a model is not simply a replication, but rather, is a simplification of reality. The more complex and all-embracing models become, the more expense, time and effort is required to run them, but without them necessarily being of greater use.

5.10 Conclusions

The difficulty of such multi-modal, multicentre and multi-disciplinary projects is the challenge presented to the group to maintain a single focus, whilst simultaneously working on their individual aspects. It is also a challenge to understand the needs of others; for example the radiologist understanding the needs of the modellers, the modellers understanding the needs of the cardiologists and the cardiologists understanding the needs of the IT experts etc. Certainly following on from this project the whole team were much more sensitive to the needs of others in the group and regular team meetings helped maintain a sense of unity and focus among all in the group. It remains to be seen how personalised models of the LV will be used in the future. Regarding the aim to predict response to CRT, there is much more to be done.

However, based on this work, it appears that models, which are complex and unwieldy (EP models for example) may not necessarily have greater clinical utility than those which could be considered simple yet elegant (3D geometrical models for example).

In summary, it has been demonstrated that simple computational models can be used to model the heart as it fails and as it responds to a therapy such as CRT, but using more complex models to predict response to the same therapy is far more challenging and whilst it was demonstrated by using statistical atlas of the LV to demonstrate response based on volume change, this clearly is not a multi-dimensional model of the LV as was envisaged by the Grand Challenge. In the next chapter, biomarkers and biophysical markers will be used to investigate whether these can be used to predict response or if they offer any insight into the HF syndrome as LV function improves and whether this leads to improvements in other organ systems.

Chapter 6 Bio and Biophysical Markers

In this chapter, novel biomarkers and biophysical markers of LV performance and the HF syndrome, are used to investigate whether response to CRT can be predicted at baseline, or alternatively whether improvements in the markers themselves, could be used as surrogates for clinical response.

6.1 Biophysical Markers

6.1.1 Introduction

A biophysical marker is a mechanical property of a tissue, organ or animal, which can be measured objectively and imparts insight into the processes underlying health, disease or treatment.

6.1.2 Flow Mediated Dilatation (FMD)

6.1.2.1 Endothelial Function

The vascular endothelium is a monocellular layer lining the entire cardiovascular system, which has a number of important functions including roles within fluid homeostasis, blood pressure regulation, thrombosis and fibrinolysis. Furchgott et al (1980)²⁹⁶ demonstrated that the rabbit aorta responded to a vasodilator e.g. acetylcholine (Ach) if the endothelium was intact, but not if removed. They hypothesised that the endothelium produced a substance, which they called endothelium-derived relaxation factor (EDRF) in response to the Ach which led to vasodilation. Later, the same phenomenon was confirmed in humans²⁹⁷, EDRF was identified as nitric oxide (NO) and found to be released in a response to a given change in shear stress following increase in flow²⁹⁸ but NO was reduced by NO antagonists²⁹⁹. Reducing arterial flow induces a shear stimulus, which leads to tissue ischaemia distal to the occlusion and upon release of the occlusion there will be a corresponding increase in flow. This phenomenon, 'reactive hyperaemia', is due to a build-up of potent vasodilators such as potassium, carbon monoxide and adenosine phosphate (ADP) distal to the occlusion. Upon release of the occlusion, there is an increase in flow to the distal tissues, a concomitant increase in shear stress stimulating the endothelium, which then releases potent vasodilators, such as NO, prostaglandins and

endothelium-derived hyperpolarising factor. These diffuse into the vessel wall to reach the underlying vascular smooth muscle cells causing relaxation and therefore vasodilation. This process leads to a reduction in vascular resistance and thus augments and accommodates the increase in flow. Vascular tone, vessel diameter, resistance and flow return to normal as the vasodilators are swept away in the flow. According to Corretti et al (2002)³⁰⁰ this mechanism is believed to be a function of calcium-activated potassium channels contained within the endothelial cell membrane. These channels open in response to shear stress, leading to the hyperpolarisation of the cell and increased Ca^{2+} entry, which in turn activates endothelial nitric oxide synthase (eNOS) generating NO.

6.1.2.2 Endothelial Dysfunction

Derangement of the vascular endothelium is known as endothelial dysfunction and is instigated by risk factors for vascular disease such as smoking and diabetes. Dysfunction refers to an imbalance of the factors regulating vasodilation and vasoconstriction, specifically a reduction in NO, which leads to vasoconstriction, increased PVR and increased LV afterload. In a pivotal paper using flow mediated dilatation (FMD), Celermajer et al (1992)³⁰¹ demonstrated that endothelial dysfunction was present, before any evidence of gross atherosclerotic plaque formation, in adults who smoked and in children with familial hypercholesterolaemia. Measurement of endothelial function has subsequently been identified as a research tool in the investigation of cardiovascular disease and can be measured by either recording the change in the size of an artery using methods such as FMD and plethysmography³⁰² or the measurement of biomarkers produced by the endothelium such as selectins or von Willebrand's factor³⁰³.

6.1.2.3 Flow mediated dilation

FMD refers to "any vasodilation of an artery following an increase in luminal blood flow and internal wall shear stress"³⁰⁴. Celermajer et al (1992)³⁰¹ developed the technique for the measurement of this, briefly using a blood pressure sphygmomanometer cuff inflated to 300 mmHg to occlude the forearm or calf arteries and then using USS to measure the diameter of the brachial or femoral artery before and after the cuff is released with the resulting reactive hyperaemia. This was

to investigate impaired endothelial function in asymptomatic children and young adults in with latent atherosclerotic risk factors. The difference in diameter of the artery from baseline to peak dilation following cuff released is FMD and measured in %. FMD is a measure of endothelium-dependent and thus NO-mediated arterial function. As reported by Pyke and Tschakovsky (2005)³⁰⁵, FMD can be thought of as an NO bioavailability assay. NO is believed to be anti-atherogenic and to have a role in the development of cardiovascular disease; a low FMD equates to poor NO bioavailability and a concomitant increase in cardiovascular disease.

It is believed that NO mediated FMD is a specific response to a specific type of stress measured in a carefully controlled way. For example, the sphygmomanometer cuff used to occlude the forearm arteries must not be inflated for more than five minutes³⁰⁶, the hand must be resting during this period³⁰⁷ and the ultrasound (USS) probe must be positioned distal, not proximal, to the cuff³⁰⁸ (see figure 69). If not, then myogenic and metabolic factors will influence the brachial artery reactivity measured. It is important to note that NO blockade, using agents such as N-monomethyl-L-arginine can significantly attenuate FMD³⁰⁹, despite there being no reduction in the measured shear stress. However, there is some redundancy in the system, as during blockade of NO, prostanoids administered can cause a measurable FMD response³¹⁰, which can then in turn be blocked by non-steroidal anti-inflammatory drugs such as indomethacin³⁰⁶. This is in turn, why being fasted before assessment is important, to remove such extraneous variables.

Nitrogen mediated dilation (NMD) refers to the maximal dilatory response of an artery to a NO donor, such as glycerine tri-nitrate (GTN), given in order to measure endothelial independent dilation. This is also commonly, but not always, performed in endothelial dysfunction studies using FMD, as NMD reflects vascular smooth muscle, not endothelial function. In FMD (see figure 71) one is assessing how much NO will be released by the endothelium in response to a change in shear stress, NMD is assessing the maximal response of the vascular smooth muscle in response to a fixed and administered quantity of NO (see figure 72).

Figure 69: FMD acquisition; patient, brachial USS, sphygmomanometer and arm jig

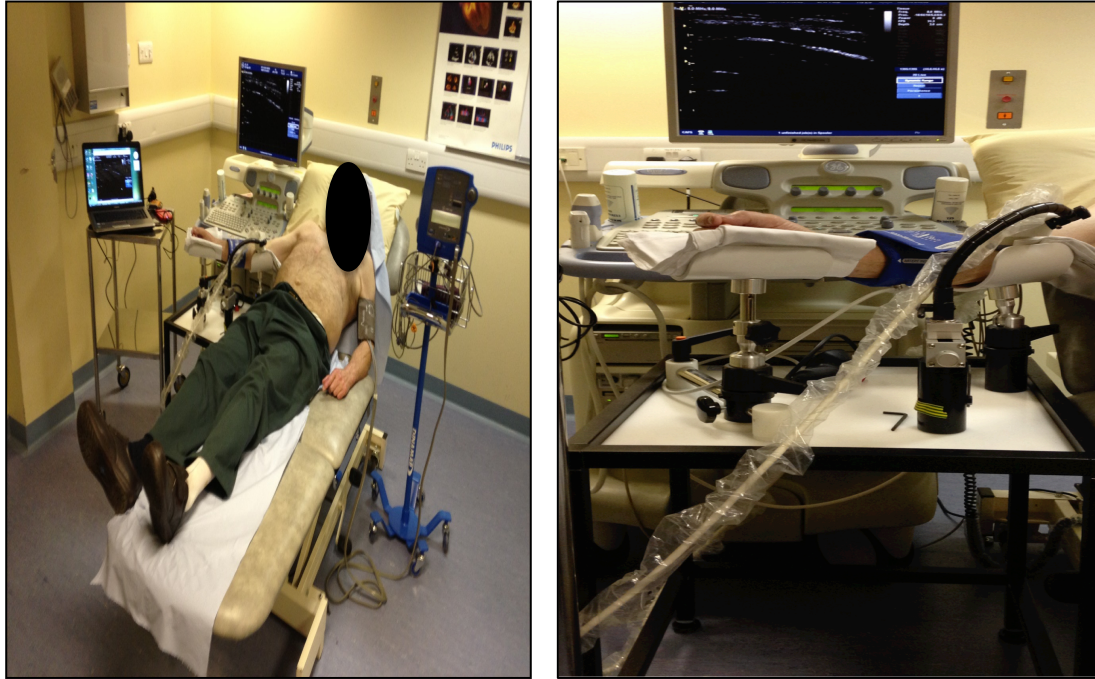


Figure 69 demonstrates on the left, one of the Sheffield patients laying on a couch and undergoing FMD measurement and on the right, close up of the arm jig, sphygmomanometer, brachial ultrasound and in the background the brachial artery 2D ultrasound image being displayed.

Figure 70: MIA-IIc brachial analyser software with B-mode USS of brachial artery

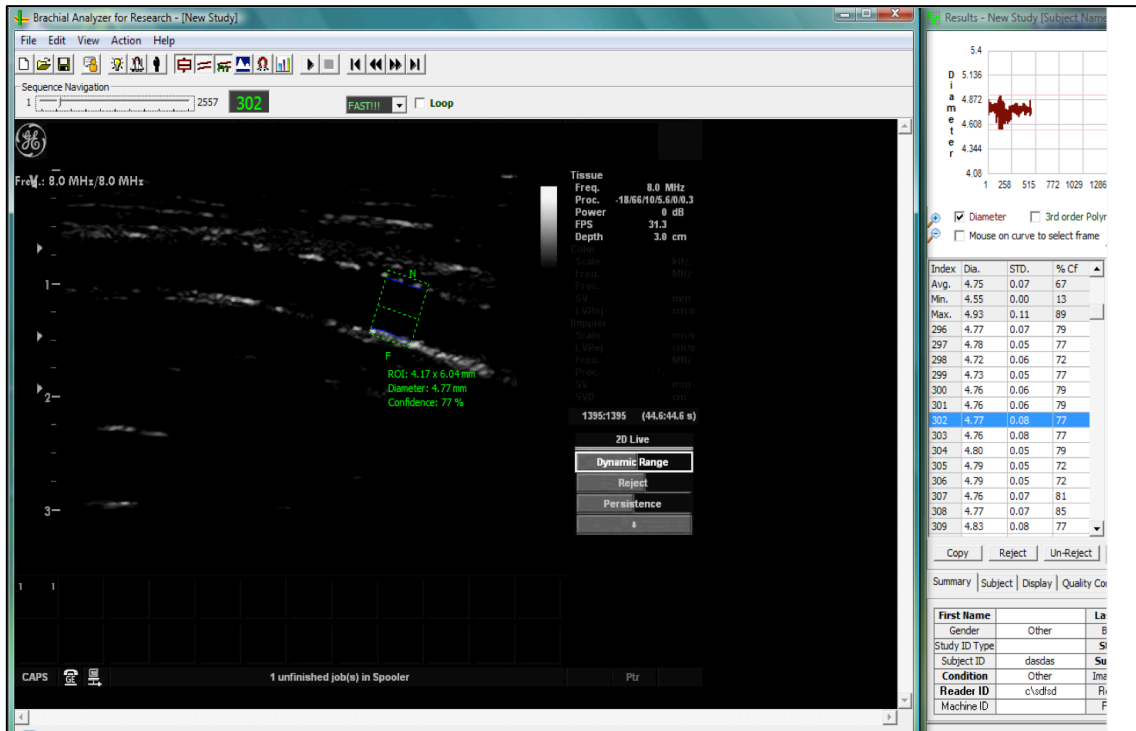


Figure 70 demonstrates the MIA-IIc brachial analyser software in use, on the left the B mode ultrasound of the brachial artery, the green box denoting the area of interest and the blue lines, the automatic endothelium tracker and on the right, the real time measure of the brachial artery diameter, with standard deviation and % confidence.

Figure 71: FMD response following cuff deflation at frame 1800 (6 minutes)

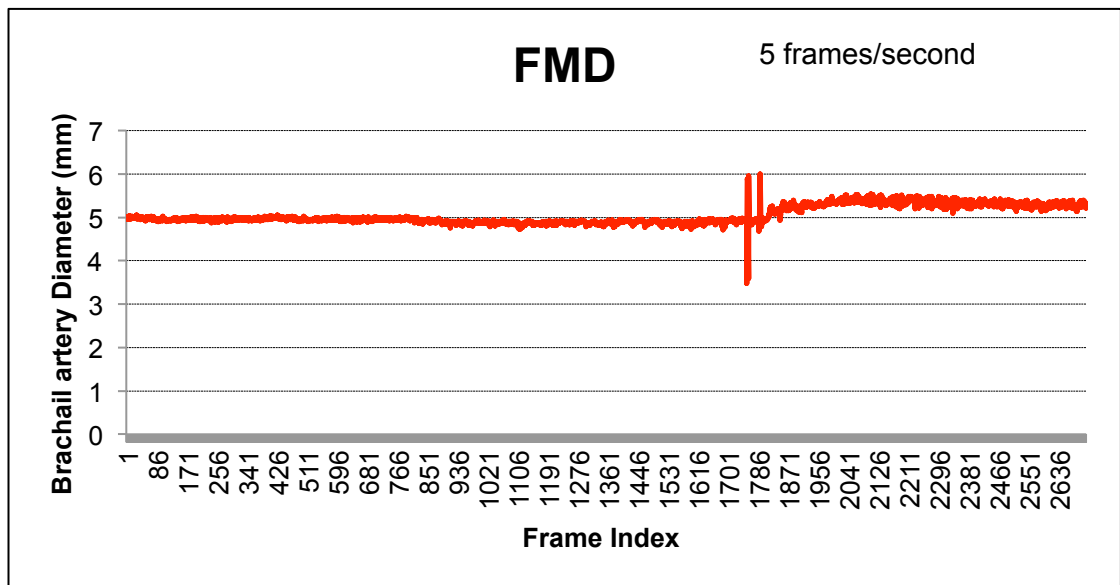


Figure 71 demonstrates the brachial artery diameter measured in a patient, with FMD response due to reactive hyperaemia seen following 1800 approximately, leading to transient dilation of the brachial artery.

Figure 72: NMD response following administration of GTN at frame 300 (1 minute)

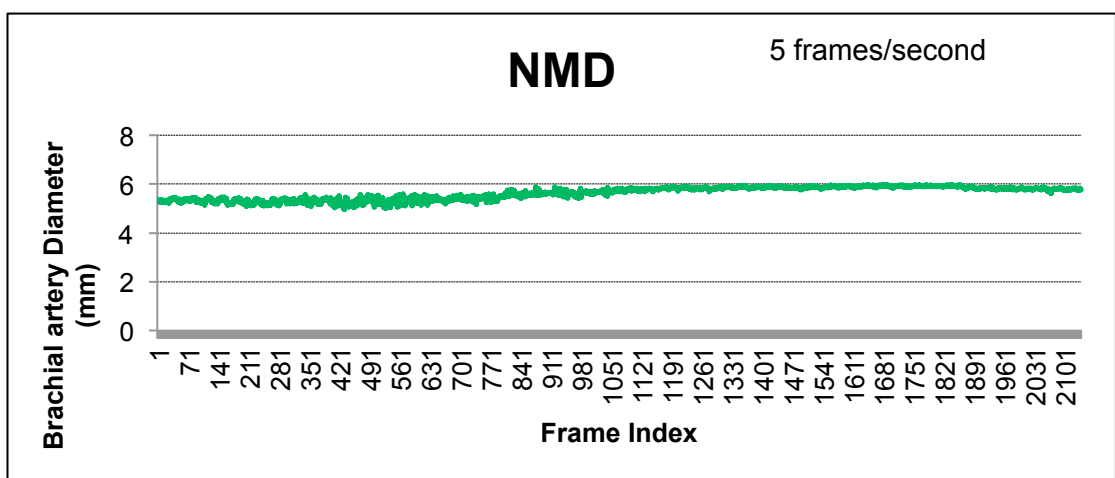


Figure 72 demonstrates the brachial artery diameter measured in a patient, with NMD response due to administration of sub-lingual GTN seen following 600 approximately, leading to sustained dilation of the brachial artery.

6.1.2.4 Pathophysiology

FMD has become popular in clinical studies, providing additional prognostic information over and above traditional risk factors, and is a reliable and reproducible way of quantifying endothelial function. Endothelial dysfunction is common in cardiovascular disease, and as a result there will be a reduction in FMD. FMD is approximately $19.8 \pm 6.2\%$ in healthy adults and $11.2 \pm 7.4\%$ in patients with HF-LVSD, although there is large variation between different studies for healthy individuals and patients with HF-LVSD (see table 54)³¹¹⁻³¹⁵. This variation is due to a lack of consensus in terms of both the acquisition and analysis of FMD^{313 316}. The exact mechanism for the reduction of FMD in HF-LVSD is unclear, but according to Katz et al (2005)³¹¹ it is believed to be due to a combination of “decreased activity of L-arginine–NO synthetic pathway, increased degradation of NO by reactive oxygen species, and hypo-responsiveness in vascular smooth muscle”. NO-dependent endothelial dysfunction is further impaired in HF patients during exercise³¹⁷. This may relate to reduced nutritive flow to skeletal muscle and contribute to the muscle hypothesis of HF symptoms, providing an explanation as to why such patients become breathless on exertion as tissue demand exceeds supply⁷⁹. FMD is not just a physiological phenomenon; it has clinical significance in the care of HF-LVSD patients as FMD independently predicts morbidity and mortality³¹⁸. This is believed to be because endothelial dysfunction leads to “increased arterial stiffness and reduced compliance, increase ventricular afterload and left ventricular end-diastolic stress and enhance dilation and failure” and FMD reflects “impaired function of the large epicardial coronary arteries, as well as the coronary microcirculation, which may cause or contribute to myocardial ischemia”³¹³. Drugs such as allopurinol³¹⁹, growth hormone³²⁰ and omega-3 polyunsaturated fatty acids³²¹ can improve FMD and endothelial function, but as yet such an improvement has not translated into tangible clinical benefit.

Table 54: Typical FMD values in HF studies

Author	Year	Study	Category	FMD (%)
Katz	2005	Prognosis	Good	2.55 ± 0.29
			Poor	0.47 ± 0.60
Klosinska	2009	Aetiology	Ischaemic	1.89 ± 1.69
			Non-Ischaemic	3.90 ± 1.71
Meyer	2005	NYHA class	I	14.5
			IV	4.5
Androne	2006	Ethnicity	African-Americans	0.77 ± 0.43
			Caucasians	1.86 ± 0.24
Deftereos	2010	Exercise	Before	6.2 ± 0.4
			After	9.2 ± 0.4

6.1.2.5 CRT

FMD has been shown to predict response to CRT, as measured by LVEF, MLWHFQ and 6MWT, as according to Akar et al (2008)³²² “every 1% reduction in baseline flow-mediated dilation correlated with an approximately 5% increased likelihood of response”. This study was carried out in 33 patients, 19 of which were responders to CRT with response assessed at 3 months only. A lower FMD at baseline was predictive of response, suggesting it is those patients with the most severe endothelial dysfunction who benefit from CRT. However this work had several shortcomings; GTN was not administered, meaning that some of the changes may have been due to non-endothelium dependent mechanisms, patients with AF who comprise a third of HF-LVSD patients were excluded, 6MWD was used rather than CPET to measure functional performance and finally, the follow-up period of 3 months was very short. As Akar states, performing FMD will greatly inform the prediction of response as, in contrast to EF% or NYHA class, it provides additional information independent of symptoms and thus may allow differentiation of patients who clinically appear to be very similar. An earlier trial showed that improvement of FMD in response to CRT could be augmented by an exercise programme³²³. Enomoto et al (2011)³²⁴, using arterial tonometry rather than FMD to measure endothelial dysfunction, found that CRT significantly improved endothelial function, noting that whilst there was a significant, and positive, correlation between the improvement in endothelial function and cardiac output there was no prediction of response

6.1.2.6 Hypotheses

Working hypotheses –

1) Measures of endothelial function improve significantly in patients who are classed as responders to CRT as determined from a combination of symptoms, echocardiography and exercise testing.

2) Clinical response to CRT is predicted by measures of endothelial function measured at baseline.

Null hypotheses –

1) Measures of endothelial function do not improve significantly in patients who are classed as responders to CRT as determined from a combination of symptoms, echocardiography and exercise testing.

2) Clinical response to CRT is not predicted by measures of endothelial function measured at baseline.

6.1.2.7 Measurement

The methodology adopted was based on the recommendations of the International Brachial Reactivity Task Force (2002) ³⁰⁰ and written in conjunction with MB, a co-author of the more recent (2011) guidelines ³⁰⁴ on the measurement of FMD.

A custom-built rig (see figure 52), developed by the Clinical Engineering Department at STHT, was used. The rig supported the right upper arm and forearm, enabling the arm to be splinted in the anatomical position (elbow extended and forearm supinated), an ultrasound (USS) probe was positioned proximal to the elbow in such a way that enabled adjustments to be made, if necessary, during data acquisition. A sphygmomanometer cuff was positioned distal to the elbow. Blood pressure was measured at baseline on the ipsilateral (left) arm. The investigator recorded time and operated the laptop and sphygmomanometer whilst a sonographer (DWL or JA) recorded USS images of the right brachial artery. DWL and JA were both senior British Society of Echocardiography (BSE) accredited sonographers, experienced in vascular

ultrasound. Both had attended an FMD training course and had significant experience in performing FMD scans.

A Vivid 7 ultrasound machine and 2D Doppler probe with 8MHz linear array (GE Healthcare, Buckinghamshire, UK) was used to image the brachial artery. Because the software for analysing FMD is not integral to the Vivid 7 machine, the scan image was captured, displayed and recorded in real-time using frame-grabber software (Epiphan Systems, Palo Alto, US) and the data were analysed and stored on an encrypted laptop computer (Toshiba Corporation, Tokyo, Japan).

The brachial artery is located 1-2cm deep to the skin, in the antecubital region, typically lying between the medial epicondyle and the biceps tendon. For patients where there was difficulty locating the artery by palpation, pulsed wave Doppler was used.

FMD was calculated with using the brachial analyser software (Medial Imaging Applications llc, Coraville, USA) which includes an automated edge detection algorithm for measurement of the diameter of the brachial artery, by tracking the lines of Pignoli.

All patients arrived in the department between 08:00-08:30, having been specifically asked both in their appointment letter several weeks prior, and reminded by telephone the day before, not to consume any food, fluids, tobacco, caffeine or alcohol from midnight. Once the equipment was in place, they were allowed to rest in a quiet, dark and temperature-controlled room (22-24°C) for a period of 30 minutes prior to assessment. The patients lay supine on a couch and the position of the probe and distance from the landmark to the probe was documented in order to ensure that the artery was scanned as close to the same place as possible at each of the 3 visits. During assessment, the patients were asked not to talk, move their head, body and in particular the right arm or hand. They were advised when the cuff was to be inflated and then deflated.

The USS image was optimised so that the artery was viewed longitudinally and the intima could be seen, with maximal contrast between the intima, the vessel lumen and

surrounding tissue. The sonographers obtained a suitable B-mode image of the artery and the image was then checked on the laptop for suitability using the image grabbing software (as it often appeared different on the monitor) and then recording began.

FMD

1) Baseline recording

“Base” was typed on the USS display to indicate the baseline period. Recording was started on the frame grabber software capturing the B-mode USS of the brachial artery for 1 minute.

2) Inflation phase

The text on the screen was changed to “cuff” and the sphygmomanometer cuff was then inflated at 30mmHg above systolic blood pressure, for 5 minutes.

3) Deflation phase

The text on the screen changed to “defl”, the cuff was deflated and the images recorded for a further 3 minutes.

The patients were then allowed a 20 minute rest to ensure that the artery had recovered sufficiently before the next test began.

NMD

1) Baseline recording

“Base” was typed on the USS display to indicate the baseline period. Recording was started simultaneously on the frame grabber software and B-mode USS image of the brachial artery and was recorded for 1 minute.

2) GTN phase

The text on the screen was changed to “GTN” and the patient was given 800 micrograms (2 puffs) of sublingual GTN and recording continued for 5 minutes.

3) Peak phase

The text on the screen changed to “peak”, and the images recorded for a further 1 minute.

Analysis

The individual FMD and NMD files were imported into the brachial analyser software.

For FMD analysis, the vertical axis was calibrated to ensure that the correct diameter (mm) was measured, a region of interest encompassing the brachial artery was chosen and then checked to ensure the intima was detected by the edge detection software (see figure 53). The analysis was then run. This created a series of diameters with time. The data were then exported into a database, giving the diameter of the brachial artery for every frame (where detected) but only the baseline and deflation periods were needed.

For NMD analysis, the process was repeated but this time only peak diameter following GTN administration was assessed.

As the frame rate of the USS was 5 frames per second, with the FMD and NMD scans taking 9 and 7 minutes respectively, 2100 or 2700 frames were captured per study. The mean vessel diameter over the baseline one minute was measured using the automated edge-detection software. All frames determined by the software to have a confidence interval < 70% were deleted and the remaining frames were checked manually for accuracy e.g. to ensure that the endothelium that was detected and measured.

The following calculations were made:

- Baseline diameter (averaged over 1 minute)
- Peak diameter following cuff deflation or GTN (averaged over 5 seconds)
- FMD% (baseline diameter/peak diameter following cuff deflation *100)
- Time to peak (TTP) (time from cuff deflation to peak diameter)
- NMD% (baseline diameter/peak diameter following GTN*100)

6.1.2.8 Results

Table 55: Baseline brachial artery parameters in responders and nonresponders

Baseline		Responders		Nonresponders		Student's T test
		Mean	SD	Mean	SD	p value
Diameter	mm	4.43	0.89	4.40	0.55	= 0.94
FMD	%	2.74	1.98	7.43	3.73	< 0.05
NMD	%	16.95	8.96	17.65	7.97	= 0.33
TTP	sec	71.75	26.09	66.60	34.25	= 0.66

Table 56: Brachial artery parameters in responders

Responders		Time point (months)						One way ANOVA with repeated measures	
		Baseline		6		12		p value	p value
		Mean	SD	Mean	SD	Mean	SD	Baseline vs. 6	Baseline vs. 12
Diameter	mm	4.43	0.89	4.47	0.54	4.59	0.53	= 0.84	
FMD	%	2.91	1.85	4.13	2.03	3.41	0.24	= 0.61	
NMD	%	16.95	8.96	14.54	7.12	15.27	8.34	= 0.54	
TTP	sec	71.75	26.09	70.64	27.41	73.82	33.41	= 0.99	

Table 57: Brachial artery parameters in nonresponders

Nonresponders		Time point (months)						One way ANOVA with repeated measures	
		Baseline		6		12		p value	p value
		Mean	SD	Mean	SD	Mean	SD	Baseline vs. 6	Baseline vs. 12
Diameter	mm	4.96	0.55	4.43	0.58	4.71	0.36	= 0.68	
FMD	%	7.43	3.73	6.04	4.50	5.81	1.70	= 0.51	
NMD	%	17.65	7.97	15.65	3.78	14.91	7.44	= 0.18	
TTP	sec	66.60	34.25	75.28	25.65	77.20	28.94	= 0.43	

Figure 73: FMD (mean and SD) in responders (white) and nonresponders (black)

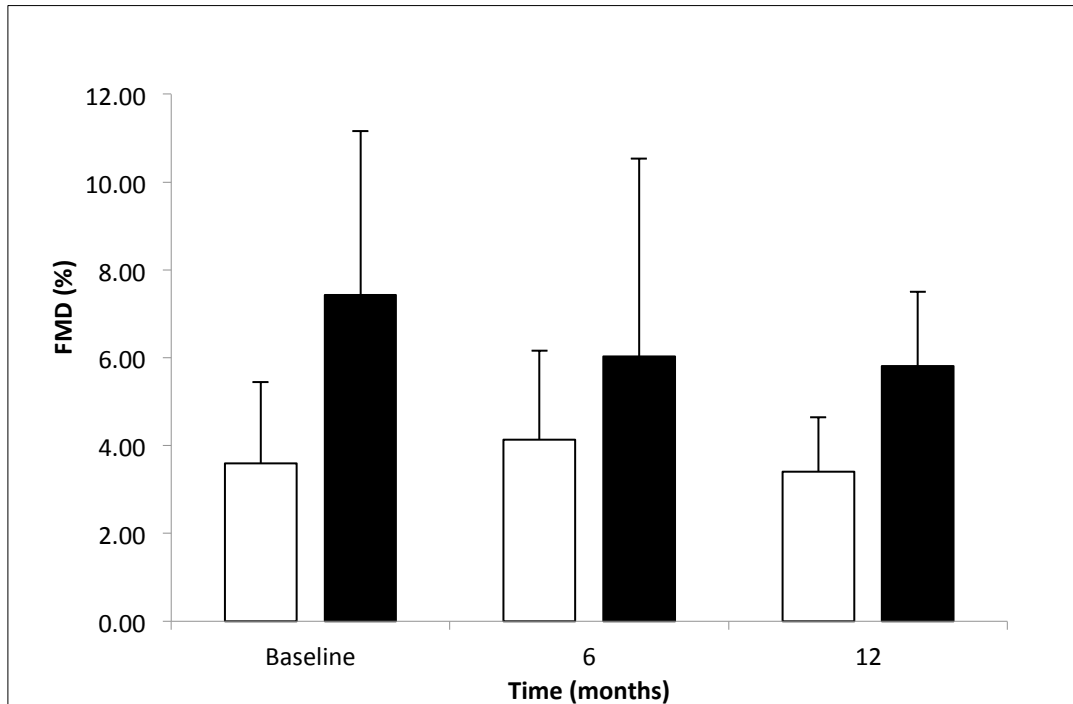


Figure 73 demonstrates the mean and standard deviation of FMD at baseline and during subsequent follow-up in responders and non-responders.

Figure 74: NMD (mean and SD) in responders (white) and nonresponders (black)

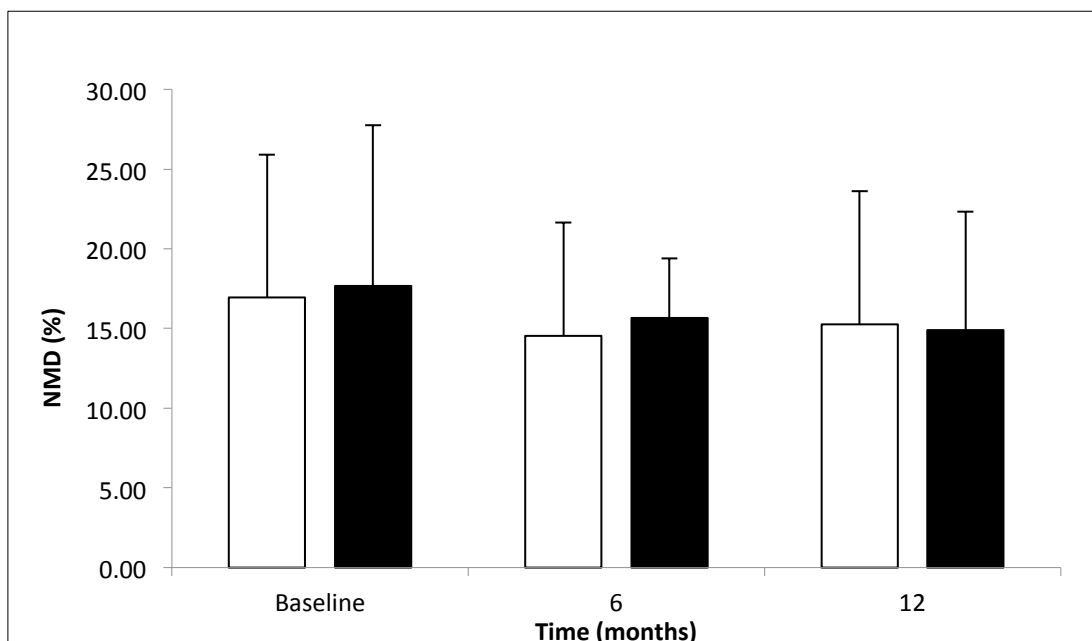


Figure 74 demonstrates the mean and standard deviation of NMD at baseline and during subsequent follow-up in responders and non-responders.

Figure 75: Logistic regression of probability of CRT response and baseline FMD

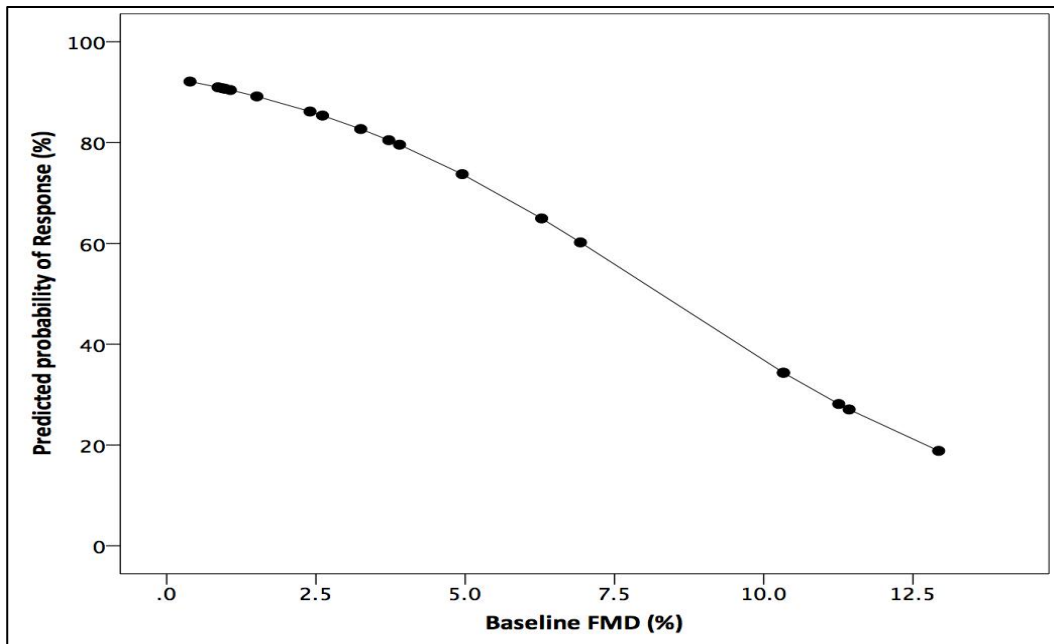


Figure 75 demonstrates the relationship by logistic regression of the FMD at baseline and predicted probability of subsequent response to CRT during follow-up.

Figure 76: FMD and NMD box plots at baseline in responders and nonresponders

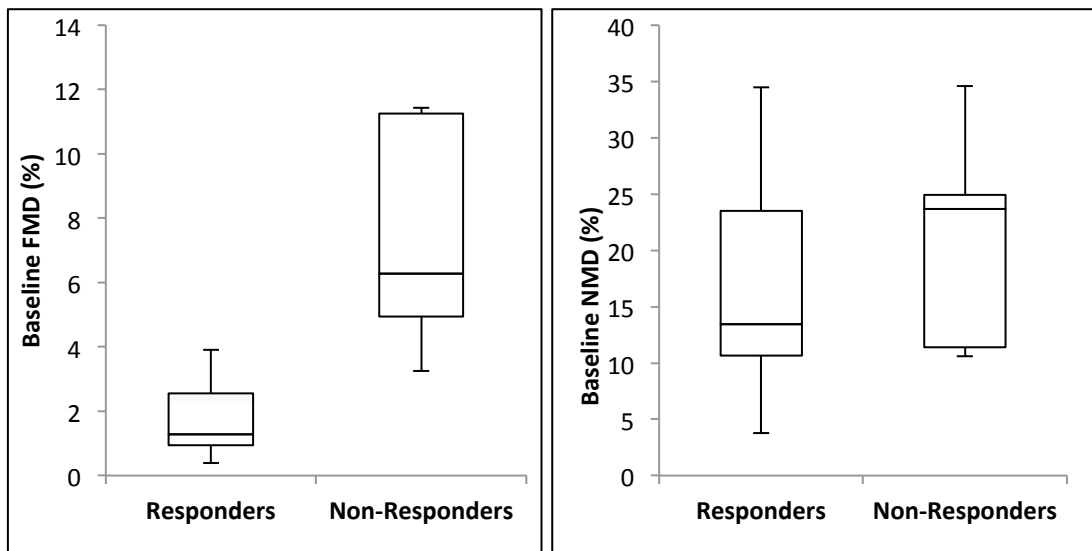


Figure 76 demonstrates box plots, on the left the difference between the baseline FMD and in responders and non-responders and on the right the difference between the baseline NMD in responders and non-responders.

No statistically significant difference was evident in brachial artery diameter, TTP or NMD (see figure 74 and 76) between responders and nonresponders at baseline (see table 55). The only statistically significant difference found between the groups at baseline was for FMD using a 2-tailed Student's T-test (see figure 73 and 76). Table 56 and 57 demonstrate the changes in diameter, FMD, NMD and TTP during follow up in responders and non-responders respectively.

A one-way ANOVA with repeated measures and Greenhouse-Geisser correction determined that there was no significant difference during follow-up in responders, in terms of brachial artery diameter ($F(1.74, 19.42) = 0.14, p = 0.83$), FMD ($F(1.57, 17.23) = 0.42, p = 0.61$), NMD ($F(1.88, 20.69) = 0.60, p = 0.54$) and TTP ($F(1.97, 19.76) = 0.08, p = 0.99$). Similarly in nonresponders, there was no statistically difference during follow-up brachial artery diameter ($F(1.83, 7.32) = 0.75, p = 0.49$), FMD ($F(1.55, 6.22) = 0.66, p = 0.51$), NMD ($F(1.83, 7.32) = 2.13, p = 0.18$) and TTP ($F(1.03, 3.10) = 0.82, p = 0.43$).

As can be seen by figure 75, for every 1% reduction in baseline flow-mediated dilation (FMD), there was an approximate 8% increase in the likelihood of CRT response.

The first working hypothesis, that clinical response to CRT is predicted by measures of endothelial function measured at baseline can be accepted thus the null hypothesis, can be rejected. The second working hypothesis that measures of endothelial function improve significantly in patients who are classed as responders to CRT determined from a combination of symptoms, echocardiography and CPET testing is rejected, and the null hypothesis that measures of endothelial function do not improve significantly in patients who are classed as responders to CRT can be accepted.

6.1.2.9 Discussion

These results demonstrate a similar trend to that reported by Akar et al (2008)³²², namely that FMD performed at baseline is a predictor of response to CRT. Whilst statistical significance was not proven, FMD tended to improve in responders and deteriorate in nonresponders and trend was found at both 6 and 12 months follow-up

thus outside the 3 month follow-up period of the Akar study. Like Akar's work, this supports the notion that FMD is a tool that can be used to differentiate clinically similar patients based on endothelial function, which can then be used to select patients more likely to respond and therefore derive benefit from CRT. At baseline, all 19 patients were eligible for CRT yet only 74% of these responded to treatment. It is important to note that the responders could all be predicted from the FMD; this supports the concept that patients with the most severe endothelial dysfunction are more likely to respond. However since CRT has no direct effect on peripheral endothelial function, improvement in FMD as a result of CRT is likely to be due to "endothelium-derived nitric oxide due to improved haemodynamics, peripheral shear stress, cardiac loading conditions, and neurohormonal activation." According to Akar et al (2008)³²². This is logical as it is known that blood pressure, stroke volume and natriuretic peptides improve in responders following CRT implantation. It remains uncertain why responders at baseline have a lower FMD than nonresponders, as whilst patients with ischaemic cardiomyopathy often have poorer endothelial function³⁰⁹, it is patients with non-ischaemic cardiomyopathy who often demonstrate a greater response to CRT^{312 325}. Certainly Akar et al (2008)³²² do not comment upon this. In this work, half the patients had HF-LVSD of an ischaemic origin, but there was no significant difference in any measures of endothelial function between the two groups (data not shown).

Importantly, there was no significant difference in the actual diameter of the brachial artery, either at baseline between the groups or during follow-up. This is consistent with Akar's findings. Any difference in diameter, due to either inaccuracy in measurement or to a physiological effect of CRT would undoubtedly have an influence on the FMD and NMD recorded.

As discussed above, the study by Akar et al (2008)³²² followed up patients at a single time-point of 3 months only. This was shorter than for the majority of large CRT trials, which follow patients at 6 or 12 months, to allow time for a clinically significant response to occur. Furthermore, Akar et al (2008)³²² did not use peak VO₂ as a measure of response (arguably a more objective measure of exercise capacity than 6MWD), a CRT optimisation protocol for all patients (as per current best practice) nor

investigate the role of non-endothelium dependent mechanisms as they assumed the difference was purely endothelial-mediated. Whilst not previously investigated, Akar et al (2008)³²² were correct in their assumption that prediction of response to CRT using FMD, was purely an endothelium dependent mechanism, as in this work there no significant differences between the groups at baseline or within the groups at follow-up using NMD. This means that selection for CRT, on the basis of impairment endothelial function measured at the brachial artery, is a function of disease of the endothelium alone (FMD) and is not influenced by the performance of vascular smooth muscle (NMD). A more recent study by Santini et al (2013) followed up HF-LVSD patients post CRT-D for 12 months and concluded that FMD did not predict response to CRT at baseline but it did correlated with markers of response and improved markedly, from $4.1\% \pm 3.8\%$ to $8.8\% \pm 4.8\%$ ³²⁶. However, they do not report the measurement of the brachial artery diameter between the groups as a possible confounder, nor used NMD to exclude the possibility of changes in smooth muscle tone corrupting their findings. Furthermore 16/57 patients were unable to complete the 6MWT at baseline due to being bedridden, presumably with HF-LVSD symptoms or osteoarthritis and the authors then classified subsequently walking any distance as a positive response to CRT. Also, the exclusive use of CRT-D devices, suggests this was sicker population and despite the authors defining abnormal FMD as $> 5\%$, the mean FMD in all patients recorded was $4.1\% \pm 3.8\%$.

FMD is grossly dependent on patient anatomy, compliance with the procedure, operator-skill and technique (for both acquisition and analysis). It is strongly recommended that B-mode ultrasound be used in order to identify the double lines of Pignoli. These represent the endothelium and can therefore allow precise measurement of the artery diameter by automated edge-detection software. There is variation in how the peak post-deflation diameter is measured, with some studies choosing a single frame at 60s (which may miss the true peak as it may not occur precisely at 60s) and others choosing mean diameters over periods of 3, 5 or 10 seconds when the peak is seen. Logically shorter periods will give higher peak diameters, and longer periods lower. The guidelines recommend that an assessment period of 3 minutes is conducted post-deflation, as for most patients, the peak will

occur before 2 minutes and the peak chosen around this, this was the methodology chosen in this work and the peak diameter averaged over a period of 5 seconds.

The time from cuff deflation to the peak in measured artery diameter, or time to peak diameter (TTP) is the time during which the shear stress stimulus determining FMD arises. It was initially hypothesised that this period might be a useful measurement of endothelial function. Thijssen et al (2011)³⁰⁴ noted however, that despite a level of variation both between and within groups, TTP does not appear to be a useful biomarker and furthermore is also partially NO independent i.e. not completely endothelial dependent³²⁷. The lack of significant difference in TTP, either between groups at baseline or within groups during follow-up in this study, suggests that TTP is of limited importance and simply demonstrates the time for the shear stress stimulus to produce maximal dilation is consistent in both groups at baseline and following CRT implantation. This also demonstrates that, if the arbitrary 60s had been chosen to record peak post-cuff deflation rather than recording for a 3-minute period, the actual peak diameter would have been missed for majority of patients as the mean TTP was found to be 70s. This would lead to inaccuracies in the FMD measurement, most likely result in an underestimate of FMD.

Whilst most patients improved symptomatically irrespective of group, only responders improved significantly in all 4 markers of response but there was no correlation between functional performance data, such as peak VO₂, 6MWT and FMD. Akar et al (2008) found a positive correlation between FMD and the 6MWD, but not in other markers and this lack of correlation in our study may be due to a lack of significant improvement in 6MWD, the issues experienced with 6MWD measurement described previously or perhaps the small sample size.

Although our sample size is small in comparison to large CRT trials, it was a similar size to the study by Akar et al (2008)³²² and, most importantly, adequately powered to find a difference between the 2 groups as per the recommendations of the International Brachial Reactivity Task Force (2002)³⁰⁰. FMD studies typically use very large supra-systolic occlusive pressures of 250mmHg to ensure an adequate shear response, negating the need to measure systolic BP. However, no issues were found with using

30mmHg above systolic pressure, other than the need to ensure that an accurate reading of systolic BP was made at the outset of the test. This was more acceptable to patients and did not cause any undue pain or distress. The sphygmomanometer required constant monitoring in order to maintain the 30mmHg above the systolic pressure and adjustment of the USS probe was also required to ensure acceptable image quality with patient movement. Unfortunately, despite patients being told to lie still and quiet they sometimes moved during the FMD study with both voluntary e.g. talking, gesticulating and involuntary e.g. coughing, sneezing movements. This led to artefacts, inconsistencies and dropout in the data and this type of noisy data was removed during analysis.

Despite the patients coming from South Yorkshire, North Derbyshire, Nottinghamshire and Lincolnshire, there were few problems with starting the FMD at 09:00 each morning, with the patients always arriving fasted and with their morning medications (to be taken later). The mean time of arrival was 09:11:27 ± 16:19 for all patients over 12 months, with over 80% of appointments on time and no significant difference during follow-up or between responders and nonresponders. Some patients arrived earlier and some later, often due to traffic or taxis running late, problems that were unavoidable. This is important as FMD is time-dependent and as some of the patients suffered from were insulin dependent diabetes mellitus, they could not remain fasted indefinitely.

Many of the patients in this study were frail with considerable comorbidities, all of which may influence FMD, and the relative presence, absence and fluctuation of these, may also have influenced CRT response and measured FMD ³²⁸. Previous CRT trials have not commented on the presence of comorbidity, but such heterogeneous patients are common in the real world.

Despite concerns reported by Akar et al (2008)³²² no problems were encountered with using GTN to investigate NMD. No patients reported symptoms of, or measurable, hypotension, despite often low baseline blood pressures < 120 mmHg systolic. GTN spray was used, rather than a tablet, as this allowed for a controlled and contemporaneous dose of NO to be delivered. As stated in the methods, the mean

time of starting the data collection was approximately 09:00, with some small variations between groups at baseline and during follow-up.

Ideally a single sonographer would perform all the FMD measurements, however due to logistical issues both JPA and DWL performed the FMD studies. This potentially creates an issue with differing technique and reproducibility, however there were no differences in the time started or baseline brachial diameter, so the influence whilst acknowledged, was minimised. Analysis was always performed immediately after acquisition and before any assessment of response and so all staff blinded in this regard. Furthermore, the use of the automated edge detection software minimised any investigator bias in influencing the FMD measured. Future work could involve using larger populations, a multicentre trial and perhaps even a prospective RCT on patients who all seem similarly suitable for CRT. It could also be interesting to delineate further between populations of HF-LVSD e.g. ischaemic and non-ischaemic aetiology. Furthermore the role of FMD and CRT optimisation could be investigated, correlating gains in aortic VTI with improvement in FMD, for example.

6.1.2.10 Conclusion

FMD was the only measure of endothelial function that predicted response to CRT at 6 and 12 months. Whilst FMD initially improved during follow-up in responders and deteriorated in nonresponders, these changes were not statistically significant. It remains unclear as to why responders have significantly worse endothelial function at baseline than nonresponders. Further research assessing endothelial function in other ways is necessary to answer this question. Finally, the use of FMD could be considered as the patient selection criterion for a randomised control trial in CRT, but whether this would be approved ethically or by patients remains to be seen.

6.1.3 Ballistocardiography

6.1.3.1 Introduction

First discovered in the late 19th Century³²⁹, ballistocardiography (BCG) or cardiac ballistics, refers to the indirect and non-invasive investigation of cardiac haemodynamics by measurement of body motion during cardiac systole. Various methods have been described; using a force plate, an accelerometer placed directly

upon the sternum, induction coils, electromagnetic bed, all of which potentially have the ability to amplify and measure the small forces imparted on the body by the heart.

The principle underpinning BCG is Newton's second and third laws of motion. The heart accelerates a volume of blood by exerting a force (Newton's second law) and the surrounding tissue must exert an equal and opposite force on the heart (Newton's third law). This leads to a change in the reaction force between the body and its surroundings. The BCG signal produced is tracked in 3 orthogonal planes, X, Y and Z. Z represents the axial plane of the body, Y the sagittal and X the anteroposterior, the dominant signal however is in the Z direction, as this is the main axis along which blood flows (e.g. along the aorta) from cranial to caudal. These 3 signals can be recorded, analysed and compared for; different populations e.g. male/female, different disease conditions e.g. healthy/IHD or before and after intervention e.g. surgery for aortic stenosis. According to the key work by Starr et al (1939)³³⁰ who first studied the concept in earnest, it was concluded that healthy, young adults all shared a similar pattern when their BCG was recorded in the longitudinal plane, with the pattern being accepted as that of the normal population (see figure 77).

Figure 77: BCG and ECG data, from a healthy adult over 10 minutes

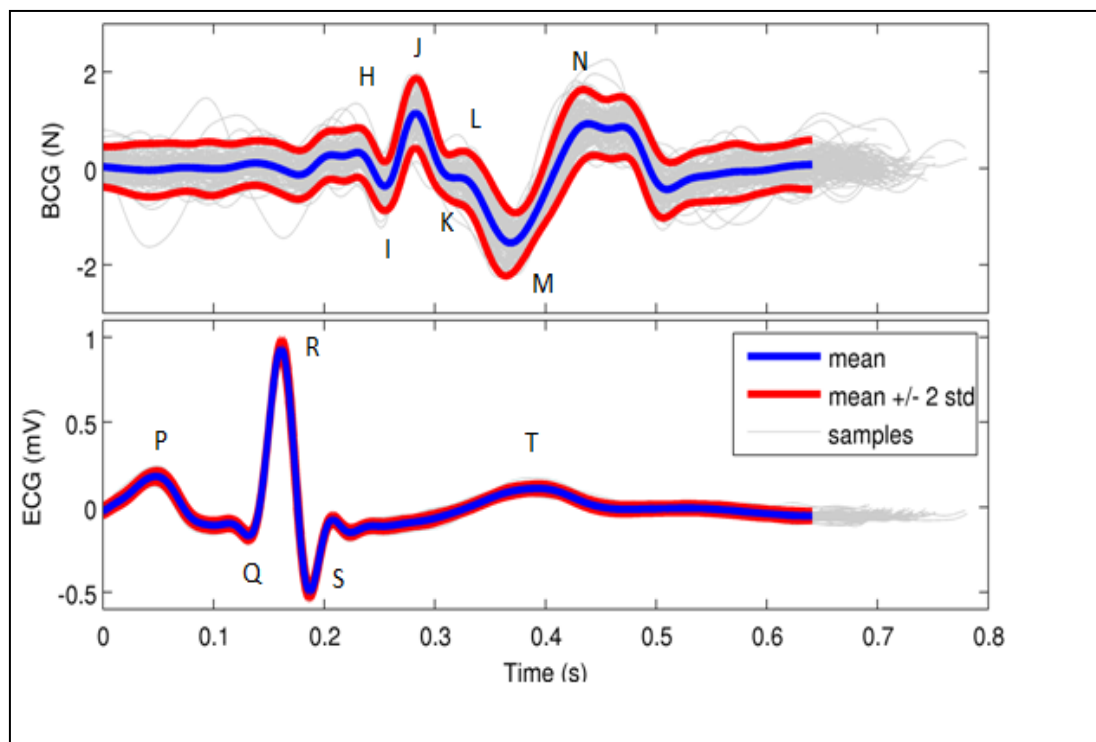


Figure 77 demonstrates the signal averaged BCG (top) and ECG (bottom) with mean values in blue and mean \pm 2 stand deviations in red, with waves of the BCG and ECG labelled according to their recognised alphabetical terms.

As for the PQRST complex of the ECG, Starr attached arbitrary letters to the BCG signal corresponding to specific points in the cardiac cycle. These are HIJKLMN with HIJK being the systolic and LMN the diastolic waves. According to Gubner et al (1953)³³¹, it is believed the small positive H wave represents the end of ventricular diastole, specifically “forces associated with the abrupt deceleration in the flow of blood returning to the heart”. The negative I wave marks the onset of ejection, with the “footward recoil of the body from the acceleration of the blood upwards in the pulmonary artery and ascending arch of the aorta”³³¹. The subsequent J wave, the dominant signal in the BCG, then follows “with impact on the crown of the 2 arches, the direction of forces is abruptly reversed and there is a sharp recoil of the body in a headward direction” this together with I, is representative of the cardiac ejection force³³¹. The K wave “is caused by the deceleration of blood flow in the descending aorta as it is slowed by the peripheral resistance and as the ejection velocity falls off at the end of systole”³³¹. LMN waves are complex, and their exact meaning has been debated, but in view of their timing shortly following the T wave e.g. ventricular repolarisation they are likely to represent ventricular diastole.

In normal healthy individuals, there is a significant amount of respiratory variation in the BCG signal, reflecting the influence of respiration on RV filling and ejection. Inspiration will increase RV filling, augmenting the BCG signal, but on expiration the signal is almost extinguished, due to the reduction in RV filling. LV filling and ejection is influenced significantly less by respiration and so, as concluded by Starr et al (1950)³³² from experiments on cadavers, who were laid on a ballistocardiograph whilst fluid was injected into pulmonary artery and aorta and the BCG recorded, the RV and LV contribute equally to the BCG signal.

Like the ECG, the BCG can be analysed quantitatively or qualitatively. An example of quantitative analysis in the ECG is measuring the height of the ST segment to diagnose

a STEMI, similarly in the BCG the amplitude or timing of certain waves could be measured. Starr believed that changes in the BCG signal could be used to diagnose diseases such as aortic stenosis or IHD based on the presence, absence or alteration in the BCG signal. However BCG measures the force of ejection rather than cardiac output and thus, as for measurements of SV or EF, the BCG signal is not just determined by the LV. Thus it is not specific to diseases of the LV, but rather represents the function of the heart and indeed the arterial system as a whole. This is particularly important, as the BCG signal changes with age and so the BCG from a healthy 70 year old could appear similar to a 50 year old with clinical IHD.

In terms of qualitative assessment the analysis can be carried out in two ways; for example in the ECG the absence of the P wave can be diagnostic for AF, as we know this signifies a lack of organised atrial electrical and therefore, mechanical activity. It is believed that the BCG signal can be interpreted in a similar way, for example the absence of the K wave may suggest coarctation of the aorta and augmentation of the same wave may suggest atherosclerosis, as these are the BCG patterns found in such patients. However, unlike the ECG, it is not clear whether all patients with such diseases will be represented in such a way or indeed if such a BCG signal is caused by those diseases alone, and so this may be a problematic approach.

An alternative qualitative approach was described by Brown et al (1950)³³³ who compiled a four stage grading system for the BCG, which placed primacy on the respiratory variation as follows:

“Grade 1 – regularity of complexes is preserved. Amplitude in inspiration is normal; in expiration amplitude is decreased and varies in definitiveness.

Grade 2- one half or more of the complexes are abnormal, mainly in expiration. The inspiratory amplitude is decreased somewhat also.

Grade 3 – Abnormalities are present in inspiration and expiration, but the complexes are still identifiable.

Grade 4 – All the waves are unidentifiable and of low amplitude”

Signal-averaging is a signal-processing tool, applied in the time domain, which is employed to amplify a signal, contained within a portion of data, relative to the noise.

This is done by repeatedly measuring the same signals in the same manner and then using statistical analysis to extract the desired data. Signal-averaging is already used in cardiology, in particular, for signal-averaged ECG (SAECG), which is used to identify late potentials, which are small signals occurring within the QRS complex, as these are associated with malignant tachyarrhythmias e.g. ventricular tachycardia (VT). As mentioned above, one of the problems with early BCG work was the unfavourable signal-to-noise (SNR) ratio, but there are also difficulties in gating the BCG to the ECG. Using modern technology, both the ECG and BCG can be gated and signal-averaged; which in theory will remove issues such as postural sway, respiratory motion, ectopic beats and other artefacts, which could degrade or pollute the signal. This means that Brown's qualitative assessment of the BCG signal will be made redundant as it is averaged over many cardiac cycles and so a quantitative assessment must be used e.g. timing and amplitude of the various waves.

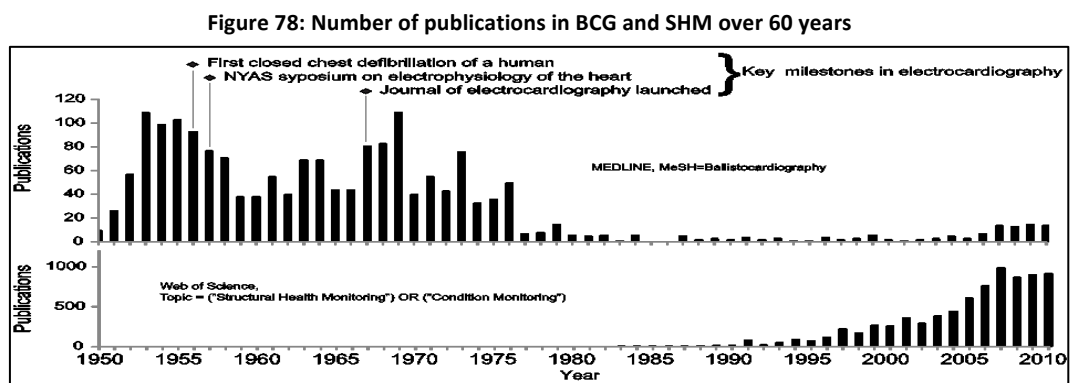


Figure 78 demonstrates the number of publications in ballistocardiography and structural heart monitoring from 1950 to 2010, with the fall and subsequent rise in ballistocardiography and latterly the rise in structural heart monitoring.

BCG technology went out of favour in the 1970s (see figure 78) for a variety of reasons, including an unfavourable signal-to-noise ratio (SNR), the advent of seemingly more sophisticated and accurate imaging modalities (both invasive such as cardiac angiography and non-invasive such as cardiac ultrasound), the large variation in acquisition techniques, the choice of signal and analysis and a lack of agreement over what constituted BCG and what the BCG waveform actually represents. However, whilst other imaging techniques allow direct visualisation of the heart and diagnosis,

they do not permit simple, repeatable and non-invasive interrogation of its actual force. The corollary to BCG would be the LV PV loop (as discussed earlier) that is predominantly a research tool, invasive and not used currently in clinical practice. Thus applications for such BCG technology include non-invasive remote monitoring, along with weight and BP, in order to assess cardiac function on a daily basis. For example if an HF-LVSD patient feels unwell, a recording could either reassure if normal (for that patient) or, prompt early admission or review if there was a significant reduction in cardiac force, perhaps pre-empting a clinical decompensation ³³⁴. Assuming, of course, that it could be proved that such a reduction in cardiac force, measured non-invasively, was clinically useful. In engineering terms, such measurement would be termed structural health monitoring (SHM), which essentially is defined as a damage detection system used for monitoring the performance of a system. Interestingly, during the time in which BCG has become less popular, SHM has increased in popularity, through telemedicine and remote-monitoring systems in medicine.

Phibbs et al (1967)³³⁵ used an ultra-low frequency (ULF) BCG to investigate individuals with predominantly acute cardiomyopathy due to infectious, autoimmune and inflammatory aetiology, rather than those with chronic HF-LVSD, of an idiopathic or ischaemic DCM aetiology. As expected, no specific pattern was identifiable as to the cause of the DCM, but the patient cohort all shared a similar alteration in their BCG signal. These changes, although not present in all cases, included deep K wave, reduced J wave, deep H wave and late/reduced I wave (see figure 79). It was interesting to note that the peak changes recorded in the BCG signal mirrored clinical severity, and improved as the course of the clinical condition improved, but there was little discussion nor reasoning as to why this might be the case. Gubner et al (1953)³³¹ however had previously delineated the reasoning behind such changes with HF; hypothesising that the late/reduced I wave and reduced/sluggish J wave peak reflecting impaired contractile force, prominent H wave denoting a stiff ventricle, and there may also be a large diastolic L wave reflecting abnormal return flow to the heart.

Giovanrandi et al (2011)³³⁶ demonstrated the use of BCG to optimise the interventricular delay for CRT programming (see figure 80), demonstrating that higher

J wave amplitude corresponded to an optimised interventricular delay of 1.5 vs 1 in controls, but this has not been correlated with altered echocardiographic or symptomatic outcomes.

Figure 79: BCG and ECG data, from a HF failure patient and a control

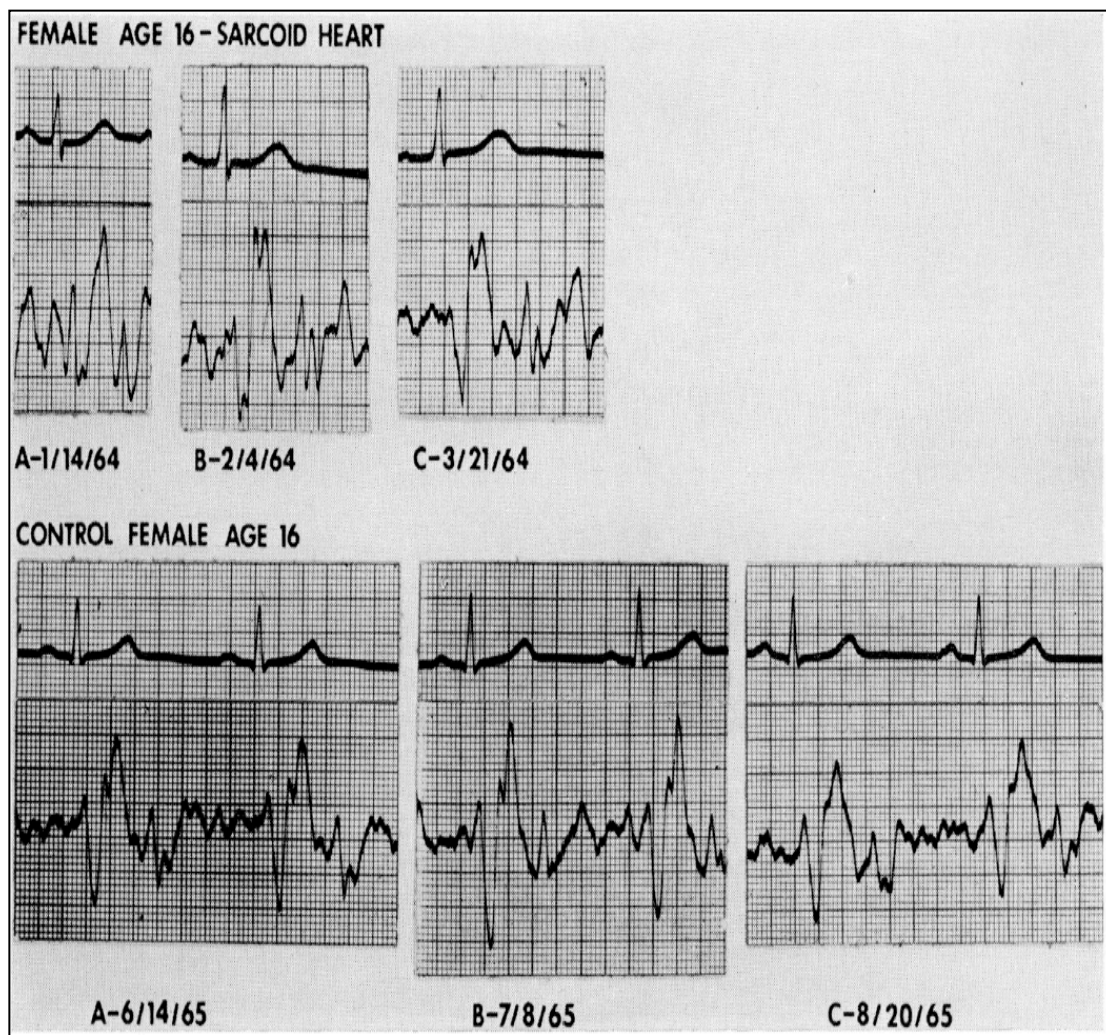


Figure 79 demonstrates simultaneous ECG (above) and BCG (below) traces, from a 16 year old female patient with sarcoidosis leading to heart failure taken several months apart with changes in clinical state mirroring changes in BCG and a control patient of the same age and gender without changes in clinical state or BCG. Note in both cases, the ECG is consistent over time.

Figure 80: Use of BCG to optimise interventricular delay in CRT

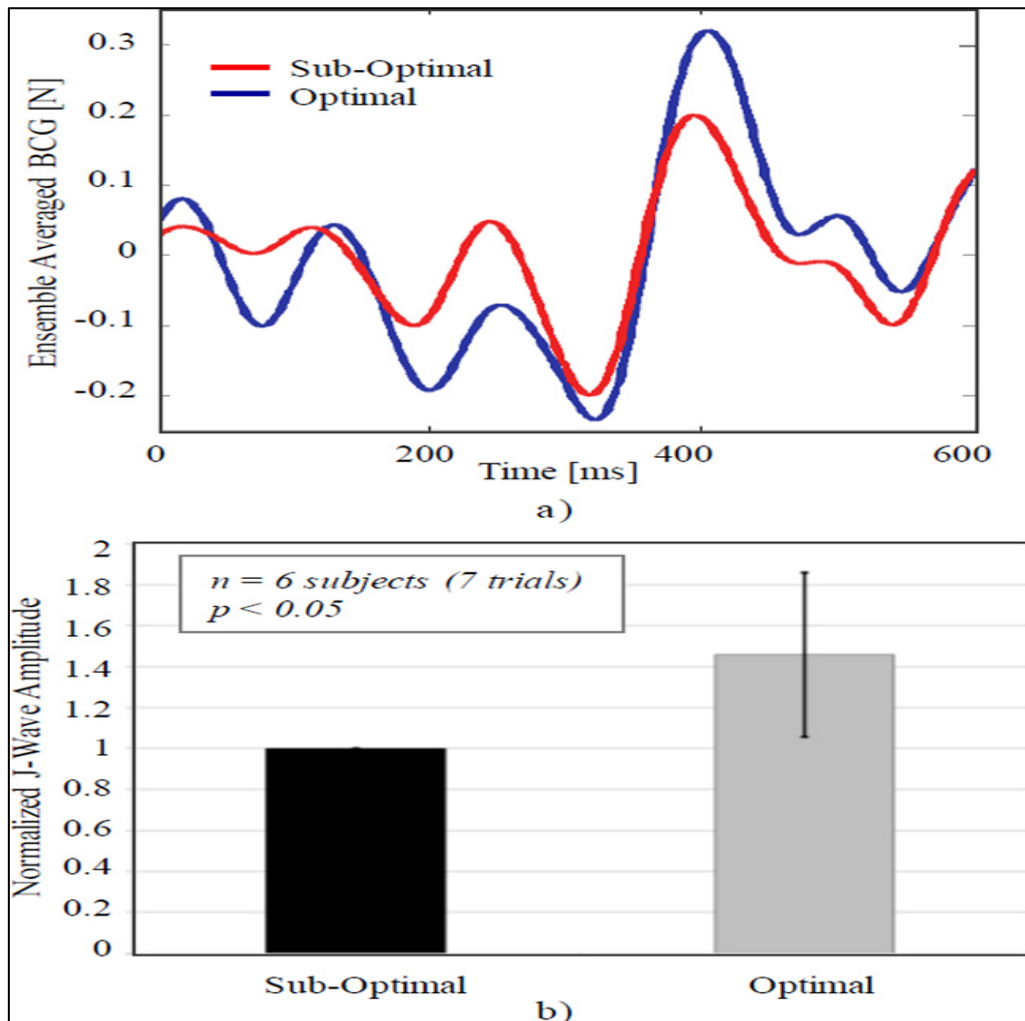


Figure 80 demonstrates the use of BCG to optimise CRT interventricular delay, above the signal averaged BCG with optimal CRT settings in blue and suboptimal settings in red (from a single patient) and below the difference in normalised J wave amplitude from the 6 subjects between optimal and sub-optimal CRT interventricular delay.

It is known that the BCG signal is fundamentally different in patients with IHD or HF and in the elderly. However what is not clear is how the BCG signal might change following CRT, in responders and nonresponders, if at all. Equally it remains to be determined whether quantitative or qualitative analysis of the baseline BCG signal can lead to prediction of response to CRT. Do any of the changes in the BCG signal post CRT implantation correlate with cardiac specific marker of response, for example SV or EF? Once again, it should be noted that whilst the BCG is not specifically a record of the LV, if systolic function improves one might expect this to manifest by a change (whether qualitative or quantitative) in the BCG signal.

6.1.3.2 Hypotheses

Working hypotheses –

- 1) *There will be a conformational change in the BCG signal post-CRT implantation in those who respond.*
- 2) *The baseline signal could predict this response.*

Null hypotheses –

- 1) *There will be no conformational change in the BCG signal post CRT implantation.*
- 2) *The baseline signal does not predict this response.*

6.1.3.3 Materials

The equipment used for this test included: A Kistler multicomponent dynamometer (Type 9257 B), a Kistler multichannel charge amplifier (Type 5070 A) (Kistler Group, Winterthur, Switzerland), a bespoke metal platform on which the patients stood, provided by the Department of Mechanical Engineering at USFD. Four ECG leads (right, left, foot and neutral), four white sensor (solid gel) electrodes (Ambu A/S, Copenhagen, Denmark), a laptop (Toshiba, Tokyo, Japan), a g.USBamp biosignal amplifier (g-tec, Graz, Austria) (figure 81).

Figure 81: Kistler signal amplifier, force plate and metal platform



Figure 81 demonstrates the hardware used to measure BCG, the metal platform on which the force plate was attached to and then the signal amplifier which recorded the BCG signal itself.

6.1.3.4 Methods

Key to the whole process was the use of the gUSB biosignal amplifier, which could record BCG and ECG data simultaneously, producing a real-time visual ECG and BCG

trace. This allowed the BCG signal to be interpreted in the light of the cardiac cycle by gating it to the ECG. The patient was asked to stand still and remain silent for a period of 10 minutes whilst BCG data was captured-i.e. for around 600-800 cardiac cycles.

1. The force platform was placed on flat ground and checked for movement during loading taking care to site it away from electrical appliances, especially mobile phones and laptop power supplies, for example.
2. The laptop and g.USBamp were connected and switched on.
3. The g.Recorder software was started. File > Load Setup... and Grand Challenge configuration was chosen (as detailed below).

The configuration screens were identical to those shown in figure 82. namely; –

In individual channel settings, Channel Number 1.1, 1.3, 1.5, 1.9 and 1.13 were called RA, LA, LL BCGX, BCGY and BCGZ. The box called “Acq” selected for all but 1.4, the “type” chosen as ECG, the sensitivity range set between -1000 (low) to +1000 (high), with 0 offset and unit recorded in uV.

In amplifier settings, common ground and common reference Group A-D were selected. Under options, “Master” was selected, under mode “Measure” was selected and under Analog Output, “square” was selected, amplitude 5mV, offset 0 mV and frequency 10 Hz. Sampling rate set to 1200 Hz, channels 1,3,5,9 and 13 selected and finally under “Channel settings” bipolar selected at channels 3, 5 and 9 for bipolar, high pass, low pass and notch 0 was selected but for 1 and 3, bipolar 0 with high pass 0.1Hz, low pass 200Hz and notch 50 Hz.

Figure 82: Configuration screens for g.Recorder software

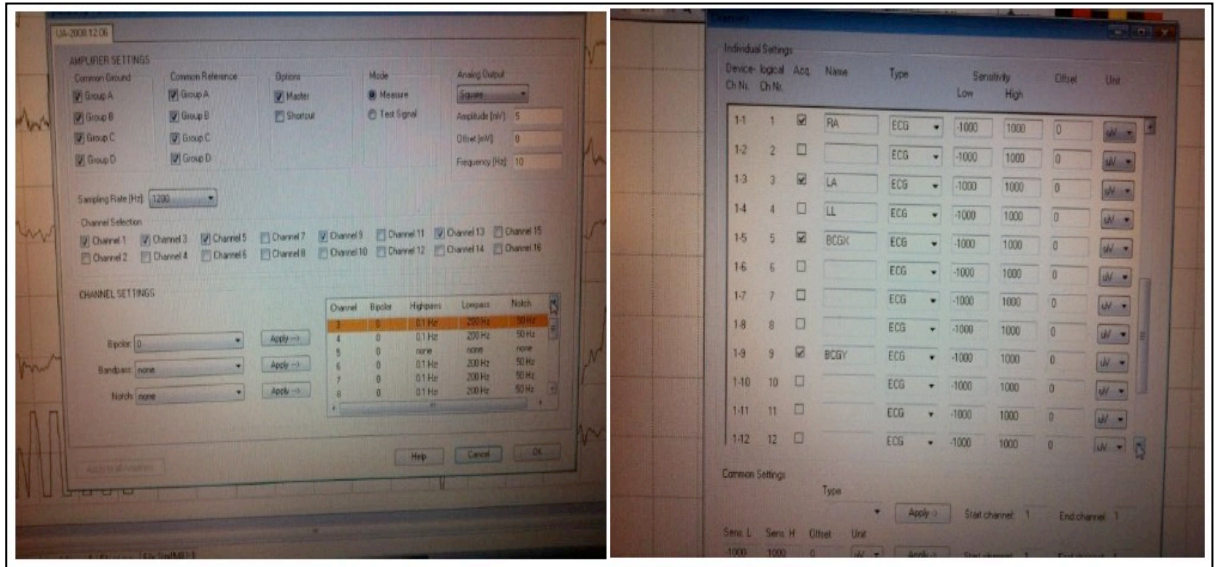


Figure 82 demonstrates the configuration screens seen when setting up the gUSB signal biosignal amplifier, on the left the general settings including ground, reference, channel selection, output and sampling and on the right the individual settings for each channel used for ECG and BCG, including name, type, sensitivity, offset and unit.

6. The Kistler charge amplifier was switched on and the configuration matched that shown in figure 83.

Figure 83: Configuration screens for Kistler charge amplifier.



Figure 83 demonstrates the configuration screens seen on the Kistler charge amplifier, channel 1 (X axis) set to -7.952 pC/N, channel 2 (Y axis) set to -7.935 pC/N and channel 3 (Z axis) set to -3.720 pC/N, all with DC long, low pass filter off and units of 100 N/V.

Each channel was checked in turn, selecting the channel with the blue dial (rotated to select the 'channel' indicator, and clicked to modify, rotate and click to reselect, press ESC button to return). Key points for all 3 channels.

- a. Channel = On
 - b. Direct current = Long
 - c. Low pass filter = Off
 - d. 100 Newtons/Volt
 - e. Channel 1 (X axis) = -7.952, Channel 2 (Y axis) -7.395, Channel 3 (Z) -3.720 pC/N as shown for each channel.
7. ECG leads were attached to the patient and together with the BCG leads were then attached to the g.USBamp as shown in Figure 84.

Figure 84: Connection guide for BCG and ECG leads into g.USBamp

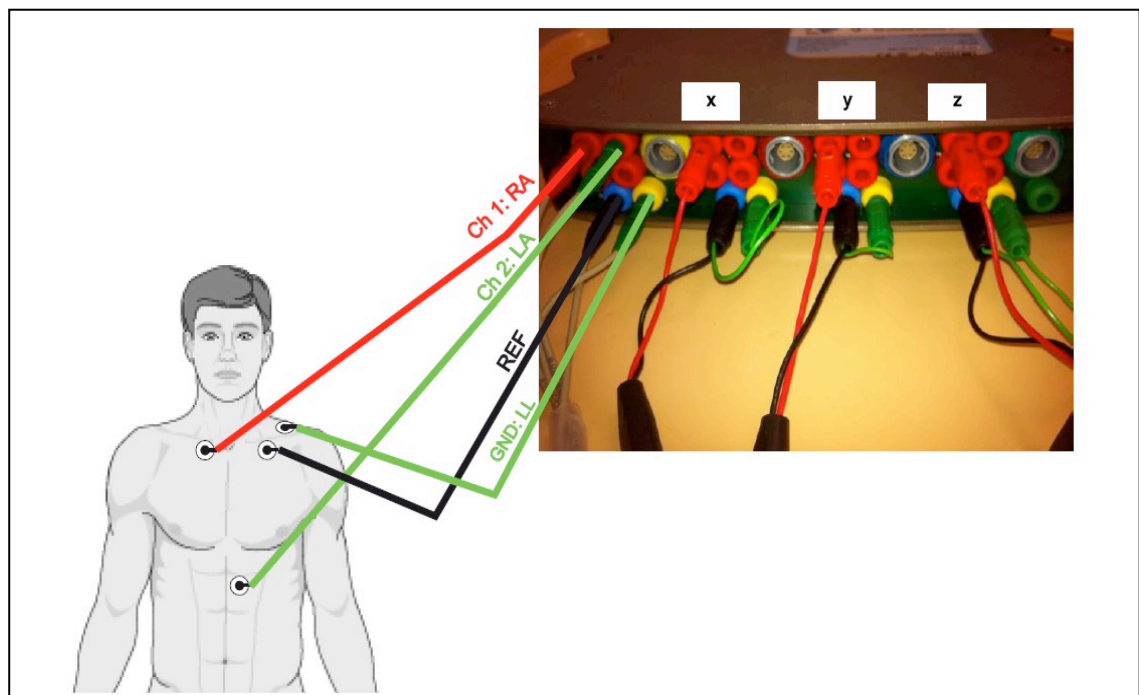


Figure 84 demonstrates the ECG electrode placement on the patient with the corresponding ECG lead placement and also the BCG lead placement in the gUSB biosignal amplifier

9. The computer screen was checked to ensure that the ECG signal is visible..
10. The patient was prepared: shoes on, feet a shoulder width apart, standing on the centre of the force platform.

11. On g.Recorder, File > Record (or the red button) was selected, and the patient's identification number entered.
12. 'Measure' was pressed on the Kister signal conditioner.
13. OK was pressed on the g.Recorder and then 'Recording' screen was pressed and data began to be recorded.
14. The Kistler signal conditioner was monitored to ensure that the red 'overload' light was not illuminated.
15. The g.Recorder screen was monitored to check that the BCG signal (bottom of screen) did not saturate (become flat).
16. The signal was recorded for a few minutes before stopping.
17. The g.BSanalyze software was loaded. The hdf5 file that had been saved was loaded and then saved as a .mat file.

Troubleshooting configuration; steps 8-12 were replaced as follows:

8. All loads/weights were removed from the force platform.
9. On g.Recorder, File > Record (or the red button) was selected and the filename details entered.
10. 'Measure' was pressed on the Kister signal conditioner.
11. 'OK' was pressed on the g.Recorder and then 'Recording' screen was pressed. Data recording then began.
12. A 200g weight was placed on the force platform. The BCGZ channel (bottom of screen) on g.Recorder was observed to ensure that a step change in the signal trace was seen.

Following step 15, the system was returned to the Matlab prompt and the .mat file was loaded into Matlab. 'Plot(P_C_S.data(1,:,5)*100)' was typed in response to the Matlab prompt, and the graph showed a step from 0N to 2N (i.e. 200 grams)

The data files in .mat format were sent to NS and PG, from the Mechanical Engineering Department at the USFD. The ECG voltage signals were summed in order to obtain a single waveform proportional to Wilson's central terminal. Signal-averaging techniques, were used to identify the start of a heartbeat using a trigger (> 0.2mV in amplitude) on the ECG and the remainder of the QRS complexes were discarded. Also,

beat-to-beat variability (caused by factors such as ectopic heartbeats or spurious signals) meant that some triggers gave erroneous heartbeats with abnormally low or high heartbeat periods were removed from the ensemble average by manually specifying a range of admissible heartbeat periods for each patient.

The ECG and the BCG signal were bandpass filtered using a Chebyshev Type II filter with pass band 0.8 to 40 Hz, stop band 0.4 to 60Hz, passband ripple 1dB, and stopband attenuation 20dB. This removed low frequency transients and high frequency noise from the two signals. The ECG QRS complex was then used as a gate or trigger mechanism, where signal values increasing above 0.5 mV in the QR segment caused a trigger. The trigger signal was then used to determine heart rate and to normalise the ECG/BCG time domain so that the signal morphology was independent of heart rate. This was performed by separating the time series into individual heart beats (characterised by the trigger signal), and interpolating between the data points to obtain 1000 linearly spaced signal values for each heart beat period. Ensemble averages of the resulting signals were then compared to ensemble averages of the original signals. The normalised cross-correlation coefficient of the original and time-normalised signals were then obtained and compared, using the following approach. First, the mean of the input ECG signal x and force signal y were removed:

Equation (6):

$$\hat{x} = x - \bar{x}$$

Equation (7):

$$\hat{y} = y - \bar{y}$$

The cross correlation coefficient was then obtained: and normalised using the number of samples N , and standard deviations $s(x)$ and $s(y)$.

Equation (8):

$$\hat{R}_{xy}(m) = \begin{cases} \sum_{n=0}^{N-m-1} \hat{x}_{n+m} \hat{y}_n^* & m \geq 0 \\ \hat{R}_{yz}^*(-m) & m < 0 \end{cases}$$

Finally, the Fourier transform of the time-normalised and original signals were obtained and compared.

Equation (9):

$$R_{xy}(m) = \frac{1}{N s(x)s(y)} \widehat{R}_{xy}(m)$$

Files were returned as .pdf files, (see figure 85) with the timing and force of the HIJKLMN waves extracted. BCG waves were all timed against the start of the QRS complex and, using the standardised nomenclature, the BCG waveforms were labelled and the peak/trough force recorded for each. This was repeated for each patient at each time point. Of the 21 patients recruited 10 patients had BCG acquired at baseline, 6 weeks (pre and post optimisation) 6 and 12 months CRT post-implantation. These comprised 9 responders and 1 nonresponder (see Chapter 5). Markers of response were recorded at baseline, 6 and 12 months only.

Figure 85: Example figure of SABCG and ECG results

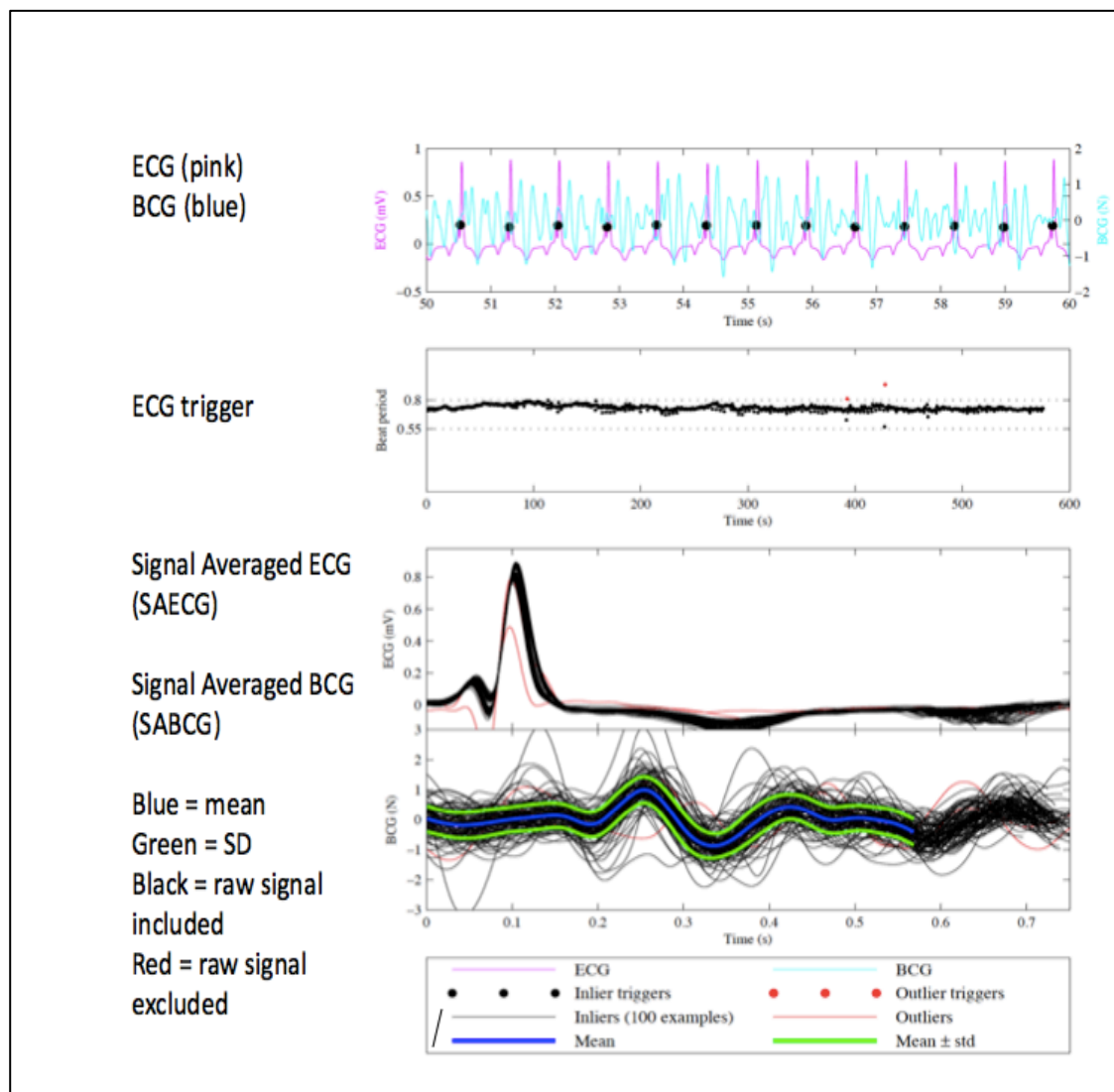


Figure 85 demonstrates the signal averaged BCG ‘report’ created for each patient, following their simultaneous BCG and ECG recording.

6.1.3.5 Results

Table 58: Markers of response in responders during follow-up

Marker	Units	Baseline*		6 months		12 months	
		Mean	SD	Mean	SD	Mean	SD
PVO ₂	ml/kg/min	12.59	1.74	13.89	2.57	14.60	1.52
LVEDV	ml	200.89	43.69	178.33	38.08	159.13	36.63
MLWHFQ	/110	41.78	15.47	29.88	23.97	23.56	19.89
6MWD	m	374.22	84.15	411.22	47.09	413.63	72.27

*PVO₂ – peak oxygen consumption, LVEDV – left ventricular end-diastolic volume, MLWHFQ – Minnesota living with heart failure questionnaire, 6MWD – 6 minute walk distance. *Baseline refers to first pacemaker clinic follow-up post CRT implantation.*

Table 59: Parameters at which may influence SABCG

Parameter		Units	Baseline		6 months		12 months	
			Mean	SD	Mean	SD	Mean	SD
BP	Systolic	mmHg	131.4	19.2	133.2	19.9	136.3	22.7
	Diastolic		73.8	10.0	79.6	10.2	77.6	15.7
	PP		57.7	12.7	53.7	12.9	58.6	19.1
	MAP		93.0	12.4	97.4	12.8	97.1	15.9
Physical	Weight	kg	89.4	18.0	89.4	14.4	86.5	18.1
	Height	m	1.7	0.1	1.7	0.1	1.7	0.1
Echo	EF	%	27.4	11.7	35.0	15.7	36.1	15.9
	SV	ml	43.3	11.6	53.3	19.4	46.6	22.1
CRT	BiVP*	%	91.0	6.6	94.4	5.7	94.7	2.9
ECG	QRSd	ms	159.9	26.9	160.9	17.6	163.1	20.8

**Baseline refers to pre-CRT implantation in all parameters, other than BiVP, where it refers to 6 weeks follow-up. BiVP – biventricular pacing, EF – ejection fraction, MAP – mean arterial pressure, PP – pulse pressure, QRSd = QRS duration, SV = stroke volume.*

Table 60: SABCG force and time at baseline and follow-up

SABCG in Responders		SABCG wave														
		H		I		J		K		L		M		N		
		Mean	SD	Mean	SD	Mean	SD	Mean	SD	Mean	SD	Mean	SD	Mean	SD	
Time point	Baseline	Time (s)	0.20	0.05	0.27	0.07	0.35	0.08	0.43	0.08	0.52	0.07	0.46	0.08	0.60	0.10
		Force (Nm)	0.54	0.42	-0.77	0.70	0.84	0.38	-0.83	0.77	0.76	0.61	-0.73	0.23	0.41	0.64
	Pre-Opt	Time (s)	0.21	0.10	0.28	0.11	0.35	0.11	0.42	0.11	0.43	0.11	0.55	0.10	0.62	0.12
		Force (Nm)	0.64	0.79	-1.09	1.08	0.82	0.88	-0.77	0.82	0.56	0.36	-0.41	0.43	0.36	0.53
	Post-Opt	Time (s)	0.19	0.07	0.26	0.09	0.33	0.09	0.41	0.09	0.47	0.08	0.55	0.08	0.56	0.08
		Force (Nm)	0.42	0.33	-0.71	0.60	0.87	0.63	-0.88	0.89	0.63	0.57	-0.37	0.35	0.23	0.27
	6 months	Time (s)	0.16	0.06	0.20	0.07	0.28	0.08	0.34	0.08	0.41	0.07	0.48	0.07	0.55	0.08
		Force (Nm)	0.41	0.42	-0.48	0.54	0.86	0.49	-0.85	0.48	0.77	0.41	-0.70	0.60	0.43	0.32
	12 months	Time (s)	0.17	0.04	0.21	0.04	0.27	0.05	0.34	0.05	0.40	0.05	0.47	0.04	0.55	0.04
		Force (Nm)	0.21	0.21	-0.19	0.21	0.71	0.32	-0.80	0.52	0.56	0.46	-0.68	0.43	0.38	0.31

***Time = duration post onset of QRS complex. Note "Opt" = CRT optimisation.**

Table 61: Comparing the force and timing of each SABCG wave in responders

One way ANOVA with repeated measures P value	H		I		J		K		L		M		N	
	Time (s)	Force (Nm)	Time (s)	Force (Nm)	Time (s)	Force (Nm)	Time (s)	Force (Nm)	Time (s)	Force (Nm)	Time (s)	Force (Nm)	Time (s)	Force (Nm)
Baseline	0.44	0.81	0.07	0.12	0.12	0.66	0.25	0.69	0.58	0.81	0.13	0.19	0.37	0.65
Pre-Opt														
Post-Opt														
6 months														
12 months														

Figure 86: SABCG from responders at all time points

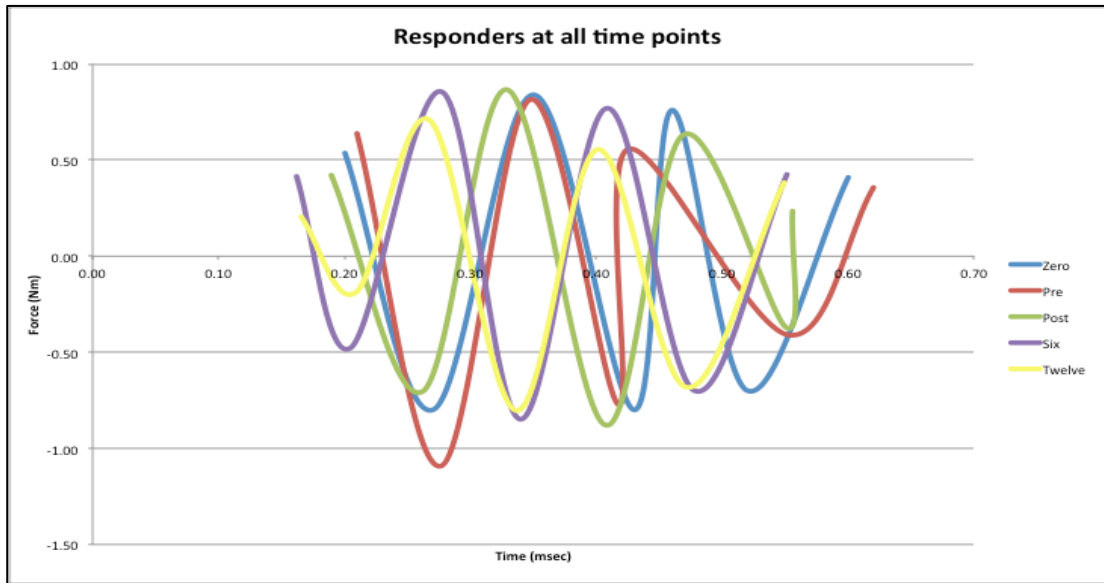


Figure 86 demonstrates the normalised signal average BCG waves from all responders during follow-up, from time zero (blue) to 12 months (yellow).

Figure 87: SABCG from responders at all timepoints (II)

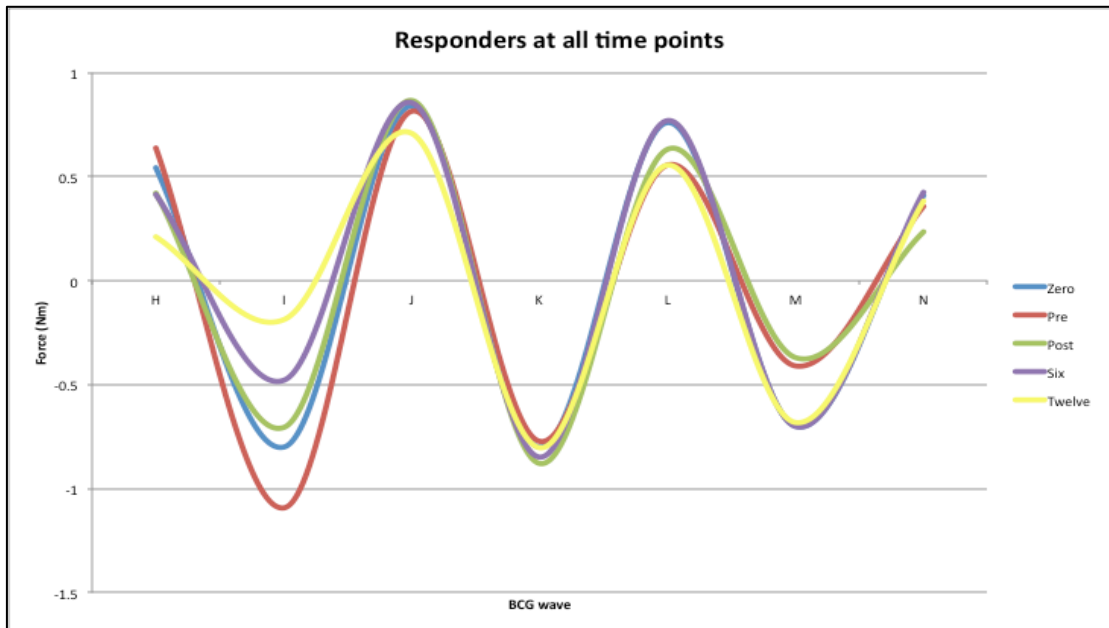


Figure 87 demonstrates the normalised signal average BCG waves from all responders during follow-up, from time zero (blue) to 12 months (yellow), organised by wave.

Figure 88: SABCG from responders pre and post optimisation of CRT device

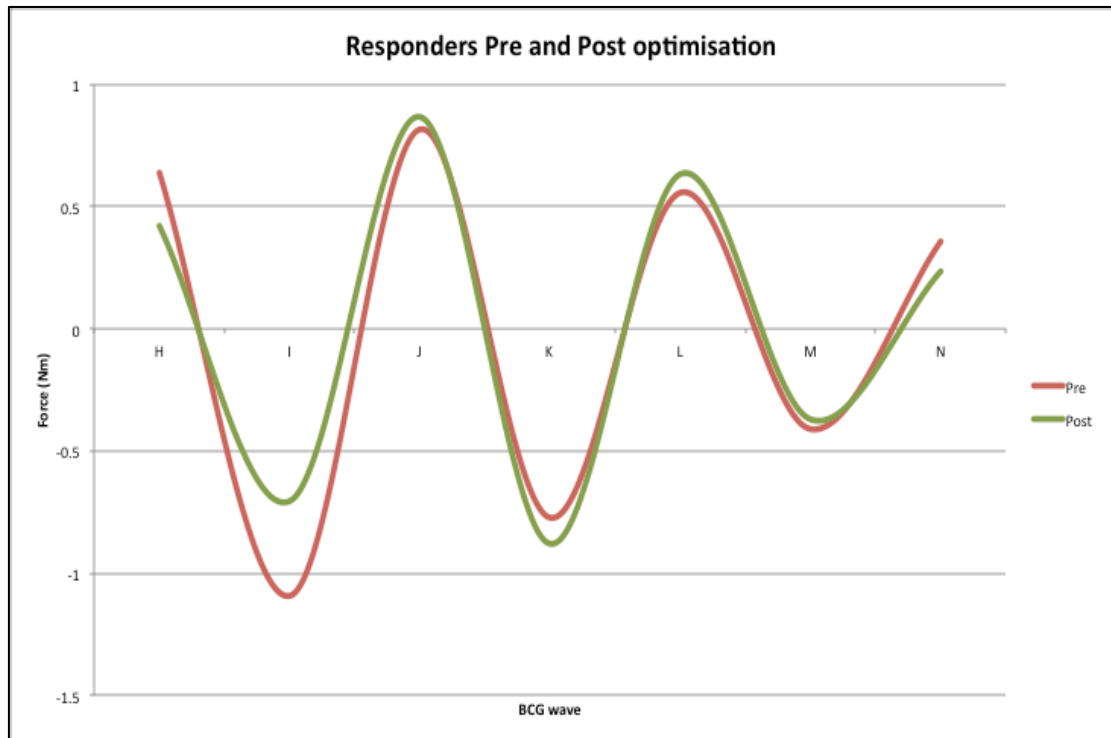


Figure 88 demonstrates the normalised signal average BCG wave from responders before (red) and after CRT optimisation (green) to 12 months.

Figures 86 and 87 demonstrate changes in the BCG SA waveform over time for the 9 responders. In figure 86, the waves consistently arrive earlier from baseline to 12 months and in figure 87 the amplitude of the waves is tempered over time. The increase in the J wave following optimisation seen in figure 88 has been reported previously, but there was also a much larger increase in the I wave in this cohort. There is no consistent pattern in the nonresponder during follow-up with respect to the timing (figure 89) or amplitude of the BCG signal. However, there appears to be an increase in the amplitude for all BCG waves following optimisation.

Comparing the BCG signal averaged data at baseline (figure 90) between responders and the nonresponder, it can be seen the responders have much larger positive waves e.g. J and L, and whilst the early negative wave (I) is smaller, the later negative wave (M) is larger. Finally, figure 91 demonstrates the SD in both time and force in responders at baseline.

Figure 89: BCG signal averaged data from the nonresponder at all time points

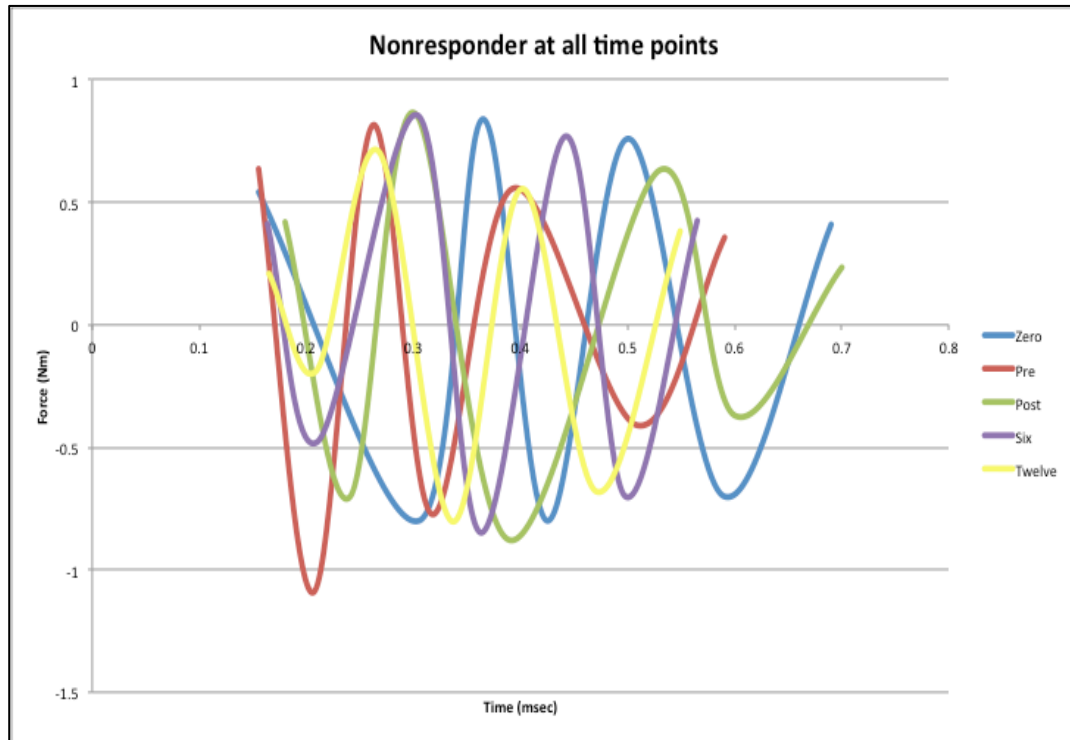


Figure 86 demonstrates the normalised signal average BCG waves from the non-responders during follow-up, from time zero (blue) to 12 months (yellow).

Time zero (baseline) is prior to implantation, pre- and post- refer to before and after optimisation at 6 weeks post-implantation, and six and twelve refer to months post-implantation.

Figure 90: SABCG at baseline in responders and nonresponder

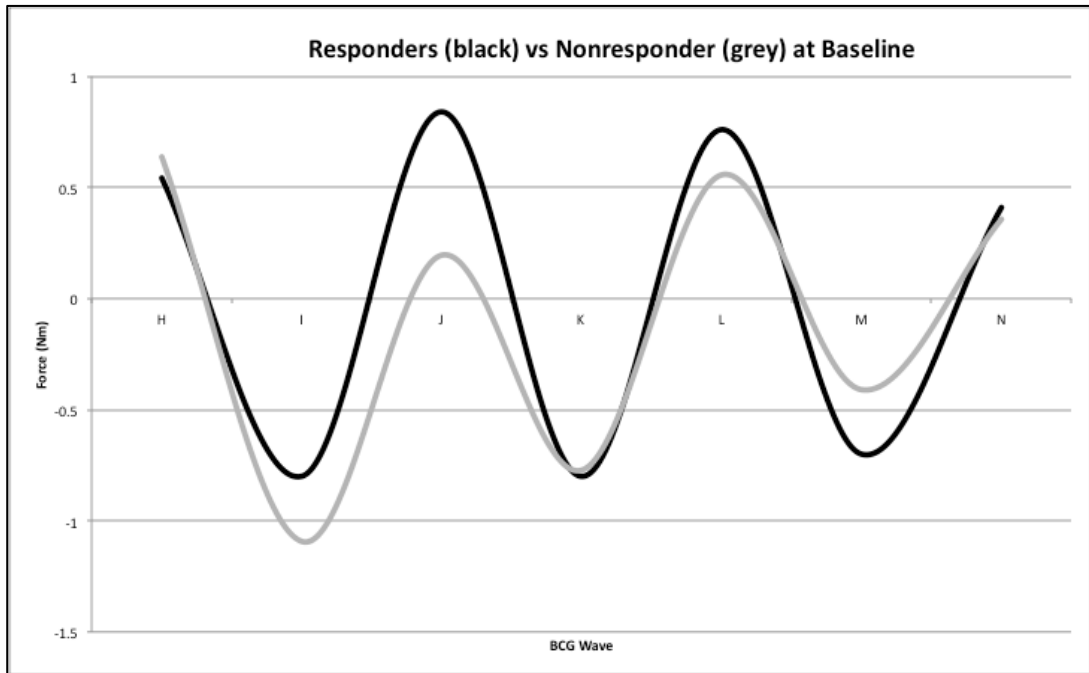


Figure 86 demonstrates the normalised signal average BCG waves from responders and single non-responder at baseline, organised by wave.

Figure 91: SABCG at baseline in responders, demonstrating SD

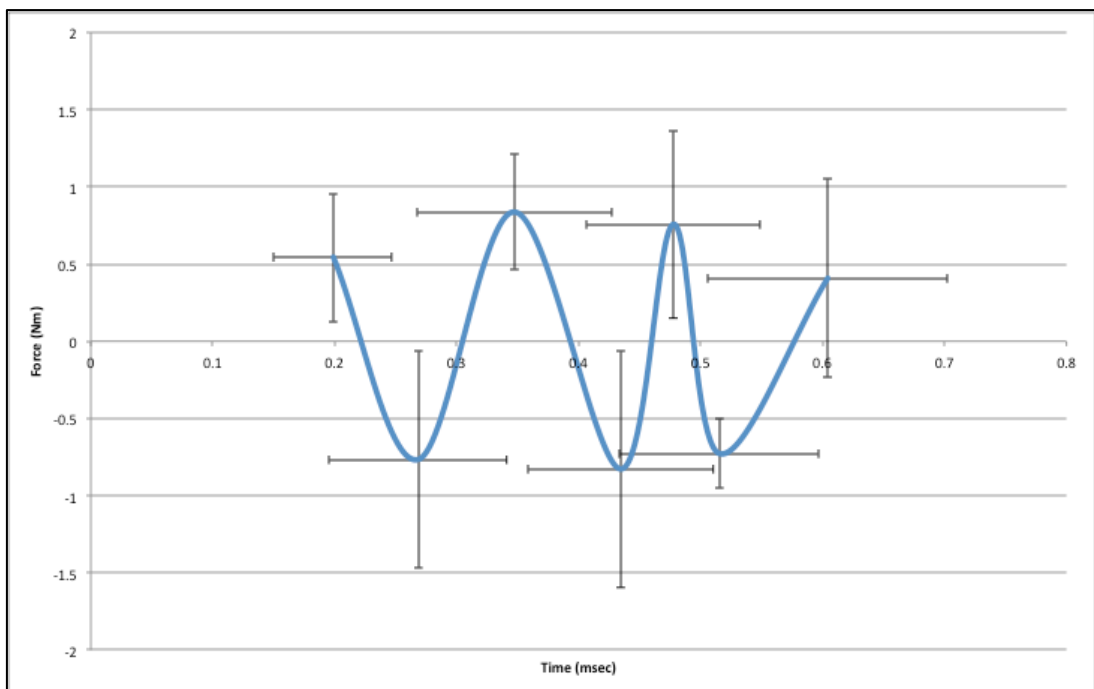


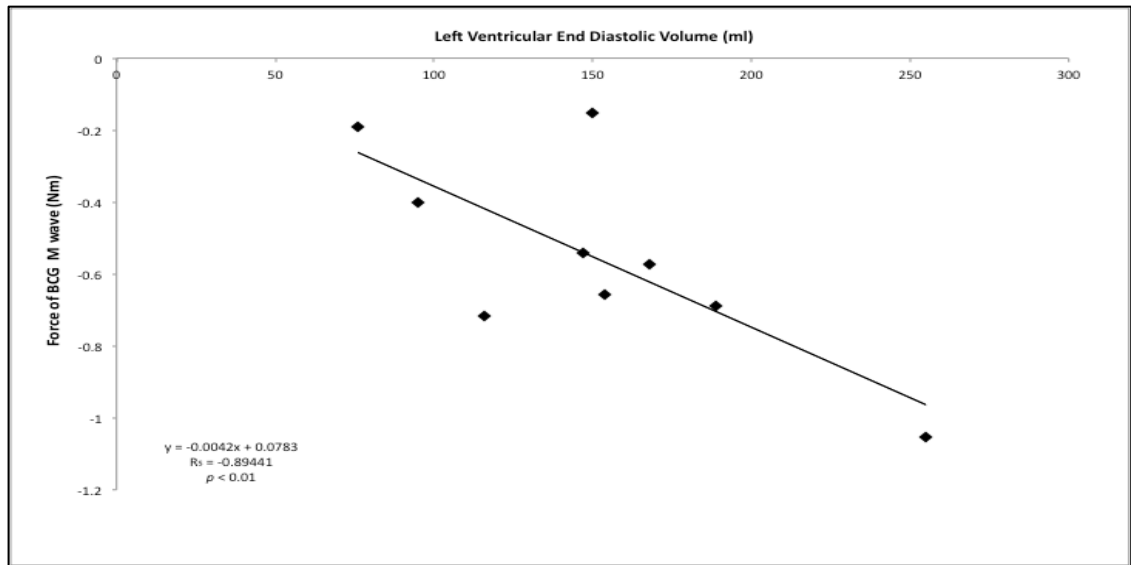
Figure 86 demonstrates the normalised signal average BCG waves from all responders in blue at baseline with standard deviation of time and force.

Table 58 demonstrates markers of response in the cohort of patients who underwent SABCG testing, table 59 demonstrates other possible factors influencing the SABCG signal and table 60 demonstrates the mean and SD of each SABCG wave at each time point. Due to the small sample size, there was no comparison made between responders and the nonresponder at baseline. Using a one-way ANOVA with repeated measures, the only difference between the BCG waveforms in responders, which trended towards significant, is the reduction in the force of I, from time point zero (baseline) compared to 12 months follow-up (see table 61). Similarly, there was no statistically significant change in the timing of the waves during follow-up (see table 61). Although, as was found previously, there was an increase in the J wave following optimisation, this was not statistically significant in either responders or the nonresponder.

In terms of correlations between the 4 markers of response and the 7 SABCG waves, the largest were the M and the N wave at 6 and 12 months. These showed a significant correlation with LVEDV and peak VO_2 respectively. There were other correlation trends, including with the J wave, but none of these reached statistical significance. The directions of the significant correlations were consistent and as expected with M and LVEDV having a negative correlation, and N and peak VO_2 having a positive correlation. Figures 92 and 93 demonstrate the significant correlation between the M and N waves at 6 months, with LVEDV and peak VO_2 respectively.

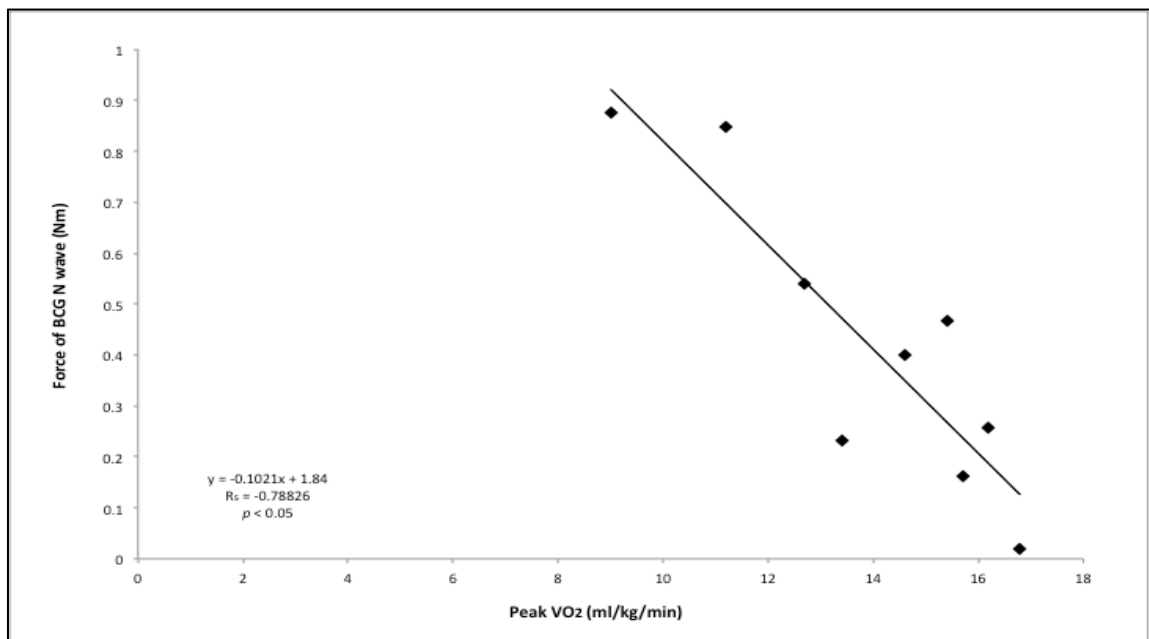
In terms of relationship between the 7 SABCG waves and other parameters that may influence the BCG signal, there were significant correlations with pulse pressure I and J wave at baseline, QRS duration and K wave at baseline, stroke volume and weight with M wave at 6 months and systolic blood pressure and I wave at 12 months. In terms of the 4 markers of response there were other correlations at the various time points but, once again, these were not statistically significant. Figures 94 and 95 demonstrate the significant correlation between the K and I waves at 12 months and baseline with the QRSd and PP respectively.

Figure 92: Correlation between M wave and LVEDV, at 6 months, in responders



The correlation between the force of the M wave from BCG with the left ventricular end diastolic volume at 6 months, in responders.

Figure 93: Correlation between N wave and peak VO₂, at 6 months, in responders



The correlation between the force of the N wave from BCG with the peak VO₂ at 6 months, in responders.

Figure 94: Correlation between K wave and QRSd, at 12 months, in responders

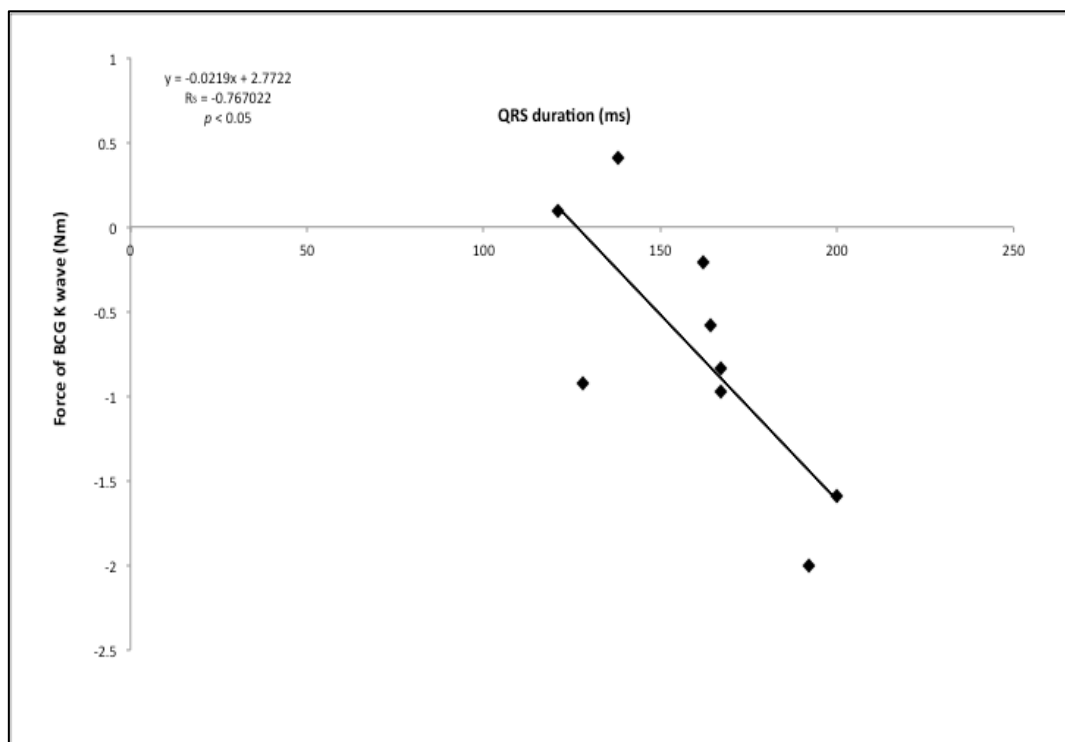


Figure 94 demonstrates the correlation between the signal average BCG K wave force and the QRS duration at 12 months in responders.

Figure 95: Correlation between I wave and PP, at baseline, in responders

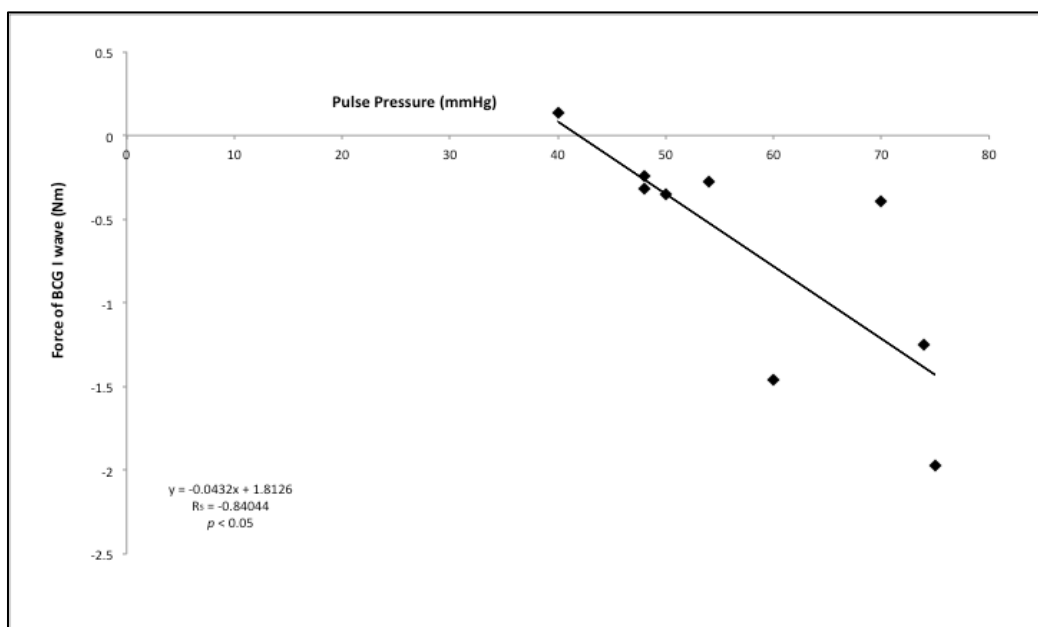


Figure 95 demonstrates the correlation between the signal average BCG I wave force and the pulse pressure at 12 months in responders.

6.1.3.6 Discussion

This work demonstrates, for the first time, the change in BCG signal during follow-up. SABCG was remarkably stable in all the patients tested over time, with the same HIJKLMN waveform pattern seen. Whilst there was no statistically significant difference to this finding, the whole waveform in responders appears to shift to the left, appearing earlier after the QRS complex with each successive point in time. This seems logical as CRT is a device for patients in whose hearts are electromechanically dyssynchronous i.e. with a delay in both conduction and contraction. The work also appears to support the earlier work of Giovangrandi et al (2011)³³⁶ demonstrating that CRT optimisation leads to an increase in the J wave, but the differences recorded did not reach statistical significance nor sustained at 6 or 12 months follow-up.

As discussed above by Gubner et al (1953)³³¹ and Phibbs et al (1967)³³⁵, in HF, a late/reduced amplitude I wave and reduced/sluggish J wave would be anticipated, reflecting impaired contractile force, prominent H wave denoting a stiff ventricle and a large L wave reflecting abnormal ventricular filling. Of all of these, CRT would be expected to have the greatest influence on the J wave as this best represents the cardiac force. Coupled with an increase in EF%, an increase in J wave amplitude might be expected following implantation, following optimisation and also during subsequent 6 and 12 months follow-up. Whilst the EF% increased during follow-up, the recorded difference was not significant and there was no increase in the SV either. In hindsight, measuring any acute increase in EF% and SV pre and post-optimisation, or indeed implantation (with SABCG recording simultaneously) might have been interesting. What is apparent is a decrease of the early part of the signal-averaged BCG signal specifically the I wave, with the amplitude reducing at each successive time point. This consistent pattern is not seen for any other of the waves but, as for the J wave, an increase rather than a reduction in the I wave would be expected following an increase in cardiac force following CRT implantation, and certainly following positive response. Such results may be a consequence of the small sample size and regression to the mean, both in terms of the physiological parameters and also the SABCG. There is no clear pattern emerging for SABCG the nonresponder, although as for responders, the

early part of the signal, both J waves and I reduce over time. There is however, a small increase in J wave amplitude following optimisation. At baseline there appeared to be a significant difference in J wave amplitude between responders and the nonresponders. Thus both the null hypotheses can be accepted; there is no significant change in the BCG signal in responders and this response could not be predicted at baseline. In terms of correlations, there are a variety of relationships between the individual elements of the signal averaged BCG signal and the 4 markers of response and, whilst these academically interesting, they are not of clinical significance, particularly since these are lacking in consistency in terms of both direction and strength. Part of the problem of interpreting SABCG, is the variety of methods used to both record and analyse the signal; there is no normal range reported for the waves in the literature, thus making comparison of this cohort to others, whether healthy controls or HF-LVSD patients, challenging

Clearly statistical comparisons are limited by the small number of patients recruited to the study compounded by the disparity in number between responders and nonresponders. This being said, the only other study investigating BCG in CRT patients found a significant increase in J wave in 6 patients following VV optimisation. However this study used seated BCG and no detail was given for the patients or for the method of CRT optimisation. The study described here predominantly looks at responders, whereas the 6 patients in the previous study had yet to have their response assessed. Indeed, a significant difference before and after optimisation, whilst scientifically interesting, would be clinically irrelevant if the patients fail to go onto respond to CRT.

Despite being asked to stand still and in silence for 10 minutes, the patients talked, moved and fidgeted to varying degrees. This could have affected the overall BCG signal, even with averaging. Patients might have had undiagnosed aortic or peripheral artery atherosclerosis. Whilst the former is unlikely considering that the patients all had transthoracic echocardiography and cMR, other comorbidities such as CKD, fluid balance disturbances or indeed diseases influencing RV function, such as PH or COPD might influence the BCG signal.

A 10 minute recording time was chosen as, even with multiple ectopic heartbeats, AF, or irregular breathing this was assumed to provide an adequate sampling period. Due to the configuration of the bespoke platform, measurement with the patient standing rather than sitting or lying was found to be most appropriate. A seated platform would eliminate movement artefacts from both intentional e.g. fidgeting and also unintentional movements, such as postural sway. Ten minutes was perhaps, in hindsight, too long a period to expect the patient to remain still; it may have been better to ask the patient to stand as still as possible for 1 min, review the data and trying again if movement artefacts were seen. Unfortunately this was not possible with the methodology used.

Interference was initially found to be an issue for the ECG signal but not for the BCG signal. This was put down to the proximity of the ECG chest leads to a power source. The ECG electrodes used proved to be very sensitive and a gel type electrode was finally used to good effect.

The force plate and conditioner were very heavy duty and robust and, coupled with the solid steel platform, were designed for general engineering applications rather than for specific clinical use. Nevertheless, the system provided a stable platform on which the patient could comfortably stand. In retrospect, more could have been done to eliminate movement artefacts; it would have useful to have noted the timings of any large movements so this data could be removed and the timing of the respiratory cycle could have also been recorded to allow data recorded during expiration to be identified and used in previous studies. It would also be interesting to perform simultaneous ECG, BCG and cardiac imaging recordings to ascertain precisely what was happening during the cardiac cycle, perhaps with the force plate built into an echocardiography couch.

Ideally BCG recording would be a 'one-button' procedure, with the patient being connected to the ECG leads and then the recording button being pressed. Indeed talks were held with Boston Scientific during the project, to develop such a device. As the prototype technology used was quite rudimentary, it required substantial input from the experimenter to ensure that both ECG and BCG were recorded, the force plate,

signal conditioner and g.USBamp were set up correctly and to encourage the patient not to move or talk for the 10 minute test period. It took several attempts with the initial patients to fine-tune the settings on the g.USBamp and the charge amplifier, to optimise the position of the ECG leads and the type of ECG electrode, to minimise interference, optimise the signal and ensure consistency during recordings and between patients. As a result, only 10 patients (9 responders and 1 nonresponder) underwent BCG recordings. This was clearly a very small group. In addition, there were no ethnic minorities in this group and only one woman. It will clearly be essential to replicate the results in a much larger population before any firm conclusions can be drawn.

Future work could include evaluation of whether the technology could be incorporated into the scales that patients are often given, along with an automated sphygmomanometer, as part of the remote monitoring package from CRT device companies such as Boston Scientific and St Jude. Remote monitoring and telemedicine is becoming increasingly popular, with researchers investigating which measures may help to identify patients who are likely to deteriorate with the aim of pre-empting this and preventing a hospital admission; left atrial pressure (LAP) monitors are one example of technologies that are used in this way. If there was a conformational change in the BCG signal (due to a reduction in cardiac force, for example) prior to a significant deterioration, then this could alert the clinical HF failure team and lead to early assessment and intervention (perhaps up-titration of diuretics, for example). It would have been interesting to follow a longitudinal measurement of BCG, tracking deterioration and subsequent recovery, but none of the 10 patients deteriorated clinically during the 12 months follow-up post CRT implantation nor, indeed, were admitted to hospital.

It would be interesting investigate potential differences in BCG signals with HF-LVSD aetiology e.g. for ischaemic versus non ischaemic; as whilst previous work has demonstrated that there was no pattern of BCG particular to one cause of acute HF of varying aetiologies, this might not bare true for chronic HF-LVSD. Furthermore, what changes, if any, occurred in patients when the CRT settings were altered, such as RV only, LV only and biventricular pacing options.

The mean age of patients with HF is 76, this cohort is no exception, and so they have "aged" hearts and the BCG signal is abnormal in most patients over the age of 60, most typically a reduction in the I and J wave amplitude, generally believed to reflect a reduction in contractile force of the heart, but the problem, as mentioned already, is that these are also identical to changes in those with IHD³³⁷. Does this mean that everyone over the age of 60 has some degree of IHD or does everyone over the age of 60 have age-related impaired contractile force of the heart that mirrors the BCG pattern of IHD? Unfortunately for our patients, whilst the HF-LVSD may improve with the CRT, in most cases it will not fully resolve and by implanting the CRT we are fundamentally altering the electrical timings and mechanical forces of the heart and so 'before' and 'after' BCG signals may appear completely different. Due to the lack of data available it is difficult to differentiate electrical response e.g. reduction in QRS, versus mechanical e.g. increase in EF% against symptomatic response e.g. improvement in NYHA and thus the BCGs influence in each.

Another potential area is the assessment of patients with aortic stenosis (AS); this patient group represent a significant and as yet unresolved problem in contemporary cardiology. Currently patients with asymptomatic AS are monitored by echocardiography, with the frequency of scans increasing as the disease severity progresses. If this could be performed simultaneously with BCG or alone by BCG, giving insight into the contractile performance of the LV, this may give insight into those who require surgical intervention, despite their echocardiographic parameters remaining unchanged. Often this patient group will remain stable for many years, with annual clinical and echocardiographic assessments but suddenly the LV may deteriorate and symptoms develop which may render them unsuitable for surgery. This sudden change is often missed. If there was a BCG marker that pre-empted clinical or echocardiographic deterioration, this would be a powerful tool.

6.1.3.7 Conclusions

This is the first investigation into the changes in SABCG in patients implanted with CRT, both responders and nonresponders. Previous work has been limited to the

investigation of the BCG signal during optimisation of the CRT device. This work adds to the existing evidence base, demonstrating that there is difference, albeit not significant, in the BCG signal between responders and nonresponders at baseline. In addition the BCG signal appeared to change during the 12-month follow-up period in responders. Whilst again this was not significant optimisation using the iterative method did not lead to significant increase in J wave as found previously.

6.1.4 Hand Grip Strength

6.1.4.1 Definition

Hand grip strength (HGS) is a measure of the maximum force that can be generated by the hand and forearm musculature during a single isometric contraction. HGS correlates well with overall body strength and for this reason it is used as a marker of exercise capacity, general health, and nutritional status. HGS can be assessed quantitatively using a hand-operated dynamometer. HGS deteriorates during the natural ageing process but also due to chronic diseases affecting organs such as the lungs, kidney and heart.

6.1.4.2 Introduction

HGS can be used to stratify HF patients according to their NYHA functional class³³⁸ or peak VO_2 ³³⁹ and is an independent predictor of survival³⁴⁰⁻³⁴². Strong correlation has been identified between the severity of HF-LVSD and, as a consequence, the degree of metabolic abnormality within skeletal muscle and it is thought that the reduction in HGS in HF-LVSD patients is a consequence of oxidative stress and disuse due to fatigue which, in turn, leads to skeletal muscle atrophy and a vicious cycle ensues³⁴³.

6.1.4.3 Pathophysiology

Weight loss was first recognised as part of the HF syndrome, as far back as the time of Hippocrates (circa 400 BC), who noted that the "The flesh is consumed and becomes water... the feet and legs swell; the thighs melt away"³⁴⁴. However, it was not until the late 1990s that this weight loss in HF, termed 'cardiac cachexia', was identified as an independent risk factor for death³⁴⁵. At the same time, the muscle hypothesis of HF-LVSD proposed that "exercise performance in heart failure patients is predominantly limited by skeletal muscle and less by the performance of cardiac muscle"³⁴⁶. As noted previously, there is a paucity of evidence to suggest that resting measures of LV

function have any correlation with functional capacity such as NYHA class³⁴⁷. Perhaps it is not weight loss *per se* that determines morbidity, but rather sarcopenia, “defined as the age-associated loss of skeletal muscle mass and function”³⁴⁸. As alluded to in chapter 2, in HF-LVSD it is known that there are reductions in; the skeletal muscle power of both upper and lower limbs, mitochondrial number, the surface density of cristae and enzyme activity e.g. 3-Hydroxyacyl-CoA-dehydrogenase, nutritive flow to muscle, slow twitch type II fibres and aerobic metabolism, all of which lead to a loss of skeletal muscle performance. Previous trials have shown that medications such as ACEi, help to preserve weight but do not affect the strength of skeletal muscle^{349 350}.

Figure 96: The muscle hypothesis of HF symptoms

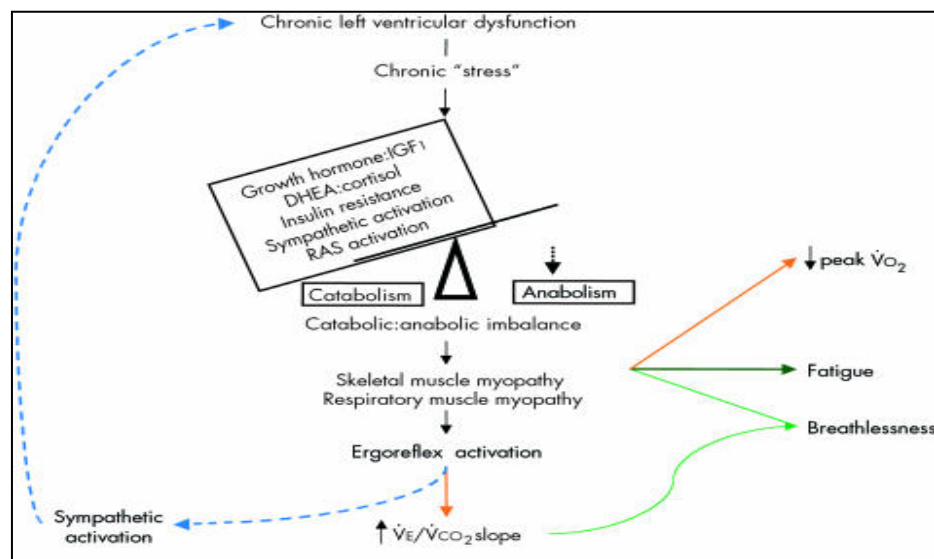


Figure 96 demonstrates the muscle hypothesis of heart failure symptoms, how chronic left ventricular dysfunction, leads to stress, a catabolic state, myopathy, sympathetic activation and then feeding back to further left ventricular dysfunction, with associated fatigue and breathlessness.

As the prevalence of sarcopenia in the general population over the age of 65 is between 10-20% due to factors such as inactivity and malnutrition, a young patient with severe HF may have similar grip strength to an older patient with mild HF³⁵¹. However, this also means that it is challenging to attribute changes in muscle mass and function in the HF population, when the average age at diagnosis is 76 and other diseases often co-exist.

6.1.4.4 Testing

A variety of different types of apparatus, techniques and protocols are used to measure HGS. The Jamar dynamometer (Lafayette Instrument Company, Indiana, USA) is considered to be the gold standard and the benchmark against which others are compared according to the American Society of Hand Therapists³⁵². The Jamar device is based on a hydraulic system, but systems using strain, pneumatic and mechanical assessment methods are also available. Unfortunately, the results of the different types of HGS test are not immediately interchangeable; HGS may be reported in terms of different units with some measuring grip pressure rather than force. As reported by Roberts et al (2011)³⁵³, the advantages of the Jamar device are that it is simple to operate, relatively inexpensive, small, portable and, since it is widely used, a large amount of normative data is available from the literature. However oil can leak from the hydraulic system over time leading to inaccuracies, strain can be exerted on the small joints of the hand and it is quite heavy (approximately 500g). The Jamar device measures grip strength in kilograms (kgf) or pounds (lbf) of force. Test–retest reliability is considered good ($r = 0.88$ to 0.93) and inter-rater reliability excellent ($r = 0.99$)³⁵⁴. Measurement of HGS is sensitive to patient encouragement, time of day, posture³⁵⁵, the position of the upper limb joints (shoulder, elbow, and wrist)³⁵⁶⁻³⁵⁹ and even the position of the dynamometer³⁶⁰ handle. For these reasons it is important to adopt a standardised approach throughout the tests.

6.1.4.5 Reference Range

Reference values are available for HGS in healthy adults; 32-56kgf is considered normal in men and 19-30kgf in women. These data were obtained from collation of outputs from a number of different studies, carried out on over 7000 adults with an age range of 20–95 years and using a number of different methods³⁶¹⁻³⁶³. For the Jamar dynamometer, a value of 32-45kgf is considered normal for men and 19–28kgf for women, taken from data acquired from more than 700 healthy adults³⁶⁴. The majority of patients with HF-LVSD will be over 60 years of age and the range for this age group is 22-42kgf and 14-24kgf for men and women respectively, however these data are based on a healthy cohort. The patients might be expected to achieve somewhat lower values (see table 62)^{338-340 343 347}.

6.1.4.6 CRT

No papers were found in the literature investigating HGS before and after CRT, or indeed, for any other therapy that improves LV function e.g. heart transplantation or LVAD. When considering the influence of CRT it is difficult to predict whether baseline HGS might be higher in nonresponders or responders.

Figure 97: Picture of the Jamar hand dynamometer

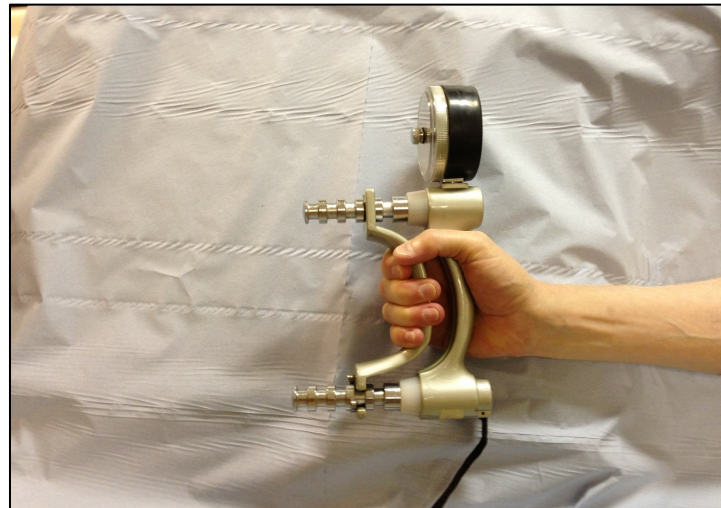


Figure 97 demonstrates the Jamar hand dynamometer in use, with the hand grip in position two and the dial facing away from the patient.

Table 62: HGS values from studies conducted on HF patients

Author	Year	Study	Dynamometer	Findings	HGS (kg)
Andrews	1997	Prognosis	Not Stated	Good	34.13
				Poor	33.13
Senden	2004	Gender	Jamar	Men	48.9 ± 10.5
				Women	30.6 ± 5.4
Castillo-Martinez	2007	NYHA class	Smedley	II	28.4 ± 10.7
				III	24.8 ± 10.4
Izawa	2009	Handedness	Jamar	Left	30.3 ± 8.0
				Right	36.3 ± 9.2
Gary	2011	Exercise Programme	Jamar	Before	43.3 ± 12.0
				After	45.4 ± 11.3

6.1.4.7 Hypotheses

Working hypotheses –

1) HGS improves significantly in patients who are classed as responders to CRT, determined from a combination of symptoms, echocardiography and exercise testing.

2) Clinical response to CRT is predicted by HGS measured at baseline.

Null hypotheses –

1) HGS shows no significant improve in patients who are classed as responders to CRT, as determined from a combination of symptoms, echocardiography and exercise testing.

2) Clinical response to CRT is not predicted by HGS measured at baseline.

6.1.4.8 Methods

For reasons discussed above, care was taken to establish and follow a single protocol for all patients. HGS was measured at baseline, and at 6 and 12 months follow-up post-CRT implantation, using a Jamar analogue dynamometer (figure 97). The patient was asked to perform 3 maximal grips for each hand. Tests were performed between 10:00-11:00 am. The patient was positioned according to the American Society of Hand Therapists (ASHT) guidance for HGS assessment, that is; seated, with the shoulders adducted and neutrally rotated, the wrist neutral (at between 0-30 degrees), the elbow flexed at 90 degrees and the forearm in a neutral position (halfway between pronation and supination) and resting on flat surface³⁵².

The dynamometer handle was set in the second position, comfortable for most individuals. In order to avoid any extraneous influences the dial was positioned facing away from the patient and the patient's previous performance was not relayed to them. Furthermore, standardised verbal instructions and encouragement were given as per Mathiowetz et al (1984)³⁵⁴, specifically "I want you to hold the handle like this and squeeze as hard as you can". The examiner demonstrates and then gives the dynamometer to the subject. After the subject is positioned appropriately, the

examiner says, 'Are you ready? Squeeze as hard as you can'. As the subject begins to squeeze, the examiner says, 'Harder! ... Harder! ... Relax'.

The patient was told to stop after 5 seconds and allowed 2.5 minutes rest. This test was repeated 3 times for each hand. Alternate hands were used in order to minimise muscle fatigue. The mean maximal value for each hand was selected for comparison across all patients and during follow-up. Medications, handedness, weight and current or previous occupation were recorded as these might influence the results.

The maximum HGS recorded for each hand was recorded for each 3 group of attempts (X, Y, Z) and the mean maximal HGS for each hand was calculated ($R \text{ or } L = X+Y+Z/3$). The right hand was always assessed first and then the left, regardless of dominance.

Measurement of HGS was performed double-blind with neither the patient knowing their previous performance nor the experimenter having access to this data. Where possible the relatives attending with the patient were kept away during testing to avoid any extraneous influence.

6.1.4.9 Results

Table 63: Patient demographics at baseline

Baseline	Responders		Nonresponders		Student's T-test
	Mean	SD	Mean	SD	<i>p</i> value
Age (years)	65.4	10.8	71.2	4.4	= 0.53
Weight (kg)	90.3	18.5	81.3	18.5	= 0.47
BMI (kg/m ²)	30.0	4.4	27.7	4.6	= 0.18
Height (m)	1.73	0.10	1.71	0.05	= 0.73

Table 64: Baseline HGS of responders and nonresponders

Baseline		Responders		Nonresponders		Student's T-test
		Mean	SD	Mean	SD	<i>p</i> value
		Kgf	Kgf	Kgf	Kgf	
GS	Left	34.4	11.4	33.0	5.3	= 0.42
	Right	35.7	12.5	31.2	12.2	= 0.25

Table 65: HGS of responders at baseline and during follow-up

Responder		Baseline		6 months		12 months		One way ANOVA with repeated measures <i>p</i> value	
		Mean	SD	Mean	SD	Mean	SD	Baseline vs	
		Kgf	Kgf	Kgf	Kgf	Kgf	Kgf	6 months	12 months
GS	L	34.4	11.4	39.7	10.8	40.3	11.3	< 0.01	< 0.001
	R	35.7	12.5	39.8	11.5	42.2	11.2	< 0.01	< 0.001

Table 66: HGS of nonresponders at baseline and during follow-up

Nonresponder		Baseline		6 months		12 months		One way ANOVA with repeated measures <i>p</i> value	
		Mean	SD	Mean	SD	Mean	SD	Baseline vs	
		Kgf	Kgf	Kgf	Kgf	Kgf	Kgf	6 months	12 months
GS	L	33.0	5.3	27.6	8.9	25.0	11.7	= 0.30	
	R	31.2	12.2	30.8	9.9	29.8	8.1	= 0.66	

Figure 98: Left and right HGS in responders (grey) and non-responders (black)

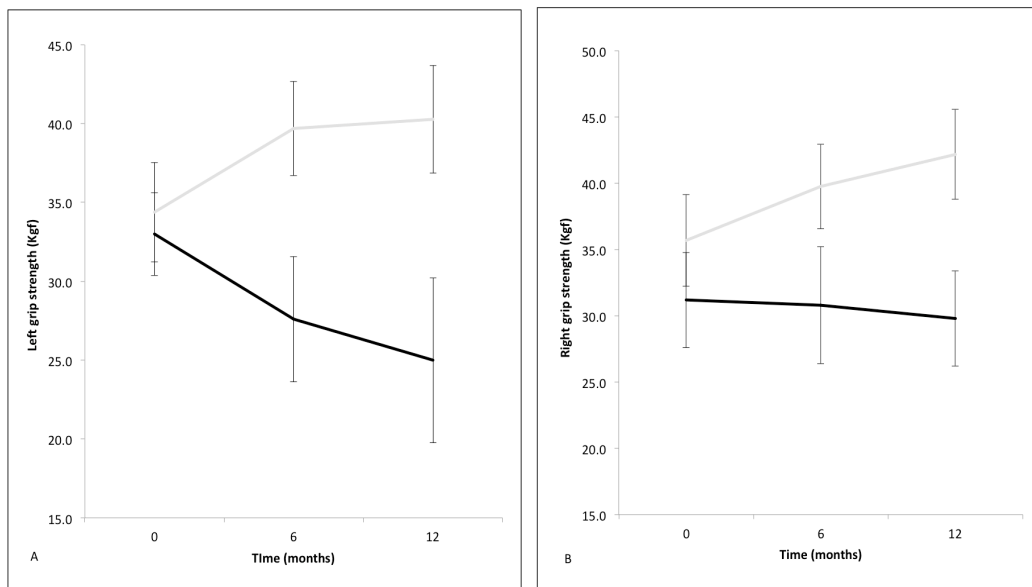


Figure 98 demonstrates the left and right hand grip strength changes in responders (grey) and non-responders (black) following CRT implantation.

There were no statistically significant differences between the HGS of responders and non-responders at baseline (see table 64). Figure 97 demonstrates changes in HGS during follow-up with standard error, demonstrating a clear improvement in responders, without any overlap.

A one-way ANOVA with repeated measures and Greenhouse-Geisser correction determined mean HGS in responders was statistically different between time points in the left ($F(1.77, 17.71) = 21.03, p < 0.001$) and the right ($F(1.36, 13.58) = 16.03, p < 0.01$) hand. Post hoc tests using the Bonferroni correction revealed that HGS increased statistically significantly between baseline and six months and baseline and twelve months in both hands (see table 65 and figure 97).

A one-way ANOVA with repeated measures and Greenhouse-Geisser correction determined that there were no statistically different between time points in the left ($F(1.05, 4.22) = 1.29, p = 0.30$) or right ($F(1.12, 4.49) = 0.24, p = 0.66$) hand (see table 66 and figure 97) in non-responders.

Based on the above findings the first working hypothesis; that HGS improves significantly in patients who are classed as responders to CRT was accepted and the null hypothesis rejected. The second working hypothesis was rejected and the null hypothesis, that the clinical response to CRT cannot be predicted by baseline HGS, was accepted

6.1.4.10 Discussion

This study suggests that HGS improves in patients who successfully respond to CRT, as measured by significant improvements in peak VO_2 , LVEDV and MLWHFQ. These are novel data and this finding has not been reported previously. This suggests that HGS is a potential marker of response, as with MLWHFQ, peak VO_2 and LVEDV, HGS significantly improves in responders with no such improvement observed in nonresponders. Indeed, for nonresponders HGS was found to have decreased at follow-up but this change was not statistically significant. There was a difference in the recorded HGS at baseline between the groups, with HGS being higher in responders than nonresponders, but the lack of statistical difference, means that HGS cannot be used to predict response based on the findings from this study. Responders were also younger, heavier, taller and had a higher BMI at baseline, suggesting that they were more nutritionally replete, but this was not statistically significant. Opasich et al (1997)⁷⁵ also found height and weight to be predictors of muscle strength in HF-LVSD. Although there was no direct measure of activity, these results suggest that, by improving cardiac function in responders, CRT better enables patients to perform activities of daily living (ADL) and so regain strength in their skeletal muscles.

Compared to data reported in other HF-LVSD studies this cohort of patients all had a similar HGS and what would be considered at the lower end of normal in a healthy population. As all the of patients were classified as NYHA III this might be expected, for example Castillo-Martinez et al (2009) for example, report a wider spread of HGS for their study, on patients with HF-LVSD between NYHA II-IV ³³⁸.

One might predict that CRT responders might have a lower HGS than nonresponders, denoting a more severe HF-LVSD syndrome at baseline, and greater propensity to

benefit from the CRT. Alternatively a higher HGS at baseline may indicate those patients whose HF symptoms originate from cardiac rather than from skeletal muscle dysfunction and so improving the pump function of the heart will improve their symptoms. In either case, one might expect sustained or higher HGS at follow-up in responders, denoting an increased physical activity. Equally, one might expect nonresponders to have a reduced HGS at follow-up due to the continuing decline of their physical health and activity due to HF-LVSD, although it is important to remember that the decline in HF is non-linear³⁶⁵.

Whilst muscle mass does not automatically equate to muscle strength, a simple, cheap and non-invasive way to support the findings from HGS testing, would be to measure forearm circumference, to see if this improved following CRT, which in conjunction with an improvement in HGS, could demonstrate a reversal in sarcopenia^{342 366}. But this would not differentiate lean from fat mass. Whilst there are studies demonstrating a positive correlation between anthropometric measures and HGS, these are in healthy populations and not following an intervention in individuals with HF-LVSD. The main limitation of this work is that HGS was measured in isolation without simultaneous measure of lean body mass, due to the absence of available equipment locally. Thus rather than sarcopenia, this work should be considered a measure of dynapenia³⁶⁷. However, there can be gains in strength in the absence of muscle hypertrophy, due to increased recruitment of existing motor units and so testing the strength of other muscle groups such as the quadriceps could also be considered to confirm the changes from the upper limb³⁶⁸. Other comparative non-invasive measurements, equipment, cost and time permitting, could have been made using bio-impedance scales to measure changes in lean mass or using magnetic resonance imaging to measure muscle volume⁷⁴. A study has demonstrated a positive correlation between lean body mass and grip strength in patients with chronic HF³⁶⁹.

Whilst there was a difference in weight and body mass index (BMI) between the responders and nonresponders, this was not significant, and furthermore, it was demonstrated that, rather than suffering from cardiac cachexia as might be expected in end-stage HF-LVSD, most patients were overweight. Perhaps this represents the rest of the UK, with over two-thirds of the population being overweight or obese.

Muscle biopsy can be used to confirm the reversal of any metabolic changes in patients with improved HGS but repeated biopsy might be unacceptable to patients and ethically questionable. HGS is a simple, non-invasive and repeatable measure of peripheral muscle strength yet, as mentioned earlier, no trial has been performed to assess the effects of treatments such as heart transplant, LVAD or CRT on HF-LVSD patients. It would be interesting to see, as reduced HGS is associated with increase mortality and morbidity in HF-LVSD, whether improvement following CRT was also associated with reduced morbidity or mortality. This cannot be confirmed with our study, due to the short follow-up and small numbers of participants. A recent study³⁷⁰ demonstrated that exercise training in HF-LVSD patients led to increases in muscle force and reductions in the levels of MuRF-1, a component of the ubiquitin-proteasome system involved in muscle proteolysis, which is increased in the skeletal muscle of patients with heart failure. It would be interesting to see what impact CRT also had on such a biomarker of sarcopenia.

Future studies would require larger groups of patients to confirm these preliminary findings. It would be interesting to investigate whether there is a difference in HGS for patients with ischaemic and non-ischaemic HF-LVSD. It would also be interesting to investigate what other components of peripheral muscle performance such as endurance or power could be improved by CRT. The only similar published study, performed in a similar cohort of patients with advanced HF who had an LVAD implanted, demonstrated an improvement in HGS of 26% at 6 months follow up³⁷¹.

Many of the patients in this study suffered from concomitant disease. Since patients with chronic diseases, such as COPD and CKD also experience reductions in peripheral muscle strength, it is possible that those with a greater number of comorbidities would have a lower HGS. However no correlation was found between the extent of comorbidities and HGS in this study^{372 373}. Three patients scored highly e.g. normal HGS; this is likely because they were 15–20 years younger than the other patients.

There was certainly a learning curve associated with using the device, with patients tending to score higher on their second or third attempt. For this reason all attempts

were included and then the mean of the three attempts calculated. As in previous studies, both left and right hands were assessed, but there was no significant difference between the R and L hands for all patients assessed. Only one patient was left-handed. The influence of handedness is still an area of contention as whilst one might assume that the dominant side would be the stronger this is yet to be born out in the evidence.

6.1.4.11 Conclusion

As HGS did not differ significantly between responders and nonresponders at baseline, this work does not support the use of HGS as a predictive marker of response to CRT. However a significant increase in HGS was recorded in responders at follow up suggesting that it could be used as a marker of response and, moreover, is a unique measure of the HF syndrome, not covered currently by others markers of response. HGS negatively correlates with 6MWD and so in this regard, demonstrates similar level of utility in terms of providing a marker of response.

Further work could involve investigating exactly what changes occur to the forearm musculature, whether these changes are mirrored in the leg and whether such changes in HGS result in a change in muscle volume or lean weight. As a simple, quick and non-invasive test, there are few negatives to adopting routine use of such HGS in assessing for CRT response.

6.2 Biomarkers

6.2.1 Introduction

A biomarker is "a characteristic that is objectively measured and evaluated as an indicator of normal biologic processes, pathogenic processes, or pharmacologic responses to a therapeutic intervention."³⁷⁴

6.2.2 Uric acid

6.2.2.1 Introduction

Patients with HF-LVSD are at risk of hyperuricaemia, i.e. elevated levels of uric acid (UA). This may occur for several reasons; medications commonly prescribed in HF-LVSD (such as aspirin and diuretics) reduce renal excretion of UA, comorbidities

common in HF include CKD, hyperparathyroidism, hypertension, diabetes, hypercholesterolemia and obesity all of which are associated with a higher incidence of hyperuricaemia and, finally, elevated UA is a consequence of chronic inflammation as a result of “activation of xanthine oxidase, through free radical release, causing leukocyte and endothelial cell activation.”³⁷⁵. UA impairs nutritive blood flow³⁷⁶ and is predictive of LV filling pressures³⁷⁷, haemodynamic compromise³⁷⁸ and the development³⁷⁹ and subsequent deterioration of HF-LVSD³⁸⁰ (table 67). A meta-analysis concluded that HF-LVSD mortality increased 13% for every 1 mg/dL increase of serum UA level³⁸¹.

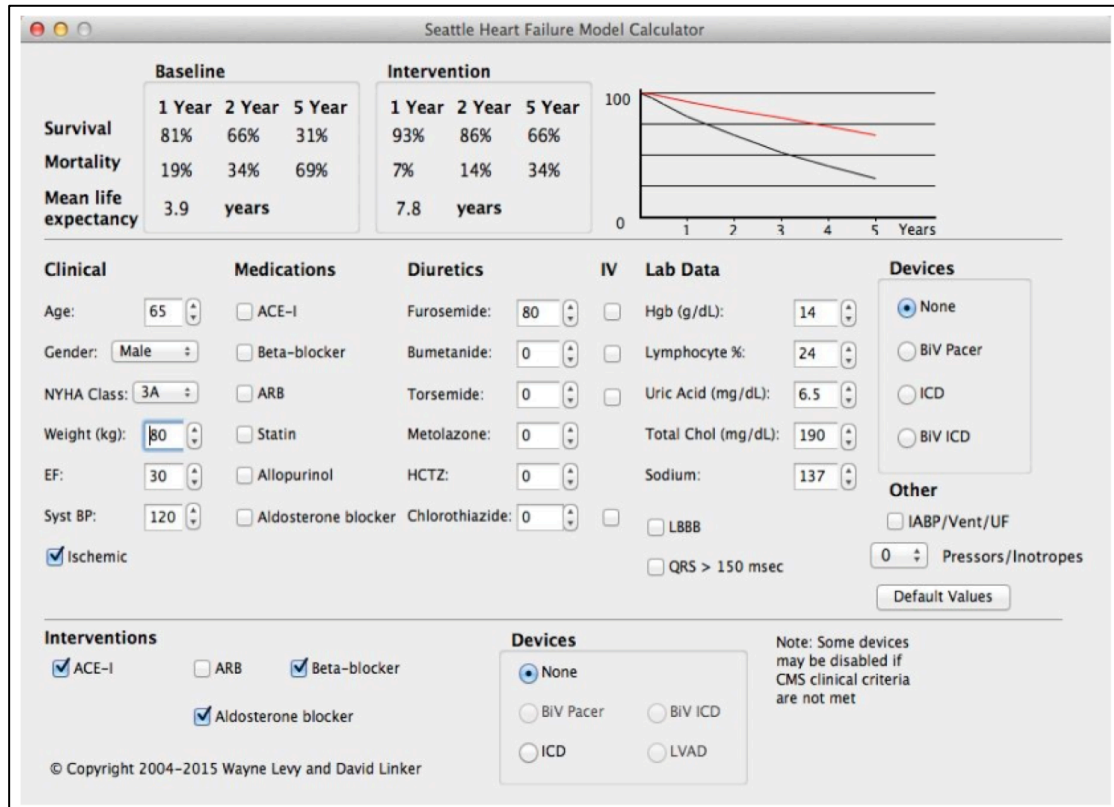
6.2.2.2 Pathophysiology

An increase in serum UA is a physiological result of cell breakdown in a hypoxic environment; deoxyribonucleic acid (DNA) purine bases such as adenosine are converted into hypoxanthine, xanthine and finally uric acid by xanthine oxidase, which is then excreted in urine. The normal ranges of serum UA in healthy adult men and women are 200-430 and 140-360umol/l, respectively. Xanthine oxidase inhibitors reduce UA and have been shown to improve peripheral blood flow³⁸² and BNP³⁸³ in HF. However a debate remains as to whether elevated UA is a cause or consequence of HF. Despite this uncertainty, serum measurement of UA is incorporated into the Seattle heart failure model (figure 99) because of its recognised independent power in predicting mortality in HF-LVSD⁵³. However there is no evidence to suggest that reducing UA levels in HF-LVSD, leads to improved outcomes³⁸⁴.

Table 67: UA levels in heart failure and their significance

Author	Year	UA level (umol/l)	Finding
Anker	2003	> 163	Predicts worse prognosis
Pascual-Figal	2007	> 108	Predicts development
Krishnan	2009	> 130	Predicts severe symptoms

Figure 99: Screen shot of the Seattle Heart Failure Model



6.2.2.3 UA after CRT

There are only two trials reported that specifically investigate UA and CRT. The first was published as an abstract by Dzeja et al (2011) and describes an assessment of the metabolic profile of the heart, including serum UA concentrations, before and after 10 minutes of CRT. The authors found that myocardial substrate metabolism was improved with CRT switched on but did not comment on UA uptake by the myocardium³⁸⁵. A more recent paper by Rinkuniene et al (2014), reported that lower UA levels at baseline were associated with better echocardiographic response to CRT at 12 months in cohort of 80 patients³⁸⁶.

Whilst not directly related to CRT, there is some evidence to suggest that improvement of cardiac function may lead to a meaningful reduction in UA. This data comes from a study of fifty-five patients with end-stage HF-LVSD. For these patients UA levels were found to drop by over 25% after heart transplantation with the greatest decrease observed after 12 months; similar results might be expected in CRT responders³⁸⁷. UA correlates with nutritive flow to lower limb muscles as measured by

plethysmography³⁴⁵, FMD has been identified as a predictor of response to CRT and both these parameters are measures of endothelial function. One might predict that serum UA might mirror changes in FMD or even, given the work described previously by Akar et al (2008)³²², predict response to CRT. These 2 papers suggest that UA levels may change in patients who have improved cardiac function and therefore respond to CRT. If FMD predicts response and is lower in responders at baseline it might be expected that responders will have higher levels of serum UA at baseline.

6.2.2.4 Hypotheses

Working hypotheses –

1) UA improves significantly in patients who are classed as responders to CRT, determined by symptoms, echocardiography and exercise testing.

2) Clinical response to CRT is predicted by UA measured at baseline.

Null hypotheses –

1) UA does not improve significantly in patients who are classed as responders to CRT, determined by symptoms, echocardiography and exercise testing.

2) The clinical response to CRT is not predicted by UA measured at baseline.

6.2.2.5 Method

Clotted blood samples were taken at baseline (within 2 weeks pre-CRT implantation), then 6 and 12 months post-CRT implantation (+/- 2 weeks) and hand-delivered to the laboratory.

Serum UA was analysed clinical chemistry department at STHT using a commercial enzymatic colorimetric test (ACN 8700, Roche, UK). Laboratory staff were blinded to the markers of response. The reaction on which the test is based is as follows; uricase cleaves UA to form allantoin and hydrogen peroxide and then hydrogen peroxide oxidises 4-aminophenazone to give a quinone-diimine dye, the colour intensity of which is directly proportional to the UA concentration and is determined by measuring the increase in absorbance

In Sheffield, test samples of 201 and 581umol/l are run with an accuracy of 201 (± 3 SD, 1.57 CV%) pg/ml and 581 (± 10 SD, 1.73 CV%)³⁸⁸. CV% is the coefficient of variation and equal to $((\text{STDEV}/\text{Mean}) * 100)$ a commonly used measure to express assay performance.

6.2.2.6 Results

Table 68: Baseline characteristics of responders and nonresponders

Baseline		Responders		Nonresponders		Student's T-test P-value
		Mean	SD	Mean	SD	
Uric Acid	umol/l	399	100	442	101	= 0.45
Creatinine	mmol/l	98	20	108	19	= 0.25
eGFR	ml/min/1.73m ²	65	10	60	10	= 0.49
Diuretic dose (mg)	Loop diuretic eq	70	57	89	71	= 0.34
	MRA eq	23	11	29	17	= 0.31

Table 69: UA and renal function in responders at baseline and follow-up

Responders		Time point (months)						One way ANOVA with repeated measures P value	
		Baseline		6		12		Baseline vs.	
		Mean	SD	Mean	SD	Mean	SD	6 months	12 months
Uric Acid	umol/l	399	100	427	138	441	128	= 0.11	
Creatinine	mmol/l	98	20	102	23	104	23	= 0.28	
eGFR	ml/min/1.73m ²	65	10	65	14	61	10	= 0.57	

Table 70: UA and renal function in nonresponders at baseline and follow-up

Nonresponders		Time point (months)						One way ANOVA with repeated measures P value	
		0		6		12		Baseline vs.	
		Mean	SD	Mean	SD	Mean	SD	6 months	12 months
Uric Acid	umol/l	442	101	472	141	484	163	= 0.53	
Creatinine	mmol/l	106	19	108	26	114	12	= 0.34	
eGFR	ml/min/1.73m ²	61	10	60	13	58	7	= 0.61	

Figure 100: UA in responders (white) and nonresponders (black)

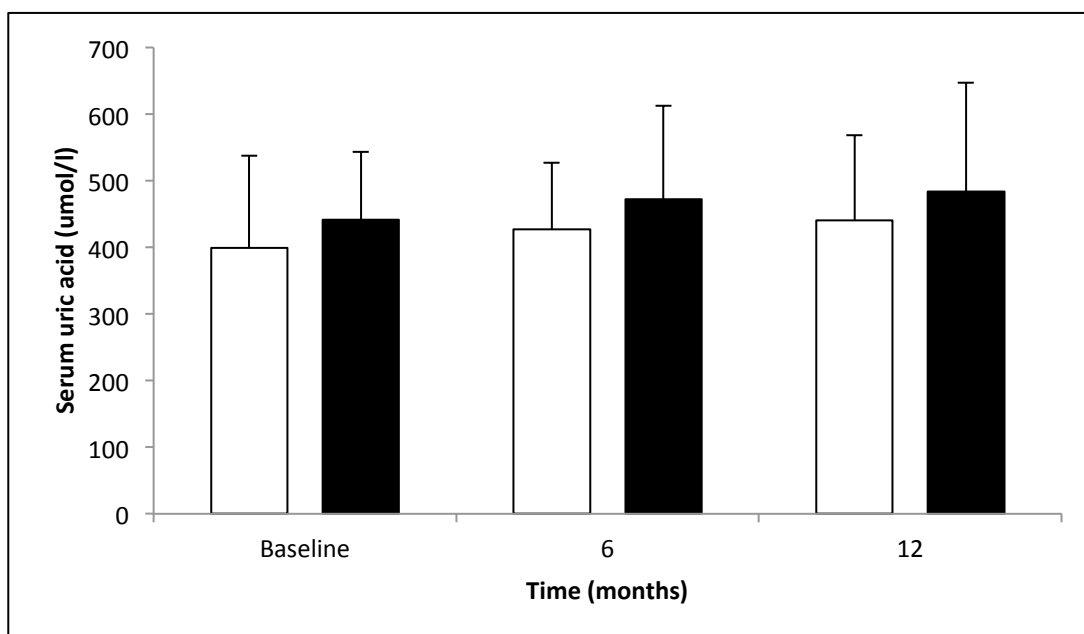


Figure 100 demonstrates the changes in serum uric acid in responders (white) and non responders (black) following CRT implantation.

There was no statistically significant difference in baseline values of UA between responders and nonresponders (table 68 and figure 100).

During subsequent follow-up, whilst there was an increase in UA in both groups, this was not statistically significant. During follow up, renal function deteriorated in both groups and the dose of diuretics prescribed fell in responders and increased in nonresponders but these differences were not significant (tables 69 and 70).

6.2.2.7 Discussion

The results demonstrate that serum UA levels measured at baseline did not differentiate between responders and nonresponders neither did UA levels change significantly following CRT. For these reasons, both the null hypotheses can be accepted and the working hypotheses rejected. Whilst lower baseline levels of serum UA were recorded for responders, levels of UA rose in a similar way in both groups during follow-up. This lack of interaction between CRT and UA was not previously known.

UA is an indirect marker of inflammation, hypoxia and cell death and so it might be reasonable to predict that improving stroke volume (and therefore cardiac output) by CRT, would lead to improvements in such a metric since, as found following heart transplant, CRT can bring about a reduction in myocardial oxygen demand and improve blood flow and therefore tissue perfusion. Similarly, nonresponders might be expected to have a more advanced HF-LVSD syndrome at baseline, demonstrating higher levels of UA, and so differentiating themselves from responders, particularly since other studies have demonstrated that UA impairs nutritive flow in HF-LVSD and since there is a significant difference between the endothelial function of responders and nonresponders at baseline. However, rather than having a direct causative role, it seems likely that the increasing level of UA is a 'fellow traveller' in the advancing HF-LVSD syndrome. In any case, changes in UA are likely to be multifactorial.

All patients had some degree of chronic renal impairment, with the average patient being in chronic kidney disease (CKD) stage 2 and with an estimated glomerular filtration rate (eGFR) 60-65ml/min/1.73m². Whilst renal function and diuretic dose were recorded in our cohort of patients, other factors, which could influence UA level such as diet, for example, were not recorded and so variations may reflect such influences. Other authors investigating HF-LVSD and UA did not comment on such variables either but simply measured weight and renal function. Asking patients to fast from midnight the day before their assessment controlled for dietary intake and fluid status. Importantly, none of the patients had a history of gout or were taking UA lowering agents.

Arora et al (2009)³⁸⁷, demonstrated that UA levels dropped from abnormal to near normal following heart transplant, with the decrease being sustained at 6 years follow-up, and levels falling higher in the subgroup of UA > 502umol/l than the < 502umol. These patients were younger (10-15 years), had a lower NT-proBNP (mean 120ng/ml) and were likely to have been physiologically fitter than this cohort. They found that hsCRP and NT-proBNP were significantly lower in the UA group < 502umol/l, supporting their hypothesis that UA is a marker of inflammation and oxidative stress, a finding which was not replicated in this study. In contrast to the work by Rinkuniene et al (2014)³⁸⁶, UA levels at baseline were not associated with echocardiographic response, however the cohort size was 4 times larger and the majority of patients had HF-LVSD of a non-ischaemic origin.

6.2.2.8 Conclusion

There is insufficient evidence, based on this study, to recommend the use of UA as either a marker or predictor of response. There is a no statistically significant difference between serum UA levels at baseline in responders and nonresponders and responders have lower levels of UA than nonresponders. Serum UA levels increased in both groups during follow up but these increases were not significant. There was, however, a statistically significant correlation between UA levels and peak VO₂. Once again, the study would need to be repeated in much larger and more heterogeneous HF-LVSD group before the results can be generalised to the HF-LVSD population as a whole.

6.2.3 Troponin T

6.2.3.1 Introduction

Elevated levels of serum troponin (Tn) are common in patients with HF-LVSD³⁸⁹ and have been shown to correlate with a worse prognosis³⁹⁰, more severe disease³⁹¹ and clinical outcomes such as cardiac transplantation³⁹². Increasing levels of Tn also correlate with an increasing risk of HF-LVSD³⁹³, with HF mortality³⁹⁴ and adverse remodelling/LV dilation³⁹⁵. Depending on the assay used and population sampled, approximately 30% of HF-LVSD patients (range 6-80%) have detectable circulating levels of Tn³⁹⁶.

6.2.3.2 Pathophysiology

Troponins are a group of proteins pivotal to the contraction of striated muscle with troponin I (TnI), troponin C (TnC) and troponin T (TnT) found in cardiac muscle. Following myocardial infarction or ischaemia, myocyte breakdown leads to release of Tn into the circulation. Serum Tn is measured in routine clinical practice to detect such myocardial injury and to diagnose conditions such as AMI. Distinct isoforms of TnT and TnI exist in skeletal (31 and 21kDa respectively) and cardiac (37 and 24kDa respectively) muscle, allowing their differentiation. Serum cardiac Tn can be elevated in other conditions, both cardiac-related e.g. pulmonary embolism and non-cardiac e.g. extreme exercise. Therefore simply measuring a rise in Tn gives no insight into the cause, as it may be due to an ischaemic cardiac event e.g. plaque thrombosis, a cardiac but not ischaemic event e.g. pulmonary embolus or an ischaemic but not cardiac event e.g. acute blood loss; hence the importance of both taking serial Tn measurements and also placing the results in a clinical context. The framework for the universal definition of myocardial infarction (table 71) is used for the interpretation of such results, based on work by Thygesen et al (2012)³⁹⁷.

6.2.3.3 Mechanism

As more sensitive and advanced assays, such as high sensitivity (hs) TnT, have been developed the threshold of detection of circulating Tn has decreased and a greater number of HF-LVSD patients have been found to have detectable levels of circulating Tn (table 72)^{389-391 393 395}. The mechanism of elevated TN in HF-LVSD is unclear, but

according to Kociol et al (2010)³⁹⁶ it is related to factors such as increased ventricular wall shear and oxidative stress, inflammation, neurohormonal activation and altered Ca²⁺ handling leading to myocyte necrosis, apoptosis, injury and hence release of Tn.

Table 71: Universal classification of myocardial infarction

Category		Type
1		Spontaneous
2		Secondary to an ischaemic imbalance
3		Resulting in death when biomarkers unavailable
4	A	Related to PCI
	B	Related to stent thrombosis
5		Related to CABG

6.2.3.4 CRT

Aarones et al (2011)³⁹⁸ published the first data suggesting that hsTnT could be used to predict response to CRT, demonstrating that patients with a baseline value of less than 15ng/ml were more likely to respond. Patients were tested at baseline and then 3, 6, and 12 months post-CRT implantation. Most were found to have abnormal hsTnT levels at baseline. No comment was made about optimisation of the devices and the patients' symptoms were assessed by NYHA functional class alone. It is notable that elevated hsTnT was more common in patients with ischaemic heart disease and transmural scar on cMR. The authors believed this reflected low-grade ongoing ischaemia or microvascular obstruction, despite the relative absence of symptoms and satisfactory revascularisation as assessed by pre-procedural angiography. Tn levels along with other variables, such as hsCRP, NYHA class, creatinine and red blood cell count, were incorporated into the HF-CRT score by Nauffal et al (2015)³⁹⁹ who demonstrated that, on multivariate analysis, patients with a Tn greater than 28ng/l at baseline were more likely to die, required an LVAD or heart transplant.

Table 72: Tn levels in heart failure and their significance

Author	Year	Troponin	Level (ng/ml)	Finding
Missov	1997	TnI	72.1±15.8	Raised Tn is common
Latinin	2007	hsTnT	> 12	Predicts severity
Peacock	2008	TnI	> 100	Predicts mortality
Sundstrom	2008	TnI	> 10	Predicts development
Fertin	2010	TnI	> 50	Predicts remodelling

6.2.3.5 Hypotheses

Working hypotheses

1) *hsTnT improves significantly in patients who are classed as responders to CRT, determined by symptoms, echocardiography, and exercise testing.*

2) *The clinical response to CRT could be predicted by hsTnT measured at baseline.*

Null hypotheses

1) *hsTnT does not improve significantly in patients who are classed as responders to CRT, determined by symptoms, echocardiography and exercise testing.*

2) *The clinical response to CRT could not be predicted by hsTnT measured at baseline.*

6.2.3.6 Method

Clotted blood samples were taken from the patients at baseline (before CRT implantation within 2 weeks) and at 6 and 12 months post CRT implantation (+/- 2 weeks) and hand-delivered to the laboratory.

The hsTnT samples were analysed by the clinical chemistry department at the SHTT using a commercially available electrochemiluminescence immunoassay (Elecsys, Roche, UK). The assay employs two monoclonal antibodies specifically directed against TNT. The antibodies recognise two troponin T epitopes at amino acid position 125-131 and 136-147. The hsTnT calibrators, contain recombinant human cardiac TnT, isolated from cell culture of E. coli BL21 containing a vector with human cardiac TnT isoform gene. After fermentation, the cells are disrupted and recombinant human cardiac TnT is then purified by ion exchange chromatography. Western blotting, immunological activity and protein content characterise purified recombinant human cardiac TnT.

In Sheffield, hsTnT test samples of 201 and 581ng/ml are run with an accuracy of 201 (± 3 SD, 1.57 CV%) pg/ml and 581 (± 10 SD, 1.73 CV%)³⁸⁸.

6.2.3.7 Results

Table 73: Baseline hsTnT in responders and nonresponders

Baseline		Responders		Nonresponders		Student's T-test
		Mean	SD	Mean	SD	p value
hsTnT	ng/l	21.1	4.5	16.0	9.6	= 0.38

Table 74: hsTnT in responders

Responders		Time point (months)						One way ANOVA with repeated measures p value	
		Baseline		6		12		Baseline vs.	
		Mean	SD	Mean	SD	Mean	SD	6 months	12 months
hsTnT	ng/l	21.1	4.5	12.9	8.0	15.2	11.8	0.53	

Table 75: hsTnT in nonresponders

Nonresponders		Time point (months)						One way ANOVA with repeated measures p value	
		Baseline		6		12		Baseline vs	
		Mean	SD	Mean	SD	Mean	SD	6 months	12 months
hsTnT	ng/l	16.0	9.6	24.7	13.8	33.9	4.5	0.25	

Figure 101: hsTnT in responders (white) and nonresponders (black)

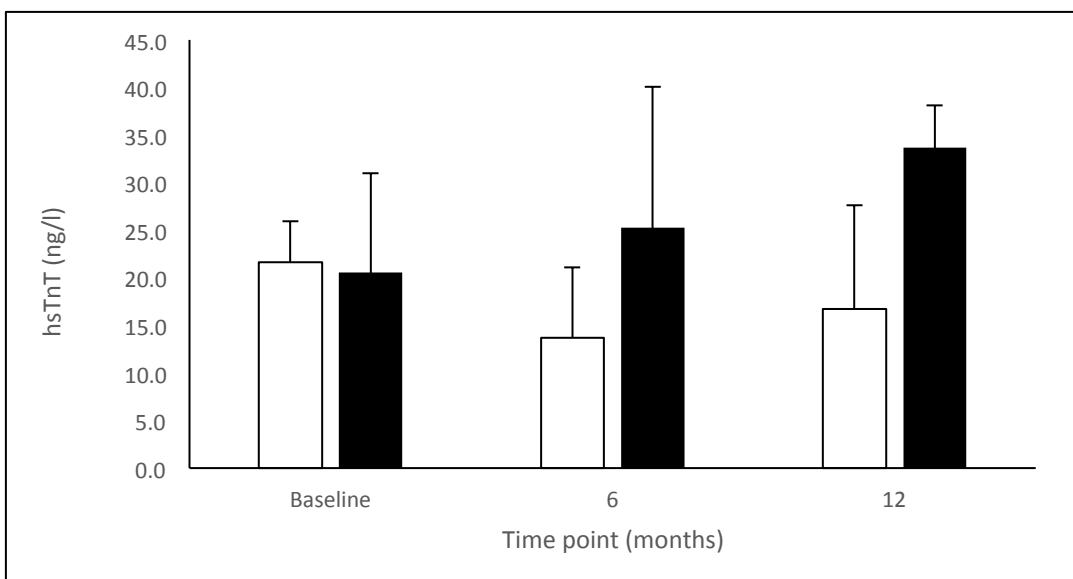


Figure 101 demonstrates the changes in high sensitivity troponin T in responders (white) and non responders (black) following CRT implantation.

There was no significant statistical difference between the groups at baseline (table 73). The decrease in serum hsTnT recorded in responders and the increase observed in nonresponders (table 74, 75 and figure 101) did not reach statistical significance.

6.2.3.8 Discussion

Based on the results of this study, there was not sufficient difference between TnT in responders and nonresponders at baseline to warrant its consideration as a predictor of CRT response. There is also no merit in using hsTnT during follow up as a marker of response, as although levels fell in CRT responders, the reductions were not statistically significant. Whilst levels of hsTnT improved over 12 months in responders they increased in nonresponders. The normal range hsTnT is 0-14ng/ml and only 50% of the patient cohort (including three responders) had an abnormal hsTnT at baseline, and so from this perspective it seems unlikely that even with larger cohort there would be significant difference. For these reasons, both null hypotheses were accepted and the working hypotheses rejected.

A significantly a larger study was carried out by Aaronson et al (2011)³⁹⁸ who recruited over 80 patients. The majority of this patient cohort had abnormal hsTnT at baseline and HF-LVSD of an ischaemic origin. Interestingly, in contrast to the present study, the responders were found to have lower values of hsTnT at baseline, denoting possibly, a less severe HF-LVSD syndrome. The nonresponders in that study had a lower LVEF and higher NT-proBNP at baseline suggesting the lack of response might be multifactorial furthermore hsTnT levels were not repeated to what influence CRT had on cardiac remodelling. The authors made no comment as to why responders had lower circulating levels of hsTnT at baseline, although it is known that patients with non-ischaemic HF-LVSD are more likely to respond to CRT. Our cohort comprised 50% patients with HF-LVSD of ischaemic origin but no difference was observed between the groups.

There was no significant difference in renal function or haemoglobin and none of the patients had a clinical decompensation or myocardial infarction during 12 months follow-up, which might have led to confounding influence. As there was no control group and there is always the possibility that, because HF-LVSD is a naturally fluctuant condition with a variable course, as for natriuretic peptides, hsTnT may vary significantly even without intervention such as CRT. Attempts to minimise this included taking the sample fasted, pre-medication and pre-exercise at the same time each assessment.

It is important to note that none of the patients with elevated hsTnT had symptoms, signs or an ECG indicative of AMI and all completed CPET to exhaustion without any sustained ill effects. None of the patients had an AMI or clinical decompensation in the intervening periods between follow-up assessments; TnT levels can take days to fall and so assessment shortly after a decompensation could lead to over-estimation of hsTnT.

6.2.3.9 Conclusion

It can be concluded that, although hsTnT was found to be higher at baseline in responders and improved at follow up and was found to be lower at baseline in nonresponders and then deteriorated. However, since the measured differences were not significant it would be inappropriate to advocate use of hsTnT as either a predictor or a marker of CRT response.

6.2.4 Brain Natriuretic Peptide

6.2.4.1 Introduction

Brain natriuretic peptide (BNP) is a 32 amino acid polypeptide, which is primarily released by the ventricular myocardium in response to stretch. Increase wall stretch is typically associated volume overloaded states such as HF-LVSD. Measurement of serum BNP is used in the clinical diagnosis of all causes of HF, particularly where there is limited or delayed access to echocardiography, and helps the clinician to differentiate from other conditions that can cause breathlessness, such as pneumonia. Normal levels are BNP < 100pg/ml and N-terminal pro-BNP (NT proBNP) < 400pg/ml.

6.2.4.2 Pathophysiology

BNP acts to increase natriuresis and diuresis and to reduce renin and systemic vascular resistance by a combination of arterial and venous dilation. This reduces circulating blood volume, volume overload and concomitant stretch on the poorly functioning myocardium, restoring fluid homeostasis. The role of BNP in the diagnosis of HF is clear, but what remains unclear, is its potential use in monitoring or, indeed, predicting response to therapy.

6.2.4.3 CRT

Several papers have investigated the relationship between CRT and BNP, but only one has specifically considered prediction of response (see table 76). Delgado et al (2006)⁴⁰⁰ studied a cohort of 70 patients, assessment of response was based upon symptomatic NYHA class and follow-up was restricted to 3 months. This study demonstrated that the responder group had lower mean BNP at baseline and this decreased during follow-up. In contrast, for the nonresponder group, BNP it was higher at baseline and increased at follow-up. This finding is significant as it suggests that nonresponders have more severe heart failure, as higher levels of BNP correlate with more severe HF-LVSD. Whilst patients can feel 'better' and have haemodynamic improvements immediately following CRT implantation, the large RCTs have followed up patients at 6 or 12 months looking for response and used an objective measure of symptoms e.g. MLWHFQ, CPET or echocardiographic evidence of remodelling. In comparison the study by Delgado, using a notion of 'response' based purely on NYHA

class at 3 months is short-term and lacks rigour. Kubanek et al (2006)⁴⁰¹ after studying a whole range of biomarkers, found that reduction in BNP at 3 months post-CRT, was the strongest predictor of response to CRT at 24 months, with responders demonstrating reductions in BNP by 40% as opposed to increasing by 27% in nonresponders at 3 months. More recently, a number of studies have concluded that BNP and NT-proBNP retain their prognostic significance in this HF-LVSD patients receiving CRT and that there is significant reduction in responders, however none of these investigated whether a baseline natriuretic peptide level could be used to predict response during follow-up⁴⁰²⁻⁴⁰⁴. Elevated BNP (> 440pg/ml), in combination with detectable hsTNT, NHYA functional class, LVEF and QRSd during multivariate Cox regression, were found by Shalaby et al (2015)⁴⁰⁵ to be predictive of worse outcomes following CRT-D implantation at 12 months.

6.2.4.4 Mechanism

It makes sense that BNP levels fall in those who improve symptomatically with CRT, as this denotes a reduction in LV volume overload and suggests that some degree of ventricular reverse remodelling has occurred. In addition, a higher level of BNP at baseline might suggest the patient has more severe HF, with more to gain from CRT, and so is more likely to respond.

Table 76: NP's in HF and CRT and their significance

Author	Year	Natriuretic peptide	Level (pg/ml)	Finding
Pitazlis	2005	BNP	> 91.5	Predicts morbidity at 1 month
Fruhwald	2006	NT-proBNP	~537	Lower at 18 months vs controls
El-Saed	2009	BNP	> 492	Predicts mortality at 2 years
Berger	2009	NT-proBNP	> 1814	Predicts mortality at 4 years

6.2.4.5 Hypotheses

Working hypotheses –

1) NT-proBNP improves significantly in patients who are classed as responders to CRT, determined by symptoms, echocardiography and exercise testing.

2) The clinical response to CRT can be predicted by baseline measures of NT-proBNP.

Null hypotheses –

1) NT-proBNP does not improve significantly in patients who are classed as responders to CRT, determined by symptoms, echocardiography and exercise testing.

2) The clinical response to CRT cannot be predicted by baseline measures of NT-proBNP.

6.2.4.6 Methods

A blood sample was taken at baseline (before CRT implantation within 2 weeks) and at 6 and 12 months post CRT implantation (+/- 2 weeks) and using a tube containing ethylenediaminetetraacetic acid (EDTA) to prevent clotting.

NT-proBNP was analysed in the clinical chemistry department at STHT using a commercially available electrochemiluminescence immunoassay (Elecsys proBNP II, Roche, UK) containing 2 monoclonal antibodies specific to epitopes on the on N-terminal part of BNP (1-76). In Sheffield, test samples of 136.00pg/ml, 350.03 and 3729.93pg/ml are run with an accuracy of 136.00 (± 1.98 SD, 1.54 CV%) pg/ml, 350.03 (± 11.02 SD, 3.15 CV%) pg/ml and 3729.93(± 72.81 , 1.95 CV%)³⁸⁸.

6.2.4.7 Results

Table 77: NT-proBNP level in responders and nonresponders

Baseline		Responders		Nonresponders		Student's T-test P value
		Mean	SD	Mean	SD	
NT-proBNP	pg/ml	2251.64	901.25	1525.40	312.36	0.54

Table 78: NT-proBNP levels in responders

Responders		Time point (months)						One way ANOVA with repeated measures p value	
		0		6		12		Baseline vs 6 months	Baseline vs 12 months
		Mean	SD	Mean	SD	Mean	SD		
NT-proBNP	pg/ml	2251.64	901.25	1840.43	768.48	1732.08	976.14	= 0.17	

Table 79: NT-proBNP levels in nonresponders

Non responders		Time point (months)						One way ANOVA with repeated measures p value	
		0		6		12		Baseline vs 6 months	Baseline vs 12 months
		Mean	SD	Mean	SD	Mean	SD		
NT-proBNP	pg/ml	1525.40	312.36	1399.20	783.09	1066.20	426.73	= 0.65	

Figure 102: NT-proBNP levels in responders (white) and nonresponders (black)

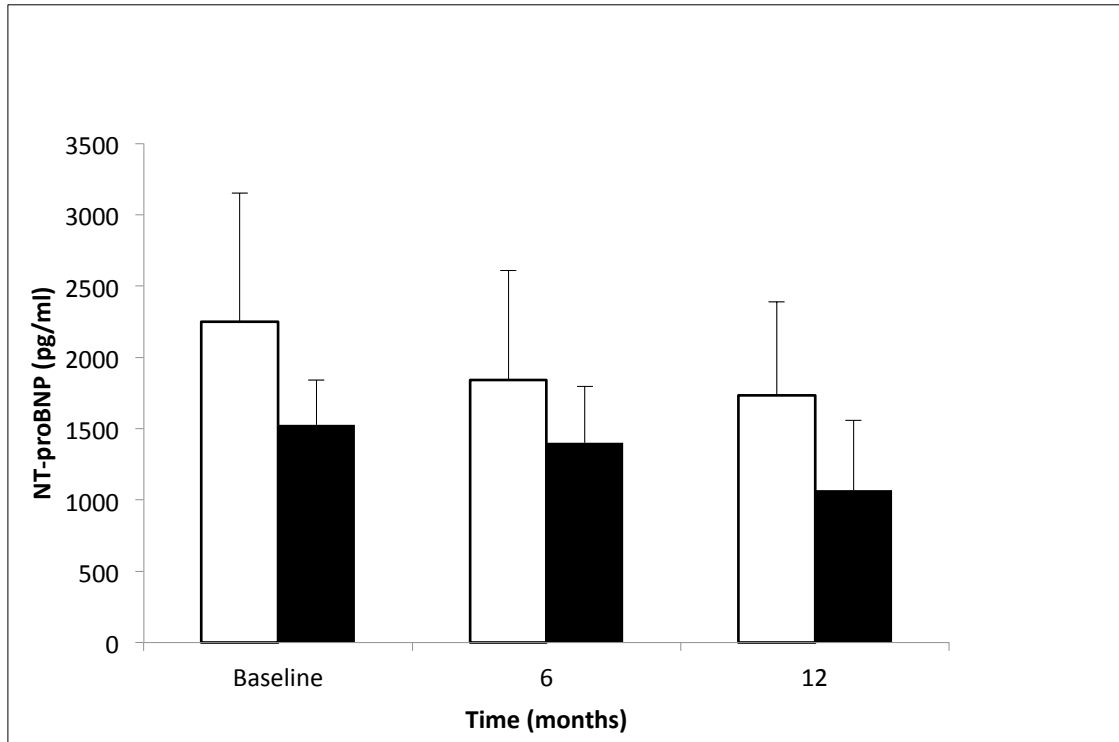


Figure 102 demonstrates the changes in NT-proBNP in responders (white) and non responders (black) following CRT implantation.

The difference in NT-proBNP baseline between responders and nonresponders was not statistically significant (table 77).

During follow up, the decreases in NT-proBNP in responders at 6 and at 12 months were not statistically significant (table 78 and figure 102). Likewise, whilst levels of NT-proBNP for nonresponders also decreased at both 6 and at 12 months, this was not statistically significant (table 79 and figure 102).

From the above data, it is clear that the first working hypothesis can be rejected and null hypothesis that there is no significant difference between responders and nonresponders to CRT in NT-proBNP levels at baseline can be accepted. The second working hypothesis can be rejected and null hypothesis that NT-proBNP does not

improve significantly in patients who are classed as responders to CRT, determined by symptoms, echocardiography and CPET testing.

6.2.4.8 Discussion

The results show that whilst there is not a sufficient difference between responders and nonresponders at baseline to warrant the introduction of NT-proBNP as a screening tool to predict CRT response, as indeed non-responders appeared to have a lower NT-proBNP than responders, there also appears to be no merit in using NT-proBNP during follow up as a marker of response. NT-proBNP did not improve statistically significantly in responders. For some responders it took 12 months to achieve a change in NT-proBNP, defined as > 10% reduction but some nonresponders also achieved a > 10% reduction in NT-proBNP at 6 months, which was sustained at 12 months despite a lack of improvement in other markers of response. The reason behind such a reduction, albeit non-significant reduction following CRT implantation may be due to a combination of acute haemodynamic improvements and chronic reduction in functional mitral regurgitation, LV filling pressures and LV volumes and improved cardiac synchrony and energetics. Following the large initial reduction at 6 months in responders, but only a smaller reduction at 12 months, it appears that the reduction in NT-proBNP maybe a measure of the stimulus to remodel but not of the remodelling process itself ⁴⁰³.

Despite the patients being a homogenous group with respect to the severity of their disease e.g. NYHA class III and appearing similar in terms of markers of response prior to CRT, they had a wide spread of NT-proBNP levels at baseline. Comparing our data to that from the large CRT trials, in the CARE-HF study ⁴⁴, a NT-proBNP level < 214.5 pg/ml were more likely to benefit from CRT, adding to the earlier notion that it is patients with milder HF-LVSD that are more likely to respond to CRT. Importantly, the CARE-HF trial used the same inclusion criteria as this study. Fruhwald et al (2007) ⁴⁰³ conducted an analysis of the CARE-HF cohort and reported that the mean level of NT-proBNP at baseline was approximately 2000 pg/ml with a significant difference between the CRT and control groups, with the CRT group having NT-proBNP levels some 537 and 567 pg/ml lower than the controls at 3 and 18 months, respectively.

In the MIRACLE ICD trial ⁴⁹, patients implanted with CRT had a median change in BNP of 68 pg/ml compared to controls at 6 months, thus contradicting the findings of the CARE-HF study that CRT leads to significant improvements in natriuretic peptides, albeit in a much smaller cohort. However, no baseline value of BNP is reported and the difference at 6 months was not statistically different to that found after medical therapy. Finally the MIRACLE ICD II trial ¹⁵⁶, showed that patients suitable for CRT had mean NT-proBNP levels of approximately 600pg/ml at baseline, which improved by 200pg/ml in CRT group but this change was not statistically significant. However, that trial included only mildly symptomatic HF-LVSD patients albeit of similar ages, QRSd and EF% as the patients in our study, perhaps accounting for the lower natriuretic peptides at baseline.

Another study, with a similar cohort to our current study (NYHA III, QRSd >150ms, LVEF < 35%) found that NT-proBNP was 3200 pg/ml in all patients at baseline, with no significant difference between either group, but at 6 months following CRT this had reduced to < 2000 pg/ml in responders but unchanged in nonresponders ⁴⁰⁶.

Thus it can be seen that our data fits with the literature, namely that there are no significant differences between responders and nonresponders to CRT at baseline (although there is a trend for lower BNP in responders, not found in this work) but there is a reduction in BNP during follow-up in responders, but which in this work, was not statistically significant.

What was not detailed in any of these trials, is the average time that patients suffered from HF-LVSD before receiving CRT or, as mentioned already, the level of comorbidity experienced by these patients. This cohort of 19 patients is representative of HF-LVSD patients in general and each has an average of 5 comorbidities, in addition to HF-LVSD. The question remains as to what influence such comorbidity has on natriuretic peptides, if deterioration in such comorbidities negates any gains from CRT as measured by NT-proBNP and whether such comorbidity has an additive effect.

Sinha et al (2003)⁴⁰⁷ found that turning CRT off led to increases in BNP and deterioration in symptoms. This was rapidly reversed on reinstating the CRT.

Improvements in BNP correlated with improvements in LVEDV thus supporting the notion that BNP is a valid, albeit surrogate marker of response to CRT and can be used to monitor efficacy of CRT post implantation.

The half-life of NT-proBNP is of the order of hours, whilst that of BNP is around half an hour, and as HF-LVSD is a naturally variable condition, with fluid states fluctuating, this infers that for patients with severe HF-LVSD that even taking diuretics or having a large drink may influence NT-proBNP levels. To attempt to mitigate against these confounders, the blood samples were taken first thing in the morning, before food, fluids, exertion or medications.

6.2.4.9 Conclusion

In general, this data fits with the literature, in that there was no significant difference between responders and nonresponders to CRT at baseline but also there was no statistically significant reduction in NT-proBNP at follow-up in responders. This suggests that NT-proBNP shouldn't, be used as a marker of response for patients following CRT, in conjunction with other markers such as peak VO_2 , LVEDV and MLWHFQ, on the basis of this work. The lack of significant difference at baseline rules out the use of NT-proBNP as a predictor of response at least in the context of the present study.

6.2.5 Parathyroid Hormone/Vitamin D

6.2.5.1 Introduction

Elevated levels of circulating parathyroid hormone (PTH), i.e. hyperparathyroidism, are associated with the cause⁴⁰⁸, development⁴⁰⁹ and risk of hospitalisation of patients with HF-LVSD independent of conventional HF risk factors and those influencing mineral metabolism, such as Vitamin D (VitD). PTH is also an independent marker of morbidity⁴¹⁰ and mortality⁴¹¹ in HF-LVSD. Furthermore, since there is a significant and positive correlation between PTH and peak VO_2 ⁴¹² and between PTH and FMD in HF-LVSD⁴¹³, PTH levels might be expected to mirror improvements in CPET and FMD following an intervention such as CRT.

VitD deficiency (hypovitaminosis D < 50nmol/l) is common in HF with some studies indicating that over 90% of patients are VitD deficient (in comparison to an estimated 15% of the normal population), furthermore VitD levels are negatively correlated with functional class, LVEF⁴¹⁴, 6MWT⁴¹⁵ and VO₂⁴¹⁶ and are predictor of mortality^{417 418}. The evidence as to whether VitD supplementation improves morbidity in the presence of deficiency in HF-LVSD is mixed^{419 420}. Indeed in patients without HF-LVSD, VitD deficiency is usually accompanied by a reduction in exercise capacity and muscle strength.

6.2.5.2 Pathophysiology

Parathyroid hormone or parathormone is an 84 polypeptide endocrine hormone which circulates in the blood both as active, intact PTH and as inactive C and N terminal fragments. PTH is secreted by the parathyroid glands in response to low circulating levels of either Calcium (Ca²⁺) or Magnesium (Mg²⁺). Secretion is inhibited by high circulating levels of Ca²⁺ and, paradoxically, by very low levels of Mg²⁺. Release of PTH indirectly stimulates osteoclasts within bone, which in turn increases bone turnover, raising serum Ca²⁺ levels, which via negative feedback reduces secretion of PTH. PTH also acts to reduce the resorption of phosphate (PO₄²⁻) by the kidney in the distal tubules and renal collecting ducts, lowering serum PO₄²⁻, which increases the amount of ionised serum Ca²⁺ as less Phosphate ions are available to form water-insoluble salts with calcium. PTH increases the activity of the 1- α -hydroxylase enzyme, which converts 25-hydroxycholecalciferol (calcidiol) from the liver to 1,25-dihydroxycholecalciferol (calcitriol) from the kidney to the active form of VitD, which amongst other roles, increases the absorption of Ca²⁺ by the intestine.

The normal reference range of serum PTH is 15-65pg/ml with elevated levels (> 65pg/ml) found in HF-LVSD (table 80)^{70 408 410 411 421}. Elevated levels of PTH are classified into 3 categories as detailed below, based on the underpinning pathology and associated calcium levels.

- Primary – the cause originates within the parathyroid gland e.g. hyperplasia or malignancy and so the Ca²⁺ level will be elevated appropriately.
- Secondary – the cause originates outside of the parathyroid gland. For example, in chronic renal failure (CRF), reduced calcitriol production leads to

chronic hypocalcaemia. Typically Ca^{2+} level is normal (normocalcaemic) due to appropriately elevated PTH. Secondary hyperparathyroidism is the form found in HF-LVSD.

- Tertiary - prolonged secondary hyperparathyroidism leads to unregulated and excess PTH production, typically found in end-stage CRF and the Ca^{2+} level is low. VitD is a fat-soluble essential vitamin obtained from dietary sources such as dairy produce or synthesised from cholesterol during skin exposure to direct sunlight and acts as a steroid hormone in the body. The form ingested or synthesised is termed cholecalciferol, in the liver this is hydroxylated into 25-hydroxycholecalciferol (the form of VitD measured by blood tests) and in the kidney further hydroxylated to 1,25-hydroxycholecalciferol (the biologically active form of VitD). This latter form acts to increase uptake of Ca^{2+} from the gut. The role of VitD deficiency in HF-LVSD remains unclear, although several mechanisms have been postulated including gene expression, cytokine up regulation or activation of the renin-angiotensin-aldosterone system (RAAS) ⁴²².

6.2.5.3 Mechanism

The causal link between PTH and HF-LVSD is unclear, according to Hagstrom et al (2006)⁴⁰⁸, the interplay between PTH and the heart is clear was it “directly affects cardiac function, increasing heart rate and coronary blood flow and altering the automaticity of the heart” but Sugimoto et al (2009)⁷⁰ suggests a more distinct role in HF-LVSD, as PTH “promote vascular pathology leading to atherosclerosis and ischaemic HF but also distinct cardiac pathology, such as myocardial calcification, fibrosis, and hypertrophy, that could lead to non-ischaemic HF”. Hypothetically, it could also be related to the cardio-renal syndrome with reduced activity 25-hydroxyvitamin D3 1-alpha-hydroxylase, but PTH dysfunction in primary renal disease is secondary to hypocalcaemia and not normocalcaemia. Most recently, Sugimoto et al (2013)⁴²³ investigated the interrelationship between PTH and haemodynamic state in HF-LVSD, finding that increased PCWP and stroke volume index (SVI) correlated, positively and negatively respectively with circulating levels of intact PTH. By extension, one might expect patients who respond positively to CRT will be found to have lower PTH during follow-up.

Table 80: PTH levels found in HF

Author	Year	PTH level (pg/ml)	Conclusion in HF
Giannakoulas	2006	> 89	Predicts reduced exercise capacity
Sugimoto	2009	> 47	Predicts hospitalisation
Hagstrom	2010	> 5.23	Predicts development
Schierbeck	2011	> 5.0	Predicts mortality
Altay	2011	> 96.4	Predicts severity

6.2.5.4 CRT

It might be expected that in responders to CRT there was a progressive improvement in PTH or VitD levels from baseline to the onset of response, if indeed PTH or VitD reflect exercise capacity, endothelial function improvement as a consequence of CRT.

6.2.5.5 Hypotheses

Working hypotheses –

1) *PTH and/or VitD improve significantly in patients who are classed as responders to CRT, determined by symptoms, echocardiography and exercise testing.*

2) *Clinical response to CRT can be predicted by baseline measures of PTH and/or VitD.*

Null hypotheses –

1) *PTH and/or VitD does not improve significantly in patients who are classed as responders to CRT, determined by symptoms, echocardiography and exercise testing.*

2) *Clinical response to CRT cannot be predicted by baseline measures of PTH and/or VitD.*

6.2.5.6 Methods

All patients had bloods taken at baseline, in a clotted blood tube, for analysis of PTH, Ca²⁺, Mg²⁺, VitD, albumin, alkaline phosphatase (ALP), renal function (urea, creatinine, sodium, potassium and eGFR) and PO₄²⁻ with repeat bloods taken at 6 and 12 months

post CRT implantation. PTH samples were analysed at the clinical chemistry department at the NGH, using an electrochemiluminescence immunoassay (Elecsys, Roche, UK). The assay for PTH employs a monoclonal antibody which reacts with the N-terminal fragment and a monoclonal antibody labelled with a ruthenium complex reacts with the C-terminal fragment of PTH. The antibodies used in this assay are reactive with amino acid epitopes on the PTH fragments. Two monoclonal PTH-specific antibodies form a sandwich complex, after addition of microparticles the complex becomes bound to the solid phase. The microparticles are magnetically captured onto the surface of an electrode. Unbound substances are then removed and an applied voltage induces chemiluminescent emission which can be measured by a photomultiplier. The lab analysing the results were blinded to the outcomes of the Grand Challenge patients, so as not to influence them. Test samples of 22.5, 157 and 475 pg/ml are run with an accuracy of 22.5 pg/ml ($0.35 \pm \text{SD}$, 1.58 CV%), 157 pg/ml ($1.14 \pm \text{SD}$, 0.73 CV%) and 475 pg/ml ($3.97 \pm \text{SD}$, 0.84 CV%)³⁸⁸. The VitD samples were analysed according to a commercially available chemiluminescence method (IS2700, immunodiagnostic systems, UK); a specific antibody to 25-hydroxycholecalciferol labelled with acridinium is added, magnetic particles linked to 25-hydroxycholecalciferol are then added and 'captured' using a magnet. The light emitted by the acridinium label is inversely proportional to the concentration of 25-hydroxycholecalciferol in the sample. In Sheffield, test samples of 33, 88 and 185 nmol/l are run with an accuracy of 33 nmol/l ($3.4 \pm \text{SD}$, 10.4 CV%), 88 nmol/l ($7.9 \pm \text{SD}$, 8.9 CV%) and 185 nmol/l ($8.2 \pm \text{SD}$, 4.4 CV%)³⁸⁸.

6.2.5.7 Results

Table 81: Calcium metabolism of responders and nonresponders at baseline

Calcium metabolism at baseline						
Test	unit	Responders		Nonresponders		Students T-Test
		Mean	SD	Mean	SD	P value
Calcium	mmol/l	2.32	0.06	2.38	0.13	= 0.22
Magnesium	mmol/l	0.87	0.16	0.87	0.14	= 0.25
Phosphate	mmol/l	1.07	0.06	0.95	0.14	= 0.15
Albumin	g/l	44.3	3.9	43.8	2.9	= 0.67
ALP	IU/l	68.0	19.4	97.6	66.8	= 0.21
PTH	ng/l	76.1	37.4	73.5	37.8	= 0.47
VitD	nmol/l	44.6	32.6	51.8	17.9	= 0.20

Table 82: Calcium metabolism of responders at baseline and follow-up

Responders		Time point (months)						One way ANOVA with repeated measures <i>p</i> value	
Test	unit	Baseline		6		12		Baseline vs 6	Baseline vs 12
		Mean	SD	Mean	SD	Mean	SD	P value	P value
Calcium	mmol/l	2.32	0.06	2.29	0.09	2.29	0.07	= 0.27	
Magnesium	mmol/l	0.87	0.16	0.87	0.05	0.88	0.06	= 0.88	
Phosphate	mmol/l	1.07	0.06	0.96	0.17	1.03	0.18	= 0.41	
Albumin	g/l	44.3	3.9	45.8	4.6	43.5	4.0	= 0.07	
ALP	IU/l	68.0	19.4	62.6	14.7	59.5	16.1	= 0.24	
PTH	ng/l	76.1	37.4	76.4	39.3	97.0	51.0	= 0.50	
VitD	nmol/l	44.6	32.6	70.7	28.3	45.7	20.7	= 0.45	

Table 83: Calcium metabolism of nonresponders at baseline and follow-up

Non Responders		Time point (months)						One way ANOVA with repeated measures <i>p</i> value	
Test	unit	Baseline		6		12		Baseline vs 6	Baseline vs 12
		Mean	SD	Mean	SD	Mean	SD	P value	P value
Calcium	mmol/l	2.38	0.13	2.29	0.14	2.35	0.06	= 0.78	
Magnesium	mmol/l	0.87	0.14	0.87	0.21	0.88	0.18	= 0.88	
Phosphate	mmol/l	0.95	0.14	0.89	0.16	0.79	0.13	= 0.76	
Albumin	g/l	43.8	2.9	39.9	2.7	44.8	2.5	= 0.52	
ALP	IU/l	97.6	66.8	83.7	55.3	75.7	25.0	= 0.59	
PTH	ng/l	73.5	37.8	85.6	41.8	72.8	24.1	= 0.69	
VitD	nmol/l	51.8	17.9	38.6	22.2	40.8	19.4	= 0.50	

Figure 103: Serum PTH in responders (white) and nonresponders (black)

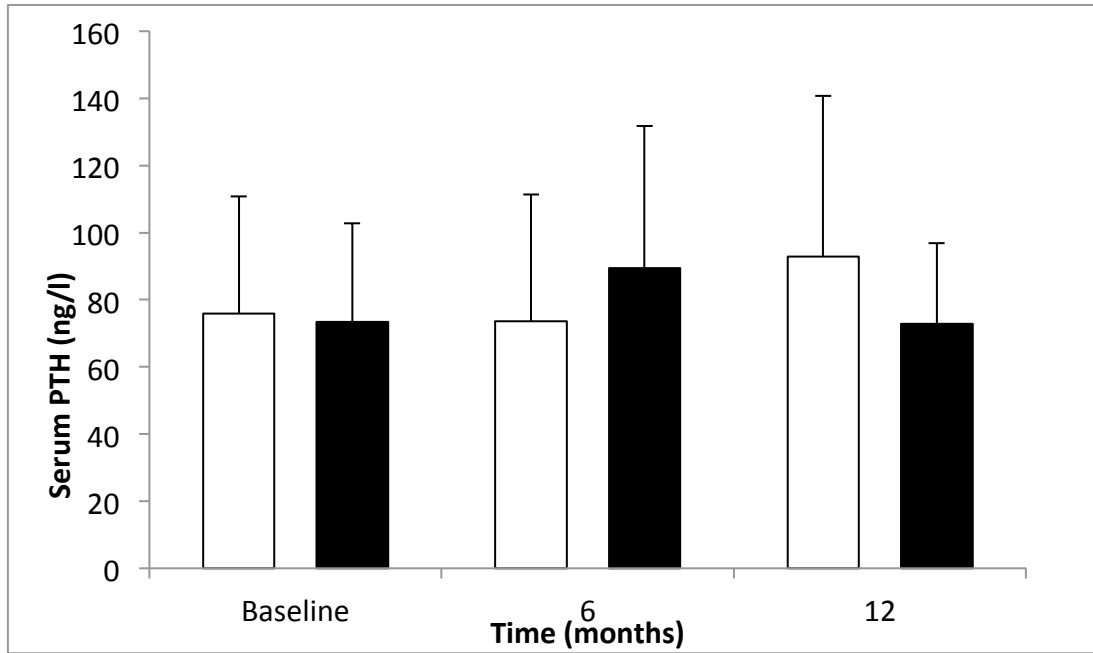


Figure 103 demonstrates the changes in PTH in responders (white) and non responders (black) following CRT implantation.

Figure 104: Serum Vitamin D in responders (white) and nonresponders (black)

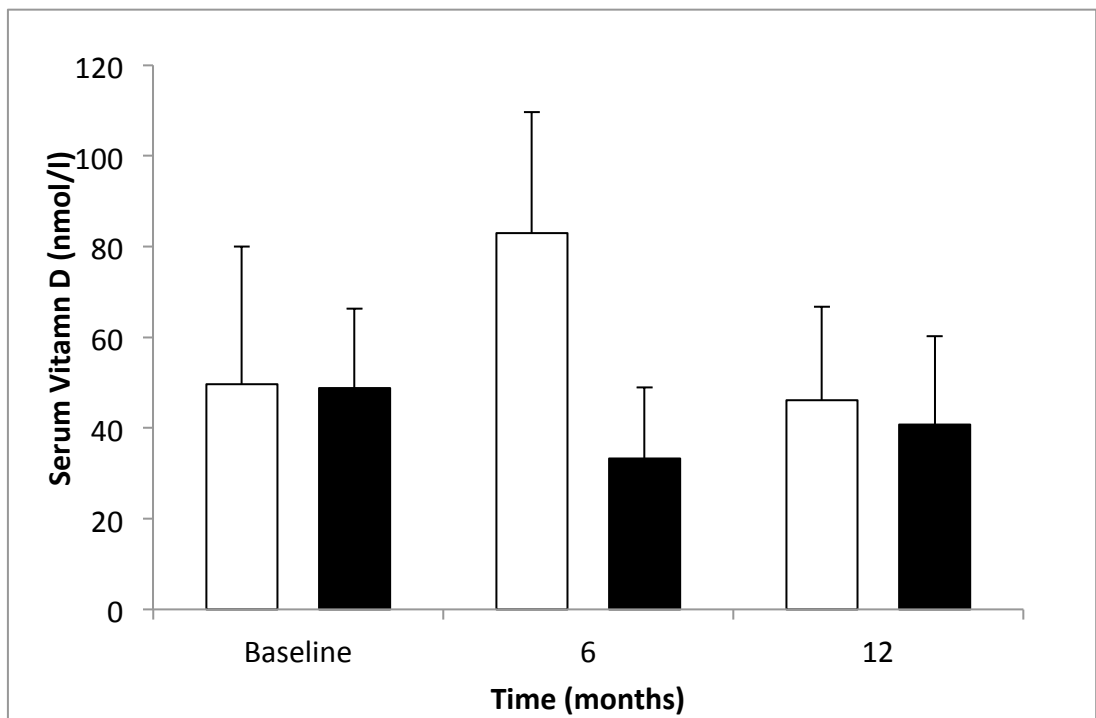


Figure 104 demonstrates the changes in serum vitamin D in responders (white) and non responders (black) following CRT implantation.

There was no significant difference at baseline between responders and nonresponders with respect to any marker of calcium metabolism, although responders had lower serum VitD levels and better renal and liver function (see table 81, figure 103 and 104). During follow-up, the responders showed increases in PTH, ALP, creatinine and VitD, but these were not significant (see table 82, figure 103 and 104). The nonresponders demonstrated increased PTH, creatinine and decreased VitD during follow-up but again these changes did not reach statistical significance (see table 83, figure 103 and 104).

Hence the data collected does not support the working hypotheses that PTH and VitD improve significantly in patients who are classed as responders to CRT, determined by symptoms, echocardiography and CPET testing or that clinical response to CRT can be predicted by baseline measures of PTH and VitD and so both the null hypotheses were accepted.

6.2.5.8 Discussion

As no significant differences were detected in baseline levels between responders and nonresponders the current work does not support the use of PTH or VitD as a predictor response to CRT. Moreover, in the absence of significant differences in either PTH or VitD at follow up they cannot be used as markers of response.

This study demonstrates, improvement in VitD levels following CRT in responders and deterioration in nonresponders at 6 months, which then appeared to return to baseline at 12 months. This suggests the possible influence of cardiac function, albeit indirectly, upon endocrine function in a HF-LVSD population, independent of changes in calcium, phosphate and magnesium and of liver and renal function. Furthermore, whilst the differences in VitD were not significant at baseline, those with lower levels appeared more likely to respond.

Patients were recruited over a 12-month period and analysis of recruitment indicates that 25% of each group were recruited in each of the 4 seasons and lived an average of 16 ± 14 miles (26 ± 22 km) from Sheffield. This rules out differences in latitude,

weather or sun exposure in influencing VitD levels. Liver function, renal function and diuretic dose remained stable over the 12-month period for all patients and so these can also be excluded as possible confounding factors. Dietary measures of VitD, calcium or phosphate which may have influenced the blood results, despite samples being taken fasted, were not recorded (using a food diary, for example).

VitD deficiency in HF is likely to have a multifactorial origin, due to factors such as age, inactivity and also chronic disease. Possible mechanisms for such differences in VitD status in the two patient groups and also subsequent improvements, may well relate to increased outdoor activity in responders and deterioration in nonresponders. CRT is known to reduce inflammation and so may also modulate cytokine release and down regulate VitD metabolism⁴²⁴. This could provide a mechanism for the changes seen. Last but not least, improvement of cardiac function leads to down-regulation of the RAAS and since VitD is a modulator of renin, this may also influence VitD metabolism^{423 425}. This remains to be established since none of the papers cited above addressed whether improved cardiac function leads to improvement in impaired endocrine function.

In keeping with other trials investigating PTH and VitD in HF-LVSD, more than 50% of this cohort had low VitD (< 50nmol/l) and 75% had abnormally high PTH levels (> 65ng/l). Other non-interventional trials, have demonstrated that, for HF-LVSD patients, VitD deficiency is associated with a poorer prognosis at follow-up.

In the present study, it was perhaps surprising that no differences were found in PTH levels between the groups at baseline, nor changes within the groups during follow-up. Recent evidence has shown that PTH levels, even within the normal range, reflect the haemodynamic state of patients with HF⁴²³, according to pulmonary capillary wedge pressure but in the context of secondary hyperparathyroidism due to HF, it is unclear what the relationship will be between PTH and haemodynamics.

VitD supplementation could be considered in both responders and nonresponders to CRT who were deficient to investigate whether this could improve response. The fact that the patients had normal Ca²⁺ and ALP levels indicates that the

hyperparathyroidism in these patients is secondary to chronic disease and not disease of the parathyroid gland *per se*. It would also be interesting to investigate patients with low VitD, following CRT to see if any in VitD levels are met with increases in peripheral muscle function or bone mass⁴¹⁹.

6.2.5.9 Conclusion

There was no significant difference in baseline levels either PTH or VitD between responders and nonresponders and, hence these results do not support the use of either PTH or VitD as a predictor of response. Similarly, whilst there were detectable changes during follow-up, these differences were neither sustained nor large enough to be considered as markers of response. It would be interesting to investigate whether supplementing VitD in nonresponders or responders would increase either the number of responders or the degree of clinical response.

6.2.6 High sensitivity C-Reactive Peptide

6.2.6.1 Introduction

C-reactive protein (CRP) is elevated in HF-LVSD and it is an independent prognostic marker of morbidity⁴²⁶ and mortality⁴²⁷. Furthermore it correlates with the development⁴²⁸, functional class⁴²⁹, symptoms⁴³⁰ and further myocardial injury in HF⁴³¹.

6.2.6.2 Pathophysiology

Any inflammatory insult, such as infection, arthritis, ischaemia or malignancy, leads to the recruitment of the non-specific and innate immune system, and this is known as the acute phase response. At the area local to the insult, cytokines such as interleukins (IL) and tumour necrosis factor (TNF) are released from inflammatory cells, which stimulate the liver to produce a number of substances known as acute phase reactants such as fibrinogen, ferritin, serum amyloid A and CRP. These have wide-ranging effects on coagulation, vascular permeability and the immune system. In particular, CRP acts by binding to phosphocholine on the cell membrane of necrotic and apoptotic cells, which in turn activates the complement system via the C1Q complex, facilitating cell opsonisation, lysis and chemotaxis and so facilitating the removal of the dying cells.

Clinically CRP is used as diagnostic aid in cases of uncertainty (for unknown causes of breathlessness, for example) and for monitoring the response to a treatment e.g. anti-inflammatories. Other commonly used, but indirect measures of the acute phase response include plasma viscosity (PV) and the erythrocyte sedimentation rate (ESR). Increasingly CRP has been recognised as having a role in IHD and latterly HF (see table 84)^{83 424 426 430 432}. In a seminal paper by Ridker et al (1997)⁴³³, elevated levels of CRP were demonstrated to be predictive of the future risk of MI, independent of lipid levels or other risk factors such as smoking.

Table 84: Typical values of CRP in HF

Author	Year	CRP (mg/ml)	Level	Conclusion in HF
Alonso-Martinez	2002	hsCRP	> 5.5	Predicts symptoms
Vasan	2003	CRP	> 5	Predicts development
Yin	2004	hsCRP	> 5.7	Predicts morbidity
Shinohara	2011	CRP	> 7.4	Predicts CRT response
Johansson	2011	CRP	> 2.4	Predicts low mood

6.2.6.3 Mechanism

Elevated CRP levels in cardiovascular disease have been found to improve with cholesterol lowering agents e.g. Rosuvastatin⁴³⁴ and β -blocker therapy⁴³⁵ e.g. Carvedilol and it is believed these agents may have an anti-inflammatory action. As HF-LVSD and its causes, such as atherosclerosis, are inflammatory in origin and thus it makes sense that a treatment that improves HF-LVSD may improve markers of inflammation. However there are many other markers of inflammation other than CRP and many other causes of an elevated CRP other than HF, also inflammatory conditions often coexist. CRT has been shown to improve FMD, a surrogate measure of endothelial function and also systemic inflammation³²². One of the problems with early CRP research, alluded to by Yin et al (2004)⁸³ was that “the mildly elevated CRP concentrations in these patients fall well within the range in healthy subjects, and standard clinical assays for CRP lack sensitivity within the low reference range and thus cannot be used effectively for risk prediction. Because inexpensive commercial assays for high-sensitivity CRP (hsCRP) are now available, the potential for the hsCRP assay to enhance the prognostic and therapeutic capabilities is of considerable interest, but its value has not been fully established”.

6.2.6.4 CRT

Preliminary work by Przybyla et al (2011) ⁴³⁶ concluded that CRP levels did not change after CRT, but it is important to note that the period of follow-up was limited to 3 months and, in addition, the authors made no comment on clinical response to CRT, which may determine whether there might be a meaningful change in CRP following implantation. Another paper, which recruited exclusively non-ischaemic HF-LVSD patients, and defined response based upon echocardiographic changes at 6 months, reported a significant decrease in hsCRP with response to CRT ⁴²⁴. However, for reasons discussed previously, reliance on a single measure such as echocardiographic LV changes, as a marker of response is problematic, highlighted by the authors themselves. Finally, work by Kamioka (2012), showed that baseline hsCRP was able to predict both echocardiographic response to CRT at 6 months and also risk of cardiac death ⁴³⁷.

6.2.6.5 Hypothesis

Working hypothesis –

1) hsCRP improves significantly in patients who are classed as responders to CRT, determined by symptoms, echocardiography and exercise testing.

2) The clinical response to CRT can be predicted by baseline measures of hsCRP

Null hypothesis –

1) hsCRP does not improve significantly in patients who are classed as responders to CRT, determined by symptoms, echocardiography and exercise testing.

2) The clinical response to CRT cannot be predicted by baseline measures of hsCRP.

6.2.6.6 Methods

Clotted blood samples for serum analysis were taken from the patient before CRT implantation (within 2 weeks of the procedure) and at 6 and 12 months post CRT implantation (+/- 2 weeks).

Serum hsCRP was analysed using a commercially available immunonephelometry assay (Cardiophase hsCRP, Siemens, UK). Polystyrene particles coated with monoclonal antibodies specific to human CRP aggregate when mixed with samples containing CRP. These aggregates scatter a beam of light passed through the sample and the intensity of the scattered light is proportional to the concentration of CRP. The result is evaluated by comparison with a standard of known concentration.

In Sheffield, the lowest level detectable is 0.2mg/l and test samples of 2.3, 4.6 and 9.4mg/l are run with an accuracy of 2.3 ($0.25 \pm \text{SD}$, 11 CV%) mg/l, 4,6 ($0.36 \pm \text{SD}$, 8 CV%) mg/l and 9.4 ($0.75 \pm \text{SD}$, 8 CV%)⁴³⁸.

6.2.6.7 Results

Table 85: hsCRP in responders and nonresponders at baseline

Baseline		Responders		Nonresponders		Student's T-test
		Mean	SD	Mean	SD	P value
hsCRP	mg/l	8.1	0.8	1.6	1.0	0.41

Table 86: hsCRP in responders at baseline and follow-up

Responders		Time point						One way ANOVA with repeated measures <i>p</i> value	
		Baseline		6		12		Baseline vs	
		Mean	SD	Mean	SD	Mean	SD	6 months	12 months
hsCRP	mg/l	8.1	0.8	3.5	2.3	2.0	1.3	0.11	

Table 87: hsCRP in nonresponders at baseline and follow-up

Nonresponders		Time point						One way ANOVA with repeated measures <i>p</i> value	
		Baseline		6		12		Baseline vs	
		Mean	SD	Mean	SD	Mean	SD	6 months	12 months
hsCRP	mg/l	1.6	1.0	4.7	3.2	2.8	2.7	0.34	

Figure 105: Serum hsCRP in responders (white) and nonresponders (black)

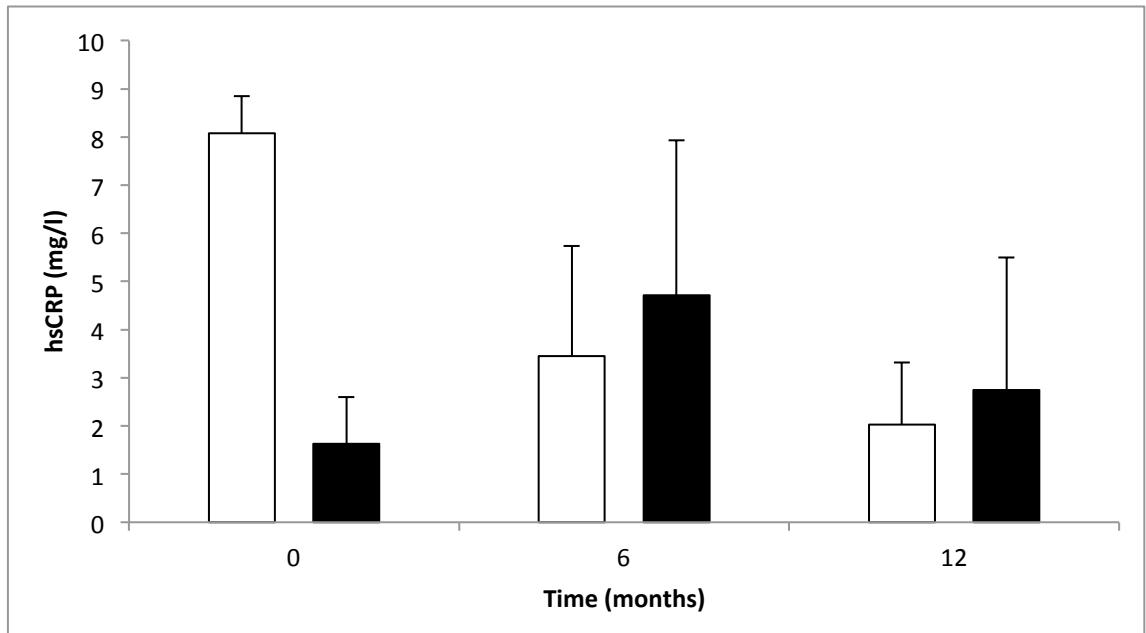


Figure 105 demonstrates the changes in serum high sensitivity CRP in responders (white) and non responders (black) following CRT implantation.

There was no statistically significant difference in hsCRP between responders and nonresponders at baseline (see table 85 and figure 105). During follow-up, the responders demonstrated a decrease in hsCRP and the nonresponders demonstrated a non-significant increase but neither of these changes was significant (see tables 86, 87 and figure 105).

6.2.6.8 Discussion

The results demonstrate that whilst there is a difference between responders and nonresponders at baseline, this difference was not of sufficient magnitude for hsCRP to be used to help predict response to CRT at baseline. Interestingly, this work, it was those patients with the higher levels of hsCRP that were more likely to respond to CRT, suggesting that patients who have a higher level of systemic inflammation and so a more severe HF-LVSD may derive greater benefit. Nonresponders had a lower baseline level of hsCRP but this increased during follow-up. Most likely this reflects continuing progression of the disease rather than being associated with CRT *per se*.

Normal levels of hsCRP are < 3mg/l; the majority of patients in this cohort had abnormal hsCRP levels both at baseline and during subsequent follow-up. In terms of

previous studies, this work appears to mirror previous findings, as discussed in the introduction, with patients receiving CRT having elevated levels of CRP. In terms of changes in CRP during follow up, although Przybyla et al (2011)⁴³⁶ found no changes they also did not differentiate between responders and nonresponders, whilst Shinohara et al (2011)⁴²⁴ did find a reduction in hsCRP after 6 months in responders, they did not suggest a possible mechanism. Kamioka (2012)⁴³⁷ demonstrated that responders had much lower levels of hsCRP at baseline (1.4 vs 3.3mg/l) which predicted response, but they did not measure hsCRP post-implantation. Finally, Cai et al (2014)⁴³⁹, found that hsCRP decreased in responders and increased in responders, but any difference at baseline between the groups was not given, follow-up was limited to 6 months and response defined as improvement > 1 NYHA functional class and > 5% improvement in LV EF%. Thus the heterogeneity of studies makes it difficult to draw firm conclusions of the role of CRP in terms of predicting or measuring response to CRT.

The hsCRP can be raised for many reasons such as infection, infarction and inflammation. Indeed, the link between cardiovascular and infectious disease is well known⁴⁴⁰. However, throughout the project patients were afebrile and asymptomatic, with no significant changes in the white cell count, suggesting infection was unlikely to have played a role. It is, of course, possible that patients may have had sub-clinical infection, leading to extraneous elevations of hsCRP, which then became symptomatic following assessment, but as the interval between assessments was 6 months, this would have been difficult to detect. As has been detailed previously, renal and liver function remained stable during the study, once again ruling out this as contributing towards any elevation in hsCRP.

Why did the responders have a higher hsCRP at baseline? As mentioned previously, there were no significant differences in the patients at baseline in terms of demographics, HF-LVSD severity, markers of response or novel biomarkers. It would also be interesting to measure other markers of inflammation such as TNF or IL, for example, to investigate what, if any, effect CRT has on those and to determine whether they mirror the changes in CRP with higher levels in responders at baseline and improvement during follow-up. Serum hsCRP was chosen over ESR, another

commonly used marker of systemic inflammation, since ESR normally rises with age and thus age could confound the results. Some patients did have comorbidities, such as COPD and malignancy for example, that could, in isolation, lead to elevated hsCRP but little is known about how the presence of comorbidities influences inflammation in HF-LVSD.

According to Yin et al (2004)⁸³ “at concentrations known to predict adverse vascular events, CRP directly quenches the production of nitric oxide, which, in turn, inhibits angiogenesis, an important compensatory mechanism in chronic ischemia. In so doing, CRP may facilitate the development and worsening of CHF” and so “risk-reduction strategies designed to lower CRP and TNF- α levels may be effective by improving nitric oxide bioavailability and endothelial function”. As FMD as a measure of endothelial function, has been shown to improve following CRT, this may explain the reduction in hsCRP following response to CRT in this cohort.

As discussed by Anand (2005)⁴²⁷ the ability of therapies to reduce CRP and the prognostic significance of this, requires further investigation and that “left ventricular dysfunction, hepatic or renal organ damage induced by low cardiac output, hypoperfusion, hypoxia, and venous congestion may all be sources of increased interleukin-6 and hence CRP production” all of which are common in HF-LVSD. So the mechanism remains unknown and levels remain similar in patients with HF-LVSD of an ischaemic and non-ischaemic origin, suggesting the CRP is independent of atherosclerosis. This raises the question; is CRP merely an epiphenomenon in HF-LVSD or does it actually drive the process? Other studies found that a higher hsCRP was found in patients with more severe HF-LVSD syndrome e.g. significantly worse symptoms, 6MWD etc but this study actually demonstrated hsCRP at baseline was higher in responders who, as has already been discussed, had less symptoms and were able to walk further at baseline⁴⁴¹.

6.2.6.9 Conclusion

There was sufficient difference at baseline between responders and nonresponders, to support the use of hsCRP as predictor of response. Similarly, whilst hsCRP levels changed during follow-up, these differences were not significant and so could not be

proposed as a marker of response. It would be interesting to validate these findings by the measurement of other markers of inflammation such as TNF or IL.

6.2.7 Proteinuria

6.2.7.1 Introduction

The presence of proteinuria, i.e. abnormal levels of protein in the urine, correlates with the development, prognosis, morbidity⁴⁴² and mortality of HF-LVSD⁴⁴³, independent of renal function, blood pressure⁴⁴⁴ or diabetic status⁴⁴⁵.

6.2.7.2 Pathophysiology

Proteinuria is a measure of renal dysfunction; specifically the permeability of the glomerular molecules and thus their presence over a threshold in the urine is pathological. This is referred to as microalbuminuria or urinary microalbumin (UMA) if the level of protein released into the urine is 30-300mg/24 hours or macroalbuminuria if the level is greater than 300mg/24 hours. Proteinuria (either micro- or macroalbuminuria) is a marker of endothelial and microvascular dysfunction, arising typically as a complication of poorly controlled or untreated diseases such as diabetes or hypertension and leading to nephron loss and eventually nephropathy. UMA may be reduced, and the rate of nephron loss interrupted, by ACEi or ARB therapy in HF-LVSD⁴⁴⁶ and, as alluded to by Struthers et al (2007)⁴⁴⁷, is a marker of silent organ damage, being present even before serum markers of kidney function are deranged. UMA correlates with NT-proBNP⁴⁴⁸, HbA1c⁴⁴⁹ and is present in approximately 20-30% of patients with stable HF-LVSD (see table 88), with macroalbuminuria (> 300mg/24 hours) present in a further 5-10%⁴⁵⁰.

6.2.7.3 Mechanism

Renal impairment is very common in HF-LVSD, it follows the progression of the disease and carries a poorer prognosis⁴⁵¹. The cardio-renal syndrome (CRS) refers to the simultaneous failure of both the heart and the kidney; often failure of one precipitates the decline of the other, directly by reduced perfusion, indirectly by neurohormonal mechanisms or iatrogenically following diuretic treatment. There are 5 subtypes of CRS but type 2 “chronic HF leading to chronic renal failure” is the most relevant here⁴⁵². The exact mechanism of CRS is unclear and equally, as with endothelial

dysfunction, the role microalbuminuria in HF, whether through a causal link or simply as a fellow traveller, remains to be established. According to Jackson et al (2009) “increased excretion might be a marker of diffuse vascular injury, systemic inflammation, activation of the renin-angiotensin system, altered glomerular haemodynamics, or abnormal tubular function. Many, if not all, of these pathophysiological abnormalities also occur in heart failure”⁸¹.

Table 88: Levels of UMA in HF

Author	Year	Measure	Albuminuria (%)			Conclusion in HF
			Normal	Micro	Macro	
VandeWal	2005	UACR	63	32	5	Common in HF
Jackson	2009	UACR	58	30	12	Predicts mortality
Masson	2009	UACR	41	40	19	Predicts mortality
Jackson	2011	UACR	65	28	7	Correlates with BNP
Blecker	2011	UACR	93	6	1	Predicts development

6.2.7.4 CRT

In normal, or mildly impaired renal function, the presence of proteinuria (either micro- or macro-) has been shown to pose an increased risk of HF-LVSD and furthermore, its presence in 30% of HF patients means it might represent a novel predictor of response to CRT⁴⁵³.

No papers that specifically investigate CRT and UMA could be found in the published literature and it is not known how CRT will impact on UMA. Whilst nephron loss is irreversible, CRT may stabilise renal function and protect the remaining nephrons. The MIRACLE study reported a significant improvement in renal function, measured by serum creatinine, was found following CRT, suggesting that it may offer some renal protection but UMA was not investigated⁴⁵⁴. Whilst UMA is reduced and nephron loss halted by therapies targeted at the renin-angiotensin-aldosterone system (RAAS), the only paper looking at UMA following improvement of myocardial performance was Hartmann et al (1996). This group measured UMA in heart transplant patients and

found that UMA actually deteriorated following transplantation over a period of 5 years ⁴⁵⁵. However, this finding was complicated by the nephrotoxic and secondary hypertensive effects of the immunosuppressive agents used. Possible mechanisms include improved endothelial function and glomerular haemodynamics and reduced systemic inflammation; all known benefits of CRT. Since poor renal function is associated with worse outcomes following CRT ⁴⁵⁶, and has recently been considered as a contra-indication to implantation ⁴⁵⁷, this also suggests, by extension, that the presence of UMA may be associated with poorer outcomes.

6.2.7.5 Measurement

UMA can be measured by one of three ways;

- a single sample of mid-stream urine (MSU) can be taken and the quantity of albumin present measured,
- the same sample can be used to measure the albumin/creatinine ratio (ACR), or
- urine can be collected for a 24 hour period and the total amount of albumin measured.

The latter measure is considered the gold standard.

Measurement of UMA can be influenced by factors including body temperature, infection, activity and time of day and so is best measured from the first voided urine.

The normal range for UMA is < 30mg/l of urine and the normal albumin/creatinine ratio (UACR) is < 3.5 mg/mmol and < 2.5 mg/mmol in male and female patients, respectively. A 24 hour urine collection was deemed not to be feasible considering how infrequently the patients were assessed, the distances travelled and how much they were already undertaking, so a spot measurement of the ACR was chosen from a first void MSU sample taken on arrival to the research facility ⁴⁵⁸. Accurate measurement of UMA depends on not only the level of albumin in the urine but also the concentration of the urine being analysed, hence in spot samples it is necessary to make a concurrent measure of the urinary creatinine concentration.

6.2.7.6 Hypotheses

Working hypotheses –

1) *UMA improves significantly in patients who are classed as responders to CRT, determined by symptoms, echocardiography and exercise testing.*

2) *The clinical response to CRT can be predicted by baseline measures of UMA*

Null hypotheses –

1) *UMA does not improve significantly in patients who are classed as responders to CRT, determined by symptoms, echocardiography and exercise testing.*

2) *The clinical response to CRT cannot be predicted by baseline measures of UMA.*

6.2.7.7 Methods

Each patient was asked to provide a urine sample at 08:30-09:30 on the morning of their appointment, prior to any medications, food, fluids or activity.

The urinary albumin was measured by an immunoturbidimetric assay (ACN 8235 Tinaquant Albumin Gen.2, Roche, UK). Anti-albumin antibodies react albumin in the urine to form antigen/antibody complexes which, following agglutination, can be measured turbidimetrically.

The assay used to measure urinary creatinine was a kinetic colorimetric assay (ACN 8691 Creatinine Jaffé Gen.2, Roche, UK). When placed in an alkaline solution, creatinine forms a yellow-orange complex with picrate and the rate of dye formation is proportional to the creatinine concentration.

In Sheffield, test samples 14.51 and 55.75mg/l for urinary albumin are run to an accuracy of the 14.51mg/l (± 0.94 SD, 6.51 CV%) and 55.75mg/l (± 1.83 SD, 1.83 CV%). For urinary creatinine 5.42mmol/l (± 0.11 SD, 2.00 CV%) and 11.14mmol/l (± 0.30 SD, 2.73 CV%) according to TG (personal communication, 2013) ⁴³⁸.

6.2.7.8 Results

Table 89: Baseline UACR in responders and nonresponders

Baseline	Responders	Nonresponders	Student's T-test
----------	------------	---------------	------------------

		Mean	SD	Mean	SD	P value
UACR	mg/mmol	7.0	2.8	2.3	1.7	= 0.75

Table 90: UACR in responders at baseline and during follow-up

Responders		Time point (months)						One way ANOVA with repeated measures <i>p</i> value	
		Baseline		6		12		Baseline vs	
		Mean	SD	Mean	SD	Mean	SD	6 months	12 months
UACR	mg/mmol	7.0	2.8	8.1	0.7	8.8	1.3	= 0.56	

Table 91: UACR in nonresponders at baseline and during follow-up

Nonresponders		Time point (months)						One way ANOVA with repeated measures <i>p</i> value	
		Baseline		6		12		Baseline vs	
		Mean	SD	Mean	SD	Mean	SD	6 months	12 months
UACR	mg/mmol	2.3	1.7	1.9	0.9	13.3	0.4	= 0.50	

Figure 106: UACR in responders (white) and nonresponders (black)

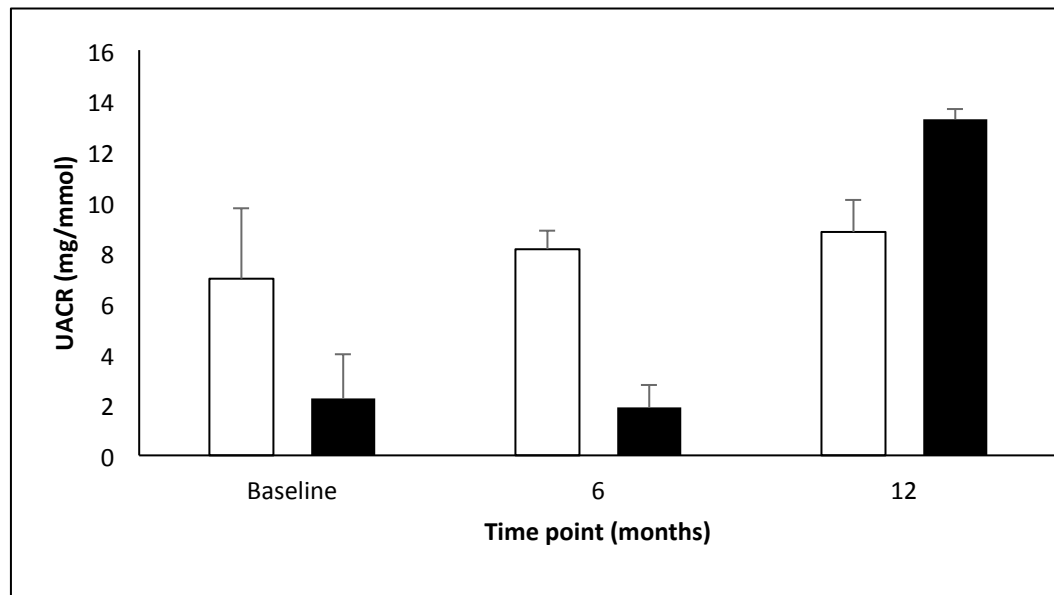


Figure 106 demonstrates the changes in the urinary albumin:creatinine ratio in responders (white) and non responders (black) following CRT implantation.

Although UMA appeared higher in responders, there was no statistically significant difference in UMA at between responder and nonresponder groups at baseline (see table 89 and figure 106). During follow-up, no change in UMA was recorded for responders; nonresponders demonstrated increase but this was not statistically significant (see tables 90, 91 and figure 106).

6.2.7.9 Discussion

The lack of significant difference between the UACR of responders and nonresponders at baseline means that this cannot be used at present as a predictor of response to CRT. Furthermore, there is no significant difference during follow-up in either responders or nonresponders for this biomarker to be considered a marker of response. One could argue that those patients without UMA may derive more benefit from CRT and have a lower likelihood of non-response as they are suffering from a single organ disease such as with idiopathic dilated cardiomyopathy and have not yet developed the HF-LVSD syndrome, affecting musculoskeletal, endocrine, renal systems etc.

As mentioned in the introduction, UMA is found in approximately 30% of HF-LVSD patients and clearly this would limit its utility in predicting response to CRT at baseline. In the present study, 30% of patients had UMA and a further 10% had macroalbuminuria at baseline, demonstrating that this cohort is similar to those from other HF-LVSD trials investigating UMA. A significant number of those with frank proteinuria were diabetic and these also comprised most of the responder group. This probably accounts for the non-significantly higher level of proteinuria at baseline in responders than nonresponders.

As discussed in the introduction, HF therapies such as ARBs have been shown to protect the remaining nephrons and prevent the onset of proteinuria but this was not found to be the case after CRT in the current study; where UACR deteriorated regardless of ARBs. It must be mentioned that ARBs have been shown to prevent the onset but not the progression of proteinuria in diabetic HF-LVSD patients⁴⁴⁶. Thus, since the diabetic HF-LVSD patients in this study already had significant UMA, the lack of a significant effect of CRT is perhaps not surprising. Furthermore, Jackson et al

(2009)⁸¹ reported contradictory findings, reporting that in their study, ARBs had no effect on proteinuria. It must be said, however that these conflicting results were the result of *post-hoc* analyses carried out on data from large studies and not obtained from prospective RCTs. Similarly, when the present patient cohort is considered as a whole, e.g. inclusive of both responders and nonresponders, there was no significant difference in UMA following CRT. Of note is that, whilst UACR deteriorated during follow-up, as did renal function, there was no significant difference in either group nor was there a significant difference in diuretic dose during follow-up. Perhaps in a cohort with stabilised or significantly improved renal function following CRT, a similarly significant difference in UMA might be found. The presence of UMA was no hindrance to CRT response, but the lack of a significant effect of CRT on UMA despite exerting beneficial effects on endothelial function; shear stress and systemic inflammation may simply suggest that the progression of CRS, like HF-LVSD itself, is unrelenting.

An alternative method to UACR could have been to use the recently discovered serum biomarker neutrophil gelatinase associated lipocalin (NGAL) as a marker of renal injury. This specific renal tubular protein responds earlier to renal injury than other biomarkers and has yet to be investigated in relation to CRT and HF-LVSD⁴⁵⁹.

Several factors can influence the day-to-day variation in UMA, in the range between 31-54% and so ideally a mean of three urine collections has been recommended to determine the UACR/UMA level of a given subject^{460 461}. However this was not deemed feasible in this study and furthermore was not carried out in other HF-LVSD studies. The urine was taken at the same time of day for each patient/visit and the patients rested overnight in order to minimise any inter-sample variation. Also, the patients were all asymptomatic, afebrile and without neutrophilia, ruling out the influence of a urinary infection as a cause of variability in UMA.

6.2.7.10 Conclusion

The lack of significant difference in UACR between responders and nonresponders at baseline or during follow-up means that by this measure at least, UMA cannot be used to predict or assess response to CRT. It appears that, as with HF-LVSD itself, following the onset of UMA the progression is unrelenting. Future work could involve using

other measures of UMA such as 24hr urine collection or other measures of renal injury such as NGAL.

6.3 Conclusions

In conclusion, of the biophysical markers investigated, FMD was able to predict response at baseline and HGS was used to demonstrate response during follow-up, however the BCG and non of the biomarkers were significantly different during follow-up in responders nor at baseline between responders, ruling them out as predictors or measures of response. In the next chapter, the clinical utility of the work in chapters 6 and 7 will be discussed.

Chapter 7 Evaluation of Clinical Relevance

This chapter discusses the clinical relevance of the work described in the preceding chapters, on modelling, biomarkers and biophysical markers.

7.1 Models

The LPM was used to analyse existing LV PV data and add tangible parameters to both the AHA/ACC and NYHA classifications and to model patients undergoing CRT therapy with the aim of predicting and assessing response. The LPM proved invaluable in gaining insight into the failing heart, from healthy normal to end-stage HF-LVSD, giving both clinically meaningful parameters such as elastance (E_{max}) and EF%, showing how they changed as the LV failed and also scientifically novel data revealing for the first time that, modelled in this way, resistance (R) and compliance (C) did not change during the process of HF-LVSD. In this work, the LPM was used to analyse existing data and perhaps the “so what?” question remains unanswered, as to model the LV, and therefore the patient, one still needs to perform the invasive measures in the first instance. Ideally one would model the LV without invasive measures, however to validate, at least initially, the model must be based on objective and robust measures of the system, in this case volume and pressure. This of course, makes the false assumption that symptoms and therefore HF-LVSD class is purely determined by LV function, when there are many other body systems intimately linked to the LV, but which are challenging to model and hard to quantify. The difficulties in this work, led to the next section and using the patients record, to attempt to model the LV in patients undergoing CRT implantation, without invasive measures. This was in itself interesting and hopefully would help to further personalise the 3D models used in the project.

As alluded to earlier, the “so what?” question, differentiates the academically interesting from the clinically useable. If using the LPM at baseline could predict which patients would respond to CRT this could be both. However, how the LV PV loop, and therefore underpinning LPM parameters, changed during follow-up is academically

interesting without having real clinical utility. The lack of correlation between the model parameters e.g. Emax and markers of response (established or novel) compounds this irrelevance, as it appears that the models' parameters lack real world validity. Furthermore, this LPM work, suffered from the same fate as the 3D modelling, that in the real world, hearts are difficult to image accurately, and reproducibly and single measures of physiological parameters do not necessarily best represent the system. As a result, the model represents a single snapshot of a component of the system rather than the working system in its entirety and measurements acquired a second before or after might give very different results. This also calls into question the utility of creating models based on healthy normal individuals and then forcing these onto morbidly unwell patients, with abnormal anatomy and physiology.

Simply recruiting a patient to a research study does not mean they will have excellent echo "windows" with beautifully delineated LV endocardium enabling accurate assessment of LV volumes. Ideally such patients would be proactively selected, but then this creates a further challenges for recruitment e.g. more patients will be deemed unsuitable and for ethical approvals e.g. pre-scan all possible candidates (unless patients are already known). However, this work has demonstrated that the LV can be modelled non-invasively, as patients respond the model adapts and reproduces pathophysiology (with the available information) accurately and with a larger cohort this may lead to identifying patients *a priori* who will respond to CRT which would be invaluable, save £10k's per year and not expose patients to the risk of implantation for a device that may not ultimately benefit them.

In terms of appraisal of the 3D segmentation tool, it became apparent that whilst superficially the 3D whole heart segmentation looked realistic, when viewed in the context of the cMR SSFP original image, the tool found it difficult to differentiate the extra-cardiac tissue from the epicardium and so overestimating the size of the LV. Objectively when comparing the gold standard hand segmentation to the automated segmentation, it became clear that significant differences were found in the 2 surfaces. Although the tool performed better in segmenting the endocardium with a bright blood pool, the resulting segmentation was far from accurate. The process of hand segmentation is laborious and hence in clinical practice a semi-automated tool is

used. This emphasises that there is more work to be done before the heart can be accurately and routinely model the heart for use in clinical practice using automated segmentation tools. This is especially important if that model is then used to determine suitability for, or response to, a therapy. This was, arguably perhaps, the most clinically relevant aspect of the whole GC project, namely could the process of creating a 3D model be automated? And could this 3D model then predict response to the therapy delivered? Whilst the second question remains unanswered, the answer to the first question remains a resounding no. Before such a project could be rolled out to further centres as part of an RCT, either the process would need to be automated or funding would be needed in each centre for a clinician or researcher to hand-segment the LV. Indeed, when other members of the GC project used the automated segmentations at least in terms of geometry any differences between responders and nonresponders were lost, hence it was found necessary to default back to hand-segmented meshes.

The 3D modelling held the greatest potential for clinical relevance at the start of the project, certainly there was hope that if the project was successful the multi-scale model could be rolled out to other centres as part of the multicentre trial. Unfortunately, no such model was realised, despite the promise shown in the preliminary pilot study. As a consequence, the both the EP model and statistical atlas were used in an attempt to deconstruct the all-encompassing complex model, into its constituent parts and assess the potential of these individually. Both produced significant results, with the EP model appearing to predict multimodal response to CRT based on type II activation pattern and the atlas demonstrating that response based on LV reverse remodelling alone could be predicted by 2 modes of variation, in length and sphericity. However, the EP model was unable to simulate 50% of the patients from USFD and 100% of patients from GSTT, taking considerable time and computational power to run and the statistical atlas required complex mathematical algorithms to prove response on a single criterion, which in itself is now rarely used in isolation in large clinical trials. This suggests that there is still much work to be done, in terms of translating biomedical modelling into the clinical setting. Whilst both were academically interesting and certainly a signpost for future work, such a workflow would need to be fully automated and run in minutes, not days to enable clinicians to

make decisions in real time on their patients, for example when planning complex device therapy e.g. CRT. Furthermore, it would be unacceptable for a clinical tool to be unable to analyse data from 50% of the patients, as this would be unusable to the clinician and unsatisfactory to the patient. In this regard, it is unsurprising that such modelling work is now being pared down, back to basics, to allow for faster simulations, less computational demands and less difficulty in analysing data.

7.2 Biophysical

With respect to FMD, this study supports its potential for the pre-assessment of CRT candidates ensuring that only those patients who are likely to respond receive the device therapy. This is the second study to confirm the utility of FMD but the reason as to why reduced endothelial function should be associated with increased likelihood to derive benefit from CRT remains unclear. As a test that in the order of about 30 minutes provided that; the patient is appropriately prepared, staff trained are suitably prepared in both the acquisition and analysis and provision is can be made for such assessment within routine clinical practice, FMD could be of great use. This is particularly the case in view of a climate of NHS cuts, austerity and increasing emphasis on personalised medicine using the best available evidence. At a cost of around £100 per scan, compared to £10-15k per CRT-P/D device, particularly if the scan avoids implanting a CRT device in a patient who will derive none of the benefits but all of the risks, it makes financial and clinical sense to first replicate these findings in a larger and more heterogenous population before then conducting a RCT to see whether such data bears true. However, whether this would be acceptable to patients or indeed an ethics committee remains to be seen but perhaps is no different to performing an ECG to measure QRS width prior to CRT implantation.

HGS elegantly demonstrates how a HF-LVSD therapy which improves LV function, can also lead to secondary gains in other areas of the HF-LVSD syndrome, muscle function. To the best of the author's knowledge, this is the first study to demonstrate that responders to CRT gain improvements in HGS and is likely to be as a result of the increase in activities of daily living, walking to the shops, gardening, cleaning etc, that a positive response to CRT allows. At present in STHT, patients are assessed for response during a clinic appointment at 6 months following CRT with the patient

simply being asked if they 'feel better' and stratifying their functional status based on their response to the NYHA classification. The use of the GS could be a helpful tool to aid more accurate categorisation of response for although nearly all patients had improved symptoms and functional capacity according to the MLWHFQ and 6MWD at follow-up, only responders had an improved HGS. To perform a serial peak VO_2 , 2DTTE or BNP assessment for all patients to assess response would be prohibitively expensive, time consuming and fraught with confounding variables such as motivation, inter-operator variability and fluid/volume status. There was also quite a large difference in HGS between responders and nonresponders at baseline, although this was not significant. Were this study to be repeated in a much larger cohort and a significant difference determined at baseline between responders and nonresponders this would increase the utility of HGS, in terms of predicting, not just measuring, response. As HF-LVSD is not simply a single organ disease, particularly at its end-stage, it becomes ever more important to take non-cardiac factors into account when assessing suitability for, and response to, treatment.

Finally, the most novel of this work, the BCG, was used to study the influence of cardiac force on the potential response to CRT and, following the implantation of a device, its impact on cardiac force. Unfortunately, due to challenges in setting up such industrial equipment for clinical use, and 2 patients subsequently dropping out, only 10 patients underwent this with 9 responders and 1 nonresponder, making comparisons between them challenging.

It is important to emphasise that, unlike for the ECG, despite many years of research into BCG, it is still not clear exactly what the BCG signal means even with the use of signal averaging. It would have been useful to carry out a simultaneous 2DTTE with ECG during BCG monitoring, but that was not feasible with the equipment used. This would have given greater insight as to what each component of the wave meant in the context of the cardiac cycle, for the composition of the JVP for example. Nevertheless, it was possible to demonstrate that real time ECG and BCG acquisition is possible. Whether recruiting a larger group, at baseline and comparing responders/nonresponders may allow a clearer picture of the role of BCG to emerge remains to be seen. Unlike for FMD or HGS, the utility of BCG as a marker or predictor of response based on this study alone remains unclear.

In terms of biophysical markers, FMD and HGS demonstrated their clinical relevance for assessing patients prior to, and following, CRT therapy respectively. The true role and value of BCG is yet to be realised, but showed promise in this pilot work.

7.3 Biomarkers

A range of putative cardiac and non-cardiac biomarkers were investigated in this project but none were shown to fulfil their promise in terms of significantly differentiating responders from nonresponders at baseline or showing significant alteration during follow-up after CRT in either responders or nonresponders. The reasons for this are multifactorial and may simply relate to the small and homogenous patient cohort, as certainly some differences did exist at baseline and during follow-up. There appeared to be 3 trends emerging from the biomarkers in responders:

- 1) Higher at baseline and decreasing after CRT; hsTNT, NT-proBNP and hsCRP.
- 2) Lower at baseline and increasing after CRT; UA, vitamin D and PTH.
- 3) Higher at baseline and increasing after CRT; UMA.

Despite providing assessment of the HF-LVSD syndrome in terms of cardiac, endocrine, renal, endothelial and cellular function, since none of the measured differences proved to be statistically significant (other than NT-proBNP during follow-up in responders) it is difficult to draw any firm conclusions.

In terms of clinical utility, such tests cost between £0.40 and £20 but until a statistically significant difference is established, it would be difficult to justify their inclusion in the routine assessment of CRT patients at baseline. As the significant improvement in NT-proBNP became widely known during the project and so the positive finding in this regard is no longer surprising and furthermore, this marker improved in some patients who were not classified as responders, despite their lack of response in terms of any other established criteria.

In order to remove any influence on the reporting of NT-proBNP levels, samples were analysed by staff blinded to the patients' condition and the investigator took total responsibility for taking, labelling and transporting the blood samples. All markers of response, such as LVEDV, 6MWT, peak VO₂ and MLWHFQ were recorded on the same day as the biomarkers to ensure any changes were contemporaneous; assessment on different days could have led to errors e.g. influenced by diet, activity, fluid balance, medication etc.

Responders to CRT appeared to be generally 'fitter' at baseline; in terms of fewer symptoms, small LV volumes, stronger GS, and greater 6MWD but this was not supported by the statistical analysis and furthermore, serum NT-proBNP and hsTNT and peak VO₂ were all lower in responders. This might indicate that, despite all these patients being classed as NYHA III, perhaps further sub-categorisation was needed, even in seemingly such a homogenous group. In principle, the AHA/ACC or NYHA classification could be sub-divided further or a new classification that better reflects the HF-LVSD syndrome as a whole could be proposed rather than simply limited to categorisation of breathlessness or the aetiology of the HF¹²⁴.

This aspect of the project gave insight into the syndrome that is HF-LVSD, as nearly all patients had values that would be considered abnormal, in one or more biomarkers, despite not being previously diagnosed with such conditions e.g. microalbuminuria or being symptomatic e.g. gout. This finding highlights how much comorbidity remains undiagnosed in such patients but also potential harms from over-diagnosis in research trials. NT-proBNP, is currently used in primary, but other than for research studies, not secondary care. This is due to the wide availability of 2DTTE in a hospital setting, which is considered to be the gold standard for diagnosing HF-LVSD and ruling out other causes of dyspnoea (and raised NPs), such as valve disease, PE or HFPEF. Assessment of NPs should be used as part of the assessment for patients following CRT implantation. This may have distinct benefits over simply asking patients if they 'feel better' and estimating NYHA class based on their symptoms of breathlessness. Used, in conjunction with the 6WMD and with GS, NT-proBNP might allow an objective assessment of functional capacity, skeletal muscle function and neurohormonal status, all or which are key factors in driving symptoms and thus determining CRT response.

7.4 Conclusions

The only tests that demonstrated real world clinical utility were the HGS, as a quick and easy adjunct to identifying patients who were CRT responders and the FMD as a method to identify patients pre-implant who would respond, but these findings would need replicating in a large and diverse cohort, before drawing firm conclusions.

Chapter 8 Discussion, Conclusions and Future work

This chapter draws together all the themes in order to discuss what has been learned, what this means and what further research needs to be done.

8.1 Discussion

The thesis has two complimentary themes, which run throughout; these are measuring and predicting response to cardiac resynchronisation. In the former, the role of patient-specific three-dimensional computational models and biophysical properties are investigated as potential predictors of response, and, in the latter, the influence of cardiac resynchronisation on the heart failure syndrome using biomarkers.

The overall aim of the GC project was to produce around 50 patient specific 3D LV models at baseline, from cMR derived whole heart segmentations, which were fitted to meshes featuring biomechanical and electrophysiological properties, and run to see if such simulations would predict response to CRT. Despite a successful pilot study, even 5 years after officially starting the project, this aim is still to be realised, even if the EP model and statistical analysis LV shape of the LV at baseline is significant at predicting response, the lack of even a single working multi-modal 3D model proves just how much of challenge the GC project was.

Mean age of patients was perhaps surprising given that the average age of HF diagnosis is 76 but the mean age of patients in the large CRT trials was mid to late sixties. This is important as it shows that the inclusion criteria were respected, the results are translatable to a HF-LVSD population receiving such devices (who should all be taking both a β -blocker and an ACE-I/ARB) and can be compared against other CRT trials with similar levels of OMT. Only 2 (10%) of the patients were female, as compared to between 15-30% in the large CRT trials. However, whilst the 19 patients studied were homogenous, clearly all this work would need repeating in much larger and more diverse cohorts, in terms of gender and ethnicity, before the results could be applied to either the HF-LVSD population as a whole and especially in respect to those groups underrepresented in this work. Furthermore, such a small sample size lacks statistical power and is at risk of type II errors, and so the results must be considered in this light.

The LPM work gave successful outcomes, firstly in the context of being able to use existing data in the public domain to unearth new parameters from existing PV LV data. A broad spectrum of data from healthy normal individuals through to patients with end-stage HF-LVSD was used. This had not been done before indeed the only similar work modelling HF-LVSD found in the literature used seemingly arbitrary measures for elastance and boundary conditions. This study therefore allows modellers to choose precise parameters for patients in varying degrees of LV dysfunction, based on the largest systematic review of LV PV data to date and in the knowledge that it is only elastance, which is important. This inspired the next body of work, exploring how such a model could be used in the absence of invasive measures. This resulted in the first non-invasive PV loops being created for patients with CRT and then modelled. Again, it was demonstrated that elastance was the only important parameter, mirroring the earlier work, but also demonstrating how similar the responders and nonresponders were at baseline. Such a model is necessarily reductive and thus a representation, not a reproduction, of reality but it did give insight into what improvements in contractility responders could expect from CRT.

In terms of measurement of response, as this is only the fifth published study to use peak VO_2 in patients before and after CRT, so it certainly adds to the existing evidence base. Indeed, this was the first to follow-up patients at 12 months using the same metric, and demonstrating further gains in peak VO_2 during subsequent follow-up which are mirrored in other metrics. Indeed, it was the single marker of response that determined a positive and significant change in the other markers e.g. if there was a significant improvement in peak VO_2 , there was improvement in the other 3 markers but not vice versa.

The lack of significant correlations between biomarkers such as UA, PTH and hsCRP is unsurprising given that no statistically significant differences were found either between or within groups for any of these tests. More surprising however, is the lack of correlation between NT-proBNP and hsTnT, as both are markers of LV wall shear stress and neurohormonal activation. Also, although hsTnT was higher in responders at baseline, NT-proBNP was found to be lower. However, as again these differences

did not achieve statistical significance, it is difficult to draw any meaningful conclusions.

The small improvement in hsTnT in responders during follow-up may be accounted for by improvements in LV wall shear stress and neurohormonal activation due to CRT. The deterioration in nonresponders suggests that they continue to decline despite of the influence of CRT. In terms of response, it makes sense that hsTnT correlates with LVEDV, as according to Laplace's law, decreasing LV diameter leads to decreased LV wall tension, a more uniform pattern of contraction and improved systolic function. As with NT-proBNP, this, in turn, results in reduced wall shear stress and so reduction in hsTnT.

By using FMD, GS and serum biomarkers, the concept of the HF-LVSD syndrome has been further elucidated, and whilst it is acknowledged that the cohort size was small it was comprehensively assessed. It is clear how common multi-organ dysfunction is likely to be, it is likely influence on response to CRT and the potential influence of CRT on the syndrome. This work also adds to the evidence base on the interaction of cardiac specific therapy and its wider effects on the whole patient, not just on the heart. Indeed, other than BNP and FMD, none of the other markers had been investigated previously in the context of CRT and predicting/measuring response or in conjunction with each other. When considering the bio and biophysical marker result in the context of each other and also the markers of response, it is perhaps surprising that there was no significant correlation between and UMA and other biomarkers of endothelial or microvascular dysfunction such as UA or FMD. This might be explained by the small sample size and lack of significant difference (other than FMD) between markers of endothelial or microvascular dysfunction at baseline or follow-up in either group. The lack of a significant positive correlation with NT-proBNP and UMA is also intriguing, as this contradicts earlier work⁴⁶². Parvez et al (2012)⁴⁶³ demonstrated that in an AMI population, UMA was significantly higher in patients that died or were diagnosed with a STEMI, compared to survivors or those with a NSTEMI. However, it is unclear what this actually tells us, there was no significant difference in UMA at baseline or following CRT. It may suggest that like hsTnT, UMA is a fellow traveller in the HF-LVSD syndrome and so as LV function deteriorates it is inevitable that both UMA and hsTnT will also rise, or possibly, as in this study, in nonresponders only.

There was no correlation between UA and FMD, despite previous evidence of a correlation between UA levels and nutritive flow in lower limbs of HF-LVSD patients ³⁴⁵. However, correlation does not equate to causation and brachial FMD is not the same measure as lower limb strain gauge venous occlusion plethysmography and patients in the study by Anker (1997) comprised 50% patients in NYHA class I or II and so were a 'fitter' cohort in this respect. There was no significant correlation with VitD, UACR, hsCRP, NTproBNP or hsTNT with any markers of response or other bio/biophysical marker. Its not immediately apparent why this was the case, but presumably a result of a small sample size.

There was however a significant correlation between HGS, both left and right, and 6MWD (see figure 107). This correlation with 6MWD suggests that HGS is a real-world assessment of fitness; indeed at 12 months follow-up, every 1.5 kgf increase in HGS correlated with a 10m increase in 6MWD. This could be used in addition to 6MWD during follow-up, as a surrogate measure of improvement for patients with lower limb osteoarthritis or indeed as a standalone test of response, particularly where space is at a premium for the corridor test. There was no significant correlation between UA and other biomarkers but there was a significant negative correlation between peak VO₂ and significant positive correlation with LVEDV suggesting that, as UA increases cardiorespiratory and left ventricular function decline (see figure 108). Other investigators have shown a correlation between LVEDV and UA levels in a similar HF-LVSD population ⁴⁶⁴.

The BCG work remains something of an unknown quantity, by virtue of less than half of the 21 patients recruited being assessed by this modality. Nevertheless, this is the first clinical trial to compare such groups at baseline and follow-up after CRT to assess for response. Differences were seen both at baseline and during follow-up. If such findings are replicated in larger populations then it could establish BCG as a marker to both measure and predict response to CRT.

Figure 107: Correlation between 6MWD and GS in the left (A) and right (B) hands

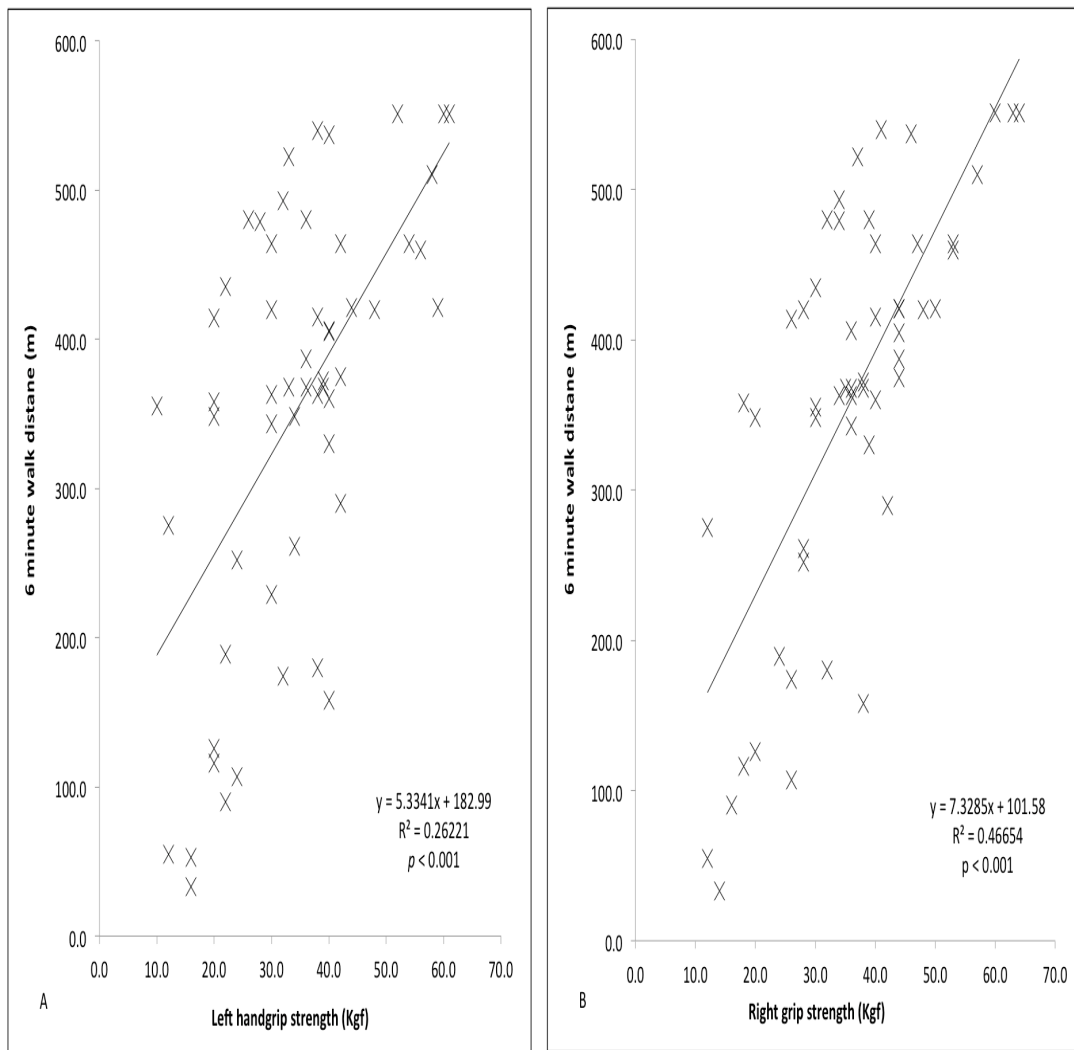


Figure 107 demonstrates the correlation between the 6 minute walk distance in both groups and the hand grip strength in the left and right hands, at all time points.

Whilst there is much interest in predicting response to CRT, this is largely driven by the need to identify responders in order to implant more devices, rather than to protect nonresponders from unnecessary harm. The scientific definition of response is necessarily arbitrary and less clear than many would believe, with grey (not black and white) being the norm; all the patients reported feeling better following CRT implantation, yet only 70% fulfilled responder criteria as defined *a priori*. This begs the question 'what is more important; the patient and their symptoms? Or their physiology and improvements in functional capacity, neurohormonal status and LV function?' Clinically, the assessment of response is still brief, subjective and unscientific despite

the device costing £10-15k; the patient is simply asked how they are feeling and dyspnoea rated on NYHA to assess response. There is much the jobbing HF or EP/Devices clinician can learn from the body of research into the assessment of response, especially that the placebo effect is strong and real. Whilst, as discussed, there may be modifiable reasons, such as AF or BiVP%, why the patient fails to respond, in reality this is uncommon and perhaps we should be having more honest conversations with patient with end-stage HF-LVSD, especially in conjunction with multi-morbidity, rather than doing something because we can, and feel we should.

Figure 108: Correlation coefficient between UA and peak VO₂ and UA and LVEDV

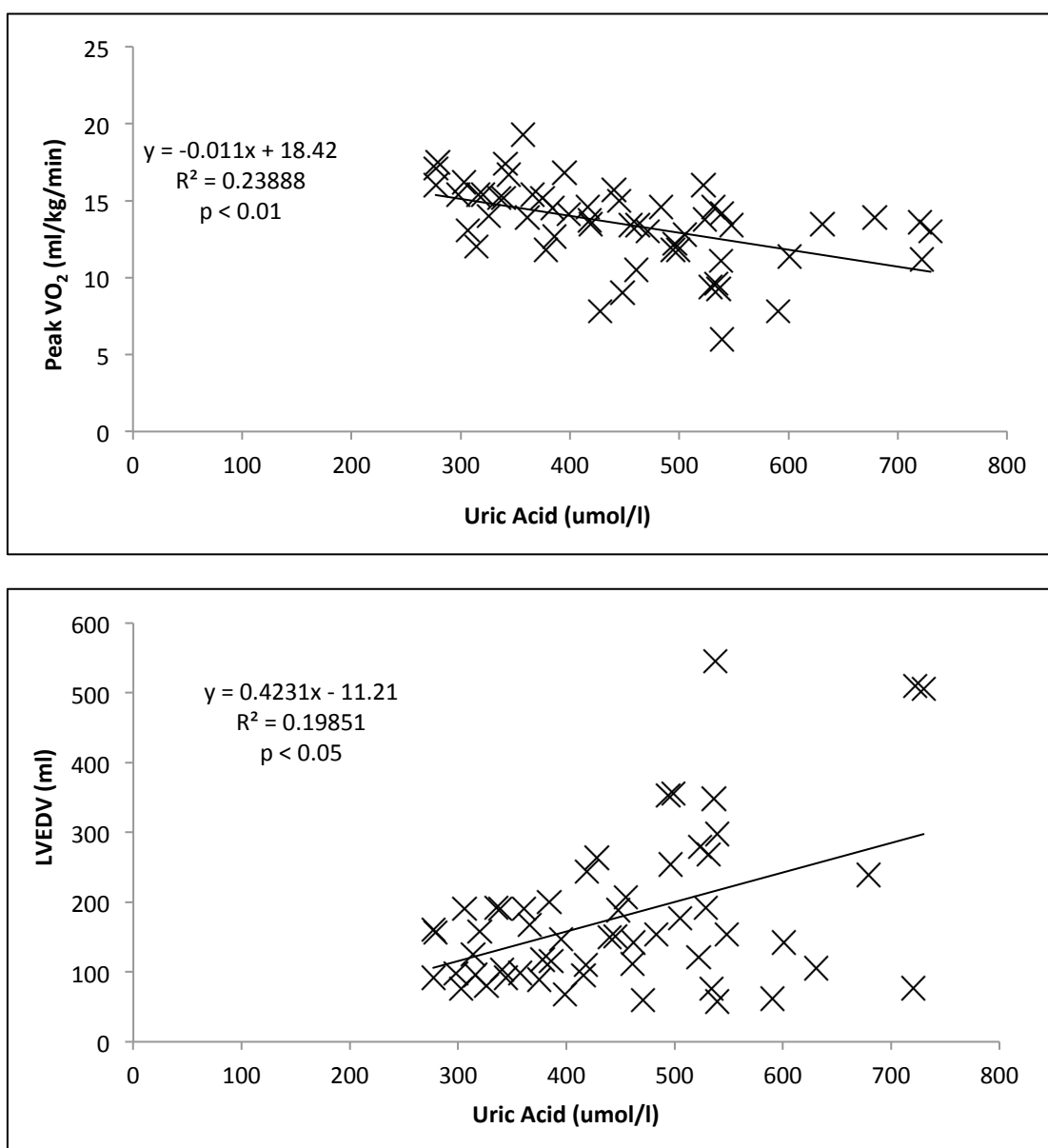


Figure 108 demonstrates the correlation between uric acid in both groups and peak VO₂ (above) and left ventricular end diastolic volume (below) at all time points.

8.2 Conclusions

The question “Why do only two thirds of patients respond to CRT?” remains unanswered. However, on the basis of this work, we have greater understanding of the physiology behind such response, how to better select responders *a priori* and finally how to more precisely define the concept of response. However, it remains to be seen whether multi-level 3D patient specific models will enable further insight into the question posed, enable researchers and clinicians to predict response to CRT *in-silico* and even whether such a quest is purely of academic interest.

8.3 Future Work

Much has been learned during this project, both in the conduct of clinical research but also as a consequence of the hypothesis generating results, which need replication in larger and more diverse groups.

8.3.1 General

Whilst some of the results have proved interesting, many of the differences recorded have not reached statistical significance and the influence of the small sample size remains to be established. Longer, and possibly, more frequent follow-up appointments would also be interesting to see if the changes demonstrated at 12 months continue subsequently following implantation and to identify what is the tipping point in response e.g. if a patient does not respond by 4 months then they will not respond at all.

A small matched control group, to assess individual, chronological and learning effect variation over time for assessment tools such as peak VO₂, natriuretic peptides, for example patients who are unable to have a CRT implanted and also to assess any possible learning effect.

Despite what was written in the introduction, with many trials struggling to recruit women and ethnic minorities to their studies, unfortunately only two women (a third had to be withdrawn) and no ethnic minorities (one patient was approached but declined to take part) were recruited to this study and one must not assume that HF-LVSD in women or ethnic minorities is the same as in white men, as it often isn't and one must not assume that they will respond to therapies as well or in the same way.

In an ideal world, the cohort of patients would comprise 50% with ischaemic and 50% with non-ischaemic HF-LVSD. Unfortunately, this is the real world and risk factors for HF are often the same that cause other comorbidities e.g. smoking, diabetes, hypertension, leading to chronic lung, liver, kidney diseases and also malignancy. Such diseases are also common in such deprived populations in South Yorkshire, where the patients were sampled. One of the reasons patients may not “respond” to CRT, is due to the presence of coexisting disease, which is actually the predominant causes of the breathlessness and may deteriorate subsequent to implantation and thus perhaps all patients with COPD should be excluded or lung function measured at each time point to mitigate for such variation.

8.3.2 Modelling

With the advent of cMR compatible implantable pacemaker devices, it won't be long until there are cMR compatible CRT devices and so using cMR in place of, or alongside, 2DTTE, before and after implantation (for volumes to determine response but also for segmentation) is a possibility. It would be of great interest as one could accurately and reliably assess the LV reverse remodelling response to CRT, irrespective of echo windows etc.

A further interesting avenue for the future would be to record actual LV PV from invasive catheter data and then use these to either create Zero-D models and model the response of the patients to CRT or validate non-invasive PV loops. During implantation and during pacing settings e.g. RV, LV, BiV the PV loop could be used to generate novel data, seeing the effect it has on LV function, LV elastance and thus the PV loop. Since starting the project the Siemens E9 echo machine has been released that can acquire a full LV 3D volume in one cardiac cycle and so negating the influence of AF and ectopy which was an issue even in patients with good echo windows.

8.3.3 Biophysical

The ED work needs to be repeated at 6 and 12 months in a much larger population, and if the findings are still positive, an adequately powered and double blind RCT should be carried out. This will confirm whether FMD can be used to predict response to CRT and what influence CRT has on endothelial dysfunction as measured by FMD.

In terms of the BCG signal, the process needs further refinement e.g. what is the optimal recording duration? What is the key signal e.g. J wave in predicting and measuring response? And what changes can we expect following CRT in terms of timing? Further work could involve the development of a sitting force plate, utilisation of home monitoring for predicting deterioration and measurement of RV, LV and BiV pacing with simultaneous 2DTTE and/or LV PV loop acquisition would help understand the origins of the BCG signal, the role of the RV and how it correlates in other imaging modalities such as EF% or elastance. Also, whether different methods of optimisation influence the BCG signal and thus lead to higher yield of response, as has been suggested by earlier work on CRT optimisation and CRT.

It would have been interesting to perform GS in a control group of subjects to explore variation over time and also consider other measures of sarcopenia in conjunction with GS, such as muscle mass, muscle biopsy, forearm circumference or knee extension/flexion strength to see if the changes in the upper limb GS were mirrored in these other markers.

8.3.4 Biomarkers

Diet and outdoor activity can all influence vitD levels, which in turn can influence Ca^{2+} and PTH levels and whilst it was not recorded this time around, to be sure that the result was solely as a result of the CRT device, one would also need to record baseline activity, particularly outdoors and also keep a food diary, with reference to dairy products.

Following the start of the project, NGAL as a measure of kidney injury became established and so it would have been interesting to measure this before and after implantation, in conjunction with eGFR, creatinine and UMA. Whilst 24 hour urine collection is the most accurate way to quantify proteinuria, it is quite a commitment and as the patients were already giving up nearly 6 days of their time over 1 year, this was too much to ask. Plus logistically, some were coming from > 50 miles away and so collection would be an issue.

Further work could involve measuring novel biomarkers such as mid-regional ANP, ST2, growth differentiation factor 15, galectin-3, and specific microRNAs such as MiR423-5p and determining their role in predicting and measuring CRT response.

Permissions

Figure 1 and 4: Reproduced with permission from Morris et al (2015) ⁴⁶⁵.

Figure 11: Reproduced with permission from Knebel et al (2004) ⁴⁶⁶.

Figure 12: Reproduced with permission from Tanaka et al (2010) ¹⁰².

Figure 32: Reproduced with permission from Steendijk et al (2006) ²²⁴.

Figure 44: Reproduced with permission from Sermesant et al (2008) ⁴⁶⁷.

Figure 78: Reproduced with permission from Phibbs et al (1967) ³³⁵.

Figure 79: Reproduced with permission from Giogravandi et al (2011) ³³⁶.

Figure 96: Reproduced with permission from Anker et al (1997) ⁴⁶⁸.

Figure 99: Reproduced with permission from Mozaffarian et al (2007) ⁵³.

Appendix

Minnesota Living with Heart Failure Questionnaire

MINNESOTA LIVING WITH HEART FAILURE® QUESTIONNAIRE

The following questions ask how much your heart failure (heart condition) affected your life during the past month (4 weeks). After each question, circle the 0, 1, 2, 3, 4 or 5 to show how much your life was affected. If a question does not apply to you, circle the 0 after that question.

Did your heart failure prevent you from living as you wanted during the past month (4 weeks) by -	No	Very Little			Very Much	
	0	1	2	3	4	5
1. causing swelling in your ankles or legs?	0	1	2	3	4	5
2. making you sit or lie down to rest during the day?	0	1	2	3	4	5
3. making your walking about or climbing stairs difficult?	0	1	2	3	4	5
4. making your working around the house or yard difficult?	0	1	2	3	4	5
5. making your going places away from home difficult?	0	1	2	3	4	5
6. making your sleeping well at night difficult?	0	1	2	3	4	5
7. making your relating to or doing things with your friends or family difficult?	0	1	2	3	4	5
8. making your working to earn a living difficult?	0	1	2	3	4	5
9. making your recreational pastimes, sports or hobbies difficult?	0	1	2	3	4	5
10. making your sexual activities difficult?	0	1	2	3	4	5
11. making you eat less of the foods you like?	0	1	2	3	4	5
12. making you short of breath?	0	1	2	3	4	5
13. making you tired, fatigued, or low on energy?	0	1	2	3	4	5
14. making you stay in a hospital?	0	1	2	3	4	5
15. costing you money for medical care?	0	1	2	3	4	5
16. giving you side effects from treatments?	0	1	2	3	4	5
17. making you feel you are a burden to your family or friends?	0	1	2	3	4	5
18. making you feel a loss of self-control in your life?	0	1	2	3	4	5
19. making you worry?	0	1	2	3	4	5
20. making it difficult for you to concentrate or remember things?	0	1	2	3	4	5
21. making you feel depressed?	0	1	2	3	4	5

©1986 Regents of the University of Minnesota. All rights reserved. Do not copy or reproduce without permission. LIVING WITH HEART FAILURE® is a registered trademark of the Regents of the University of Minnesota.

11/10/04

Borg Breathlessness scale

0 - Nothing at all

1 - Very light

2 - Fairly light

3 - Moderate

4 – Some-what hard

5 - Hard

6

7 - Very hard

8

9

10 - Very, very hard

Borg Rating of Perceived Exertion (RPE) scale

6 - No exertion at all

7 - Extremely light

8

9 - Very light

10

11 - Light

12

13 - Somewhat hard

14

15 - Hard (heavy)

16

17 - Very hard

18

19 - Extremely hard

20 - Maximal exertion

Patient Information Sheet



PATIENT INFORMATION SHEET

Project: Grand Challenge Modelling Project

You are being invited to take part in a research study. Before you decide it is important for you to understand why the research is being done and what it will involve. Please take time to read the following information carefully. Talk to others about the study if you wish.

Part 1 tells you the purpose of this study and what will happen to you if you take part. Part 2 gives you more detailed information about the conduct of the study.

Ask us if there is anything that is not clear or if you would like more information. Take time to decide whether or not you wish to take part.

PART 1

Outline explanation

It has been recommended by your heart doctor that you have a cardiac resynchronisation therapy (CRT) device implanted. This is a special kind of pacemaker that usually consists of 3 electrical leads which are placed in the heart to improve the way it beats. Although this type of pacemaker makes many people feel better, around a third of patients do not improve with this treatment in terms of their ability to exercise and quality of life.

What is the purpose of the study?

At present it is not clear which patients will get better after CRT. The aim of this study is to see if the measurements we take during heart scans can be used to make computer models of the heart which help us to predict who will improve with CRT.

Why have I been chosen?

You have been chosen to take part as you are eligible for CRT on the basis of our current guidelines.

Do I have to take part?

No. It is up to you to decide whether or not to take part. If you do, you will be given this information sheet to keep and be asked to sign a consent form at the time, or if you prefer once you have had chance to read the information, we will telephone you to ask any questions and then see if you still want to take part. You are still free to withdraw at any time, and do not need to give a reason. A decision to withdraw at any time, or a decision not to take part, will not affect the standard of care you receive.

What will happen to me if I take part?

You will be given a consent form to sign.

As part of your routine care before having CRT, you will be seen in the outpatient department. You will fill in a questionnaire, have a blood test, a urine test, a walking test, a bicycle test and an ultrasound scan of your heart called an echo scan. These tests are routine and take around 2 hrs in total. Some patients will be asked to raise their legs (supported by a cushion) for 5 minutes during the echo scan.

On the same day you will also have a scan called a magnetic resonance imaging (MRI) scan. This gives us further detailed information about the heart. The MRI scan involves lying still in a scanner for around an hour. The MRI does not involve X-rays and is part of the routine work-up for the type of pacemaker you are having.

Patients in Sheffield will also have the following tests performed:

1) A grip strength test. This gives us further information about the strength of your peripheral muscles e.g. forearm, in relation to your heart muscle. This involves gripping

a measuring device with your hand as hard as possible, maintained for about 5 seconds, with the best of 3 attempts recorded. There will be a rest of 30 seconds between each attempt. Taking around 5 minutes.

2) A measure of the blood flow in your brachial e.g. arm artery will also be recorded, this is called flow mediated dilatation. This is performed using an ultrasound probe e.g. without X-rays, looking at the diameter of your artery before and after the flow is stopped using a blood pressure cuff for a maximum of 5 minutes. This is then repeated again using a small tablet of Glyceryl Tri-Nitrate, a medication commonly used to treat angina attacks. This will be absorbed into your blood and will relax your blood vessels, causing them to widen and increasing the blood flow through them. The whole test will take around 40 minutes.

3) An indirect measure of the force of blood ejected from the heart, using a device called a force plate. This involves, standing, sitting and lying on a fixed platform, the force is recorded by the platform and requires no invasive measurements. This will take around 5-10 minutes. During the optimisation of your device only, the pacemaker settings will be altered, to see what effect this has on the force of your heart beat, before being returned to their optimum.

Once your CRT is implanted we would like to follow you up at 6 and 12 months with a repeat of the questionnaire, walking and cycling tests and echo scan of your heart. Sheffield patients will also have repeat blood and urine tests at these follow-ups. Some St Thomas' Hospital patients will have extra echo images taken at their 6 week and 3 month device checks.

This information will be used to develop computer models that may be helpful in the future for predicting which patients will get better with CRT.

How does this differ from "standard practice" i.e. routine care (if you were not to take part in the study)?

The assessment with the blood test, questionnaire, walking test, cycling test and echo scan before the CRT implant are all routine. The MRI scan is also part of our routine assessment for CRT.

In addition to routine care:

1) The echo scan before the CRT implant may be 10 minutes longer than usual

2) You will have a repeat questionnaire, walking test, cycling test and echo scan at 6 and 12 months after the CRT implant. Some St Thomas Hospital patients will have extra echo images taken at their 6 week and 3 month device checks. You would need to attend at these times even if you were not in a study to have your CRT device checked. Sheffield patients will also have repeat blood and urine tests, grip, force plate and blood flow tests at these follow-ups,

3) The MRI scan may take slightly longer than a standard scan.

What do I have to do?

You will need to have the routine tests which include the blood test, questionnaire, walking test, cycle test, echo scan and MRI prior to your CRT. You will then have your CRT implant. We will need to see you at 6 weeks and 3 months for a standard check of your CRT (this is not part of the research). We will also see you at 6 and 12 months after your CRT has been implanted to repeat the initial assessments (but not the MRI scan).

What is the procedure that is being tested?

We are looking at the electrical and mechanical function of the heart using echo and MRI. This allows us to develop computer models of the heart that we hope will help us to predict which patients are likely to get better with CRT.

What are the contraindications of taking part?

If carried out properly, MRI is harmless. We have safety procedures and well-trained staff to minimise any possible risks associated with the procedure. Because MRI uses a strong magnet, it is not safe for some people to be scanned. This includes people who have a heart pacemaker or some other types of metal in the body. You will be asked to fill in a screening form to make sure that you can have a MRI scan.

What are the possible disadvantages and risks of taking part?

The MRI scan may be uncomfortable as you need to lie flat for around an hour. Most people tolerate this procedure very well.

You may experience some discomfort such as pins and needles in your hand during the inflation of the blood pressure cuff for the brachial artery measurements, but this will

only be short lived and will cease as soon as the pressure is released. You may also experience some light headedness or headaches after taking the Glyceryl Tri-Nitrate tablet, again this will be short lived and is a common and transient side effect of the tablet. (Sheffield patients only).

You will be required to have more tests than usual at your follow-up appointments.

The radiation dose (26mSv) from having the CRT implanted is the same as if you do not take part in this research study. It is the about the same as 12 years of natural background radiation.

What are the possible benefits of taking part?

You will also have more detailed follow-up following your CRT implant.

You will receive the benefits of cardiovascular health screening.

What happens when the research study stops?

You will continue to have normal follow-up in clinic.

What if there is a problem?

Any complaint about the way you have been dealt with during the study or any possible harm you might suffer will be addressed. The detailed information on this is given in Part 2.

Will my taking part in the study be kept confidential?

Yes. All the information about your participation in this study will be kept confidential.

The details are included in Part 2.

Contact Details:

St Thomas' Hospital patients: Prof. Reza Razavi. St Thomas' Hospital, 4th Floor Lambeth Wing.

Telephone 02071885440

Sheffield patients: Dr Paul Sheridan, CVBRU, Northern General Hospital, Sheffield
Tel: (0)114 2714950).

This completes Part 1 of the Information Sheet.

If the information in Part 1 has interested you and you are considering participation, please continue to read the additional information in Part 2 before making any decision.

PART 2

What if relevant new information becomes available?

Sometimes during the course of a research project, new information becomes available about the procedure that is being studied. If this happens, your research doctor will tell you about it and discuss whether you want to or should continue in the study.

What will happen if I don't want to carry on with the study?

If you withdraw from the study, we will need to use the data collected up to your withdrawal. We will ask you to keep in contact with us to let us know your progress.

What if there is a problem?

Complaints: If you have a concern about any aspect of this study, you should ask to speak with the researchers who will do their best to answer your questions (St Thomas' Hospital patients: contact Prof. Reza Razavi on 02071885440 and Sheffield patients: contact Dr Paul Sheridan on (0)114 2714950). Should you wish to complain formally, you can do this through the NHS Complaints Procedure. Details can be obtained from the hospital.

Harm: In the event that you are harmed during the research study there are no special compensation arrangements. If you are harmed and this is due to someone's negligence then you may have grounds for a legal action for compensation against Guy' & St. Thomas' NHS Trust but you may have to pay your legal costs. The normal National Health Service complaints mechanisms will still be available to you.

Will my taking part in this study be kept confidential?

Procedures for handling, processing, storage and destruction of your data are compliant with the Data Protection Act 1998. All information which is collected about you during the course of the research will be kept strictly confidential. Any information about you which leaves the hospital will have your name and address removed so that you cannot be recognised from it. Your data will be collected from the referral letter and patient notes, as well from your oral information; Data will be automatically stored securely, in an encrypted format; Authorised persons such as researchers, regulatory authorities and Research and Development (for monitoring of

the quality of the research) will have access to these data; Data will be retained for 15 years.

What will happen to the results of the research study?

We aim to publish these in a research paper so as to advance the knowledge of echo, MRI and CRT. All patient identities are treated as strictly confidential and anonymous in any publication.

Who is organising and funding the research?

The research is organised by Prof Reza Razavi, St Thomas' Hospital, London and funded by the EPSRC Grand Challenge Project.

Who has reviewed the study?

The study has been independently reviewed by the St Thomas' Hospital Ethics Committee (Project Ref: 10/H0802/71).

A copy of the information sheet and a signed consent form to keep will be given to you.

Thank you for considering taking part in this study.

Protocol

Grand Challenge Modelling Project

Background & Rationale

Heart failure is a complex condition that despite advances in diagnosis and pharmacological treatments in the past two decades, continues to have significant morbidity and mortality. The incidence and prevalence of heart failure increases steeply with age. The average age of first diagnosis is 76yrs in the UK. The incidence of heart failure in the UK is 140 per 100,000 men and 120 per 100,000 women. Around 3% of people aged between 65-75years have heart failure. This increases to 7% of those aged 75-84 and 14% of those aged over 85years. Heart failure has a poor prognosis with about 40% of patients dying within 1 year of diagnosis [1].

Cardiac resynchronisation therapy (CRT) has revolutionised the treatment of heart failure. The aim of CRT is to improve the heart's pumping efficiency by resynchronising the pumping action of the chambers of the heart. Disruption of the usual sequence of ventricular activation is well recognised as a major factor in the development of heart failure in patients with both ischaemic and non-ischaemic aetiology. Delayed and dyssynchronous left ventricular (LV) contraction reduces myocardial efficiency, causes abnormal diastolic interaction between the ventricles and increases mitral regurgitation [2]. CRT pacing devices allow regulation of the atrioventricular delay and restoration of synchronous contraction by pacing the right atrium and both ventricles.

According to National Institute of Clinical Excellence (NICE) guidelines, patients should be considered for CRT if :

- i) They are currently experiencing or have recently experienced New York Heart Association (NYHA) class III-IV symptoms AND
- ii) They have a QRS duration of greater than 150ms on their ECG or a QRS duration of 120-149ms and mechanical dyssynchrony on echocardiography AND

iii) They have a LV ejection fraction (LVEF) less than 35%

There are numerous randomised control trials that show morbidity and mortality benefits with CRT (CARE HF, COMPANION, MIRACLE, MUSTIC-SR, CONTAK-CD). A recent review of CRT [3] summarized the current evidence base of the efficacy and safety of CRT in patients with LV dysfunction. This review found that CRT is a cost-effective therapy for patients with NYHA class III and IV heart failure combined with optimal medical management. CRT improves ventricular function, remodelling, symptoms, and exercise capacity, while reducing the frequency of heart failure hospitalization from 37% to 22% [2].

Despite these impressive results around 30% of patients do not derive clinical benefit from CRT despite meeting implant criteria [4]. Important effects on the functional status of the patient are difficult to quantify and very significant placebo effects can be seen with this type of intervention. Functional assessments therefore need to be performed in conjunction with less subjective measurements of ventricular performance and exercise capacity, including serial echocardiography, maximal oxygen uptake (V02 max) and six minute walk tests (6MWT).

Trials have demonstrated an overall mean increase in V02 max of approximately 1-2ml/kg/min, in exercise duration of 30-60 seconds, and in six minute walk test distances of 20-40 metres in patients undergoing CRT [5]. Echocardiographic data demonstrate a reduction in LV dimensions and reduced severity of mitral regurgitation.

Variability in response rates to CRT is due to the marked heterogeneity of the heart failure population as well as methods by which response is measured. Different aetiologies as well as varying degrees of dyssynchrony, burden and location of scar and ischaemia, arrhythmias, co-morbidity and baseline level of function all contribute.

The response to CRT is critically dependent upon pacing cardiac regions which can

maximally reduce left ventricular activation time and induce homogeneous left ventricular depolarisation [6]. To date, one of the major criteria used to determine patient suitability for CRT is by using the QRS duration as an indicator of dyssynchrony. This does not take into account all of the variables that decide whether a patient will respond to CRT.

Many methods have been researched with the aim of improving patient selection for CRT. It is important to identify “non-responder” patients and consider the possible underlying reasons. In practice this process will involve:

Improvements in the assessment of patients prior to CRT

Optimisation of pacing lead position

Optimisation of device programming

Patient Selection for CRT

Guidelines from the American Heart [7] and European society of Cardiology [8] recommend that CRT is indicated in patients with symptomatic heart failure despite optimal drug therapy, with evidence of dyssynchrony as defined by prolonged QRS duration on the surface ECG (>120ms), without requirement for echocardiographic evidence of dyssynchrony.

QRS duration as a predictor of electrical evidence of dyssynchrony is relatively insensitive in identifying patients who will benefit from CRT [9-10]. The surface ECG provides a relatively crude assessment of myocardial activation and may not show areas of localised delays which have important mechanical consequences.

We plan to investigate the mechanical, electrical and haemodynamic function of the LV in patients prior to their CRT implant by using echocardiography and cardiac magnetic resonance imaging. Developments in the functional imaging of the heart, in particular with respect to the measurement of electrical activity, deformation, flows

and fibre orientation provide data that can be used to develop biophysical models. Biophysical models are personalised computer-generated simulations that have been developed due to advances in recent years in imaging, image processing, computer hardware and simulation technology.

The aim is that biophysical models can be used for diagnosis as well as for the planning of interventions. While the scientific importance and enormous clinical potential for this computerised modelling have been acknowledged this has yet to be implemented in clinical practice.

Trial Objectives, Design and Statistics

Trial Objectives

To design biophysical models of left ventricular mechanical, electrical and haemodynamic function from data acquired from echocardiography and cardiac magnetic resonance imaging that can predict the mechanical, electrical and haemodynamic response to CRT.

Trial Design

Pre-assessment

Prior to patients having a CRT device implanted they will undergo a number of investigations during a pre-assessment clinic:

- i) An assessment of symptoms with a Minnesota Living with Heart Failure Questionnaire (MLWHFQ) and
- ii) 6MWT
- iii) A cardio-pulmonary exercise test (CPET) to assess VO₂ max.
- iv) Baseline blood tests (FBC, U&E, NT-proBNP).
- v) Echocardiography
- vi) Cardiac magnetic resonance (CMR)

These tests are validated and give baseline information about patients' prior to them having their implant. They also allow direct comparison of patient performance status pre and post implant. The pre-assessment with MLWHFQ, 6MWT, CPET and echocardiogram will take around 2hours.

The CMR will ideally be performed on the same day as the other pre-assessment tests. It gives further information about the function of the left ventricle. It also allows assessment of the left ventricle for scar tissue which may be a cause for patients not responding to CRT (6). The scan takes 60 to 90 minutes.

Cardiac Resynchronisation Therapy

The CRT device will be implanted at least 1 week after the pre-assessment tests. Implantation will be as per standard clinical practice.

Pre-discharge

Patients will have routine device checks prior to discharge.

6 week Check

Patients will undergo an echo-guided optimisation of their device at 6 weeks.

6 and 12 month Follow-up

We aim to follow-up patients at 6 months and 12 months. The follow-up appointments will involve the same assessments as the initial pre-assessment with a MLWHFQ, 6MWT, CPET, blood tests and repeat echocardiogram. These tests will be performed as an outpatient and will last around 2 hours.

These follow-up assessments will be compared to pre-CRT tests to determine whether patients have 'responded'.

End of Study

Data analysis is performed at the end of the study.

Response to CRT will be determined from:

Echo parameters – change in left end systolic volume (ESV), change in left ventricular ejection fraction (LVEF) and change in dyssynchrony measures.

Change in VO₂ max and 6MWT distance

Change in MLWHFQ score

After 12 months, patients will have standard cardiology out-patient follow-up.

ST THOMAS HOSPITAL ONLY SUBSETS

Frank Starling Law Subset

In a subset of up to 20 patients we will spend an extra 10 minutes during their pre-assessment echocardiogram determining each patient's haemodynamic response to a passive leg-raise (PLR) test. This will involve measuring an echo parameter (Aortic VTI) at baseline, 5 minutes after raising the patient's legs to a 45° angle to the body and then again 5 minutes after lowering their legs. It has been shown that the change in aortic VTI when performing PLR in critically ill patients predicts their response to a fluid challenge. We hypothesize that a positive response to a fluid challenge requires an intact Frank Starling mechanism. We further hypothesize that only patients with an intact Frank Starling mechanism as determined by a 12.5% increase in stroke volume (measured using aortic VTI) in response to PLR will respond to CRT [11-12].

Extra Imaging Subset

In a subset of up to 10 patients we will spend an extra 5 minutes during their 6 week optimisation echo taking extra images. In the same subset we will also bring them back at 3 months post-implant to repeat their echocardiogram. The extra echo images in this subset will allow our computer modellers to gain even more detailed data on how the heart remodels after CRT. This in turn should allow them to predict with even more accuracy how an individual heart will respond to biventricular pacing.

SHEFFIELD HOSPITAL ONLY SUBSET

In a subset of 20 patients we will be conducting several extra tests.

In addition to the blood tests mentioned below, at Pre-Assessment and 12 months

follow-up, we will also be analysing the same samples for Uric Acid, Thyroid Function, Liver Function, high sensitive CRP, Troponin T, Parathyroid Function, Vitamin D and a urine test for Microalbumin. These have all been identified as predictors of morbidity and mortality in heart failure and thus we hypothesise they will help to predict response to CRT. The blood tests will be using the samples already taken and a first morning urine will be collected by the patients and brought to the clinic, at pre-assessment and 12 months follow-up, taking only 5 minutes. [13-20]

Patients with heart failure have impaired vascular endothelial function, this not only predicts mortality but also response to CRT. Thus, we feel performing Flow Mediated Dilatation, as a marker of vascular health, will greatly inform the model. This will be measured at pre-assessment, 6 months and at 12 months follow-up and will take around 40 minutes. It will involve the patient arriving fasted (for 8-12 hours), kept in a temperature controlled room for 10 minutes for equilibration, the brachial artery is then imaged (non-invasively) using an ultrasound probe with ECG monitoring pre and post occlusion with a pneumatic tourniquet for 5 minutes, at 50mmHg above systolic (maximum) blood pressure. The patient is then allowed to rest for 20 minutes before the procedure is repeated following administration of sub-lingual Glyceryl Tri-Nitrate [21-24].

Patients with end-stage heart failure develop cardiac cachexia, it is not just a loss of muscle mass but it is an alteration in strength, fibre type, metabolism, mitochondria and hyperaemia. We believe that once grip strength is impaired this may indicate a heart failure that will not respond to CRT as it is advanced and thus measurement of this prior to CRT will enable us to predict response [25-28].

Ballistocardiography, is investigation of cardiac haemodynamics by non-invasive and indirect measurements using a force plate. This involves a patient standing, sitting and lying on a plate, calibrated to measure small forces, such as those produced by the resting heart. We propose that such measurement is a novel and useful adjunct into predicting patient response to CRT. These are routine parameter changes, which are safe and well tolerated. [29]

Primary Endpoint

Do the biophysical models created from pre-implant echo and CMR data predict who will respond to CRT? Response to CRT will be determined by change in ESV, LVEF, VO2 max, 6MWT distance and MLWHFQ score.

Trial Statistics

Assuming a 65% 'responder' rate to CRT, a sample size of 50 would give a 95% confidence interval plus/minus 17% for sensitivity and plus/minus 23% for specificity assuming a worst case scenario where the computer models perform no better than chance (ie sensitivity and specificity = 50%) at predicting who will 'respond'.

Sample Size

50 patients in the UK.

Patients

Inclusion Criteria

> 18 years of age

Patients that clinically require cardiac resynchronisation therapy.

Heart failure with NYHA Class III-IV symptoms despite optimal medical therapy

LVEF < 35%

QRS duration > 150ms or

QRS duration 120-149ms with echocardiographic evidence of dyssynchrony

Exclusion Criteria

Contraindication to CMR scan

Pregnancy

Claustrophobia

ICD/Pacemaker

Severe Renal Impairment (GFR < 30)

Ethics & Regulatory Approvals

The trial will be conducted in compliance with the principles of the Declaration of Helsinki October 2008, the principles of GCP and all of the applicable regulatory requirements.

Quality Assurance, Data Handling, Publication Policy and Finance

Quality assurance will be maintained by Trust Clinical and Research Governance. Data protection will be maintained according to Trust Guidelines. The Research Unit will comply with all aspects of the Data Protection Act 1998. All information collected during the course of the study will be kept strictly confidential. Information will be held securely on paper and electronically at the Research Unit, which includes appropriate storage, restricted access and disposal arrangements of patient personal clinical details. Electronic transfer of data will be encrypted.

References:

1. Barnett D, Phillips S, Longson C. Cardiac resynchronisation therapy for the treatment of heart failure: NICE technology appraisal guidance. *Heart*, 93(9), 1134-1135 (2007).
2. Abraham WT, Hayes DL. Cardiac resynchronization therapy for heart failure. *Circulation*, 108(21), 2596-2603 (2003).
3. Mcalister F, Ezekowitz J, Hooton N et al. Cardiac Resynchronization Therapy for Patients With Left Ventricular Systolic Dysfunction: A Systematic Review. *JAMA: The Journal of the American Medical Association*, 297(22), 2502-2514 (2007).
4. Fox D. Optimisation of cardiac resynchronisation therapy: addressing the problem of "non-responders". *Heart*, 91(8), 1000-1002 (2005).
5. Saxon L. Resynchronization Therapy for the Treatment of Heart Failure. *Circulation*, 108(9), 1044-1048 (2003).
6. Lambiase P. Non-contact left ventricular endocardial mapping in cardiac resynchronisation therapy. *Heart*, 90(1), 44-51 (2004).
7. Strickberger SA, Conti J, Daoud EG et al. Patient selection for cardiac resynchronization therapy: from the Council on Clinical Cardiology Subcommittee on Electrocardiography and Arrhythmias and the Quality of Care and Outcomes Research Interdisciplinary Working Group, in collaboration with the Heart Rhythm Society. *Circulation*, 111(16), 2146-2150 (2005).
8. Vardas P, Auricchio A, Blanc J et al. Guidelines for cardiac pacing and cardiac resynchronization therapy: The Task Force for Cardiac Pacing and Cardiac Resynchronization Therapy of the European Society of Cardiology. Developed in Collaboration with the European Heart Rhythm Association. *European Heart Journal*, 28(18), 2256-2295 (2007).

9. Pitzalis MV, Iacoviello M, Romito R et al. Cardiac resynchronization therapy tailored by echocardiographic evaluation of ventricular asynchrony. *Journal of the American College of Cardiology*, 40(9), 1615-1622 (2002).
10. Reuter S, Garrigue S, Barold SS et al. Comparison of characteristics in responders versus nonresponders with biventricular pacing for drug-resistant congestive heart failure. *Am J Cardiol*, 89(3), 346-350 (2002).
11. Lamia B, Ochagavia A, Monnet X et al. Echocardiographic prediction of volume responsiveness in critically ill patients with spontaneously breathing activity. *Intensive Care Med*, 33(7), 1125-1132 (2007).
12. Cavallaro F, Sandroni C, Marano C et al. Diagnostic accuracy of passive leg raising for prediction of fluid responsiveness in adults: systematic review and meta-analysis of clinical studies. *Intensive Care Med*, 36(9), 1475-1483 (2010).
13. Kim H, Shin HW, Son J, Yoon HJ, Park HS, Cho YK, et al. Uric Acid as prognostic marker in advanced nonischemic dilated cardiomyopathy: comparison with N-terminal pro B-type natriuretic peptide level. *Congest Heart Fail*;16(4):153-8.
14. Pingitore A, Landi P, Taddei MC, Ripoli A, L'Abbate A, Iervasi G. Triiodothyronine levels for risk stratification of patients with chronic heart failure. *Am J Med* 2005;118(2):132-6.
15. Iacoviello M, Guida P, Guastamacchia E, Triggiani V, Forleo C, Catanzaro R, et al. Prognostic role of sub-clinical hypothyroidism in chronic heart failure outpatients. *Curr Pharm Des* 2008;14(26):2686-92.
16. Butler J, Kalogeropoulos A, Georgiopoulos V, Belue R, Rodondi N, Garcia M, et al. Incident heart failure prediction in the elderly: the health ABC heart failure score. *Circ Heart Fail* 2008;1(2):125-33.
17. Yin WH, Chen JW, Jen HL, Chiang MC, Huang WP, Feng AN, et al. Independent prognostic value of elevated high-sensitivity C-reactive protein in chronic heart failure. *Am Heart J* 2004;147(5):931-8.
18. Vazquez R, Bayes-Genis A, Cygankiewicz I, Pascual-Figal D, Grigorian-Shamagian L, Pavon R, et al. The MUSIC Risk score: a simple method for predicting mortality in ambulatory patients with chronic heart failure. *Eur Heart J* 2009;30(9):1088-96.
19. Jackson CE, Solomon SD, Gerstein HC, Zetterstrand S, Olofsson B, Michelson EL, et al. Albuminuria in chronic heart failure: prevalence and prognostic importance. *Lancet* 2009;374(9689):543-50.

20. Sugimoto T, Tanigawa T, Onishi K, Fujimoto N, Matsuda A, Nakamori S et al. Serum intact parathyroid hormone levels predict hospitalisation for heart failure. *Heart* 2009; 95(5): 395-398.
21. Akar JG, Al-Chekakie MO, Fugate T, Moran L, Froloshki B, Varma N, et al. Endothelial dysfunction in heart failure identifies responders to cardiac resynchronization therapy. *Heart Rhythm* 2008;5(9):1229-35.
22. Shechter M, Matetzky S, Arad M, Feinberg MS, Freimark D. Vascular endothelial function predicts mortality risk in patients with advanced ischaemic chronic heart failure. *Eur J Heart Fail* 2009;11(6):588-93.
23. Kubo SH, Rector TC, Williams RE, et al. Endothelium dependent vasodilation is attenuated in patients with heart failure. *Circulation*. 1991;84:1589–1596
24. Corretti, M. C., T. J. Anderson, et al. "Guidelines for the ultrasound assessment of endothelial-dependent flow-mediated vasodilation of the brachial artery: A report of the International Brachial Artery Reactivity Task Force." *JACC* 2002. 39(2): 257-265
25. Mancini DM, Walter G, Reichek N, Lenkinski R, McCully KK, Mullen JL, et al. Contribution of skeletal muscle atrophy to exercise intolerance and altered muscle metabolism in heart failure. *Circulation* 1992;85(4):1364-73.
26. Opasich C, Ambrosino N, Felicetti G, Aquilani R, Pasini E, Bergitto D, et al. Heart failure-related myopathy. Clinical and pathophysiological insights. *Eur Heart J* 1999;20(16):1191-200.
27. Sullivan MJ, Green HJ, Cobb FR. Skeletal muscle biochemistry and histology in ambulatory patients with long-term heart failure. *Circulation* 1990; 81(2):518-27.
28. Mettauer B, Zoll J, Sanchez H, Lampert E, Ribera F, Veksler V, et al. Oxidative capacity of skeletal muscle in heart failure patients versus sedentary or active control subjects. *J Am Coll Cardiol* 2001;38(4):947-54.
29. Sunnerhagen KS, Cider A, Schaufelberger M, Hedberg M, Grimby G. Muscular performance in heart failure. *J Card Fail* 1998;4(2):97-104.
30. Kriz J, Seba, P. Force plate monitoring of human haemodynamics. *Nonlinear Biomed Phys* 2008; 2(1):1.

Consent form

Study Title
Grand Challenge Modeling Project
Study Code
10/H0802/71

Please initial box

I confirm that I have read and understand the information sheet dated 1st January 2011 for the above study and have had the opportunity to ask questions.

I understand that my participation is voluntary and that I am free to withdraw at any time, without giving any reason, without my medical care or legal rights being affected.

I understand that sections of any of my medical notes may be looked at by responsible individuals from regulatory authorities where it is relevant to my taking part in research. I give permission for these individuals to have access to my records. I have been informed that the data concerning me will be computerised and that I have the right to access these data and to rectify them. I agree to the anonymised data collected being used for scientific communications.

I agree to my GP being informed of my participation in this study and to any feedback of information from my GP.

I agree to take part in the above study.

_____ Name of patient	_____ Date (DD/MM/YY)	_____ Signature
_____ Name of person taking consent (if different from investigator)	_____ Date (DD/MM/YY)	_____ Signature
_____ Name of investigator	_____ Date (DD/MM/YY)	_____ Signature

3 copies required: → one for the patient → one for the investigator → one for patient notes

Grand Challenge 1st January 2011. Version 3.0

Letter of invitation



**Research Study:
STH15700
The Grand Challenge**

Modelling Project

Professor Rod Hose and Dr Paul J Sheridan

An Invitation on behalf of the Academic Unit of Cardiovascular Medicine and Medical Physics

Dear

You have received an appointment to attend the Pre-assessment Clinic before you are admitted for Cardiac Resynchronisation Therapy (CRT) with the department of cardiology at the Northern General Hospital, Sheffield. This department is part of the Sheffield Teaching Hospitals Foundation Trust which supports clinical research to enhance the understanding of diseases and improve the treatment of patients.

During your attendance at the pre-assessment clinic you may be asked to consider taking part in the previously mentioned clinical study aimed at modeling the heart and so predicting response to CRT. I can assure you that whether you decide to take part or not will have no affect on your clinical treatment or management. Before you decide to take part you will require more information about the study and to understand what is involved.

A consultant cardiologist will be able to explain the research study to you before you make a decision.

Yours Sincerely

Dr Paul J Sheridan MB ChB PhD MRCP

GP letter



Date

Dear Dr

Re:

.....

The Grand Challenge Modelling Project STH15700

I am writing to inform you that your patient has been enrolled into the above research study.

The purpose of the study is to determine whether we can predict response to CRT (cardiac synchronisation therapy) for patients with severe heart failure (NYHA 3-4). As such, the patients will all be receiving a more detailed assessment before and after CRT implantation, including blood tests, quality of life questionnaire, exercise tests, cMR and 3D echo, this will take place over a 12 month period.

We are not testing any new devices or drug therapies, rather using the information gathered above to construct a 3D model of the heart in heart failure and then with CRT in situ.

We hope this will allow us to more accurately choose patients suitable for CRT.

If you have any questions regarding any of the above, please feel free to contact me on 0114 2434343 ext 66776.

Yours sincerely

Dr Paul J Sheridan
Consultant Cardiologist and Electrophysiologist
South Yorkshire Cardiac Centre
Northern General Hospital
Sheffield

References

1. British Heart Foundation Cardiovascular Disease Statistics [Available from: <https://www.bhf.org.uk/publications/statistics/cvd-stats-2015>].
2. Effects of enalapril on mortality in severe congestive heart failure. Results of the Cooperative North Scandinavian Enalapril Survival Study (CONSENSUS). The CONSENSUS Trial Study Group. *N Engl J Med* 1987;316(23):1429-35.
3. Gillum RF. Epidemiology of heart failure in the United States. *Am Heart J* 1993;126(4):1042-7.
4. Butter C, Auricchio A, Stellbrink C, et al. Effect of resynchronization therapy stimulation site on the systolic function of heart failure patients. *Circulation* 2001;104(25):3026-9.
5. Nelson G, Berger R, Fetters B, et al. Left ventricular or biventricular pacing improves cardiac function at diminished energy cost in patients with dilated cardiomyopathy and left bundle-branch block. *Circulation* 2000;102(25):3053 - 59.
6. Bristow M, Saxon L, Boehmer J, et al. Cardiac-resynchronization therapy with or without an implantable defibrillator in advanced chronic heart failure. *N Engl J Med* 2004;350:2140 - 50.
7. Sermesant M, Chabiniok R, Chinchapatnam P, et al. Patient-specific electromechanical models of the heart for the prediction of pacing acute effects in CRT: a preliminary clinical validation. *Med Image Anal* 2012;16(1):201-15.
8. Dickstein K, Cohen-Solal A, Filippatos G, et al. ESC Guidelines for the diagnosis and treatment of acute and chronic heart failure 2008. The Task Force for the Diagnosis and Treatment of Acute and Chronic Heart Failure 2008 of the European Society of Cardiology. Developed in collaboration with the Heart Failure Association of the ESC (HFA) and endorsed by the European Society of Intensive Care Medicine (ESICM). *Eur Heart J* 2008;29:2388 - 442.
9. Davies M, Hobbs F, Davis R, et al. Prevalence of left-ventricular systolic dysfunction and heart failure in the Echocardiographic Heart of England Screening study: a population based study. *Lancet* 2001;358(9280):439-44.
10. Murphy NF, Simpson CR, McAlister FA, et al. National survey of the prevalence, incidence, primary care burden, and treatment of heart failure in Scotland. *Heart* 2004;90(10):1129-36.

11. Cowie MR, Wood DA, Coats AJ, et al. Incidence and aetiology of heart failure; a population-based study. *Eur Heart J* 1999;20(6):421-8.
12. McDonagh TA, Morrison CE, Lawrence A, et al. Symptomatic and asymptomatic left-ventricular systolic dysfunction in an urban population. *Lancet* 1997;350(9081):829-33.
13. Stewart S, MacIntyre K, Capewell S, et al. Heart failure and the aging population: an increasing burden in the 21st century? *Heart* 2003;89(1):49-53.
14. Hobbs FD, Roalfe AK, Davis RC, et al. Prognosis of all-cause heart failure and borderline left ventricular systolic dysfunction: 5 year mortality follow-up of the Echocardiographic Heart of England Screening Study (ECHOES). *Eur Heart J* 2007;28(9):1128-34.
15. Najafi F, Jamrozik K, Dobson AJ. Understanding the 'epidemic of heart failure': a systematic review of trends in determinants of heart failure. *Eur J Heart Fail* 2009;11(5):472-9.
16. Khand AU, Shaw M, Gemmel I, et al. Do discharge codes underestimate hospitalisation due to heart failure? Validation study of hospital discharge coding for heart failure. *Eur J Heart Fail* 2005;7(5):792-7.
17. Morgan S, Smith H, Simpson I, et al. Prevalence and clinical characteristics of left ventricular dysfunction among elderly patients in general practice setting: cross sectional survey. *BMJ* 1999;318(7180):368-72.
18. Hellermann JP, Jacobsen SJ, Gersh BJ, et al. Heart failure after myocardial infarction: a review. *Am J Med* 2002;113(4):324-30.
19. Blackledge HM, Tomlinson J, Squire IB. Prognosis for patients newly admitted to hospital with heart failure: survival trends in 12 220 index admissions in Leicestershire 1993-2001. *Heart* 2003;89(6):615-20.
20. Bourassa MG, Gurne O, Bangdiwala SI, et al. Natural history and patterns of current practice in heart failure. The Studies of Left Ventricular Dysfunction (SOLVD) Investigators. *J Am Coll Cardiol* 1993;22(4 Suppl A):14A-19A.
21. Goldacre MJ, Mant D, Duncan M, et al. Mortality from heart failure in an English population, 1979-2003: study of death certification. *J Epidemiol Community Health* 2005;59(9):782-4.
22. Sutcliffe S, Phillips C, Watson D, et al. Trends in heart failure mortality in England and Wales since 1950. *Eur J Intern Med* 2007;18(8):576-80.

23. Mehta PA, Dubrey SW, McIntyre HF, et al. Improving survival in the 6 months after diagnosis of heart failure in the past decade: population-based data from the UK. *Heart* 2009;95(22):1851-6.
24. Unal B, Critchley JA, Capewell S. Explaining the decline in coronary heart disease mortality in England and Wales between 1981 and 2000. *Circulation* 2004;109(9):1101-7.
25. Keeley EC, Boura JA, Grines CL. Primary angioplasty versus intravenous thrombolytic therapy for acute myocardial infarction: a quantitative review of 23 randomised trials. *Lancet* 2003;361(9351):13-20.
26. Roger VL, Go AS, Lloyd-Jones DM, et al. Heart disease and stroke statistics--2011 update: a report from the American Heart Association. *Circulation* 2011;123(4):e18-e209.
27. Jencks SF, Williams MV, Coleman EA. Rehospitalizations among patients in the Medicare fee-for-service program. *N Engl J Med* 2009;360(14):1418-28.
28. Rutledge T, Reis VA, Linke SE, et al. Depression in heart failure a meta-analytic review of prevalence, intervention effects, and associations with clinical outcomes. *J Am Coll Cardiol* 2006;48(8):1527-37.
29. Shavers-Hornaday VL, Lynch CF, Burmeister LF, et al. Why are African Americans under-represented in medical research studies? Impediments to participation. *Ethn Health* 1997;2(1-2):31-45.
30. Taylor AL, Ziesche S, Yancy C, et al. Combination of isosorbide dinitrate and hydralazine in blacks with heart failure. *N Engl J Med* 2004;351(20):2049-57.
31. Sosin MD, Bhatia GS, Zarifis J, et al. An 8-year follow-up study of acute admissions with heart failure in a multiethnic population. *Eur J Heart Fail* 2004;6(5):669-72.
32. Lip G, Zarifis J, Beevers DG. Acute admissions with heart failure to a district general hospital serving a multiracial population. *Int J Clin Pract* 1997;51(4):223-7.
33. Cruickshank JK, Beevers DG, Osbourne VL, et al. Heart attack, stroke, diabetes, and hypertension in West Indians, Asians, and whites in Birmingham, England. *Br Med J* 1980;281(6248):1108.
34. Lip GY, Khan H, Bhatnagar A, et al. Ethnic differences in patient perceptions of heart failure and treatment: the West Birmingham heart failure project. *Heart* 2004;90(9):1016-9.

35. Martinez-Selles M, Garcia Robles JA, Prieto L, et al. Systolic dysfunction is a predictor of long term mortality in men but not in women with heart failure. *Eur Heart J* 2003;24(22):2046-53.
36. Ghali JK, Krause-Steinrauf HJ, Adams KF, et al. Gender differences in advanced heart failure: insights from the BEST study. *J Am Coll Cardiol* 2003;42(12):2128-34.
37. O'Meara E, Clayton T, McEntegart MB, et al. Sex differences in clinical characteristics and prognosis in a broad spectrum of patients with heart failure: results of the Candesartan in Heart failure: Assessment of Reduction in Mortality and morbidity (CHARM) program. *Circulation* 2007;115(24):3111-20.
38. Nieminen MS, Harjola VP, Hochadel M, et al. Gender related differences in patients presenting with acute heart failure. Results from EuroHeart Failure Survey II. *Eur J Heart Fail* 2008;10(2):140-8.
39. Cohn JN, Tognoni G. A randomized trial of the angiotensin-receptor blocker valsartan in chronic heart failure. *N Engl J Med* 2001;345(23):1667-75.
40. Pitt B, Remme W, Zannad F, et al. Eplerenone, a selective aldosterone blocker, in patients with left ventricular dysfunction after myocardial infarction. *N Engl J Med* 2003;348(14):1309-21.
41. Komajda M, Follath F, Swedberg K, et al. The EuroHeart Failure Survey programme - a survey on the quality of care among patients with heart failure in Europe. Part 2: treatment. *Eur Heart J* 2003;24(5):464-74.
42. Hsich EM, Pina IL. Heart failure in women: a need for prospective data. *J Am Coll Cardiol* 2009;54(6):491-8.
43. Zareba W, Moss AJ, Jackson Hall W, et al. Clinical course and implantable cardioverter defibrillator therapy in postinfarction women with severe left ventricular dysfunction. *J Cardiovasc Electrophysiol* 2005;16(12):1265-70.
44. Cleland J, Daubert J, Erdmann E, et al. The effect of cardiac resynchronization on morbidity and mortality in heart failure. *N Engl J Med* 2005;352:1539 - 49.
45. Saxon LA, De Marco T, Schafer J, et al. Effects of long-term biventricular stimulation for resynchronization on echocardiographic measures of remodeling. *Circulation* 2002;105(11):1304-10.
46. Stellbrink C, Breithardt OA, Franke A, et al. Impact of cardiac resynchronization therapy using hemodynamically optimized pacing on left ventricular remodeling in

patients with congestive heart failure and ventricular conduction disturbances. *J Am Coll Cardiol* 2001;38(7):1957-65.

47. Kuhlkamp V. Initial experience with an implantable cardioverter-defibrillator incorporating cardiac resynchronization therapy. *J Am Coll Cardiol* 2002;39(5):790-7.

48. Cazeau S, Leclercq C, Lavergne T, et al. Effects of multisite biventricular pacing in patients with heart failure and intraventricular conduction delay. *N Engl J Med* 2001;344:873 - 80.

49. Young JB, Abraham WT, Smith AL, et al. Combined cardiac resynchronization and implantable cardioversion defibrillation in advanced chronic heart failure: the MIRACLE ICD Trial. *JAMA : the journal of the American Medical Association* 2003;289(20):2685-94.

50. Fox KF, Cowie MR, Wood DA, et al. Coronary artery disease as the cause of incident heart failure in the population. *Eur Heart J* 2001;22(3):228-36.

51. Maggioni AP, Dahlstrom U, Filippatos G, et al. EURObservational Research Programme: the Heart Failure Pilot Survey (ESC-HF Pilot). *Eur J Heart Fail* 2010;12(10):1076-84.

52. Fonarow GC, Abraham WT, Albert NM, et al. Influence of beta-blocker continuation or withdrawal on outcomes in patients hospitalized with heart failure: findings from the OPTIMIZE-HF program. *J Am Coll Cardiol* 2008;52(3):190-9.

53. Mozaffarian D, Anker SD, Anand I, et al. Prediction of mode of death in heart failure: the Seattle Heart Failure Model. *Circulation* 2007;116(4):392-8.

54. Baldasseroni S, Opasich C, Gorini M, et al. Left bundle-branch block is associated with increased 1-year sudden and total mortality rate in 5517 outpatients with congestive heart failure: a report from the Italian network on congestive heart failure. *Am Heart J* 2002;143(3):398-405.

55. Packer M, Poole-Wilson PA, Armstrong PW, et al. Comparative effects of low and high doses of the angiotensin-converting enzyme inhibitor, lisinopril, on morbidity and mortality in chronic heart failure. ATLAS Study Group. *Circulation* 1999;100(23):2312-8.

56. Mair FS, Crowley TS, Bundred PE. Prevalence, aetiology and management of heart failure in general practice. *Br J Gen Pract* 1996;46(403):77-9.

57. McMurray JJ, Stewart S. Epidemiology, aetiology, and prognosis of heart failure. *Heart* 2000;83(5):596-602.

58. Killip T, 3rd, Kimball JT. Treatment of myocardial infarction in a coronary care unit. A two year experience with 250 patients. *Am J Cardiol* 1967;20(4):457-64.
59. Maisel AS, Krishnaswamy P, Nowak RM, et al. Rapid measurement of B-type natriuretic peptide in the emergency diagnosis of heart failure. *N Engl J Med* 2002;347(3):161-7.
60. Starling EH, Visscher MB. The regulation of the energy output of the heart. *J Physiol* 1927;62(3):243-61.
61. Schwinger RH, Bohm M, Koch A, et al. The failing human heart is unable to use the Frank-Starling mechanism. *Circ Res* 1994;74(5):959-69.
62. Hobbs A, Foster P, Prescott C, et al. Natriuretic peptide receptor-C regulates coronary blood flow and prevents myocardial ischemia/reperfusion injury: novel cardioprotective role for endothelium-derived C-type natriuretic peptide. *Circulation* 2004;110(10):1231-5.
63. Del Ry S, Passino C, Maltinti M, et al. C-type natriuretic peptide plasma levels increase in patients with chronic heart failure as a function of clinical severity. *Eur J Heart Fail* 2005;7(7):1145-8.
64. Aghel A, Tang WH. Tolvaptan: the evidence for its therapeutic value in acute heart failure syndrome. *Core Evid* 2008;3(1):31-43.
65. Anand I, McMurray J, Cohn JN, et al. Long-term effects of darusentan on left-ventricular remodelling and clinical outcomes in the EndothelinA Receptor Antagonist Trial in Heart Failure (EARTH): randomised, double-blind, placebo-controlled trial. *Lancet* 2004;364(9431):347-54.
66. Fischer D, Rossa S, Landmesser U, et al. Endothelial dysfunction in patients with chronic heart failure is independently associated with increased incidence of hospitalization, cardiac transplantation, or death. *Eur Heart J* 2005;26(1):65-9.
67. Farquharson CA, Butler R, Hill A, et al. Allopurinol improves endothelial dysfunction in chronic heart failure. *Circulation* 2002;106(2):221-6.
68. Kobayashi N, Tsuruya Y, Iwasawa T, et al. Exercise training in patients with chronic heart failure improves endothelial function predominantly in the trained extremities. *Circ J* 2003;67(6):505-10.
69. Pingitore A, Landi P, Taddei MC, et al. Triiodothyronine levels for risk stratification of patients with chronic heart failure. *The American journal of medicine* 2005;118(2):132-36.

70. Sugimoto T, Tanigawa T, Onishi K, et al. Serum intact parathyroid hormone levels predict hospitalisation for heart failure. *Heart* 2009;95(5):395-98.
71. Anker SD, Clark AL, Teixeira MM, et al. Loss of bone mineral in patients with cachexia due to chronic heart failure. *Am J Cardiol* 1999;83(4):612-5, A10.
72. Guazzi M, Pontone G, Brambilla R, et al. Alveolar--capillary membrane gas conductance: a novel prognostic indicator in chronic heart failure. *Eur Heart J* 2002;23(6):467-76.
73. Schaufelberger M, Eriksson BO, Grimby G, et al. Skeletal muscle alterations in patients with chronic heart failure. *Eur Heart J* 1997;18(6):971-80.
74. Mancini DM, Walter G, Reichel N, et al. Contribution of skeletal muscle atrophy to exercise intolerance and altered muscle metabolism in heart failure. *Circulation* 1992;85(4):1364-73.
75. Opasich C, Ambrosino N, Felicetti G, et al. Heart failure-related myopathy. Clinical and pathophysiological insights. *Eur Heart J* 1999;20(16):1191-200.
76. Sullivan MJ, Green HJ, Cobb FR. Skeletal muscle biochemistry and histology in ambulatory patients with long-term heart failure. *Circulation* 1990;81(2):518-27.
77. Hambrecht R, Fiehn E, Yu J, et al. Effects of endurance training on mitochondrial ultrastructure and fiber type distribution in skeletal muscle of patients with stable chronic heart failure. *J Am Coll Cardiol* 1997;29(5):1067-73.
78. Mettaufer B, Zoll J, Sanchez H, et al. Oxidative capacity of skeletal muscle in heart failure patients versus sedentary or active control subjects. *J Am Coll Cardiol* 2001;38(4):947-54.
79. Wilson JR, Martin JL, Schwartz D, et al. Exercise intolerance in patients with chronic heart failure: role of impaired nutritive flow to skeletal muscle. *Circulation* 1984;69(6):1079-87.
80. Meyer FJ, Borst MM, Zugck C, et al. Respiratory muscle dysfunction in congestive heart failure: clinical correlation and prognostic significance. *Circulation* 2001;103(17):2153-8.
81. Jackson CE, Solomon SD, Gerstein HC, et al. Albuminuria in chronic heart failure: prevalence and prognostic importance. *Lancet* 2009;374(9689):543-50.
82. Kim H, Shin HW, Son J, et al. Uric Acid as prognostic marker in advanced nonischemic dilated cardiomyopathy: comparison with N-terminal pro B-type natriuretic peptide level. *Congest Heart Fail* 2010;16(4):153-8.

83. Yin W-H, Chen J-W, Jen H-L, et al. Independent prognostic value of elevated high-sensitivity C-reactive protein in chronic heart failure. *American heart journal* 2004;147(5):931-38.
84. Martos R, Baugh J, Ledwidge M, et al. Diastolic heart failure: evidence of increased myocardial collagen turnover linked to diastolic dysfunction. *Circulation* 2007;115(7):888-95.
85. Watanabe J, Levine MJ, Bellotto F, et al. Left ventricular diastolic chamber stiffness and intramyocardial coronary capacitance in isolated dog hearts. *Circulation* 1993;88(6):2929-40.
86. Yu C-M, Hayes DL, Auricchio A. *Cardiac Resynchronisation Therapy*. 2nd ed. Oxford: Blackwell Publishing, 2008.
87. Myerburg RJ, Nilsson K, Gelband H. Physiology of canine intraventricular conduction and endocardial excitation. *Circ Res* 1972;30(2):217-43.
88. Durrer D, van Dam RT, Freud GE, et al. Total excitation of the isolated human heart. *Circulation* 1970;41(6):899-912.
89. Verheule S, Wilson E, Everett Tt, et al. Alterations in atrial electrophysiology and tissue structure in a canine model of chronic atrial dilatation due to mitral regurgitation. *Circulation* 2003;107(20):2615-22.
90. Cheng S, Keyes MJ, Larson MG, et al. Long-term outcomes in individuals with prolonged PR interval or first-degree atrioventricular block. *JAMA : the journal of the American Medical Association* 2009;301(24):2571-7.
91. Park S-J, On YK, Byeon K, et al. Short- and long-term outcomes depending on electrical dyssynchrony markers in patients presenting with acute heart failure: Clinical implication of the first-degree atrioventricular block and QRS prolongation from the Korean Heart Failure registry. *American heart journal* 2013;165(1):57-64.e2.
92. Bussink BE, Holst AG, Jespersen L, et al. Right bundle branch block: prevalence, risk factors, and outcome in the general population: results from the Copenhagen City Heart Study. *Eur Heart J* 2013;34(2):138-46.
93. Eriksson P, Hansson PO, Eriksson H, et al. Bundle-branch block in a general male population: the study of men born 1913. *Circulation* 1998;98(22):2494-500.
94. Hawkins NM, Wang D, McMurray JJV, et al. Prevalence and prognostic impact of bundle branch block in patients with heart failure: Evidence from the CHARM programme. *European Journal of Heart Failure* 2007;9(5):510-17.

95. Ghio S, Constantin C, Klersy C, et al. Interventricular and intraventricular dyssynchrony are common in heart failure patients, regardless of QRS duration. *Eur Heart J* 2004;25(7):571-8.
96. Emkanjoo Z, Esmailzadeh M, Mohammad Hadi N, et al. Frequency of inter- and intraventricular dyssynchrony in patients with heart failure according to QRS width. *Europace : European pacing, arrhythmias, and cardiac electrophysiology : journal of the working groups on cardiac pacing, arrhythmias, and cardiac cellular electrophysiology of the European Society of Cardiology* 2007;9(12):1171-6.
97. Cazeau S, Bordachar P, Jauvert G, et al. Echocardiographic Modeling of Cardiac Dyssynchrony Before and During Multisite Stimulation: A Prospective Study. *Pacing and Clinical Electrophysiology* 2003;26(1p2):137-43.
98. Pitzalis M, Iacoviello M, Romito R, et al. Cardiac resynchronization therapy tailored by echocardiographic evaluation of ventricular asynchrony. *J Am Coll Cardiol* 2002;40:1615 - 22.
99. Chung ES, Leon AR, Tavazzi L, et al. Results of the Predictors of Response to CRT (PROSPECT) Trial. *Circulation* 2008;117(20):2608-16.
100. Seo Y, Ishizu T, Sakamaki F, et al. Mechanical Dyssynchrony Assessed by Speckle Tracking Imaging as a Reliable Predictor of Acute and Chronic Response to Cardiac Resynchronization Therapy. *Journal of the American Society of Echocardiography* 2009;22(7):839-46.
101. Delgado V, Ypenburg C, van Bommel RJ, et al. Assessment of Left Ventricular Dyssynchrony by Speckle Tracking Strain Imaging: Comparison Between Longitudinal, Circumferential, and Radial Strain in Cardiac Resynchronization Therapy. *Journal of the American College of Cardiology* 2008;51(20):1944-52.
102. Tanaka H, Nesser H-J, Buck T, et al. Dyssynchrony by speckle-tracking echocardiography and response to cardiac resynchronization therapy: results of the Speckle Tracking and Resynchronization (STAR) study. *European Heart Journal* 2010.
103. Lecoq G, Leclercq C, Leray E, et al. Clinical and electrocardiographic predictors of a positive response to cardiac resynchronization therapy in advanced heart failure. *European Heart Journal* 2005;26(11):1094-100.
104. Ruschitzka F, Abraham WT, Singh JP, et al. Cardiac-resynchronization therapy in heart failure with a narrow QRS complex. *N Engl J Med* 2013;369(15):1395-405.

105. Bleeker GB, Bax JJ, Fung JW, et al. Clinical versus echocardiographic parameters to assess response to cardiac resynchronization therapy. *Am J Cardiol* 2006;97(2):260-3.
106. Galderisi M, Cattaneo F, Mondillo S. Doppler echocardiography and myocardial dyssynchrony: a practical update of old and new ultrasound technologies. *Cardiovascular ultrasound* 2007;5:28.
107. Kapetanakis S, Kearney MT, Siva A, et al. Real-Time Three-Dimensional Echocardiography. *Circulation* 2005;112(7):992-1000.
108. Harrington D, Anker SD, Coats AJ. Preservation of exercise capacity and lack of peripheral changes in asymptomatic patients with severely impaired left ventricular function. *Eur Heart J* 2001;22(5):392-9.
109. Harlan WR, oberman A, Grimm R, et al. Chronic congestive heart failure in coronary artery disease: clinical criteria. *Ann Intern Med* 1977;86(2):133-8.
110. Hunt SA, Abraham WT, Chin MH, et al. 2009 focused update incorporated into the ACC/AHA 2005 Guidelines for the Diagnosis and Management of Heart Failure in Adults: a report of the American College of Cardiology Foundation/American Heart Association Task Force on Practice Guidelines: developed in collaboration with the International Society for Heart and Lung Transplantation. *Circulation* 2009;119(14):e391-479.
111. Al-Mohammad A, Mant J, Laramée P, et al. Diagnosis and management of adults with chronic heart failure: summary of updated NICE guidance. *BMJ* 2011;341:c4130.
112. REMES J, MIETTINEN H, REUNANEN A, et al. Validity of clinical diagnosis of heart failure in primary health care. *European Heart Journal* 1991;12(3):315-21.
113. Fuat A, Hungin APS, Murphy JJ. Barriers to accurate diagnosis and effective management of heart failure in primary care: qualitative study. *BMJ* 2003;326(7382):196.
114. Craig J BI, Cummins E et al. . The use of B-type natriuretic peptides (BNP and NT-proBNP) in the investigation of patients with suspected heart failure. In: Scotland NQI, ed. *Health Technology Assessment Report (6)*. Glasgow, 2005.
115. De Marco T, Delgado RI, Agocha A, et al. Confusion at Large: Incorrect Assignment of Patients to the AHA/ACC Stages of Heart Failure in the ADVANCENT Registry. *J Cardiac Fail* 2004;10 (4 suppl)(S96).
116. van den Broek SA, van Veldhuisen DJ, de Graeff PA, et al. Comparison between New York Heart Association classification and peak oxygen consumption in the

assessment of functional status and prognosis in patients with mild to moderate chronic congestive heart failure secondary to either ischemic or idiopathic dilated cardiomyopathy. *Am J Cardiol* 1992;70(3):359-63.

117. Muntwyler J, Abetel G, Gruner C, et al. One-year mortality among unselected outpatients with heart failure. *European Heart Journal* 2002;23(23):1861-66.

118. Forrester JS, Diamond GA, Swan HJ. Correlative classification of clinical and hemodynamic function after acute myocardial infarction. *Am J Cardiol* 1977;39(2):137-45.

119. MacIver DH, Townsend M. A novel mechanism of heart failure with normal ejection fraction. *Heart* 2008;94(4):446-49.

120. Marantz P, Tobin J, Wassertheil-Smoller S, et al. The relationship between left ventricular systolic function and congestive heart failure diagnosed by clinical criteria. *Circulation* 1988;77(3):607-12.

121. Bellenger NG, Burgess MI, Ray SG, et al. Comparison of left ventricular ejection fraction and volumes in heart failure by echocardiography, radionuclide ventriculography and cardiovascular magnetic resonance. Are they interchangeable? *European Heart Journal* 2000;21(16):1387-96.

122. McMurray J, Adamopoulos S, Anker S, et al. The Task Force for the Diagnosis and Treatment of Acute and Chronic Heart Failure 2012 of the European Society of Cardiology. Developed in collaboration with the Heart Failure Association (HFA) of the ESC. *Eur Heart J* 2012;33:1787 - 847.

123. Curtis JP, Sokol SI, Wang Y, et al. The association of left ventricular ejection fraction, mortality, and cause of death in stable outpatients with heart failure. *J Am Coll Cardiol* 2003;42(4):736-42.

124. Ammar KA, Jacobsen SJ, Mahoney DW, et al. Prevalence and Prognostic Significance of Heart Failure Stages: Application of the American College of Cardiology/American Heart Association Heart Failure Staging Criteria in the Community. *Circulation* 2007;115(12):1563-70.

125. The Cardiac Insufficiency Bisoprolol Study II (CIBIS-II): a randomised trial. *Lancet* 1999;353(9146):9-13.

126. Effect of enalapril on survival in patients with reduced left ventricular ejection fractions and congestive heart failure. The SOLVD Investigators. *N Engl J Med* 1991;325(5):293-302.

127. Chan JY-S, Fang F, Zhang Q, et al. Biventricular pacing is superior to right ventricular pacing in bradycardia patients with preserved systolic function: 2-year results of the PACE trial. *European Heart Journal* 2011;32(20):2533-40.
128. Kass DA. Pathobiology of cardiac dyssynchrony and resynchronization. *Heart Rhythm* 2009;6(11):1660-5.
129. Saxon L, De Marco T, Schafer J, et al. VIGOR Congestive Heart Failure Investigators. Effects of long-term biventricular stimulation for resynchronization on echocardiographic measures of remodeling. *Circulation* 2002;105:1304 - 10.
130. Auricchio A, Stellbrink C, Sack S, et al. Long-term clinical effect of hemodynamically optimized cardiac resynchronization therapy in patients with heart failure and ventricular conduction delay. *J Am Coll Cardiol* 2002;39(12):2026-33.
131. Gras D, Leclercq C, Tang AS, et al. Cardiac resynchronization therapy in advanced heart failure the multicenter InSync clinical study. *Eur J Heart Fail* 2002;4(3):311-20.
132. Abraham W, Fisher W, Smith A, et al. Multicenter InSync Randomized Clinical evaluation. Cardiac resynchronization in chronic heart failure. *N Engl J Med* 2002;346:1845 - 53.
133. Higgins SL, Hummel JD, Niazi IK, et al. Cardiac resynchronization therapy for the treatment of heart failure in patients with intraventricular conduction delay and malignant ventricular tachyarrhythmias. *J Am Coll Cardiol* 2003;42(8):1454-9.
134. Bristow M, Saxon L, Boehmer J, et al. Cardiac Resynchronization Therapy with or without an Implantable Defibrillator in Advanced Chronic Heart Failure. *N Eng J Med* 2004;350:2140 - 50.
135. Tang AS, Wells GA, Talajic M, et al. Cardiac-resynchronization therapy for mild-to-moderate heart failure. *N Engl J Med* 2010;363(25):2385-95.
136. NICE. Implantable cardioverter defibrillators and cardiac resynchronisation therapy for arrhythmias and heart failure. technology appraisal guidance [TA314]: National Institutes for Health and Care Excellence., 2014.
137. Fox M, Mealing S, Anderson R, et al. The clinical effectiveness and cost-effectiveness of cardiac resynchronisation (biventricular pacing) for heart failure: systematic review and economic model. *Health Technology Assessment* 2007;11(47).
138. Tracy CM, Epstein AE, Darbar D, et al. 2012 ACCF/AHA/HRS Focused Update of the 2008 Guidelines for Device-Based Therapy of Cardiac Rhythm AbnormalitiesA Report of the American College of Cardiology Foundation/American Heart Association Task

Force on Practice Guidelines. *Journal of the American College of Cardiology* 2012;60(14):1297-313.

139. Dickstein K, Bogale N, Priori S, et al. The European cardiac resynchronization therapy survey. *Eur Heart J* 2009;30(20):2450-60.

140. Cunningham D, Charles R, Cunningham M, et al. Cardiac Rhythm Management UK National Clinical Audit Report. National Institute for Cardiovascular Outcomes Research 2011.

141. Jones S, Gammage M, Linker N, et al. Clinical guidance by consensus for the follow up of implantable cardiac devices for cardiac rhythm management. London: HRUK & SCST, 2008.

142. Landolina M, Gasparini M, Lunati M, et al. Long-Term Complications Related to Biventricular Defibrillator Implantation: Rate of Surgical Revisions and Impact on Survival: Insights From the Italian ClinicalService Database. *Circulation* 2011;123(22):2526-35.

143. Lewis EF, Moye LA, Rouleau JL, et al. Predictors of late development of heart failure in stable survivors of myocardial infarction: the CARE study. *J Am Coll Cardiol* 2003;42(8):1446-53.

144. Cazeau S, Ritter P, Bakdach S, et al. Four chamber pacing in dilated cardiomyopathy. *Pacing and clinical electrophysiology : PACE* 1994;17(11 Pt 2):1974-9.

145. Foster AH, Gold MR, McLaughlin JS. Acute hemodynamic effects of atrio-biventricular pacing in humans. *The Annals of thoracic surgery* 1995;59(2):294-300.

146. Cazeau S, Ritter P, Lazarus A, et al. Multisite pacing for end-stage heart failure: early experience. *Pacing and clinical electrophysiology : PACE* 1996;19(11 Pt 2):1748-57.

147. Blanc JJ, Etienne Y, Gilard M, et al. Evaluation of different ventricular pacing sites in patients with severe heart failure: results of an acute hemodynamic study. *Circulation* 1997;96(10):3273-7.

148. Kass D, Chen C, Curry C, et al. Improved left ventricular mechanics from acute VDD pacing in patients with dilated cardiomyopathy and ventricular conduction delay. *Circulation* 1999;99:1567 - 73.

149. Leclercq C, Cazeau S, Le Breton H, et al. Acute hemodynamic effects of biventricular DDD pacing in patients with end-stage heart failure. *J Am Coll Cardiol* 1998;32(7):1825-31.

150. Saxon LA, Kerwin WF, Cahalan MK, et al. Acute effects of intraoperative multisite ventricular pacing on left ventricular function and activation/contraction sequence in patients with depressed ventricular function. *J Cardiovasc Electrophysiol* 1998;9(1):13-21.
151. Gras D, Mabo P, Tang T, et al. Multisite pacing as a supplemental treatment of congestive heart failure: preliminary results of the Medtronic Inc. InSync Study. *Pacing and clinical electrophysiology : PACE* 1998;21(11 Pt 2):2249-55.
152. Packer M. Proposal for a new clinical end point to evaluate the efficacy of drugs and devices in the treatment of chronic heart failure. *Journal of cardiac failure* 2001;7(2):176-82.
153. Linde C, Leclercq C, Rex S, et al. Long-term benefits of biventricular pacing in congestive heart failure: results from the MULTIsite STimulation in cardiomyopathy (MUSTIC) study. *J Am Coll Cardiol* 2002;40:111 - 18.
154. Auricchio A, Stellbrink C, Butter C, et al. Clinical efficacy of cardiac resynchronization therapy using left ventricular pacing in heart failure patients stratified by severity of ventricular conduction delay. *J Am Coll Cardiol* 2003;42(12):2109-16.
155. Abraham W, Fisher W, Smith A, et al. Cardiac resynchronization in chronic heart failure. *N Engl J Med* 2002;346:1845 - 53.
156. Abraham WT, Young JB, Leon AR, et al. Effects of cardiac resynchronization on disease progression in patients with left ventricular systolic dysfunction, an indication for an implantable cardioverter-defibrillator, and mildly symptomatic chronic heart failure. *Circulation* 2004;110(18):2864-8.
157. Leclercq C, Cazeau S, Lellouche D, et al. Upgrading from Single Chamber Right Ventricular to Biventricular Pacing in Permanently Paced Patients with Worsening Heart Failure: The RD-CHF Study. *Pacing and Clinical Electrophysiology* 2007;30:S23-S30.
158. Moss AJ, Hall WJ, Cannom DS, et al. Cardiac-Resynchronization Therapy for the Prevention of Heart-Failure Events. *New England Journal of Medicine* 2009;361(14):1329-38.
159. Beshai JF, Grimm RA, Nagueh SF, et al. Cardiac-Resynchronization Therapy in Heart Failure with Narrow QRS Complexes. *New England Journal of Medicine* 2007;357(24):2461-71.

160. Curtis AB, Worley SJ, Adamson PB, et al. Biventricular Pacing for Atrioventricular Block and Systolic Dysfunction. *New England Journal of Medicine* 2013;368(17):1585-93.
161. Wiklund I, Lindvall K, Swedberg K, et al. Self-assessment of quality of life in severe heart failure. An instrument for clinical use. *Scand J Psychol* 1987;28(3):220-5.
162. Guyatt GH, Nogradi S, Halcrow S, et al. Development and testing of a new measure of health status for clinical trials in heart failure. *J Gen Intern Med* 1989;4(2):101-7.
163. Green CP, Porter CB, Bresnahan DR, et al. Development and evaluation of the Kansas City Cardiomyopathy Questionnaire: a new health status measure for heart failure. *J Am Coll Cardiol* 2000;35(5):1245-55.
164. O'Leary CJ, Jones PW. The left ventricular dysfunction questionnaire (LVD-36): reliability, validity, and responsiveness. *Heart* 2000;83(6):634-40.
165. Rector T, Kubo S, Conn J. Patients' self-assessment of their congestive heart failure: II. Content, reliability and validity of a new measure—the Minnesota Living with Heart Failure Questionnaire. *Heart Failure* 1987(3):198-209.
166. Sneed NV, Paul S, Michel Y, et al. Evaluation of 3 quality of life measurement tools in patients with chronic heart failure. *Heart & Lung: The Journal of Acute and Critical Care* 2001;30(5):332-40.
167. Gorkin L, Norvell NK, Rosen RC, et al. Assessment of quality of life as observed from the baseline data of the Studies of Left Ventricular Dysfunction (SOLVD) trial quality-of-life substudy. *The American Journal of Cardiology* 1993;71(12):1069-73.
168. Dunderdale K, Thompson DR, Miles JNV, et al. Quality-of-life measurement in chronic heart failure: do we take account of the patient perspective? *European Journal of Heart Failure* 2005;7(4):572-82.
169. Freemantle N, Tharmanathan P, Calvert MJ, et al. Cardiac resynchronisation for patients with heart failure due to left ventricular systolic dysfunction — a systematic review and meta-analysis. *European Journal of Heart Failure* 2006;8(4):433-40.
170. Wells G, Parkash R, Healey JS, et al. Cardiac resynchronization therapy: a meta-analysis of randomized controlled trials. *Canadian Medical Association Journal* 2011;183(4):421-29.
171. Hill AV, Lupton H. Muscular exercise, lactic acid and the supply and utilization of oxygen. *QJM* 1923(16):135-71.

172. Diaz-Infante E, Mont L, Leal J, et al. Predictors of lack of response to resynchronization therapy. *Am J Cardiol* 2005;95:1436 - 40.
173. Lipkin DP, Scriven AJ, Crake T, et al. Six minute walking test for assessing exercise capacity in chronic heart failure. *BMJ* 1986;292(6521):653-55.
174. Olsson LG, Swedberg K, Clark AL, et al. Six minute corridor walk test as an outcome measure for the assessment of treatment in randomized, blinded intervention trials of chronic heart failure: a systematic review. *Eur Heart J* 2005;26(8):778-93.
175. Cahalin LP, Mathier MA, Semigran MJ, et al. The Six-Minute Walk Test Predicts Peak Oxygen Uptake and Survival in Patients With Advanced Heart Failure. *CHEST Journal* 1996;110(2):325-32.
176. Casanova C, Celli BR, Barria P, et al. The 6-min walk distance in healthy subjects: reference standards from seven countries. *European Respiratory Journal* 2011;37(1):150-56.
177. El Desoky ES, Derendorf H, Klotz U. Variability in response to cardiovascular drugs. *Curr Clin Pharmacol* 2006;1(1):35-46.
178. Follath F, Cleland JGF, Klein W, et al. Etiology and response to drug treatment in heart failure. *J Am Coll Cardiol* 1998;32(5):1167-72.
179. Ganesan AN, Brooks AG, Roberts-Thomson KC, et al. Role of AV Nodal Ablation in Cardiac Resynchronization in Patients With Coexistent Atrial Fibrillation and Heart Failure: A Systematic Review. *Journal of the American College of Cardiology* 2012;59(8):719-26.
180. Upadhyay GA, Choudhry NK, Auricchio A, et al. Cardiac Resynchronization in Patients With Atrial Fibrillation A Meta-Analysis of Prospective Cohort Studies. *Journal of the American College of Cardiology* 2008;52(15):1239-46.
181. ATS Statement. *American Journal of Respiratory and Critical Care Medicine* 2002;166(1):111-17.
182. Wu G, Sanderson B, Bittner V. The 6-minute walk test: How important is the learning effect? *American Heart Journal*;146(1):129-33.
183. Leach RM, Davidson AC, Chinn S, et al. Portable liquid oxygen and exercise ability in severe respiratory disability. *Thorax* 1992;47(10):781-89.

184. Adsett J, Mullins R, Hwang R, et al. Repeat six-minute walk tests in patients with chronic heart failure: are they clinically necessary? *European Journal of Cardiovascular Prevention & Rehabilitation* 2011;18(4):601-06.
185. Hughes T. Personal Communication., 2013.
186. Lang RM, Bierig M, Devereux RB, et al. Recommendations for chamber quantification. *European journal of echocardiography : the journal of the Working Group on Echocardiography of the European Society of Cardiology* 2006;7(2):79-108.
187. Gottdiener JS, Bednarz J, Devereux R, et al. American Society of Echocardiography recommendations for use of echocardiography in clinical trials. *Journal of the American Society of Echocardiography : official publication of the American Society of Echocardiography* 2004;17(10):1086-119.
188. Masani N, Wharton G, Allen J, et al. *Echocardiography: Guidelines for Chamber Quantification*. British Society of Echocardiography 2011.
189. Hayes DL, Boehmer JP, Day JD, et al. Cardiac resynchronization therapy and the relationship of percent biventricular pacing to symptoms and survival. *Heart Rhythm* 2011;8(9):1469-75.
190. Koplan BA, Kaplan AJ, Weiner S, et al. Heart Failure Decompensation and All-Cause Mortality in Relation to Percent Biventricular Pacing in Patients With Heart Failure: Is a Goal of 100% Biventricular Pacing Necessary? *Journal of the American College of Cardiology* 2009;53(4):355-60.
191. Santos J, Brofman P. Six-minute walk test and quality-of-life in heart failure: A correlative study with a Brazilian sample. *Insuficiencia cardiaca* 2008;3(2).
192. Dictionary OE. "model, n. and adj.": Oxford University Press.
193. Steinhart B, Thorpe KE, Bayoumi AM, et al. Improving the Diagnosis of Acute Heart Failure Using a Validated Prediction Model. *Journal of the American College of Cardiology* 2009;54(16):1515-21.
194. A heart failure diagnosis model based on support vector machine. *Biomedical Engineering and Informatics, 3rd International Conference on*; 2010; Yantai. IEEExplore.
195. Shi Y, Lawford P, Hose R. Review of zero-d and 1-d models of blood flow in the cardiovascular system. *Biomed Eng Online* 2011;10:33.

196. Watanabe H, Sugiura S, Kafuku H, et al. Multiphysics simulation of left ventricular filling dynamics using fluid-structure interaction finite element method. *Biophys J* 2004;87(3):2074-85.
197. Segers P, Rietzschel ER, De Buyzere ML, et al. Three- and four-element Windkessel models: Assessment of their fitting performance in a large cohort of healthy middle-aged individuals. *Proceedings of the Institution of Mechanical Engineers, Part H: Journal of Engineering in Medicine* 2008;222(4):417-28.
198. O'Rourke M, Avolio A. Pulsatile flow and pressure in human systemic arteries. Studies in man and in a multibranched model of the human systemic arterial tree. *Circ Res* 1980;46(3):363-72.
199. SUGA H. Importance of Atrial Compliance in Cardiac Performance. *Circ Res* 1974;35(1):39-43.
200. Werner J, Bohringer D, Hexamer M. Simulation and prediction of cardiotherapeutical phenomena from a pulsatile model coupled to the Guyton circulatory model. *Biomedical Engineering, IEEE Transactions on* 2002;49(5):430-39.
201. Simulate Heart Failure by a Mathematical Model. *Bioinformatics and Biomedical Engineering , 2009 ICBBE 2009 3rd International Conference on; 2009 11-13 June 2009.*
202. Lim E, Dokos S, Cloherty SL, et al. Parameter-Optimized Model of Cardiovascular–Rotary Blood Pump Interactions. *Biomedical Engineering, IEEE Transactions on* 2010;57(2):254-66.
203. Hsu P-L, Cheng SJ, Saumarez RC, et al. An Extended Computational Model of the Circulatory System for Designing Ventricular Assist Devices. *ASAIO Journal* 2008;54(6):594-99 10.1097/MAT.0b013e318185e1ce.
204. Di Molfetta A, Santini L, Forleo GB, et al. Use of a comprehensive numerical model to improve biventricular pacemaker temporization in patients affected by heart failure undergoing to CRT-D therapy. *Med Biol Eng Comput* 2010;48(8):755-64.
205. Ursino M. Interaction between carotid baroregulation and the pulsating heart: a mathematical model. *American Journal of Physiology - Heart and Circulatory Physiology* 1998;275(5):H1733-H47.
206. Segers P, Stergiopoulos N, Schreuder JJ, et al. Left ventricular wall stress normalization in chronic pressure-overloaded heart: a mathematical model study. *Am J Physiol Heart Circ Physiol* 2000;279(3):H1120-7.

207. Shi Y, Korakianitis T. Numerical simulation of cardiovascular dynamics with left heart failure and in-series pulsatile ventricular assist device. *Artif Organs* 2006;30(12):929-48.
208. Cole RT, Lucas CL, Cascio WE, et al. A LabVIEW model incorporating an open-loop arterial impedance and a closed-loop circulatory system. *Ann Biomed Eng* 2005;33(11):1555-73.
209. Stergiopoulos N, Westerhof BE, Westerhof N. Total arterial inertance as the fourth element of the windkessel model. *Am J Physiol* 1999;276(1 Pt 2):H81-8.
210. Alexopoulos D, Lazzam C, Borricco S, et al. Isolated chronic mitral regurgitation with preserved systolic left ventricular function and severe pulmonary hypertension. *Journal of the American College of Cardiology* 1989;14(2):319-22.
211. Tsuruta H, Sato T, Ikeda N. Mathematical model of cardiovascular mechanics for diagnostic analysis and treatment of heart failure: Part 2. Analysis of vasodilator therapy and planning of optimal drug therapy. *Med Biol Eng Comput* 1994;32(1):12-8.
212. Arnold JM, Marchiori GE, Imrie JR, et al. Large artery function in patients with chronic heart failure. Studies of brachial artery diameter and hemodynamics. *Circulation* 1991;84(6):2418-25.
213. Duprez DA, De Buyzere ML, Rietzschel ER, et al. Inverse relationship between aldosterone and large artery compliance in chronically treated heart failure patients. *Eur Heart J* 1998;19(9):1371-6.
214. Giannattasio C, Achilli F, Failla M, et al. Arterial stiffness in heart failure patients: dependence on diastolic dysfunction and plasma aldosterone levels. *European Heart Journal Supplements* 2004;6(suppl F):F30-F34.
215. Hunt SA, Baker DW, Chin MH, et al. ACC/AHA Guidelines for the Evaluation and Management of Chronic Heart Failure in the Adult: Executive Summary A Report of the American College of Cardiology/American Heart Association Task Force on Practice Guidelines (Committee to Revise the 1995 Guidelines for the Evaluation and Management of Heart Failure). *Circulation* 2001;104(24):2996-3007.
216. Tsuruta H, Sato T, Shirataka M, et al. Mathematical model of cardiovascular mechanics for diagnostic analysis and treatment of heart failure: Part 1. Model description and theoretical analysis. *Med Biol Eng Comput* 1994;32(1):3-11.

217. Kass DA, Baughman KL, Pak PH, et al. Reverse remodeling from cardiomyoplasty in human heart-failure - external constraint versus active assist. . *Circulation* 1995;91(9):2314-18.
218. Tulner SAF, Steendijk P, Klautz RJM, et al. Surgical ventricular restoration in patients with ischemic dilated cardiomyopathy: Evaluation of systolic and diastolic ventricular function, wall stress, dyssynchrony, and mechanical efficiency by pressure-volume loops. *Journal of Thoracic and Cardiovascular Surgery* 2006;132(3):610-20.
219. Ferrari M, Kadipasaoglu KA, Croitoru M, et al. Evaluation of myocardial function in patients with end-stage heart failure during support with the Jarvik 2000 left ventricular assist device. *Journal of Heart and Lung Transplantation* 2005;24(2):226-28.
220. Kawaguchi AT, Sugimachi M, Sunagawa K, et al. Perioperative hemodynamics in patients undergoing partial left ventriculectomy. *J Card Surg* 2001;16(1):48-55.
221. Lorusso R, Milan E, Volterrani M, et al. Cardiomyoplasty as an isolated procedure to treat refractory heart failure. *Eur J Cardiothorac Surg* 1997;11(2):363-72.
222. Redington AN, Gray HH, Hodson ME, et al. Characterisation of the normal right ventricular pressure-volume relation by biplane angiography and simultaneous micromanometer pressure measurements. *Br Heart J* 1988;59(1):23-30.
223. Aroney CN, Herrmann HC, Semigran MJ, et al. Linearity of the left ventricular end-systolic pressure-volume relation in patients with severe heart failure. *J Am Coll Cardiol* 1989;14(1):127-34.
224. Steendijk P, Tulner SA, Bax JJ, et al. Hemodynamic Effects of Long-Term Cardiac Resynchronization Therapy. *Circulation* 2006;113(10):1295-304.
225. Dekker ALAJ, Phelps B, Dijkman B, et al. Epicardial left ventricular lead placement for cardiac resynchronization therapy: Optimal pace site selection with pressure-volume loops. *J Thorac Cardiovasc Surg* 2004;127(6):1641-47.
226. Kim MH, Devlin WH, Das SK, et al. Effects of β -Adrenergic Blocking Therapy on Left Ventricular Diastolic Relaxation Properties in Patients With Dilated Cardiomyopathy. *Circulation* 1999;100(7):729-35.
227. MacGowan GA, Haber HL, Cowart TD, et al. Direct Myocardial Effects of OPC-18790 in Human Heart Failure: Beneficial Effects on Contractile and Diastolic Function Demonstrated by Intracoronary Infusion With Pressure–Volume Analysis. *Journal of the American College of Cardiology* 1998;31(6):1344-51.

228. Feldman MD, Pak PH, Wu CC, et al. Acute Cardiovascular Effects of OPC-18790 in Patients With Congestive Heart Failure : Time- and Dose-Dependence Analysis Based on Pressure-Volume Relations. *Circulation* 1996;93(3):474-83.
229. Sonntag S, Sundberg S, Lehtonen LA, et al. The calcium sensitizer levosimendan improves the function of stunned myocardium after percutaneous transluminal coronary angioplasty in acute myocardial ischemia. *Journal of the American College of Cardiology* 2004;43(12):2177-82.
230. Smith M, Russell RO, Feild BJ, et al. Left Ventricular Compliance and Abnormally Contracting Segments in Postmyocardial Infarction Patients. *Chest* 1974;65(4):368-78.
231. ten Brinke EA, Klautz RJ, Tulner SA, et al. Long-term effects of surgical ventricular restoration with additional restrictive mitral annuloplasty and/or coronary artery bypass grafting on left ventricular function: Six-month follow-up by pressure-volume loops. *J Thorac Cardiovasc Surg* 2010;140(6):1338-44.
232. Magorien D, Shaffer P, Bush C, et al. Assessment of left ventricular pressure-volume relations using gated radionuclide angiography, echocardiography, and micromanometer pressure recordings. A new method for serial measurements of systolic and diastolic function in man. *Circulation* 1983;67(4):844-53.
233. Thormann J. The influence of clinical intervention on pressure-volume relationships--the conductance (volume) technique. *Eur Heart J* 1992;13:69-79.
234. Thormann J, Hueting J, Kremer P, et al. Enoximone: True inotropic effects? Do they cause ischemia? Analysis of end-systolic pressure-volume relations using the conductance (volume) Catheter technique. *Cardiovascular Drugs and Therapy* 1990;4(5):1403-15.
235. Thormann J, Huting J, Kremer P, et al. Do class 1 antiarrhythmic drugs impair myocardial contractility? The class 1A example of ajmaline (conductance catheter technique). *J Cardiovasc Pharmacol* 1990;16(2):182-90.
236. Thormann J, Kramer W, Kremer P, et al. Influence of the new class-I antiarrhythmic agent diprafenone on the end-systolic pressure-volume relationship (conductance technique). *Cardiovascular Drugs and Therapy* 1989;3(2):145-54.
237. Schreuder JJ, Biervliet JD, van der Velde ET, et al. Systolic and diastolic pressure-volume relationships during cardiac surgery. *J Cardiothorac Vasc Anesth* 1991;5(6):539-45.

238. Schreuder JJ, Maisano F, Donelli A, et al. Beat-to-Beat Effects of Intraaortic Balloon Pump Timing on Left Ventricular Performance in Patients With Low Ejection Fraction. *The Annals of thoracic surgery* 2005;79(3):872-80.
239. Schreuder JJ, van der Veen FH, van der Velde ET, et al. Beat-to-Beat Analysis of Left Ventricular Pressure-Volume Relation and Stroke Volume by Conductance Catheter and Aortic Modelflow in Cardiomyoplasty Patients. *Circulation* 1995;91(7):2010-17.
240. Hayward CS, Kalnins WV, Kelly RP. Gender-related differences in left ventricular chamber function. *Cardiovascular Research* 2001;49(2):340-50.
241. Hayward CS, Kalnins WV, Rogers P, et al. Left ventricular chamber function during inhaled nitric oxide in patients with dilated cardiomyopathy. *Journal of Cardiovascular Pharmacology* 1999;34(5):749-54.
242. Urheim S, Bjornerheim R, Endresen K, et al. Quantification of left ventricular diastolic pressure-volume relations during routine cardiac catheterization by two-dimensional digital echo quantification and left ventricular micromanometer. *Journal of the American Society of Echocardiography : official publication of the American Society of Echocardiography* 2002;15(3):225-32.
243. Remmelink M, Delewi R, Yong ZY, et al. More pronounced diastolic left ventricular dysfunction in patients with accelerated idioventricular rhythm after reperfusion by primary percutaneous coronary intervention. *J Invasive Cardiol* 2010;22(12):574-8.
244. Remmelink M, Sjauw KD, Henriques JP, et al. Acute left ventricular dynamic effects of primary percutaneous coronary intervention from occlusion to reperfusion. *J Am Coll Cardiol* 2009;53(17):1498-502.
245. Kashimura T, Kodama M, Aizawa Y. Left ventricular pressure–volume loops during mechanical alternans in a patient with dilated cardiomyopathy. *Heart* 2007;93(2):151.
246. Herrmann HC, Ruddy TD, William G, et al. Inotropic effect of enoximone in patients with severe heart failure: demonstration by left ventricular end-systolic pressure-volume analysis. *J Am Coll Cardiol* 1987;9(5):1117-23.
247. Kelly R, Ting C, Yang T, et al. Effective arterial elastance as index of arterial vascular load in humans. *Circulation* 1992;86(2):513-21.
248. Mitchell M. Engauge Digitizer Fairfax,VA, USA.: Sourceforge; 2005 [Available from: <http://digitizer.sourceforge.net/index.php?c=7>].

249. Shi Y. Lumped-parameter cardiovascular model with Windkessel after-load. *CellML* 2007; (30/5/2012). <http://models.cellml.org/exposure/ea64608ab564ee085bef7cde3ed1731e> (accessed 30/5/2012).
250. Lloyd CM, Lawson JL, Hunter PJ, et al. The CellML Model Repository. *Bioinformatics* 2008;24(18):2122-23.
251. Chen C-H, Fetics B, Nevo E, et al. Noninvasive single-beat determination of left ventricular end-systolic elastance in humans. *J Am Coll Cardiol* 2001;38(7):2028-34.
252. Nagueh SF, Middleton KJ, Kopelen HA, et al. Doppler tissue imaging: a noninvasive technique for evaluation of left ventricular relaxation and estimation of filling pressures. *J Am Coll Cardiol* 1997;30(6):1527-33.
253. Pieragnoli P, Perego GB, Ricciardi G, et al. Cardiac resynchronization therapy acutely improves ventricular-arterial coupling by reducing the arterial load: assessment by pressure-volume loops. *Pacing and clinical electrophysiology : PACE* 2015;38(4):431-7.
254. Zócalo Y, Bia D, Armentano RL, et al. Resynchronization improves heart-arterial coupling reducing arterial load determinants, 2013.
255. Hunter PJ, Pullan AJ, Smaill BH. Modeling total heart function. *Annu Rev Biomed Eng* 2003;5:147-77.
256. Rhode K, Sermesant M. Modeling and Registration for Electrophysiology Procedures Based on Three-Dimensional Imaging. *Curr Cardiovasc Imaging Rep* 2011;4:116-26.
257. Lamata P, Niederer S, Nordsletten D, et al. An accurate, fast and robust method to generate patient-specific cubic Hermite meshes. *Med Image Anal* 2011;15(6):801-13.
258. Lohner R. Automatic unstructured grid generators. *Finite Elements in Analysis and Design* 1997;25:111-34.
259. Zuluaga MA, Cardoso MJ, Modat MM. Segmentation from MRI and CTA using a Local Normalised Correlation Coefficient Criterion. In "Functional Imaging and Modeling of the Heart". Berlin: Springer, 2013:174-81.
260. Angelie E, de Koning PJ, Danilouchkine MG, et al. Optimizing the automatic segmentation of the left ventricle in magnetic resonance images. *Med Phys* 2005;32(2):369-75.

261. Pednekar A, Kurkure U, Muthupillai R, et al. Automated left ventricular segmentation in cardiac MRI. *IEEE Trans Biomed Eng* 2006;53(7):1425-8.
262. Cohn JN, Ferrari R, Sharpe N. Cardiac remodeling--concepts and clinical implications: a consensus paper from an international forum on cardiac remodeling. Behalf of an International Forum on Cardiac Remodeling. *J Am Coll Cardiol* 2000;35(3):569-82.
263. Konstam MA, Kramer DG, Patel AR, et al. Left ventricular remodeling in heart failure: current concepts in clinical significance and assessment. *JACC Cardiovasc Imaging* 2011;4(1):98-108.
264. Young AA, Frangi AF. Computational cardiac atlases: from patient to population and back. *Exp Physiol* 2009;94(5):578-96.
265. Medrano-Gracia P, Cowan BR, Ambale-Venkatesh B, et al. Left ventricular shape variation in asymptomatic populations: the Multi-Ethnic Study of Atherosclerosis. *J Cardiovasc Magn Reson* 2014;16:56.
266. Leyva F, Nisam S, Auricchio A. 20 years of cardiac resynchronization therapy. *J Am Coll Cardiol* 2014;64(10):1047-58.
267. Yu CM, Wing-Hong Fung J, Zhang Q, et al. Understanding nonresponders of cardiac resynchronization therapy--current and future perspectives. *J Cardiovasc Electrophysiol* 2005;16(10):1117-24.
268. Yu CM, Bleeker GB, Fung JW, et al. Left ventricular reverse remodeling but not clinical improvement predicts long-term survival after cardiac resynchronization therapy. *Circulation* 2005;112(11):1580-6.
269. Heusch G, Libby P, Gersh B, et al. Cardiovascular remodelling in coronary artery disease and heart failure. *Lancet* 2014;383(9932):1933-43.
270. Ganau A, Devereux RB, Roman MJ, et al. Patterns of left ventricular hypertrophy and geometric remodeling in essential hypertension. *J Am Coll Cardiol* 1992;19(7):1550-8.
271. Verma A, Meris A, Skali H, et al. Prognostic implications of left ventricular mass and geometry following myocardial infarction: the VALIANT (VALsartan In Acute myocardial iNfarcTion) Echocardiographic Study. *JACC Cardiovasc Imaging* 2008;1(5):582-91.

272. Cleland JG, Daubert JC, Erdmann E, et al. Longer-term effects of cardiac resynchronization therapy on mortality in heart failure [the CARdiac RESynchronization-Heart Failure (CARE-HF) trial extension phase]. *Eur Heart J* 2006;27(16):1928-32.
273. Birnie DH, Tang AS. The problem of non-response to cardiac resynchronization therapy. *Curr Opin Cardiol* 2006;21(1):20-6.
274. Dreger H, Borges AC, Baumann G, et al. Successful reduction of intraventricular asynchrony is associated with superior response to cardiac resynchronization therapy. *Cardiovascular ultrasound* 2010;8:35.
275. Antonio N, Teixeira R, Coelho L, et al. Identification of 'super-responders' to cardiac resynchronization therapy: the importance of symptom duration and left ventricular geometry. *Europace : European pacing, arrhythmias, and cardiac electrophysiology : journal of the working groups on cardiac pacing, arrhythmias, and cardiac cellular electrophysiology of the European Society of Cardiology* 2009;11(3):343-9.
276. Hsu JC, Solomon SD, Bourgoun M, et al. Predictors of super-response to cardiac resynchronization therapy and associated improvement in clinical outcome: the MADIT-CRT (multicenter automatic defibrillator implantation trial with cardiac resynchronization therapy) study. *J Am Coll Cardiol* 2012;59(25):2366-73.
277. Castellant P, Fatemi M, Bertault-Valls V, et al. Cardiac resynchronization therapy: "nonresponders" and "hyperresponders". *Heart Rhythm* 2008;5(2):193-7.
278. Rickard J, Kumbhani DJ, Popovic Z, et al. Characterization of super-response to cardiac resynchronization therapy. *Heart Rhythm* 2010;7(7):885-9.
279. Steffel J, Ruschitzka F. Superresponse to cardiac resynchronization therapy. *Circulation* 2014;130(1):87-90.
280. Fornwalt BK, Sprague WW, BeDell P, et al. Agreement is poor among current criteria used to define response to cardiac resynchronization therapy. *Circulation* 2010;121(18):1985-91.
281. Lewandowski AJ, Augustine D, Lamata P, et al. Preterm Heart in Adult Life: Cardiovascular Magnetic Resonance Reveals Distinct Differences in Left Ventricular Mass, Geometry, and Function. *Circulation* 2013;127(2):197-206.
282. Vadakkumpadan F, Trayanova N, Wu KC. Image-based left ventricular shape analysis for sudden cardiac death risk stratification. *Heart Rhythm* 2014;11(10):1693-700.

283. Auricchio A, Fantoni C, Regoli F, et al. Characterization of left ventricular activation in patients with heart failure and left bundle-branch block. *Circulation* 2004;109(9):1133-9.
284. Abraham J, Abraham TP. Is echocardiographic assessment of dyssynchrony useful to select candidates for cardiac resynchronization therapy? Echocardiography is useful before cardiac resynchronization therapy if QRS duration is available. *Circ Cardiovasc Imaging* 2008;1(1):79-84; discussion 84.
285. Sohal M, Shetty A, Duckett S, et al. Noninvasive assessment of LV contraction patterns using CMR to identify responders to CRT. *JACC Cardiovasc Imaging* 2013;6(8):864-73.
286. Prinzen FW, Kroon W, Auricchio A. U-shaped mechanical activation 4 U? *JACC Cardiovasc Imaging* 2013;6(8):874-6.
287. Lamata P, Sinclair M, Kerfoot E, et al. An automatic service for the personalization of ventricular cardiac meshes. *J R Soc Interface* 2014;11(91):20131023.
288. Keener J, Sneyd J. *Mathematical Physiology*. 1 ed. New York: Springer, 1998.
289. ten Tusscher KH, Panfilov AV. Alternans and spiral breakup in a human ventricular tissue model. *Am J Physiol Heart Circ Physiol* 2006;291(3):H1088-100.
290. Caldwell BJ, Trew ML, Sands GB, et al. Three distinct directions of intramural activation reveal nonuniform side-to-side electrical coupling of ventricular myocytes. *Circ Arrhythm Electrophysiol* 2009;2(4):433-40.
291. Roberts DE, Hersh LT, Scher AM. Influence of cardiac fiber orientation on wavefront voltage, conduction velocity, and tissue resistivity in the dog. *Circ Res* 1979;44(5):701-12.
292. Roberts DE, Scher AM. Effect of tissue anisotropy on extracellular potential fields in canine myocardium in situ. *Circ Res* 1982;50(3):342-51.
293. Clerc L. Directional differences of impulse spread in trabecular muscle from mammalian heart. *J Physiol* 1976;255(2):335-46.
294. Roth BJ. Electrical conductivity values used with the bidomain model of cardiac tissue. *IEEE Trans Biomed Eng* 1997;44(4):326-8.
295. Costa CM, Hoetzel E, Rocha BM, et al. Automatic Parameterization Strategy for Cardiac Electrophysiology Simulations. *Comput Cardiol (2010)* 2013;40:373-76.
296. Furchgott RF, Zawadzki JV. The obligatory role of endothelial cells in the relaxation of arterial smooth muscle by acetylcholine. *Nature* 1980;288(5789):373-76.

297. Ignarro LJ, Buga GM, Wood KS, et al. Endothelium-derived relaxing factor produced and released from artery and vein is nitric oxide. *Proc Natl Acad Sci U S A* 1987;84(24):9265-9.
298. Rubanyi GM, Romero JC, Vanhoutte PM. Flow-induced release of endothelium-derived relaxing factor. *Am J Physiol Heart Circ Physiol* 1986;250(H1145-H1149).
299. Cooke JP, Stamler J, Andon N, et al. Flow stimulates endothelial cells to release a vasodilator that is potentiated by reduced thiol. *Am J Physiol Heart Circ Physiol* 1990;259:H804-12.
300. Corretti MC, Anderson TJ, Benjamin EJ, et al. Guidelines for the ultrasound assessment of endothelial-dependent flow-mediated vasodilation of the brachial artery: a report of the International Brachial Artery Reactivity Task Force. *J Am Coll Cardiol* 2002;39(2):257-65.
301. Celermajer DS, Sorensen KE, Gooch VM, et al. Non-invasive detection of endothelial dysfunction in children and adults at risk of atherosclerosis. *Lancet* 1992;340(8828):1111-5.
302. de Berrazueta JR, Guerra-Ruiz A, García-Unzueta MT, et al. Endothelial dysfunction, measured by reactive hyperaemia using strain-gauge plethysmography, is an independent predictor of adverse outcome in heart failure. *European Journal of Heart Failure* 2010;12(5):477-83.
303. Kistorp C, Chong AY, Gustafsson F, et al. Biomarkers of endothelial dysfunction are elevated and related to prognosis in chronic heart failure patients with diabetes but not in those without diabetes. *European Journal of Heart Failure* 2008;10(4):380-87.
304. Thijssen DH, Black MA, Pyke KE, et al. Assessment of flow-mediated dilation in humans: a methodological and physiological guideline. *Am J Physiol Heart Circ Physiol* 2011;300(1):H2-12.
305. Pyke KE, Tschakovsky ME. The relationship between shear stress and flow-mediated dilatation: implications for the assessment of endothelial function. *J Physiol* 2005;568(Pt 2):357-69.
306. Mullen MJ, Kharbanda RK, Cross J, et al. Heterogenous nature of flow-mediated dilatation in human conduit arteries in vivo: relevance to endothelial dysfunction in hypercholesterolemia. *Circ Res* 2001;88(2):145-51.

307. Doshi SN, Naka KK, Payne N, et al. Flow-mediated dilatation following wrist and upper arm occlusion in humans: the contribution of nitric oxide. *Clin Sci (Lond)* 2001;101(6):629-35.
308. Agewall S, Hulthe J, Fagerberg B, et al. Post-occlusion brachial artery vasodilatation after ischaemic handgrip exercise is nitric oxide mediated. *Clin Physiol Funct Imaging* 2002;22(1):18-23.
309. Joannides R, Haefeli WE, Linder L, et al. Nitric oxide is responsible for flow-dependent dilatation of human peripheral conduit arteries in vivo. *Circulation* 1995;91(5):1314-9.
310. Corson MA, James NL, Latta SE, et al. Phosphorylation of endothelial nitric oxide synthase in response to fluid shear stress. *Circ Res* 1996;79(5):984-91.
311. Katz SD, Hryniewicz K, Hriljac I, et al. Vascular Endothelial Dysfunction and Mortality Risk in Patients With Chronic Heart Failure. *Circulation* 2005;111(3):310-14.
312. Klosinska M, Rudzinski T, Grzelak P, et al. Endothelium-dependent and -independent vasodilation is more attenuated in ischaemic than in non-ischaemic heart failure. *European Journal of Heart Failure* 2009;11(8):765-70.
313. Meyer B, Mortl D, Strecker K, et al. Flow-mediated vasodilation predicts outcome in patients with chronic heart failure: comparison with B-type natriuretic peptide. *J Am Coll Cardiol* 2005;46(6):1011-8.
314. Androne AS, Hryniewicz K, Hudaihed A, et al. Comparison of Metabolic Vasodilation in Response to Exercise and Ischemia and Endothelium-Dependent Flow-Mediated Dilation in African-American Versus Non-African-American Patients With Chronic Heart Failure. *The American Journal of Cardiology* 2006;97(5):685-89.
315. Deftereos S, Giannopoulos G, Raisakis K, et al. Comparison of Muscle Functional Electrical Stimulation to Conventional Bicycle Exercise on Endothelium and Functional Status Indices in Patients With Heart Failure. *The American Journal of Cardiology* 2010;106(11):1621-25.
316. Kubo SH, Rector TS, Bank AJ, et al. Endothelium-dependent vasodilation is attenuated in patients with heart failure. *Circulation* 1991;84(4):1589-96.
317. Katz SD, Krum H, Khan T, et al. Exercise-induced vasodilation in forearm circulation of normal subjects and patients with congestive heart failure: role of endothelium-derived nitric oxide. *J Am Coll Cardiol* 1996;28(3):585-90.

318. Shechter M, Matetzky S, Arad M, et al. Vascular endothelial function predicts mortality risk in patients with advanced ischaemic chronic heart failure. *Eur J Heart Fail* 2009;11(6):588-93.
319. George J, Carr E, Davies J, et al. High-Dose Allopurinol Improves Endothelial Function by Profoundly Reducing Vascular Oxidative Stress and Not by Lowering Uric Acid. *Circulation* 2006;114(23):2508-16.
320. Napoli R, Guardasole V, Matarazzo M, et al. Growth hormone corrects vascular dysfunction in patients with chronic heart failure. *Journal of the American College of Cardiology* 2002;39(1):90-95.
321. Moertl D, Hammer A, Steiner S, et al. Dose-dependent effects of omega-3-polyunsaturated fatty acids on systolic left ventricular function, endothelial function, and markers of inflammation in chronic heart failure of nonischemic origin: A double-blind, placebo-controlled, 3-arm study. *American heart journal* 2011;161(5):915.e1-15.e9.
322. Akar JG, Al-Chekakie MO, Fugate T, et al. Endothelial dysfunction in heart failure identifies responders to cardiac resynchronization therapy. *Heart rhythm : the official journal of the Heart Rhythm Society* 2008;5(9):1229-35.
323. Belardinelli R, Capestro F, Misiani A, et al. Moderate exercise training improves functional capacity, quality of life, and endothelium-dependent vasodilation in chronic heart failure patients with implantable cardioverter defibrillators and cardiac resynchronization therapy. *European Journal of Cardiovascular Prevention & Rehabilitation* 2006;13(5):818-25.
324. Enomoto K, Yamabe H, Toyama K, et al. Improvement effect on endothelial function in patients with congestive heart failure treated with cardiac resynchronization therapy. *Journal of cardiology* 2011;58(1):69-73.
325. Castellant P, Fatemi M, Orhan E, et al. Patients with non-ischaemic dilated cardiomyopathy and hyper-responders to cardiac resynchronization therapy: characteristics and long-term evolution. *Europace : European pacing, arrhythmias, and cardiac electrophysiology : journal of the working groups on cardiac pacing, arrhythmias, and cardiac cellular electrophysiology of the European Society of Cardiology* 2009;11(3):350-55.

326. Santini L, Capria A, Di Molfetta A, et al. Endothelial dysfunction is a marker of systemic response to the cardiac resynchronization therapy in heart failure. *Journal of cardiac failure* 2013;19(6):419-25.
327. Liuni A, Luca MC, Lisi M, et al. Observations of time-based measures of flow-mediated dilation of forearm conduit arteries: implications for the accurate assessment of endothelial function. *Am J Physiol Heart Circ Physiol* 2010;299(3):H939-45.
328. Eickhoff P, Valipour A, Kiss D, et al. Determinants of systemic vascular function in patients with stable chronic obstructive pulmonary disease. *Am J Respir Crit Care Med* 2008;178(12):1211-8.
329. Gordon JW. *Anat & Physiol* 1877;11(533).
330. Starr I, Rawson AJ, Schroeder HA, et al. Studies on the estimation of cardiac output in man, and of abnormalities in cardiac function from the heart's recoil and the blood's impact: the ballistocardiogram. *Am J Physiol* 1939;127(1).
331. Gubner RS, Rodstein M, Ungerleider HE. [Ballistocardiography; an appraisal of technic, physiologic principles, and clinical value]. *Circulation* 1953;7(2):268-86.
332. Starr I, Horwitz O, Mayock RL, et al. Standardization of the ballistocardiogram by simulation of the heart's function at necropsy; with a clinical method for the estimation of cardiac strength and normal standards for it. *Circulation* 1950;1(5):1073-96.
333. Brown HR, Hoffman MJ, DeLalla V. Ballistocardiogram findings in patients with angina pectoris. *Circulation* 1950;1(132).
334. Inan OT, Etemadi M, Wiard RM, et al. Robust ballistocardiogram acquisition for home monitoring. *Physiol Meas* 2009;30(2):169-85.
335. PHIBBS B, LOWE CR, HOLMES RW. The Ultra Low Frequency Force Ballistocardiograph in Acute Cardiomyopathy. *Circulation* 1967;36(1):92-100.
336. Ballistocardiography: A method worth revisiting. *Annual International Conference of the IEEE*; 2011 Aug. 30 2011-Sept. 3 2011.
337. Starr I, Hildreth EA. The effect of aging and of the development of disease on the ballistocardiogram; a study of eighty subjects, originally healthy, followed from ten to fourteen years. *Circulation* 1952;5(4):481-95.

338. Castillo Martínez L, Colín Ramírez E, Orea Tejeda A, et al. Bioelectrical impedance and strength measurements in patients with heart failure: comparison with functional class. *Nutrition* 2007;23(5):412-18.
339. Gary RA, Cress ME, Higgins MK, et al. Combined Aerobic and Resistance Exercise Program Improves Task Performance in Patients With Heart Failure. *Archives of Physical Medicine and Rehabilitation* 2011;92(9):1371-81.
340. Izawa KP, Watanabe S, Osada N, et al. Handgrip strength as a predictor of prognosis in Japanese patients with congestive heart failure. *European Journal of Cardiovascular Prevention & Rehabilitation* 2009;16(1):21-27.
341. Izawa KP, Watanabe S, Yokoyama H, et al. Muscle Strength in Relation to Disease Severity in Patients with Congestive Heart Failure. *American Journal of Physical Medicine & Rehabilitation* 2007;86(11):893-900 10.1097/PHM.0b013e318154b592.
342. Senden PJ, Sabelis LW, Zonderland ML, et al. The effect of physical training on workload, upper leg muscle function and muscle areas in patients with chronic heart failure. *International Journal of Cardiology* 2005;100(2):293-300.
343. Andrews R, Walsh JT, Evans A, et al. Abnormalities of skeletal muscle metabolism in patients with chronic heart failure: evidence that they are present at rest. *Heart* 1997;77(2):159-63.
344. Katz AM, Katz PB. Diseases of the heart in the works of Hippocrates. *Br Heart J* 1962;24:257-64.
345. Anker SD, Leyva F, Poole-Wilson PA, et al. Relation between serum uric acid and lower limb blood flow in patients with chronic heart failure. *Heart* 1997;78(1):39-43.
346. Coats AJS, Clark AL, Piepoli M, et al. Symptoms and quality of life in heart failure: the muscle hypothesis. *British Heart Journal* 1994;72(2 Suppl):S36-S39.
347. Senden PJ, Sabelis LWE, Zonderland ML, et al. Determinants of maximal exercise performance in chronic heart failure. *European Journal of Cardiovascular Prevention & Rehabilitation* 2004;11(1):41-47.
348. Fulster S, Tacke M, Sandek A, et al. Muscle wasting in patients with chronic heart failure: results from the studies investigating co-morbidities aggravating heart failure (SICA-HF). *Eur Heart J* 2013;34(7):512-9.
349. Anker SD, Negassa A, Coats AJ, et al. Prognostic importance of weight loss in chronic heart failure and the effect of treatment with angiotensin-converting-enzyme inhibitors: an observational study. *Lancet* 2003;361(9363):1077-83.

350. Schellenbaum GD, Smith NL, Heckbert SR, et al. Weight Loss, Muscle Strength, and Angiotensin-Converting Enzyme Inhibitors in Older Adults with Congestive Heart Failure or Hypertension. *Journal of the American Geriatrics Society* 2005;53(11):1996-2000.
351. Sayer AA. Sarcopenia. *BMJ* 2010;341.
352. Fess EE. *Grip Strength*. 2nd ed. Chicago: American Society of Hand Therapists, 1992.
353. Roberts HC, Denison HJ, Martin HJ, et al. A review of the measurement of grip strength in clinical and epidemiological studies: towards a standardised approach. *Age and Ageing* 2011;40(4):423-29.
354. Mathiowetz V, Weber K, Volland G, et al. Reliability and validity of grip and pinch strength evaluations. *Journal of Hand Surgery* 1984;9A:222-6.
355. Balogun JA, Akomdafe CT, Amusa LO. Grip Strength: Effects of testing posture and elbow position. *Archives of Physical Medicine and Rehabilitation* 1991;72:280-83.
356. Mathiowetz V RC, Donahoe L. Effect of elbow position on grip and key pinch strength. *J Hand Surg Am* 1985;10(5):694-7.
357. The effects of instruction, verbal encouragement, and visual feedback on static handgrip strength. *Proceedings of the Human Factors and Ergonomics Society 43rd Annual Meeting*; 1999.
358. Su CY, Lin JH, Chien TH, et al. Grip strength in different positions of elbow and shoulder. *Arch Phys Med Rehabil* 1994;75(7):812-5.
359. Spijkerman DC, Snijders CJ, Stijnen T, et al. Standardization of grip strength measurements. Effects on repeatability and peak force. *Scand J Rehabil Med* 1991;23(4):203-6.
360. Beaton DE, O'Driscoll SW, Richards RR. Grip strength testing using the BTE work simulator and the Jamar dynamometer: a comparative study. *J Hand Surg [Am]* 1995;20(2):293-98.
361. Mitsionis G, Pakos EE, Stafilas KS, et al. Normative data on hand grip strength in a Greek adult population. *Int Orthop* 2009;33(3):713-7.
362. Rantanen T, Guralnik JM, Foley D, et al. Midlife Hand Grip Strength as a Predictor of Old Age Disability. *JAMA: The Journal of the American Medical Association* 1999;281(6):558-60.

363. Günther CM, Bürger A, Rickert M, et al. Grip Strength in Healthy Caucasian Adults: Reference Values. *The Journal of Hand Surgery* 2008;33(4):558-65.
364. Peters MJH, van Nes SI, Vanhoutte EK, et al. Revised normative values for grip strength with the Jamar dynamometer. *Journal of the Peripheral Nervous System* 2011;16(1):47-50.
365. Lunney JR, Lynn J, Foley DJ, et al. Patterns of functional decline at the end of life. *JAMA : the journal of the American Medical Association* 2003;289(18):2387-92.
366. ANAKWE RE, HUNTLEY JS, MCEACHAN JE. Grip Strength and Forearm Circumference in a Healthy Population. *Journal of Hand Surgery (European Volume)* 2007;32(2):203-09.
367. Clark BC, Manini TM. Sarcopenia \neq dynapenia. *J Gerontol A Biol Sci Med Sci* 2008;63(8):829-34.
368. Skelton DA, Greig CA, Davies JM, et al. Strength, power and related functional ability of healthy people aged 65-89 years. *Age Ageing* 1994;23(5):371-7.
369. Oreopoulos A, Ezekowitz JA, McAlister FA, et al. Association between direct measures of body composition and prognostic factors in chronic heart failure. *Mayo Clin Proc* 2010;85(7):609-17.
370. Gielen S, Sandri M, Kozarez I, et al. Exercise training attenuates MuRF-1 expression in the skeletal muscle of patients with chronic heart failure independent of age: the randomized Leipzig Exercise Intervention in Chronic Heart Failure and Aging catabolism study. *Circulation* 2012;125(22):2716-27.
371. Khawaja T, Chokshi A, Ji R, et al. Ventricular assist device implantation improves skeletal muscle function, oxidative capacity, and growth hormone/insulin-like growth factor-1 axis signaling in patients with advanced heart failure. *J Cachexia Sarcopenia Muscle* 2014;5(4):297-305.
372. Gosker HR, Lencer NH, Franssen FM, et al. Striking similarities in systemic factors contributing to decreased exercise capacity in patients with severe chronic heart failure or COPD. *Chest* 2003;123(5):1416-24.
373. Chang Y-T, Wu H-L, Guo H-R, et al. Handgrip strength is an independent predictor of renal outcomes in patients with chronic kidney diseases. *Nephrology Dialysis Transplantation* 2011.

374. Atkinson AJ, Colburn WA, DeGruttola VG, et al. Biomarkers and surrogate endpoints: Preferred definitions and conceptual framework*. *Clin Pharmacol Ther* 2001;69(3):89-95.
375. Leyva F, Anker SD, Godsland IF, et al. Uric acid in chronic heart failure: a marker of chronic inflammation. *European Heart Journal* 1998;19(12):1814-22.
376. Pascual-Figal DA, Hurtado-Martínez JA, Redondo B, et al. Hyperuricaemia and long-term outcome after hospital discharge in acute heart failure patients. *European Journal of Heart Failure* 2007;9(5):518-24.
377. Kittleson MM, St John ME, Bead V, et al. Increased levels of uric acid predict haemodynamic compromise in patients with heart failure independently of B-type natriuretic peptide levels. *Heart* 2007;93(3):365-67.
378. Tamariz L, Harzand A, Palacio A, et al. Uric Acid as a Predictor of All-Cause Mortality in Heart Failure: A Meta-Analysis. *Congestive Heart Failure* 2011;17(1):25-30.
379. Krishnan E. Hyperuricemia and Incident Heart Failure / CLINICAL PERSPECTIVE. *Circulation: Heart Failure* 2009;2(6):556-62.
380. Anker SD, Doehner W, Rauchhaus M, et al. Uric Acid and Survival in Chronic Heart Failure. *Circulation* 2003;107(15):1991-97.
381. Huang H, Huang B, Li Y, et al. Uric acid and risk of heart failure: a systematic review and meta-analysis. *Eur J Heart Fail* 2014;16(1):15-24.
382. Hare JM, Mangal B, Brown J, et al. Impact of Oxypurinol in Patients With Symptomatic Heart Failure: Results of the OPT-CHF Study. *Journal of the American College of Cardiology* 2008;51(24):2301-09.
383. Gavin AD, Struthers AD. Allopurinol reduces B-type natriuretic peptide concentrations and haemoglobin but does not alter exercise capacity in chronic heart failure. *Heart* 2005;91(6):749-53.
384. Givertz MM, Anstrom KJ, Redfield MM, et al. Effects of Xanthine Oxidase Inhibition in Hyperuricemic Heart Failure Patients: The Xanthine Oxidase Inhibition for Hyperuricemic Heart Failure Patients (EXACT-HF) Study. *Circulation* 2015;131(20):1763-71.
385. Dzeja P, Nemutlu E, Xu Y-Z, et al. Abstract 18444: Effects of Cardiac Resynchronization Therapy on Transcardiac Metabolomic Profile and Substrate Utilization American Heart Association, 2011:A18444.

386. Rinkuniene D, Bucyte S, Ceseviciute K, et al. Predictors of positive response to cardiac resynchronization therapy. *BMC Cardiovascular Disorders* 2014;14(1):55.
387. Arora S, Aukrust P, Ueland T, et al. Elevated serum uric acid levels following heart transplantation predict all-cause and cardiac mortality. *European Journal of Heart Failure* 2009;11(10):1005-13.
388. Gillot T. Personal Communication., 2013.
389. Missov E, Calzolari C, Pau B. Circulating Cardiac Troponin I in Severe Congestive Heart Failure. *Circulation* 1997;96(9):2953-58.
390. Latini R, Masson S, Anand IS, et al. Prognostic Value of Very Low Plasma Concentrations of Troponin T in Patients With Stable Chronic Heart Failure. *Circulation* 2007;116(11):1242-49.
391. Peacock WF, De Marco T, Fonarow GC, et al. Cardiac Troponin and Outcome in Acute Heart Failure. *New England Journal of Medicine* 2008;358(20):2117-26.
392. Miller WL, Hartman KA, Burritt MF, et al. Profiles of Serial Changes in Cardiac Troponin T Concentrations and Outcome in Ambulatory Patients With Chronic Heart Failure. *Journal of the American College of Cardiology* 2009;54(18):1715-21.
393. Sundström J, Ingelsson E, Berglund L, et al. Cardiac troponin-I and risk of heart failure: a community-based cohort study. *European Heart Journal* 2009;30(7):773-81.
394. deFilippi CR, de Lemos JA, Christenson RH, et al. Association of Serial Measures of Cardiac Troponin T Using a Sensitive Assay With Incident Heart Failure and Cardiovascular Mortality in Older Adults. *JAMA: The Journal of the American Medical Association* 2010;304(22):2494-502.
395. Fertin M, Hennache B, Hamon M, et al. Usefulness of Serial Assessment of B-Type Natriuretic Peptide, Troponin I, and C-Reactive Protein to Predict Left Ventricular Remodeling After Acute Myocardial Infarction (from the REVE-2 Study). *The American Journal of Cardiology* 2010;106(10):1410-16.
396. Kociol RD, Pang PS, Gheorghiade M, et al. Troponin Elevation in Heart Failure: Prevalence, Mechanisms, and Clinical Implications. *Journal of the American College of Cardiology* 2010;56(14):1071-78.
397. Thygesen K, Alpert JS, Jaffe AS, et al. Third universal definition of myocardial infarction. *J Am Coll Cardiol* 2012;60(16):1581-98.

398. Aarones M, Gullestad L, Aakhus S, et al. Prognostic value of cardiac troponin T in patients with moderate to severe heart failure scheduled for cardiac resynchronization therapy. *American heart journal* 2011;161(6):1031-37.
399. Nauffal V, Tanawuttiwat T, Zhang Y, et al. Predictors of mortality, LVAD implant, or heart transplant in primary prevention cardiac resynchronization therapy recipients: The HF-CRT score. *Heart Rhythm* 2015.
400. Delgado RM, Palanichamy N, Radovancevic R, et al. Brain Natriuretic Peptide Levels and Response to Cardiac Resynchronization Therapy in Heart Failure Patients. *Congestive Heart Failure* 2006;12(5):250-53.
401. Kubánek M, Málek I, Bytešník J, et al. Decrease in plasma B-type natriuretic peptide early after initiation of cardiac resynchronization therapy predicts clinical improvement at 12 months. *European Journal of Heart Failure* 2006;8(8):832-40.
402. El-Saed A, Voigt A, Shalaby A. Usefulness of Brain Natriuretic Peptide Level at Implant in Predicting Mortality in Patients with Advanced But Stable Heart Failure Receiving Cardiac Resynchronization Therapy. *Clinical Cardiology* 2009;32(11):E33-E38.
403. Fruhwald FM, Fahrleitner-Pammer A, Berger R, et al. Early and sustained effects of cardiac resynchronization therapy on N-terminal pro-B-type natriuretic peptide in patients with moderate to severe heart failure and cardiac dyssynchrony. *Eur Heart J* 2007;28(13):1592-7.
404. Berger R, Shankar A, Fruhwald F, et al. Relationships between cardiac resynchronization therapy and N-terminal pro-brain natriuretic peptide in patients with heart failure and markers of cardiac dyssynchrony: an analysis from the Cardiac Resynchronization in Heart Failure (CARE-HF) study. *European Heart Journal* 2009;30(17):2109-16.
405. Shalaby AA, Abraham WT, Fonarow GC, et al. Association of BNP and Troponin Levels with Outcome among Cardiac Resynchronization Therapy Recipients. *Pacing and clinical electrophysiology : PACE* 2015;38(5):581-90.
406. Magne J, Dubois M, Champagne J, et al. Usefulness of NT-pro BNP monitoring to identify echocardiographic responders following cardiac resynchronization therapy. *Cardiovascular ultrasound* 2009;7(1):39.
407. Sinha AM, Filzmaier K, Breithardt OA, et al. Usefulness of brain natriuretic peptide release as a surrogate marker of the efficacy of long-term cardiac resynchronization therapy in patients with heart failure. *Am J Cardiol* 2003;91(6):755-8.

408. Hagstrom E, Ingelsson E, Sundstrom J, et al. Plasma parathyroid hormone and risk of congestive heart failure in the community. *Eur J Heart Fail* 2010;12(11):1186-92.
409. Bozic B, Loncar G, Prodanovic N, et al. Parathyroid Hormone Response to Vitamin D Insufficiency in Elderly Males With Chronic Heart Failure. *Physiol Res* 2011;60(Suppl . 1):s115-s63.
410. Altay H, Zorlu A, Binici S, et al. Relation of Serum Parathyroid Hormone Level to Severity of Heart Failure. *The American Journal of Cardiology* 2011.
411. Schierbeck LL, Jensen TS, Bang U, et al. Parathyroid hormone and vitamin D— markers for cardiovascular and all cause mortality in heart failure. *European Journal of Heart Failure* 2011;13(6):626-32.
412. Agapitou V, Dimopoulos S, Mpouchla A, et al. Serum intact parathyroid hormone levels independently predict exercise capacity in stable heart failure patients. *International Journal of Cardiology* 2011;146(3):462-64.
413. Loncar G, Bozic B, Dimkovic S, et al. Association of increased parathyroid hormone with neuroendocrine activation and endothelial dysfunction in elderly men with heart failure. *J Endocrinol Invest* 2011;34(3):e78-85.
414. Ameri P, Ronco D, Casu M, et al. High prevalence of vitamin D deficiency and its association with left ventricular dilation: An echocardiography study in elderly patients with chronic heart failure. *Nutrition, Metabolism and Cardiovascular Diseases* 2010;20(9):633-40.
415. Boxer RS, Dauser DA, Walsh SJ, et al. The Association Between Vitamin D and Inflammation with the 6-Minute Walk and Frailty in Patients with Heart Failure. *Journal of the American Geriatrics Society* 2008;56(3):454-61.
416. Boxer RS, Kenny AM, Cheruvu VK, et al. Serum 25-hydroxyvitamin D concentration is associated with functional capacity in older adults with heart failure. *American Heart Journal* 2010;160(5):893-99.
417. Gotsman I, Shauer A, Zwas DR, et al. Vitamin D deficiency is a predictor of reduced survival in patients with heart failure; vitamin D supplementation improves outcome. *European Journal of Heart Failure* 2012;14(4):357-66.
418. Pilz S, März W, Wellnitz B, et al. Association of Vitamin D Deficiency with Heart Failure and Sudden Cardiac Death in a Large Cross-Sectional Study of Patients Referred for Coronary Angiography. *Journal of Clinical Endocrinology & Metabolism* 2008;93(10):3927-35.

419. Witham MD, Crighton LJ, Gillespie ND, et al. The effects of vitamin D supplementation on physical function and quality of life in older patients with heart failure: a randomized controlled trial. *Circulation Heart failure* 2010;3(2):195-201.
420. Stockton KA, Mengersen K, Paratz JD, et al. Effect of vitamin D supplementation on muscle strength: a systematic review and meta-analysis. *Osteoporos Int* 2011;22(3):859-71.
421. Giannakoulas G, Karvounis H, Koliakos G, et al. Parathyroid hormone-related protein is reduced in severe chronic heart failure. *Peptides* 2006;27(7):1894-97.
422. Agarwal M, Phan A, Willix R, et al. Is Vitamin D Deficiency Associated With Heart Failure? A Review of Current Evidence. *Journal of Cardiovascular Pharmacology and Therapeutics* 2011;16(3-4):354-63.
423. Sugimoto T, Dohi K, Onishi K, et al. Interrelationship between haemodynamic state and serum intact parathyroid hormone levels in patients with chronic heart failure. *Heart* 2013;99(2):111-15.
424. Shinohara T, Takahashi N, Saito S, et al. Effect of cardiac resynchronization therapy on cardiac sympathetic nervous dysfunction and serum C-reactive protein level. *Pacing and clinical electrophysiology : PACE* 2011;34(10):1225-30.
425. Forman JP, Williams JS, Fisher ND. Plasma 25-hydroxyvitamin D and regulation of the renin-angiotensin system in humans. *Hypertension* 2010;55(5):1283-8.
426. Alonso-Martínez JL, Llorente-Diez B, Echegaray-Agara M, et al. C-reactive protein as a predictor of improvement and readmission in heart failure. *European Journal of Heart Failure* 2002;4(3):331-36.
427. Anand IS, Latini R, Florea VG, et al. C-Reactive Protein in Heart Failure. *Circulation* 2005;112(10):1428-34.
428. Suleiman M, Khatib R, Agmon Y, et al. Early Inflammation and Risk of Long-Term Development of Heart Failure and Mortality in Survivors of Acute Myocardial Infarction: Predictive Role of C-Reactive Protein. *Journal of the American College of Cardiology* 2006;47(5):962-68.
429. Sánchez-Lázaro IJ, Almenar L, Reganon E, et al. Inflammatory markers in stable heart failure and their relationship with functional class. *International Journal of Cardiology* 2008;129(3):388-93.

430. Johansson P, Lesman-Leegte I, Svensson E, et al. Depressive symptoms and inflammation in patients hospitalized for heart failure. *American heart journal* 2011;161(6):1053-59.
431. Nakagomi A, Seino Y, Endoh Y, et al. Upregulation of Monocyte Proinflammatory Cytokine Production by C-Reactive Protein is Significantly Related to Ongoing Myocardial Damage and Future Cardiac Events in Patients With Chronic Heart Failure. *Journal of cardiac failure* 2010;16(7):562-71.
432. Vasan RS, Sullivan LM, Roubenoff R, et al. Inflammatory Markers and Risk of Heart Failure in Elderly Subjects Without Prior Myocardial Infarction. *Circulation* 2003;107(11):1486-91.
433. Ridker PM, Cushman M, Stampfer MJ, et al. Inflammation, aspirin, and the risk of cardiovascular disease in apparently healthy men. *N Engl J Med* 1997;336(14):973-9.
434. McMurray JJV, Kjekshus J, Gullestad L, et al. Effects of Statin Therapy According to Plasma High-Sensitivity C-Reactive Protein Concentration in the Controlled Rosuvastatin Multinational Trial in Heart Failure (CORONA). *Circulation* 2009;120(22):2188-96.
435. Nagatomo Y, Yoshikawa T, Kohno T, et al. Effects of β -Blocker Therapy on High Sensitivity C-Reactive Protein, Oxidative Stress, and Cardiac Function in Patients With Congestive Heart Failure. *Journal of cardiac failure* 2007;13(5):365-71.
436. Przybyła A, Czarnecka D, Kusiak A, et al. The influence of cardiac resynchronization therapy on selected inflammatory markers and aldosterone levels in patients with chronic heart failure. *Przegl Lek* 2011;68(7):359-61.
437. Kamioka M, Suzuki H, Yamada S, et al. High sensitivity C-reactive protein predicts nonresponders and cardiac deaths in severe heart failure patients after CRT implantation. *Int Heart J* 2012;53(5):306-12.
438. Whitfield P. Personal Communication, 2013.
439. Cai C, Hua W, Ding LG, et al. High sensitivity C-reactive protein and cardiac resynchronization therapy in patients with advanced heart failure. *J Geriatr Cardiol* 2014;11(4):296-302.
440. OPARIL S, OBERMAN A. Nontraditional Cardiovascular Risk Factors. *The American Journal of the Medical Sciences* 1999;317(3):193-207.

441. Windram JD, Loh PH, Rigby AS, et al. Relationship of high-sensitivity C-reactive protein to prognosis and other prognostic markers in outpatients with heart failure. *American heart journal* 2007;153(6):1048-55.
442. Masson S, Latini R, Milani V, et al. Prevalence and Prognostic Value of Elevated Urinary Albumin Excretion in Patients With Chronic Heart Failure / CLINICAL PERSPECTIVE. *Circulation: Heart Failure* 2010;3(1):65-72.
443. Villacorta H, Ferradaes PdV, Mesquita ET, et al. Microalbuminúria é um marcador prognóstico independente em pacientes com insuficiência cardíaca crônica. *Arquivos Brasileiros de Cardiologia* 2012;98:62-69.
444. Gerstein HC, Mann JFE, Yi Q, et al. Albuminuria and Risk of Cardiovascular Events, Death, and Heart Failure in Diabetic and Nondiabetic Individuals. *JAMA: The Journal of the American Medical Association* 2001;286(4):421-26.
445. Figueiredo EL, Leão FVG, Oliveira LV, et al. Microalbuminuria in Nondiabetic and Nonhypertensive Systolic Heart Failure Patients. *Congestive Heart Failure* 2008;14(5):234-38.
446. Capes SE, Gerstein HC, Negassa A, et al. Enalapril prevents clinical proteinuria in diabetic patients with low ejection fraction. *Diabetes Care* 2000;23(3):377-80.
447. Struthers A, Lang C. The potential to improve primary prevention in the future by using BNP/N-BNP as an indicator of silent 'pancardiac' target organ damage. *European Heart Journal* 2007;28(14):1678-82.
448. van de Wal RMA, Asselbergs FW, Plokker HWT, et al. High Prevalence of Microalbuminuria in Chronic Heart Failure Patients. *Journal of cardiac failure* 2005;11(8):602-06.
449. Orea-Tejeda A, Colín-Ramírez E, Hernández-Gilsoul T, et al. Microalbuminuria in systolic and diastolic chronic heart failure patients. *Cardiology Journal* 2008;15(2):143-49.
450. Jackson CE, MacDonald MR, Petrie MC, et al. Associations of albuminuria in patients with chronic heart failure: findings in the ALiskiren Observation of heart Failure Treatment study. *European Journal of Heart Failure* 2011;13(7):746-54.
451. McAlister FA, Ezekowitz J, Tonelli M, et al. Renal insufficiency and heart failure: prognostic and therapeutic implications from a prospective cohort study. *Circulation* 2004;109(8):1004-9.

452. Ronco C, Haapio M, House AA, et al. Cardiorenal Syndrome. *Journal of the American College of Cardiology* 2008;52(19):1527-39.
453. Blecker S, Matsushita K, Köttgen A, et al. High-Normal Albuminuria and Risk of Heart Failure in the Community. *American Journal of Kidney Diseases* 2011;58(1):47-55.
454. Boerrigter G, Costello-Boerrigter LC, Abraham WT, et al. Cardiac Resynchronization Therapy Improves Renal Function in Human Heart Failure With Reduced Glomerular Filtration Rate. *Journal of cardiac failure* 2008;14(7):539-46.
455. Hartmann A, Andereassen AK, Holdaas H, et al. Five years' follow-up of renal glomerular and tubular functions in heart transplant recipients. *J Heart Lung Transplant* 1996;15(10):972-9.
456. Lin G, Gersh BJ, Greene EL, et al. Renal function and mortality following cardiac resynchronization therapy. *European Heart Journal* 2010.
457. European Heart Rhythm A, European Society of C, Heart Rhythm S, et al. 2012 EHRA/HRS expert consensus statement on cardiac resynchronization therapy in heart failure: implant and follow-up recommendations and management. *Europace : European pacing, arrhythmias, and cardiac electrophysiology : journal of the working groups on cardiac pacing, arrhythmias, and cardiac cellular electrophysiology of the European Society of Cardiology* 2012;14(9):1236-86.
458. AmericanDiabetesAssociation. Clinical practice recommendations 2001: diabetic nephropathy. *Diabetes Care* 2001;24(suppl 1):S69-S72.
459. Damman K, van Veldhuisen DJ, Navis G, et al. Urinary neutrophil gelatinase associated lipocalin (NGAL), a marker of tubular damage, is increased in patients with chronic heart failure. *European Journal of Heart Failure* 2008;10(10):997-1000.
460. Viberti GC, Mackintosh D, Bilous RW, et al. Proteinuria in diabetes mellitus: role of spontaneous and experimental variation of glycemia. *Kidney Int* 1982;21(5):714-20.
461. Mogensen CE. Microalbuminuria as a predictor of clinical diabetic nephropathy. *Kidney Int* 1987;31(2):673-89.
462. Peng T, Gao H, Shen L, et al. Correlation of brain natriuretic peptide and microalbuminuria in patients with heart failure. *West Indian Med J* 2011;60(6):658-61.
463. Parvez A, Khan SA, Rizvi I, et al. Prevalence of microalbuminuria in acute myocardial infarction and its correlation with Cardiac Troponin - I. *Biomedical Research* 2012;23(1):93-97.

464. Sakai H, Tsutamoto T, Tsutsui T, et al. Serum level of uric acid, partly secreted from the failing heart, is a prognostic marker in patients with congestive heart failure. *Circ J* 2006;70(8):1006-11.
465. Morris P, Warriner D, Morton A. *Eureka: Cardiovascular Medicine*. London: JP Publishing, 2015.
466. Knebel F, Reibis RK, Bondke H-J, et al. Tissue Doppler echocardiography and biventricular pacing in heart failure: Patient selection, procedural guidance, follow-up, quantification of success. *Cardiovascular ultrasound* 2004;2(1):17.
467. Sermesant M, Peyrat J-M, Chinchapatnam P, et al. Toward Patient-Specific Myocardial Models of the Heart. *Heart Failure Clinics* 2008;4:289-301.
468. Anker SD, Ponikowski P, Varney S, et al. Wasting as independent risk factor for mortality in chronic heart failure. *Lancet* 1997;349(9058):1050-3.